Synthesis of Novel Chemical Adjuvants for the Modulation and Study of CD1-d Mediated Immunological Processes

By

Padraic Quaid

A thesis submitted to the

University of Birmingham

For the degree of

DOCTOR OF PHILOSOPHY

School of Chemistry

College of Engineering

and Physical Sciences

University of Birmingham

May 2017

UNIVERSITY OF
BIRMINGHAM

University of Birmingham Research Archive

e-theses repository

This unpublished thesis/dissertation is copyright of the author and/or third parties. The intellectual property rights of the author or third parties in respect of this work are as defined by The Copyright Designs and Patents Act 1988 or as modified by any successor legislation.

Any use made of information contained in this thesis/dissertation must be in accordance with that legislation and must be properly acknowledged. Further distribution or reproduction in any format is prohibited without the permission of the copyright holder.

For my Family and Friends

Abstract

Antigen-presenting cells play a vital role in the immune system as presentation of antigens via cell-surface glycoproteins, such as MHC-I and CD1d, elicits an immune response. Antigen loading occurs in the endoplasmic reticulum with the help of chaperone proteins such as calreticulin. The natural ligand of calreticulin is an *N*-linked dodecasaccharide; however, it has been shown that a truncated Glc_1Man_3 tetrasaccharide can also be recognised. A biotinylated Glc_1Man_3 was designed to bind to both calreticulin and streptavidin to allow isolation of the calreticulin–tetrasaccharide complex through pull-down experiments. The stereoselective synthesis of this biotinylated oligosaccharide is described. CD1d-mediated presentation of glycolipids to the T-cell receptor of *i*NKT cells leads to an immune response. While α-galactosyl ceramide is the prototypical ligand, its activation of *i*NKT cells produces a mixture of T_H1 and T_H2 cytokines, which limits its therapeutic application. Analogues that induce a biased cytokine response are therefore desirable. Analysis of the crystal structure of the CD1d–α-GalCer–TCR complex reveals that the 6-*OH* and ring oxygen are not involved in binding. Analogues where these parts of the molecule have been excised, have led to the introduction of ThrCer and its cyclitol analogue ThrCer-6. We report a new and improved synthesis of ThrCer-6 and a series of analogues that were designed to elicit biased cytokine responses. Studies towards the preparation of ThrCer analogues involving modifications to the pseudo-glycosidic linkage are also described. Finally, the synthesis of ceramide analogues with the potential for conjugation through a photoreactive group to the CD1d protein are discussed.

Declaration

The work recorded in this thesis was carried out in the School of Biosciences at the University of Birmingham, U.K. during the period of September 2012 to December 2015. The work in this thesis is original except where acknowledged by reference.

No portion of this work is being, or has been submitted for a degree, diploma or any other qualification at any other university.

Acknowledgments

Firstly, I would like to thank my supervisors, Dr. Liam R. Cox and Prof. Gurdyal S. Besra for giving me the opportunity to work on a rewarding project. Your continued guidance and support through the lab work and patience while writing my thesis was invaluable and has helped develop my skills as a researcher and as a chemist. I would also like to thank the School of Chemistry and the analytical facility for their help throughout my PhD.

Next I want to thank the lab, you are all a great bunch and showed me that biologists aren't all bad, Monika in particular, our chats over coffee with Nat were always 'insightful'. To the chemists, Pete, Vee and Nat I want to thank you for taking me under your wings, I was never lost as I always got an answer to any question I asked, I was extremely lucky to have landed in next to such a talented bunch. Bogdan and Giacomo too, we had good craic in the lab, running columns and listening to tunes. Natacha, I want to especially thank you for being there for me when either chemistry or life got me down.

To the Kings of Jacoby Place, Joe, Liam and Niall, having you in Brum always made the place feel more like home. Trevor, I wouldn't have even got this far without you and I always said I'd give you a mention!

To my family, I am eternally grateful for your continued support through my many years of education. Thank you for helping me become the man I am today.

Finally, to Lorraine, my best bud, your belief in me when my belief in myself had faltered is your greatest gift to me and I can't wait to see what our future holds!

Contents

List of Abbreviations

°C	degrees centigrade
%	percent
Ac	acetyl
Å	angstrom
AG	activating group
AGL	agelasphin
α-GalCer	α-galactosyl ceramide
APC	antigen Presenting Cell
Ar	aromatic, aryl
Arg	arginine
Asn	asparagine
Asp	aspartic acid
β2m	β2-microglobulin
BCR	B-cell receptor
Bn	benzyl (CH_2Ph)
Boc	*tert*-Butyl carbamate
Bu	butyl
Bz	benzoyl
CD	cluster of differentiation

COSY	correlation spectroscopy
CRT	calreticulin
CSA	(1*S*)-(+)-10-camphorsulfonic acid
DC	dendritic Cells
DIPEA	*N,N*-Diisopropylethylamine (Hünig's base)
DIBALH	diisobutylaluminium hydride
DMAP	4-dimethylaminopyridine
DME	dimethoxyethane
DMF	*N,N*-dimethylformamide
DMSO	dimethylsulfoxide
DMTST	dimethyl(methylthio)sulfonium trifluoromethanesulfonate
DN	double negative
DP	double positive
EDCI.HCl	1-ethyl-3-(3-dimethylaminopropyl)carbodiimide hydrochloride
ER	endoplasmic Reticulum
Et	ethyl
FGI	functional group interconversion
g	grammes
Glc	glucose
GSH	glutathione
GST	glutathione S-transferase

h	hour(s)
hCD1d	human CD1d
HLA	human leukocyte antigen
HMBC	heteronuclear multiple bond correlation experiment
HMDS	hexamethyldisilazane
HMPA	hexamethylphosphoramide
HSQC	heteronuclear single-quantum correlation spectroscopy
IFN	interferon
Ig	immunoglobulin
IL	interleukin
Ile	isoleucine
*i*NKT cell	invariant natural killer T cell
IR	infrared
K_d	dissociation constant
L	litre
m	milli
M	molar
MAIT cell	mucosal associated invariant T cell
Man	mannose
Me	methyl
Met	methionine

mg	milligrammes
MHC	major histocompatability complex
MHz	megahertz
min	Minute
mL	Millilitres
m.p.	Melting point
M.S.	Molecular Sieves
n	Nano
NBS	*N*-Bromosuccinimide
NHS	*N*-Hydroxysuccinimide
NIS	*N*-Iodosuccinimide
NK cell	natural killer cell
NMR	nuclear magnetic resonance
Nosyl (Ns)	2- or 4-nitrobenzenesulfonyl
OD	optical density
PAL	photoaffinity labelling
PAMPs	pathogen-associated molecular patterns
PG	protecting group
Ph	phenyl
Phe	phenylalanine
PhG	photoreactive group

PMB	*para*-Methoxybenzyl
Pr	propyl
PRRs	pattern recognition receptors
PTSA	*para*-Toluenesulfonic acid
rt	room temperature
s	second(s)
T_C	cytotoxic T-lymphocytes
T_H	helper T cell
TBAF	tetrabutylammonium fluoride
TBDMS	*tert*-butyldimethylsilyl
TBDPS	*tert*-butyldiphenylsilyl
TBTA	tris(benzyltriazolylmethyl)amine
TCR	T cell receptor
TFA	trifluoroacetic acid
THF	tetrahydrofuran
ThrCer	threitol ceramide
TLC	thin layer chromatography
TMS	trimethylsilyl
TMU	tetramethylurea
Tf	trifluoromethanesulfonyl
Tosyl (Ts)	*para*-toluenesulfonyl

Trp	tryptophan
Tyr	tyrosine
µ	micro

Chapter 1

General Introduction

1. General Introduction

1.1. Immunity

The immune system is the body's way of fighting the invasion by pathogens, be they viral, bacterial, fungal or other external invaders. Vertebrates employ two different types of immunity to tackle the problem of attack by opportunistic pathogens; these are termed innate and adaptive immunity (Table 1.). Innate immunity is the defence mechanism that is activated following *immediate* exposure to a pathogen. It is non-specific and functions the same irrespective of whether or not there has been a previous infection by the same pathogen. In contrast, adaptive or acquired immunity is *pathogen-specific* and is based around the recognition of antigens that are specific to a particular pathogen. While innate immunity provides a rapid response and is found in all animal- and plant-life, adaptive immunity is a slower response and is specific to vertebrates.[1]

	Innate	Adaptive
Self/non-self discrimination	Present, reaction is against foreign	Present, reaction is against foreign
Lag phase	Absent, response is immediate	Present, response takes a few days
Specificity	Limited, the same response is mounted to a wide variety of agents	High, the response is directed only to the agent that initiated it
Diversity	Limited, hence limited specificity	Extensive, resulting in a wide range of antigen receptors
Memory	Absent, subsequent exposure to an agent generates the same response	Present, subsequent exposure to the same agent induces amplified responses

Table 1.1. Principal differences between innate and adaptive immunity.

1.2. Innate Immunity

The skin acts as the first physical barrier of the innate immune system with the surface epithelial cells physically blocking entry by pathogens. Mucous membranes also trap microbes and other particles to prevent their entry. Other secretions can prevent infection; these include tears and saliva, both of which contain lysozyme. This enzyme is able to kill bacterial pathogens by breaking up their cell wall. It does this by catalysing the hydrolysis of 1, 4-β-glycosyl linkages found in the peptidoglycan component of the cell wall. Stomach acid functions similarly by placing the pathogen in a low pH environment, which it may not be able to withstand.

When pathogens get through these external barriers and first lines of defence an internal response is required. This internal response will come from phagocytic and Natural Killer (NK) cells as well as antimicrobial proteins following an inflammatory response. This response does not require any previous exposure to the invading pathogen as no immunological memory is required for an innate immune response.

The internal response is initiated by the recognition of Pathogen-Associated Molecular Patterns (PAMPs) by innate cells, such as macrophages and Dendritic Cells (DCs), which contain Pattern Recognition Receptors (PRRs) on their cell surfaces.[2] PAMPs are conserved non-self molecules that are associated with particular pathogens. A large range of PRRs are present on innate cells which can identify a similarly large range of different PAMPs.[3] PRR-containing innate cells are present in all tissues to maximise potential exposure. Following exposure to a pathogen, phagocytic cells can then be instigated to perform phagocytosis. This mechanism works with the cell first engulfing the pathogen to form an endosome within the cell. This cell then binds to lysosome, which contains enzymes and acids that digest and kill the cell. [4]

1.3. Adaptive immunity

Adaptive immunity is unique in that it possesses immunological memory, which was first mentioned in history in 430 B.C., when Thucydides, the Greek historian noted that following a plague that had swept through Athens, those who had survived were able to tend to the sick without being re-infected. However, it wasn't until Edward Jenner (1749–1823) in the 18th century and his experiment with cowpox that we began to understand this side of the immune system. Jenner deliberately infected people with cowpox and subsequently showed that they were immune to small pox. This observation led to the basis of vaccination whereby antigenic material is administered to induce an immune response, developing adaptive immunity to a pathogen. Louis Pasteur developed vaccination further along with his proposal of the germ theory of disease which stated that microorganisms were the cause of infection. Further study has improved our understanding of the immune system much further with the discovery of antibodies and the processes about which adaptive immunity and immunological memory take place.

The adaptive immune response relies on the activation of lymphocytes, which are white blood cells known as T cells and B cells. B cells are required for the formation of antibodies or immunoglobulin (Ig) and are involved in humoral or antibody-mediated immunity. T cells on the other hand are involved in cell-mediated immunity, which depend on the activation of antigen-specific cytotoxic T-lymphocytes (T_C). A special type of T cell known as the helper T cell (T_H) plays a vital part in both cell-mediated and humoral immunity responses.

All lymphocytes begin as stem cells in the bone marrow. In humans, stem cells that migrate to the thymus for maturation become T cells, whilst stem cells that remain within the bone marrow to mature become B cells. Both types of cells are only activated upon recognition by an antigen.

1.3.1. Antigen recognition of B cells and T cells

Both B cells and T cells express antigen-specific receptors on their cell surface. The B-cell receptor (BCR) is a trans-membrane Y-shaped protein formed from a combination of heavy- and light-chain polypeptides linked together by disulfide bonds as shown in Figure 1.1.

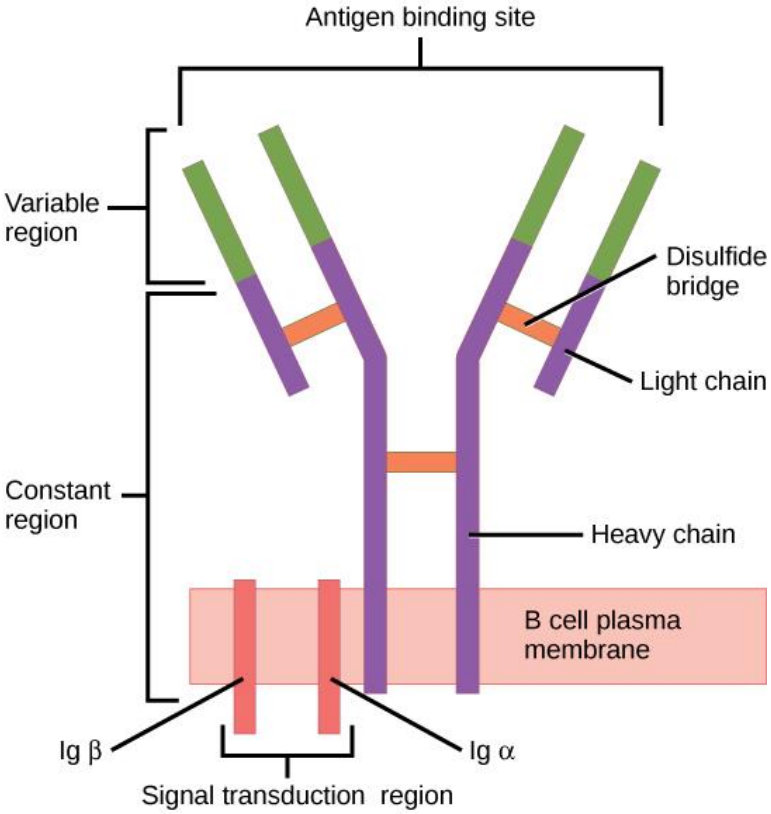

Figure 1.1. Structure of B-cell receptor. Figure adapted from ref.[5] Permission not required.

B-cell receptors have a similar structure to antibodies but are bound to the cell surface. By contrast, antibodies are soluble and free-flowing molecules that are secreted from activated B cells and found within the blood. T-cell receptors (TCRs) consist of two peptide chains, alpha (α) and beta (β) linked together by disulfide bonds as shown in Figure 1.2. These molecules are also membrane-bound.

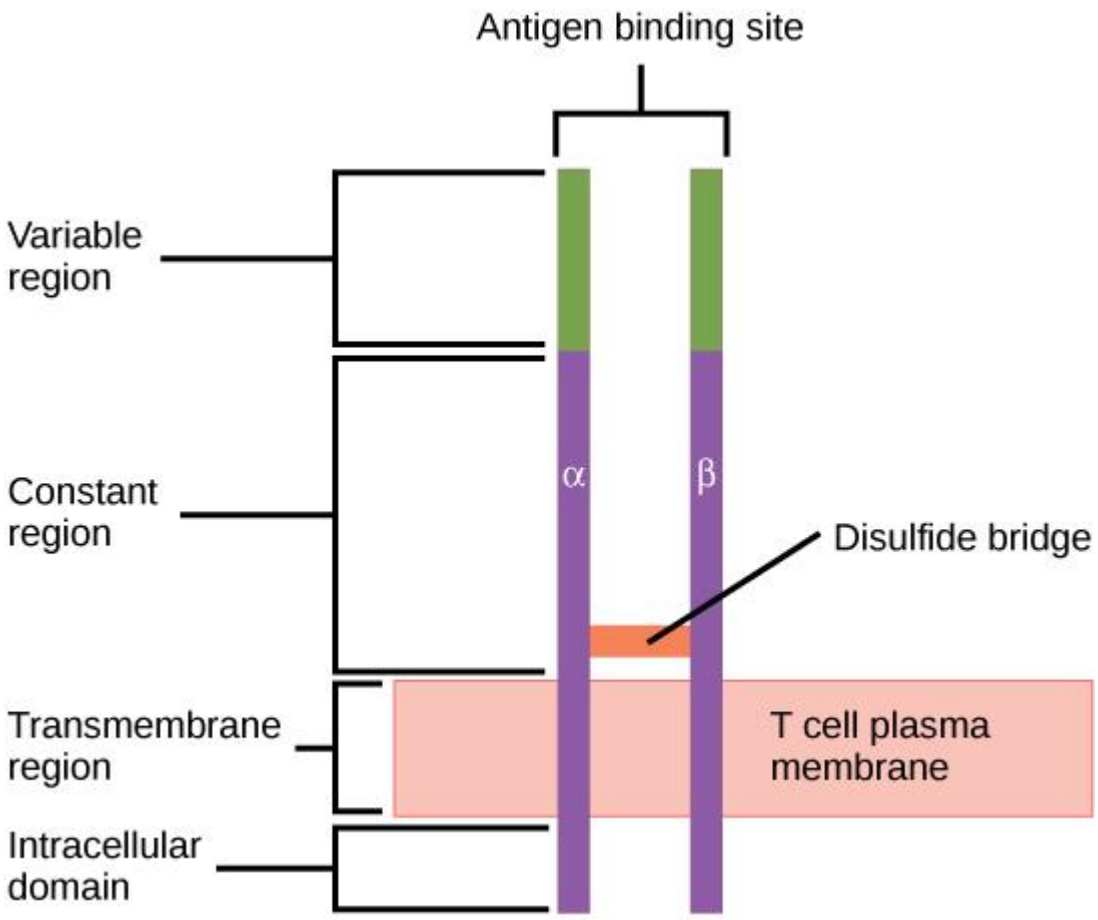

Figure 1.2. Structure of a T-cell receptor. Adapted from ref.[5] Permission not required.

T cells and B cells differ in the way the antigen is presented to their associated receptors. The BCR binds to epitopes of its cognate antigen in its native exogenous form. The TCR recognises its antigen after it has been processed within an infected antigen-presenting cell (APC) and bound to a major histocompatibility complex class 1 (MHC-I) molecule on the surface of the infected cell. The resulting antigen–MHC complex is then presented to the TCR, an example of which is shown in Figure 1.3.

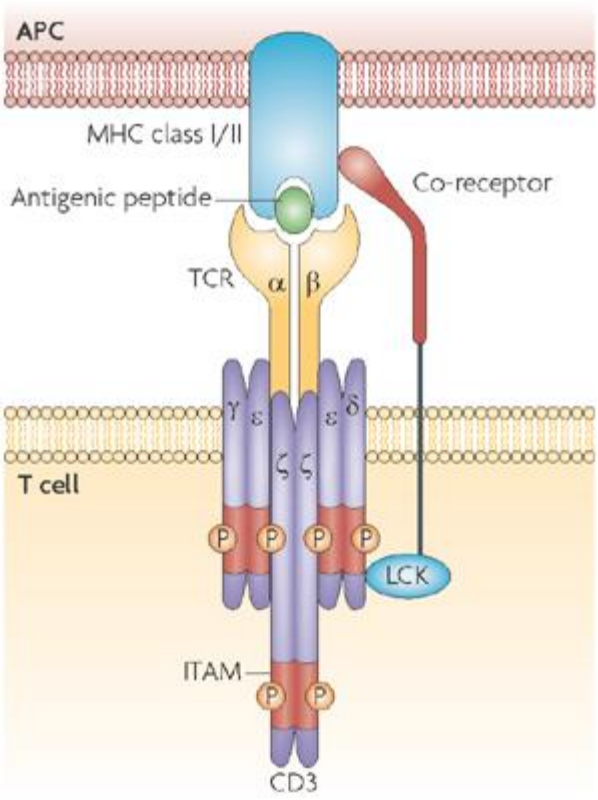

Figure 1.3. The TCR–antigen–MHC complex. Figure adapted from ref.[6] Permission to reproduce figure was obtained through RightsLink® - licence number 4106410895166.

1.3.2. Development of lymphocytes

The development of B- and T cells occurs in two stages, before and after binding to its specific antigen. The diversity within the receptors, needed to recognise a large range of potential pathogenic proteins and differentiate self from non-self are developed while the cells are

maturing. Proliferation of activated cells and the formation of immunological memory are developed *post* binding to the specific antigen.

Diversity among the millions of antigen receptors found on the surface of the millions of cells is developed during the synthesis of the proteins within the cell prior to expression. Both BCRs and TCRs are made of conserved regions and variable regions. As seen in Figures 1.1. and 1.2., the constant regions are found at the end of the protein which is embedded within the cell membrane. These regions do not change between different receptors and maintain a similar function around the cell wall. A variable region is found at the other end, which is exposed outwards away from the cell wall. It is this variable region that recognises pathogenic proteins through protein–protein interactions. The mechanism for this is shown in Figure 1.4. for the β-chain however the α-chain has a similar mechanism although it is encoded from another part of the DNA. The variable region comes about by the rearranging of the germline DNA by a recombinase, which randomly deletes part of the undifferentiated DNA strand for the protein which is then transcribed and translated to give a polypeptide of a specific sequence, with this sequence being different from the last. These different polypeptides can then assemble to form a specific protein with a unique binding site. A large number of potential recombinations leads to an even larger number of specific receptors. Before maturation, the receptors are tested for self-reactivity as a receptor that reacts with self-antigens will be detrimental to the body by causing autoimmunity. Any cell with a receptor shown to be self-reactive either undergoes apoptosis or is non-functionalised before final maturation.[1]

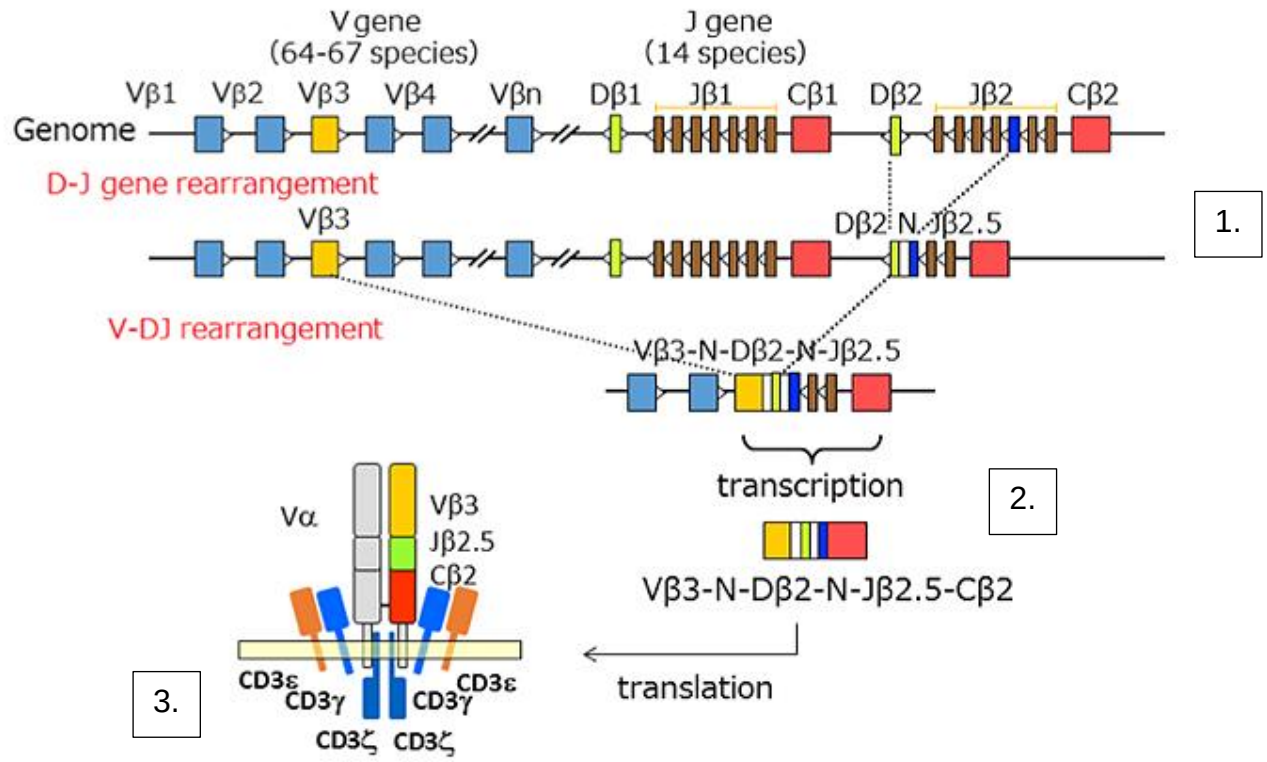

Figure 1.4. Diversity of the TCR from the processing of the germline DNA. Adapted from ref.[7] Permission not required.

1. Shows the germline DNA for the β chain.
2. Shows the rearrangement of the DNA followed by transcription and translation.
3. Shows the final unique TCR, with a similar mechanism used to synthesise the α–chain

Proliferation of activated cells is achieved by a process of clonal selection. When a specific antigen receptor binds to its epitope the cell undergoes cell divisions to yield a large number of clones, each expressing the same desired antigen receptor. These clones will be made into memory cells or into effector cells for an immediate immune response. B-cell effector cells are known as plasma cells, which secrete antibodies whilst T-cell effector cells are T helper and cytotoxic T cells, which go on to react further to kill the invading pathogen. Following the primary immune response, which results in the formation of memory cells, any subsequent infection by the same pathogen will activate the memory cells, which then proliferate to

generate a large number of desired clones at a faster rate than was the case at the first infection. This is known as immunological memory.

1.3.3. Activation of cells for an immune response

A humoral immune response involves the use of antibodies to fight infection in the blood and lymph, while a cell-mediated immune response involves cytotoxic T cells, which kill infected cells. Both responses are initiated following the activation of helper T cells (T_H) by a dedicatedl Antigen-Presenting Cell (APC) presenting the specific antigen bound to a MHC II molecule. The accessory protein CD4 found on the surface of the T cell binds as a co-receptor to the MHC to stabilise the complex. This complex activates an intracellular pathway that leads to the secretion of cytokines which activates T helper cells, causing them to proliferate and form clones which can then go on to activate B cells and cytotoxic T cells.

B Cells

Activation of B Cells occurs following recognition of the BCR with a pathogenic protein with the desired epitope. Receptor-mediated endocytosis then takes the antigen into the cell where it is broken down by proteases into peptide fragments, which are then bound to a MHC II molecule and presented on the cell surface. The antigen–MHC Class II complex then binds to a previously activated T_H cell *via* receptors for the same epitope. The newly formed complex secretes cytokines that then activate the B cell, which proliferates and multiplies to yield plasma cells. These plasma cells no longer produce the membrane-bound receptor but instead secrete them as antibodies (Figure 1.5.).

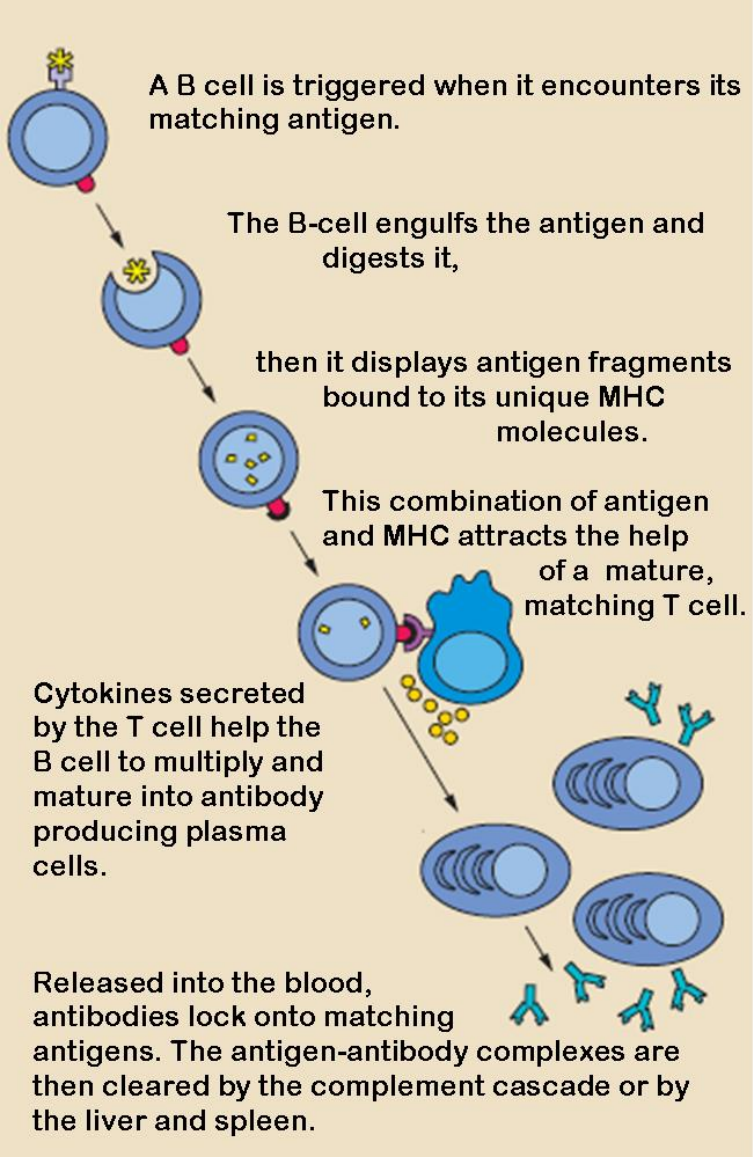

Figure 1.5. Production of antibodies *via* activation of B cells. Adapted from ref.[8] Permission not required

Antibodies do not kill pathogens themselves but instead mark them for destruction. Following recognition of a pathogenic epitope by an antibody there are various ways in which the target can be prevented from causing further harm. The first is through neutralisation, which blocks off the surface of a virus, preventing it from binding to a host cell. Next is opsonisation, which is the process whereby the target is marked for phagocytosis. This is done by the binding of opsonins to the target which then attracts macrophages and neutrophils. Finally, through the

use of a complement system also bound to the antibody, a membrane attack complex is formed which forms a pore in the cell wall causing the cell to lyse.

T Cells

As shown previously, T_H cells are vital in both humoral and cell-mediated immunity. As there are different cells involved in both processes, T_H cells need to be able to signal to a particular cell while not signalling to another. This differentiation is achieved through the use of cytokines. Cytokines are cell-signalling molecules which are released by one cell to elicit a response from another. A range of cytokines can be produced with the cytokine profile being important for governing how the body subsequently tackles the infection. Although there are many different types of cytokine present in the body, they can be divided into two main groups based on their function: those that are pro-inflammatory and those that are essentially anti-inflammatory but promote allergic responses. T_H cells are regarded as being the most prolific cytokine producers. They bring about two responses termed T_H1 and T_H2. T_H1-type cytokines afford a pro-inflammatory response, responsible for attacking intracellular foreign pathogens and for also exacerbating autoimmune responses. Interferon gamma (IFN-γ) is the principal Th1 cytokine. The T_H2 response is needed to oppose the T_H1 response as excessive pro-inflammatory responses may lead to tissue damage. T_H2-type cytokines include interleukins (IL) 4, 5, and 13, which are associated with the promotion of IgE (a type of antibody) and also interleukin-10, which has more of an anti-inflammatory response.[9]

Cell-mediated immunity is so called as it is predicated on the fact that a host cell has become infected. The host cell now produces foreign proteins required by the pathogen to survive and multiply. Fragments of these proteins are then presented by MHC-I molecules on the cell surface. MHC-I and the MHC-II molecules previously seen differ in the type of antigen they present. MHC-II molecules, which are only found on certain APCs, present exogenous antigens, which have been taken in from the outside and, by endocytosis or phagocytosis,

taken into the cell before being processed into fragments that are then presented by the MHC-II molecule. MHC-I molecules are found on the surface of most cells. They present endogenous proteins, which are antigens made within the host cell, be they self-proteins or non-self.

While T_H cells which have a CD4 co-receptor and interact with the MHC-II, another T cell, known as the Killer T cell interacts with the MHC-I. This killer or cytotoxic T cell (T_C) is responsible for the apoptosis of infected cells. When an infected cell presents a non-self antigen in the context of a MHC-I molecule, it is recognised by the TCR of a cytotoxic T cell, with the co-receptor CD8 helping to bind the complex. The T_C cell then secretes cytotoxins like perforin or granzyme, which effect cell death. Once apoptosis is complete the T_C cell is released allowing it to search for, and attack, other infected cells.

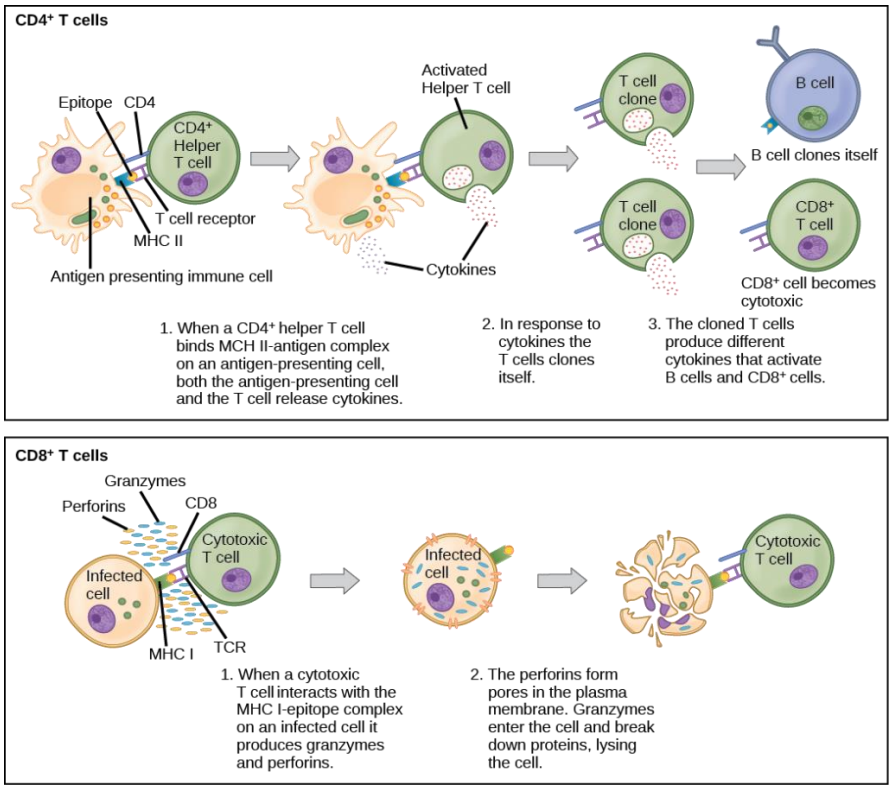

Figure 1.6. Difference between helper T (T_H) cells and Killer T (T_C) cells. Adapted from ref.[5] Permission not required.

1.4. Different types of T cells

We have seen that antigen recognition is vitally important in the adaptive immune response through the presentation of foreign peptide fragments by the MHC to TCRs located on cytotoxic and helper T cells. There are, however, several other types of T cells, which contain altered TCRs. Instead of interacting with MHC–peptide complexes, these TCRs recognise MHC-like molecules that present alternative small-molecule antigens including glycolipids, lipids and vitamin metabolites. These T cells include Natural Killer T (NKT) cells, Mucosal Associated Invariant T (MAIT) cells and gamma delta (γδ) T cells are of particular interest due to their ability to bridge the gap between innate and adaptive immunity through producing / reacting to cytokines and chemokines, which can lead to the activation of a range of other cells in a resulting immune response.

1.4.1. γδ-T cells

Gamma-delta (γδ) T cells are so named due to their unique γδTCR, which is formed like other T cells in the thymus. The γδ TCR is achieved by V(D)J recombination which is mediated by the recombination activation gene (RAG). γδ T cells have not been widely studied and a full understanding of their workings is not yet available; however, they have been shown to possess a distinct combination of characteristics not seen in other T cells. For example, whilst other naive T cells move to the lymph nodes and spleen for maturation, γδ T cells have been shown to migrate to alternative tissues such as the dermis and intestines. Vγ9Vδ2^{+} T cells are the predominant subset of γδ T cells. These cells recognise phosphoantigens (low molecular-mass alkyl diphosphates) as their prototypical antigens of which (*E*)-4-Hydroxy-3-methyl-but-2-enyl pyrophosphate (HMB-PP) **1** has been shown to be the most potent. HMB-PP is an intermediate in the non-mevalonate pathway to the biosynthesis of isopentenyl pyrophosphate **2** (IPP) and dimethylallyl pyrophosphate **3** (DMAPP) (Scheme 1.1.). These molecules are used as starting materials in the biosynthesis of more complex molecules used in cell processes. The non-mevalonate pathway is used by many bacterial and pathogenic species but not by

vertebrate cells, which use the mevalonate pathway. It is not known whether HMB-PP **1** binds directly to the TCR or if it is presented following complexation to another molecule.

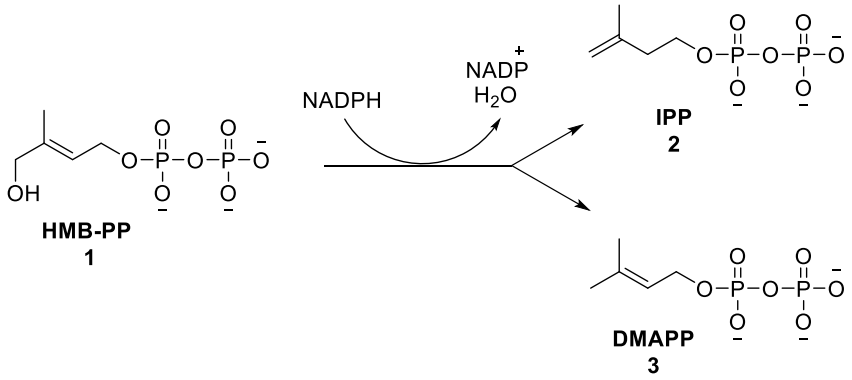

Scheme 1.1. HMB-PP is a precursor to IPP and DMAPP in the non-mevalonate pathway.

Along with releasing high concentrations of IFNγ and tumour necrosis factor (TNF), $\gamma\delta$ T cells also produce granzymes for lysis of infected cells. Through the release of a range of chemokines and cytokines, they can also interact with other important cells. For example, they can produce high concentrations of CXC-chemokine ligand 13 (CXCL13), which regulates the organisation of B cells.[10]

1.4.2. MAIT cells and MR1

Mucosal-Associated Invariant T (MAIT) cells are enriched in mucosal areas and are also found in the liver. They make up around 5% of the total T-cell population and are characterised by their expression of a semi-invariant $\alpha\beta$ T-cell receptor (Vα7.2-Jα33/12/20). This TCR is restricted by the MHC-like protein MR1, which is non-polymorphic and highly evolutionarily conserved. Until recently it was not known what the natural ligand was for MR1 and activated MAIT cells but it has since been discovered that MR1 presents unstable pyrimidine intermediates derived from the biosynthesis of riboflavin, which occurs in bacteria but not in humans.

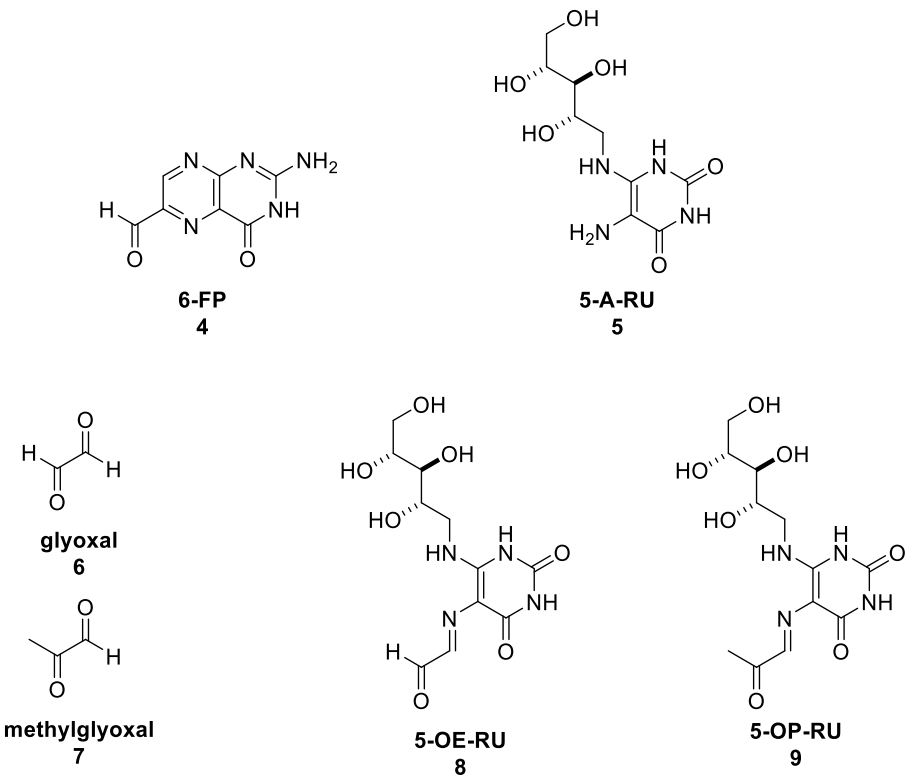

Figure 1.7. Ligands of MR1 which present to MAIT cells.

Kjer-Nielsen *et al.*[11] found that whilst 6-formyl pterin **4** (6-FP) binds to MR1, the resulting complex does not activate MAIT cells. Following further studies, it was shown that 5-amino-6-D-ribitylaminouracil **5** (5-A-RU) was important as an intermediate but that this molecule itself was unable to bind MR1 or activate MAIT cells.[12] [5-(2-Oxoethylideneamino)-6-D-ribitylaminouracil] **8** (5-OE-RU) and [5-(2-oxopropylideneamino)-6-D-ribitylaminouracil] **9** (5-OP-RU), both of which are formed following non-enzymatic condensation of 5-A-RU with either glyoxal **6** or methylglyoxal **7**, respectively, were shown to bind to MR1 and form reversible Schiff base complexes with Lys43 of the human MR1 protein. Glyoxal and methylglyoxal are formed during other metabolic pathways. 5-OP-RU is currently believed to be the natural ligand of MR1 on the basis of a mass-to-charge ratio (*m/z*) of 329.11 seen for a ligand bound to MR1 which matched 5-OP-RU. This MR1–5-OP-RU complex can also activate MAIT cells.[13]

Similarly to γδ T cells, MAIT cells produce IFN-γ and TNF following activation and are also involved in the granule exocytosis pathway.[14, 15]

1.4.3. *i*NKT cells and CD1

Natural Killer (NK) T cells were first discovered in 1987[16-18] and so named from their co-expression of an αβ TCR along with NK markers, like NK 1.1, which are normally found on natural killer cells. It has since been shown that not all NKT cells express this marker and that there are in fact three distinct types of NKT cell (see Table 1.2.). [19]

	Type I Cells (classical NKT Cells)	**Type II Cells (non-classical NKT Cells)**	**NKT-like cells (CD1d-independent NK1.1$^+$ T cells)**
CD1d dependent	Yes	Yes	No
α-GalCer reactive	Yes	No	No
TCR α-Chain	Vα14-Jα18 (mice) Vα24-Jα18 (humans)	Diverse, but some Vα3.2-Jα9, Vα8 (mice)	Diverse
TCR β-Chain	Vβ8.2, Vβ7 and Vβ2 (mice) Vβ11 (humans)	Diverse, but some V β 8.2 (mice)	Diverse
NK1.1 (CD161)	+ (resting mature) – /low (immature or post activation)	+/–	+
Subsets	CD4$^+$ and DN (mice) CD4$^+$, CD8$^+$ and DN (humans)	CD4$^+$ and DN (mice)	CD4$^+$, CD8$^+$ and DN

Table 1.2. Showing the contrasting features of the different populations of NKT cells. Figure adapted from ref.[19] Permission to reproduce table was obtained through RightsLink® - licence number 4174380942019 .

Whilst they express the cell-surface marker NK1.1, NKT-like cells are not CD1d-dependent; indeed, they may be classical MHC-restricted T cells which also express the NK1.1 marker. Type 1 (classical or invariant) and type 2 (non-classical) NKT cells differ in the TCR they express on their cell surfaces. There is more diversity in the TCRs found on type 2 NKT cells although these are still CD1d-dependent. In contrast, type 1 *i*NKT cells contain a semi-invariant TCR in mice and an invariant TCR in humans. As summarised in Table 2., the α chain is invariant with one variation possible for both humans (Vα24-Jα18) and mice (Vα14-Jα18). The semi-invariance in mice is seen in the composition of the β chains (Vβ8.2, Vβ7 or Vβ2) that are predominantly paired with the α chain. In humans, the β chain is composed exclusively of Vβ11. Of the three types of NKT cell, type 1 or *invariant* (*i*) NKT cells have been the most studied. In mice, Type I NKT cells represent ~0.5% of the T-cell population in the blood and peripheral lymph nodes although they are also found in the spleen and liver at higher concentrations. Type I NKT cells in humans display a similar tissue distribution albeit at lower concentrations.

CD1d is a member of the CD1 family of glycoproteins, which are expressed on the surface of antigen-presenting cells including dendritic cells or macrophages. These MHC-like proteins present glycolipid antigens rather than peptides to the TCR. Although not the natural ligand for this protein, alpha-Galactosyl Ceramide **10** (α-GalCer) has been used as the prototypical model glycolipid in *i*NKT-cell research since its discovery in 1995.[20]

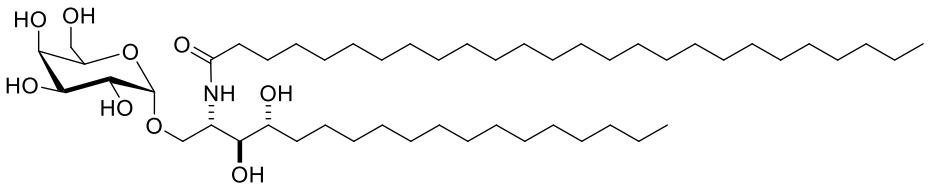

α-GalCer
10

Figure 1.8. α-Galactosyl Ceramide

Other natural ligands have been shown to bind to CD1d and be presented to the TCR of NKT cells. These include the microbial ligands α-galacturonylceramide and α-glucuronylceramide **11** (GSL1) found in the cell wall of the gram-negative bacteria sphingomonas and the self-ligand isoglobotrihexosylceramide **12** (iGb3). [21]

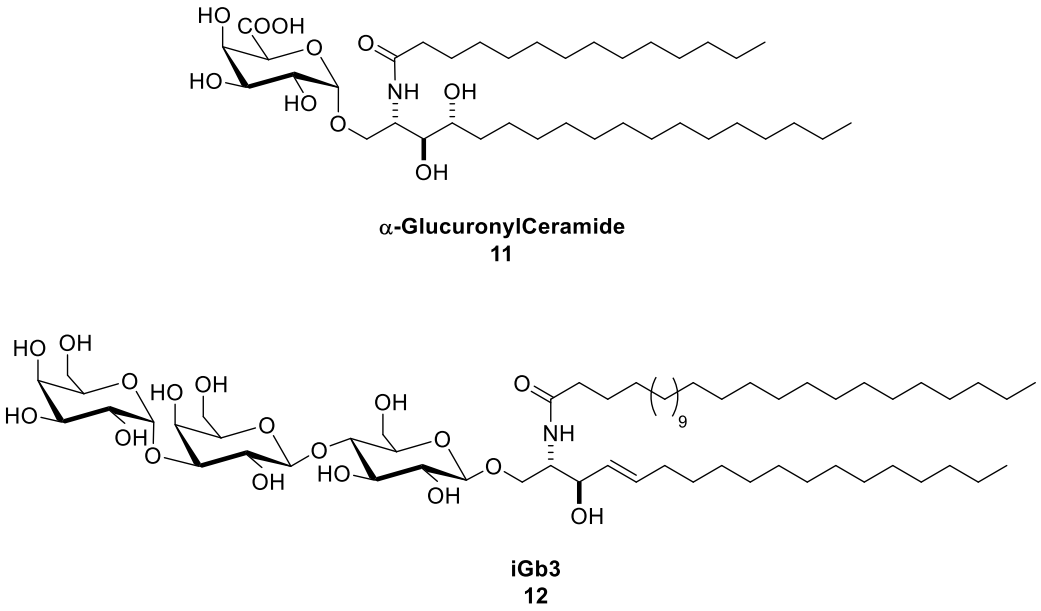

Figure 1.9. α-glucuronylceramide **11** and isoglobotrihexosylceramide **12**.

These innate-like T cells secrete a range of cytokines upon activation. While MAIT cells can produce high concentrations of IFNγ when activated, NKT cells are of particular interest in that they can be activated to produce a cytokine profile involving cytokines such as IFNγ for a T_H1 (pro-inflammatory) response as well cytokines, such as interleukin-10 (IL-10) that can lead to a T_H2 (anti-inflammatory) response. Although these cytokine profiles lead to opposing responses, it has been shown that the concentrations of the various cytokines can be altered depending on the ligand–CD1d complex that is activating the T cell. In this way, by changing the ligand it is possible to modulate the immune response in different ways.

1.5. Aims and objectives

The immune system contains a complex array of diverse cells, which have differing roles to ensure that invading pathogens are discovered and killed before they can do damage to the host. The aim of my Ph.D. will be to use chemical synthesis to help further understand the mechanisms and workings of these biological processes. Specifically, we will focus on two aspects of the immune response. The first part will discuss the synthesis of biotinylated Glc_1Man_3 tetrasaccharide **13** and its role in binding to calreticulin, an ER resident protein involved in the folding of proteins, including the cell surface proteins MHC-I and CD1d.

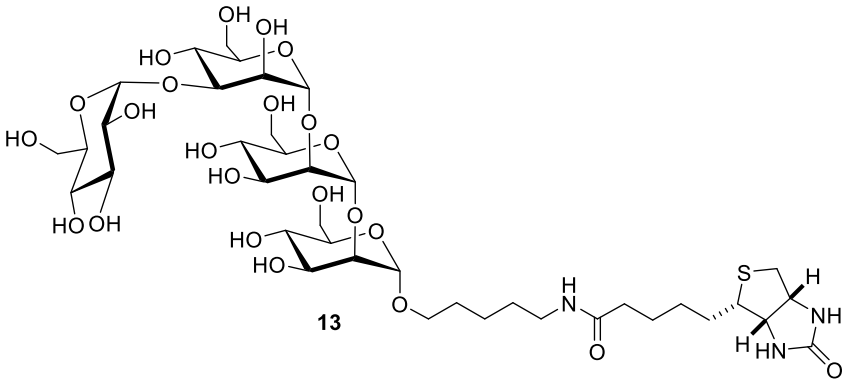

13

Figure 1.10. Tetrasaccharide **13**.

The second part of this project will focus on the development of glycolipid and non-glycolipid molecules, which activate *i*NKT cells. Non-glycosidic analogues ThrCer **14** and and ThrCer-6 **16**, which were developed from α-GalCer **10** have previously been synthesised within the group. This project involves synthesis of the second generation of these compounds which contain modifications of the acyl chain as well as at the pseudo-glycosidic linkage. These molecules would then be tested for their ability to induce an immune response from *i*NKT cells and in particular measure their T_H1/T_H2 cytokine response.

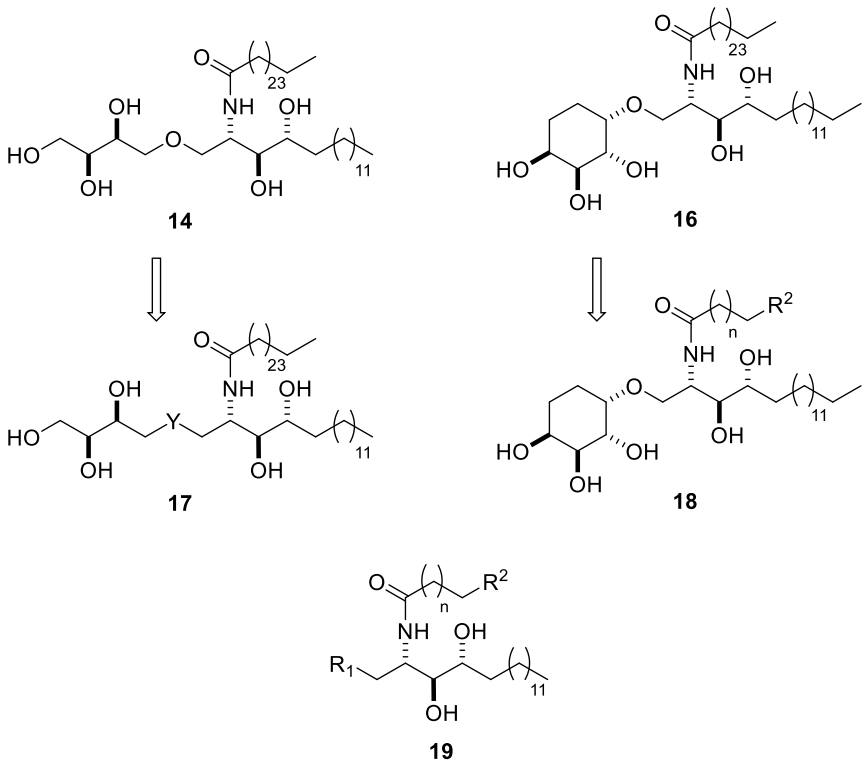

Figure 1.11. Target molecules which potentially activate *i*NKT cells.

Chapter 2

Synthesis of biotinylated Glc_1Man_3 tetrasaccharide

2. Synthesis of biotinylated Glc_1Man_3 tetrasaccharide

Introduction

The Major Histocompatibility Complex (MHC) and Human Leukocyte Antigen (HLA) as it is known in humans comprise a set of cell-surface proteins that are required for the adaptive immune response. They function by binding peptides. The resulting MHC–peptide–complex can then be recognised by T-cell receptors located on the surface of different T cells. If the peptide is not recognised as being from the host then an immune response is initiated.

2.1. MHC-II

There are two major sub-classes of MHC molecules, class I and class II. MHC class II molecules are normally only expressed on the surface of Antigen-Presenting Cells (APC) such as Dendritic Cells (DC). These molecules bind exogenous peptides, *i.e.* peptides from non-self proteins that have been degraded in the endocytic pathway. As seen in Figure 2.1. the MHC-II molecule is comprised of an α and a β chain that are assembled in the endoplasmic reticulum (ER) where they form a complex with the so-called Invariant chain (Ii). The Invariant chain blocks the peptide antigen binding site thereby preventing peptides present in the ER from binding prematurely. Following transport of the Ii–MHC-II complex to the MHC class II compartment (MIIC), the Invariant chain is digested by cathepsin proteases. A class-II associated Ii peptide (CLIP) remains in the MHC binding site after this digestion. A late endosome, containing digested exogenous protein, fuses with the MIIC bringing these foreign peptides into contact with the MHC molecule. An MHC-like molecule, HLA-DM facilitates the removal of CLIP enabling exogenous protein peptide to bind to the MHC-II. The length of the peptide can extend up to 12 amino acids due to the binding groove being open-ended. The peptide-bound MHC complex is then transported from the MIIC to the cell surface where it is presented to $CD4^+$ T cells.

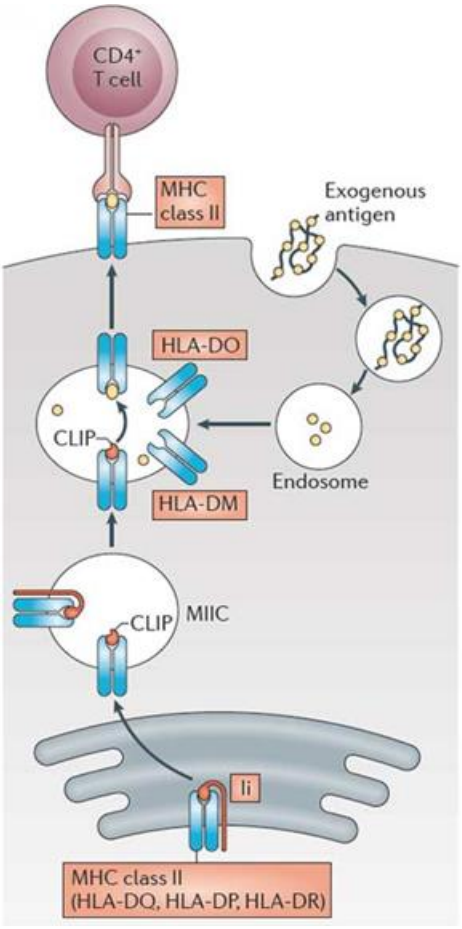

Figure 2.1. The mechanism for presentation of an MHC II–peptide complex to a TCR. Figure adapted from ref.[22] Permission to reproduce figure was obtained through RightsLink® - licence number 4106420148928.

2.2. MHC-I

While both MHC class I and class II molecules present peptides on the cell surface, the types of peptides, the synthesis of the loaded antigen complex and the type of TCR that recognises the MHC–peptide complex are different. Peptides presented by class I molecules are endogenous, *i.e.*, they are derived from proteins that have been synthesised within the cell

before being digested by proteasomes. Healthy cells will generate peptides that when presented on the cell surface, are not recognised as TCRs do not recognise self-antigens. However, when a foreign pathogen like a virus enters the cell and hijacks cell function, peptides arising from the pathogen are recognised as non-self and will therefore initiate an immune response.

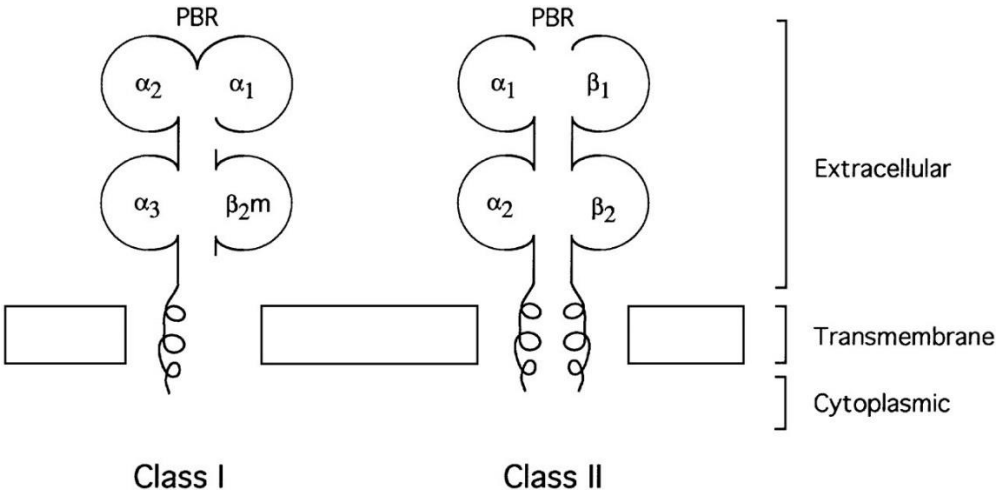

Figure 2.2. Difference between the structure of MHC-I and MHC-II molecules. Adapted from ref.[23] Permission not required

Figure 2.3. shows the processes involved in the presentation of an MHC-I–peptide complex. Following transcription and translation of proteins in the nucleus of a cell some are broken down into smaller peptide units. The bulk of peptides that are loaded on to MHC molecules are generated by the *26S* proteasome, which consists of a *20S* core barrel and two *19S* caps (Item 1). This multi-domain protein produces peptides in the cytosol. The transporter associated with antigen-processing (TAP) then pumps these peptides from the cytosol into the ER lumen (Item 2). Meanwhile the MHC class I molecule is already within the ER and being assembled and folded in readiness for peptide loading (Item 3). Unlike the MHC class II molecule, which has two homogenous α and β chains, the MHC-I molecule consists of one heavy α chain and a β2-microglobulin (β2m), which is non-covalently bonded to the α3 domain (Figure 2.2). Two other common chaperones, ERp57 and calreticulin help to fold and stabilise

the MHC-I molecule. Calreticulin is a carbohydrate binding protein known as a lectin which binds *N*-glycosylated MHC-I molecules to help form a stable interaction between the MHC-I molecule and tapasin. Tapasin itself is required to stabilise the interaction between TAP and the MHC-I molecule. Together, the complex of the unloaded MHC-I, TAP, tapasin, calreticulin and ERp57 is known as the peptide loading complex (PLC) (Item 4). Together, the molecules of the PLC stabilise the peptide binding groove of the MHC molecule in a configuration for optimum loading of a peptide (Item 5). The ER aminopeptidase associated with antigen presentation (ERAAP) will trim the peptides if required before loading and release of the loaded MHC-I complexes from the PLC (Item 6). The Golgi apparatus then helps to transport the complex to the cell surface to allow presentation (Item 7–8). This complex is recognised $CD8^+$ cytotoxic T-cells with the α3 domain interacting with CD8 (Item 9).

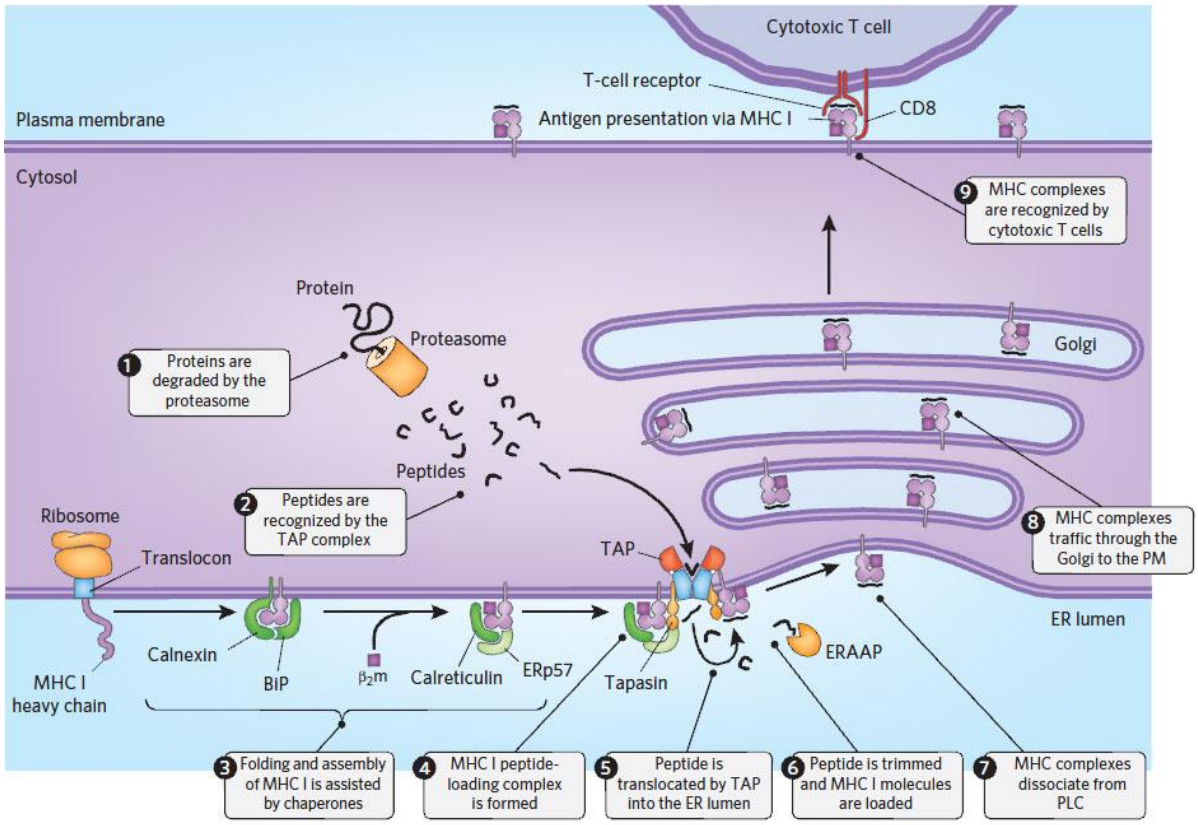

Figure 2.3. The mechanism for presentation of an MHC I–peptide complex to a TCR. Figure adapted from ref.[24] Permission to reproduce figure was obtained through RightsLink® - licence number 4106420255336.

2.3. Calreticulin

Calreticulin has two major functions. It acts as a chaperone for the folding of glycopeptides into functional proteins. It is this function that makes it vital in MHC-I synthesis. However, it is named for its other function, which is to regulate calcium levels within the ER. As shown schematically in Figure 2.3., the protein is divided into three domains. The C-domain contains a high concentration of acidic amino acids, which allows for high-capacity, low-affinity calcium binding. The terminal KDEL sequence prevents calreticulin from leaving the ER as it is retrieved from the Golgi apparatus by retrograde transport using the COPI protein complex. The P-domain is proline-rich forming a long, arm-like domain that contains the ERp57 binding site. Finally, the N-domain is a globular domain containing the glycan binding site. This domain largely consists of a β-sandwich formed by two concave β-sheets.

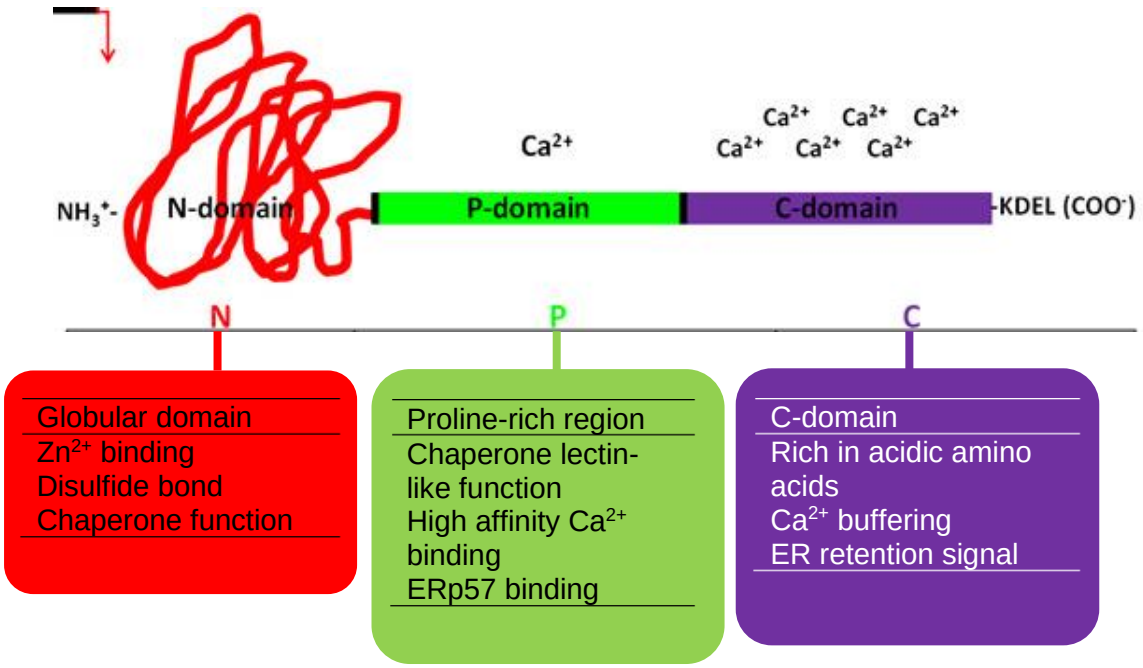

Figure 2.4. Structure and function of regions of the calreticulin protein.[25]

2.3.1. N-linked Glycan

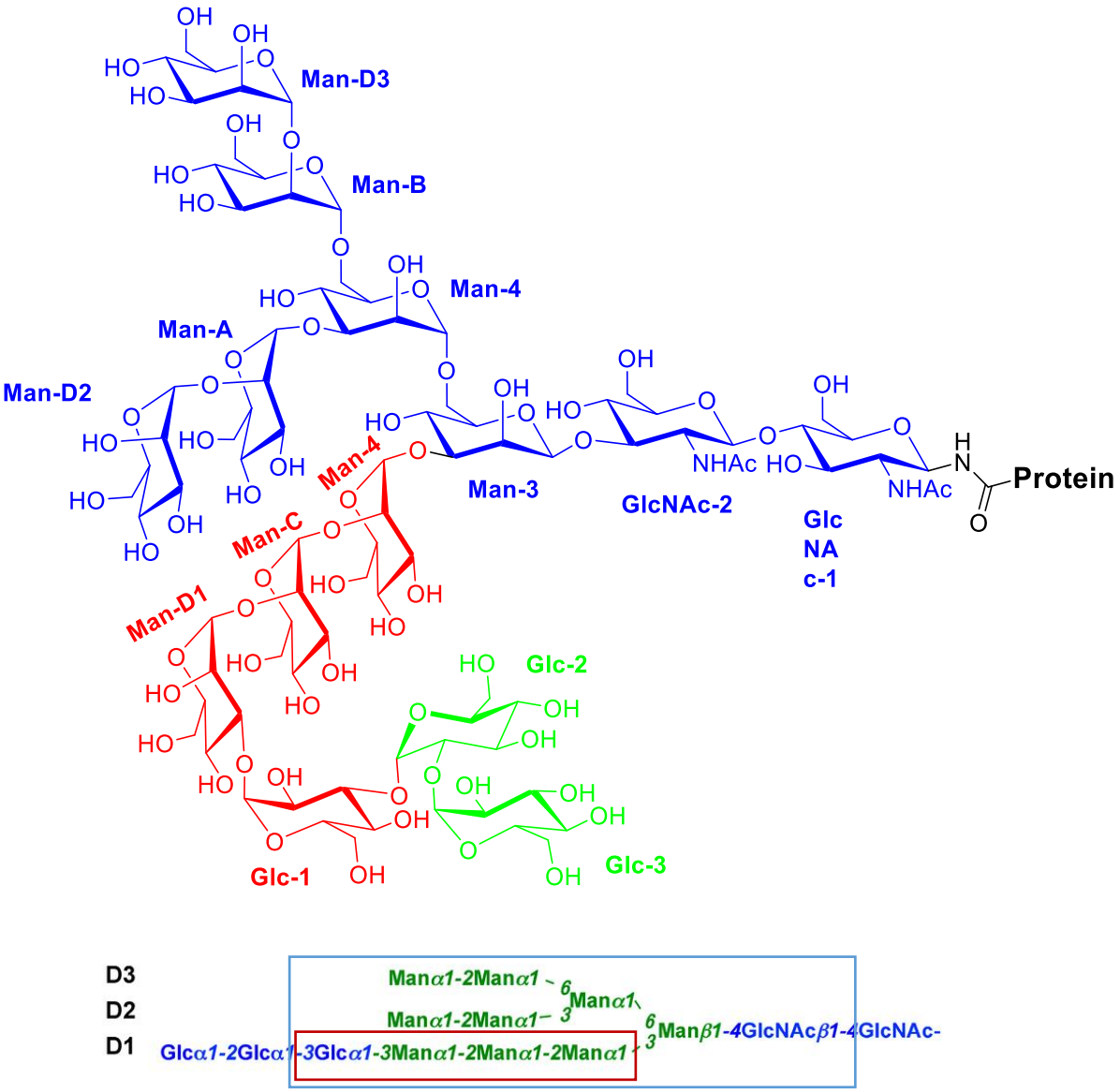

Figure 2.5. Structure of the oligosaccharide $Glc_3Man_9GlcNAc_2$ donor used for post-translational protein modification in the ER [26]

N-Glycosylation is an important post-translational modification that occurs on nascent peptides in the ER. The enzyme oligosaccharyltransferase catalyses the transfer of the oligosaccharide $Glc_3Man_9GlcNAc_2$ (Figure 2.4.) from dolicholdiphosphate to an asparagine (Asn) residue in a sequence of Asn-X-Ser/Thr, where X is any amino acid except proline. Processing of the resulting glycoprotein then occurs with α-glucosidase I/II removing the two terminal glucose units (Glc-3 then Glc-2) to yield the dodecasaccharide within the blue box of Figure 2.4. At this stage the glycan can now bind to calreticulin and protein folding can occur. Once correct folding has been achieved, removal of the final terminal glucose (Glc-1) by α-glucosidase II leads to release of the glycoprotein.

2.3.2. Crystal structure and lectin binding of calreticulin

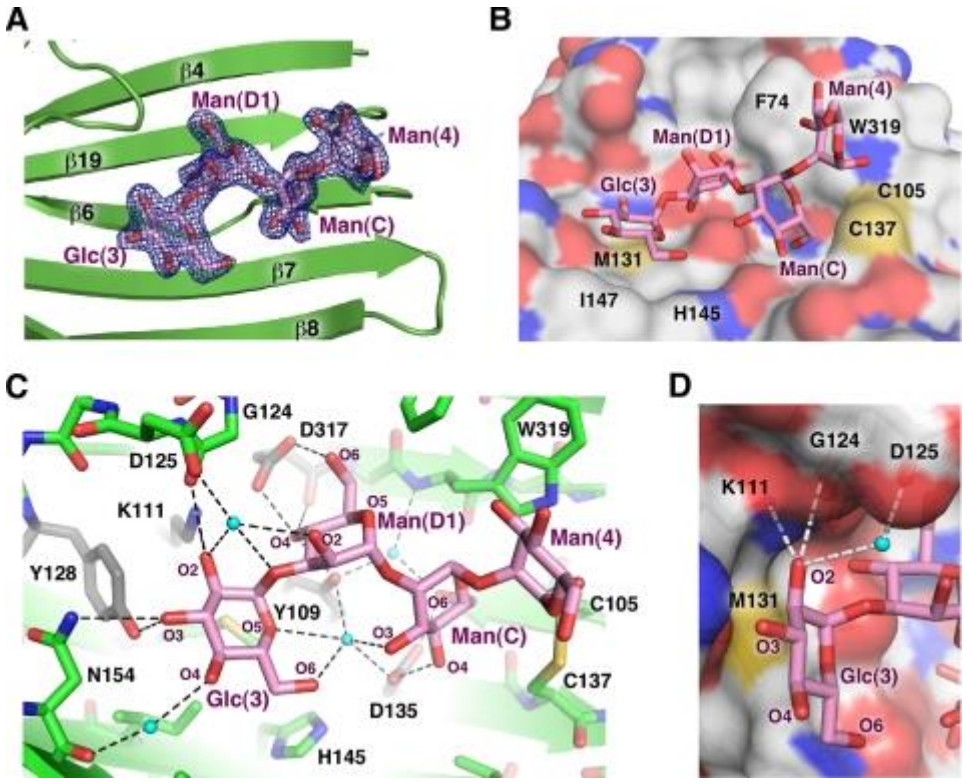

Figure 2.6. Structural basis of recognition by calreticulin of tetrasaccharide Glc_1Man_3. Figure adapted from ref. [27] Permission not required.

A. An omit map showing the binding cavity for tetrasaccharide binding; **B.** Surface representation of calreticulin showing the residues in contact with the tetrasaccharide; **C.** Dotted lines show hydrogen bonds between the tetrasaccharide and the protein including ordered water molecules; **D.** Close up detail of hydrogen bonds formed between Glc(3) and protein residues with a water molecule.

Figure 2.6. shows the crystal structure of the tetrasaccharide Glc_1Man_3 (the tetrasaccharide found in red of Figure 2.5.) bound at the lectin binding site of a mutant calreticulin in which the P-domain has been deleted and replaced with a short linker and the C-terminus has been removed by cleavage at Lys^{368}. These modifications kept the globular domain of the protein intact but allowed the tetrasaccharide–protein complex to be crystallised. The sugars of the tetrasaccharide will be referred to according to the numbering of the natural ligand, *i.e.* Glc(3)-Man(D1)-Man(C)-Man(4) (Figure 2.5.).[27]

The Glc_1Man_3 tetrasaccharide has been used as a model for studying the mode of action of calreticulin and has been shown to be an effective competitor for binding versus the natural ligand.[28] This means effective study can be done using the tetrasaccharide in place of the structurally more complex and significantly less accessible complete natural oligosaccharide. The crystal structure of the tetrasaccharide bound to calreticulin shows how the methyl glycosyl linkage of Man(4) of the tetrasaccharide is directed away from the protein, which has been interpreted as suggesting that only this tetrasaccharide portion of the natural oligosaccharide is involved in binding at the lectin site.

Sugar atom	Hydrogen bonds
Glc(3)	
1-O	Asp^{125} *via* H_2O molecule
2-O	Asp^{125} *via* H_2O molecule; Lys^{111} (side-chain); Gly^{124} (backbone carbonyl)
3-O	Tyr^{128} (side-chain); Asn^{154} (side-chain)
4-O	Asn^{154} (backbone carbonyl) *via* H_2O molecule
6-O	Asp^{135} *via* H_2O molecule; Tyr^{109} (side-chain)

Table 2.1. Hydrogen-bond interactions between calreticulin and Glc(3) residue of the Glc_1Man_3 tetrasaccharide.

Table 2.1 lists the hydrogen bonds (both direct and indirect) between the glucose terminus (Glc-3) of the tetrasaccharide and amino-acid residues in the calreticulin binding site as shown in Figure 2.5., Panel C. From these extensive contacts, it can be seen why this glucose residue is necessary for effective binding as all of the hydroxyl groups are involved in binding to the protein. The structure also shows why binding is selective to the mono-glucosylated glycan [Glc(3)-Man(D1)-Man(C)-Man(4)] rather than the di-glucosylated tetrasaccharide glycan [Glc(2)-Glc(3)-Man(D1)-Man(C)] which does not fully bind due to the glycosidic bond of the second sugar being at the 3-O position rather than the 2-O position [α-Glc-(1→3)-α-Glc-(1→3)-α-Man-(1→2)-α-Man-(1→2)] vs [α-Glc-(1→3)-α-Man-(1→2)-α-Man-(1→2)-α-Man-(1→2)] .

Sugar atom	Hydrogen bonding
Man(D1)	
2-O	Asp^{125} *via* H_2O molecule
4-O	Tyr^{109} (side chain); Asp^{317} (backbone carbonyl & side chain)
6-O	Asp^{317} (side chain)
Man(C)	
3-O	Tyr^{109} *via* H_2O molecule; Asp^{135} *via* H_2O molecule
4-O	Asp^{135} (side chain)
6-O	Asp^{135} (side chain); Tyr^{109} *via* H_2O molecule; Trp^{319} (backbone amide) *via* H_2O molecule

Table 2.2. Hydrogen-bond interactions between calreticulin and Man(D1) and Man(C) residues of the Glc_1Man_3 tetrasaccharide.

Man(D1) and Man(C) also form key hydrogen bonds with calreticulin as summarised in Table 2.2. Finally Man(4) is also necessary for effective binding. Kapoor *et al.* [29] showed that the binding constant is doubled between the tri- and tetrasaccharide (from $112.0 \pm 5.18 \times 10^{-4}$ M^-

[1] to 230.0 ± 5.6 × 10^{-4} M^{-1} measured at 279 K), as a consequence of the partial wrapping of the C(1)-O(1) bond of Man(4) with the disulfide bond between Cys^{105} and Cys^{137}.

2.4. Previous syntheses of the tetrasaccharide, methyl α-D-glucopyranosyl-(1→3)-α-D-mannopyranosyl-(1→2)- α-D-mannopyranosyl-(1→2)-α-D-mannopyranoside (35)

Owing to the problems related to the isolation of the complete oligosaccharide and its challenging synthesis and knowing that only the Glc_1Man_3 tetrasaccharide is involved in binding at the lectin site, the tetrasaccharide has been used as a model for studying the mode of action of calreticulin. There have been four syntheses of the tetrasaccharide methyl α-D-glucopyranosyl-(1→3)-α-D-mannopyranosyl-(1→2)- α-D-mannopyranosyl-(1→2)-α-D-mannopyranoside **35** published to date. One further synthesis has also been achieved in which a fluorescent label has been incorporated at the reducing end of the tetrasaccharide. The tetrasaccharide has been synthesised using both linear and convergent strategies, with the key challenges, as with all oligosaccharide syntheses, being the controlling of the stereoselectivity of the glycosylation reactions.

The synthesis of tetrasaccharide **35** requires the formation of four glycosidic linkages, three α-mannosides and one α-glucoside. The synthesis of an α-mannoside linkage is straightforward due to mannose having an axial hydroxyl at the C-2 position, which can be functionalised to increase the α selectivity of the glycosylation reaction. Steric bulk from a large C-2 protecting group (e.g. benzyl) can be used to cover the top face slowing β reactivity. Alternatively, an ester protecting group can engage in the glycosylation by neighbouring group participation, which serves to block the β face even more effectively. Both of these α-mannosylation strategies are highlighted in Scheme 2.1.

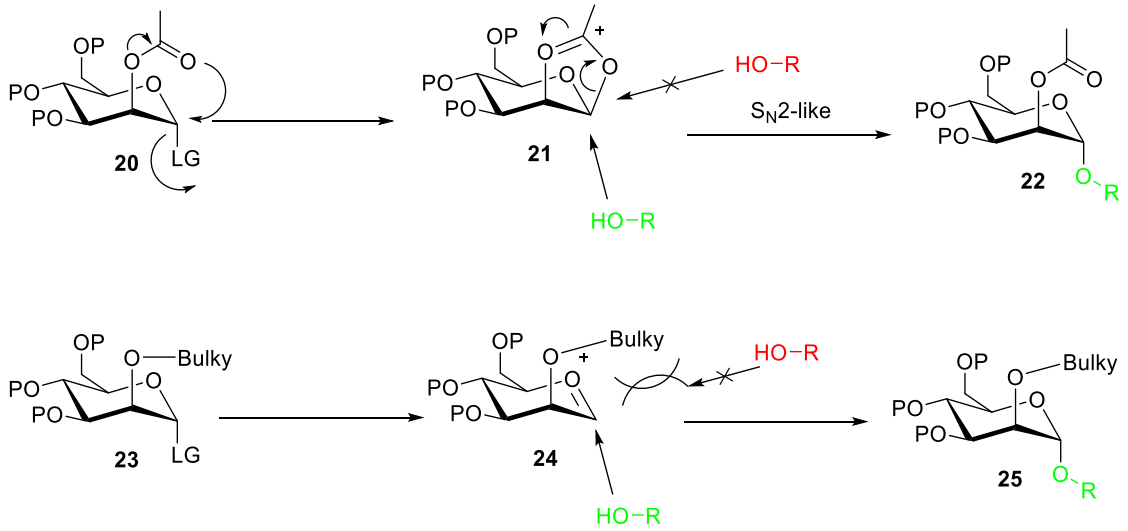

Scheme 2.1. Participating and bulky groups on the 2-*O* position in mannose can lead to α-selectivity.

The stereoselective formation of α-glucosides is however, more problematic. Glucose is the C-2 epimer of mannose with its hydroxyl in an equatorial position in its low energy $^4C_1$ conformation. This means it is more challenging to achieve α-selective glycosylation. The anomeric effect can be used advantageously to increase the α-stereoselectivity of glycosylations, as can the use of non-participating groups to prevent neighbouring group participation. The type of glycosyl donor used in particular the protecting groups employed, the solvent, the pressure and temperature can all have an effect on the stereoselectivity of the glycosylation. [30] In this regard there has been good reason to investigate both linear and convergent strategies to tetrasaccharide **35**.

Tetrasaccharide **35** was first synthesised by Jain *et al.* in 1995.[31] The key glycosylation reactions involved in this linear strategy are summarised in Scheme 2.2.

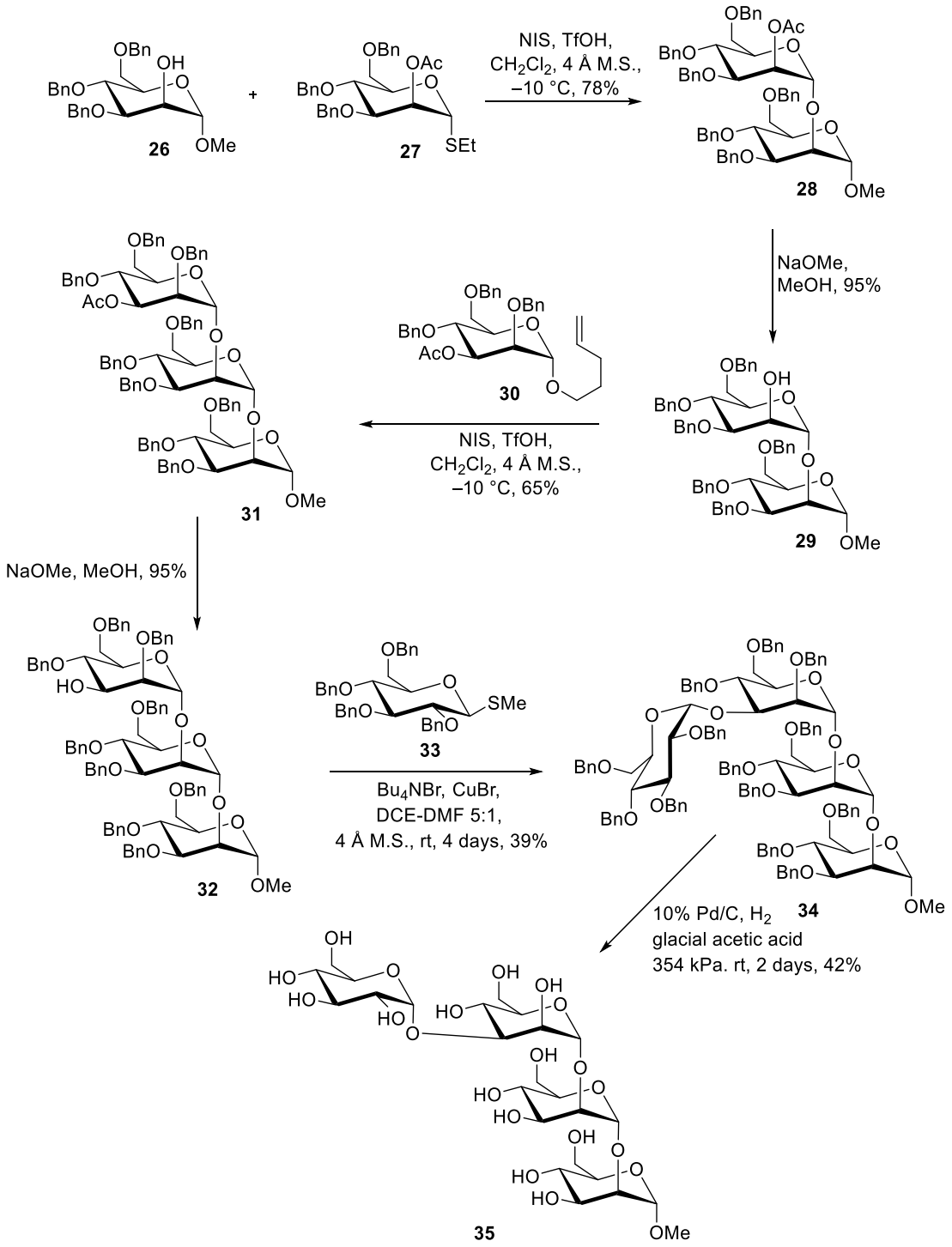

Scheme 2.2. Linear synthesis of Glc_1Man_3 tetrasaccharide by Jain *et al.*[31]

Mannosyl acceptor **26** and thiomannoside **27** were both synthesised from mannose in four steps. The first glycosylation reaction between these two reactants was performed using *N*-iodosuccinimide and triflic acid to activate the thiosugar donor **27** and yielded disaccharide **28**

in 78% yield. The high selectivity for the α product was ensured by using an acetate protecting group at the 2-*O* in the donor. Following uneventful removal of the acetate in **28** using Zemplén conditions, disaccharide **29** was used as the glycosyl acceptor in a glycosylation with *O*-pentenyl mannosyl donor **30**, which was synthesised from mannose in five steps. Although a different donor, glycosylation was performed using NIS and triflic acid under the same conditions as the first glycosylation to provide trisaccharide **31** in 65% yield. In this instance the large benzyl protecting group on 2-*O* of the mannosyl donor was sufficient to achieve the desired α selectivity. The acetate at the 3-*O* position of the newly added mannose was then saponified to yield the trisaccharide acceptor **32** in excellent yield. The final glycosylation was performed with donor **33** and acceptor **32** in the presence of tetrabutylammonium bromide and copper(I) bromide, yielding tetrasaccharide **34** in 39% yield. Although no stereoselectivity is mentioned in the paper and the mass balance is not accounted for, the procedure used is adapted from a paper by Sato *et al.* who mention complete α-selectivity when using this donor under these conditions admittedly to form a different disaccharide product.[32] Finally, hydrogenolysis of the benzyl protecting groups using 10% palladium on carbon afforded the desired tetrasaccharide **35** in 42% yield.

The problems related to a linear synthesis of tetrasaccharide **35** can be seen in this example. The preparation of acceptor **26** and donors **27** and **30** each requires 4-5 steps and an extra step to remove a protecting group to be able to proceed to the next reaction. The yield of the glycosylation reactions is often lower when employing larger oligosaccharides and may also have contributed to the poor yield in the final glycosylation reaction.

Convergent syntheses are often more efficient and the first convergent synthesis of tetrasaccharide **35** was reported by Cherif *et al.* in 2002 and is summarised in Scheme 2.3. [33]

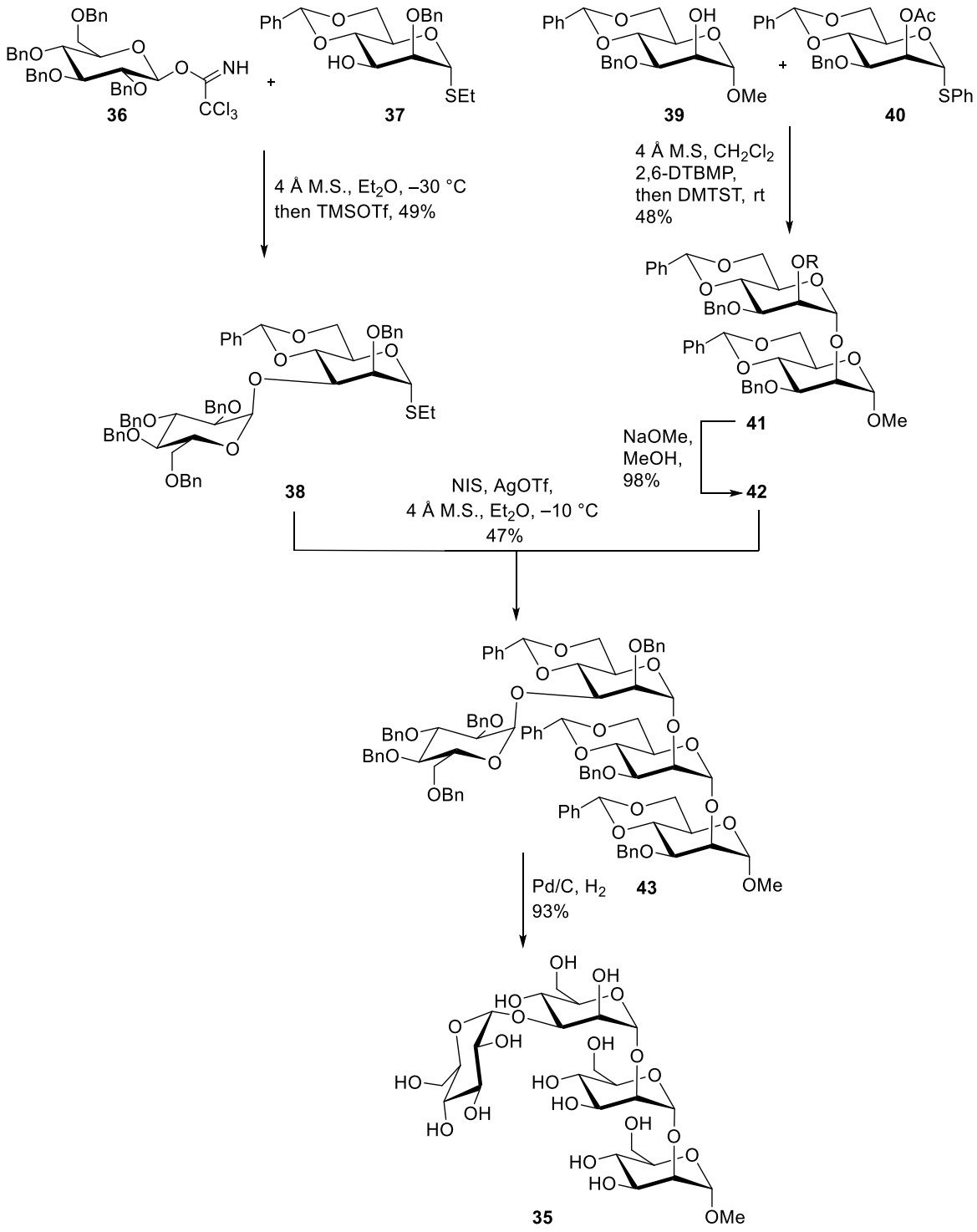

Scheme 2.3. Cherif *et al*. synthesis of tetrasaccharide **35.**

This convergent “2+2” synthesis involved the preparation of two disaccharides **38** and **42** which were then coupled to provide the tetrasaccharide **43** and subsequently target **35** after global deprotection. All of the mannosyl residues employed a benzylidene acetal to protect

the 4-O and 6-O positions. The glucosyl donor in this instance was per-benzylated trichloroacetimidate **36**. Activation of **36** using trimethylsilyl triflate in the presence of mannosyl acceptor **37** yielded disaccharide **38** in 49% yield. Whilst no α:β ratio was reported, this reaction is believed to be α-selective. The group had previously published the α-selective synthesis of disaccharide **38** using acceptor **37** with the phenyl thioglycoside rather than the ethyl thioglycoside used in the present study.[34] The previous synthesis yielded the disaccharide at 85% yield with an α:β ratio of 93:7. As a thiosugar, disaccharide **38** was primed to act as a donor in the next glycosylation reaction. The synthesis of the mannobiose coupling partner **42** was achieved using phenyl thiomannoside **40** and mannosyl acceptor **39**. Activation of the thioglycoside was achieved using dimethyl(thiomethyl)sulfonium triflate (DMTST) and 2,6-di-*tert*-butyl-4-methylpyridine and reaction with the acceptor yielded disaccharide **41** in 48% yield. This reaction is also presumed to be α although there was no mention of selectivity in the paper. The poor yield of this glycosylation might be attributed to the inefficient activation of the phenyl thioglycoside which is less reactive than its methyl or ethyl counterparts. Zemplén deacetylation provided the desired disaccharide acceptor **42**. Disaccharide donor **38** and acceptor **42** reacted under activation of the donor using NIS and silver(I) triflate to yield the desired tetrasaccharide **43** in 47% yield. This reaction was also probably α-selective, although the stereoselectivity of this final glycosylation was not reported. In glycosylation reactions, as the size of the coupling partners increases they typically become less reactive and substrate effects can become more important leading to an erosion (or improvement) of stereoselectivity. Global deprotection of tetrasaccharide **43** using hydrogen gas and palladium on carbon in methanol yielded the final tetrasaccharide **35** in 93% yield.

One of the benefits of a convergent synthesis is that there are fewer steps which often allows the synthesis of the intermediates in larger quantities and often higher overall yields. However, in this case Kapoor's linear strategy which employed similarly protected glycosides was more efficient principally owing to the improved yields of the glycosylation reactions. Yields may

have been sacrificed by Cherif *et al*. so as to achieve high levels of α–selectivity in the glycosylation steps.

The last published synthesis of the *O*-methyl tetrasaccharide **35** was accomplished by Gemma *et al.* who also employed a convergent strategy.[35] Scheme 2.4. outlines shows the synthesis of the mannobiose acceptor from benzyl-protected orthoester **44**, which was adapted from a previous paper by Ogawa *et al.* [36] Conveniently, both acceptor and donor were synthesised in one step from this starting material; thus, conversion to chloride donor **45** was achieved using chlorotrimethylsilane in CH_2Cl_2 while *in situ* ring-opening of the orthoester and deacetylation, using acetyl chloride in methanol yielded acceptor **46**. Activation of donor **45** using silver(I) triflate in the presence of acceptor **46** yielded disaccharide **47** in 82% yield. The high α selectivity can again be attributed to the acetyl protecting group at the 2-*O* position.

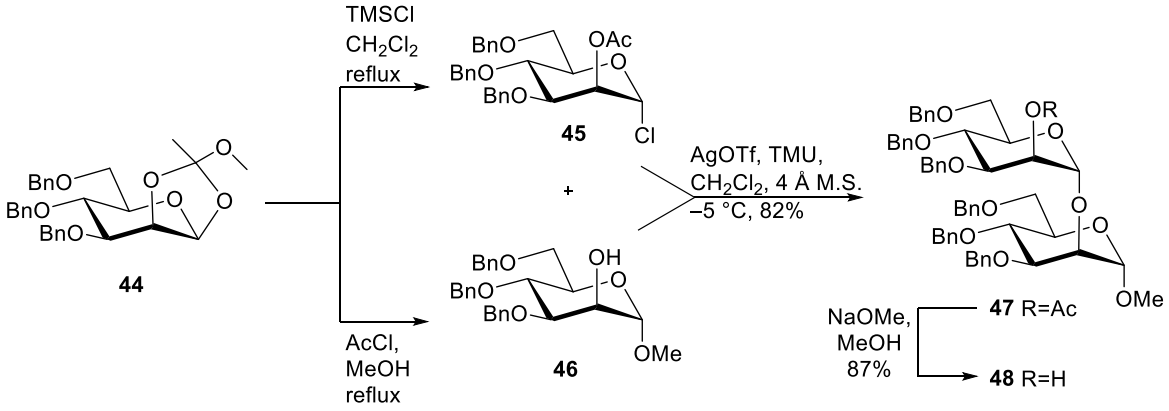

Scheme 2.4. Synthesis of mannobiose disaccharide **48** from orthoester **44**.

The second disaccharide of this synthesis was once again the more difficult due to the control of the stereoselectivity. Gemma *et al*. chose a glycosyl iodide as their donor which could be activated in the presence of a thioglycoside. Iodide **49** (which was formed from the reaction of the corresponding glycosyl acetate with trimethylsilyl iodide) and thioglycoside **50** were stirred together for 72 h in CH_2Cl_2 in the presence of triphenylphosphine oxide to yield disaccharide

51 in 70% yield. While there is no mention of the α:β ratio in the paper, Kobashi *et al.* who published the original work on the use of glycosyl phosphonium iodide donors achieved α:β ratios from 95:5 to 99:1.[37] The coupling of both disaccharides proceeded uneventfully with the tetrasaccharide formed selectively α in 88% yield using NIS with silver(I) triflate in CH_2Cl_2. Global deprotection of the benzyl groups was achieved using H_2 gas in the presence of Pd/C to yield tetrasaccharide **35** in 90% yield.

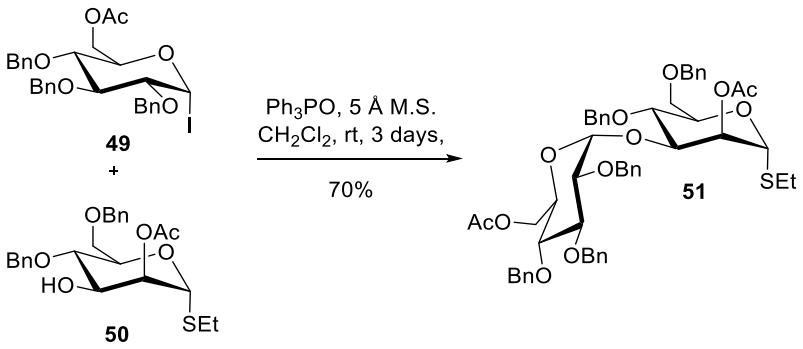

Scheme 2.5. Synthesis of disaccharide donor **51**.

Finally, Iwamoto *et al.* recently published a synthesis of the tetrasaccharide which incorporates a fluorescent label at the reducing end.[38] Tetrasaccharide **54** was synthesised using a linear strategy similar to that reported by Jain *et al*. although interestingly the same mannosyl donor was used in all of the glycosylation reactions, thereby taking advantage of the high levels of α-selectivity associated with mannosylations.

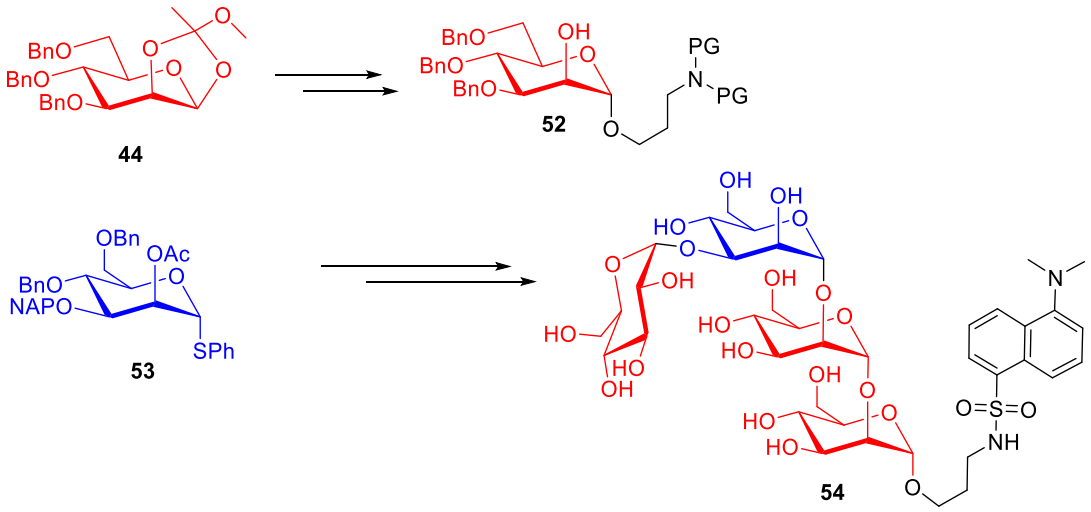

Scheme 2.6. Orthoester **44** was used as the building block for the three residues shown in red with the remaining residue of Man (D1) using thioglycoside **53**.

Orthoester **44** (shown in red, Scheme 2.6.) was a key building block in the synthesis with *N*-protected 3-aminopropanol used as the first acceptor. Thioglycoside **53** was used as the third residue (shown in blue) in the synthesis, which allowed selective deprotection of the 3-*O* position. Following this deprotection, glycosylation using chloride **45** yielded mannotetraose **55** in 90% yield. Scheme 2.7. shows the conversion of mannotetraose **55** to the desired tetrasaccharide **58** *via* an oxidation/reduction sequence which was needed to epimerise the 2-*O* position and convert the fourth mannose to a glucose residue. Deacetylation of **55** yielded tetrasaccharide **56** in excellent yield. Activated DMSO oxidation of the resulting alcohol using Alrbight-Goldman conditions yielded ulosyl **57** which underwent direct reduction using sodium triacetoxyborohydride in THF to yield tetrasaccharide **58** in 63% yield over the two steps The selectivity of the reduction of the ulosyl product to a glucosyl residue as the major product was first shown by Lemieux *et al.* in 1968.[39] Steric hindrance forces hydride attack at the opposite face to the trisaccharide in the α-position drives formation of the desired glucose residue (Figure 2.7.). Previously they had shown that the use of more sterically hindered reducing agents yielded a higher Glc:Man ratio $NaBH_4$ gave a ratio of 4:1, while the use of L-selectride

gave a ratio of 57:1 (as measures by HPLC).[40] Global deprotection and reaction of the amine with dansyl chloride yielded the desired target tetrasaccharide **27**.

The benefits of using mannosyl residues for all glycosylations can be seen in the yields achieved in these reactions, however, this route introduces more steps and a new stereocentre in which the desired compound will need to be separated from its epimer.

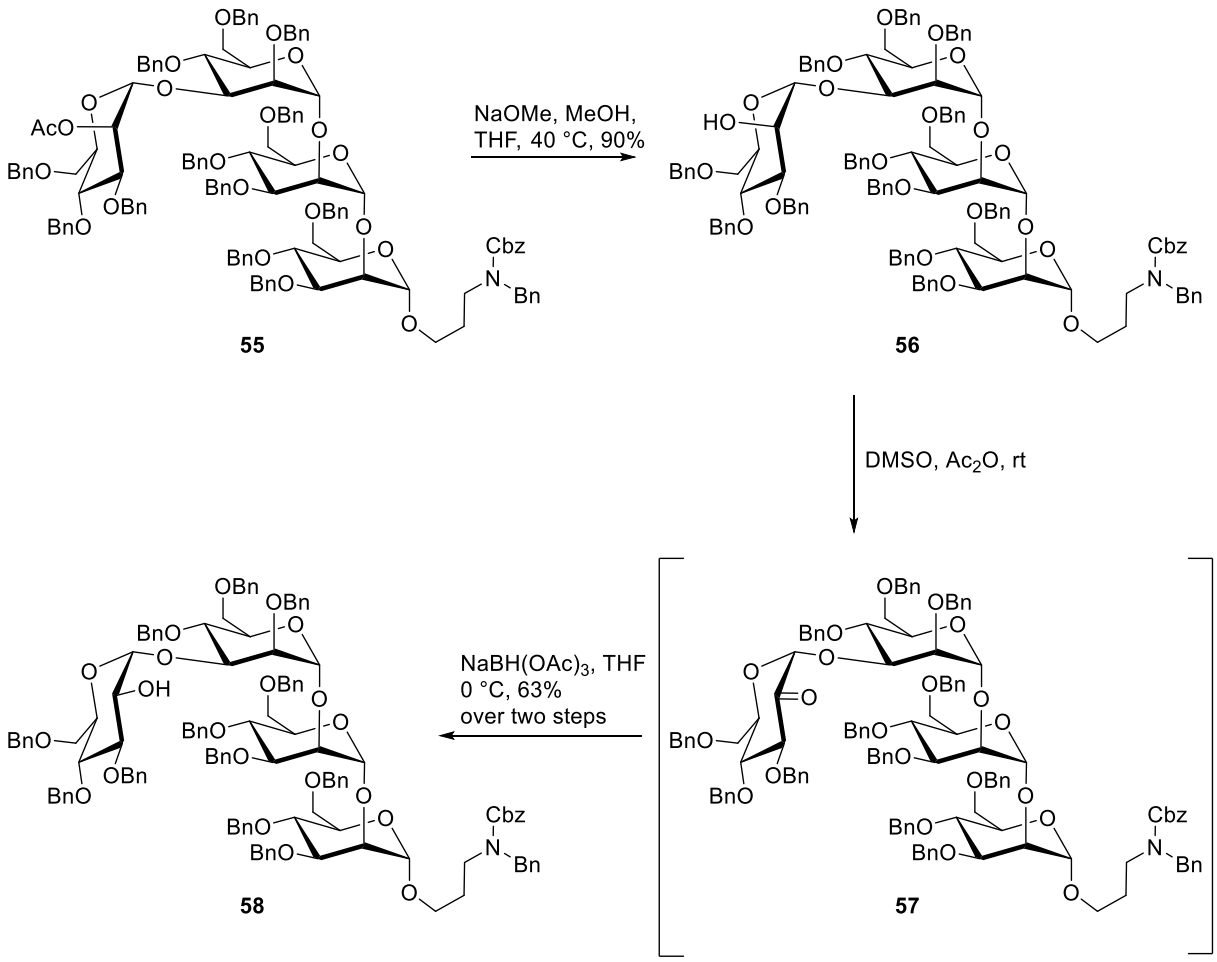

Scheme 2.7. Conversion of Man_4 tetrasaccharide **55** to Glc_1Man_3 tetrasaccharide **58** *via* ulosyl **57**.

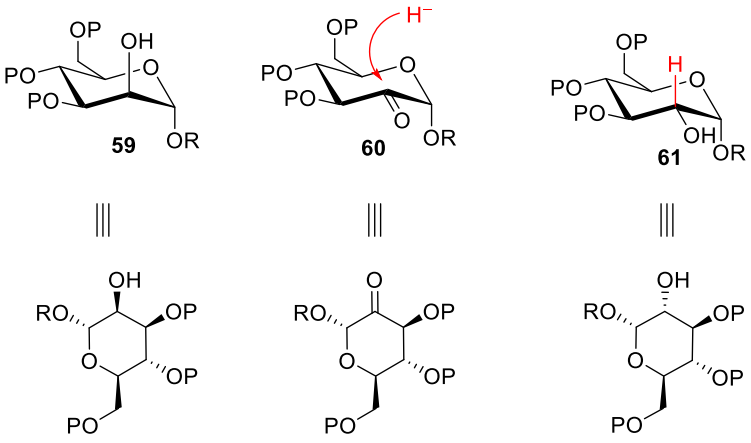

Figure 2.7. Hydride attack favoured on opposite site to the bulky anomeric group.

2.5. Biotin

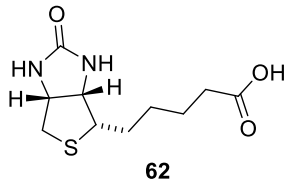

Biotin is a water-soluble B vitamin and essential for cell growth. It also has a use for biological studies. Both streptavidin and avidin bind the biotin moiety with very high affinity, with a K_d of 10^{-14} M making it one of the strongest non-covalent binding coefficients observed in nature. This feature can be exploited to extract a protein target for a ligand. Biotinylation of a molecule of interest can be used to extract the molecule–protein through the use of streptavidin-coated beads and subsequent isolation of the desired complex. To be successful the biotinylated compound must behave similarly to the unlabelled molecule under study in how it interacts with the protein. Judicious positioning of the biotin group and inclusion of a linker to separate the two parts of the molecule may therefore be required.[41]

The process is illustrated in Scheme 2.8. Starting with the biotinylated molecule of interest, step 1 shows the addition of the protein under study which yields the bound molecule–protein

complex in the presence of unbound protein. Step 2 introduces streptavidin which is bound to a surface *e.g.* on beads. Providing the binding of biotin to streptavidin does not interfere with the complex of interest, in Step 3 the complex of interest can then be isolated from unbound protein allowing study of the bound complex.

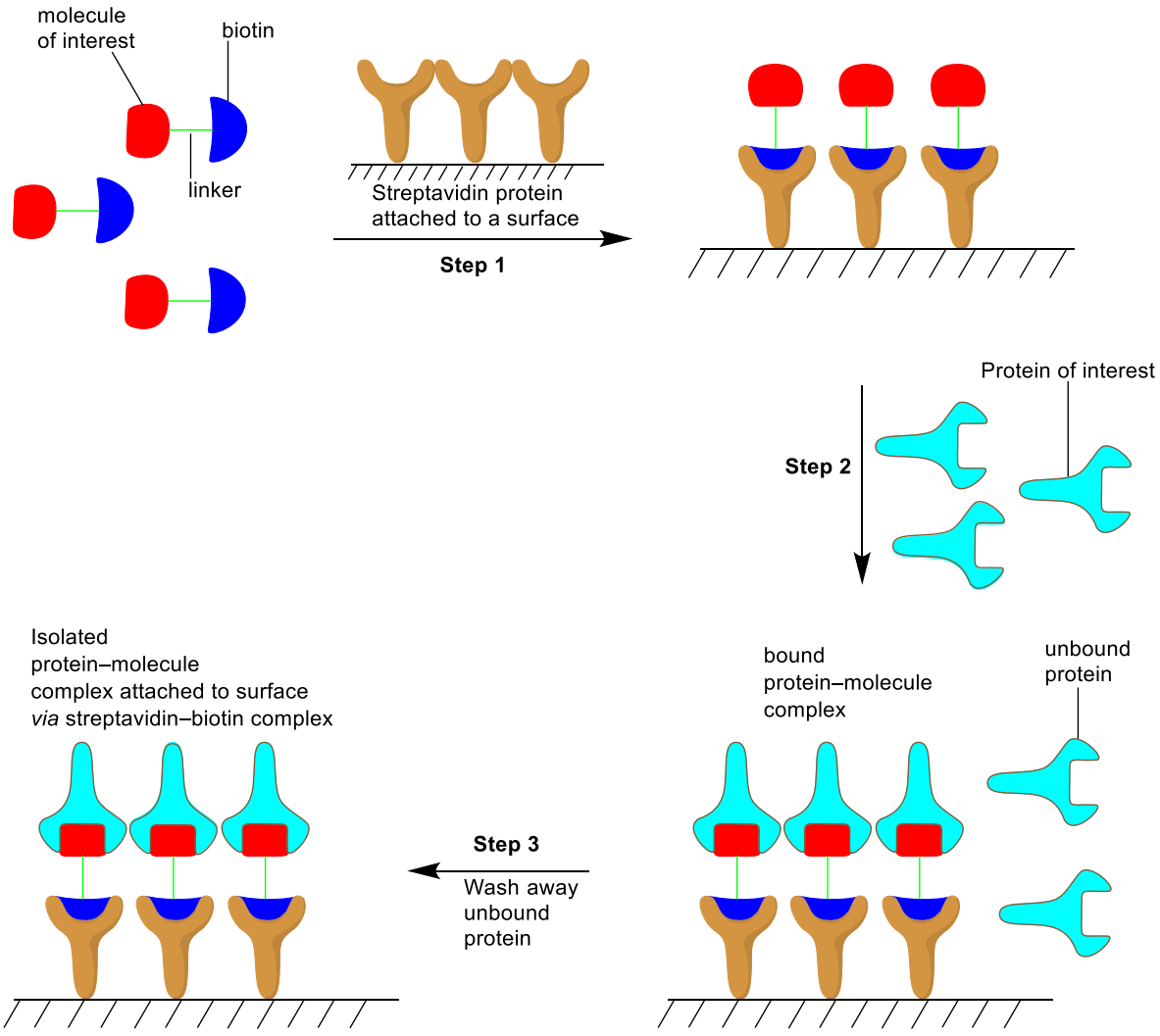

Scheme 2.8. Schematic showing biotinylated product being pulled down using streptavidin to isolate the desired ligand–protein complex.

2.6. Aims and objectives.

The aim of this project is to synthesise a biotinylated Glc_1Man_3 tetrasaccharide which retains its ability to bind at the lectin binding site of calreticulin, with the goal of developing a strategy from more efficiently isolating the calreticulin–tetrasaccharide complex. With this in mind, we elected to incorporate the biotin group at the reducing end of the tetrasaccharide *via* a five-carbon spacer. As seen in the crystal structure of the complex between calreticulin and tetrasaccharide **13,** the glycosidic bond at the reducing end points away from the protein. Moreover as Iwamoto *et al*. have previously incorporated a dansyl group at this position we postulated that incorporation of the biotin group into this site would have minimal impact on binding.

With all of this information, tetrasaccharide **13** was our synthetic target. As seen below it contains the Glc_1Man_3 tetrasaccharide shown in blue. The presence of the biotin group shown in red will allow for selective pull down of the protein–tetrasaccharide complex and a five-carbon linker shown in green connects the tetrasaccharide *via* an amide linkage.

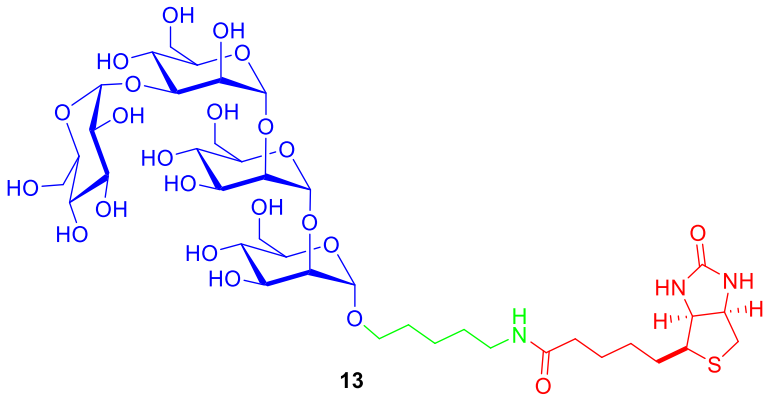

13

2.7. Synthesis of 5-biotinamido-pentanyl α-D-Glc*p*-(1→3)-α-D-Man*p*-(1→2)-α-D-Man*p*-(1→2)-α-D-Man*p* (13)

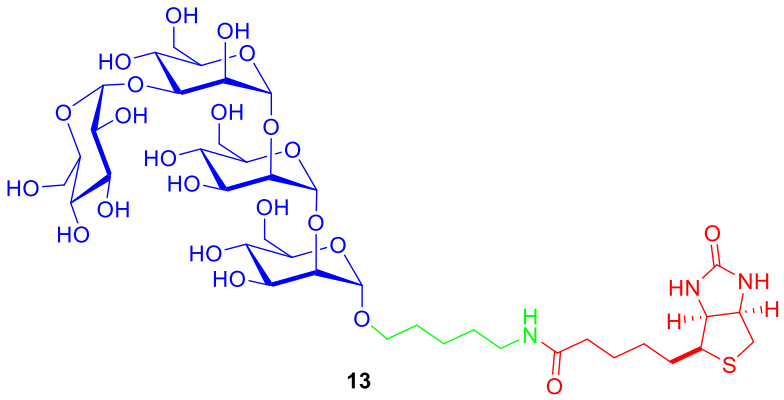

13

Our target tetrasaccharide **13** seen above can be separated into three parts, shown by the different colours. The blue shows the Glc_1Man_3 tetrasaccharide all with α-glycosidic linkages as required for binding to calreticulin. An aminopentyl chain is shown in green and acts as both a linker and spacer between the tetrasaccharide and the biotin group shown in red. Incorporation of a fluorescent label at the reducing end of the tetrasaccharide had previously been shown by Iwamoto *et al.* to not impede on protein binding therefore we postulated that incorporation of the biotin group at a similar position would work similarly.

2.7.1. Retrosynthesis

The retrosynthesis of 5-biotinamido-pentanyl α-D-Glc*p*-(1→3)-α-D-Man*p*-(1→2)-α-D-Man*p*-(1→2)-α-D-Man*p* 13 is summarised in Scheme 2.9. Owing to the unit cost of the biotin label along with a desire to minimise potential side-reactions and handling issues, we decided to incorporate the biotin in the final step of the synthesis. Through formation of an amide bond via the coupling of amine **64** with commercially available (+)-biotin *N*-hydroxysuccinimide ester **65**. The tetrasaccharide would be assembled using a convergent "2+2" synthesis, which both Cherif *et al*. and Gemma *et al*. had used successfully. Also, installing the glucose residue on to the 3-*O* hydroxyl of the Man(D1) residue would minimise the number of protection/deprotection steps. Cleavage of the glycosyl bond connecting Man(D1) and Man(C) would yield two disaccharides, GlcMan disaccharide **66** and ManMan disaccharide **67**. It was decided that the GlcMan disaccharide donor would be a thioglycoside, which is stable to a range of glycosylation conditions, allowing alternative reactions conditions to be investigated for the most challenging coupling of the glucosyl donor with the suitably protected mannose thioglycoside acceptor. Tetra-*O*-protected glucose **68** can be synthesised from glucose or purchased commercially, while mannose thioglycoside **69** can be synthesised from D-mannose **70**. The synthesis of ManMan disaccharide **66** would utilise a suitably protected mannose orthoester **71** for both residues as shown by Gemma and Iwamoto separately. The linker **72**, which can be synthesised from azide displacement of a pentanol halide **73**, would provide the acceptor for the first glycosylation reaction.

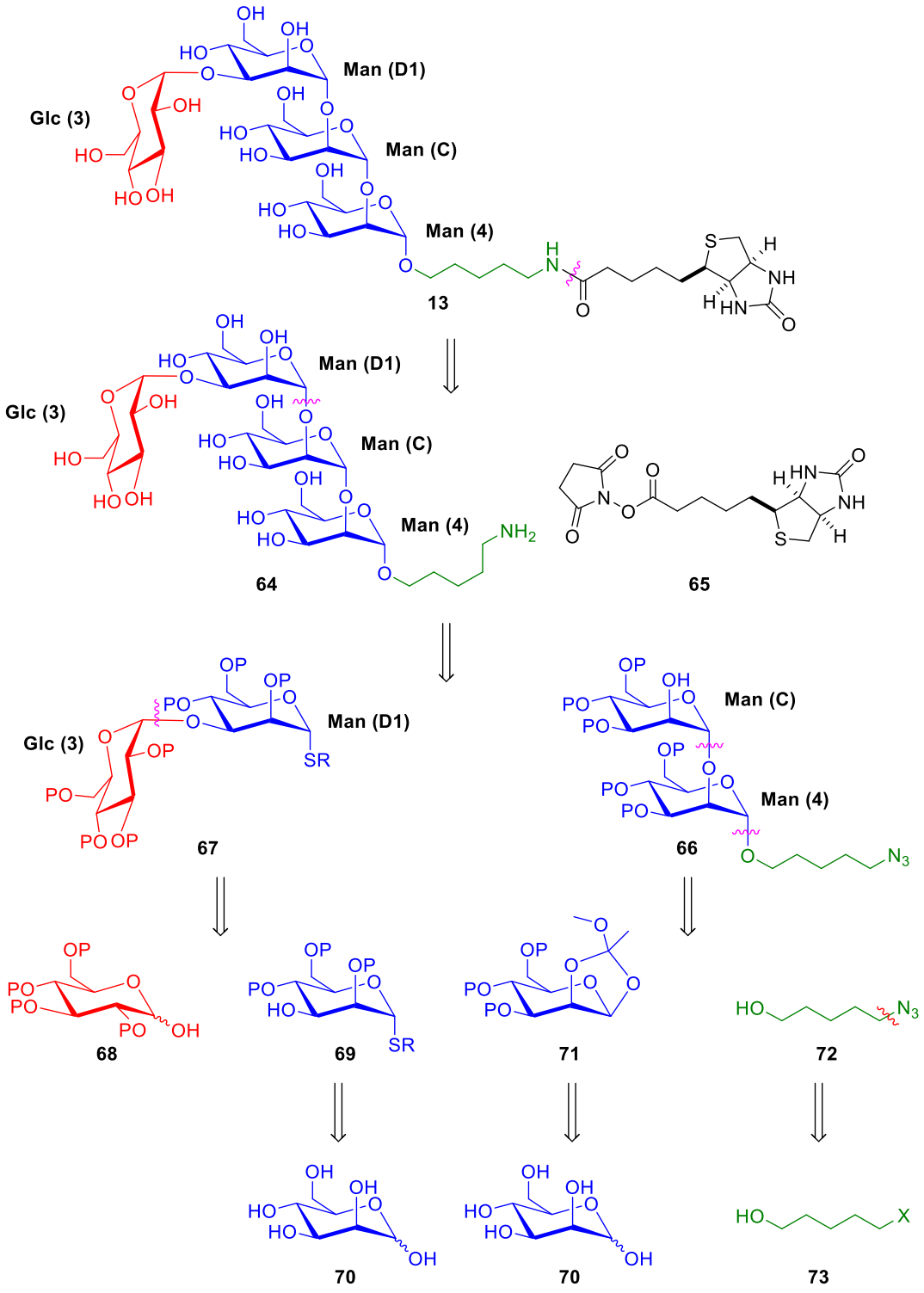

Scheme 2.9. Retrosynthetic analysis towards the synthesis of biotinylated tetrasaccharide **13**.

2.7.2. Synthesis of Mannose orthoester (44)

Starting with D-mannose, peracetylation using acetic anhydride in pyridine led to the peracetylated mannose **76** in quantitative yield with an α:β ratio of 77:23. Selective bromination at the anomeric position was achieved using 33% HBr in acetic acid solution. Due to the potential for hydrolysis of the bromide, bromide **74** was used directly in the next step and while no α:β ratio was measured, bromide **74** has been shown to exist as the α-steroisomer exclusively.[42] Orthoester **77** was synthesised from bromide **74** using 2,6-lutidine in CH_2Cl_2 and methanol in 67% yield over two steps. The acetate at the 2-*O* position displaces the bromide to form the corresponding acetoxonium ion which is trapped by methanol at the carbonyl carbon to yield the orthoester **77** (Scheme 2.10.).

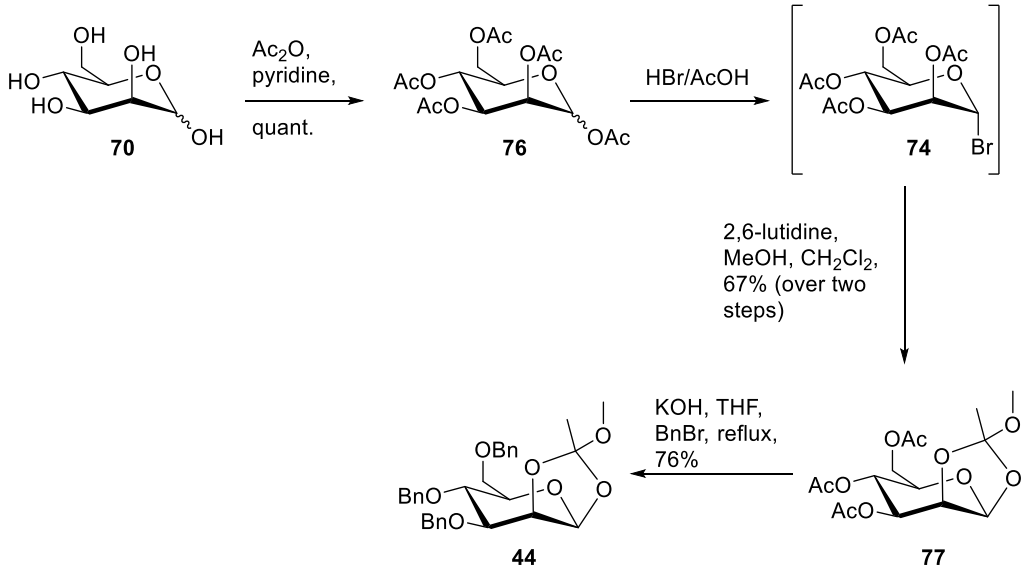

Scheme 2.10. Synthesis of benzyl orthoester **44**.

2,6-Lutidine being a non-nucleophilic base, acts as an acid scavenger but will not itself take part in the reaction. The methanol has the potential to attack from both sides, it was shown

that the major isomer was achieved in a 93:7 ratio and subsequent analysis by X-ray diffraction confirmed **exo-77** as the major product (Scheme 2.11).[42]

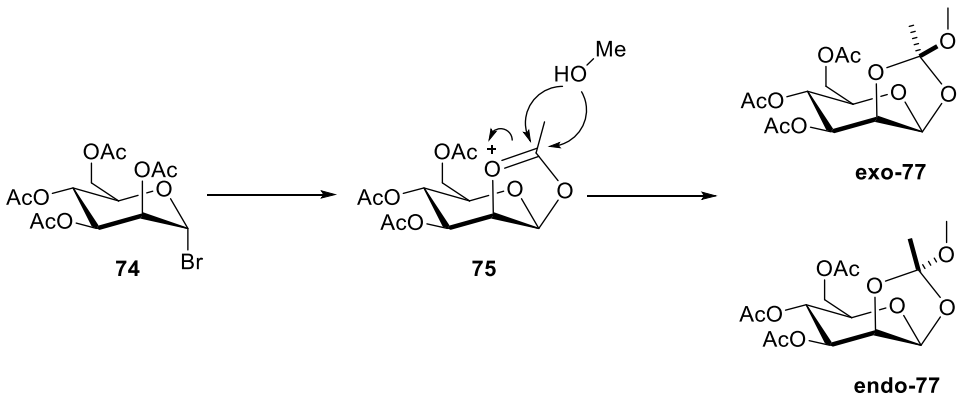

Scheme 2.11. Formation of Orthoester leads to two products depending on face of attack of methanol.

Having differentiated the 2-*O* position from the other sites, the remaining acetates were exchanged for benzyl ethers in a one-pot reaction. Thus, *in-situ* deacetylation using potassium hydroxide provided the corresponding alkoxides, which reacted with benzyl bromide to yield the target intermediate orthoester **44** in 76% yield. Orthoester **44** could be stored until required at which point it was converted to chloride **45** using TMSCl in CH_2Cl_2, to act as a mannosyl donor in a Koenigs–Knorr glycosylation.

2.7.3. Synthesis of ManMan disaccharide (83)

Scheme 2.12. outlines the synthesis of mannobiose **83** starting with acceptor **79** and using mannosyl chloride **45** as the donor in both glycosylation reactions. Azido-pentan-1-ol **79** was synthesised in quantitative yield from bromo-pentan-1-ol **78** *via* bromide displacement using sodium azide in DMF. Care had to be taken during the work-up to ensure the DMF was partitioned efficiently into the aqueous phase as the high temperature/ low pressure needed

to remove residual DMF from the organic phase led to some loss of the product. In glycosylation reactions, it is common to stir the acceptor and activator together in the presence of activated molecular sieves for up to a half an hour prior to adding the donor as a solution (which may also have been dried similarly with sieves). Our first attempt at the Koenigs–Knorr reaction using azido alcohol **79** as the acceptor and chloride **45** as the donor, we followed this general drying procedure. Alcohol **79**, 4 Å M.S., and silver(I) triflate were stirred together for 30 minutes prior to adding chloride **45**. However, the reaction did not proceed as expected and gave a complicated mixture of products as observed by TLC with no discernible major product. On repeating the reaction, TLC analysis of the mixture of sieves, activator and acceptor prior to addition of the donor revealed degradation of the acceptor which appeared to be the cause of the previous failed reaction. Precedent was found for the acid-catalysed decomposition of azide with a range of Lewis acids.[43] Under our conditions, the stoichiometric amount of AgOTf may have acted as a Lewis acid, leading to the decomposition products. To counter this problem the silver(I) triflate activator was stirred alone with molecular sieves, followed by simultaneous addition of both acceptor and donor as a solution in dichloromethane. This modification led to the desired α-mannoside **80** in 56% yield. Adding both acceptor and donor simultaneously presumably allows preferential activation of the chloride donor over competing degradation pathways with the azide. The benefits of using chloride **45** as the donor were next shown as selective deprotection of the acetate at the 2-*O* position was achieved using sodium methoxide in methanol to yield alcohol **81** in 92% yield. With our next acceptor, alcohol **81,** in hand, this was coupled with chloride donor **45** using the same conditions that had worked previously. The target disaccharide **82** was isolated in 48% yield and only the α-product was observed. Finally, removal of the acetate in **82** under Zémplen conditions yielded our first target disaccharide **83** which would serve as the acceptor in the key '2+2' glycosylation reaction.

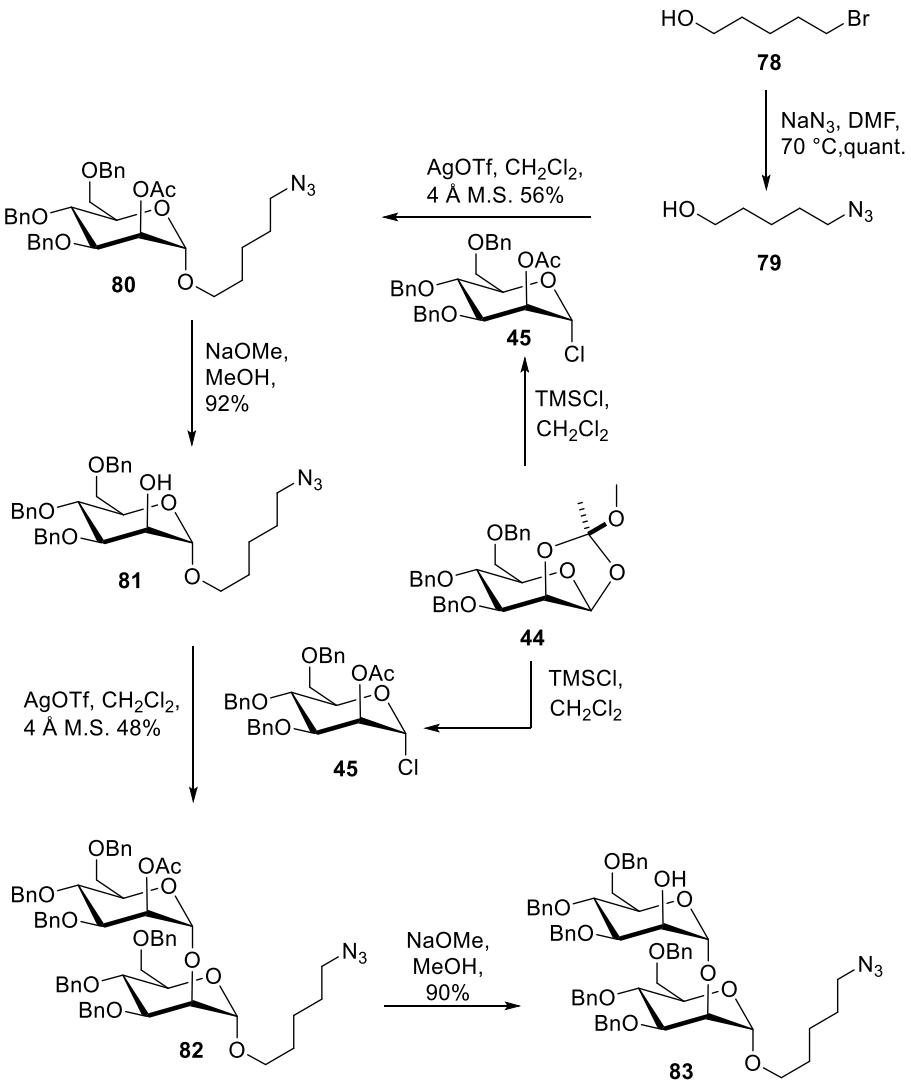

Scheme 2.12. Synthesis of ManMan disaccharide **83**.

2.7.4. Synthesis of 4,6-*O* benzylidene mannose thioglycoside (86)

With mannobiose disaccharide **83** in hand attention turned to the synthesis of the GlcMan disaccharide donor. We decided to investigate the phenyl thioglycoside rather than the ethyl thioglycoside. Although the ethyl thioglycoside is more reactive the synthesis of the phenyl thioglycoside employs thiophenol which is less toxic (and has a lower stench than ethanethiol).

Previously synthesised mannose pentaacetate **76**, was converted into phenyl thioglycoside **84** using thiophenol and boron trifluoride diethyl etherate in dichloromethane and ^{1}H NMR analysis confirmed the major product as the α-thioglycoside. Global deacetylation using sodium methoxide in methanol yielded phenylthioglycoside **85**. In order to isolate the 3-*O* hydroxyl we chose to protect the 4-*O* and 6-*O* positions as a benzylidene acetal and then explore methods for regioselectively protecting the 2-*O* position.

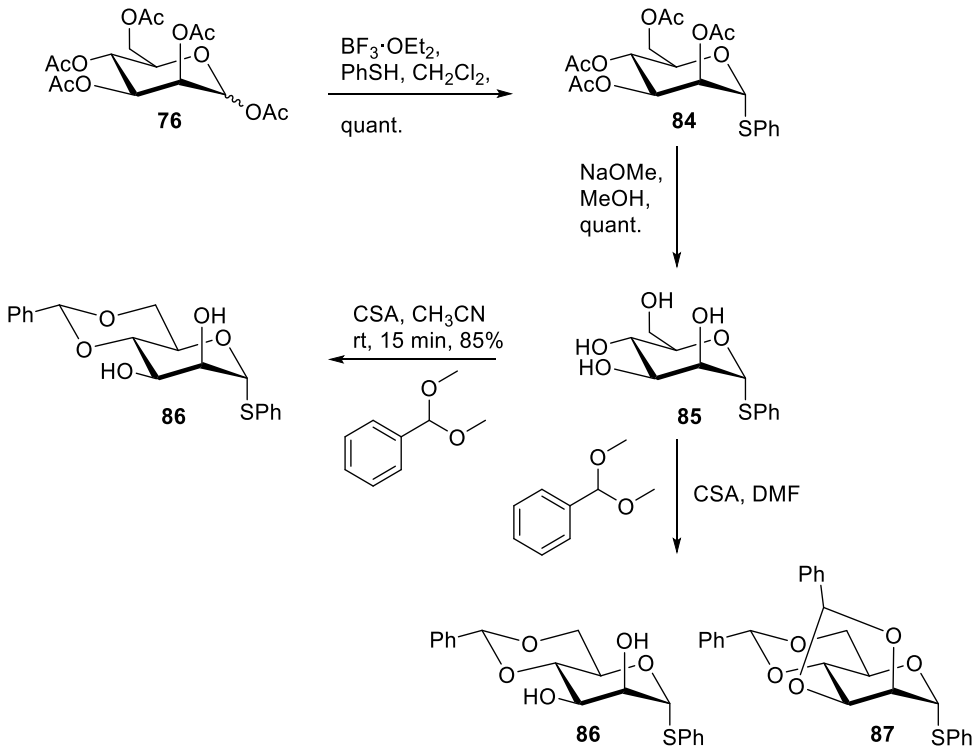

Scheme 2.13 Synthesis of Phenyl 4,6-O-benzylidene-1-thio-α-D-mannopyranose **86**.

Under thermodynamic conditions, benzylidene acetals favour the protection of 1,3-diols over 1,2-diols, while isopropylidene acetals favour the protection of 1,2-diols over 1,3-diols. As highlighted in Figure 2.8., formation of a six-membered ring in the protection of the 4-*O* and 6-*O* positions using benzaldehyde provides an acetal in which the large phenyl group can adapt an equatorial position leaving the hydrogen atom to assume axial position. In contrast, the

analogous isopropylidene acetal formed from using acetone would introduce significant 1,3-diaxial interactions as one of the methyl is forced into an axial position. A first attempt at the formation of thioglycoside **86** using benzylidene dimethylacetal in DMF with camphorsulfonic acid yielded a mixture of mono 4,6-*O* and bis 2,3:4,6-*O* benzylidene-protected thioglycosides **86** and **87** shown (Scheme 2.13). As the 2-*O* and 3-*O* hydroxyls in mannose are cis to one another, the formation of this bis-protected product is perhaps not unexpected. Purification of this mixture proved difficult. Although based on TLC the products should have been easily separated, their poor solubility caused complications when preparing a column for flash chromatography. Large volumes of solvent were required and the product also precipitated from solution on the column.

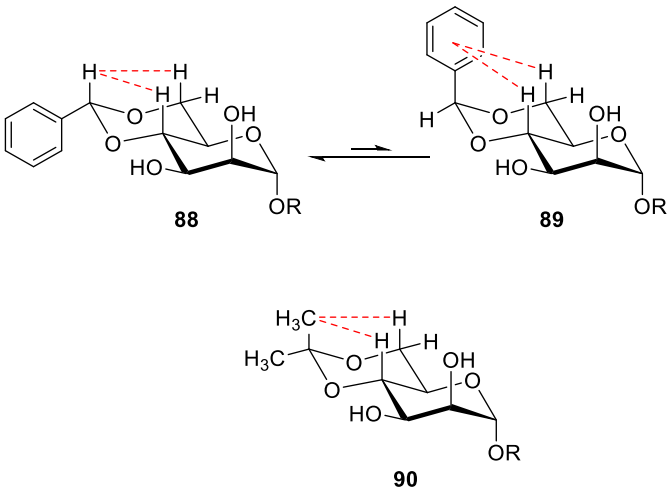

Figure 2.8. 1,3 Diaxial interactions of 4,6 protected mannose with benzylidene acetal and isopropylidene acetal.

It transpires that this is a known problem for the synthesis of benzylidene thioglycoside **86**. Previous methods to synthesise benzylidene **86** have used alternative Lewis acids and solvents.[44] More recently, Sanapala *et al*. published a synthesis of benzylidene thioglycoside **86**, achieving the desired compound in 94% yield with no presence of the bis-benzylidene product observed.[45] The key modification to the method involved the use of acetonitrile as the

solvent. We were able to replicate this reaction. While the starting material is not fully soluble in acetonitrile, following addition of the benzylidene dimethylacetal and camphorsulfonic acid the mixture became briefly homogenous before a white solid (the desired product) began to precipitate out. The reaction was quenched with triethylamine. The product was recovered in pure form in 85% yield by filtration after washing with petroleum ether (b.p. 40–60 °C). The choice of solvent was key here as desired product precipitates outs before further reaction can take place.

2.7.5. First synthesis of GlcMan disaccharide

The next step following the formation of benzylidene thioglycoside **86** was the selective protection of the 2-*O* position leaving the free 3-*OH* to act as an acceptor for the next glycosylation reaction. The target thioglycoside **92** has been previously synthesised *via* different routes from mannose thioglycoside **85**. Szurmai *et al*. found that chemoselective reductive ring opening of the dioxolane in bis 2,3:4,6-*O* benzylidene-protected thioglycoside **endo-87** and was possible using $LiAlH_4$–$AlCl_3$.[46] Interestingly, the regioselectivity of the reaction was determined by the *endo*/*exo* nature of the dioxolane benzylidene; thus, **exo-87** afforded the 3-*O*-Bn product **91** at a 20:1 ratio with the 2-*O*-Bn product **92**, whereas **endo-87** provided its 2-*O*-benzyl regioisomer at a 10:1 ratio with the 3-*O*-Bn product.

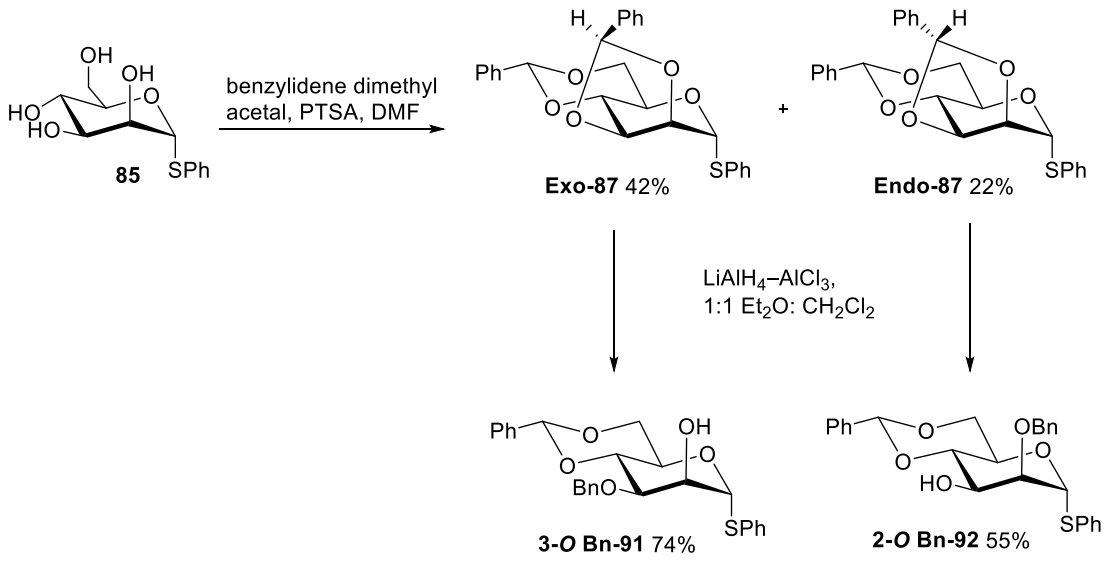

Scheme 2.14. Reductive ring opening of the dioxolane in bis 2,3:4,6-*O* benzylidene-protected thioglycoside.

Scheme 2.14 shows the formation of the 2-*O*-Bn and 3-*O*-Bn products from mannose thioglycoside **85**. While the reaction with benzylidene dimethyl acetal yielded a 1:1 mixture of endo:exo products, fractional crystalisation was then used to isolate both exo and endo isomers, at 41.8% and 22.4% respectively and only a moderate–good yield was obtained for the reductive ring openings of the dioxolane benzylidene in bis-acetals **exo-87** and **endo-87.** As we had previously encountered problems purifying bis 2,3:4,6-*O* benzylidene **87**, we chose to investigate alternative methods.

Another method for selectively differentiating the 2- and 3-*O*-positions of thioglycoside **86** involved the use of tin acetal chemistry, which Cherif *et al.* used to selectively protect the 3-*O* position as a *p*-methoxybenzyl ether (Scheme 2.15).[34] Benzyl protection of the 2-*O* position followed by selective removal of the PMB group with DDQ yielded the desired thioglycoside **92** in 63% yield over the three steps. While this approach offered a more efficient route to our target acceptor, it still required an inelegant protection–deprotection sequence.

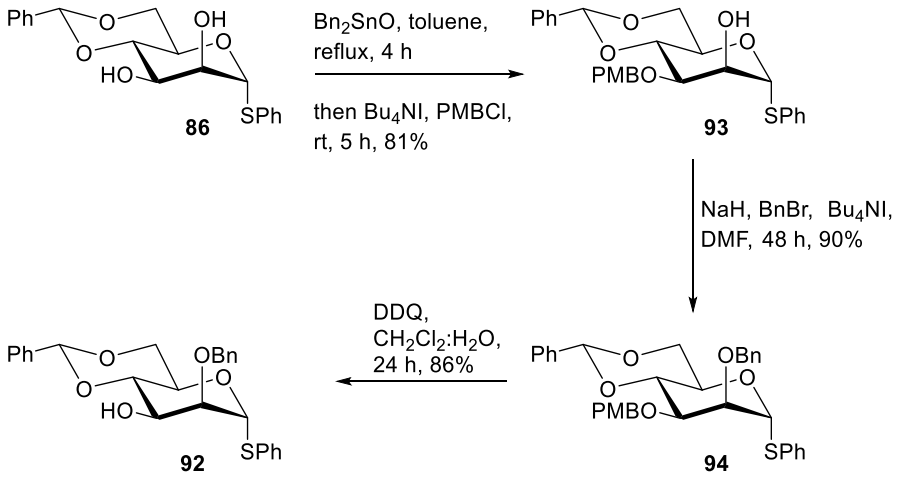

Scheme 2.15 Synthesis of alcohol **92** *via* initial 3-*O* protection.

Phase transfer-catalysed reactions have been studied on carbohydrate diols and in some cases shown to provide high yields of selectively mono-protected products.[47, 48] Of relevance to our target, Crich *et al.* described the regioselective phase transfer-catalysed benzylation of the 2-*OH* of the desired thioglycoside **92** in 75% yield.[49] Applying the same conditions to our phenyl thiomannoside, the selectively 2-*O*-benzylated product **92** was isolated in 62% yield.[50, 51]

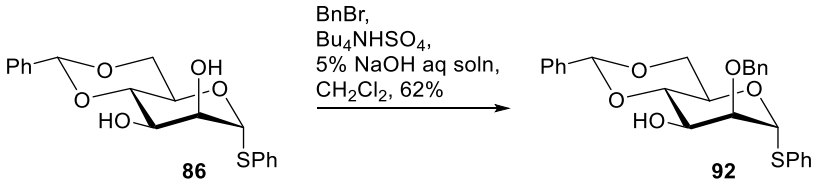

Scheme 2.16 Selective 2-*O* protection using a phase transfer catalyst.

The next key step of the synthesis involved incorporation of the α-glucose residue, which had been the most challenging in all of the previous syntheses of tetrasaccharide **13**. A range of α-selective glycosylation methods were explored; thus, glucosyl iodide, trichloroacetamide

and bromide donors were all tested for their reactivity and stereoselectivity in their reaction with acceptor **92**.

Within the group, the synthesis of α–GalCer **10** is typically achieved via the coupling of per-TMS-protected galactosyl iodide **95** and protected sphingosine **96** using conditions that were developed by Gervay-Hague (Scheme 2.17).[52-55] The product glycolipid **97** is typically isolated in excellent yield and selectively as the α-product. α-Selectivity is achieved by establishing conditions that allow rapid anomerisation of the intermediate α- and β-iodides through the inclusion of TBAI in the reaction mixture. Selective S_N2 substitution is acheived on the more reactive β-iodide. Since equilibration of the intermediate α- and β-iodides proceeds much faster than glycosylation, high α-selectivity can be achieved (Curtin-Hammett conditions).

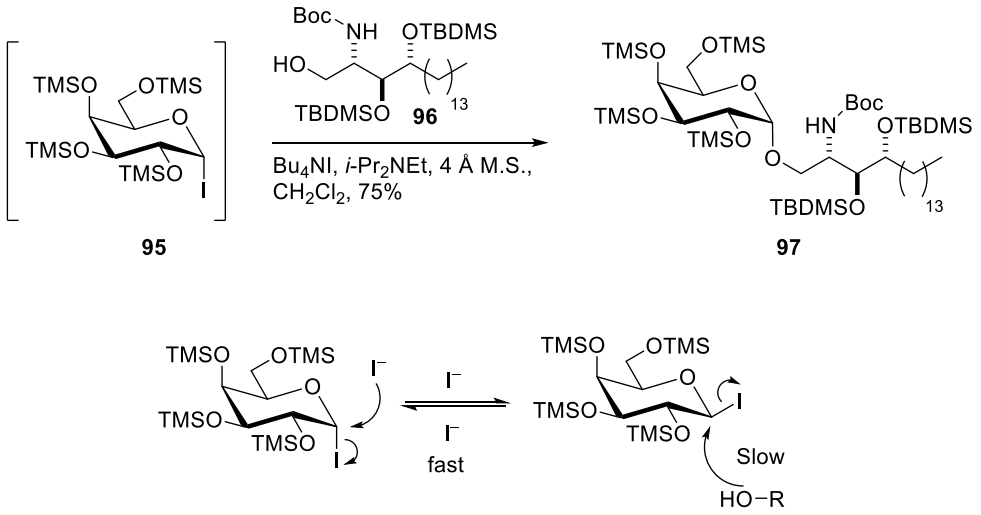

Scheme 2.17 α-selective glycosylation of glycolipid **97** as a precursor of α-GalCer.

Whilst there are no examples of glycosylations using TMS-protected galactosyl iodide donor **95** with a sugar acceptor, Davis *et al*. have performed a glycosylation using per-TMS glucosyl and galactosyl iodides and cholesterol (Scheme 2.18).[56]

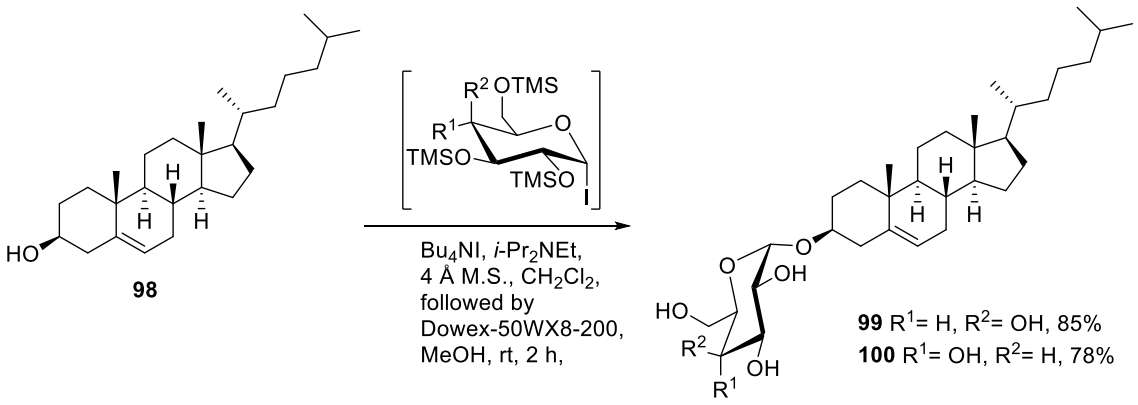

Scheme 2.18 Glycosylation of iodide **95** with cholesterol acceptor.

While the acceptor in our synthesis of α-GalCer is a primary alcohol we expected our glycosylation would proceed with similar α-stereoselectivity albeit with a less reactive secondary alcohol sugar acceptor. Per-TMS protection of glucose was achieved in 94% yield using TMSCl in pyridine with HMDS acting as a co-solvent (Scheme 2.19.). TMS-glucose **102** was then treated with TMSI in CH_2Cl_2. After 30 min, the reaction mixture was co-evaporated with anhydrous toluene to remove any unreacted TMSI and the crude glucosyl iodide product was used directly without purification in the glycosylation reaction. Thus, a solution of iodide **95** in anhydrous dichloromethane was added to a dichloromethane solution of thioglycoside **92**, TBAI and Hünig's base, which had been previously stirred over activated 4 Å molecular sieves for 30 min. Unfortunately, no glycosylation product was observed; the acceptor proved unreactive and was recovered intact.

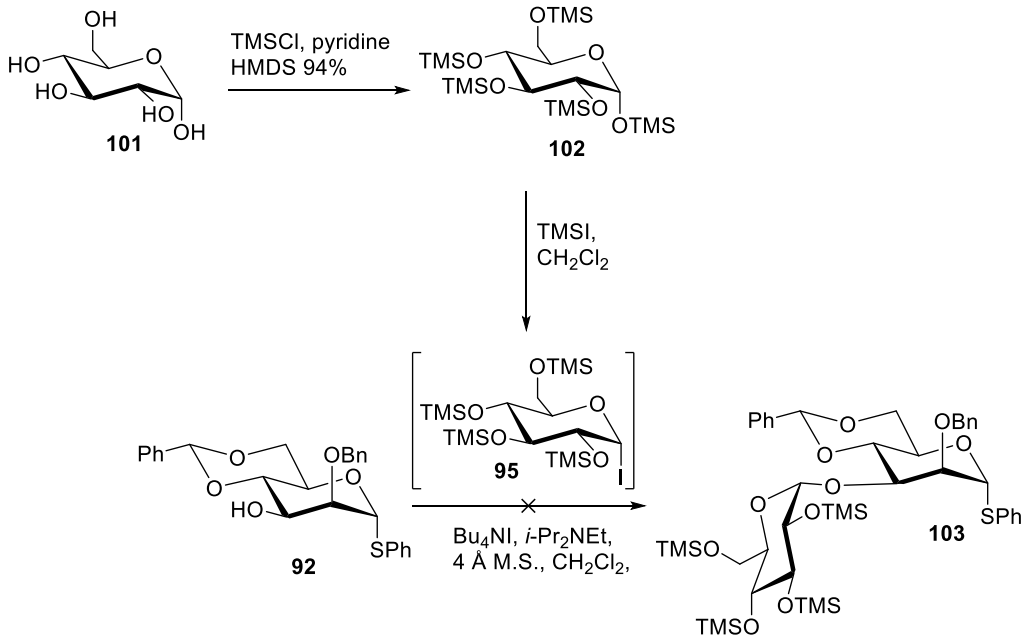

Scheme 2.19 Failed attempt at GlcMan disaccharide synthesis using per-TMS glucosyl donor.

Gemma *et al*. were also unable to effect glycosylation between donor **49** and acceptor **50** under Gervay-Hague conditions (Scheme 2.20); however, they had more success using conditions developed by Mukaiyama and Kobashi,[37] which employ a phosphine oxide activator (Scheme 2.4, p38).

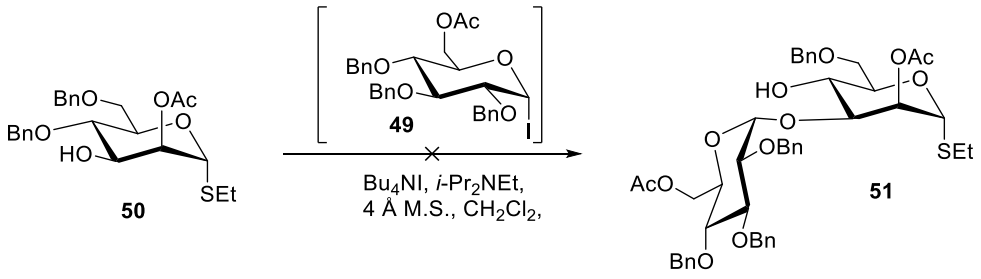

Scheme 2.20. Failed attempt at glycoyl iodide glycosylation by Gemma *et al.* using Gervay-Hague conditions.

In our syntheses of α-GalCer analogues, we have also observed that small changes to the lipid acceptor or glycosyl donor can affect the success of Gervay-Hague glycosylations.[52] In these instances, we too have often had more success with perbenzylated glycosyl halide donors.

Based on these observations, we decided to move away from glycosyl iodides and focus instead on alternative, more stable donors that had been previously established within the group.

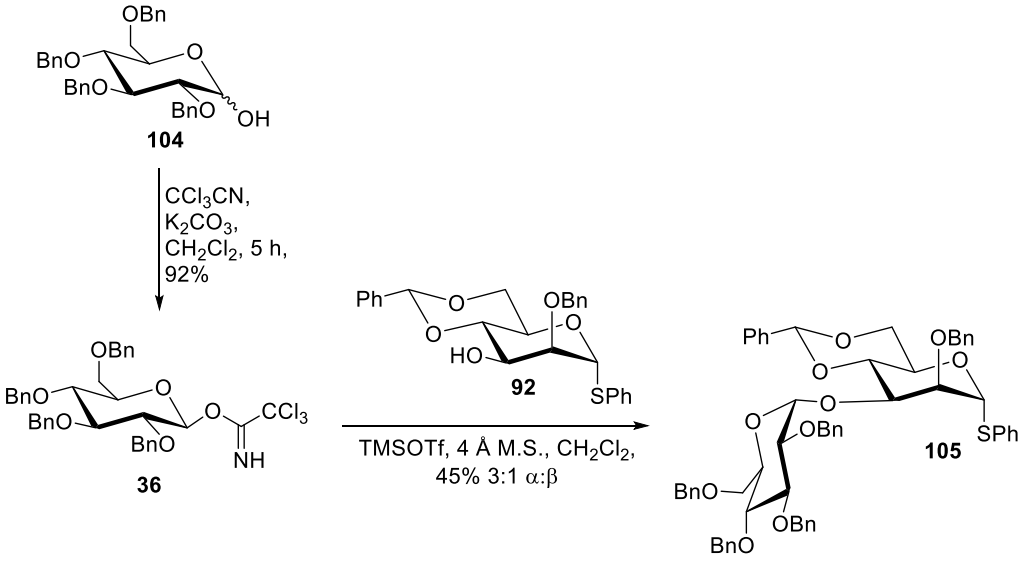

Scheme 2.21 Synthesis of GlcMan disaccharide **105** using a trichloroacetamidate donor.

Trichloroacetimidate **36** was synthesised from commercially available 2,3,4,6 tetra-*O*-benzyl glucose in one step from trichloroacetonitrile and solid potassium carbonate. The product was used directly without further purification in a glycosylation with acceptor **92** under TMSOTf activation. Full consumption of the donor **92** was observed after 1 h and disaccharide **105** was successfully isolated in a 3:1 α:β ratio and combined yield of 45%. Unfortunately, the two anomers proved inseparable by flash column chromatography.

A second method that had been previously used within the group to synthesise α-GalCer was through the use of 2,3,4,6-tetra-*O*-benzyl glucose as the donor in a dehydrative glycosylation.[57] The method developed by Nishida uses the Appel reagents, triphenylphosphine and carbon tetrabromide, to prepare the active glycosyl bromide *in situ* as summarised in Scheme 2.22.[58-60]

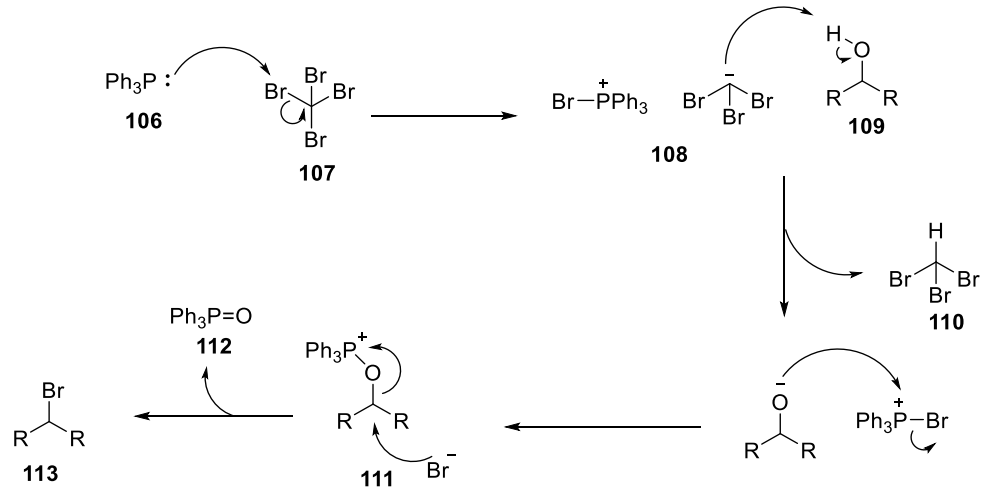

Scheme 2.22. Conversion of hydroxyl group to bromide using Appel reagents.

The first step involves reaction of triphenylphosphine and carbon tetrabromide to yield the phosphonium salt **108**. The carbanion acts as a base to deprotonate the alcohol and form bromoform. The resulting alkoxide reacts with the phosphonium cation to yield phosphonium intermediate **111**, which undergoes substitution with bromide anion to form the glycosyl bromide and triphenylphosphine oxide, which provides a strong driving force for the reaction.

Scheme 2.23 summarises the α-selective glycosylation. Under the reaction conditions, the more stable α-glycosyl bromide is in equilibrium with its highly reactive β-anomer. The inclusion of *N,N*-tetramethylurea (TMU) and presence of bromide anions facilitate the rapid equilibration; which crucially, proceeds at a much faster rate than does any reaction with the acceptor. The acceptor alcohol (R-OH) then reacts preferentially with the more reactive β-

glycosyl bromide in an S_N2 fashion to provide the α-glycoside product. The use of an excess of the Appel reagents ensures any glycosyl bromide that is hydrolysed by adventitious water is recycled. The use of non-participating groups is also vital, especially at the 2-*O* position prevent neighbouring group participation. While this was beneficial during the syntheses of α-linked mannose residues, neighbouring group participation at the equatorial 2-*O* position of a glucsoyl donor serves to block the α-face, leading to attack from the β-face.

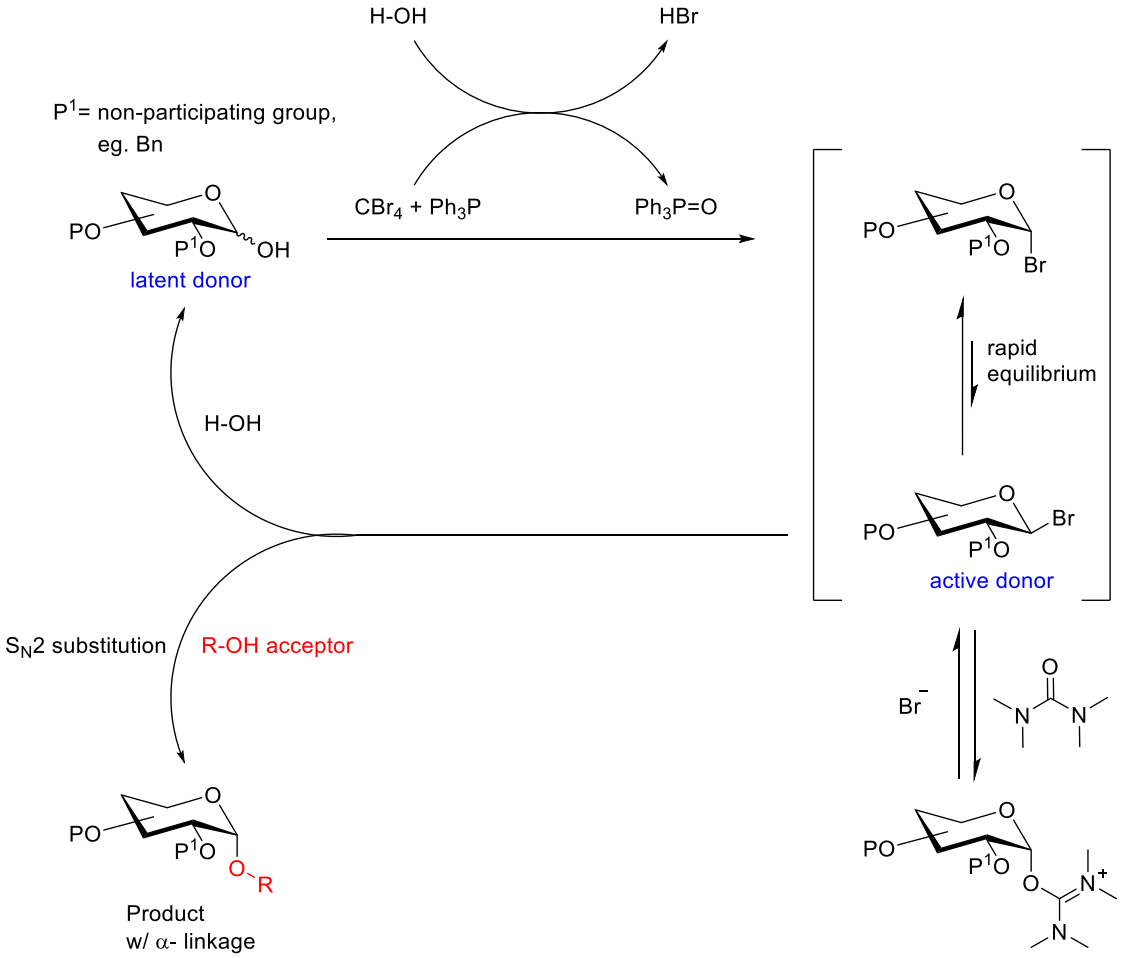

Scheme 2.23 Summarising the α-selectivity of the Koenig Knorr reaction using Appel reageants.

Using three equivalents of the Appel reagents to one equivalent of the hydroxyl sugar **114** in dichloromethane, the mixture was stirred for 3 h at room temperature until TLC analysis

showed full conversion of the starting material[1]. *N,N*-Tetramethylurea along with acceptor **92** were then added and the reaction mixture was stirred for four days, after which time, TLC analysis showed full consumption of the bromide to yield disaccharide **105** in 51% yield as a 10:1 α:β mixture. The reaction was also attempted with the addition of tetrabutylammonium iodide and tetrabutylammonium bromide to facilitate equilibration; however, these additives led to no difference in the reaction time or stereoselectivity, which was in keeping with the findings of Nishida.[61]

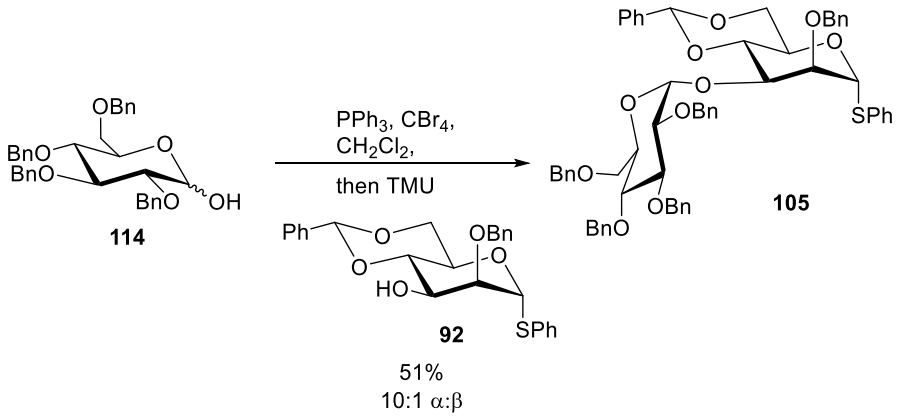

Scheme 2.24 Synthesis of GlcMan disaccharide **105**.

Nishida reported that an acetyl protecting group at the 6-*O* position of the sugar donor increased the α-stereoselectivity of the reaction, proposing long-range group participation and formation of an acetoxonium intermediate on the α-stereoface.[58] Hydroxy sugar was therefore synthesised in two steps from 2,3,4,6-tetra-*O*-benzylglucopyranose via acetylation of the anomeric and 6-*O* position and selective deprotection of the anomeric acetate (Scheme 2.25).[62, 63] While the glycosylation reaction was now completely α-stereoselective, disaccharide **118** was only isolated in 26% yield as its separation from the starting acceptor,

[1] The bromide can be visualised by TLC

which was used in excess, proved problematic. As a consequence, we decided to continue the synthesis with disaccharide **105**, which could be prepared on the larger scales needed to complete the synthesis of the tetrasaccharide target.

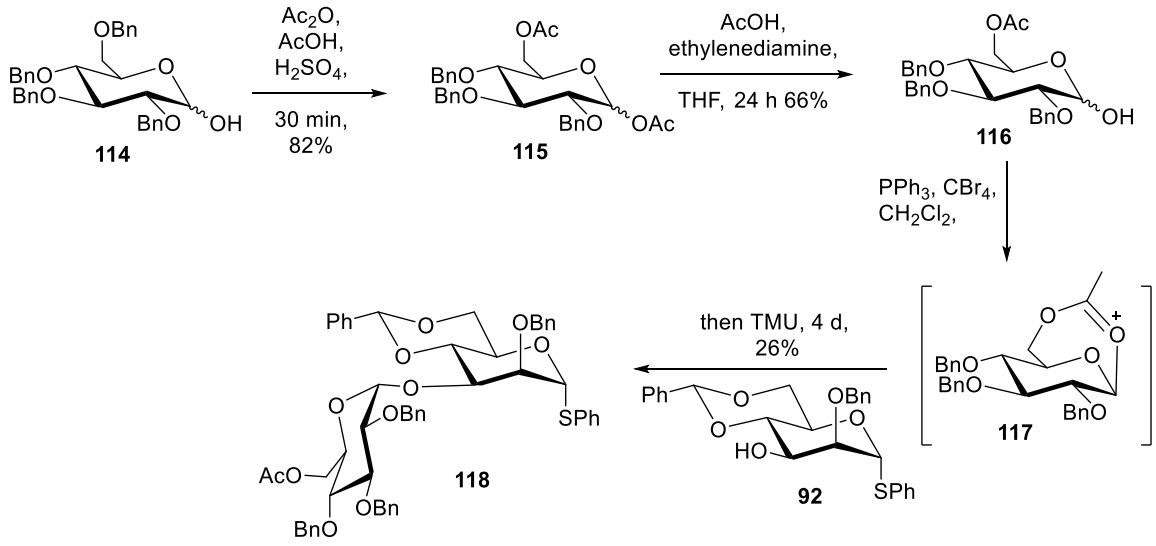

Scheme 2.25. Synthesis of GlcMan disaccharide **118**.

2.7.6. Synthesis of Glc_1Man_3 tetrasaccharide (119)

With both disaccharides in hand, the next step was the '2+2' coupling of acceptor **83** with donor **105**. Activation of the thioglycoside using (freshly recrystallised) *N*-iodosuccinimide (NIS) and trifluoromethanesulfonic acid followed by addition of the acceptor afforded a mixture of tetrasaccharide products in 22% yield. The presence of the β-isomer from the previous reaction to form the GlcMan disaccharide **105** along with any β-isomer formed in '2+2' coupling reaction meant that up to four diastereomers were possible. NMR analysis of the product confirmed the presence of a mixture. As we could not separate the diastereomers at this stage, and the next step in the synthesis was a global deprotection of the benzyl ethers and

hydrogenolysis of the azide, separating a mixture of highly polar products would be very challenging. We therefore investigated an ester protecting group at the 2-OH position of the mannose residue of the GlcMan disaccharide. During the synthesis of the ManMan disaccharide **83**, following both glycosylations, deacetylation had caused a change in polarity which usefully allowed the α- and β- diastereomers to be separated. We postulated that a similar deprotection strategy might allow for separation of the major, desired isomer from other tetrasaccharide products.

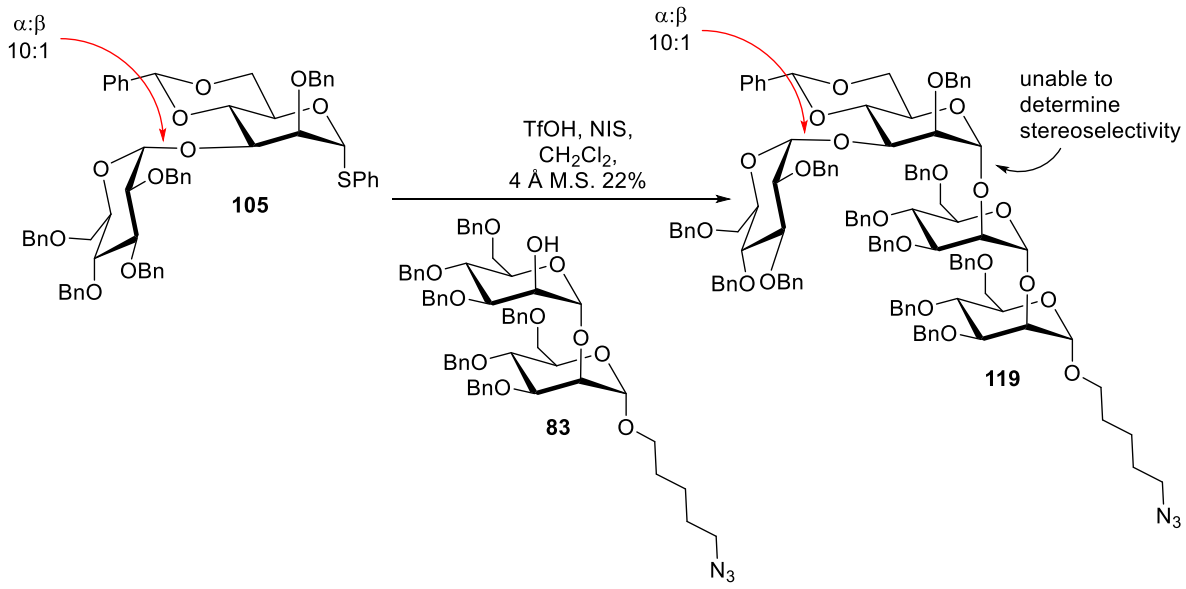

Scheme 2.25 a. Synthesis of tetrasaccharide **119**.

2.7.7. Synthesis of alternative GlcMan disaccharide (125)

We decided to protect the the 2-*O* position of the acceptor as a benzoate as there was literature precedent for the synthesis of thioglycoside acceptor **120** using the phase transfer catalyst method described previously (see p56).[64] Unlike the benzylation reaction, which required heating under reflux overnight for the reaction to reach completion, the analogous

benzoylation proceeded at 0 °C and was complete in 30 min (Scheme 2.26). The desired product **120** was isolated in 48% yield. Bis-benzoate **121** was also isolated in 26% yield with the potential for this product to be recycled back to alcohol **86** under Zemplén conditions.

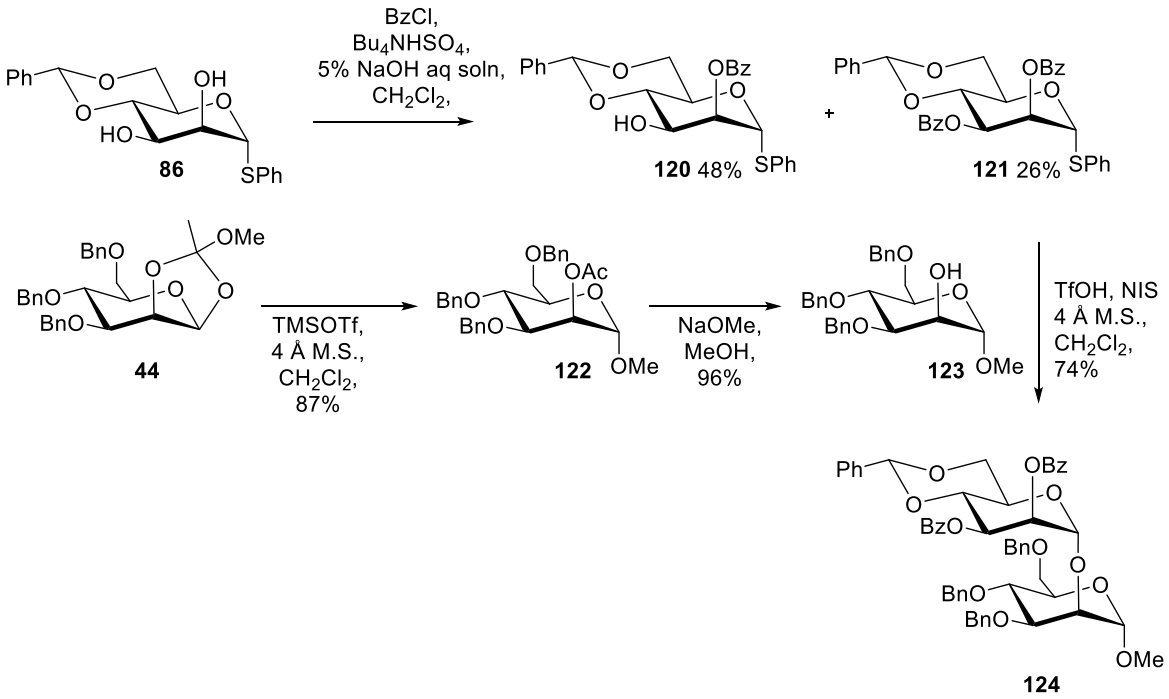

Scheme 2.26 Model glycosylation using thioglycoside **121** and mannosyl acceptor **123**.

We decided to investigate the reactivity of the thioglycoside **121**, which is a further disarmed donor compared with disaccharide **120**,[65, 66] with methyl 3,4,6-tri-*O*-benzyl mannopyrannoside **123**. Acceptor **123** was synthesised from orthoester **44** in two steps; thus, TMSOTf-mediated ring opening of the orthoester provided acetate **122**, which underwent Zemplen deacetylation to yield model acceptor **123** in 96% yield. With both model donor **121** and acceptor **123** in hand, we attempted the glycosylation using NIS / triflic acid to activate the donor. Pleasingly, the reaction proceeded uneventfully, affording the desired disaccharide **124** in 74% yield as a single α-anomer.

2.7.8. Second synthesis of GlcMan disaccharide

Having shown that thioglycoside **121** was a competent donor, we next targeted the GlcMan disaccharide containing a benzoate ester at the 2-*O* position of the mannose residue. Under Nishida's dehydrative glycosylation conditions, donor **114** reacted with acceptor **120** to yield the desired disaccharide **125** in 57% yield, an improved yield from the reaction using the 2-*O* benzyl acceptor although again as a 10:1 α:β ratio.

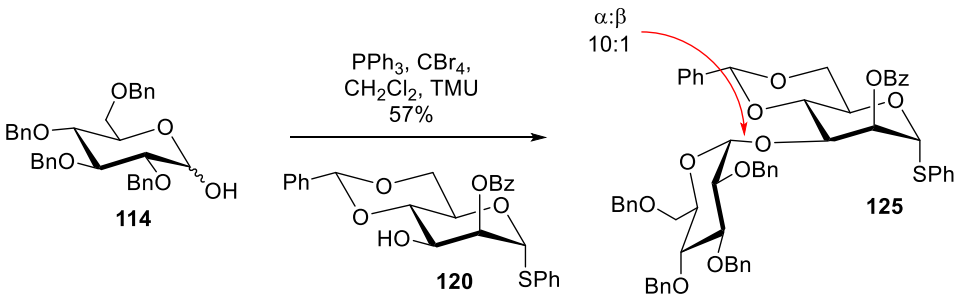

Scheme 2.27 Synthesis of disaccharide **125** using acceptor **120**.

2.7.9. Second synthesis of tetrasaccharide

Using our newly synthesised donor **125**, activation of the thioglycoside, once again with NIS / triflic acid and reaction with acceptor **83** yielded a new product which was confirmed as the tetrasaccharide **126** by mass spectrometry. As before, the product was isolated as an inseparable mixture of diastereomers; however, these were separable after debenzoylation under Zémplen conditions, allowing isolation of the desired target tetrasaccharide **127** in 35% yield over two steps from thioglycoside **125**.

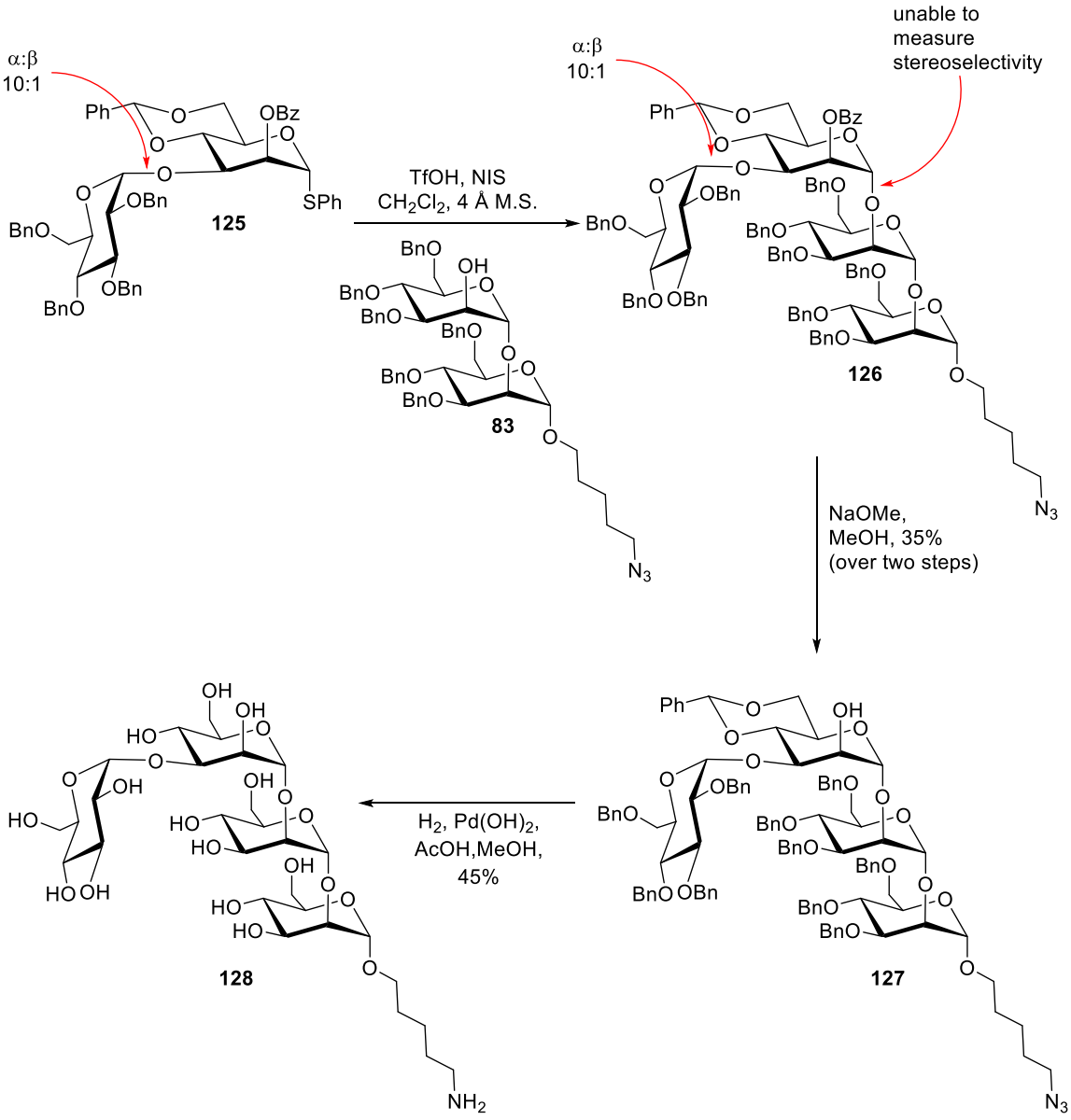

Scheme 2.29 Synthesis of tetrasaccharide **127** followed by global deprotection to **128** using hydrogenation conditions.

Our attention turned to confirming that all of the glycoside linkages in tetrasaccharide **127** were indeed α-linkages. To do this, we would use NMR spectroscopy. Figure 2.9. shows the angular relationship between the H-1 and H-2 substituents of α- and β-glucosides and α- and β-mannosides. In the case of glucose, there is a large difference in the dihedral angle between the H1 and H2 substituents in the two anomers, which makes it possible to differentiate them

by determining the magnitude of the vicinal coupling constant. In accord with the Karplus relationship, axial-axial coupling (dihedral angle ~ 180°) observed in a β-glucoside gives a $J_{1,2}$ value of 8–12 Hz whereas in the case of α-glucosides, a smaller $J_{1,2}$ value of 2–5 Hz (dihedral angle ~ 60°) is observed for this equatorial-axial coupling. Differentiating α- and β-mannosides by measuring the analogous vicinal $J_{1,2}$ coupling constants is more difficult as the dihedral angle between the two protons is around 60° for both α- and β-linkages. However, experimentally the $J_{eq\text{-}ax}$ value in α-mannosides is typically slightly larger than the $J_{ax\text{-}ax}$ value for β-mannosides (Figure 2.9.).[67, 68]

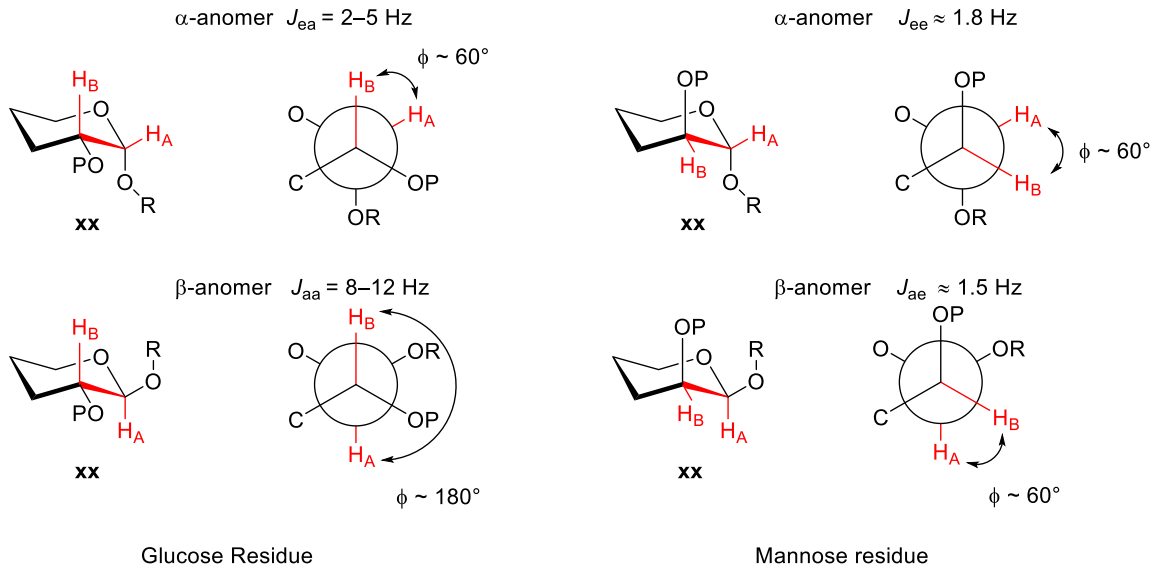

Figure 2.9. *J*-coupling values of anomeric position H-1 and H-2 of mannosyl and glucosyl residues

The NMR spectra of tetrasccharide **127** were recorded on the 900 MHz Varian spectrometer, housed in the Henry Wellcome Building NMR facility, by Sara Whittaker (NMR Operations Manager). Recording the NMR spectra on such a sensitive, high-field instrument provided the best opportunity to separate the resonances in the spectrum and to obtain the best possible resolution to confirm that only one diastereomer was present.

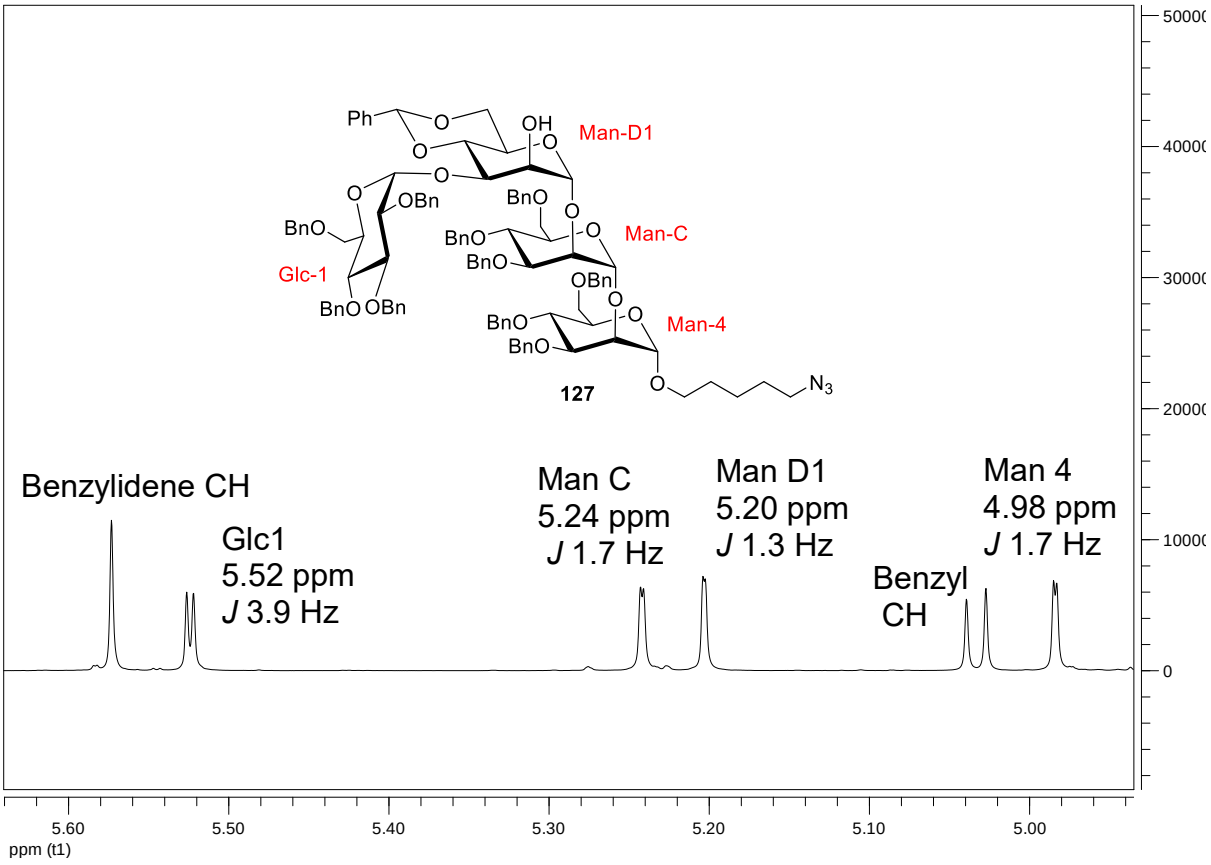

Figure 2.10. Expansion of ^{1}H NMR spectrum of tetrasaccharide **127**

Pendant ^{13}C, COSY, HSQC and HMBC experiments allowed near complete[2] full assignment of the proton and carbon resonances for the tetrasaccharide. Figure 2.10 shows a magnification of the region of the ^{1}H-NMR spectrum containing the four resonances arising from the anomeric hydrogens. The measured $J_{1,2}$ value of 3.9 Hz for the glucose residue is consistent with an α-glycosidic linkage. As expected, the measured $J_{1,2}$ values for the three mannose were residues small. The 1.7 Hz coupling constant obtained for Man-C and Man-4 was in agreement with the value reported in of a previous synthesis of the tetrasaccharide.[31]

[2] A complete assignment was not possible owing to overlapping resonances in both ^{1}H- and ^{13}C-NMR spectra.

The lower value of $J_{1,2}$ for Man-D1 can be attributed to the presence of the benzylidene group, which restricts the conformational flexibility and increases torsional strain of this particular mannoside residue. Similar observations were observed by Cherif *et al.*[33] and Despras *et al.*[69], whose measured values for $J_{1,2}$ of α-mannosides containing benzylidene protecting groups are in agreement with ours.

Having confirmed that all of the glycosidic linkages were of the correct stereochemistry, the next step was the global deprotection of the molecule with removal of the benzyl and benzylidene protecting groups, and reduction of the azide. Hydrogenation was done using $Pd(OH)_2$ catalyst with H_2 gas in methanol. $Pd(OH)_2$ is a more active catalyst than Pd/C and the addition of acetic acid has a dual purpose in that it facilitates the removal of the benzylidene group under hydrogenolysis conditions as well as protonate the amine to help reduce poisoning of the catalyst. The reaction mixture was stirred over an atmosphere of H_2 for 2 days, with the reaction being worked up and restarted with fresh catalyst after 24 h. The fully deprotected product **128**, as determined by mass spectrometry, was isolated in 45% yield following flash chromatography using a H_2O:methanol eluent.

2.7.10. Biotinylation of tetrasaccharide

The final step of the synthesis involved the coupling of the biotin to the amine via an amide linkage. Reaction of amine **128** with commercially available (+)-biotin *N*-hydroxysuccinimide ester proceeded uneventfully to provide biotinylated tetrasaccharide **13** in 68% yield (Scheme 2.30.). Conversion of the amine to the amide also facilitated purification of the final compound as $CHCl_3$:MeOH could now be used as the eluent without having to include water. However,

we were unable to isolate pure product; TLC analysis showed the presence of another compound with a similar R_f value. NMR spectroscopic analysis confirmed that the impurity was neither a carbohydrate nor did it contain biotin. As the biotin group was prerequisite for the CRT binding assay, we deemed that the impurity would not affect the outcome of these experiments.

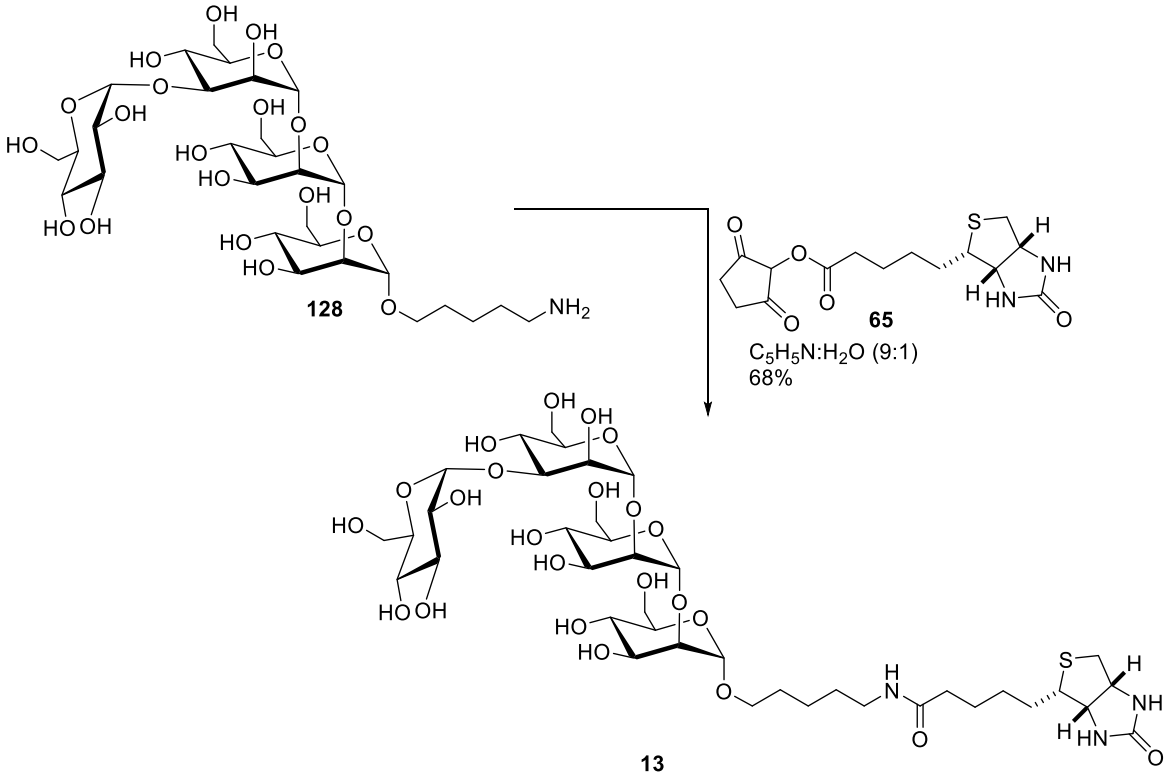

Scheme 2.30. Acylation of amine **128** to yield desired tetrasaccharide **13**

2.8. Binding studies of Calreticulin and its mutants to oligosaccharide substrates

Calreticulin (CRT) is an ER-resident lectin chaperone involved in the folding of various glycoproteins. The natural ligand for CRT is the mono-glucosylated oligosaccharide $Glc_1Man_9GlcNAc_2$, which is found on the surface of glycoproteins in the ER. Whilst the terminal glucose is essential for CRT binding, this residue is only transiently present on the oligosaccharide substrate, as this undergoes further processing in the cell. The development of CRT mutants that are able to recognise the non-glucosylated substrate, $Man_9GlcNAc_2$, are desirable as these will interact with a larger number of glycoproteins, which will facilitate the isolation of chaperone-substrate complexes. It has been shown previously that a truncated oligosaccharide containing the terminal Glc_1Man_3 tetrasaccharide can be recognised by CRT and that modifications at the reducing end do not interfere with binding.[38] To this end, biotinylated tri-mannose trisaccharide **129** and biotinylated tetrasaccharide **13** are being used as surrogate substrates to detect functional mutants in the sugar-binding domain, which alter the specificity of the lectin such that it can bind to non-glucosylated glycoproteins.

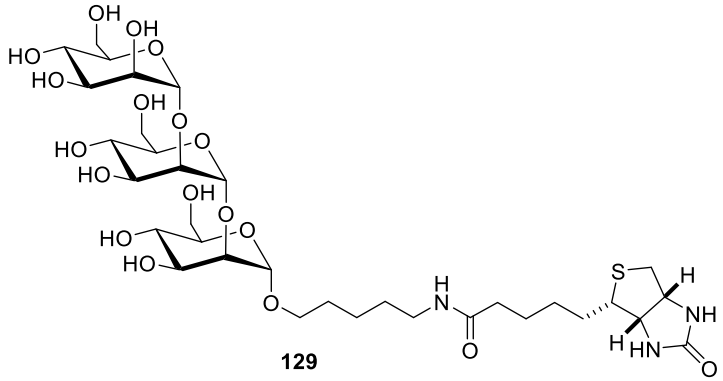

129

The biotinylated sugars can be bound to streptavidin-coated agarose beads and used in a pull-down assay with purified mutant CRTs. Alternatively, they can be bound to streptavidin-coated plates and employed in a high-throughput ELISA-based assay. Tetrasaccharide **13** serves as both a positive control in these experiments to ensure the assay is functioning, and

to test whether or not any CRT mutant, which is pulled down, has retained the binding specificity of the wildtype (WT)-CRT.

Tetrasaccharide **13** was submitted for biological testing, which was carried out by Dr Najla Arshad, a member of Prof. Peter Cresswell's group at the Department of Immunobiology at Yale University School of Medicine, US. Initial experiments used GST-fusion proteins of i) WT-CRT, ii) a known CRT mutant (Y92A) which is unable to bind to any oligosaccharides, and iii) a test CRT mutant (K111A) which was recombinantly expressed in *E. coli* and purified from the bacteria by affinity purification using GSH-agarose beads. The biotinylated oligosaccharides were incubated with streptavidin beads to allow attachment. The beads were then dispensed into tubes, protein was added to each tube and the mixture was incubated for 1.5 h at 4 °C. The recovered beads were then boiled in sample-loading buffer and subjected to SDS PAGE, to remove unbound protein, followed by Coomassie staining. 10% of the protein used in each experiment was run on the gel.

The results of these experiments are summarised in Figure 2.11. As expected, the calreticulin wildtype binds to tetrasaccharide **13** but not to trisaccharide **129**, which is in accordance with the known specificity requirement of the terminal Glc residue. This result supports our design strategy: the biotin label does not compromise the ability of CRT-WT to recognise the tetrasaccharide unit in **13** nor does the tetrasaccharide unit compromise the ability of the biotin label to attach to the streptavidin-coated beads. The mutant CRT-Y92A does not interact with either of the sugars, as expected, but neither does CRT- K111A. These initial results suggest that this mutation (of lysine to alanine) at position 111 has rendered CRT incapable of binding sugars. However, further studies are needed since the amount of CRT-WT used in the assay was more than the other two proteins, which may confound the result. New mutants are currently being isolated, which may prove to successfully bind to the trisaccharide.

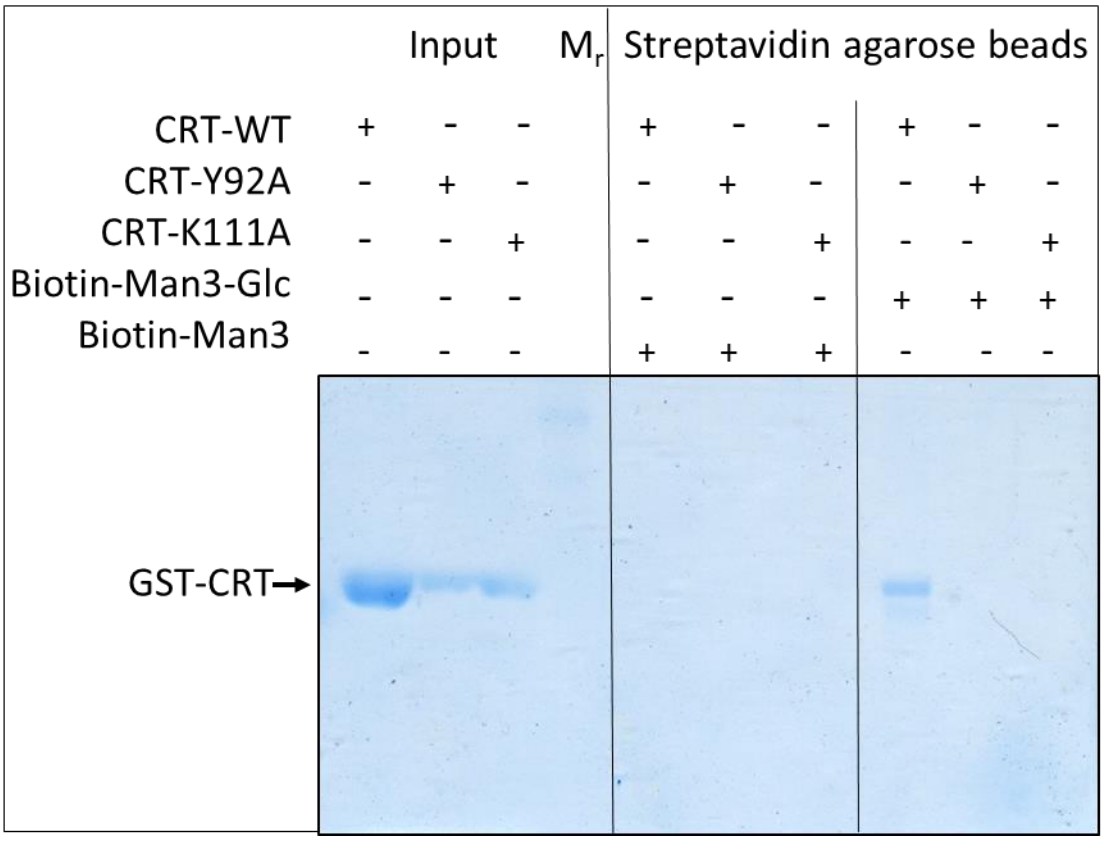

Figure 2.11. Assay showing binding of tetrasaccharide **13** to CRT-WT

2.9. Conclusions and future work

Successful synthesis of biotinylated Glc_1Man_3 **13** has been achieved using a convergent 2+2 method. Successful binding was seen between WT-CRT and the tetrasaccharide, however, thus far, no functional mutant that can bind to non-glucosylated trisaccharide has been isolated. Future work may involve the development of a cleavable linker between the tetrasaccharide and the biotin group. The conditions required to separate the biotin–streptavidin complex are harsh and would also separate the tetrasaccharide–calreticulin complex in the process. An enzymatic cleavable linker in particular would be beneficial as the conditions required are highly selective. Development of the cleavable linker would allow isolation of the tetrasaccharide–calreticulin complex in the absence of the biotin–streptavidin complex. This may be of benefit when calreticulin mutants are discovered that bind both tetrasaccharide **13** and trisaccharide **129** and it is necessary to develop a crystal structure to determine the new binding interactions of the mutant

Chapter 3

Synthesis of analogues of ThrCer-6 and ThrCer as CD1d adjuvants

3. Synthesis of analogues of ThrCer-6 and ThrCer as CD1d adjuvants

Introduction

3.1. CD1

The Cluster of Differentiation 1 (CD1) family of antigen-presenting proteins are highly conserved. They have a similar function to MHC molecules. However, in contrast to MHC molecules, which present peptide antigens to T-cell receptors (TCR), CD1 molecules bind and present a range of lipids and glycolipids to the TCR of CD1-restricted T cells. There are five different isoforms of CD1. Based on their nucleotide and amino acid sequence homology, they can be divided into three groups. Group 1 comprises CD1a, CD1b, and CD1c, which are expressed by humans, but not present in mice. Group 2 consists of CD1d, which is present in both humans and mice. CD1e is the sole representative of group 3 and has received little study.[70-72]

CD1 molecules are structurally similar to MHC class I molecules in that they comprise a heavy trans-membrane α chain, which is folded into three domains (α1, α2 and α3). This heavy chain is non-covalently associated with β_2 -microglobulin (β_2m). The structure of CD1 molecules allows for the binding of antigens of amphipathic nature which contain a hydrophilic head group and a hydrophobic tail. The antigen binding site of CD1 molecules is generated by the α1 and α2 domains, which fold to form deep, narrow pockets that are lined with mostly non-polar amino acids. The hydrophobic nature of these pockets allows for the binding of lipids through stabilisation by hydrophobic interactions. The polar, hydrophilic head group is then exposed on the surface of the protein molecule, where it is stabilised by hydrogen-bonding interactions and available for TCR recognition.

CD1 molecules have almost invariant binding grooves; however, they can still bind a range of antigens, including both intracellular and extracellular lipids of endogenous or foreign origin.

CD1a presents glycolipids such as the sphingolipid sulfatide **130** (which has also been shown to bind to CD1b, CD1c and CD1d) and mycobacterial lipopeptides including didehydroxymycobactin (DDM) **131** (Figure 3.1.). CD1b is able to bind lipids with very long lipid tails such as mycolic acids **132** (Figure 3.1.) because the molecule has two extra pockets which provide the necessary space to accommodate these longer lipids.CD1c binds and presents polyketides like mannosyl-1β-phosphomycoketide **133** which contain branched lipid tails.

CD1e is different from the other members of the CD1 family. It is not involved in surface antigen presentation. Instead, it is converted into a soluble lysosomal form and found in late endosomes. It is still immunologically relevant and is involved in intracellular lipid transport and antigen processing. It is also involved in the conversion of PIM_6 to PIM_2 by α-mannosidase.

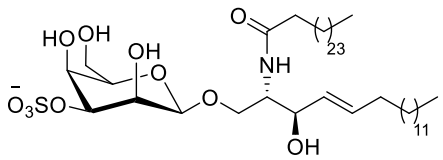

Sulfatide **130**

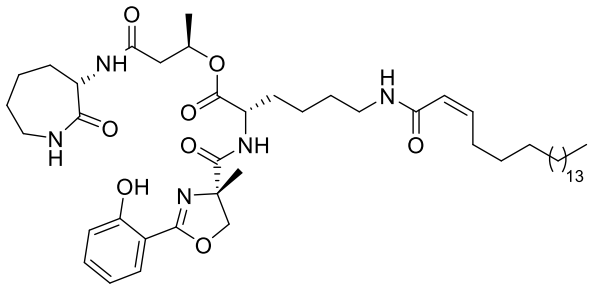

Dideoxymycobacin (DDM) **131**

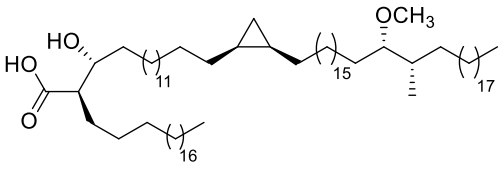

mycolic acid **132**

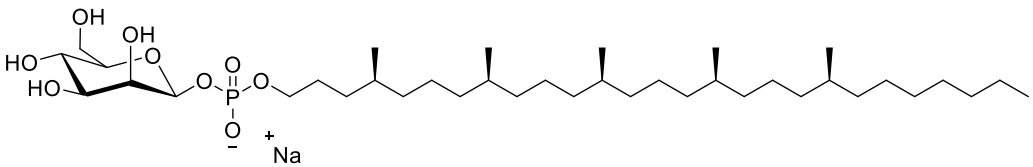

mannosyl phosphomycoketide **133**

Figure 3.1. Examples of lipid antigens presented by CD1 molecules

CD1d is recognised exclusively by the semi-invariant TCR of *i*NKT cells. It is assembled in the endoplasmic reticulum, where it is loaded with an endogenous lipid and binds to chaperones including calreticulin, calnexin, ERp57 and β_2m, which facilitates its transport first through the Golgi apparatus and then to the plasma membrane *via* the secretory pathway (Figure 3.2, a–b). Nascent CD1d molecules on the surface are then internalised *via* a clathrin-coated pit into the early or sorting endosome, with the help of adapter protein (AP) 2 (Figure 3.2, c). AP3 allows murine CD1d to traffic from early endosomes to late endosomes before being re-exported to the cell membrane (Figure 3.2, e). Human CD1d cannot interact with AP3 so gets re-exported to the cell membrane after only being in the early endosome. The trafficking into endosomes is important in allowing CD1d to encounter and bind to lipids for subsequent presentation to T-cells.[73]

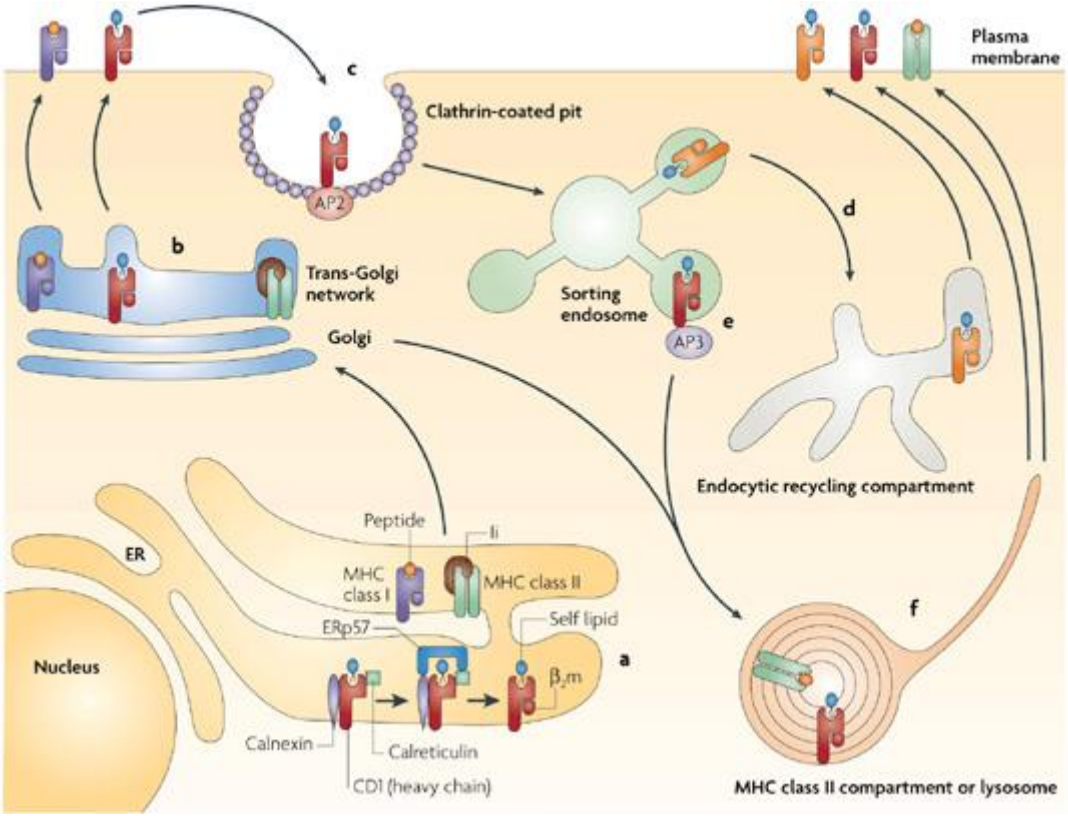

Figure 3.2. Intracellular trafficking of CD1d. Figure adapted from ref.[73] Permission to reproduce figure was obtained through RightsLink® - licence number 4106400518435.

3.2. *i*NKT cells

As previously mentioned (paragraph 1.4.3.) NKT cells are so named because of their co-expression of an αβ TCR along with NK markers, which are normally found on natural killer cells. The most studied of these are Type 1 or invariant (*i*) NKT cells, which are CD1d-restricted in that their activity is dependent on the presentation of a glycolipid-bound CD1d molecule to the invariant TCR.

Like conventional T cells, the development of *i*NKT cells begins in the thymus. The TCR is formed on a precursor thymocyte at the double positive (DP) stage. Positive selection of the *i*TCR occurs through the recognition of CD1d-expressing DP thymocytes (Figure 3.3). The endogenous glycolipid bound to the CD1d in the thymus is still unknown. Isoglobotrihexosyl ceramide (iGb3) has been suggested as the self ligand but this view has challenged.[74] More recent research has shown that both synthetic and purified sources of mammalian β-glycolipids contain a small percentage of the α-anomer (0.5–1%).[3] While this has not been tested regarding positive selection within the thymus, even a low abundance of the α-anomer would likely be sufficient to bind and activate the invariant TCR.[75] Following positive selection of immature NK 1.1$^-$ CD4$^+$CD8$^+$ NKT cells, downregulation of the CD8 receptor leaves CD4$^+$ cells. These NK1.1$^-$ cells are then transported to the periphery of the spleen or liver where they mature to NK1.1$^+$ cells.

[3] While it had previously been thought that mammals are unable to synthesise α-anomeric sugars

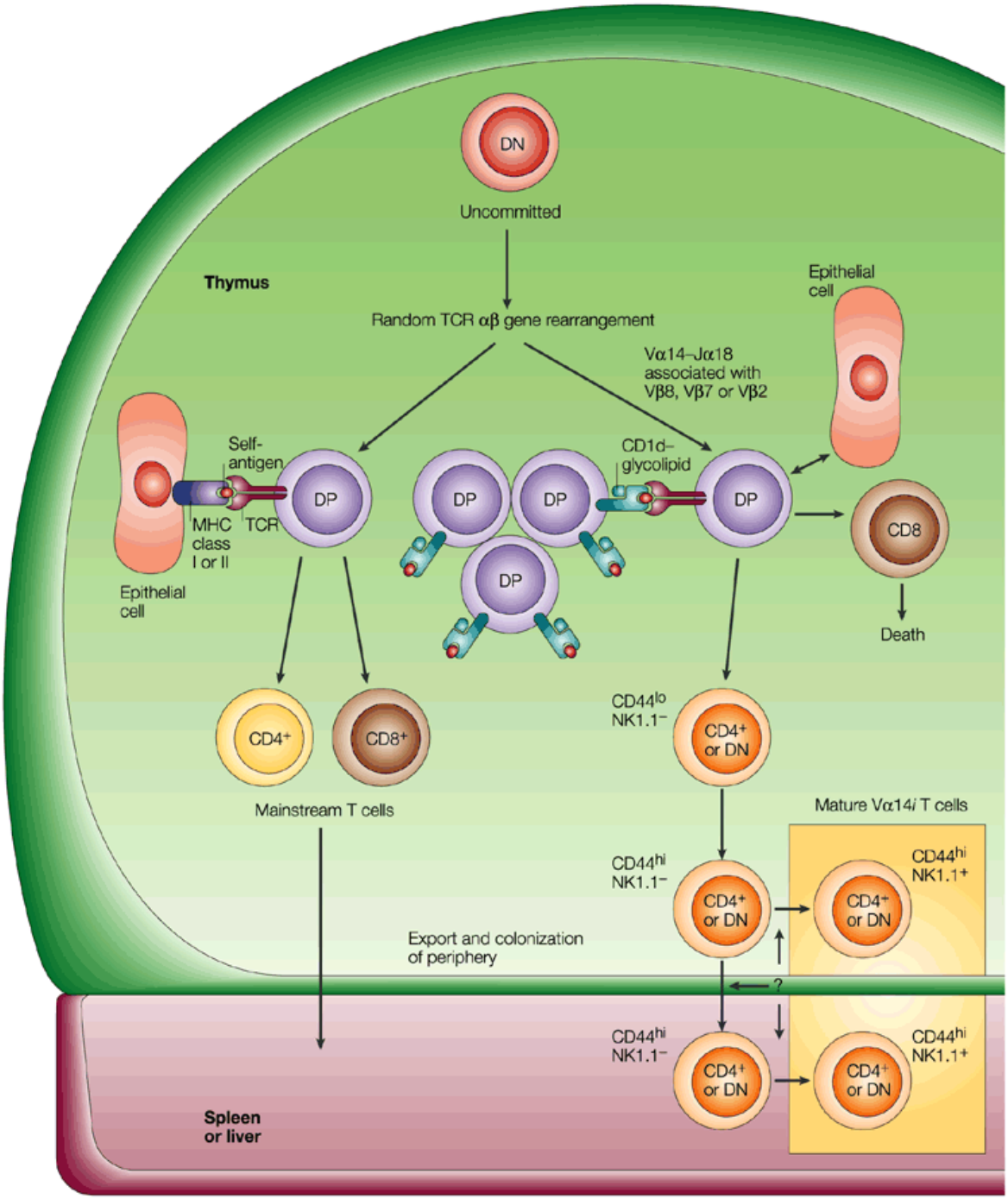

Figure 3.3 Development of Vα14i T cells in the thymus. TCR with random αβ rearrangement is first expressed by an uncommitted precursor thymocyte at the DP stage. CD1d-expressing DP thymocytes then positively select DP cells with a CD1d-specific Vα14i α-chain (Vα14–Jα18). After maturing into DN and $CD4^+$ T cells they are exported to peripheral organs where a hypothetical second signal is required for the expression of mature iNKT cells. Positive

selection of T cells with TCRs that are specific for MHC–peptide complexes leads to maturation of mainstream CD4+ and CD8+ T cells. Figure adapted from ref.[76] Permission to reproduce figure was obtained through RightsLink® - licence number 4174390432812.

3.3. Cytokines

Upon activation *i*NKT cells have the ability to induce the expression of various cytokines, which can in turn activate other cells such as NK cells, conventional T cells and B cells. Cytokines are cell-signalling protein molecules that are secreted by numerous cells. These messenger molecules allow cells to communicate with each other and are responsible for most of the biological effects in the immune system, such as cell-mediated immunity and allergicresponses. Although there are many different cytokines present in the body, they can be divided into two main groups based on their function: those that are pro-inflammatory and those that are essentially anti-inflammatory but promote allergic responses.

T lymphocytes are the major source of cytokines. Those T lymphocytes that express the cell-surface molecule CD4 are also called mature helper T cells, and these are regarded as being the most prolific cytokine producers. CD4+ T cells can give two responses, termed T_H1 and T_H2 (T helper) depending on the cytokine profile they induce. T_H1-type cytokines afford a pro-inflammatory response, responsible for attacking intracellular foreign pathogens and also for exacerbating autoimmune responses. Interferon gamma (IFN-γ) is the main T_H1 cytokine. The T_H2 response is needed to oppose the T_H1 response as excessive pro-inflammatory responses may lead to tissue damage.[77] T_H2-type cytokines include interleukins (IL) 4, 5, and 13, which are associated with the promotion of IgE (a type of antibody) and also interleukin-10, which has more of an anti-inflammatory response.[9] *i*NKT cells have been shown to be able to induce both T_H1 and T_H2 cytokines following activation. As both processes lead to separate

outcomes the potential to use *i*NKT cells to induce a biased response make them a great target for therapeutic applications

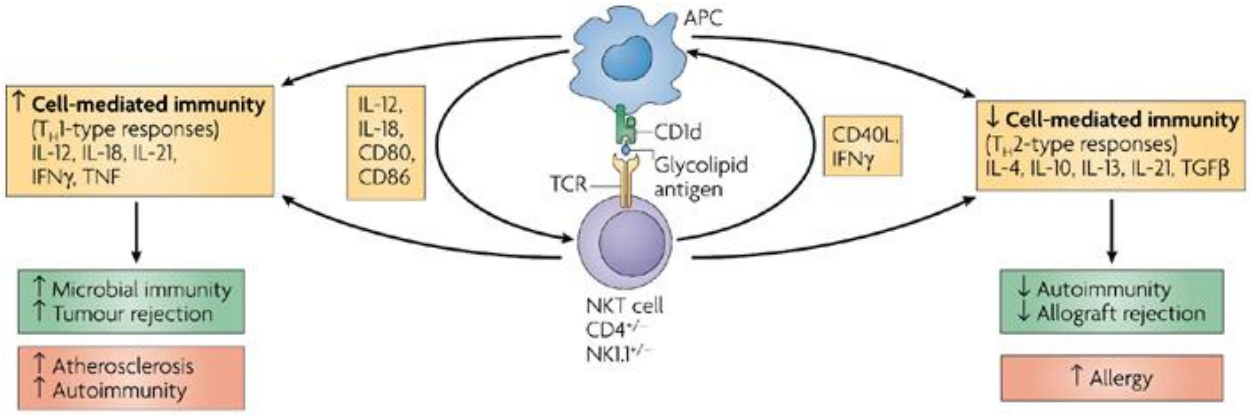

Figure 3.4. Cytokines produced by T_H1 and T_H2 responses along with the overall effect. Figure adapted from ref.[78] Permission to reproduce figure was obtained through RightsLink® - licence number 4106420478310.

3.4. α-Galactosyl Ceramide (α-GalCer)

Of the glycolipids that bind to CD1d and activate *i*NKT cells, the most studied is α-Galactosyl Ceramide (α-GalCer) **10**. In 1993, novel glycosphingolipids were isolated by Natori *et al.* from the marine sponge *Agelas mauritianus* in the Okinawa Sea.[79] Four agelasphins (AGLs) were isolated from the sponge all possessing an α-galactosylceramide structure. β-

Galactosylceramides were already known these but α-galactosylceramides were novel and the first cerebrosides to have an α-galactosyl linkage (Figure 3.5).

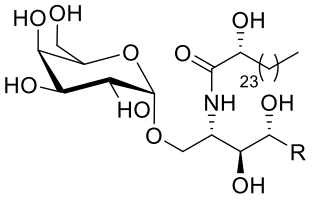

	R=
134, agelasphin-7a	$-(CH_2)_{11}CH_3$
135, agelasphin-9a	$-(CH_2)_{12}CH_3$
136, agelasphin-9b	$-(CH_2)_{11}CH(CH_3)_2$
137, agelasphin-11	$-(CH_2)CH(CH_3)C_2H_5$

Figure 3.5 Structure of four agelaspins isolated from *Agelas mauritianus*

The AGLs showed potent *in vivo* antitumor activity against a murine B16 melanoma cell line. Using AGL-9a and AGL-9b (shown to be most active) as the starting point, a range of synthetic AGLs were developed for further experimental studies. Morita *et al.* showed that the hydroxyl group alpha to the amide carbonyl was not necessary for activity nor was the terminally branched methyl group; the structurally simplified analogue, α-GalCer also known as KRN7000, displayed highly potent antitumor activity.[20]

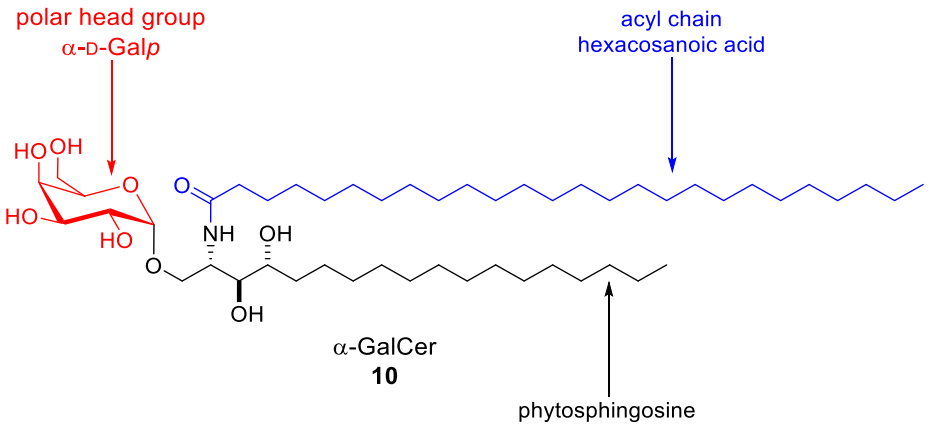

Figure 3.6 Structure of α-GalCer

α-GalCer is comprised of a D-galactopyranose sugar alpha linked to a phytosphingosine backbone which is *N*-acylated with hexacosanoic acid (Figure 3.6). It binds strongly to CD1d- with a kinetic dissociation constant (K_d) of 1.29 ± 0.08 μM.

While α-GalCer has been shown to have therapeutic effects against autoimmune diseases including type I diabetes, experimental allergic encephalomyelitis, arthritis and systemic lupus erythematosus[80] and been shown to be effective in antitumour therapy,[81, 82] it has certain properties that have prevented its application as a therapeutic agent:

1. It over-stimulates *i*NKT cells resulting in cytokine storm, DC lysis and iNKT cell anergy.
2. It possesses glycosidic and amide bonds, which can potentially be hydrolysed *in vivo* by glycosidases and amidases, respectively.
3. Activation of iNKT cells leads to the production of both T_H1 and T_H2 cytokines, which can lead to a mixed immune response, which limits its therapeutic application.

Anergy is a tolerance mechanism in which a lymphocyte is intrinsically functionally inactivated following an encounter with an antigen, meaning that after stimulation by the antigen the cell is unable to be activated upon further stimulus.

3.5. Crystal Structure CD1d Protein–GalCer

. The Crystal structure of the complex of α-GalCer glycolipid and human (h)CD1d complex has been determined and shows the binding interactions between the molecules and the structure of the α-GalCer glycolipid (Figure 3.7.–3.9.)[83]. Structures are also available for mouse and other organisms are also available in PDB.[84]

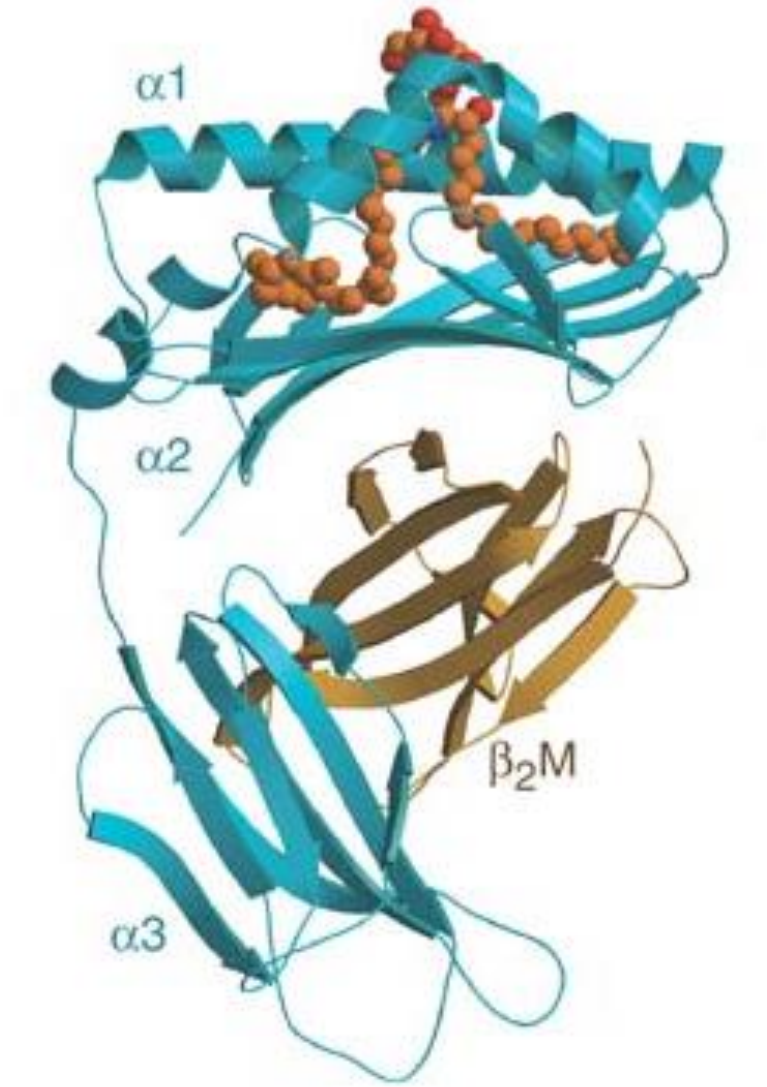

Figure 3.7 Ribbon representation of the CD1d–α-GalCer complex. PDB ID:1ZT4. Figure adapted from ref.[83] Permission to reproduce figure was obtained through RightsLink® - licence number 4106420868745.

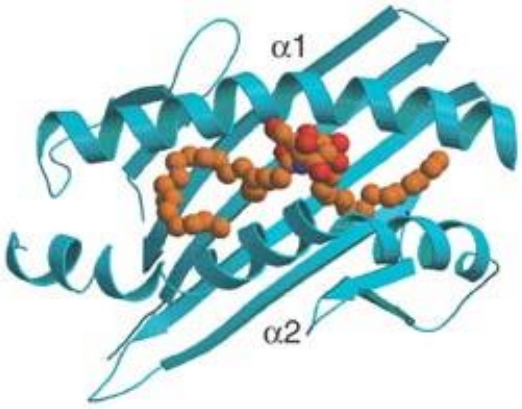

Figure 3.8. Ribbon representation of the CD1d–α-GalCer complex showing the binding groove from above. Figure adapted from ref.[83] Permission to reproduce figure was obtained through RightsLink® - licence number 4106420868745.

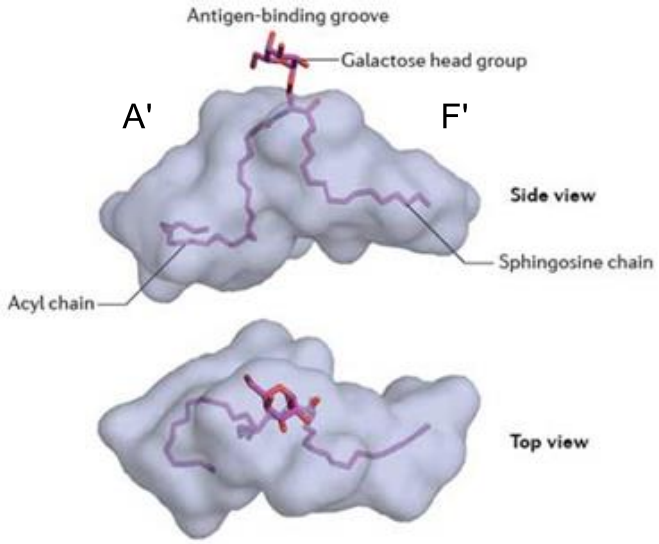

Figure 3.9. Space-filling representation of CD1d–α-GalCer complex. Figure adapted from ref.[85] Permission to reproduce figure was obtained through RightsLink® - licence number 4111590202719.

CD1d is a heterodimeric protein consisting of a heavy chain made up of three domains, α1, α2 and α3. The antigen binding groove is made up of the α1 and α2 domains and consists of two anti-parallel α-helices sitting on top of a β-pleated sheet. This groove superficially resembles the binding pocket of MHC class I molecules but is deeper and larger in volume. It is also narrower and divides into two channels, generating the so-called A' and F' pockets. MHC molecules characteristically have a number of small pockets in the wall of the binding groove to accommodate peptide side-chains. In CD1 molecules these pockets have fused together to form the two pockets A' and F', which are lined with amino acids such as phenylalanine and tryptophan imparting the hydrophobic nature of these binding sites.

The acyl chain (26 carbons) of α-GalCer fits in the A' pocket while the sphingosine chain (18 carbons) fits in the less voluminous F' pocket. Both hydrocarbon chains fully occupy these two pockets and so are indicative of the maximum chain length which can be tolerated in the antigen-binding groove of human CD1d.[83] This finding explains why CD1d exhibits much higher binding affinity than glycolipids possessing truncated chains. Figure 3.9. shows how the glycolipid is anchored in the CD1d binding groove *via* hydrophobic interactions between the lipid chains and the hydrophobic amino acids lining the binding pockets, leaving the sugar head-group exposed on the surface of the protein for recognition by the iNKT cell TCR. The hydrogen bond interactions between Asp151 and the 2-*O* hydroxy of the sugar as well as Thr154 and the anomeric oxygen are vitally important as they not only stabilise the glycolipid but also orientate the polar head group for effective presentation to the TCR.

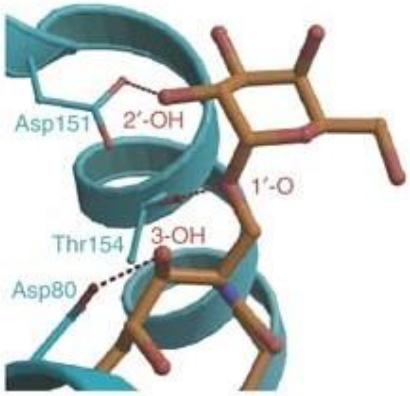

Figure 3.10. Ribbon representation showing key H-bonding interactions between α-GalCer and the CD1d molecule. Figure adapted from ref.[83] Permission to reproduce figure was obtained through RightsLink® - licence number 4106420868745.

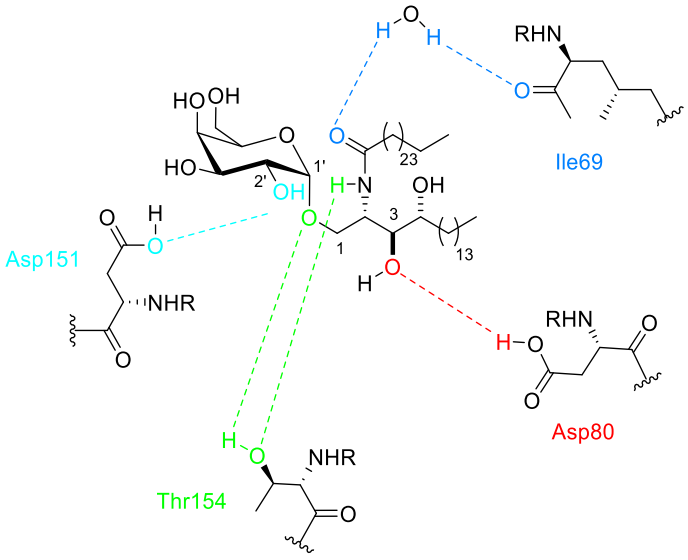

Figure 3.11. Key Hydrogen bonding interactions between hCD1d and α-GalCer.

Position on α–GalCer	Human CD1d	Mouse CD1d
1'-O	Thr154 on α2-helix of CD1d	Thr156 on α2-helix of CD1d
2'-OH	Asp151 on α2-helix of CD1d	Asp153 on α2-helix of CD1d
3-OH	Asp80 on α2-helix of CD1d	Asp80 on α2-helix of CD1d
NH	Thr154 on α2-helix of CD1d	Thr156 on α2-helix of CD1d
C=O	Ile69* on α1-helix of CD1d	Met69* on α1-helix of CD1d

Table 3.1 Key hydrogen bonds between α-GalCer and the CD1d molecule.

*This hydrogen bond involves a bridging H_2O molecule.

Table 3.1. summarises the key hydrogen bonding interactions between α-GalCer and the CD1d molecule. These interactions between the protein and the polar group on the α-GalCer molecule ensure the sugar head group is oriented parallel to the plane of the α-helices. [86-87] Thus positioning is vital for effective recognition by the iNKT cell TCR.

3.6. CD1d–Glycolipid–iNKT-cell TCR Ternary complex

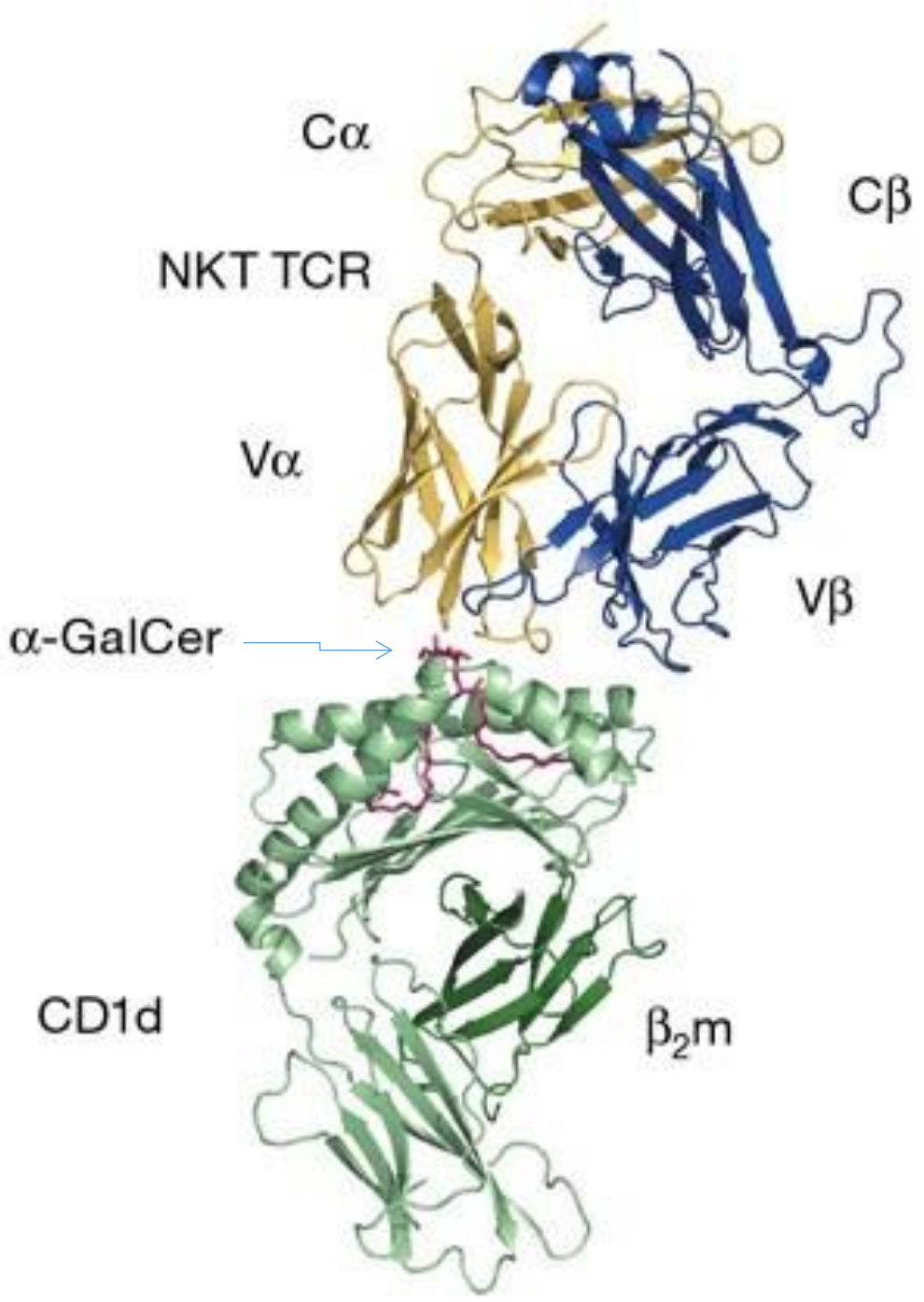

Figure 3.12 Shows the TCR–α-GalCer–CD1d complex. Figure adapted from ref.[88] Permission to reproduce figure was obtained through RightsLink® - licence number 4173120438296.

The *i*NKT-cell TCR comprises an invariant Vα24-Jα18 α-chain and a restricted Vβ11-containing β-chain. A co-crystal structure of the human NKT-cell TCR–α-GalCer–CD1d complex has also been described at 3.2 Å resolution. It shows that the TCR binds almost parallel to the antigen binding site, positioned above the F′ pocket and at the extreme enB of AB1d. The crystal structure also shows that the α-chain contributes more interactions with CD1d–α-GalCer than does the β-chain (approximately 82 compared to 32 respectively). The total buried surface area (BSA) of the TCR–α-GalCer–CD1d interface is around 910 $Å^2$ with the α-chain again contributing more to the BSA than does the β-chain (65.5% vs 34.5%, respectively).

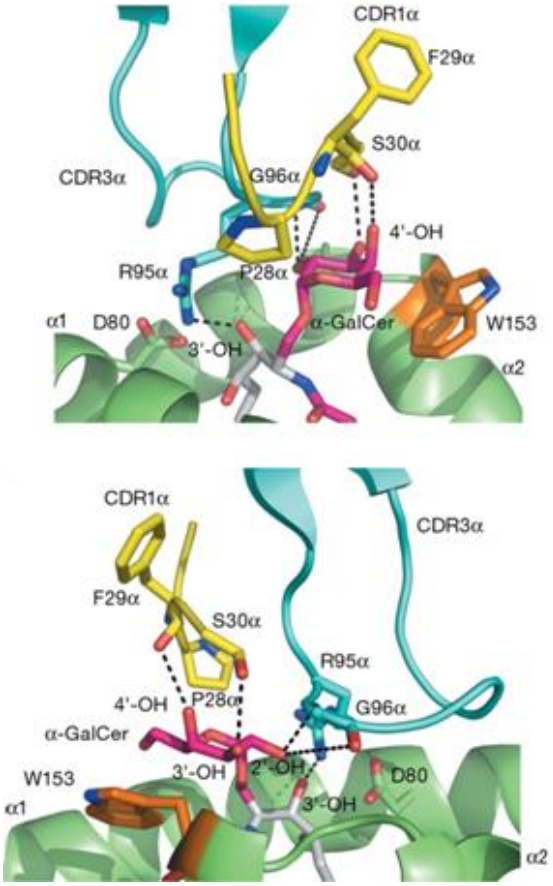

Figure 3.13 Hydrogen bonding interactions between the sugar head-group and amino-acid residues in the TCR. Figure adapted from ref.[88] Permission to reproduce figure was obtained through RightsLink® - licence number 4173120438296.

The majority of the Van der Waals, electrostatic and hydrogen bonding interactions are between the CD1d molecule and the TCR. For the Vβ-chain, the major contact is between the CDR2β loop to the α1-helix of CD1d. Contacts are found between the CDR3α loop of the Vα-chain and the α1- and α2-helix of CD1d. However, a glycolipid is required for activity meaning the interactions between the polar head group and the TCR are vital. The galactose ring is positioned underneath the CDR1α loop, which only interacts with the ligand and next to the CDR3α loop. Figure 3.13 shows the numerous hydrogen bonds that stabilise the TCR-α–GalCer interaction: the 3-OH of the sphingosine chain hydrogen bonds to the side-chain of Arg95α. The sugar 2′- and 4′-OH groups hydrogen bond with the main chain of Gly96α and Phe29α, respectively, and the 3'-OH forms a hydrogen bond to the side-chain hydroxyl residue of Ser30α. (Table 2)

These interactions are important for recognition of the TCR and are also stereospecific as α-ManCer does not activate iNKT cells. Mannose differs from galactose in the orientation of the OHs groups at C-2′ and C-4′, which result in the loss of two key hydrogen-bond interactions and no activation of the TCR even though α-ManCer does still bind to CD1d.

The α-linkage is also important for TCR recognition and activation; while β-GalCer is able to activate iNKT cells, it is a much less potent agonist than its α-anomer. It is predicted that β-GalCer adopts a more perpendicular orientation due to the altered position of the head group. Leading to disruption of contacts with the TCR CDR1α chain.

3.7. Analogues of α-GalCer

As *i*NKT cells can induce both T_H1 and T_H2 cytokines the potential for use in therapeutic application are great if a biased response can be induced. This highlights the importance of the synthesis glycolipid targets that activate *i*NKT cells. Production of the key T_H2 cytokine, IL-4 is rapid after initial *i*NKT-cell stimulation, typically showing its highest concentration when assayed after 2 hours. Production of key T_H1 cytokine, IFN-γ requires prolonged stimulation and is typically assayed 18 to 24 h after administration of the agonists.[89] While there are other factors that affect biaising, these observations led to the proposal that analogues of α-GalCer that dissociate from the ternary complex after a short period of time may elicit a T_H2-biased (more IL-4, less IFN-γ) response. Conversely, glycolipids and analogues that result in a more stable longer lasting ternary complex might be expected to shift the bias towards a T_H1 response.

3.7.1. Analogues with modifications to the sphingosine chain

Modifications that can be made to the sphingosine chain include altering the length, using alternative stereoisomers and functionalising the chain. OCH **138**, first synthesised by Yamamura *et al*., is a truncated analogue of α-GalCer. The phytosphingosine chain is shortened to nine carbons instead of the eighteen found in α-GalCer.[90] The acyl chain is also truncated by two carbons compared with that in α-GalCer. OCH has been shown to be a less potent agonist than α-GalCer but elicits a T_H2-biasing immune response by producing more IL-4 and less IFN-γ *in vitro*, compared to α-GalCer, leading to its potential application in treating autoimmune diseases. The T_H2-bias is believed to be due to the fact that OCH–CD1d complex is less stable as the alkyl chain does not fill the binding groove resulting in faster dissociation.

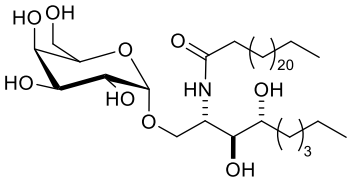

138

It has been shown independently by Iijima *et al*.[91] and Brossay *et al*.[92] that when the 3-OH and the 4-OH of the phytosphingosine unit are removed, the molecule loses the ability to proliferate spleen cells in mice. These observations have been rationalised by a loss of key H-bonding interactions between the 3-OH to the CD1d Asp80 as well as to Arg 95 of the CDR3α-loop of the TCR, leading to a differently bound confirmation which is no longer recognised by the TCR. However, if only the 4-OH is removed, the analogue **139** still initiates a strong biological response in mice. 4-Deoxy-4, 4-difluoro- α-GalCer **140,** was synthesised by Leung *et al*. to investigate the effect of removing the hydrogen-bond donating capacity and minimising the ability to accept a hydrogen bond.[93] Following only minimal loss of activity, it was argued that the Arg 95α interaction is not as vital as that with Asp 80.

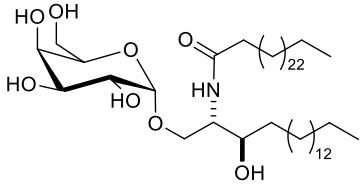

139

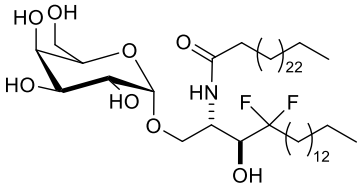

140

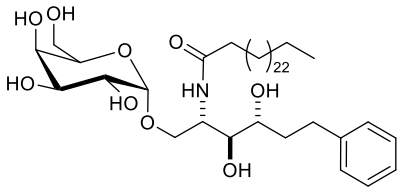

141

Analogues which contain an aromatic group at the end of a truncated phytosphingosine chain such as **141** have also been shown to provide be a potent *i*NKT cell activator that induces a more T_H1-biased cytokine response. It is suggested that the ligand binds to CD1d with a higher binding affinity due to the extra aromatic interaction caused by the aromatic group of the antigen and aromatic residues of the CD1d protein which prolongs the lifetime of bound complex leading to increased levels of IFN-γ.

3.7.2. Modifications to the Acyl chain

α-GalCer analogues containing a truncated acyl chain such as C10:0 **142** display a T_H2 biasing cytokine response whereas appending an aromatic group to the end of the acyl chains has provided analogue **143**, which has similarly been shown to induce a T_H1 cytokine bias, believed to be due to the increased stability of the CD1d– α–GalCer complex and enhancing IFN-γ secretion, which requires longer stimulation time to be released.[89] This increased stability of the glycolipid–CD1d complex is due to π–π stacking with aromatic residues lining the binding pockets.[94]

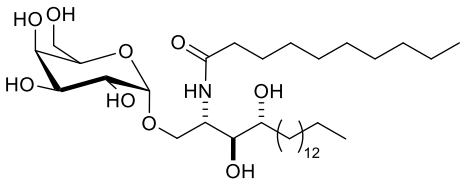

142

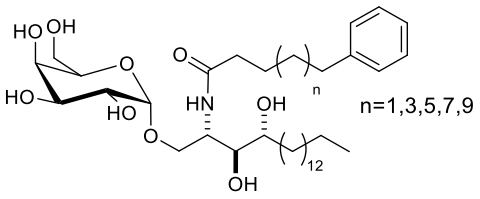

143

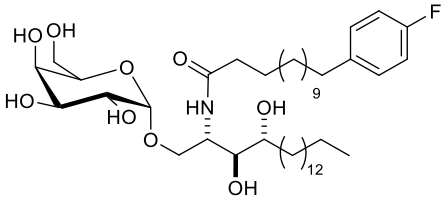

144

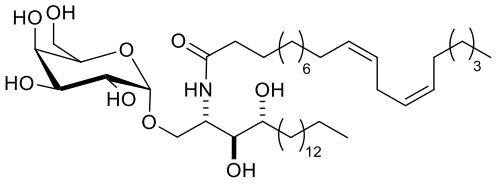

145

Another acyl chain analogue is C20:2 **145** which contains an unsaturated acyl chain with two *cis* double bonds at C_{11} and C_{14}, this compound skews the response towards T_H2, with a diminished IFN-γ production.[95] However, in contrary to α-GalCer, it does not require endosomal localisation of CD1d for efficient loading and presentation.[96]

7DW8-5 **144**, developed by Wu *et al*.[97] which contains a terminal *para*-fluoro phenyl group and has also been shown to be a highly potent *i*NKT cell activator. It has also been shown to induce a higher level of IFN-γ compared to the unfluorinated analogue.[98] 7DW8-5 **144** shows higher affinity towards CD1d which is due to the fluorine forming of a neutral hydrogen bond within the binding pocket.[99]

3.7.3. Modifications to the amide bond

The amide N-H in α-GalCer is perfectly aligned to form a hydrogen bond with the OH group of Thr154 as shown in the crystal structure of the hCD1d–αGalCer complex.[100] It was postulated that the gem-difluoro analogue **146** would increase the H-bond capability by increasing the acidity of the N-H. A stronger interaction between the amide N-H and Thr154 should stabilise the complex and lead to a T_H1 bias. However, this compound proved to be

less potent than α-GalCer, inducing less IFN-γ. In light of these experimental results, it was suggested that the H-bonding involving the amide N–H formed a network with the 2'OH of the sugar and Thr154 and Asp151 of CD1d which contributed to the correct orientation of the sugar head.[101, 102] It was postulated that introducing the fluorine substitution changed this H-bonding network which negatively impacted on the polar group stabilisation, consistent with the lower affinity with the TCR and resulting T_H2 cytokine bias. Replacing of the amide with sulfonamides, both aliphatic **147** and aromatic **148**[103] and a triazole **149**[104] have been shown to impart a T_H2 cytokine bias.

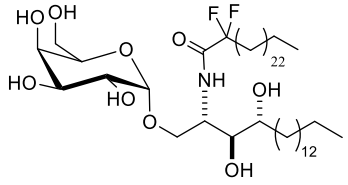

146

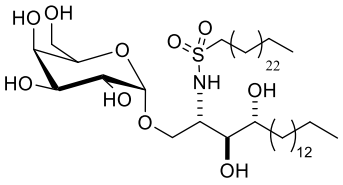

147

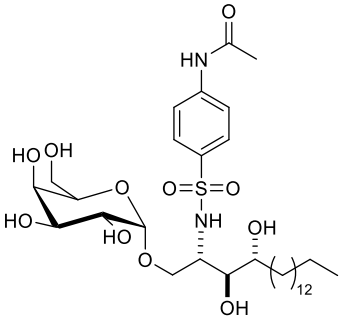

148

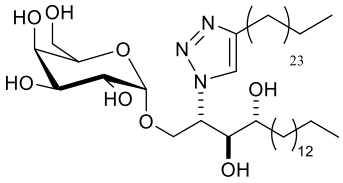

149

More recently, substitutions with thioamides **151** and **152**[87] and urea **153**[105] have been developed and shown to elicit a T_H1 response. Thioamides have increased polarity and N–H acidity *versus* amides making them better hydrogen bond donors, while the sulfur atom functions as a weaker hydrogen bond acceptor. It was postulated that the thioamide would form a strong hydrogen bond with Thr156. It was subsequently shown however that while it induced a T_H1 biased response, TCR binding affinity was actually weaker than the parent amide. This has shown that the correlation between TCR binding affinity for a CD1d−glycolipid complex and the measured cytokine profile is not the sole factor involved in determining a cytokine profile.[106, 107] Researchers have attributed differences in cytokine response profiles

to other factors, that have been attributed to altered cytokine profiles include different pharmacokinetics properties and ability to transactivate NK cells downstream of iNKT cell activation. For the latter however, thioamide **152** was shown to not transactivate NK cells, with the further studies needed to identify the factors involved in thioamide binding and activation.[87]

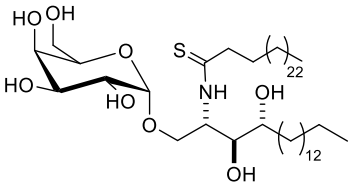

151

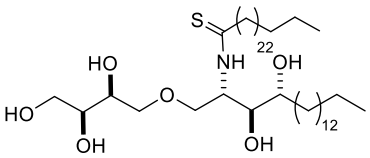

152

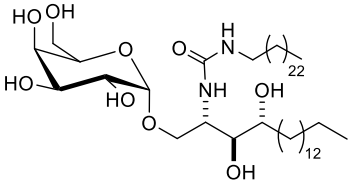

153

3.7.4. Modifications to the glycosidic bond

The glycosidic bond in α-GalCer is susceptible to hydrolysis *in vivo* by glycosidases. α-*C*–GalCer **154**, an analogue where the glycosidic oxygen is substituted with a methylene group, gives a T_H1 cytokine bias. It has been proposed that this increase in concentration of IFN-γ compared to α-GalCer is possibly due to prolonged stimulation times due to the increased metabolic stability of the *C*-glycosidic linkage.[108]

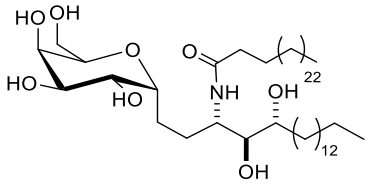

154

3.7.5. Modifications to the Sugar head group

As the sugar head group provides the most interactions with the TCR, modifications to this part of the glycolipid have been careful not to disrupt the H-bonding interactions formed by the hydroxyls at the 2, 3 and 4 positions of the ring. Based on crystallographic information of the CD1d–α-GalCer–TCR complex, (Figure 3.13. p 92) the 6'-OH is the only hydroxyl group, along with the ring oxygen, that is not involved in H-bonding to the TCR. Tashiro *et al.*[109] showed that a methoxy group at the 6 position **155** gives a T_H1 response. This has been postulated to be due to the fact that the 6 position can no longer act as a H-bond donor, increasing electron density of the 4'-*O* allowing it to interact with the TCR to form a more stable complex.

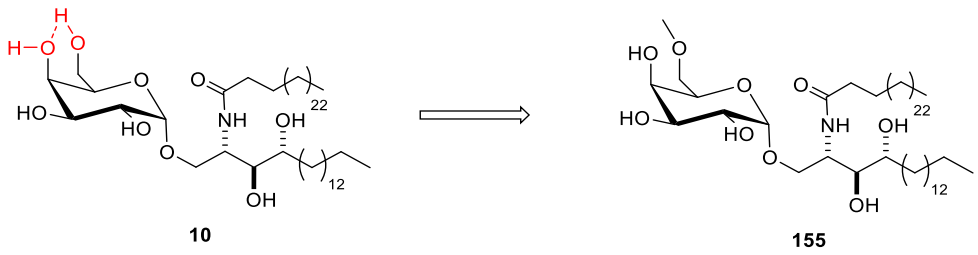

10 **155**

Nitrogen–substituted compounds at the 6 position with aryl amide **156** and urea **157** moieties have also been shown to give a T_H1 biased response. π–π Stacking of the aromatic ring with the indole of Trp153 is postulated to contribute to the stability of these compounds in the CD1d–ligand–TCR complex.[110]

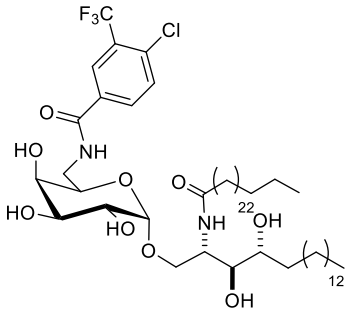

156

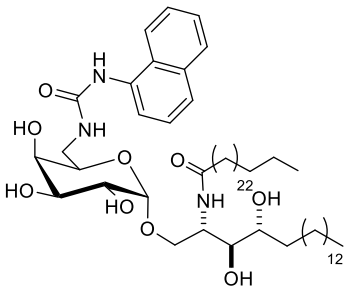

157

3.7.6. Non-glycosidic α–GalCer analogues

As crystallographic information of the TCR–α-GalCer–CD1d complex has shown, the ring oxygen or the 6′-OH is not involved in H-bonding to the TCR nor CD1d while the glycosidic oxygen is involved in H-bonding (to Thr154 on the α2 helix of hCD1d) it was envisioned that excising both groups would retain key interactions with the TCR and CD1d molecules but at the same time also exhibit increased metabolic stability. Threitol ceramide (ThrCer) **14** contains an ether bond and is an acyclic analogue of α-GalCer as it retains the key alcohols in the correct relative and absolute configuration that are required for the formation of the CD1d–Glycolipid–TCR complex. **14** should be similarly resistant to hydrolysis by α-galactosidases (as the molecule now contains an ether bond) as α-*C*-GalCer **154**. Due to the increase in entropic loss of the acyclic chain when bound in the ternary complex compared to α–GalCer it was postulated that this analogue would not overstimulate iNKT cells, which leads to cell anergy, but also retain activity. This analogue has also been developed further by substituting a urea, thioamide and carbamate at the amide position.[87] These analogues were shown to have an IFN-γ bias although at a lower activity to that of α-GalCer, although ThrCer was also seen to be less potent.[111]

Due to the conformational flexibility of the ThrCer acyclic analogue further work within the group was done to develop carbocycles that contained the L-threitol configuration within six-,

seven- and eight- membered rings **158**. The six and seven ring structures showed similar cytokine response profiles as α-GalCer, thus incorporating ThrCer into a ring recovers activity.[112, 113]

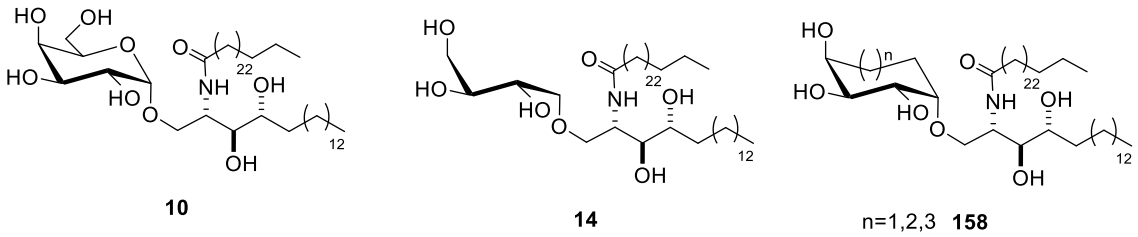

3.8. Development of ThrCer-6 analogues

The lead compound of our target analogues was ThrCer-6 **16** which was previously developed within the group. Scheme 3.1. shows the development of ThrCer-6 from α-GalCer progressing *via* ThrCer. Starting with α-GalCer, removal of the ring oxygen, C-5 and C-6(OH) yields a polar head group based on tetrose *L*-threitol, which retains the same absolute and relative configuration at C-2 and C-3 as D-galactose. Previous studies had shown that ThrCer does not show any cytokine bias and is less biologically active than α-GalCer but was still of potential therapeutic interest as it was shown to overcome the *i*NKT cell activation-induced anergy associated with α-GalCer.[114] It was postulated that constraining the threitol sugar unit into a carbocycle would recover activity whilst retaining some of the attractive features of ThrCer.To this end, the sugar was incorporated into a carbocycle by the addition of two carbon atoms to yield ThrCer-6.

In the case of α-GalCer the galactose residue adopts a $^4C_1$ chair conformation as a consequence of the anomeric effect and minimisation of unfavourable 1,3-diaxial interactions. As ThrCer-6 is not a sugar there is no anomeric stabilisation. Moreover, loss of the

hydroxymethyl group further reduces the 1,3-diaxial interactions in the pseudo "$^{1}C_{4}$" chair conformation.

It was therefore not obvious at the outset whether or not this molecule would adopt the pseudo "$^{4}C_{1}$" chair conformation required for effective TCR recognition and *i*NKT simulation. However, it was postulated that the two chair conformational isomers of ThrCer-6 would have similar energies. Providing the barrier to their interconversion was low, it was postulated that the low energy conformation was not important and binding to CD1d would ensure the required pseudo "$^{1}C_{4}$" conformation is adopted through an induced fit. Whilst these proposals have not been confirmed, ThrCer-6 exhibited greatly increased potency similar to and in some experiments, better than α-GalCer. Moreover, it also led to a T_H1 cytokine bias, similar to other carbocycles which restored biological activity and caused a T_H1 bias similar to other carbocycles previously synthesised.[113]

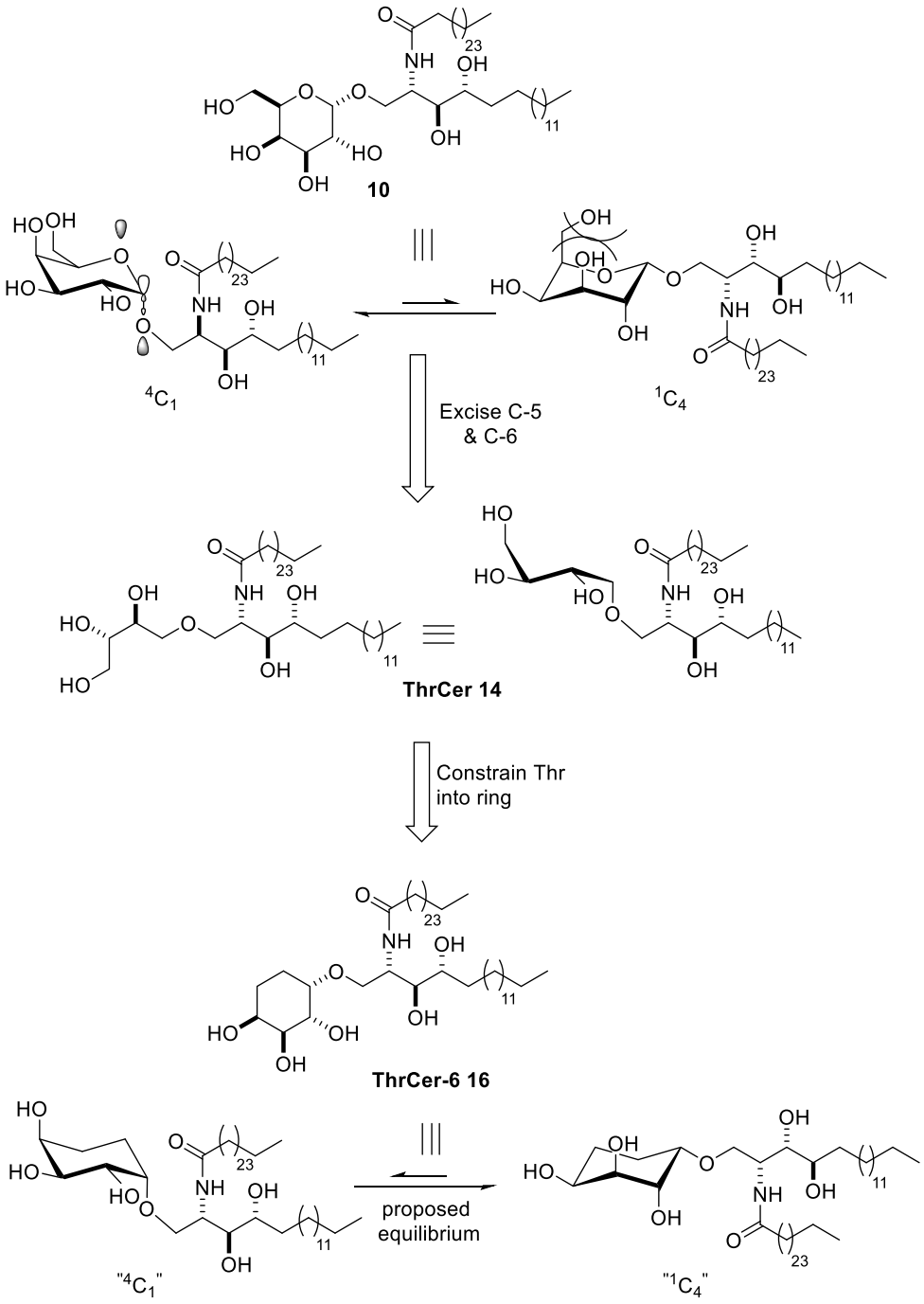

Scheme 3.1. ThrCer-6 with "$^4C_1$" chair confirmation retains correct configuration for binding

3.8.1. First Generation Synthesis of ThrCer-6

The first-generation synthesis of ThrCer-6 involved the use of protected sulfamidate **162** as the electrophilic coupling partner. Alcohol **160** (which could itself be synthesised from phytosphingosine in four steps) was reacted with thionyl chloride in the presence of imidazole and Et_3N in CH_2Cl_2 to form intermediate sulfamidite **161** which was further oxidised using ruthenium chloride and sodium periodate to sulfamidate **162** in 58% yield over the two steps (Scheme 3.2.).

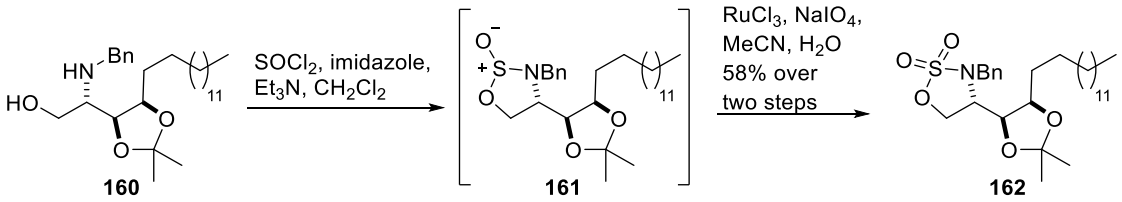

Scheme 3.2. First generation of electrophilic phytosphingosine coupling partner

Conduritol E based alcohol **163** was reacted with NaH in DMF at 0 °C followed by addition of sulfamidate **162** to yield the intermediate sodium salt **164**. This was subsequently hydrolysed using 20% H_2SO_4 in Et_2O to yield benzylamine **165** in 43% over two steps. Global deprotection under hydrogenation and acidic conditions followed by acylation with hexacosanoyl chloride in NaOAc (aq)/THF yielded ThrCer-6 **16** in 33% yield over the three steps.

The main problems associated with this route involved the protecting group on the nitrogen. Harsh conditions were required in the deprotection step when a benzyl group was used. Other groups on the nitrogen also proved problematic. When a boc protected sulfamidate was used using similar conditions to ring open the sulfamidate only loss of the Boc group was observed and a PMB group was similarly difficult to remove following ring-opening.

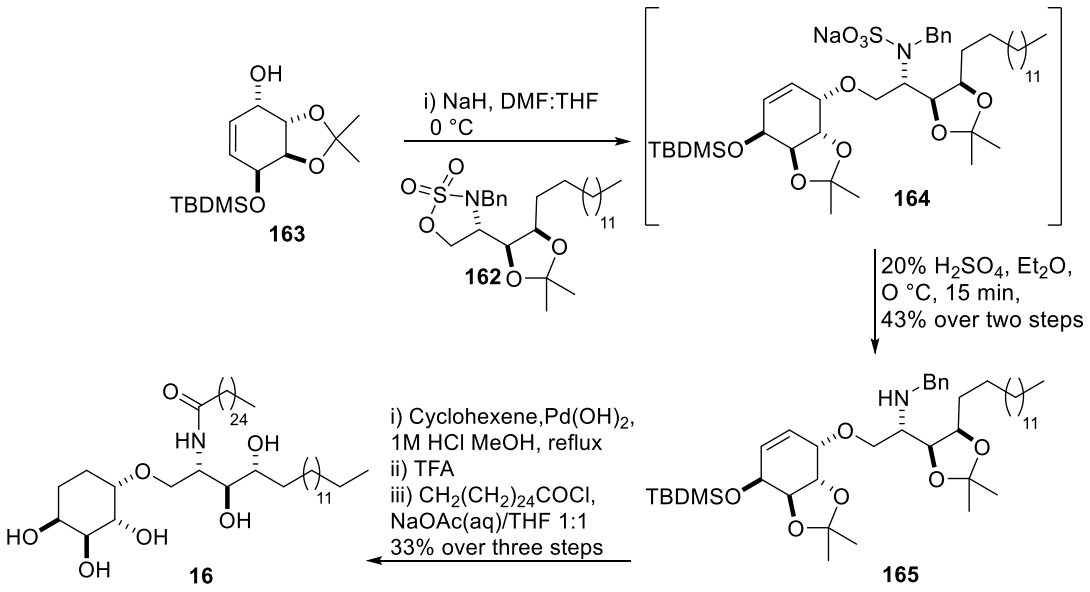

Scheme 3.3. First generation synthesis of ThrCer-6 **16**

3.8.2. Target ThrCer-6 analogues

As the first-generation synthesis of ThrCer-6 had previously involved a hydrogenolysis step to deprotect the benzylamine hydrogenation of the double bond was also effected. Compound **166** which retains the double bond was of interest as structurally the inclusion of an alkene into the carbocycle increases rigidity of the ring along with forcing all the hydroxyl groups into a different in space. Testing of this molecule could be important in further elucidating new binding potentials of the next generation of glycolipids to the TCR.

While the factors that lead to T_H1/T_H2 biases (in either direction) are not fully understood, certain structural features, for whatever reason have been shown to lead to particular responses as seen by the range of analogues discussed in the introduction. Further skewing of the T_H1/T_H2 cytokine bias of ThrCer-6 was hoped through the use of alternative acyl chains which are known to elicit a more biased response. Thioamide analogues of α-GalCer and ThrCer have previously been shown to elicit a more T_H1 response, which we hoped might translate to compound **167**.[87] An α-GalCer analogue possessing a truncated chain terminating

with a *para*-fluorobenzyl group has also shown a more T_H1 biased response; thus, compound **169** was of interest.[115] Finally compounds with a *Z*,*Z* eicosa-11,14-dienoic (C20:2) acyl chain have been shown to provide a skewed T_H2 cytokine bias, leading to compound **168** as another target.[96]

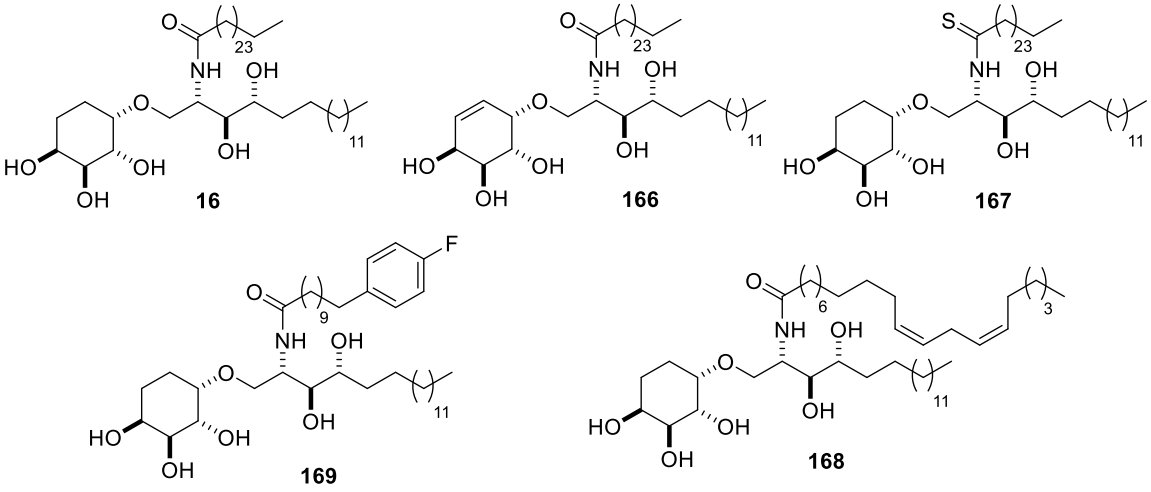

Figure 3.14. ThrCer-6 and four other target molecules

3.8.3. Retrosynthesis

The retrosynthetic analysis for targets **16**, **166**, **167**, **168** and **169** are summarised in Scheme 3.4. Cleavage of the amide bond yields amine **171** and acid **173**. Leaving the acylation to the final step is attractive as it allows late-stage incorporation of a range alternative acyl chains using a common advanced intermediate. Cleavage of amine **171** at the ether linkage separates the polar head group from the phytosphingosine-derived chain, yielding alcohol **174**, which is based on conduritol E, to act as the nucleophile and an electrophilic phytosphingosine coupling partner **175**, in this case an activated aziridine. Ring opening of protected conduritol E **174** yields diene **176** which itself can be synthesised from commercially available (2*R*, 3*R*)-dimethyl 2,3-*O*-isopropylidene tartrate **177**. The electrophilic

phytosphingosine coupling partner **175**, would be accessed from commercially available phytosphingosine **179** *via* standard functional group manipulations.

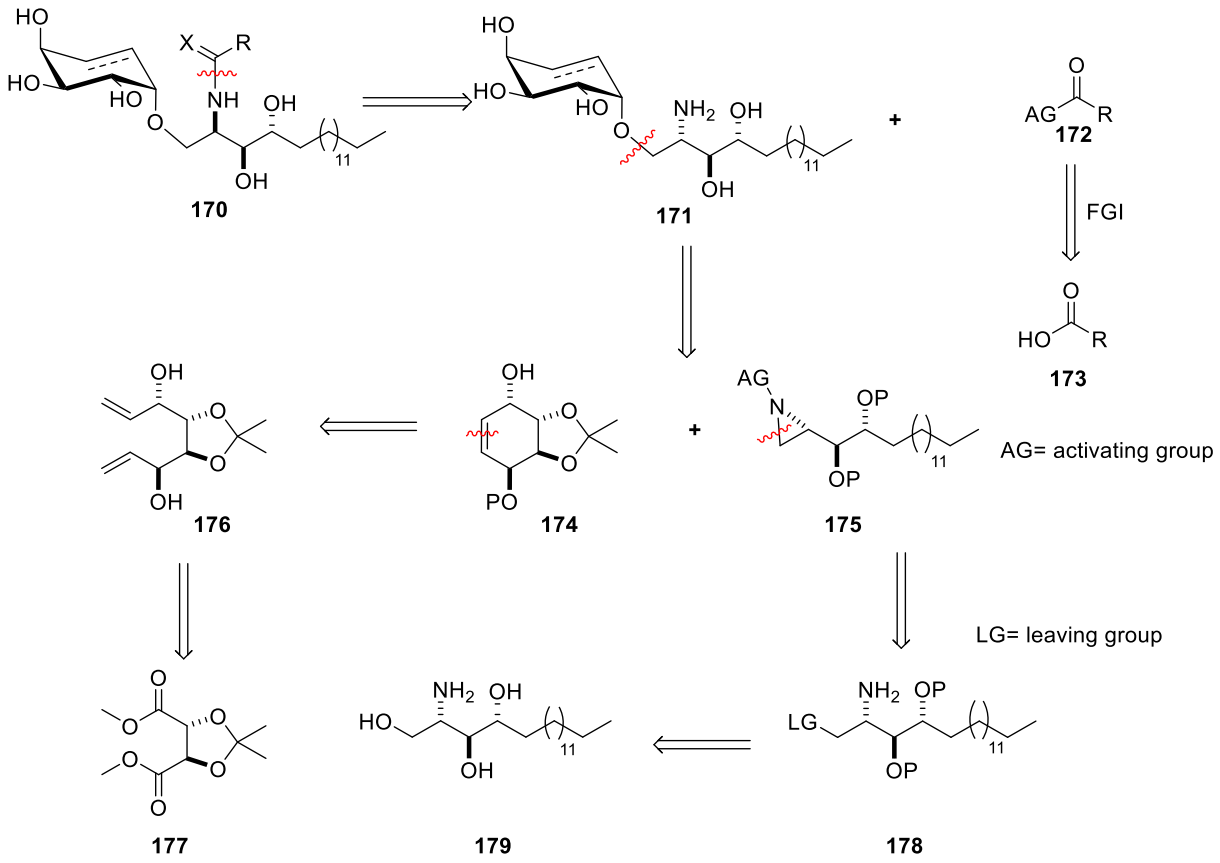

Scheme 3.4. Retrosynthetic analysis of ThrCer-6 analogues

3.8.4. Aziridine Synthesis

The first step in the synthesis of our target molecules involved the development of an electrophilic phytosphingosine coupling partner. It was postulated that an activated aziridine might prove more attractive. Whilst soft nucleophiles are more commonly used to ring-open aziridines, there is precedent for the use of oxygen nucleophiles.[116-120] Indeed Tsunoda *et al.*[121] successfully reacted tosyl aziridine **180** with the sodium alkoxide of **114** to provide glycoside **181** in 60% yield (Scheme 3.5.).

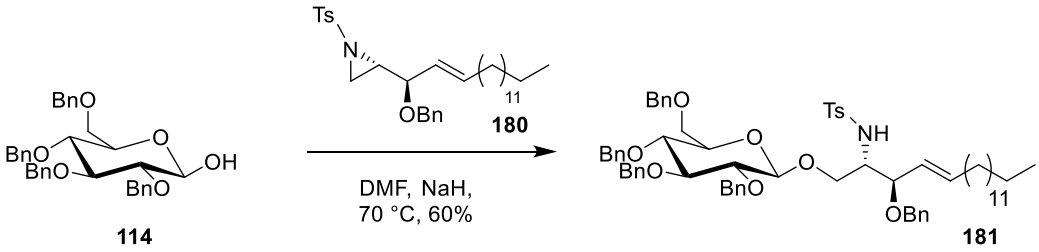

Scheme 3.5. Tsunoda *et al*. Ts-aziridine ring-opening using an oxygen nucleophile

The cleavage of the tosyl amides generally requires harsh acidic conditions or reductive conditions.[122-126] It was therefore proposed to synthesise the more reactive 4-nitrobenzenesulfonyl **187** and 2-nitrobenzenesulfonyl **188** aziridines which would allow more facile deprotection.[118] Using the acyl chain as an activating group in acyl aziridine **192** would allow direct incorporation of the desired acyl chain and reduce the number of steps to the final target.

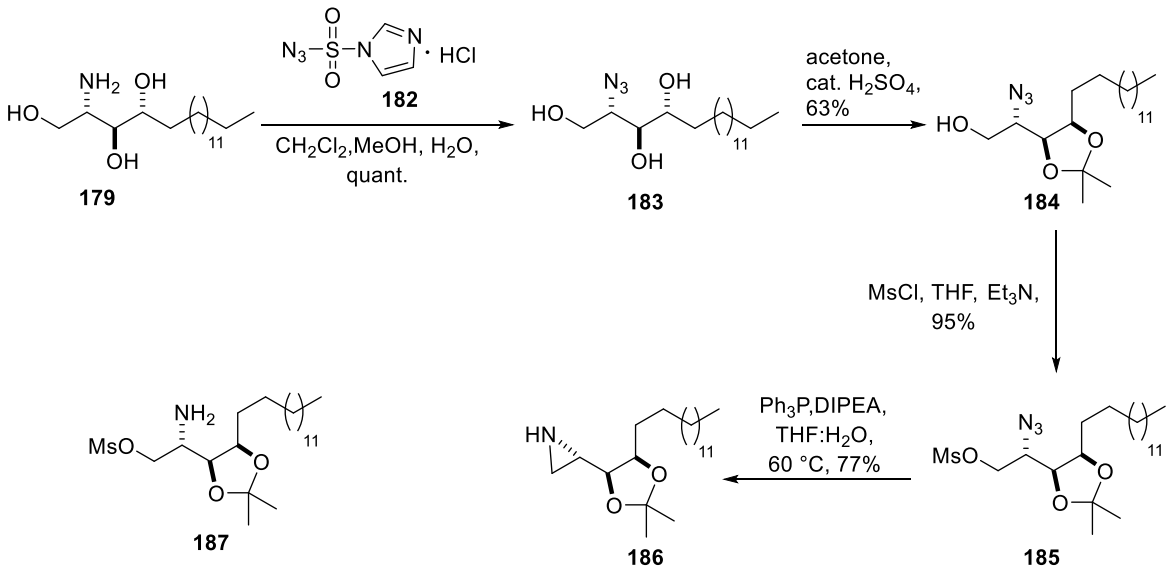

Scheme 3.6. Synthesis of phytosphingosine based aziridine **186**.

Scheme 3.6. shows the synthesis of the unprotected aziridine **186** from phytosphingosine **179**. Imidazole-1-sulfonyl azide hydrochloride **182** was used to convert the phytosphingosine **179**

to azide **183**.[127] Trifluoromethanesulfonyl azide (TfN_3) had been used previously as the diazo donor; however, imidazole-1-sulfonyl azide hydrochloride is less explosive, shelf stable (as its crystalline hydrochloride salt) and therefore more attractive than TfN_3 which needs to be prepared immediately before use.[128, 129] The internal 1,2-diol of azide **183** was next protected as an 1,2-isopropylidene using acetone under acid catalysis. Acetonide **184** was obtained in 63% yield following stirring of the reaction mixture for 2 days to promote the formation of the thermodynamic product. The remaining primary alcohol of acetonide **184** was then converted to the mesylate in quantitative yield.[130]

Trimethylphosphosine is frequently used in the group for Staudinger reactions in place of triphenylphosphine which is most commonly used. Increased volatility of the phosphine and phosphine oxide by-product often removes the need for purification *via* column chromatography. For this reason, Me_3P was first used to reduce the azide **185** to the intermediate amine which would undergo intramolecular substitution to afford aziridine **186**. However, this reaction led to a complex mixture of products, which may have arose as a consequence of the elevated temperature which was required to effect aziridine formation. The same problems were not encountered with Ph_3P. Trituration of the majority of the phosphine oxide with neat hexane, follow by purification by column chromatography provided aziridine **186** in 77% yield. While not isolated the uncyclized amine **187** was also observed. Reduction of the azide to the amine occurred rapidly with the rate limiting step being the intramolecular substitution. However, leaving the reaction longer or increasing the temperature did not increase the yield. Amine **187** proved difficult to separate from the aziridine at this stage but could be easily purified following reaction with the activating group.

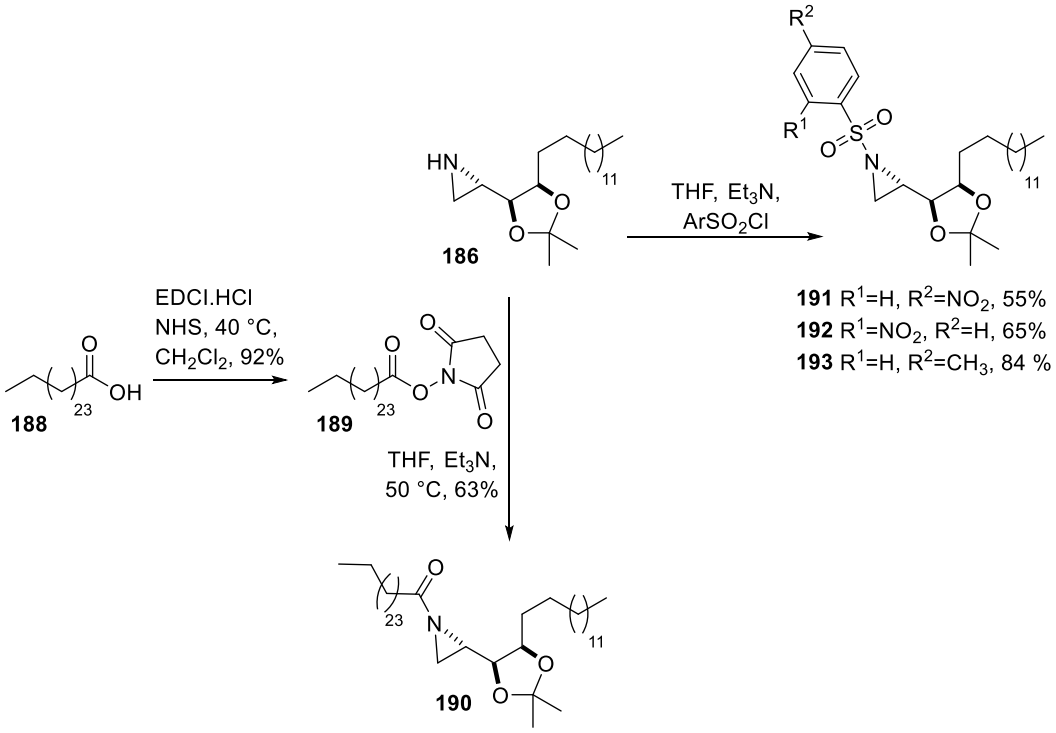

Scheme 3.7. Synthesis of activated aziridines

Acyl aziridine **190** was formed by reaction of aziridine **186** with the NHS ester of hexacosanoic acid **188**, which was prepared from using EDCI.HCl and NHS in CH_2Cl_2 in excellent yield (Scheme 3.7.). Usefully NHS ester **188** could be stored in the fridge and used when required. Sulfonyl aziridines **191**, **192** and **193** were synthesised in moderate to great yields using their respective sulfonyl chlorides in the presence of Et_3N in THF (Scheme 3.7.).

3.8.5. Ring opening- Trial studies with cyclohexanol

With a series of activated aziridines in hand the next step was to study the ring opening using cyclohexanol as a model secondary alcohol (Scheme 3.8.). Starting with acyl aziridine **190**, treatment of 2 equivalents of sodium cyclohexanoate failed to yield any of the desired ring opened product, instead yielding ester **195** and the recovery of aziridine **186** with the amide

carbonyl group evidently proving to be more electrophilic than the aziridine resulting in transacylation.

Next, ring-opening was attempted on both nosyl aziridines **191** and **192** to examine the effect of the position of the nitro group on reactivity. Once again, however, the desired ring-opened product was not obtained. This time, the major products arose from S_NAr reaction of cyclohexanoate at the nitro carbon and the sulfone carbon leading to aryl ether products **196** and **197** respectively. Loudon and Shulman reported S_NAr substitution of the nitro and a sulfone can be achieved using a sodium alkoxide.[131] Varying the reaction temperature, reaction stoichiometry and solvent led to no improvement. A similar distribution of products was observed when two and 1.25 equiv. of the sodium alkoxide were used at rt and at 40 °C. Use of THF at rt afforded aryl ether **196** as the major product, whilst in DMF, no reaction was observed at 0 °C even in the presence of four equiv. of the sodium alkoxide. Finally, tosyl aziridine **198** did provide the desired product in quantitative yield.

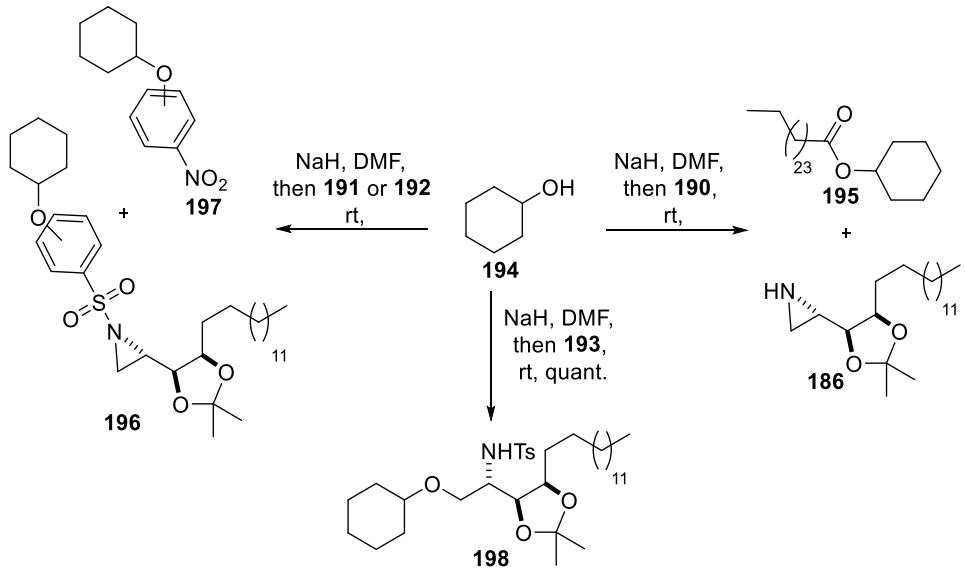

Scheme 3.8. Attempts at ring-opening Nosyl, Acyl, and Tosyl aziridine with cyclohexanol as a model cyclitol

3.8.6. Attempts at detosylation of sulfonamide (198)

Following successful ring-opening of aziridine **193** by sodium cyclohexanoate, different reaction conditions were examined to effect detosylation. While the use of HBr led to complex mixture of products, sodium naphthelanide proved more promising. The desired amine was observed; however, the large excess of naphthalene hampered purification and amine was isolated in only poor yield. This reaction also proved difficult to replicate. Finally, successful removal of the tosyl group was achieved by conversion to the boc carbamate **200**. Nyasse *et al*. showed that detosylation proceeded readily using solid magnesium powder in methanol with sonication to provide the corresponding Boc amides.[132] Gratifyingly, carbamate **200** was isolated in quantitative yield over the two steps. Boc protection was not deemed a problem as it was envisaged this group would be removed in the global deprotection step.

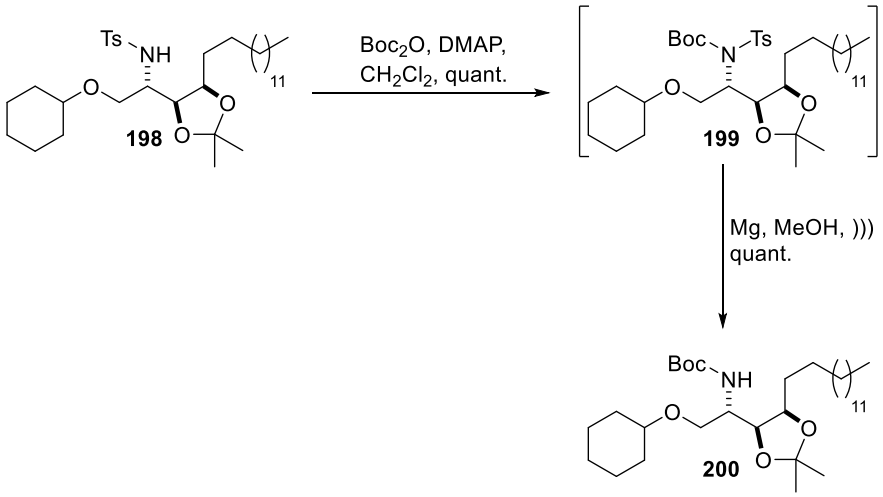

Scheme 3.9. Detosylation of sulfonamide **198**

3.8.7. Synthesis of TBDMS conduritol E (163)

The cyclohexanol coupling partner **163**, was synthesised using a modified route to what had been developed previously in the group (Scheme 3.12). Previously, DIBALH reduction of

tartrate-derived di-ester **177**, followed by *in-situ* reaction of the bis-aldehyde intermediate with vinyl magnesium bromide provided diene **176** as an inseparable 3:1 mixture of diastereoisomers (desired product was major diastereoisomer). Competing-reduction of the intermediate aldehyde was a problem in this reaction. Seeking to improve on this reaction, divinylzinc was used as Jørgensen *et al*. had reported enhanced diastereoselectivity.[133] Though not commercially available, divinyl zinc can be synthesised by reaction of vinyl magnesium bromide with $ZnCl_2$ *via* transmetallation.[134] Due to the hygroscopic nature of $ZnCl_2$, care had to be taken when fusing under vacuum, a Schlenk flask allowed the addition of THF to be made in an Argon atmosphere to give a solution of $ZnCl_2$ in THF which was then heated with vinyl magnesium bromide for 4 h. Cooling of the reaction mixture led to precipitation of Mg salts which were allowed to settle and the supernatant containing the newly formed divinyl zinc was filter cannulated directly into the reaction mixture of the DIBALH reduction. Indeed, the diastereoselectivity was improved to 5:1 and less over-reduction was observed (Scheme 3.12.).

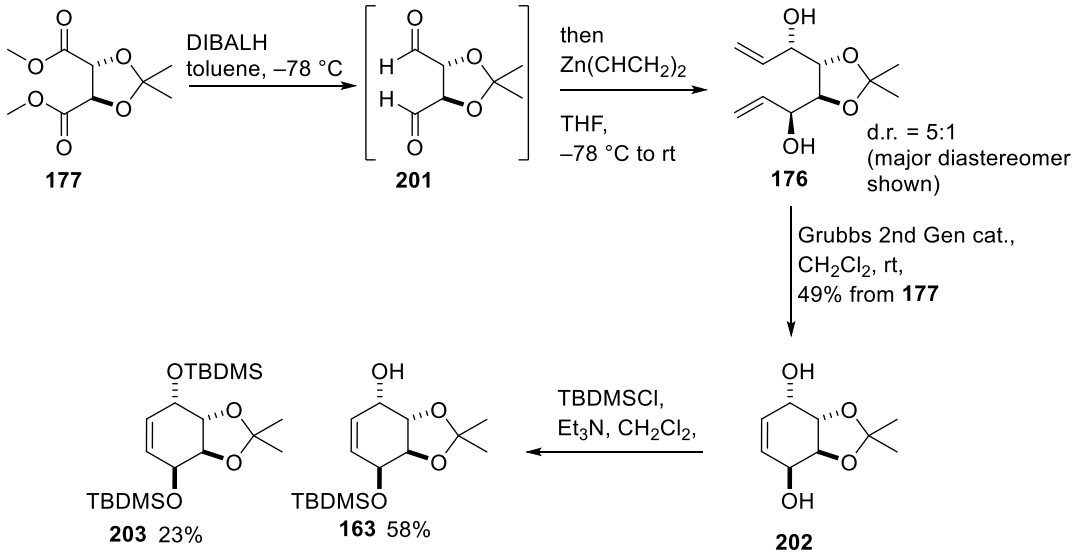

Scheme 3.10. Synthesis of TBDMS-protected conduritol E

Scheme 3.11 shows the potential products of the Barbier reaction, both diol **176** and diol **204** are symmetrical and diol **206** and diol **208** are equivalent. While the products were inseparable

at the vinyl alcohol stage, following ring-closing metathesis the major product was isolated pure. Confirmation that the major product was the desired was done using both NMR and optical rotation. As the ^{1}H NMR confirmed a symmetric molecule, conduritol F **207** as the major product was eliminated. Elimination of (–) conduritol B **205** was done by comparison of previously published NMR shift values and further confirmed following a positively signed optical rotation measurement[4] was obtained indicating (+) conduritol E.[135, 136]

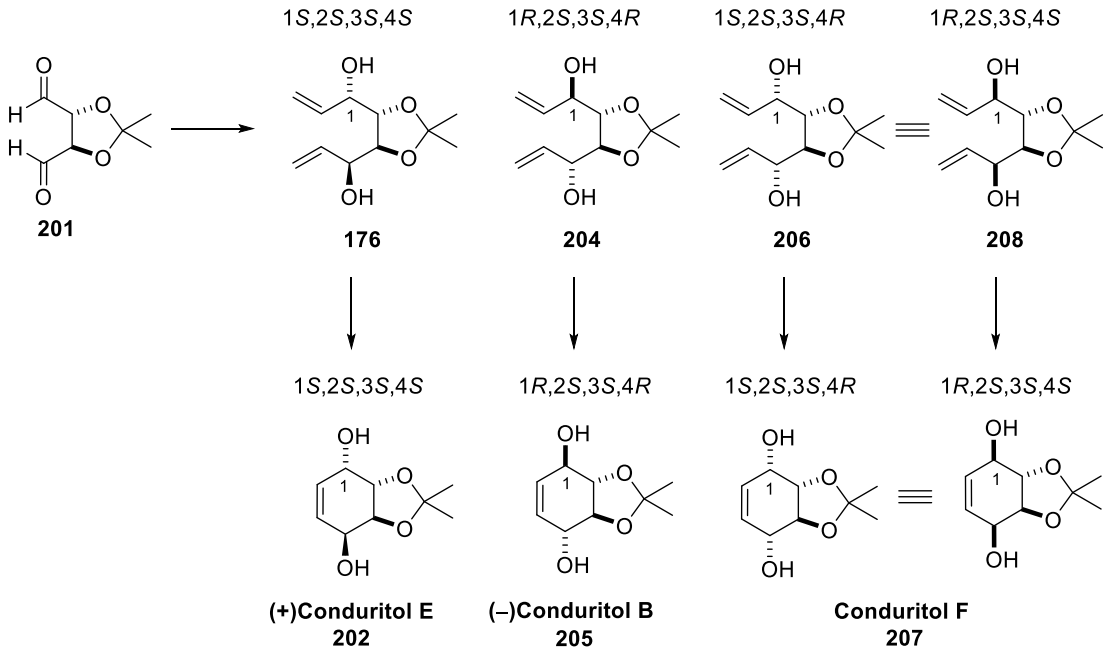

Scheme 3.11. Potential for synthesis of a range of diols following Barbier reaction leading to different conduritols after ring-closing metathesis

While no difference could be measured for the *J* coupling values, the difference in shift values for key atoms can be used to identify the correct isomer. Tables 3.2 and 3.3 compare the ^{1}H and ^{13}C spectra of (–) conduritol B **205** and (+) conduritol E **202** along with the data obtained from my synthesis of (+) conduritol E **202**. While (–) conduritol B **205** has only been

[4] $[\alpha]_D^{20}$ = +304.0 (c = 1.0, $CHCl_3$) obtained, lit.[133] (+) conduritol E $[\alpha]_D^{25}$ = +338.6 (c = 0.7, $CHCl_3$).

synthesised by Yong-Uk Kwon *et. al.*[137] (+) conduritol E has been synthesised by three groups whose data is similar and confirms the chemical shift differences.[136, 138, 139]

^{1}H		
(–) conduritol B **205** **(Published)**	(+) conduritol E **202** **(Published)**	(+) conduritol E **202 (Mine)**
1.47 (6H, s)	1.48 (6H, s)	1.48 (6H, s)
2.74 (2H, br ,s)	2.63 (2H, br s)	2.70 (2H, br s)
3.55 (2H, dd, *J* 5.6, 2.3)	3.94 (2H, dd, *J* 1.9, 1.3)	3.88–3.95 (2H, m)
4.50 (2H, dd, *J* 5.6, 2.3)	4.49 (2H, br d)	4.53 (2H, app. s)
5.69 (2H, s)	5.98 (2H, dd, *J* 3.2, 1.5)	5.98 (2H, m)

Table 3.2 Compares the ^{1}H spectra highlighting a key difference, data shown for published (+) conduritol E from ref [139]

^{13}C		
(–) conduritol B **205** **(Published)**	(+) conduritol E **202** **(Published)**	(+) conduritol E **202 (Mine)**
27.4 (*C*H$_3$)	25.9 (*C*H$_3$)	26.9 (*C*H$_3$)
71.1 (*C*H)	63.7 (*C*H)	64.8(*C*H)
81.1 (*C*H)	72.4 (*C*H)	73.4 (*C*H)
111.7 (*C*)	109.5 (*C*)	110.5 (*C*)
130.9 (*C*H)	129.4 (*C*H)	130.4 (*C*H)

Table 3.3 Comparing the ^{13}C spectra, higlighting the key differences, data shown for published (+) conduritol E from ref [139]

The stereochemical outcome can be rationalised under the predictions of the Felkin-Anh model (Scheme 3.12.).[133, 140]

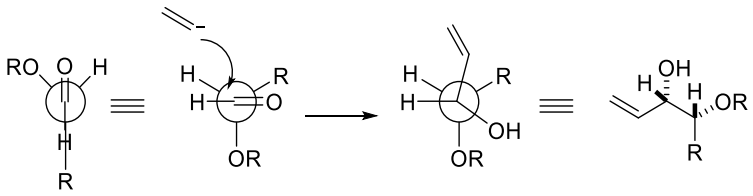

Scheme 3.12. Felkin-Anh model predicts formation of diol **176**

Next, ring-closing metathesis of diene **176** using Grubbs' second-generation catalyst yielded the corresponding cyclohexene as a mixture of diastereoisomers, which were now readily separable. Monosilyletherification of diol **202** using TBDMSCl in the presence of Et_3N provided silyl ether **163** in 58%. The bis-silylated and unreacted starting were both readily isolated and could be recycled (Scheme 3.12.).

3.8.8. Synthesis of carbamate intermediate (211) *via* Ts-aziridine ring-opening as a precursor to target (166)

Turning our attention to alcohol **163**, we found that it was not necessary to employ a two-fold excess of substrate as had previously been used during the model ring-opening experiements, when following the conditions used by Tsunoda *et al*.[121] ; thus, regioselective ring-opening of aziridine **193** with equimolar quantities of the sodium alkoxide of **163** yielded sulfonamide **209** in 58%. Detosylation of sulfonamide **209** to carbamate **211** was achieved in 86% yield by employing the two-step method developed by Nyasse *et al*. Initial Boc protection proceeded in quantitative yield using Boc_2O in the presence of DMAP to yield intermediate carbamate **210** which was next reacted with magnesium metal in methanol under sonication for 30 min to yield carbamate **211** in 86% yield. Treatment of **211** with TFA effected global deprotection of the protecting groups in a single step to provide amine **212**, which, without purification,

underwent acylation using the NHS ester of hexacosanoic acid **189** to yield our first target **166** in 62% yield over two steps (Scheme 3.13.).

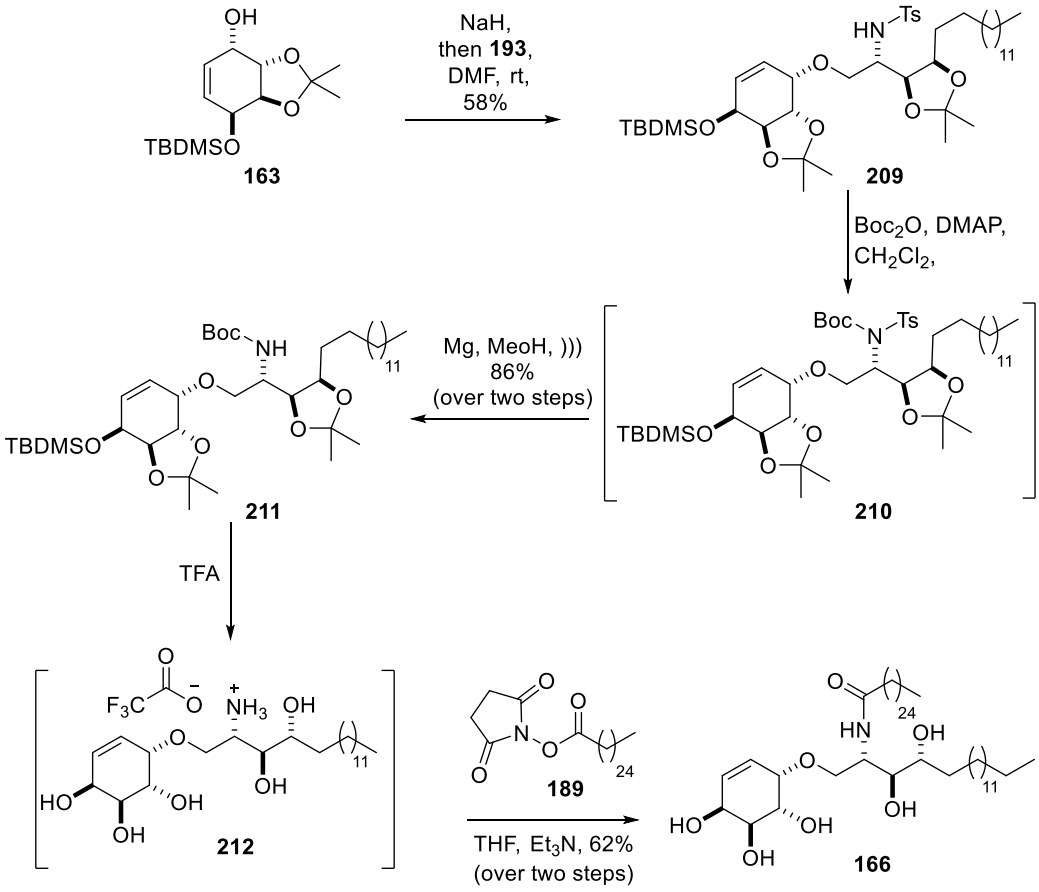

Scheme 3.13. Synthesis of target alkene **166**.

3.8.9. Synthesis of ThrCer-6 (16) and C20:2 (168) compounds

In order to complete the synthesis of the three remaining target molecules, **167**, **168** and **169**, the cyclohexene needed to be reduced. Hydrogenation of alkene **211** was effected using H_2 and Pd/C in the presence of a stoichiometric amount of Hünig's base, which prevented the premature acid-catalysed hydrolysis of the acetonide protecting groups. Subsequent global deprotection of the protecting groups provided ammonium trfilate **214**, from which amides **16**

and **168** were accessed uneventfully by acylation with the corresponding NHS esters of (*Z, Z*)-eicosa-11, 14-dienoic acid **215** and hexacosanoic acid **189**, respectively.

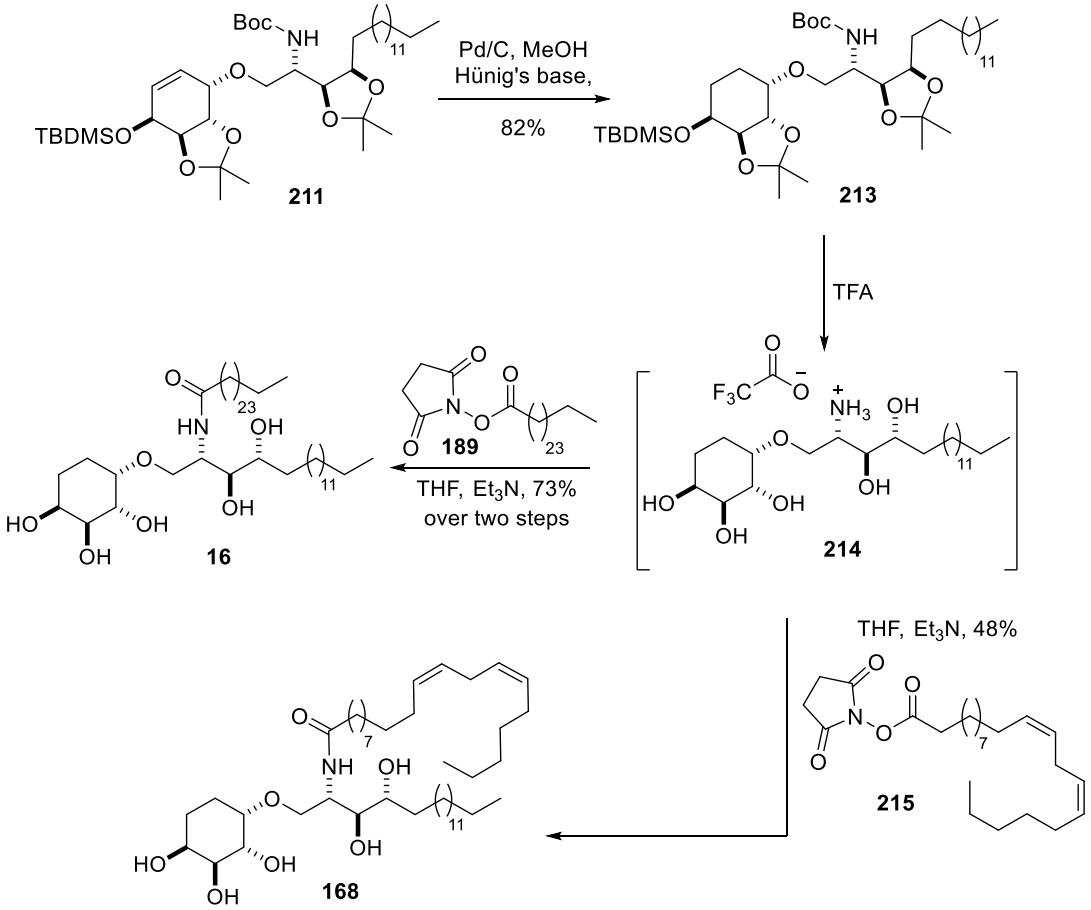

Scheme 3.14. Synthesis of ThrCer-6 (**16**) and C20:2 (**168**)

3.8.10. Synthesis of thioamide (167)

Formation of thioamide **167** was accomplished in a three-step sequence from amide **16**. Thus, peracetylation with acetic anhydride in pyridine afforded pentacetate **216**, which reacted selectively with Lawesson's reagent to provide thioamide **217** in 94% yield. Deacetylation under Zemplén conditions afforded, thioamide **167** in 74% yield.

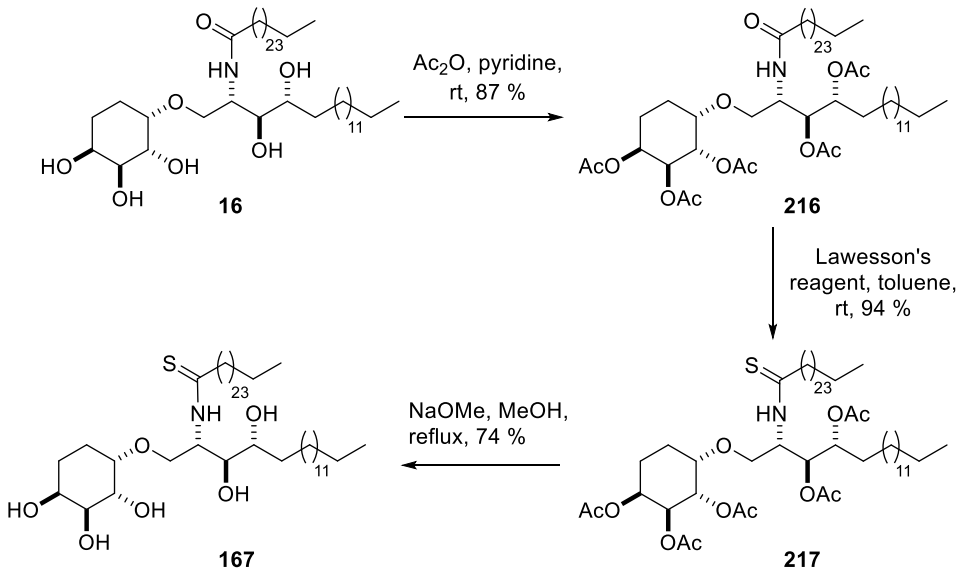

Scheme 3.15. Synthesis of thioamide **167**

3.8.11. Synthesis of amide target (169) *via* acylation with acid (221)

Synthesis of our final target, namely amide **169**, required acylation of ammonium **214** with an appropriate activated acid. Previously within the group, aryl acid **221** was synthesised using a cross-metathesis between 1-allyl-4-fluorobenzene and dec-9-enoic acid using Grubbs' second-generation catalyst. However, competing homo-coupling of the allyl benzene (the homodimer was not a substrate for desired cross-metathesis) led to a poor yield of the desired acid. Moreover, separating the cross-metathesis acid product from the starting alkenyl acid proved difficult and compounded the problem. An alternative route summarised in Scheme 3.16. was more successful.

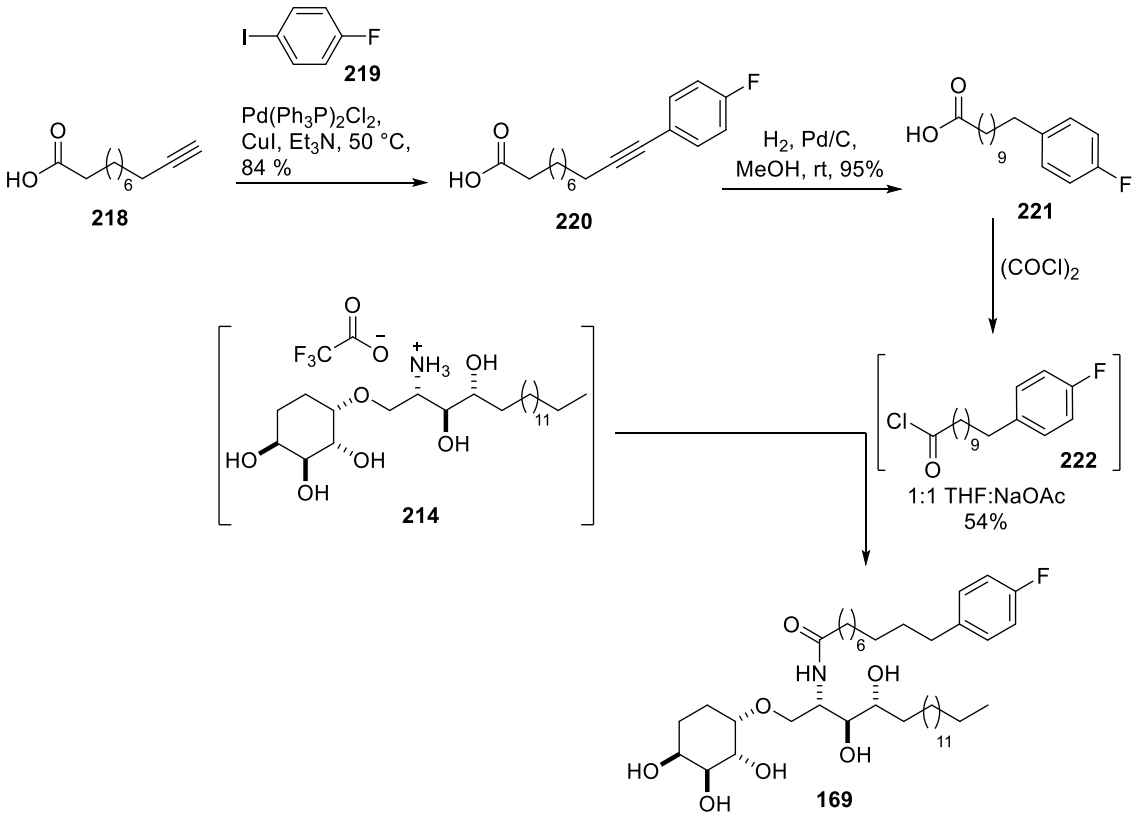

Scheme 3.16. Synthesis of amide **169** *via* acylation with acid **221**

Acid **221** was synthesised in two steps *via* a Sonagashira cross-coupling reaction between alkyne **218** and 4-fluoroiodobenzene **219**. Alkyne **220** was obtained in 79% yield with full conversion of the acid starting material **218** (facilitating purification). Subsequent hydrogenation of the alkyne using H_2/Pd/C in methanol furnished the acid in quantitative yield. Reaction of the corresponding acid chloride generated using oxalyl chloride with ammonium triflate **214** proceeded uneventfully to afford our final target molecule, amide **169** in 61% yield.

3.9. Biological evalutation of target ThrCer-6 analogues

*i*NKT cells are activated to induce an immunological response following binding with CD1d cell-surface protein in the presence of a suitable glycolipid, which is necessary for formation of the CD1d–ligand–TCR interaction. While α-GalCer **10** has been used as the prototypical model glycolipid due to its potency, it induces a mixed T_H1/T_H2 cytokine response; however, it has been shown that altering the ligand can bias the cytokine profile to produce a potentially more therapeutically useful immune response. Using ThrCer-6 **16** as the starting point and reference, four analogues were synthesised, three (**167**, **168** and **169**) containing modifications of the acyl chain, which are known to induce a biased cytokine response and one (**166)** with a conduritol polar head group.

A first set of experiments were performed by Dr Hemza Ghadbane, a member of Prof. Vincenzo Cerundolo's group at the Weatherall Institute of Molecular Medicine in Oxford, UK. The compounds were tested for *in vivo* activation of *i*NKT cells using C57 BL/6 WT and $CD1d^{-/-}$ mice. The mice were injected intravenously with lipids at concentrations ranging from 0.06 ng/ml to 1000 ng/ml (n=3 at each concentration for each compound tested) and after 48 h, blood serum was taken. The presence of IFN-γ was then determined by enzyme-linked immunosorbent assay (ELISA).[114] The results of these experiments are summarised in Figure 3.15. Starting with the conduritol analogue **166**, at lower concentrations of 0.2, 1.1, 4 and 15 ng/ml a greater IFN-γ response is produced compared to that stimulated by the parent α-GalCer, compound **10** ($P<0.05$ at each concentration). An increase in IFN-γ was also produced by compound **166** at 15 ng/ml compared to parent compound ThrCer-6, compound **16** ($P<0.05$). However, at higher concentrations, 1000 ng/ml and 250 ng/ml, both ThrCer-6 **16** and α-GalCer **10** produce a stronger IFN-γ response compared to all other compounds, **166**, **167**, **168** and **169** ($P<0.05$). Further study is needed to determine the mode of binding. The three other analogues, **167**, **168** and **169**, produced a weaker IFN-γ response than both ThrCer-6 **16** and α-GalCer **10** at all concentrations. The C20:2 analogue **168** in particular

showed a weaker response at higher concentrations, 1000ng/ml and 250/ng/ml compared to α-GalCer **10** ($P<0.05$ at each concentration) and at all concentrations compared to ThrCer-6 **16** ($P<0.05$ at each concentration). This may be due to the known ability of glycolipids incorporating a C20:2 acyl chain to induce a T_H2 response, however, it would be necessary to measure the IL-4 response to confirm any T_H2 cytokine bias. Data were analysed by two-way ANOVA to compare treatment groups, followed by a Dunnett's multiple comparison test to identify differences compared to untreated controls. Differences were considered statistically significant at $P<0.05$. The fact that no activity is seen when CD1d-deficient mice were used confirms that the observed bioactivity of the glycolipids is CD1d-dependent.

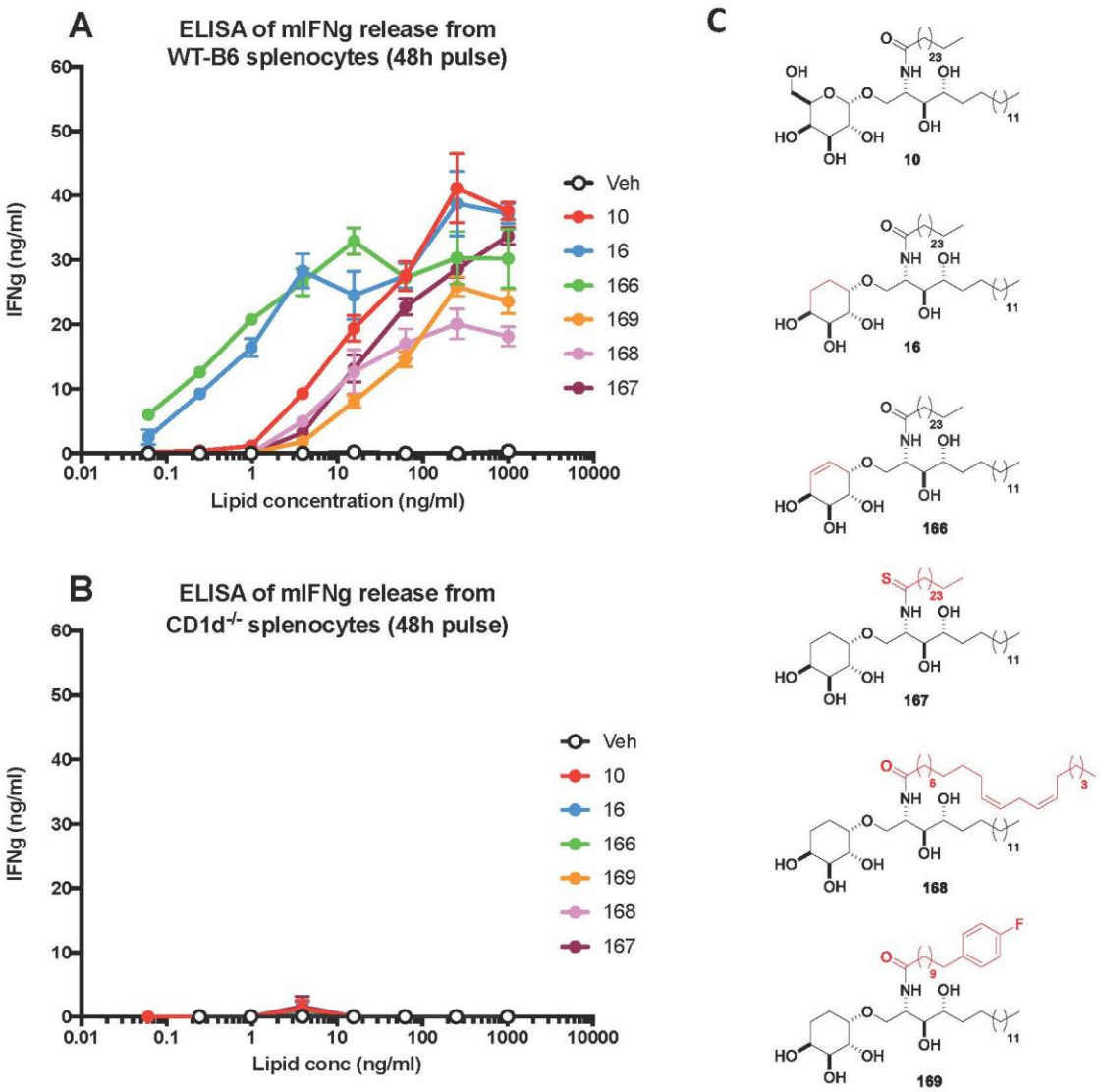

Figure 3.15. IFN-γ response of synthesised compounds in splenocytes of (A) C57 BL/6 WT mice (n=3 for each compound at each concentration) (B) CD1d$^{-/-}$ mice (n=3 for each compound at each concentration). Data presented as mean ± S.E.M (error bars). (C) Structures of glycolipids tested.

In a further set of experiments,[141] which were carried out by Shalu Sharma, a member of Prof Steven A. Porcelli's group at the Albert Einstein College of Medicine in New York, US, the

same set of compounds were incubated with human HeLa cells transfected with human CD1d in concentrations ranging from 1–100 nM. After 18 hours, the cells were washed and exposed to cultured iNKT cells (human clone HDD3). Supernatants were collected after 24 hours, and the levels of IFN-γ were measured by ELISA. All five compounds were highly stimulatory to iNKT cells.[5] The results of these experiments are summarised in Figure 3.16. At all concentrations, a stronger IFN-γ response is seen from all of the cyclitol-based glycolipids compared to that of the galactose-based control compounds. At concentrations of 100, 10 and 1 nM, compounds 166 and 167 resulted in an increase in IFN-γ ($P<0.005$, Figure 3.16). Treatment with compound 168 increased concentration of IFN-γ at 10 and 1 nM ($P<0.05$, Figure 3.16). Treatment with compound 169 increased IFN-γ at 100 and 10 nM ($P<0.05$, Figure 3.16). There was no change in IFN-γ concentration from treatment with compounds 169, KRN7000 and 7DW85. Data were analysed by two-way ANOVA to compare treatment groups, followed by a Dunnett's multiple comparison test to identify differences compared to untreated controls. Differences were considered statistically significant at $P<0.05$. The conduritol analogue **166** once again proved to be the most active, showing a two-fold stronger cytokine response over α-GalCer **10 (KRN7000)** at 100 nM concentration.

[5] The positive controls for comparison are KRN7000 (α-GalCer **10**), and another potent analogue 7DW8-5 (C_{11} *p*-fluoro analogue of α-GalCer **144**).

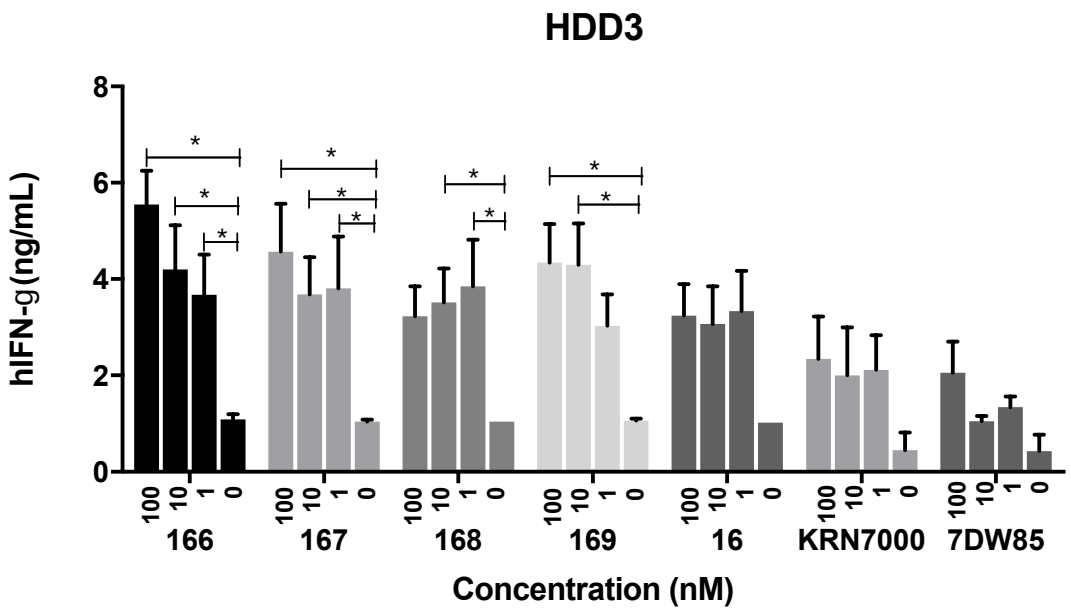

Figure 3.16. IFN-γ response of synthesised compounds using hCD1d and HDD3 human clone *i*NKT cells (*in vitro study*). For each compound tested at each concentration n=5. Data presented as mean concentration ± S.E.M (error bars). *, $p<0.05$. (2way ANOVA with multiple comparison tests).

To determine the cytokine bias, the ratio of IFN-γ:IL-4 now needs to be measured; however, these preliminary experiments reveal that this set of compounds activate *i*NKT cells in a CD1d-dependent manner, producing varying levels of IFN-γ and in some cases, a stronger response than that of the parent compound, ThrCer-6 **16** and α-GalCer **10**.

3.10. Synthesis of ThrCer analogues at the pseudo-anomeric linkage

Following on with the development of analogues with a T_H1/T_H2 skewing bias, we decided to develop analogues with alternative atoms at the pseudo-glycosidic linkage of ThrCer. The potential to generate ThrCer analogues that not only induce a biased response but also a more potent response was desirable.

Previously synthesised analogues of α-GalCer which contain alternative atoms at the glycosidic linkage have shown to have varying cytokine profiles (Figure 3.17). Of these α-*C*-GalCer **154** is the most studied, it has shown to be more potent than α-GalCer in some tests and induces a T_H1 biased cytokine profile.[142, 143] The thio analogue of α-GalCer, α-*S*-GalCer **223** has also been synthesised with more studied needed on its mode of binding as it has been shown to not activate the murine *i*NKT cells both *in vitro* and *in vivo*, but stimulated human iNKT cells in vitro.[144] Finally, only one synthesis of the amino analogue α-*N*-GalCer **224** has been published but there has been no biological testing data published on the molecule[145] However, the non-glycosidic amino analogue **225** has been shown to induce a T_H1 biased respone.[146, 147]

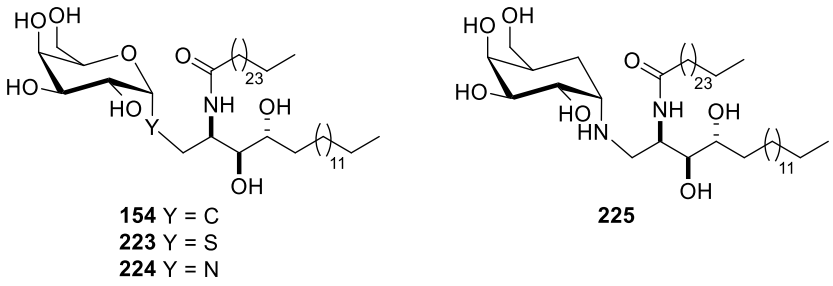

154 Y = C
223 Y = S
224 Y = N

225

Figure 3.17 Analogues of α-GalCer with alternative atoms at the glycosidic linkage

Through the use of the previously developed activated aziridines as electrophilic phytosphingosine coupling partners we targeted ThrCer **14** and three analogues *N*-ThrCer **227**, *S*-ThrCer **226** and *C*-ThrCer **228**.

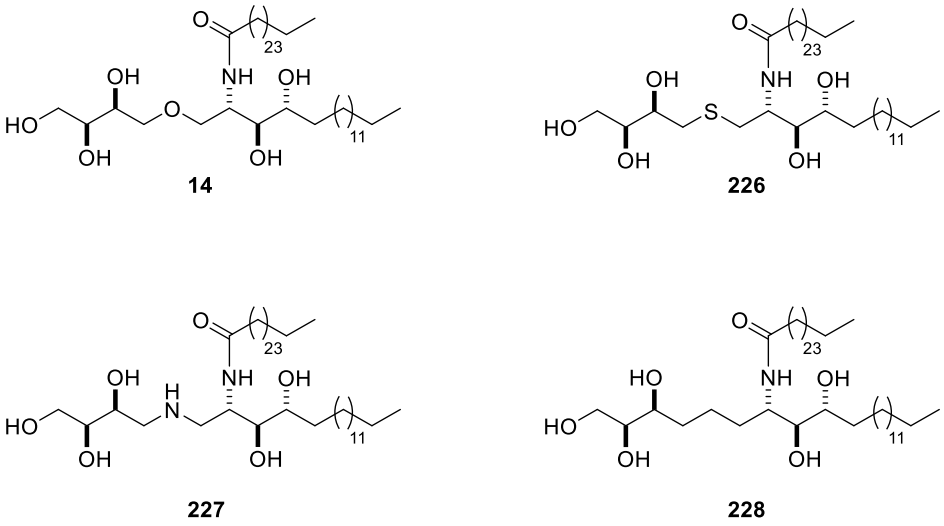

Figure 3.18 ThrCer and three analogues *S*-ThrCer, *N*-ThrCer and *C*-ThrCer

3.10.1. Retrosynthesis

A retrosynthetic analysis of these molecules is shown in Scheme 3.17 and follows a similar pattern to that of the ThrCer-6 analogues. Cleavage of the amide bond yields amine **231** and activated carboxylic acid **232**. Further disconnection of amine **231** would yield the activated aziridine **175**, which can be synthesised from phytosphingosine **179**, and a threitol-based nucleophile **233**, which can be synthesised from commercially available (+)-2,3-*O*-Isopropylidene-L-threitol **234**.

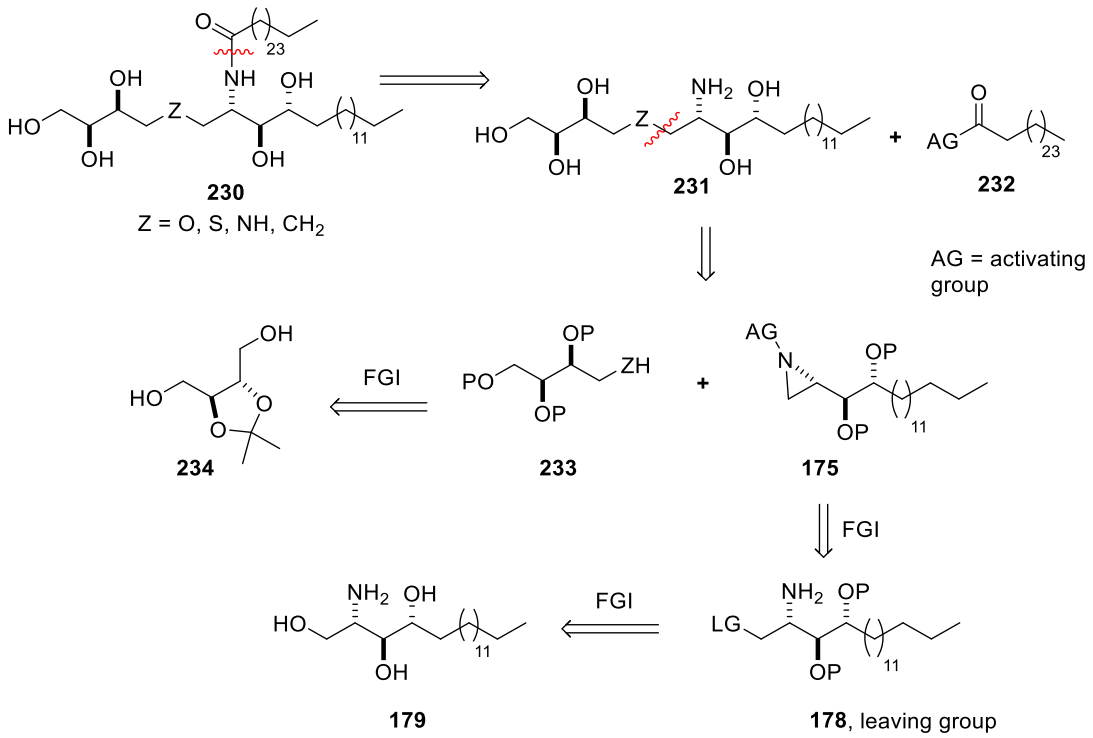

Scheme 3.17. Retrosynthetic analysis of ThrCer and its analogues.

3.10.2. Synthesis of ThrCer *via* aziridine ring-opening

The synthesis of the parent molecule, ThrCer **14**, began with (+)-2,3-*O*-Isopropylidene-L-threitol **234** which was protected as its monobenzyl ether **235** in 76% yield following reaction with NaH and BnBr. The small amount of debenzylated product was readily separated from the desired product by column chromatography. Next, ring-opening of tosyl aziridine **193** by the sodium alkoxide of benzyl ether **235** was achieved using the same conditions as had been developed for the protected conduritol E analogue **163**, in the synthesis sulfonamide **209**. In this instance tosyl amide **236** was achieved in 64% yield. Conversion of the resulting tosyl amide **236** to its Boc carbamate **238** was achieved in 65% over two steps: sulfonamide **236** was first reacted with Boc_2O to yield the sulfonamide carbamate **237**, which underwent facile detosylation by reaction with magnesium metal in MeOH under sonication to yield Boc carbamate **238**. Global deprotection was then achieved by first removing the benzyl group

using by hydrogenolysis, which afforded alcohol **239** in 79%. Alcohol **239** was then treated with neat TFA to remove the Boc carbamate and acetal protecting groups. The resulting ammonium salt **240** was treated directly with C_{26} NHS ester **189** in the presence of Et_3N to yield the first target ThrCer **14** in 62% over two steps (Scheme 3.18.).

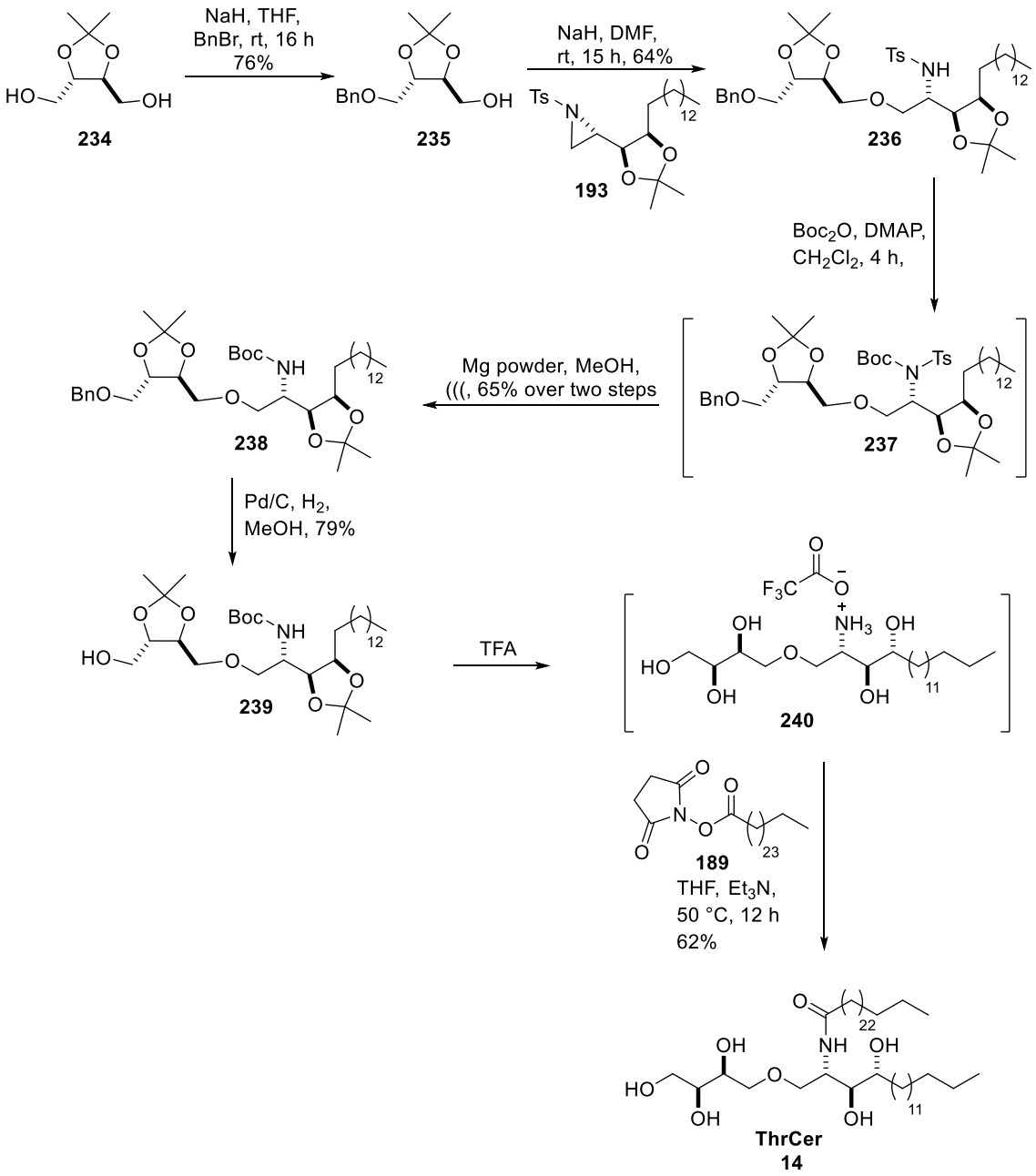

Scheme 3.18. Synthesis of ThrCer *via* aziridine ring-opening

A published syntheses of ThrCer has previously been done within the group.[148] Alcohol **241** was used as a nucleophilic phytosphingosine coupling partner in reaction with threitol triflate **242** in a Williamson etherification. Our synthesis is comparable in overall yield at 15% over 7 steps in comparison to 16% over 6 steps. However, our aziridine synthesis is much more amenable to scale up, especially with regards the coupling reaction as no large by-products such as the triflate are formed. With regards the synthesis of the other targets, an electrophilic phytosphingosine coupling partner is much more desirable due to shorter synthetic sequences required for the threitol analogues

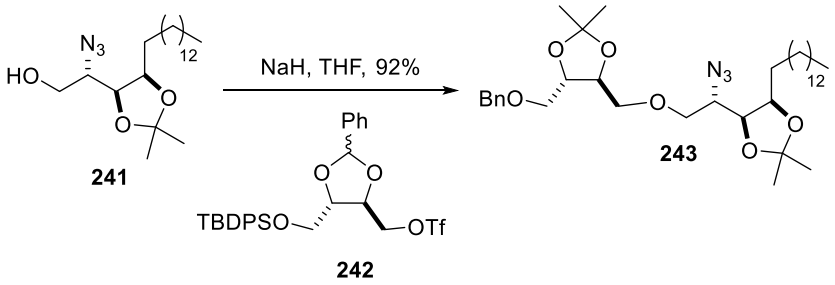

Scheme 3.19. Key coupling step of published synthesis of ThrCer

3.10.3. Attempted synthesis of *N*-ThrCer

To access the next target, amino-substituted *N*-ThrCer, it was necessary to introduce an amine into the threitol nucleophilic coupling partner. Starting with alcohol **235**, tosylation under standard conditions, followed by azide displacement yielded azide **245** in 63% yield over the two steps. Selective reduction of the azide using hydrogenation conditions, afforded amine **246** in 67% yield. Potential hydrogenolysis of the benzyl ether was avoided by conducting the hydrogenolysis for a short reaction time. Using hydrogenation rather than a Staudinger reaction to reduce the azide facilitated the work up and purification of the amine product (Scheme 3.20).

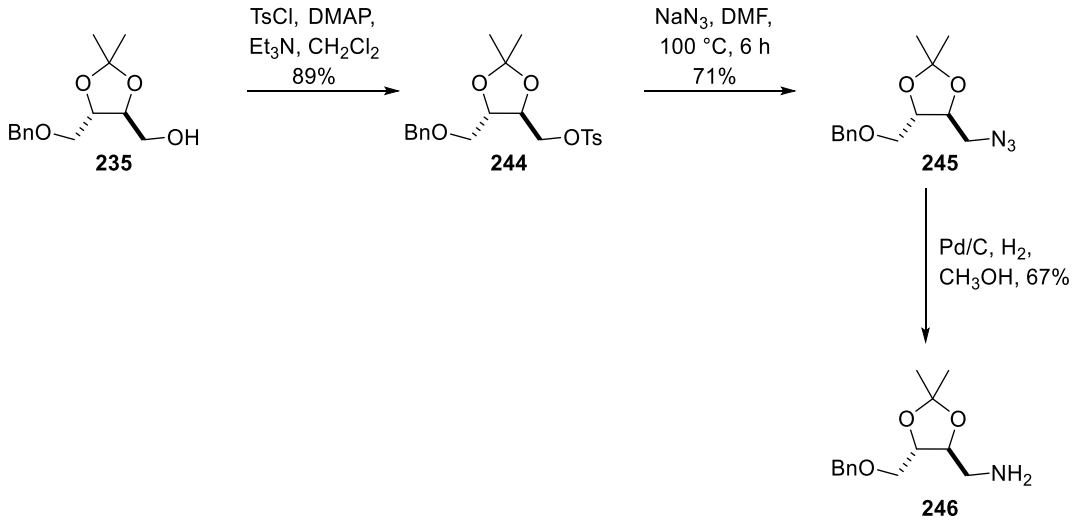

Scheme 3.20. Conversion of alcohol **235** to amine **246**

Llebaria had reported that amines could be used to effect the ring opening of a phytosphingosine-based acyl aziridine in the presence of lithium perchlorate.[149] However in our hands were unable to replicate their results, and instead isolated amide **248**, resulting from transamidation, as the major product (Scheme 3.21). The length of the acyl chain may have been a factor as the acyl aziridine used by Alcaide and Llebaria was only 8 carbons in length versus our 26 carbon chain and we have previously seen the effects of the hexacosanoyl chain on solubility in organic solvents. Reaction of the $LiClO_4$ and acyl aziridine **190** was required for 30 min prior to addition of the amine. The poor solubility may have affected the reaction of the Lewis acid with the aziridine. The amine then reacted with the unactivated acyl aziridine at the carbonyl carbon as the most electrophilic site to give amide **248** as the desired product

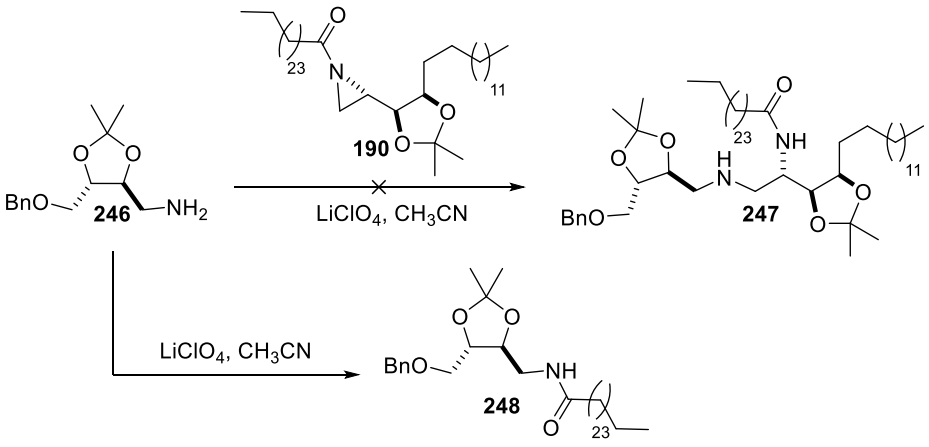

Scheme 3.21. Attempted ring opening of aziridine **190** with amine **246**

Harrak *et al.* have previously shown that nosyl aziridines can be ring-opened by both primary and secondary amines substrates.[130, 146] Using their conditions, we were able to successfully ring-open nosyl aziridine **192** in 65% yield following stirring with nosyl amide **249** in MeCN. Next removal of the nosyl group was achieved in excellent yield of 86% using PhSH and $CsCO_3$.

With amine **250** in hand we next attempted to selectively acylate at the primary amine, for which there was precedent from the work of Harrak *et al*.[146] The benefit of the attempted use of the acyl aziridine can be seen here with the route being more efficient, if ring-opening had been successful the acyl chain would be previously installed. With limited material available, a small scale reaction of diamine **250** with NHS ester **189** afforded a less polar product, which was fully deprotected using TFA followed by hydrogenolysis of the benzyl ether to yield a final product.

Mass spectrometry data of this product revealed that monoacylation had occurred. However owing to the small quantities of material we were working with, we were unable to confirm the selectivity of the acylation step (Scheme 3.22.).

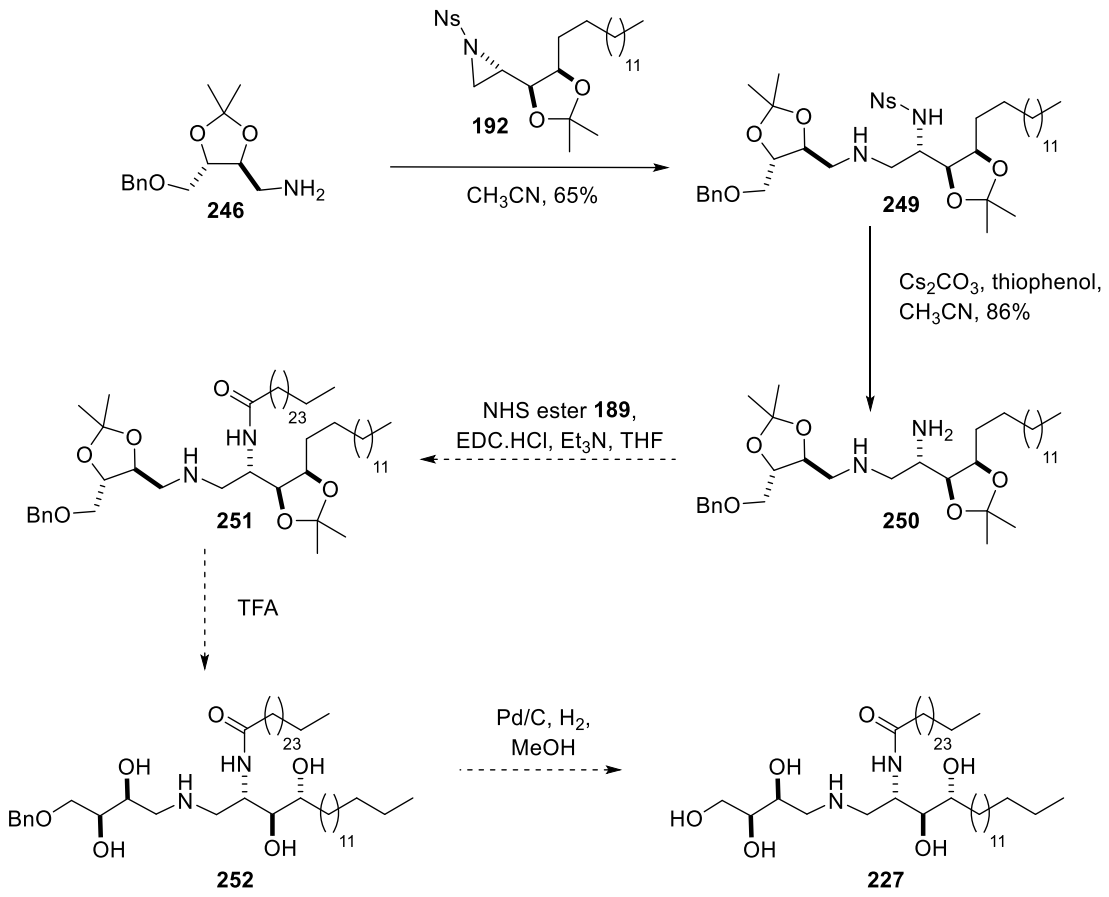

Scheme 3.22. Attempted synthesis of *N*-ThrCer **227**

3.10.4. Attempted synthesis of *S*-ThrCer

Using the previously synthesised tosylate **244**, nucleophilic substitution using thioacetic acid in the presence of Cs_2CO_3 yielded thioacetate **253** in excellent yield. Due to the potential for thiols to undergo oxidative dimerisation we elected not to isolate the thiol but rather to deprotect the thioacetate **253** using 2 equivalents of NaOMe and use the thiolate directly in a ring-opening of aziridine **193**. This strategy proved successful and sulfide **255** was isolated in 68%. While these conditions were not extended to nosyl aziridine **191** or **192**, an attempt at ring-opening the acyl aziridine **190** was made; however, this reaction proved unsuccessful even with a longer reaction time and increased temperature. Boc protection of tosyl amide **255**

followed by detosylation using Mg metal with sonication, afforded carbamate **256** in 70% yield over two steps (Scheme 3.23).

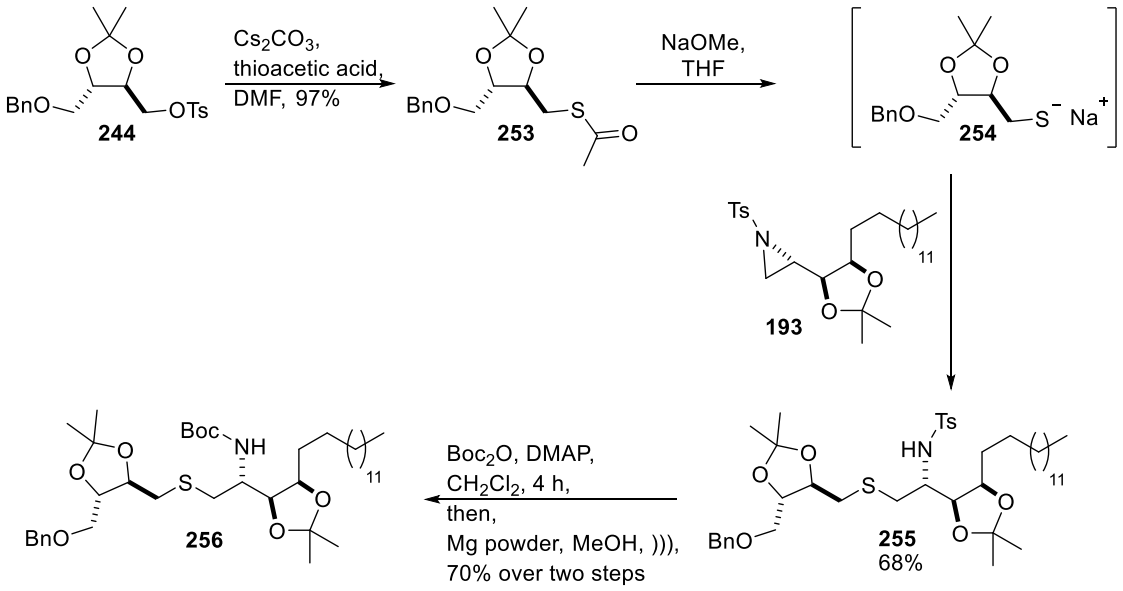

Scheme 3.23. Synthesis of carbamate **256**

After removal of the acetal and Boc protecting groups using neat TFA, acylation using NHS ester **189** in the presence of Et_3N yielded amide **258** in 47% over the two steps. All that remained was removal of the benzyl ether protecting group. Since sulphides are known to act as poisons for the Pd and Pt catalysts that are commonly used to effect hydrogenolysis of benzyl ethers, we chose to employ a Birch reduction instead. Unfortunately, and despite literature precedent, dissolving metal reduction led to complex mixture of products from which we were unable to isolate the desired product.[150, 151] Time prevented us from exploring alternative conditions (Scheme 3.24).

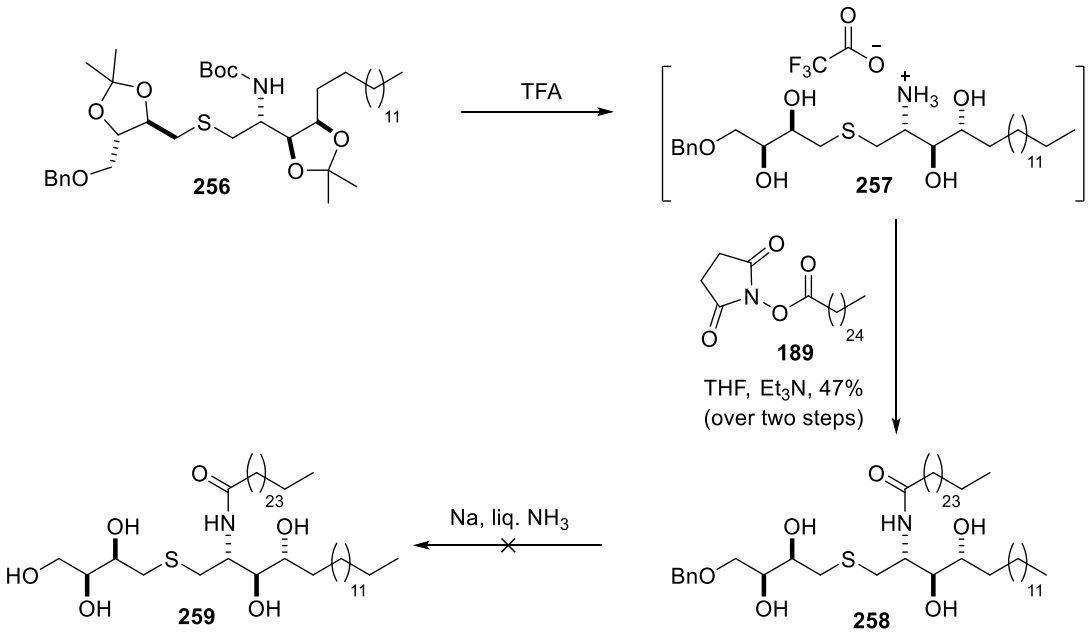

Scheme 3.24 Attempted synthesis of *S*-ThrCer

3.10.5. Studies towards the synthesis of *C*-ThrCer

The synthesis of *C*-ThrCer required a carbon nucleophile analogue of threitol. Using a 1,3 dithiane would allow us to introduce one carbon, while the umpolung nature would allow us to deprotonate the carbon to act as a nucluophile. We postulated that a double alkylation of 1,3 dithiane would allow us to unite the threitol and phytosphingosine units.1,3 Dithianes have been shown to react with epoxides, sulfamidates and carbonyls, fortunately they have also been shown to react with aziridines.[152, 153] Precedent was also found for the synthesis of protected threitol 1,3 dithiane **261** *via* displacement of an iodide.[154] This approach would also potentially allow us to access other analogues. Whilst Ra-Ni would be used to effect desulfurisation to provide our target molecule, *C*-ThrCer **228**, dithioacetal hydrolysis would provide a keto analogue **263**, which could undergo difluorination using DAST to provide a CF_2 analogue **264**, which is arguable even more attractive.

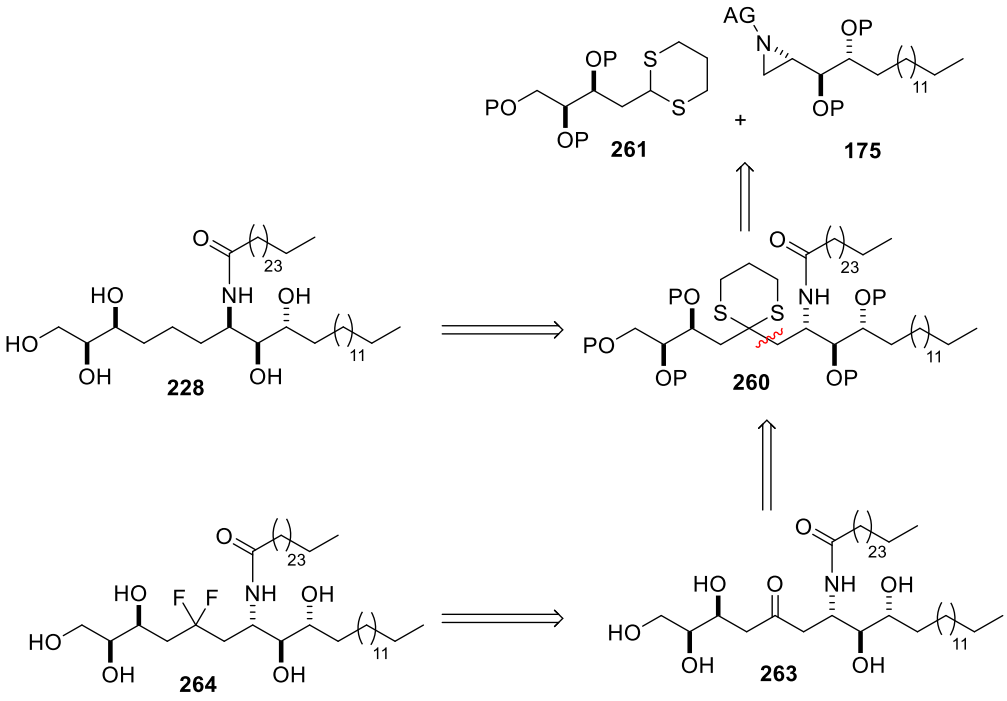

Scheme 3.25. Retrosynthesis of *C*-ThrCer

Conversion of alcohol **235** to iodide **265** was achieved using PPh_3 and imidazole in the presence of I_2, to yield the desired product in 97%. This primary alkyl iodide **265** proved to be stable and could be stored at –4 °C for at least 6 months without noticing (significant) decomposition. Following conditions used by Enders *et al*., reaction of iodide **265** with 2-lithio-2-TMS-1,3 dithiane in the presence of HMPA in THF yielded a mixture of dithiane products, TMS-dithiane **266** in 52% yield and dithiane **267** in 18% yield. TMS-dithiane **266** was deprotected to afford dithiane **267** in quantitative yield using TBAF. 2-Lithio-1,3 dithiane was also used as the nucleophile in a reaction with iodide **265** but provided lower yield (39%) of the desired dithiane **267**. Thus a solution of dithiane **267** in THF:HMPA at – 78 °C was treated with *t*-BuLi. After 15 min, aziridine **193** was added, however no reaction was seen and both starting materials were recovered in quantitative yield. The reaction was repeated using *n*-BuLi as the base and by performing the reaction at higher temperatures (up to –30 °C) but still no reaction was observed (Scheme 3.26.).

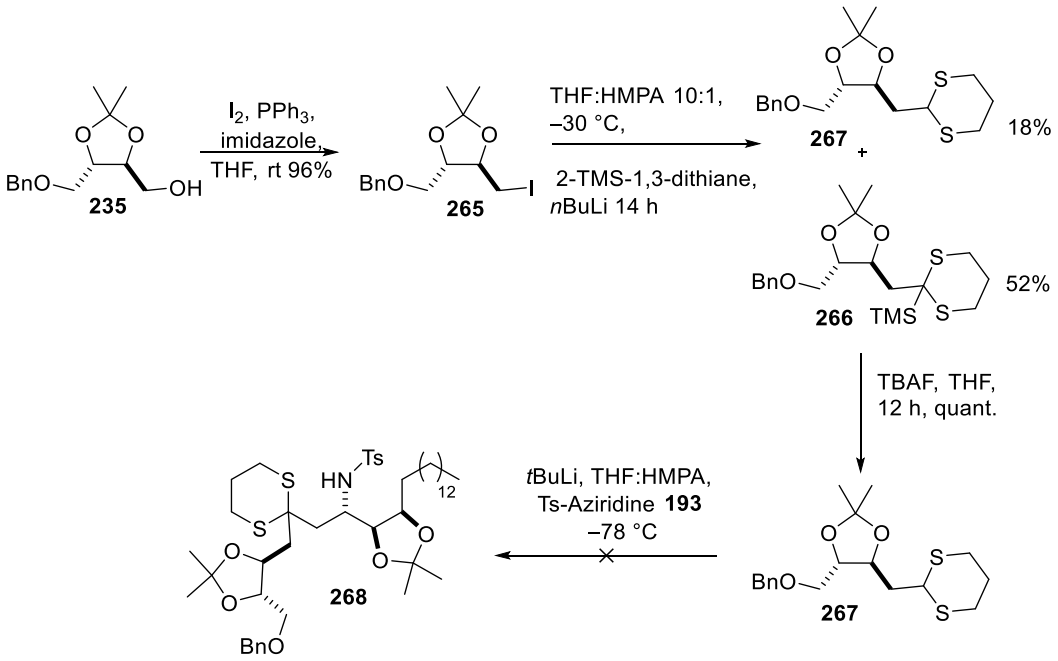

Scheme 3.26. Attempted synthesis of dithiane **268** *via* ring-opening of aziridine **193** with dithian **267**.

To investigate whether unreactivity of the aziridine or the nucleophilicity of the alkyl dithiane were the problem with the lack of product formation, we tested the ring opening of Ts-aziridine **193** with 2-lithio-2-TMS-1,3-dithiane. The desired ring-opened product, phytosphingosine TMS-dithiane **269** was isolated in 56% yield; however, the reaction was noticeably sluggish, even at –30 °C, required an excess of 2-lithio-2-TMS-1,3-dithiane and the reaction mixture still contained starting material after reacting for 24 h. The reaction was also performed in the presence of HMPA as a co-solvent; however, whilst this change led to full consumption of starting material, a complex mixture of products was observed. These observations suggest inclusion of HMPA is detrimental for the ring-opening of the aziridine coupling partner. Deprotection of TMS-dithiane **269** was achieved using TBAF to yield dithiane **270** in 87% yield (Scheme 3.27.).

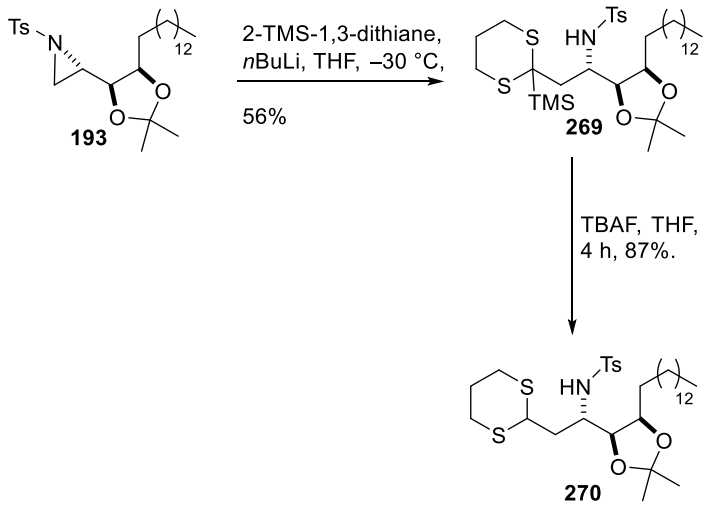

Scheme 3.27. Ring-opening of aziridine **193** with 2-lithio-2-TMS-1,3-dithiane.

3.10.6. Future Work

These studies were performed on small quantities of material and time constraints prevented further optimisation. Future work on the synthesis of *N*-ThrCer **227** would involve repeating the synthetic sequence in order to bring through enough material to elucidate the position of the C_{26} acyl chain in the final molecule. If it transpired that the acyl chain has reacted on the secondary amine, an alternative approach will be required. Another potential route to *N*-ThrCer could be to first convert amine **246** to a secondary amine such as a PMB amine, providing this amine is able to ring-open the Ns-aziridine **192**, the selective acylation should not present a problem. Moreover, PMB group might also undergo deprotection along with the acetal groups under acidic conditions, if not a dimethoxy benzyl protecting group could be used (Scheme 3.28.).

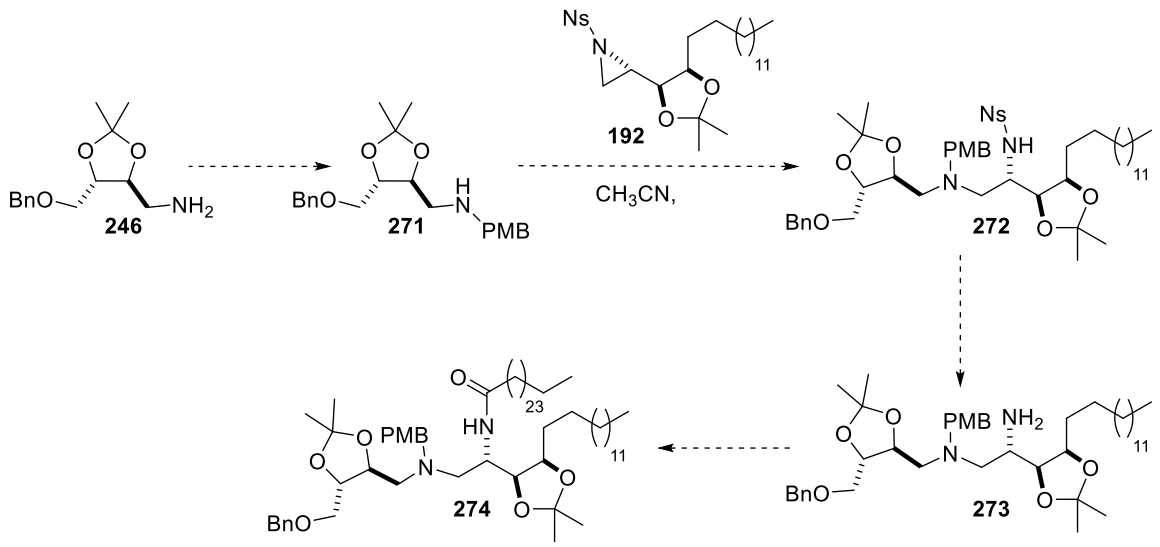

Scheme 3.28. Potential alternative route to *N*-ThrCer.

Due to the difficulty in removing the benzyl group in the final step of the S-ThrCer synthesis the use of an alternative protecting group such as a TBDPS group could be used. Removal of the silyl ether could then be achieved using TBAF (Scheme 3.29.). A previous co-worker has investigated the use of a TBDPS-protected threitol **275** in the ring-opening of Ts-aziridine **193**. In this case, the reaction led to a complex mix of products. However, this may not be an issue under the milder conditions needed for the ring-opening reaction using the thiolate.

Scheme 3.29. Using a silyl protecting group on *S*-ThrCer precursor would allow for selective deprotection conditions to the desired thioether product **226**.

As HMPA has proven detrimental when used as a co-solvent in the ring-opening reaction with our Ts-aziridine **193**, attempts to retry the ring-opening with threitol dithiane **267** without HMPA

present. If the reaction still does not proceed, we can turn our attention to phytosphingosine dithiane **270** as we have seen the efficacy of iodide **265** to displacement by a lithio-dithiane

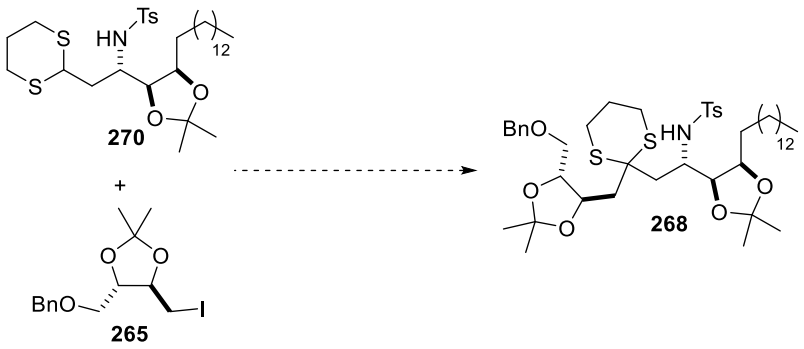

Scheme 3.30. Potential route to dithiane **268** using an electrophilic threitol coupling partner **265** and nucleophilic phytosphingosine based coupling partner **270**.

Chapter 4

Synthesis of glycolipid and ceramide analogues incorporating a photoreactive group in the acyl chain

4. Synthesis of glycolipid and ceramide analogues incorporating a novel acyl chain with a terminal photoreactive group

4.1. Introduction

Incorporating covalent ligands such as fluorophores and cross-linkers into biological systems has been key to furthering our understanding of key processes and pathways. Singh *et al*. first introduced the concept of photoaffinity labelling (PAL) in 1962.[155] PAL involves the use of a ligand which has been modified to contain a photoreactive group (PhG). Following irradiation of the photoreactive group at a certain wavelength, a reactive species is formed which reacts with molecules in close proximity. In this way, a ligand can be covalently bound to a protein or other biomolecule with which it is interacting. There are three major types of PhG that have been used in photoaffinity labelling. These include benzophenones **277**, arylazides **278**, and diazirines **279** (Figure 4.1.). The use of a particular PhG is based on certain criteria. Following introduction of the PhG, the modified ligand should still structurally resemble and behave like the starting ligand in order that it binds similarly. The PhG should have an activation wavelength which does not affect other parts of the system under study. While arylazides can be prepared easily, the short wavelength (250–350 nm) needed to effect photo-activation can cause significant damage to the protein. Diazirines are the smallest PhG and are activated upon irradiation at a wavelength of 350–380 nm, which is generally not harmful for biological systems. They are however more difficult to synthesise. Benzophenones are also activated with light of a wavelength around 350–360 nm. Moreover, they are a relatively robust functionality, stable in most organic solvents and can be incorporated readily into a synthetic sequence. However, the benzophenone group is sterically bulky compared to arylazides and diazirines and the need for longer irradiation times can lead to non-specific binding and potentially damage to the biomolecules under study.[156-159]

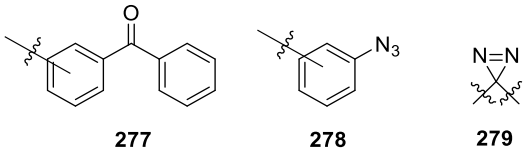

Figure 4.1. Benzophenones, arylazides, and diazirines as photoreactive functional groups

Following irradiation, the benzophenone group generates a reactive triplet carbonyl state **280** This is achieved by intersystem crossing from an n→π* singlet excited state to an energetically similar π →π* triplet state which quickly decays to the lower energy n→π* triplet excited state. The oxygen, which now has an unpaired electron acts as a radical and can abstract a proton from the neighbouring receptor, to yield a receptor radical **282** and alcohol radical **283** which can form a covalent bond to yield the crosslinked compound **284** (Scheme 4.1.)[160]

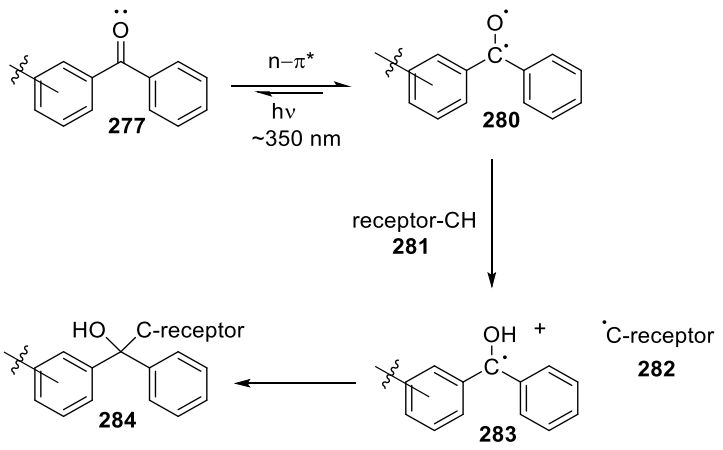

Scheme 4.1. Bioconjugation of the benzophenone functional group

Previous work within the group involved the synthesis of a series of α-GalCer analogues **285**–**292** (Figure 4.2.) which contained an acyl chain of differing lengths, terminating with a benzophenone group. As the hydrophobic tails of the glycolipid bind in the A′ and F′ pockets of CD1d, it was postulated that the benzophenone acyl chains would fit in the A′ pocket with the potential of the benzophenone group to cross-link with the protein to form a glycolipid/protein covalent complex. Because of the non-covalent nature of the interaction between the glycolipid and the CD1d protein, the glycolipid–protein complex is not stable and dissociation of the latter as well as displacement of the glycolipid by natural inhibitors *in vivo*, is very likely and results in loss of activity. A covalent interaction between the two is desired in order to create a long-lived CD1d protein/ glycolipid complex, hence increasing its stability and maintaining potent *i*NKT-cell activating properties

All compounds were shown to activate *i*NKT cells in a CD1d-dependent manner and of these compound **290** (C11:BP) showed the highest potency as the free molecule.

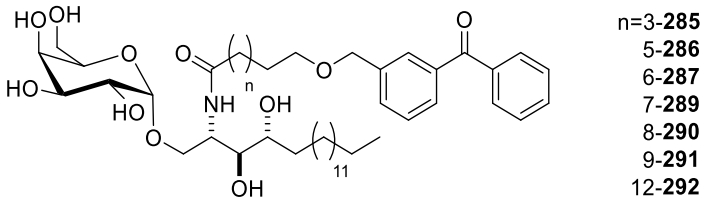

Figure 4.2. Range of benzophenone containing α-GalCer analogues

The benzophenone containing series has been shown to form stable covalent adducts. Figure 4.3. shows the difference in optical density before and after a wash both pre- and post exposure to the activating wavelength. As seen using optical density (OD), prior to activation of the benzophenone, the compounds are bound until a wash is done. However, post-

irradiation there is no reduction in OD, indicating formation of a covalent bond (n=3). Work is currently ongoing to determine the exact site of formation of the covalent bond.

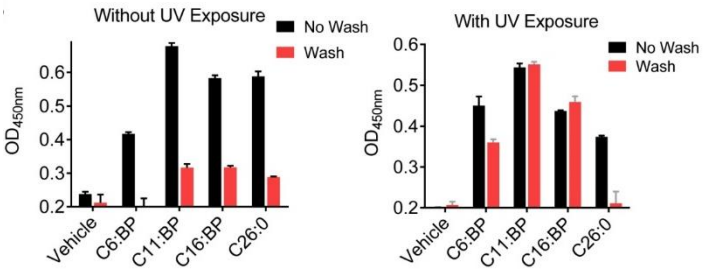

Figure 4.3. Following UV irradiation, no change in OD after wash. Both non-covalent and covalent complexes of the galactosyl ceramides with CD1d were coated on high binding plates and washed intermittently to allow dissociation of the lipids. Complexes bound to the plate were detected using L363 anitbody

Using C11:BP **290** as the model we envisioned the synthesis of its analogue **293** which did not contain an oxygen atom in the acyl chain and to test whether the substitution of the oxygen to a carbon had an effect on activity. While the ether linkage was initially chosen due to the synthetic ease, introducing an oxygen to the chain decreases hydrophobicity, which may alter binding within the hydrophobic pocket of CD1d. Formation of a more hydrophobic tether which should more closely resembles the all carbon acyl chain in α-GalCer would therefore be a better model. To this end, reaction of acid **294** with amine **295** would deliver our target molecule, glycolipid **293**

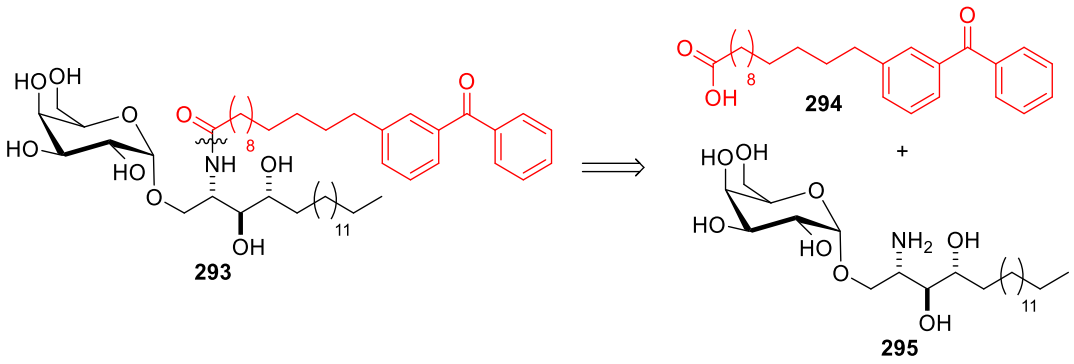

Figure 4.4. Glycolipid **293** formed by reaction of acid **294** with amine **295**

4.2. Retrosynthesis of acid (294)

Retrosynthetic analysis of acid **294** alongside a comparison with the original acid **296** used in the synthesis of glycolipid **290** is shown in Scheme 4.2. The original acid can be cleaved at the benzylic ether to give 11-bromo undecanoic acid **297**, which is commercially available, alcohol **298** which was synthesised from commercially available 3-methylbenzophenone in two steps. The acid **294** used for the new compound would need to be thirteen carbons in length to match the thirteen-atom chain of acid **296**. Introduction of an alkyne (**300**) would open up a disconnection to provide alkyne **301** and a 3-halobenzophenone **302**, which could be coupled under Sonagashira conditions. While 3-iodobenzophenone would be likely the more reactive starting material we chose to use 3-bromobenzophenone which is cheaper and commercially available. Alkyne **301** would be synthesised from 11-bromoundecanoic acid **303** *via* an alkynylation.

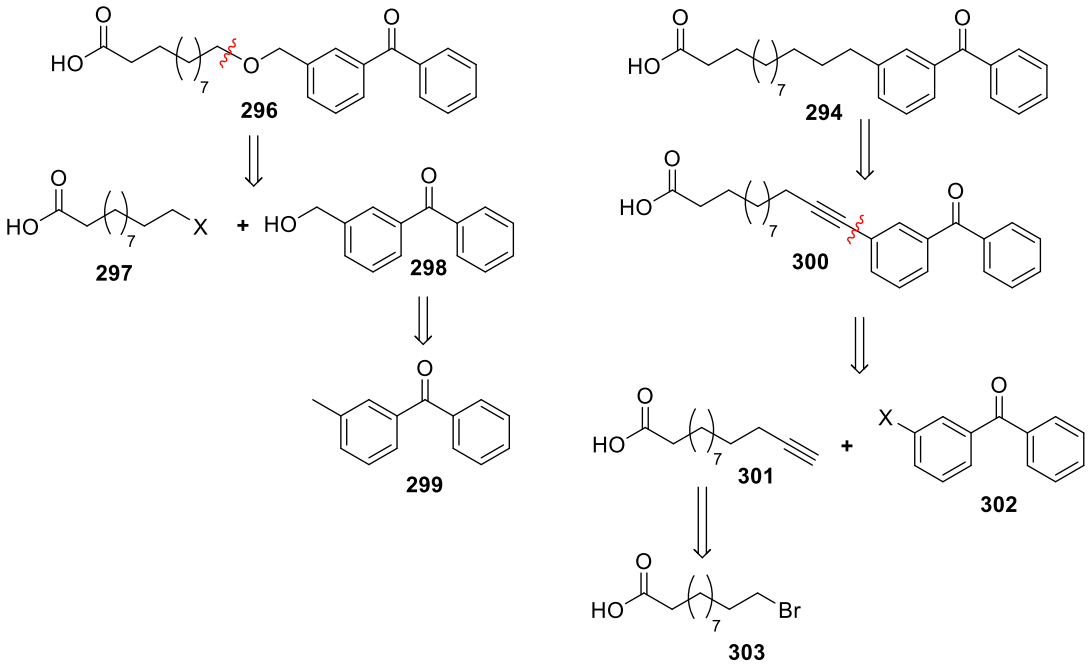

Scheme 4.2. Retrosynthetic analysis of acid **294** and acid **296**.

4.3. Synthesis of carboxylic acid (294)

Reaction of lithium (TMS)acetylide with 11-bromoundecanoic acid at –30 °C in THF:HMPA yielded TMS-alkyne **304** in 88% yield and terminal alkyne **301** after treatment with TBAF. Attempts to form alkyne **301** directly using 2.5 equivalents lithium acetylide ethylenediamine complex, were unsuccessful and just led to recovery of the starting bromo acid. For primarily practical reasons, acid **301** was converted into the corresponding methyl ester **305** by treatment with methanol in the presence of H_2SO_4.

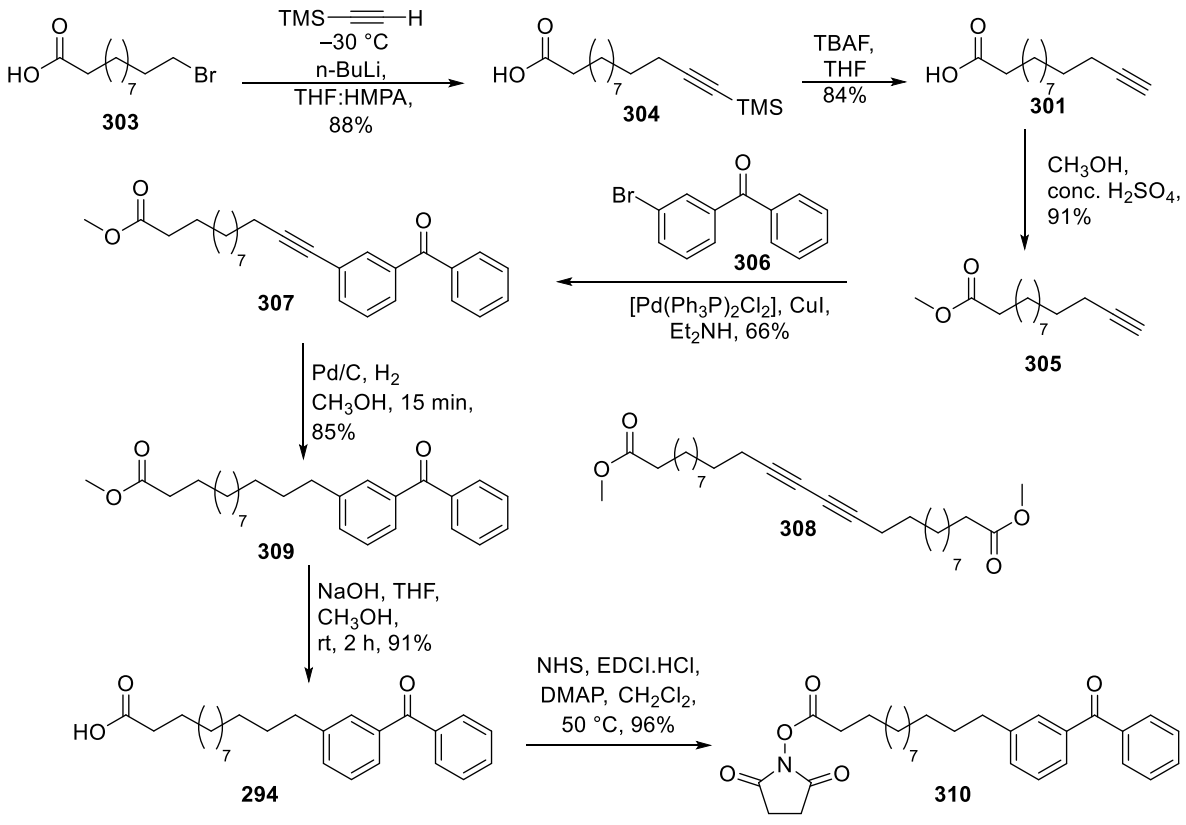

Scheme 4.3. Synthesis of acid **294**

Following Sonagashira coupling conditions used by Queseda *et al.* on similar reactants,[161, 162] coupling of alkyne **305** with 3-bromobenzophenone **306** in the presence of bis(triphenylphosphine)palladium chloride and copper(I) iodide afforded alkyne **307** in 66%

yield. Deoxygenation of the diethylamine solvent was important to prevent formation of the Glaser homocoupling diyne product **308**. Next, hydrogenation of the alkyne using Pd/C provided ester **309** in 85% yield (Scheme 4.3.).

The short reaction time for the alkyne reduction was critical to avoid reduction of the benzophenone, which we had observed in an alternative approach in which the carboxylic acid/ ester was replaced with a benzyl-protected alcohol (Scheme 4.4.). Whilst benzyl ether **314** was prepared uneventfully, attempted debenzylation and alkyne reduction led to a range of reduction products **316**–**318**, none of which was the desired alcohol **315**. Whilst hydrogenation of the alkyne proved to be rapid, the longer reaction time required to effect hydrogenolysis of the benzyl ether also led to reduction of the benzophenone to alcohol **317** and methylene derivative **318** as evidenced by resonances in the ^{1}H NMR due to the presence of CHO*H* and C*H*OH in **317** and CH_2 in **318** (Scheme 4.4.).[6]

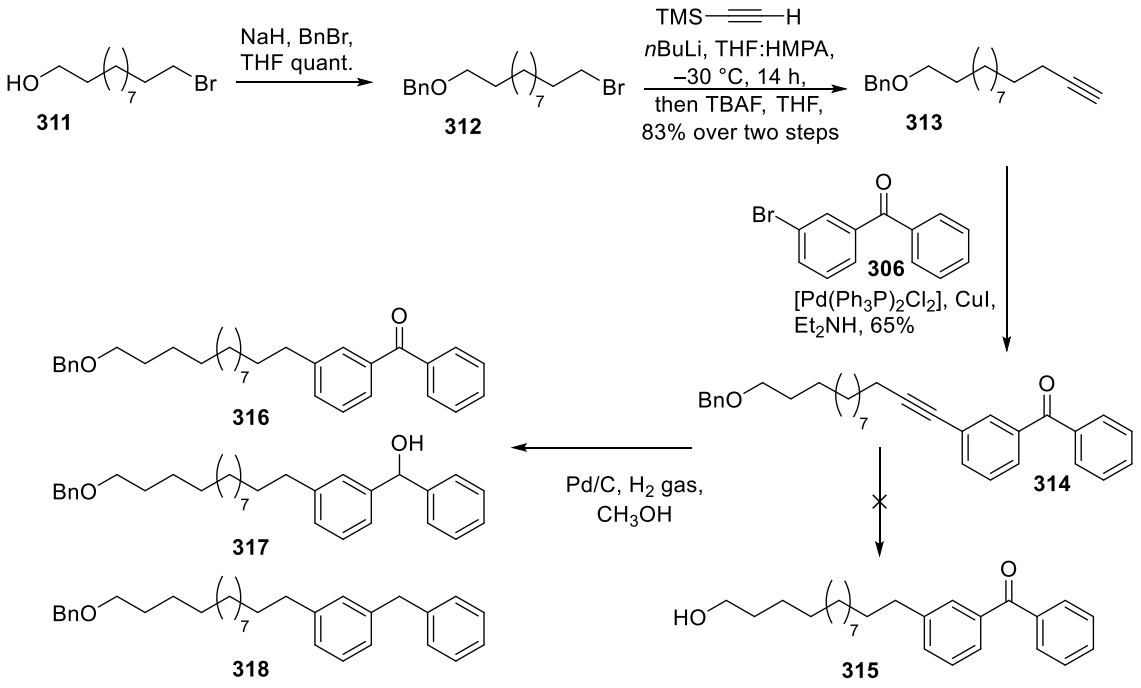

Scheme 4.4. Attempted synthesis of alcohol **315**

[6] Selected resonance: **317** [2.25 (1H, d, *J* 3.0, CHO*H*), 5.82 (1H, d, *J* 3.0, C*H*OH)], **318** [3.96 (2H, s, CH_2)]

With ester **309** in hand, saponification NaOH (aq) in MeOH:THF provided Acid **294** which was converted to NHS ester **310** in 96% yield. This activated ester could be stored at – 4 °C for at least six months without any evidence of decomposition (Scheme 4.3.).

4.4. Synthesis of ether-linked carboxylic acid (296)

Ether-linked carboxylic acid **296** was also synthesised. Starting with 3-methylbenzophenone **299**, radical bromination using *N*-bromosuccinimde in the presence of benzoyl peroxide as the initiator yielded bromide **319**, which was immediately hydrolysed without purification using $CaCO_3$ in a H_2O:dioxane mixture to yield alcohol **298** in 53% yield over two steps. Reaction of 11-bromo undecanoic acid **303** with three equivalents of the sodium alkoxide of alcohol **298** effected etherification to provide acid **296**. It was necessary to perform this reaction under dilute concentration (0.05 M) as the reaction mixture was too viscous at higher concentrations. An excess of the alcohol was also important to ensure complete consumption of 11-bromo undecanoic acid **303** which otherwise was difficult to separate from the product. Acid **296** was then converted to NHS ester **320** under the standard conditions. Separation of the desired NHS ester **320** from any NHS ester of the unreacted bromo acid which had been carried through from the previous reaction was readily achieved by flash column chromatography (Scheme 4.5.).

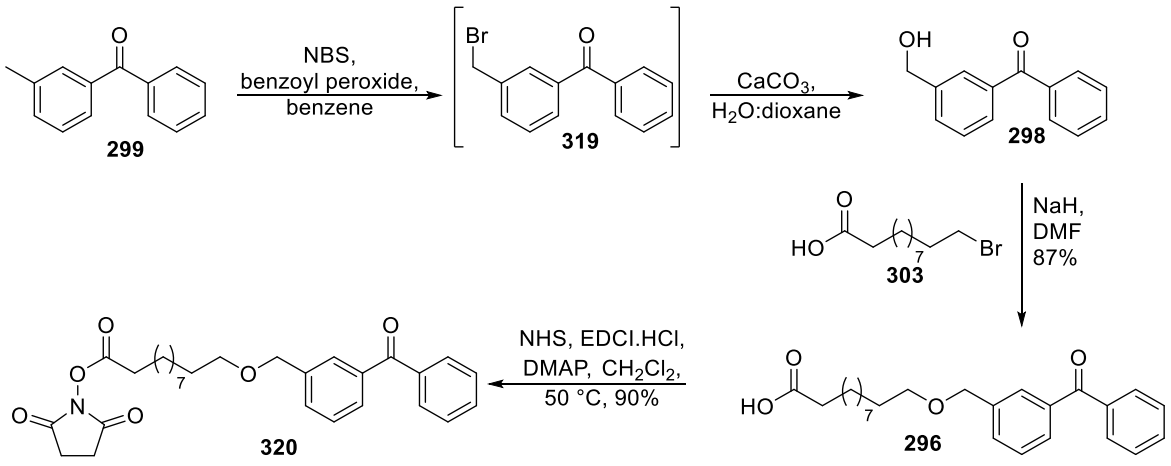

Scheme 4.5. Synthesis of acid **296**

4.5. Synthesis of glycolipid amine coupling partner (295)

With both acids in hand the next step was to synthesise the glycolipid amine coupling partner **295**. A route to a protected analogue (**97**) of glycolipid **295** was already available in the group,[52] however, we decided upon the synthesis of glycoside **321** in which an isopropylidene acetal was used to protect the vicinal diol in the phytosphingosine fragment. Previous experience had revealed that removal of the TBDMS protecting groups from ThrCer-6 analogue **213** was often sluggish under the TFA global deprotection conditions on similar substrates. Trimethylsilyl ethers were used as the protecting group for the galactose sugar head group due to their ease of protection/deprotection as well as the 'arming' effect that silyl ethers impart on the donor during glycosylation reactions. A Boc protecting group was chosen for the phytosphingosine nitrogen due to its potential for deprotection under acidic conditions. The synthesis of glycoside **321** would therefore allow for a one-step global deprotection under acidic conditions.

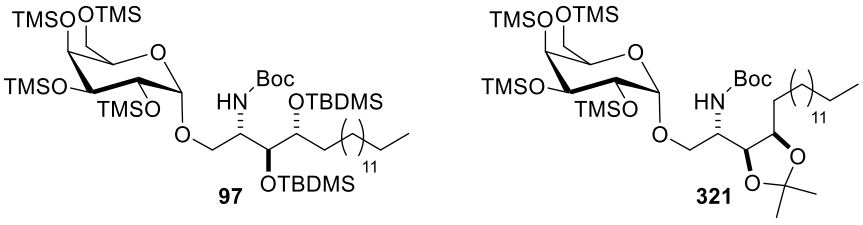

Figure 4.5. Protected analogues of amine **295**

4.5.1. Synthesis of protected phytosphingosine acceptor (321)

Starting with phytosphingosine **179**, chemoselective Boc protection of the amine was achieved using Boc_2O in the presence of Et_3N to obtain carbamate **322** in 96% yield. This compound can be recrystallised from hot EtOAc avoiding the need for purification by column chromatography. Next, selective protection of the primary alcohol using TBDPSCl in pyridine gave silyl ether **323** in 92% yield. While acceptor alcohol **325** can be synthesised from carbamate **322** in one step without the need for protection of the primary alcohol, we found that silyletherification of the primary alcohol reduced the number of side-products in the acetal forming step and an improved yield of the final acceptor target.[7] From a practical standpoint, incorporating a TBDPS ether also imparted some U.V. activity on the product which allowed for easier monitoring of the product by TLC. Silyl ether **323** was reacted with acetone under acidic conditions to yield acetal **324** in 84% yield. Fluoride mediated deprotection of the silyl ether provided target acceptor **325** in 88% yield.

[7] While the potential for the formation of the 1,3-acetonide product **326** (and in some cases the 1,4-acetonide **327**) can be reduced through longer reaction times to give the 1,2-acetonide as the thermodynamic product, this also drives the formation the bis acetal hemiaminal product **328**

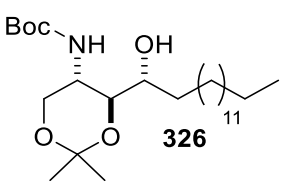

326

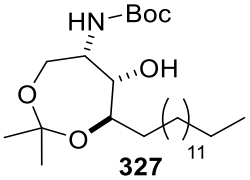

327

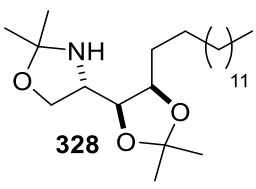

328

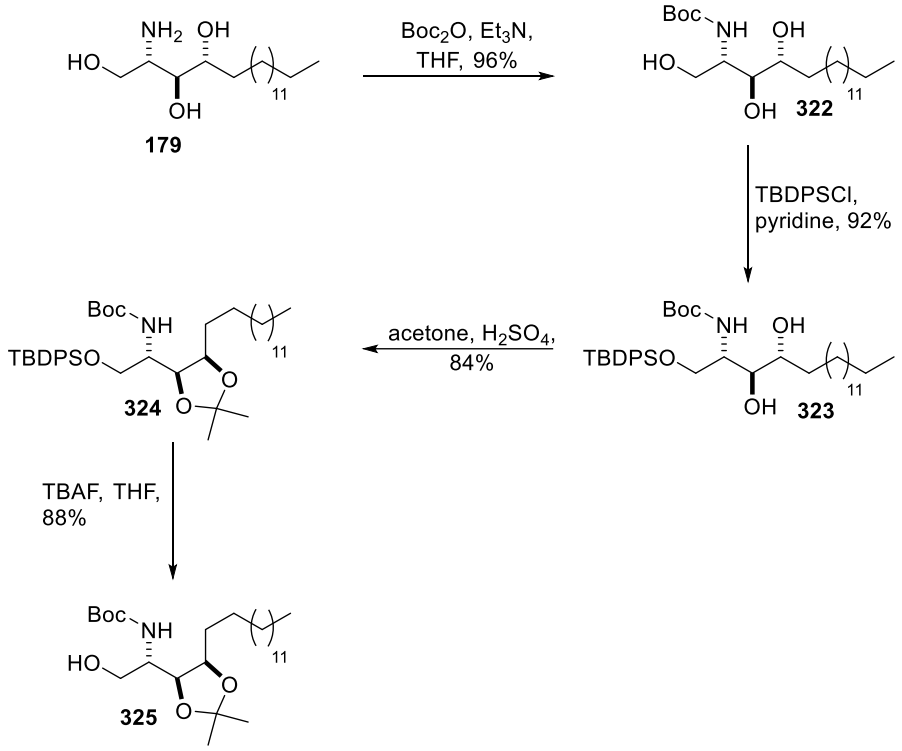

Scheme 4.6. Synthesis of target acceptor **325**

4.5.2. Synthesis of Benzophenone-derivatised α-GalCer analogues

TMS protection of galactose **329** using TMSCl in pyridine and HMDS as co-solvent gave per-TMS galactose **330** in excellent yield. Following the work developed by Gervay-Hague, conversion of the per-TMS sugar to glycosyl iodide **95** was achieved using TMSI in CH_2Cl_2. This product was used directly in the key glycosylation reaction. Acceptor **325**, TBAI and Hünig's base were stirred over activated 3 Å molecular sieves for 30 minutes prior to addition of glycosyl iodide **95**. Use of an excess of iodide **95** ensured full consumption of the starting acceptor and formation of a new product based on TLC analysis of the reaction mixture. Work-up involved trituration of the ammonium salts with Et_2O which yielded a mixture of phytosphingosine glycosylation product **321** and excess sugar. This mixture was then treated with acid using $CHCl_3$:MeOH:HCl (40 mL total volume, 10:10:3) which formed a homogenous

solution. After 15 minutes, $CHCl_3$ (17.5 mL) and H_2O (7.5 mL) were added and the solution separated into two layers, with the organic compounds in the organic layer. Following concentration of the organic layer under reduced pressure, the residue was purified to afford glycoside **331** in 48% yield and glycoside **332** in 28% yield. Both products were isolated as the α-anomer; the β-anomer was not observed by analysis of these products by NMR spectroscopy. Deprotecting the glycosylation product using the 10:10:3 method allowed separation of the majority of the excess galactose sugar which was water soluble and therefore partitioned into the aqueous layer.

Glycoside **332** was treated with TFA for 30 minutes to afford glycoside as its ammonium trifluoroacetate salt. As both acid coupling partners were very similar we investigated the acylation under two different conditions. For the synthesis of target glycoside **333**, glycoside **295** was treated with NHS ester **320** in the presence of Et_3N in THF to give amide **333** in 48% yield. Acylation of the ammonium salt of **295** using NHS ester **310** was performed in a solution of pyridine:H_2O (9:1); to provide a similar yield of 50% of the desired glycoside **334**. However, the purification was much easier using the pyridine:H_2O method. Et_3N was difficult to remove under reduced pressure and purification using column chromatography also proved difficult as Et_3N co-eluted with the product.

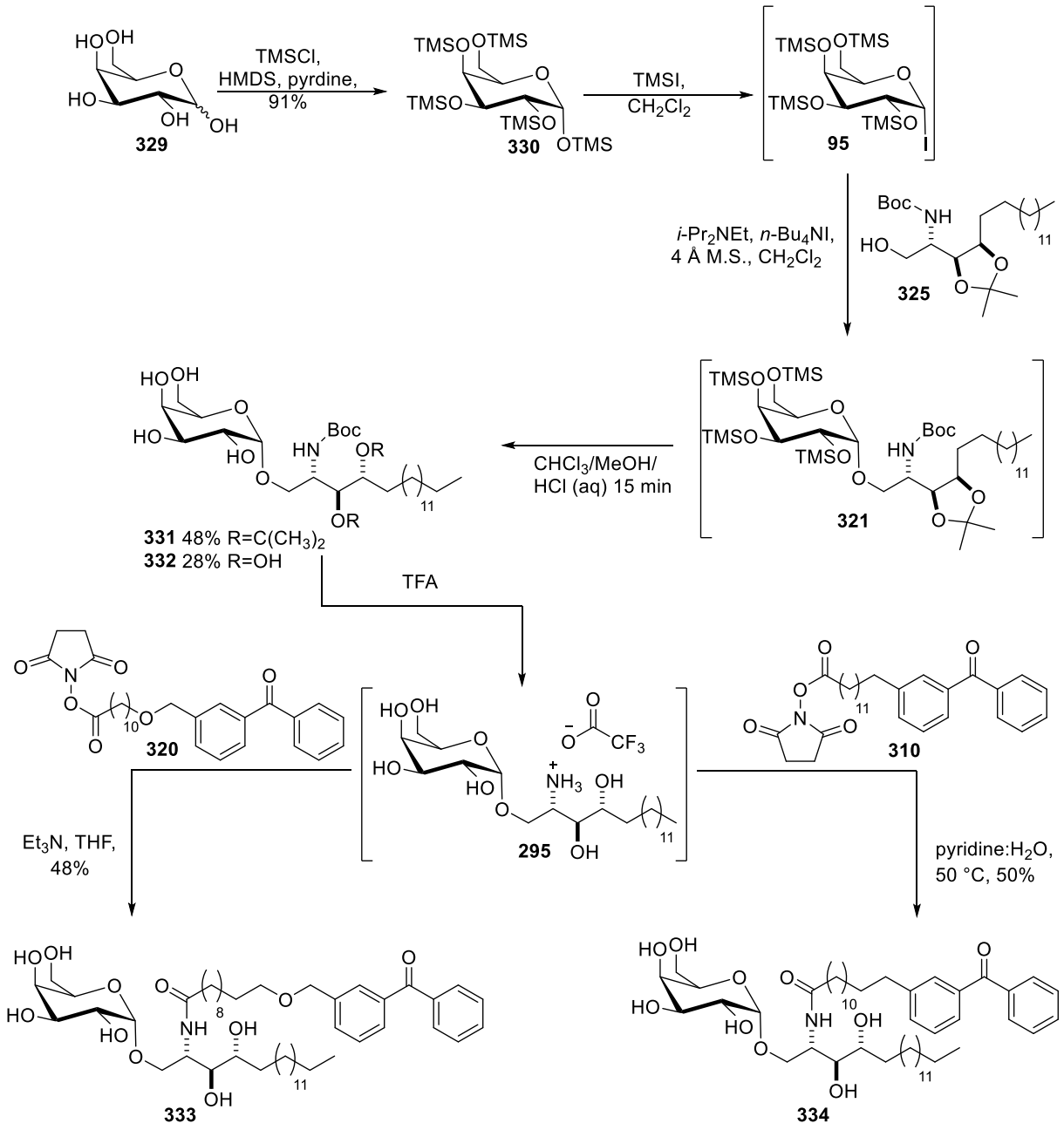

Scheme 4.7. Synthesis of Benzophenone-derivatised α-GalCer analogues **333** and **334**

4.6. Conclusions and Future Work

These compounds have been submitted to Prof. Steven A. Porcelli to comparatively study their biological properties and to determine whether the replacement of the oxygen atom with a methylene group in the acyl chain effects binding and activity towards *i*NKT cells. If the effects of the new compound are beneficial then the new acyl chain will be used going forward in the synthesis of the next generation of analogues including analogues containing the cyclic threitol polar head group. Further studies involving the development of a crystal structure of the ligand–CD1d covalent complex would also help elucidate the area of binding, and mode of conjugation of the ceramide to the CD1d

4.7. Synthesis of alkyne and azide benzophenone ceramides to for use in development of high throughput

Alkyne–azide [3+2] dipolar cycloaddition reactions have previously been used in the synthesis of analogues of α-GalCer, including substituting the amide bond with a triazole **149**.[163] Another synthesis involved the substitution of the 6-*O* position of the galactose sugar with an azide **335**, which was subsequently used to "click" with a range of alkynes.[164]

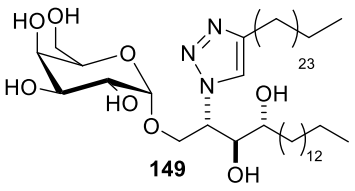

149

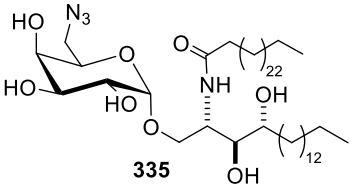

335

More recently however, and more appropriate for our needs, two syntheses have been published which have used Copper(I)-catalyzed Azide-Alkyne Cycloaddition (CuAAC) in the synthesis of glycolipid analogues which contain triazole groups at the pseudo-anomeric position (Scheme 4.8). Gorantla *et al*. reacted an azido-based phytosphingosine **337** with *N*-

propargyl-2-pyrrolidinone **336** using CuI and Hünig's base in MeCN to give triazole **338** in the key coupling step (Scheme 4.8, A).[165] McDonagh *et al* also used CuI and Hünig's base in MeCN in their reaction however, they also required MW conditions to drive the reaction as they used a less reactive α-glycosyl azide **339** and an alkyne based phytosphingosine **340** (Scheme 4.8, B)

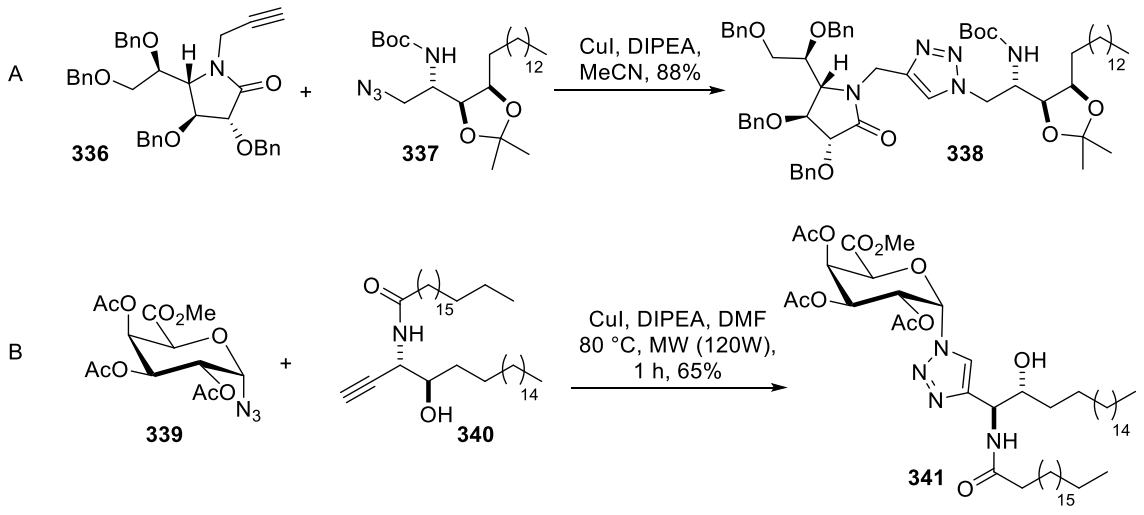

Scheme 4.8. Published reactions using "click" chemistry to form a triazole at the anomeric position of α-GalCer analogues

Using the previously developed benzophenone containing analogues, which covalently bond to CD1d, we aimed to develop a high-throughput method for the synthesis and evaluation of potentially *i*NKT cell activating, triazole containing compounds using azide **342** and alkyne **344** as the base molecules (Figure 4.6.).

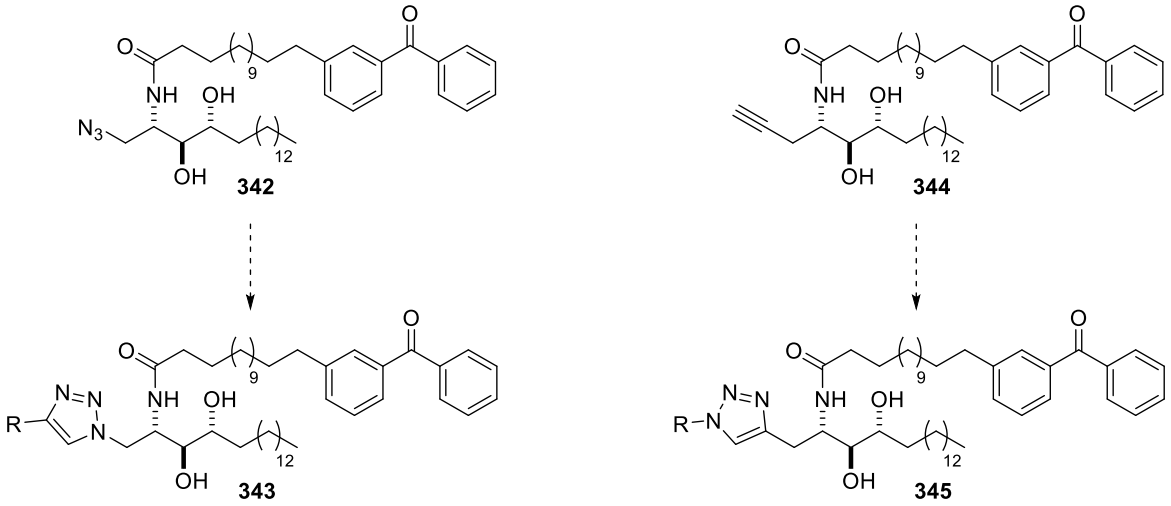

Figure 4.6. Azide **342** and alkyne **344** as precursors towards a novel library of triazole containing ceramides

Scheme 4.9. shows how azide **342** and alkyne **344** can be used in a high-throughput screening method. Starting with a 96 well plate, CD1d protein is bound to each well followed by addition of azide **342** or alkyne **344**. At this stage the ligand is only bound by electrostatic and hydrogen bonding interactions and can be washed away. However, activation using U.V. at around 350 nm will yield the covalently bound molecule. At this stage, a range of alkyne and azide containing compounds, with the potential for hydrogen bonding, can be reacted using Alkyne–azide [3+2] dipolar cycloaddition reaction conditions, to give the target triazole containing compounds. The high selectivity nature of the cycloaddition reaction, along with the fact that azides and alkynes are not found in proteins has led to the use of “click” chemistry being used to further functionalise biomolecules.[166] The triazole containing, CD1d derived compound can then be measured for its activity towards *i*NKT cells. Whilst the newly synthesised compounds won’t overlap and have the same hydrogen bonding interactions formed between the TCR and the galactosyl polar head group, the potential to yield a large library of compounds could help to find another area of the TCR to bind with and induce an immune response.

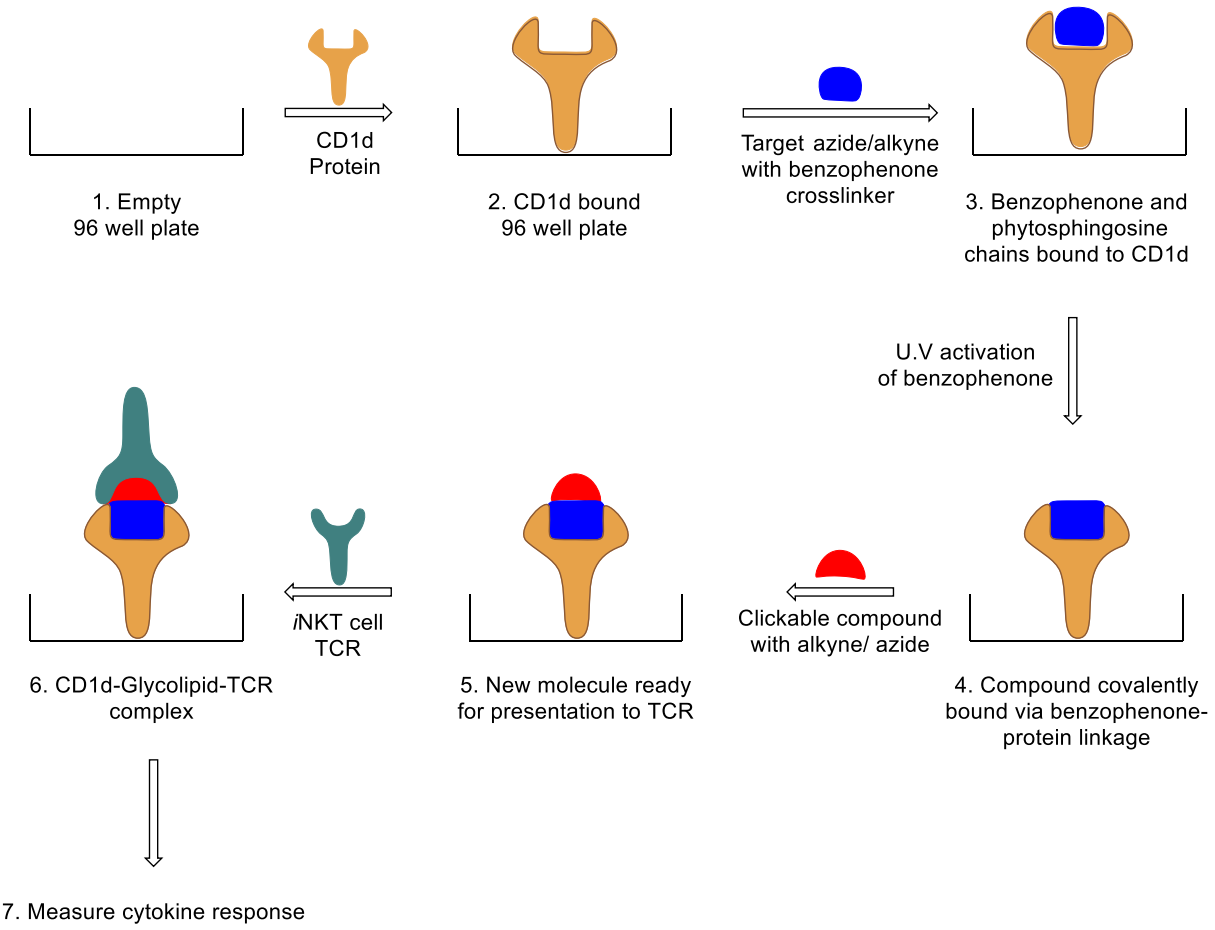

Scheme 4.9. Schematic view of the potential for high-throughput development of a large library of *i*NKT cells activating compounds

4.7.1. Retrosynthetic analysis

Starting with triazoles **343** and **345**, “retro” click of these molecules provides azide **342** and alkyne **344** along with a range of azides and alkynes. Disconnection of the amide bond of azide **342** and alkyne **344** gives amine **346** and amine **347**, respectively, and the previously synthesised benzophenone acid **294**. Both amine **346** and amine **347** can be synthesised from activated aziridine **175** which can be accessed in five steps from phytosphingosine **179**.

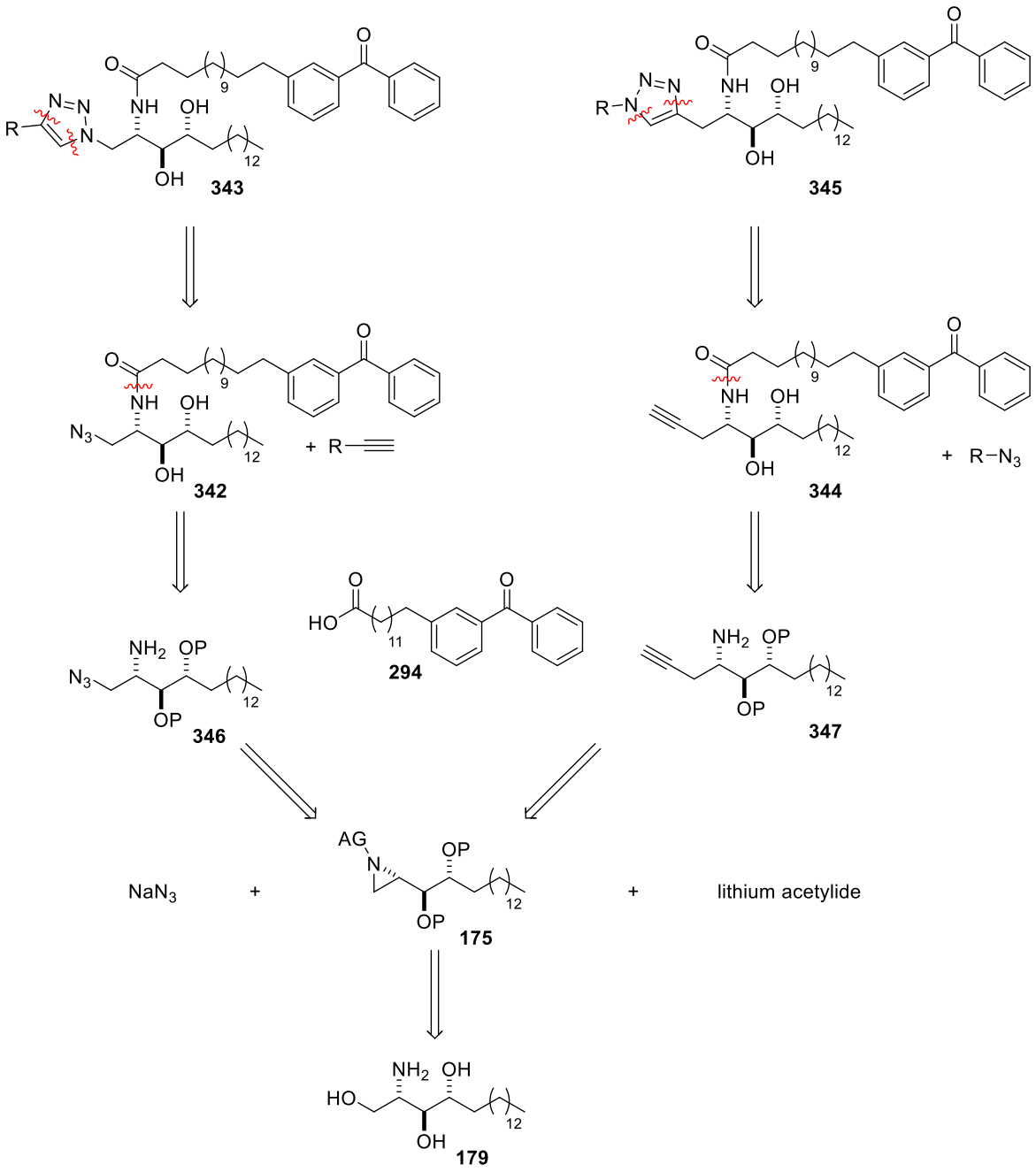

Scheme 4.10. Retrosynthetic analysis triazole containing ceramide analogues

4.7.2. Synthesis of azido ceramide (342) *via* Ns-aziridine ring-opening

Ring opening of nosyl aziridine **192** using NaN_3 in MeCN:H_2O proceeded uneventfully to give azide **348** in 72% yield. These conditions were developed by Bisai *et al*. for a range of Ts-aziridines; we have shown they extend to Ns-aziridines.[167] Harrak *et al*. also showed the successful ring opening of Ns-aziridine **192** using NaN_3 to give azide **348** in 85% yield.[130] They used a 9:1 mixture of MeOH:H_2O which led to an extended reaction time, taking 16 h rather than the 2 h needed using MeCN:H_2O. Denosylation using thiophenol in the presence of Cs_2CO_3 provided amine **349** in 83% yield. Cesium thiophenolate which is formed *in situ* reacts at the *ipso* position of the nosyl ring *via* a S_NAr reaction to give the desired amine **349** and a bis-aryl thioether bi-product which are easily separable. Next, acylation using NHS ester **310** afforded amide **350** in 76% yield. Having the molecule fully protected meant it was much easier to handle following the acylation and probably reflects the increased yield of this reaction. Finally, removal of the acetonide was achieved using TFA in CH_2Cl_2 to give target azide **342** in 56% yield. With target azide **342** in hand a test cycloaddition reaction was attempted using 4-pentyn-ol as a model alkyne. While the previously published syntheses of anomeric triazole containing compounds employed the used of CuI, DIPEA and MeCN, we chose to use conditions that would potentially be more suitable for reaction on biomolecules. Initial attempts employed conditions used previously in the group for Huisgen cycloaddition reactions with α-GalCer analogues which used a 1:1 *t*-BuOH:H_2O solvent mixture.[164, 168] No reaction was seen however, which we believe is due to solubility issues. The α-GalCer analogues used previously would be much more soluble in butanol than our azide. However, when the solvent mixture was changed to 2:1 H_2O:THF the reaction proceeded to give the desired triazole **351** in an excellent 90% yield.[169-171]

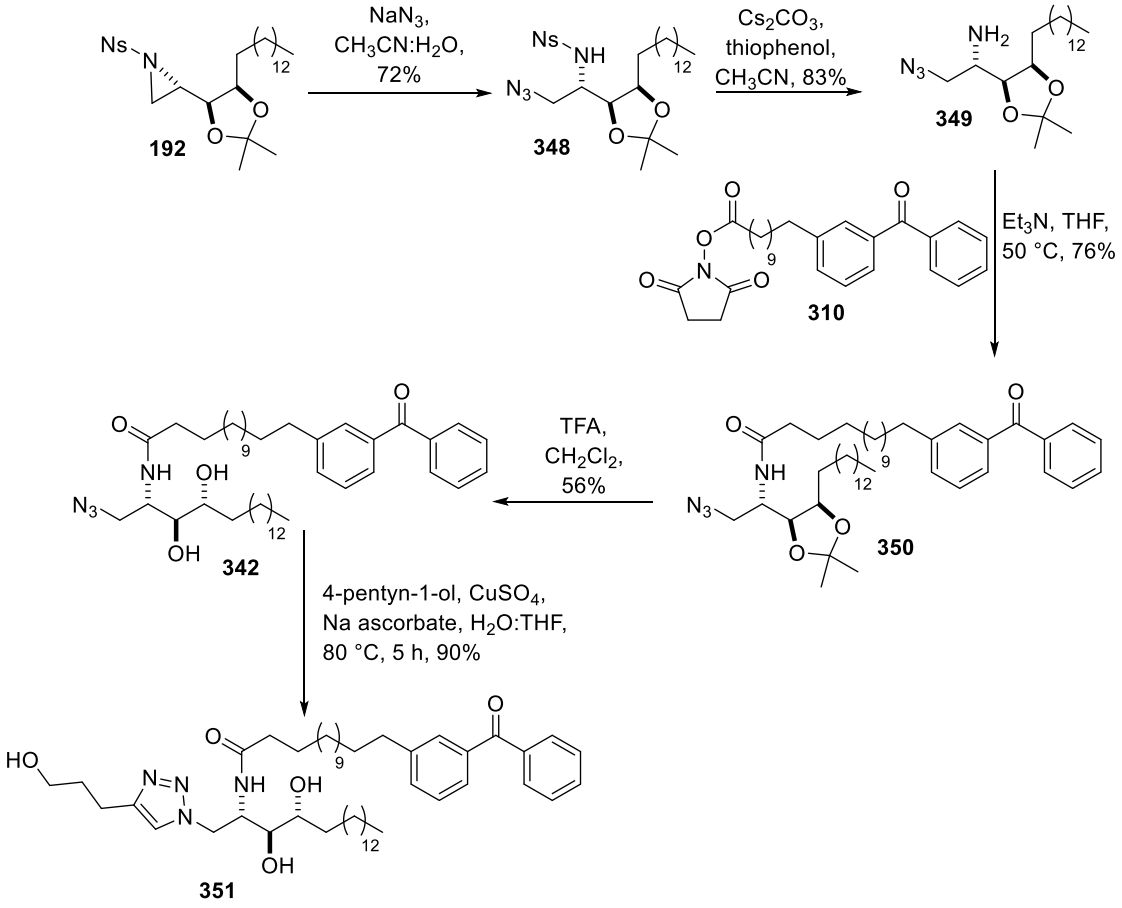

Scheme 4.11. Synthesis of triazole **351** *via* azido-ceramide **342**

As well as sodium azide, sodium cyanide was also used to ring open Ns-aziridine **192**. This afforded nitrile **352** in 64% yield using a MeCN:H_2O solution. The nosyl group was also removed from the nitrogen using cesium carbonate and thiophenol to give amine **353** in 92% yield (Scheme 4.12.). Future work on this project involves the development of tetrazole ring containing molecules *via* cycloaddition reaction with an azide.

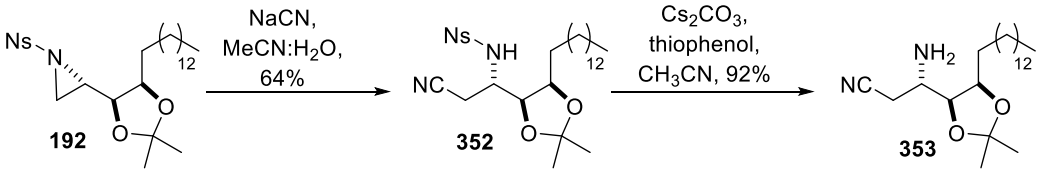

Scheme 4.12. Ring opening of nosyl aziridine using sodium cyanide followed by deprotection

4.7.3. Synthesis of alkynyl benzophenone ceramide (357) *via* Ns-Aziridine ring-opening

The synthesis of alkyne **344** was similarly achieved using Ns-aziridine **192**. While there is little literature precedent for the ring-opening of sulfonyl aziridines with lithium acetylides,[172, 173] reaction of Ns-aziridine **192** with the lithium acetylide of TMS-acetylene in THF:HMPA (10:1) at –78 °C alkyne **354** in 79% yield. The silyl group was removed using TBAF in THF to give alkyne **355** in quantitative yield. Denosylation under standard conditions afforded amine **356** in 77% yield. Acylation of amine **356** using NHS ester **310** provided amide **357** under the pyridine:H_2O conditions to afford the desired product in 77% yield. Acetal hydrolysis using TFA in wet CH_2Cl_2 yielded alkyne **344** in 85% yield. With the target alkyne in hand a test click reaction was performed: using the same conditions previously used for the synthesis of triazole **351**, 3-azidopentan-1-ol as the model azide reacted with alkyne **344** to give the desired triazole **358** in 90% yield (Scheme 4.13.).

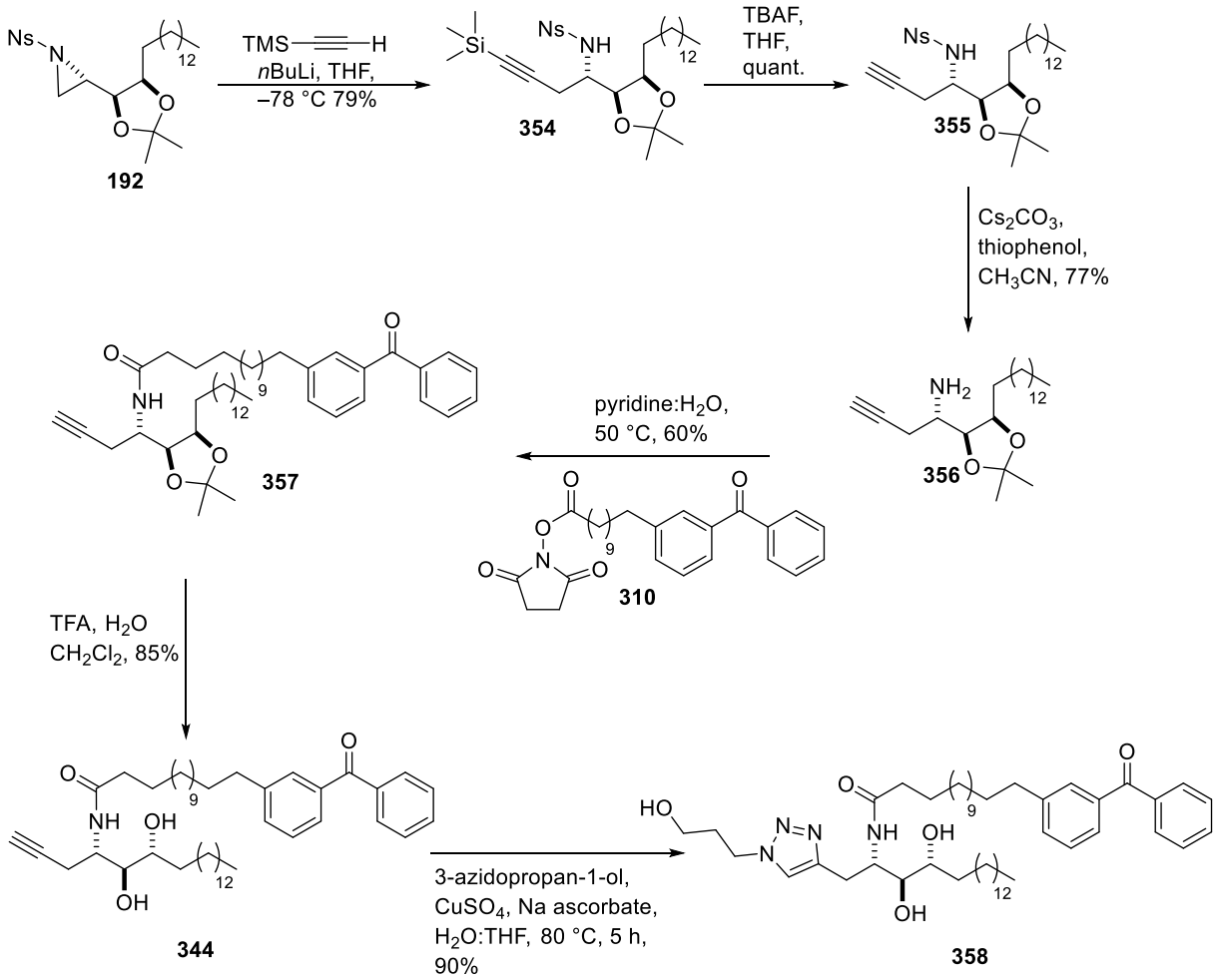

Scheme 4.13. Synthesis of triazole **358** *via* alkynyl-ceramide **344**

°

4.7.4. Conclusions and Future Work

Nosyl aziridine **192** have been successfully ring-opened with sodium azide, sodium cyanide and TMS-lithio acetylide with the azido and alkynyl compounds being subsequently acylated with acid **310** to give the target azide **342** and alkyne **344**. These compounds were then shown to be acceptable reactants towards CuAAc chemistry with successful coupling to yield triazoles **351** and **358**. The next step is the development of the covalent bonding of azide **342** and alkyne **344** with the CD1d molecule using U.V. irradiation and to test whether both the azide and alkyne functional groups are unaffected by the cross-coupling procedure. Following successful cross-coupling, design and optimisation of the “click” reaction will be necessary. Due to the potential for the copper source to interact with the biomolecule being tested, ligands such as TBTA **359** are used to coordinate and stabilise the copper and as we have seen solvent effects also play a role in the success of the reaction.

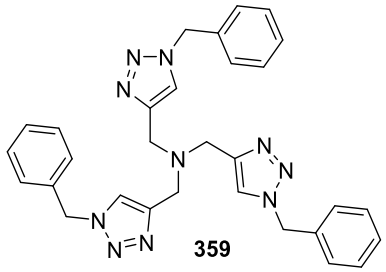

359

Chapter 5

Experimental

5. Experimental

5.1. Instrumentation

Infra-red spectra were recorded neat as thin films on Varian 660-IR FT-IR spectrometer. The intensity of each band is described as s (strong), m (medium) or w (weak) and with the prefix v (very) and suffix br (broad) where appropriate. ^{1}H-NMR, ^{19}F-NMR and proton-decoupled ^{13}C-NMR spectra were recorded in $CDCl_3$ at ambient temperature unless specified otherwise. ^{1}H-NMR spectra are reported as follows: δ_H (frequency of spectrometer, solvent) chemical shift (number of protons, multiplicity, coupling constant(s) *J* (Hz), assignment) at 400 or 300 MHz. Multiplicities of ^{1}H-NMR resonances are reported as follows: s – singlet, d – doublet, t – triplet, q – quartet, qn – quintet, m – multiplet, v – very, br – broad signal, stack and apparent (app.). The term 'stack' is used to describe a region in the spectrum where resonances arising from non-equivalent nuclei are coincident while multiplet, m, is used to describe a resonance arising from a single nucleus (or equivalent nuclei) in which coupling constants cannot be readily assigned. Chemical shifts are reported as δ values (ppm) referenced to the following solvent signals: $CDCl_3$, δ_H 7.26; $CDCl_3$, δ_C 77.0, CD_3OD, δ_H 3.31; CD_3OD δ_C 49.0. In analysing ABX (and similar) systems, where the resonance pattern forms two, clearly separated groups of lines (two sets of four lines for an ABX system), these are reported as "A of ABX" and "B of ABX", along with $J_{A–B}$, which can be directly measured from the spectra. Whilst $J_{A–X}$ cannot strictly be measured directly from the spectrum, the value obtained from the spectrum is sufficiently close to the actual value for it still to be useful; however it is acknowledged that the value quoted for $J_{A–X}$ is not the true value. The chemical shift reported for A of AB (or AX of ABX *etc*.) is the measured midpoint between the lines making up the resonance. It is acknowledged that this figure is not the true chemical shift for the resonance, which needs to be calculated. Proton-decoupled ^{13}C-NMR spectra were recorded at 100 MHz and are reported as follows: chemical shift δ_F ppm [multiplicity (CH_3, CH_2, CH or C), assignment].

Connectivities were deduced from COSY90, HSQC and HMBC experiments. Proton-coupled ^{19}F-NMR spectra were recorded at 282 MHz and are reported as follows: δ_F (frequency of spectrometer) chemical shift ppm [multiplicity, coupling constant(s) *J* (Hz), assignment] and all spectra were recorded relative to chlorotrifluoromethane as the internal standard. Optical rotations were measured in $CHCl_3$ at a concentration of 10 mg /1 mL (unless specified otherwise) using a PolAAR 2001 automatic polarimeter (Optical Activity Ltd., Huntingdon, Cambridgeshire, United Kingdom), using a 5 cm cell, at a wavelength of 589 nm (sodium D line), and are quoted as $[\alpha]_D^{Temp}$. EI (electron impact) mass spectra and TOF ES+ (time of flight electrospray) mass spectra were recorded on and are reported as (*m/z* (%)) usinga Xevo G2-XS TOF with Waters e2695 separation module, a Synapt G2-S with Waters e2695 separation module, an LCT Premier with Waters 600 controller, a GCT Premier with Agilent 789OA. The Melting points were determined using open capillaries and are uncorrected.

5.1.1. Reactions

Reactions were monitored by thin layer chromatography using pre-coated glass-backed silica plates (60A F_{254}, Merck) and visualised by UV detection (at 254 nm) and with phosphomolybdic acid (lipid stain) staining dip or α-naphthol with H_2SO_4 (sugar stain) staining dip or vanillin staining dip or $KMnO_4$ staining dip. Column chromatography was performed usin silica gel (40–60 μm mesh) and on pre-packed column cartridges (Mega Bond Elut Si 5 g – 20 mL and 2 g – 12 mL).

All reactions were conducted with magnetic stirring in oven-dried (140 °C) or flame-dried glassware under an argon atmosphere and at ambient temperature (20 to 25 °C) unless specified otherwise. Volumes of 1 mL or less were measured and dispensed with gastight syringes. Evaporation of volatiles and concentration of solutions under reduced pressure were

performed at 50–700 mbar at 40 °C. Residual solvent was removed under high vacuum (<1 mbar).

5.1.2. Chemicals and Reagents

All reagents were obtained from commercial sources and used without further purification unless specified otherwise. All solutions are aqueous and saturated unless specified otherwise.

5.1.3. General procedure for activation of molecular sieves

Powdered molecular sieves were weighed into a round-bottom flask (or the reaction vessel whenever possible) and then heated with a Bunsen flame under high vacuum for 5 min. The sieves were then allowed to cool to rt before (where necessary) immediate transfer to the reaction vessel.

5.2. Chapter 2

1,2,3,4,6-Penta-*O*-acetyl-α,β-D-mannopyranoside (76)

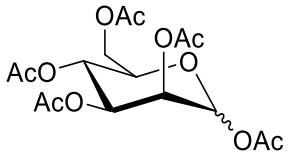

Ac_2O (61 mL, 0.55 mol) was added to a solution of D-mannose (5.0 g, 0.028 mol) in pyridine (100 mL). After stirring the resulting solution for 16 h at rt, the solvent was removed by co-evaporation with toluene (2 × 50 mL). The residue was redissolved in CH_2Cl_2 (50 mL) and washed sequentially with H_2O (2 × 50 mL), 1 M HCl (2 × 30 mL), $NaHCO_3$ solution (2 × 40 mL) and brine (1 x 50 mL) and dried using Na_2SO_4. The product was then filtered and concentrated under reduced pressure to yield pentaacetate **76** as a viscous oil and a mixture of anomers [α:β, 1.0 : 0.3 (as determined by ^{1}H-NMR), 9.95 g, 92%]: Data for mixture unless specified otherwise: R_f = 0.42 (50% EtOAc in hexane); ν_{max}(film)/cm^{-1} 2955 vw, 1743 vs (C=O), 1433 w, 1368 m, 1209 vs, 1148 s, 1087 m, 1051 s, 1025 s, 973 s, 913 w, 732 w; δ_H(400 MHz, α-anomer) [2.00, 2.05, 2.09, 2.16, 2.17 (15H, 5 × s, C(O)CH_3)], 4.02–4.07 (1H, m), 4.10 (1H, dd, *J* 12.4, 2.3), 4.28 (1H, dd, *J* 12.4, 4.9), 5.26 (1H, app t, *J* 2.2), 5.33–5.35 (2H, stack), 6.08 (1H, d, *J* 1.9, H-1); δ_C(100 MHz, α-anomer) [20.5, 20.6, 20.7, 20.8 (5 × CH_3, C(O)CH_3, resonance overlap), 62.1 (CH_2, C-6), [65.5, 68.3, 68.7, 70.6 (CH, C-2, C-3, C-4, C-5)], 90.6 (CH, C-1), [168.0, 169.5, 169.7, 170.0, 170.6 (5 × C, *C*=O)]; visible resonances for minor β-anomer: δ_H(400 MHz) 2.10, 2.21 (2 × 3H, s, C(O)CH_3), 3.80 (1H, ddd, *J* 9.9, 5.3, 2.3, H-5), 5.13 (1H, dd, *J* 10.0, 3.3, H-3), 5.48 (1H, dd, *J* 3.3, 1.0, H-2), 5.86 (1H, d, *J* 1.0, H-1); δ_H(100 MHz) 65.4 (CH), 68.2 (CH), 73.3 (CH), 90.4 (CH); *m/z* (TOF ES+) 413.1 ([M + Na]$^+$, 100%).

Data were in agreement with those reported in the literature.[42]

3,4,6-Tri-*O*-acetyl-1,2-*O*-(1-methoxyethylidene)-β-D-mannopyranose (77)

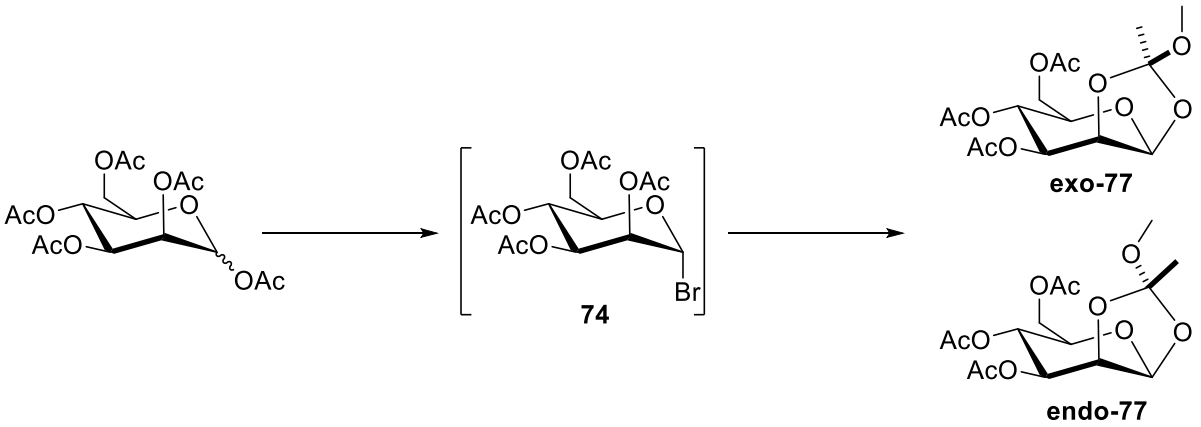

33% HBr in AcOH (50 mL, 0.20 mol) was added to a solution of pentaacetate **76** (5.0 g, 0.013 mol) in CH_2Cl_2 (50 mL) at rt. After 2 h, the solvent was co-evaporated with toluene (3 × 50 mL) to leave bromide **74**, which was used directly without further purification. Assuming full conversion to the bromide, the flask was charged with MeOH (50 mL), CH_2Cl_2 (50 mL) and 2,6-lutidine (10 mL, 0.086 mol) and the resulting solution stirred overnight at rt. The reaction mixture was then concentrated under reduced pressure and the residue was co-evaporated with toluene (2 × 30 mL). The residue was re-dissolved in $CHCl_3$ (50 mL) and washed sequentially with H_2O (3 × 50 mL) and brine (1 × 50 mL). The organic layer was dried using Na_2SO_4, filtered and concentrated under reduced pressure. The residue was purified by flash column chromatography (20% EtOAc in hexanes) to yield orthoester **77** as an off white solid and a 7.5:1 exo:endo mixture of diastereomers (as measured by ^{1}H NMR) (3.15 g, 67%): Data for mixture unless specified otherwise : R_f = 0.43 (50% EtOAc in hexanes); m.p. 101–106 °C (Et_2O), lit.[42] 110–111 °C (MeOH, Et_2O); $[\alpha]_D^{21}$ = –22.8 (c = 1.0, $CHCl_3$), lit.[42] $[\alpha]_D^{25}$ = –26.8 (c = 1.0, $CHCl_3$); ν_{max}(neat)/cm^{-1} 1741 s (C=O), 1432 w, 1385 m, 1371 m, 1257 m, 1210 vs, 1137 m, 1115 m, 1053 vs, 1029 s, 958 m, 891s; δ_H(400 MHz, *exo* anomer) 1.73 (3H, s, C(OCH$_3$)C*H$_3$*), [2.04, 2.06, 2.11 (9H, 3 × s, C(O)C*H$_3$*)], 3.27 (3H, s, OC*H$_3$*), 3.67 (1H, ddd, *J* 9.5, 4.9, 2.7, H-5), 4.13 (1H, dd, *J* 12.1, 2.7, H-6$_A$), 4.22 (1H, dd, *J* 12.1, 4.9, H-6$_B$), 4.60 (1H, dd, *J* 4.0, 2.6, H-2), 5.14 (1H, dd, *J* 9.9, 4.0, H-3), 5.29 (1H, app. t, *J* 9.8, H-4), 5.48 (1H, d, *J*

2.5, H-1); δ_C(100 MHz, *exo* anomer) [20.68, 20.72, 20.8 (CH_3, 3 × C(O)*C*H_3)], 24.3 (CH_3, C(OCH_3)*C*H_3), 49.9 (CH_3, O*C*H_3), 62.3 (CH_2, C-6), 65.4 (CH, C-4), 71.3 (CH, C-3), 70.6 (CH, C-5), 76.5 (CH, C-2), 97.3 (CH, C-1), 124.5 (C, *C*(OCH_3)CH_3), [169.4, 170.3, 170.6 (C, 3 × C=O)]; visible resonances for minor endo anomer; δ_H(400 MHz) 1.51 (3H, s, C(OCH_3)C*H*$_3$), 2.01 (3H, s, C(O)C*H*$_3$), 3.48 (3H, s, OC*H*$_3$), 4.37 (1H, dd, *J* 4.2, 2.4), 5.19 (1H, dd, *J* 10.0, 4.2), 5.38 (1H, app. t, *J* 9.9); δ_C(100 MHz) 24.0 (C(OCH_3)*C*H_3), 50.1 (O*C*H_3), 61.9 (CH_2, C-6), 65.3 (CH), 70.8 (CH), 75.4 (CH), 94.8 (CH); *m/z* (TOF ES+) 385.1 ([M + Na]$^+$, 100%).

Data were in agreement with those reported in the literature.[42]

3,4,6-Tri-*O*-benzyl-1,2-*O*-(1-methoxyethylidene)-β-D-mannopyranose (44)

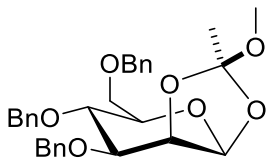

BnBr (5.00 mL, 42.1 mmol) and solid KOH (4.60 g, 82.8 mmol) were added to a solution of orthoester **77** (3.00 g, 8.28 mmol) in THF (30 mL). After heating at reflux, H_2O (50 mL) was added and the reaction mixture was diluted with CH_2Cl_2 (100 mL). The organic layer was separated, washed sequentially with $NaHCO_3$ solution (50 mL) and brine (50 mL), dried (Na_2SO_4), filtered and the filtrate concentrated under reduced pressure. The residue was purified by flash column chromatography (20% EtOAc in hexanes) to yield exo-orthoester **44** as a white solid (3.2 g, 76%)[8]: R_f = 0.6 (50% EtOAc in hexanes); m.p. 74 –76 °C (Et_2O), lit.[42] 76–78 °C (Et_2O-pentane); $[\alpha]_D^{21}$ = +27.6 (c = 1.0, $CHCl_3$), lit.[42] $[\alpha]_D^{19}$ +34.4 (c = 6.0, $CHCl_3$); ν_{max}(film)/cm^{-1} 2954 w, 2906 w, 2867 w, 1454 m, 1383 m, 1355 m, 1260 w, 1239 m, 1207 m, 1155 m, 1130 m, 1099 vs, 1066 s, 1049 vs, 1036 vs, 1026 vs, 987 m, 969 m, 931 m, 893 s, 877 m, 839 w, 822 w, 793 w, 735 s, 696 vs, 673 m, 655 m; δ_H(400 MHz) 1.66 (3H, s,

[8] No sign of endo anomer from ^{1}H NMR following purification.

C(OCH$_3$)C*H*$_3$), 3.21 (3H, s, OC*H*$_3$), 3.34 (1H, ddd, *J* 9.4, 4.4, 2.4, H-5), 3.61–3.70 (3H, stack, H-3, H-6$_{A,}$ H-6$_B$), 3.85 (1H, app. t, *J* 9.4, H-4), 4.32 (1H, dd, *J* 3.9, 2.6, H-2), 4.45–4.55 (3H, stack, PhC*H*$_2$), 4.69 (1H, A of AB, *J* 12.3, PhC*H*$_A$H$_B$), 4.73 (1H, B of AB, *J* 12.3, PhCH$_A$*H*$_B$), 4.82 (1H, d, *J* 10.8, PhC*H*$_2$), 5.27 (1H, d, *J* 2.6, H-1), 7.15–7.34 (15H, stack, Ar C*H*); δ_C(100 MHz) 24.4 (CH$_3$, C(OCH$_3$)*C*H$_3$), 49.7 (CH$_3$, O*C*H$_3$), 69.0 (CH$_2$, C-6), 72.4 (CH$_2$, Ph*C*H$_2$), 73.3 (CH$_2$, Ph*C*H$_2$), 74.1 (CH, C-4), 74.2 (CH, C-5), 75.2 (CH$_2$, Ph*C*H$_2$), 77.1 (CH, C-3), 79.0 (CH, C-2), 97.5 (CH, C-1), 124.0 (C, *C*(OCH$_3$)CH$_3$), [127.5, 127.8, 128.0, 128.3, 128.4, 128.5 (CH, Ar *C*H, resonance overlap)], [137.8, 138.2 (C, Ar *C*, resonance overlap)]; *m/z* (TOF ES+) 529.2 ([M + Na]$^+$, 100%).

Data were in agreement with those reported in the literature.[42]

5-Azidopentan-1-ol (79)

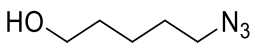

A solution of 5-bromo-1-pentanol (2.00 g, 12.0 mmol) and NaN$_3$ (2.34 g, 36.0 mmol) in DMF (15 mL) was heated at 80 °C for 12 h. After cooling to rt, H$_2$O (100 mL) was added and the resulting mixture was extracted with EtOAc (5 × 80 mL). The combined organic layers were washed sequentially with H$_2$O (200 mL) and brine (200 mL), and dried over Na$_2$SO$_4$, filtered and concentrated under reduced pressure to yield azide **79** as a pale yellow oil (1.47 g, 94%), which was used immediately without further purification: R_f = 0.6 (20% EtOAc in hexanes); ν_{max}(film)/cm^{-1} 3337 br m (O–H), 2936 m, 2865 m, 2090 vs (N$_3$), 1455 m, 1349 m, 1255 m, 1165 w, 1071 w, 1052 m, 1018 w, 877 w, 835 w; δ_H(400 MHz) 1.40–1.46 (2H, m, *H*-3), 1.54–1.65 (4H, stack, H-2, H-4), 2.36 (1H, br s, O*H*), 3.26 (2H, t, *J* 6.9, H-5), 3.62 (2H, t, *J* 6.5, H-1); δ_C(100 MHz) 22.9 (CH$_2$, C-3), [28.5, 32.0 (CH$_2$, C-2, C-4)], 51.3 (CH$_2$, C-5), 62.4 (CH$_2$, C-1); *m/z* (TOF ES+) 130.1 ([M + H]$^+$, 15%), 132.1 (100).

Data were in agreement with those reported in the literature.[174]

5′-Azidopentyl 2-*O*-acetyl-3,4,6-tri-*O*-benzyl-α-D-mannopyranoside (80)

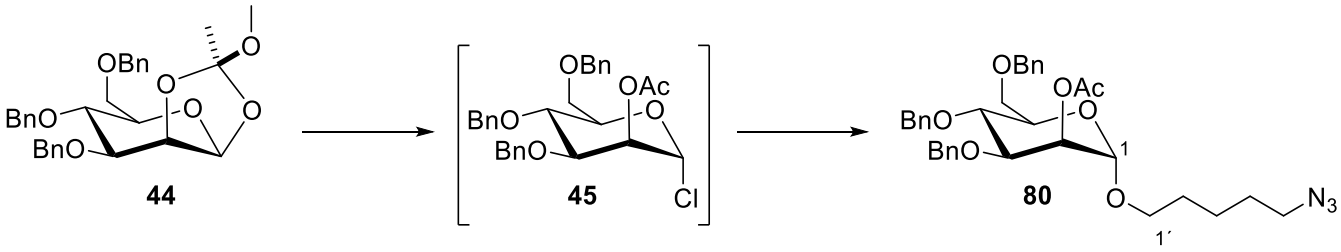

TMSCl (2.5 mL, 19.7 mmol) was added to a solution of orthoester **44** (1.00 g, 1.97 mmol) in CH_2Cl_2 (20 mL) at 0 °C. After 1 h, the reaction mixture was concentrated under reduced pressure to yield the glycosyl chloride **45** as a syrup that was used directly without further purification. In a separate flask, AgOTf (0.557 g, 2.17 mmol) and activated 4 Å MS (1 g) in CH_2Cl_2 (10 mL) were stirred at rt for 30 min. The flask was then cooled to –30 °C. A solution of alcohol **79** (0.517 g, 3.72 mmol) in CH_2Cl_2 (10 mL) was added, followed immediately by a solution of the glycosyl chloride **45** in CH_2Cl_2 (10 mL). The reaction mixture warmed to rt and then stirred for 16 h before filtering through Celite and concentrating the filtrate under reduced pressure. Purification of the residue by flash column chromatography (20% EtOAc in hexanes) yielded α-mannoside **80** as a colourless syrup (0.666 g, 56%): R_f = 0.5 (20% EtOAc in hexane); $[\alpha]_D^{21}$ = +24.0 (c = 1.0, $CHCl_3$); ν_{max}(film)/cm^{-1} 3031 vw, 2935 w, 2867 w, 2093 s (N_3), 1743 s (C=O), 1496 w, 1453 m, 1367 m, 1234 vs, 1137 s, 1076 vs, 1060 vs, 1027 s, 977 s, 911 w, 845 w, 798 w, 735 vs, 696 vs, 678 m; δ_H(300 MHz) 1.26–1.39 (2H, stack, H-3′), 1.45–1.57 (4H, stack, H-2′, H-4′), 2.07 (3H, s, C(O)CH_3), 3.18 (2H, app. t, *J* 6.9, H-5′), 3.33 (1H, app. dt, *J* 9.7, 6.3, H-1′$_A$), 3.56–3.66 (2H, stack, H-6$_A$, H-1′$_B$), 3.66–3.76 (2H, stack, H-5, H-6$_B$), 3.80 (1H, app. t, *J* 9.3, H-4), 3.90 (1H, dd, *J* 9.1, 3.3, H-3), 4.40 (1H, A of AB, *J* 10.7, PhCH_AH$_B$), 4.44 (1H, A of AB, *J* 12.1, PhCH_CH$_D$), 4.47 (1H, A of AB, *J* 11.1, PhCH_EH$_F$), 4.61 (1H, B of AB, *J* 12.1, PhCH$_C$$H_D$), 4.64 (1H, B of AB, *J* 11.1, PhCH$_E$$H_F$), 4.75 (1H, d, *J* 1.7, H-1), 4.78 (1H, B of AB, *J* 10.7, PhCH_2), 5.28 (1H, dd, *J* 3.3, 1.7, H-2), 7.05–7.11 (2H, stack, Ar C*H*), 7.16–7.31 (13H, stack, Ar C*H*); δ_C(100 MHz) 21.1 (CH_3, C(O)CH_3), 23.3 (CH_2, C-3′), [28.6, 28.9 (CH_2, C-2′, C-4′)], 51.2 (CH_2, C-5′), 67.5 (CH_2, C-1′), 68.8 (CH, C-2), 68.8 (CH_2, C-6), 71.3 (CH, C-5),

71.7 (CH_2, Ph*C*H_2), 73.4 (CH_2, Ph*C*H_2), 74.3 (CH, C-4), 75.2 (CH_2, Ph*C*H_2), 78.2 (CH, C-3), 97.7 (CH, C-1), [127.6, 127.7, 127.9, 128.0, 128.3 (CH, Ar *C*H, resonance overlap)], [137.9, 138.1, 138.2 (C, Ar *C*)] 170.5 (C, *C*=O); *m/z* (TOF ES+) 626.3 ([M + Na]$^+$, 100%); HRMS *m/z* (TOF ES+) 626.2838 [M + Na]$^+$, $C_{34}H_{41}N_3O_7Na$ requires 626.2842.

5′-Azidopentyl 3,4,6-tri-*O*-benzyl-α-D-mannopyranoside (81)

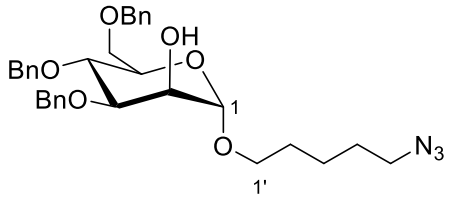

NaOMe (5 mL of a 0.5 M soln. in MeOH, 2.5 mmol) was added to a solution of acetate **80** (0.504 g, 0.835 mmol) in MeOH (30 mL). After 3 h, the reaction mixture was neutralised by the addition of acidic ion-exchange resin [Dowex H CR-S, pre-washed sequentially with MeOH (100 mL) and $CHCl_3$ (50 mL)]. The solution was filtered and the resin washed sequentially with MeOH (2 × 20 mL) and $CHCl_3$ (2 × 20 mL). The filtrate was concentrated under reduced pressure and the residue purified by flash column chromatography (25% EtOAc in hexanes) to provide alcohol **81** as a clear oil (0.427 g, 92%): R_f = 0.2 (20% EtOAc in hexanes); $[\alpha]_D^{21}$ = +43.6 (c = 1.0, $CHCl_3$); ν_{max}(film)/cm^{-1} 3435 br vw (O–H), 3030 vw, 2920 m, 2865 m, 2094 s (N_3), 1626 m, 1577 w, 1496 w, 1454 s, 1386 m, 1339 s, 1249 m, 1212 m, 1190 m, 1152 m, 1099 vs, 1055 vs, 1028 vs, 980 m, 749 s, 699 vs; δ_H(400 MHz) 1.28–1.37 (2H, stack, H-3′), 1.46–1.56 (4H, stack, H-2′, H-4′), 2.45 (1H, br s, O*H*), 3.17 (2H, app. t, *J* 6.9, H-5′), 3.34 (1H, app. dt, *J* 9.7, 6.4, H-1′$_A$), 3.58–3.71 (4H, stack, including H-1′$_B$, H-6$_A$, H-6$_B$), 3.72–3.82 (2H, stack, including H-3), 3.95 (1H, app s, H-2), 4.40–4.49 (2H, stack, PhCH_2), 4.52–4.63 (3H, stack, PhCH_2), 4.75 (1H, B of AB, *J* 10.8, Ph*CH*$_2$), 4.81 (1H, d, *J* 1.4, H-1), 7.07–7.11 (2H, stack, Ar C*H*), 7.16–7.32 (13H, stack, Ar C*H*); δ_C(100 MHz) 23.4 (CH_2, C-3′), [28.6, 28.9 (CH_2, C-2′, C-4′)], 51.2 (CH_2, C-5′), 67.3 (CH_2, C-1′), 68.4 (CH, C-2), 68.9 (CH_2, C-6), 71.0 (CH),

71.9 (CH_2, Ph*C*H_2), 73.4 (CH_2, Ph*C*H_2), 74.3 (CH), 75.1 (CH_2, Ph*C*H_2), 80.2 (CH), 99.1 (CH, C-1), [127.5, 127.7, 127.8, 128.0, 128.3 (CH, Ar *C*H, resonance overlap)], [138.0, 138.2 (C, Ar C, resonance overlap)]; *m/z* (TOF ES+) 584.3 ([M + Na]$^+$, 100%); HRMS *m/z* (TOF ES+) 584.2732 [M + Na]$^+$, $C_{32}H_{39}N_3O_6Na$ requires 584.2737.

5″-Azidopentyl [2′-*O*-acetyl-3′,4′,6′-tri-*O*-benzyl-α-D-mannopyranosyl]-(1′→2)-[3,4,6-tri-*O*-benzyl-α-D-mannopyranoside] (82)

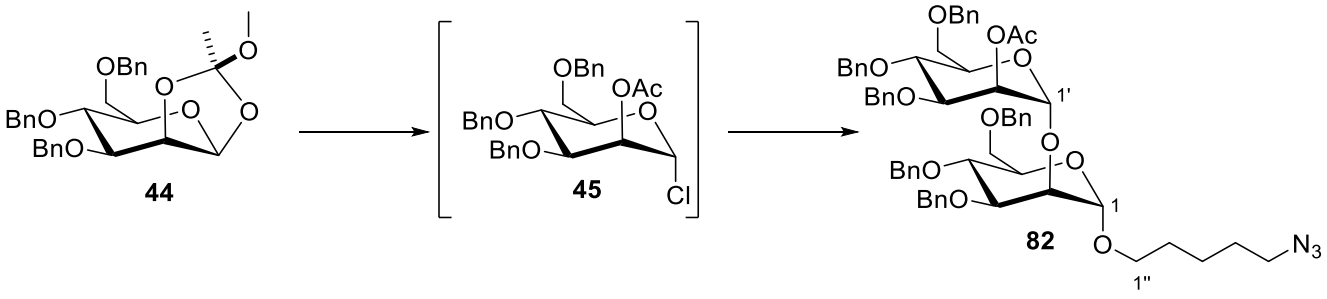

TMSCl (2.0 mL, 15.8 mmol) was added to a solution of orthoester **44** (0.302 g, 0.596 mmol) in CH_2Cl_2 (15 mL) at 0 °C. After 1 h, the reaction mixture was concentrated under reduced pressure to yield the glycosyl chloride **45** as a syrup, which was directly used without further purification. In a separate flask, a mixture of AgOTf (0.168 g, 0.656 mmol) and activated 4 Å MS (0.6 g) in CH_2Cl_2 (10 mL) was stirred at rt for 30 min. The flask was then cooled to –30 °C before a solution of alcohol **81** (0.402 g, 0.715 mmol) in CH_2Cl_2 (10 mL), followed immediately by a solution of glycosyl chloride **45** in CH_2Cl_2 (10 mL) were added. The reaction mixture was warmed to rt. After 16 h, the reaction mixture was filtered through Celite and the filtrate concentrated under reduced pressure. Purification of the residue by flash column chromatography (20% EtOAc in hexanes) yielded disaccharide **82** as a colourless syrup (0.296 g, 48%): R_f = 0.5 (20% EtOAc in hexane); $[\alpha]_D^{21}$ = +24.0 (c = 1.0, $CHCl_3$); ν_{max}(film)/cm^{-1} 3030 vw, 2914 m, 2865 m, 2096 s (N_3), 1743 s (C=O), 1605 vw, 1497 m, 1454 s, 1366 s, 1236 vs, 1138 vs, 1101 vs, 1059 vs, 1028 s, 980 m, 912 w, 846 vw, 741 vs, 699 vs; δ_H(400 MHz) 1.21–1.30 (2H, stack, H-3″), 1.40–1.51 (4H, stack, H-2″, H-4″), 2.05 (3H, s, C(O)C*H*$_3$),

3.11–3.21 (3H, stack, H-1″$_A$, H-5″), 3.51 (1H, app. dt, *J* 9.6, 6.5, H-1″$_B$), 3.60–3.78 (7H, stack, including H-6$_A$, H-6$_B$, H-6′$_A$, H-6′$_B$), 3.82 (1H, dd, *J* 9.2, 2.9), 3.86–3.93 (3H, stack, including H-2, H-3′), 4.33 (1H, A of AB, *J* 10.9, PhC*H*$_A$H$_B$), 4.36–4.43 (2H, stack, PhC*H*$_2$), 4.44–4.50 (2H, stack, PhC*H*$_2$), 4.55–4.63 (5H, stack, PhC*H*$_2$), 4.74–4.80 (3H, stack, H-1, PhC*H*$_2$), 5.00 (1H, d, *J* 1.6, H-1′), 5.46 (1H, dd, *J* 3.2, 1.9, H-2′), 7.06–7.10 (2H, stack, Ar C*H*), 7.10–7.14 (3H, stack, Ar C*H*), 7.15–7.30 (25H, stack, Ar C*H*); δ_C(100 MHz) 21.1 (CH_3, C(O)*C*H$_3$), 23.3 (CH_2, C-3″), [28.6, 28.9 (CH_2, C-2″, C-4″)], 51.2 (CH_2, C-5″), 67.3 (CH_2, C-1″), 68.7 (CH, C-2′), [69.1, 69.3 (CH_2, C-6, C-6′)], 71.7 (CH), 71.8 (CH), [71.9, 72.0, 73.3, 73.3 (CH_2, Ph*C*H$_2$)], 74.3 (CH), 74.6 (CH), 74.9 (CH), [75.0, 75.2 (CH_2, Ph*C*H$_2$)], 78.1 (CH), 79.6 (CH), 98.6 (CH, C-1), 99.5 (CH, C-1′), [127.4, 127.5, 127.6, 127.7, 128.1, 128.3 (CH, Ar *C*H, resonance overlap)], [138.0, 138.2, 138.3, 138.3, 138.4, 138.5 (C, Ar *C*)], 170.1 (C, *C*=O); *m/z* (TOF ES+) 1058.5 [M + Na]$^+$, 100%); HRMS *m/z* (TOF ES+) 1058.4780 [M + Na]$^+$, $C_{61}H_{69}N_3O_{12}Na$ requires 1058.4779.

5″-Azidopentyl [3′,4′,6′-tri-*O*-benzyl-α-D-mannopyranosyl]-(1′→2)-[3,4,6-tri-*O*-benzyl-α-D-mannopyranoside] (83)

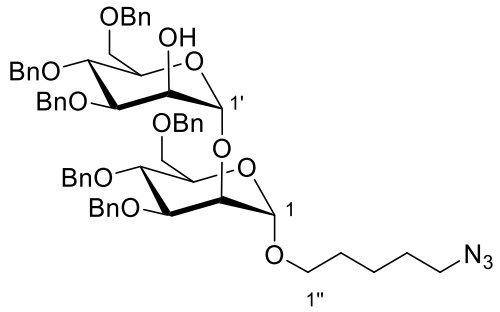

NaOMe (1.0 mL of a 0.5 M soln. in MeOH, 0.5 mmol) was added to a solution of acetate **82** (0.25 g, 0.24 mmol) in MeOH (20 mL) at rt. After 3 h, the reaction mixture was neutralised by the addition of acidic ion-exchange resin [Dowex H CR-S, pre-washed sequentially with MeOH (100 mL) and $CHCl_3$ (50 mL)]. The solution was filtered and the resin washed sequentially with MeOH (2 × 20 mL) and $CHCl_3$ (2 × 20 mL). The filtrate was concentrated under reduced pressure and the residue purified by flash column chromatography (25% EtOAc in hexanes)

to afford alcohol **83** as a colourless oil (0.215 g, 90%): R_f = 0.2 (20% EtOAc in hexanes); $[\alpha]_D^{21}$ = +29.6 (c = 1.0, $CHCl_3$); ν_{max}(film)/cm^{-1} 3372 br vw (O–H), 3030 vw, 2913 m, 2865 m, 2095 s (N_3), 1496 m, 1454 s, 1362 m, 1309 m, 1279 m, 1209 m, 1103 vs, 1058 vs, 1029 vs, 910 w, 738 vs, 699 vs; δ_H(400 MHz) 1.22–1.30 (2H, stack, H-3″), 1.37–1.51 (4H, stack, H-2″, H-4″), 2.37 (1H, br s, O*H*), 3.12–3.21 (3H, stack, H-1″$_A$, H-5″), 3.51 (1H, app. dt, *J* 9.6, 6.5, H-1″$_B$), 3.61–3.68 (4H, stack including H-4′, H-6$_A$, H-6′$_A$ and H-6$_B$ or H-6′$_B$), 3.69–3.78 (3H, stack, H-4, H-6$_B$ or H-6′$_B$ and H-5 or H-5′), 3.80 (1H, dd, *J* 9.1, 3.2, H-3′), 3.83 (1H, dd, *J* 9.1, 3.2, H-3), 3.80 (1H, ddd, *J* 9.7, 4.2, 2.7, H-5 or H-5′), 3.93–3.95 (1H, m, H-2), 4.04–4.07 (1H, m, H-2′), 4.40–4.64 (10H, stack, PhC*H*$_2$), 4.72–4.78 (2H, stack, PhC*H*$_2$), 4.82 (1H, d, *J* 1.7, H-1), 5.07 (1H, d, *J* 1.4, H-1′), 7.08–7.30 (30H, stack, Ar C*H*); δ_C(100 MHz) 23.4 (CH_2, C-3″), [28.6, 29.0 (CH_2, C-2″, C-4″)], 51.3 (CH_2, C-5″), 67.3 (CH_2, C-1″), 68.5 (CH, C-2′), [69.3, 69.4 (CH_2, C-6, C-6′)], 71.5 (CH), 71.9 (CH, C-4′), [72.2, 72.3, 73.3, 73.4 (CH_2, Ph*C*H$_2$)], 74.4 (CH), 74.8 (CH), 75.0 (CH, C-2), [75.1, 75.2 (CH_2, Ph*C*H$_2$)], 79.8 (CH, C-3), 80.0 (CH, C-3′), 98.8 (CH, C-1), 101.1 (CH, C-1′), [127.4, 127.5, 127.6, 127.7, 127.8, 127.9, 128.0, 128.3, 128.4, 128.5 (CH, Ar *C*H, resonance overlap)], [138.0, 138.2, 138.3, 138.36, 138.41, 138.6 (C, Ar *C*)]; *m/z* (TOF ES+) 1016.5 ([M + Na]$^+$, 100%); HRMS *m/z* (TOF ES+) 1016.4670 [M + Na]$^+$, $C_{59}H_{67}N_3O_{11}Na$ requires 1016.4673.

Phenyl 2,3,4,6-tetra-*O*-acetyl-1-thio-α-D-mannopyranose (84)

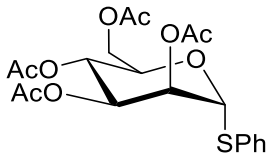

PhSH (2.00 mL, 19.6 mmol) was added to a solution of pentaacetate **76** (5.00 g, 12.8 mmol) in CH_2Cl_2 (50 mL) and the mixture was cooled to 0 °C. $BF_3{\cdot}Et_2O$ (2.0 mL, 32 mmol) was added dropwise over 5 min and the reaction mixture was warmed to rt. After 3 h, CH_2Cl_2 (50 mL) was added and the mixture was washed sequentially with 2 M NaOH solution (2 × 50 mL) and H_2O (2 × 50 mL). The organic phase was dried (Na_2SO_4), filtered and concentrated under reduced

pressure. Purification of the residue by flash column chromatography (20% EtOAc in hexanes) yielded thiosugar **84** as an off-white solid (5.6 g, quant.). R_f = 0.4 (30% EtOAc in hexanes); m.p. 79–81 °C, lit.[175] 83-85 °C; $[\alpha]_D^{21}$ = +96.4 (c = 1.0, $CHCl_3$), lit.[176] $[\alpha]_D^{24}$ = +85.6 (c = 2.0, CH_2Cl_2); ν_{max}(film)/cm^{-1} 1739 vs (C=O), 1481 vw, 1439 w, 1366 s, 1242 vs, 1217 vs, 1100 s, 1061 s, 1046 vs, 979 s, 752 s, 739 s; δ_H(400 MHz) 2.01 (3H, s, C(O)CH_3), 2.05 (3H, s, C(O)CH_3), 2.07 (3H, s, C(O)CH_3), 2.15 (3H, s, C(O)CH_3), 4.10 (1H, dd, *J* 12.2, 2.3, H-6$_A$), 4.30 (1H, dd, *J* 12.2, 5.9, H-6$_B$), 4.54 (1H, ddd, *J* 9.8, 5.9, 2.3, H-5), 5.28–5.37 (2H, stack, H-3, H-4), 5.47–5.52 (2H, stack, H-1, H-2), 7.27–7.34 (3H, stack, Ph), 7.46–7.51 (2H, stack, Ph); δ_C(100 MHz) [20.6, 20.7, 20.9 (CH_3, C(O)*C*H_3, resonance overlap)], 62.4 (CH_2, C-6), [66.3, 69.4 (CH, C-3, C-4)], 69.5 (CH, C-5), 70.9 (CH, C-2), 85.7 (CH, C-1), [128.1, 129.2, 132.1 (CH, Ar *C*H)], 132.6 (C, Ar *C*), [169.7, 169.8, 169.9, 170.6 (C, *C*=O)]; *m/z* (TOF ES+) 463.1 ([M + Na]$^+$, 100%).

Data were in agreement with those reported in the literature.[176]

Phenyl 1-thio-α-D-mannopyranose (85)

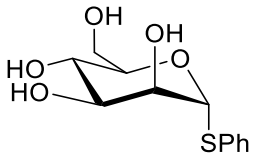

NaOMe (100 mL of a 0.5 M soln. in MeOH, 0.5 mmol) was added to a solution of tetraacetate **84** (5.00 g, 11.4 mmol) in MeOH (50 mL). After 16 h, the reaction mixture was neutralised by the addition of acidic ion-exchange resin [Dowex H CR-S, pre-washed sequentially with MeOH (100 mL) and $CHCl_3$ (50 mL)]. The solution was filtered and the resin washed sequentially with MeOH (2 × 50 mL) and $CHCl_3$ (2 × 20 mL). The filtrate was concentrated under reduced pressure. Purification of the residue by flash column chromatography (10% MeOH in $CHCl_3$) provided thiosugar **85** as a white solid (3.0 g, quant.): R_f = 0.54 (30% MeOH in $CHCl_3$); m.p. 130–134 °C; solubility issues prevented an optical rotation measurement; ν_{max}(film)/cm^{-1} 3314

br s (O–H), 2878 br w, 1583 w, 1478 m, 1455 m, 1439 m, 1411 m, 1388 m, 1329 m, 1255 m, 1215 m, 1095 vs, 1062 vs, 1040 vs, 1023 vs, 968 s, 913 s, 876 m, 849 m, 796 s, 770 s, 738 vs, 688 vs, 670 vs, 664 vs; δ_H(300 MHz) 3.69–3.85 (4H, stack, H-3, H-4, H-6_A, H-6_B), 4.01 (1H, app. dt, *J* 9.6, 3.2, H-5), 4.10 (1H, dd, *J* 3.2, 1.4, H-2), 5.44 (1H, d, *J* 1.4, H-1), 7.21–7.30 (3H, stack, Ar C*H*), 7.41–7.46 (2H, stack, Ar C*H*); δ_C(100 MHz) 61.4 (CH_2, C-6), [67.3, 72.1 (CH, C-3, C-4)], 72.4 (CH, C-2), 73.6 (CH, C-5), 88.8 (CH, C-1), [127.6, 129.2, 131.8 (CH, Ar *C*H)], 134.3 (C, Ar *C*); *m/z* (TOF ES+) 295.1 ([M + Na]$^+$, 100%).

Data were in agreement with those reported in the literature.[177]

Phenyl 4,6-*O*-benzylidene-1-thio-α-D-mannopyranose (86)

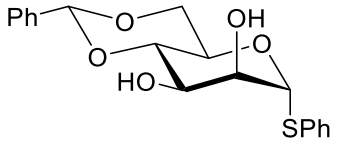

(1*S*)-(+)-10-Camphorsulfonic acid (0.681 g, 2.94 mmol) and benzaldehyde dimethyl acetal (1.90 mL, 12.2 mmol) were added to a suspension of thioglycoside **85** (3.20 g, 11.8 mmol) in CH_3CN (32 mL) at rt. After 15 min, the product had precipitated and the reaction was quenched with Et_3N (2 mL). The reaction mixture was partitioned between EtOAc (200 mL) and H_2O (150 mL). The aqueous phase was extracted with EtOAc (2 × 100 mL). The combined organic fractions were washed with brine (100 mL) and then dried (Na_2SO_4) and filtered. Removal of the solvent under reduced pressure afforded a white solid, which was washed with petroleum ether (b.p. 40–60 °C) (3 × 30 mL) to provide benzylidene **86** as a white, fluffy solid (3.62 g, 85%): R_f = 0.5 (50% MeOH in $CHCl_3$); m.p. 198–202 °C, lit.[49] 202–204 °C; solubility issues prevented an optical rotation measurement; ν_{max}(film)/cm^{-1} 3318 br w (O–H), 3197 br m, 2896 w, 1451 m, 1473 m, 1441 m, 1401 m, 1370 s, 1352 w, 1338 w, 1287 m, 1253 w, 1216 m, 1162 w, 1078 vs, 1032 s, 1007 vs, 979 s, 974 s, 860 s, 742 vs, 700 vs, 688 vs; δ_H(DMSO-d_6, 400 MHz) 3.72–3.82 (2H, stack, H-3, H-6_A), 3.97 (1H, app. t, *J* 9.3, H-4 or H-5),

4.02 (1H, app. t, *J* 3.1, H-2), 4.04–4.12 (2H, stack, H-6_B, H-5 or H-4), 5.24 (1H, d, *J* 6.0, 3-O*H*), 5.48 (1H, app. s, H-1), 5.57 (1H, d, *J* 4.1, 2-O*H*), 5.64 (1H, s, benzylidene C*H*), 7.34–7.42 (5H, stack, Ph), 7.45–7.51 (5H, stack, Ph); δ_C(DMSO-d_6,100 MHz) 65.2 (CH, C-4 or C-5), 67.5 (CH_2, C-6), 68.0 (CH, C-3), 72.3 (CH, C-2), 78.4 (CH, C-5 or C-4), 89.2 (CH, C-1), 101.1 (CH, benzylidene CH), [126.3, 127.3, 127.9, 128.8, 129.2, 131.2 (CH, Ph)], [133.6, 137.8 (C, Ph, *ipso* C)]; *m/z* (TOF ES+) 743.2 ([2M + Na]$^+$, 100%), 383.1 (75, [M + Na]$^+$).

Data were in agreement with those reported in the literature.[49]

Phenyl 2-*O*-benzyl-4,6-*O*-benzylidene-1-thio-α-D-mannopyranose (92)

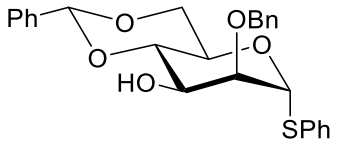

1 M NaOH solution (7 mL) was added to a mixture of diol **86** (500 mg, 1.39 mmol), Bu_4NHSO_4 (94 mg, 0.28 mmol) and BnBr (0.2 mL, 1.66 mmol) in CH_2Cl_2 (20 mL). The reaction mixture was heated under reflux for 20 h, then cooled to rt, and diluted with CH_2Cl_2 (10 mL). The phases were separated. The aqueous phase was extracted with CH_2Cl_2 (2 × 10 mL). The combined organic fractions were washed sequentially with $NaHCO_3$ solution (30 mL) and brine (30 mL), dried (Na_2SO_4), filtered, and concentrated under reduced pressure. The residue was purified by flash column chromatography (10% EtOAc in hexanes) to afford monobenzyl ether **92** as a white solid (506 mg, 81%): R_f = 0.5 (30% EtOAc in hexanes); m.p. 147–150 °C, lit.[49] 144−146 °C; $[\alpha]_D^{21}$ = +117.6 (c = 1.0, $CHCl_3$), lit.[49] $[\alpha]_D^{26}$ = +144.4 (c = 1.3, $CHCl_3$); ν_{max}(film)/cm^{-1} 3505 br w (O–H), 3029 w, 2902 m, 2863 m, 1582 m, 1476 m, 1455 s, 1387 m, 1360 m, 1272 w, 1214 m, 1153 m, 1080 vs, 1041 s, 1025 vs, 1003 s, 970 s, 916 m, 856 m, 774 m, 743 s, 697 vs, 674 m; δ_H(400 MHz) 2.23 (1H, br s, O*H*), 3.84 (1H, app. t, *J* 10.2, H-6_A), 4.00 (1H, app. t, *J* 9.3, H-4), 4.10–4.15 (2H, stack, H-2, H-3), 4.23 (1H, dd, *J* 10.2, 4.9, H-6_B),

4.32 (1H, app. dt, *J* 9.8, 4.9, *H*-5), 4.56 (1H, A of AB, *J* 11.6, PhCH_AH_B), 4.66 (1H, B of AB, *J* 11.6, PhCH_AH_B), 5.58–5.61 (2H, stack, H-1, benzylidene C*H*), 7.29–7.40 (11H, stack, Ar C*H*), 7.41–7.45 (2H, stack, Ar C*H*), 7.50–7.54 (2H, stack, Ar C*H*); δ_C(100 MHz) 64.7 (CH, C-5), 68.4 (CH_2, C-6), 69.0 (CH, C-2 or C-3), 73.1 (CH_2, $PhCH_2$), 79.5 (CH, C-4), 80.0 (CH, C-3 or C-2), 86.2 (CH, C-1), 102.1 (CH, benzylidene CH), [126.3, 127.8, 128.1, 128.26, 128.34, 128.7, 129.2, 131.8 (CH, Ar *C*H, resonance overlap)] [133.6, 137.2 (C, Ar *C*, resonance overlap)]; *m/z* (TOF ES+) 473.1 ($[M + Na]^+$, 100%).

Data were in agreement with those reported in the literature.[178]

1,2,3,4,6-Penta-*O*-trimethylsilyl-α,β-D-glucopyranose (102)

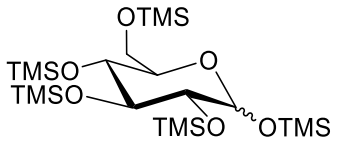

HMDS (10 mL, 0.048 mol) and TMSCl (5 mL, 0.039 mol) were added sequentially to a solution of D-glucose (1.0 g, 5.55 mmol) in pyridine (30 mL). The solution was heated at 75 ºC for 1 h under an Ar atmosphere and then cooled to rt. The mixture was poured into ice-H_2O (100 mL) and extracted with hexane (3 × 150 mL). The combined organic extracts were washed with H_2O (3 × 150 mL), dried ($MgSO_4$) and concentrated under reduced pressure to afford per-silylated glucose **102** as a colourless oil (2.82 g, 94%, α-only): R_f = 0.25 (4% EtOAc in hexane); $[\alpha]_D^{22}$ +65.6 (c 1.0, $CHCl_3$), lit.[179] $[\alpha]_D^{20}$ +62.5 (c 0.2, $CHCl_3$); ν_{max}(film)/cm^{-1} 2956 m, 2904 w, 1386 w, 1248 s, 1153 m, 1102 m, 1070 s, 1051 m, 967 m, 891 m, 864 s, 821 vs, 746 s, 682 m; δ_H(400 MHz) 0.10 (9H, s, Si(CH_3)$_3$), 0.12 (9H, s, Si(CH_3)$_3$), 0.140 (9H, s, Si(CH_3)$_3$), 0.144 (9H, s, Si(CH_3)$_3$), 0.17 (9H, s, Si(CH_3)$_3$), 3.33 (1H, dd, *J* 9.1, 3.10, H-2), 3.37–3.43 (1H, m, H-4), 3.63–3.74 (3H, stack, H-5, H-6), 3.77 (1H, app. t, *J* 8.9, H-3), 5.00 (1H, d, *J* 3.1, H-1); δ_C(100 MHz) [–0.2, 0.2, 0.5, 1.0, 1.3 CH_3, Si(*C*H_3)$_3$], 62.3, (CH_2, C-6), 72.3 (CH, C-4), 72.5

(CH, C-5), 74.0 (CH, C-3), 74.2 (CH, C-2), 93.9 (CH, C-1); *m/z* (TOF ES+) 563.25 ([M + Na]$^+$, 100%).

Data were in agreement with those reported in the literature.[52]

Trichloroacetimidate 2,3,4,6-tetra-*O*-benzyl-α,β-D-glucopyranoside (36)

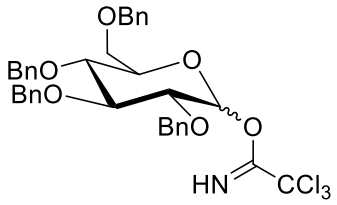

CCl_3CN (0.5 mL, 4.81 mmol) and K_2CO_3 (0.25 g, 1.85 mmol) were added to a solution of 2,3,4,6-tetra-*O*-benzyl-α,β-D-glucopyranose (200 mg, 0.37 mmol) in CH_2Cl_2 (5 mL) was stirred vigorously with for 12 h at rt. The reaction mixture was then filtered through Celite and the filtrate was concentrated under reduced pressure to give trichloroacetimidate **36** as a colourless syrup (α:β, 1 : 2.5, 221 mg 87%): Data for mixture unless specified otherwise: R_f = 0.5 (20% EtOAc in hexanes); ν_{max}(film)/cm^{-1} 3337 br w (N–H), 3030 w, 2914 m, 2867 m, 1671 s, 1496 m, 1453 s, 1359 m, 1287 s, 1209 m, 1149 m, 1055 vs, 1027 vs, 909 s, 833 s, 794 vs, 732 vs, 690 vs, 645 s; δ_H(400 MHz) 3.66–3.74 (1H, m, H-5), 3.76–3.87 (5H, stack, H-2, H-3, H-4, H-6), 4.50–5.00 (8H, stack, PhC*H*$_2$), 5.86 (1H, d, *J* 5.4, H-1), 7.27–7.40 (20H, stack, Ar C*H*), 8.75 (1H, br s, C=N*H*); δ_C(100 MHz, β-anomer) 68.2 (CH_2, C-6), 73.3 (CH_2, Ph*C*H$_2$), 74.8 (CH_2, Ph*C*H$_2$), 74.9 (CH_2, Ph*C*H$_2$), 75.5 (CH_2, Ph*C*H$_2$), 75.8 (CH, C-5), [77.2, 80.9, 84.5 (CH, C-2, C-3, C-4), 90.9 (C, *C*Cl$_3$), 98.3 (CH, C-1), [127.6, 127.7, 127.8, 127.9, 128.0, 128.3 (CH, Ar *C*H, resonance overlap)], [137.9, 138.0, 138.1, 138.4 (C, Ar *C*), 161.1 (C, *C*=NH); visible resonances for minor α-anomer: δ_H(400 MHz) 4.00–4.20 (2H, stack, H-3, H-5), 6.58 (1H, d, *J* 3.1, H-1), 8.63 (1H, s, C=N*H*); δ_C(100 MHz) 68.0 (CH_2, C-6), 72.8 (CH_2, Ph*C*H$_2$), 73.1 (CH, C-

5), 73.4 (CH_2, Ph*C*H_2), 75.3 (CH_2, Ph*C*H_2), 76.8 (CH), 79.3 (CH), 81.3 (CH), 94.4 (CH, C-1), 161.3 (C, *C*=NH); *m/z* (TOF ES+) 706.2 ([M + Na]$^+$, 10%), 577.3 (100).

Data were in agreement with those reported in the literature.[180]

Phenyl [2′,3′,4′,6′-tetra-*O*-benzyl-α-D-glucopyranosyl]-(1′→3)-[2-*O*-benzyl-4,6-*O*-benzylidene-1-thio-α-D-mannopyranoside] (105)

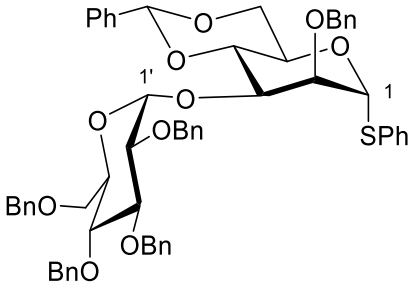

CBr_4 (0.88 g, 2.66 mmol) and Ph_3P (0.7 g, 2.66 mmol) were added sequentially to a solution of 2,3,4,6-tetra-*O*-benzyl-D-glucose **114** (437 mg, 0.81 mmol) in CH_2Cl_2 (5 mL) at rt. The reaction mixture was stirred for 3 h. In a separate flask, a solution of tetramethyl urea (TMU) (0.5 mL), Bu_4NBr (0.86 g, 2.66 mmol) and acceptor **92** (400 mg, 0.89 mmol) in CH_2Cl_2 (5 mL), were stirred over activated 3 Å MS for 30 min, after which time, this solution was added dropwise (5 min) *via* syringe to the solution containing the glycosyl donor. The reaction mixture was stirred at r.t. for 3 d until the donor was no longer being consumed (as judged by TLC). The reaction mixture was then filtered through a silica plug, washed with CH_2Cl_2 (50 mL) and concentrated under reduced pressure to provide the crude product. Purification of the residue by flash column chromatography (10% EtOAc in hexane) afforded glycoside **105** as a colourless oil oil and a mixture of anomers [α:β, 10 : 1 (as determined by ^{1}H-NMR), 402 mg, 51%]: Data for mixture unless specified otherwise: R_f = 0.6 (25% EtOAc in hexanes); $[\alpha]_D^{21}$ = + 127.2 (c = 1.0, $CHCl_3$),(α-anomer); ν_{max}(film)/cm^{-1} 2955 vw, 1743 vs, 1433 w, 1368 m, 1209 vs, 1148 s, 1087 m, 1051 s, 1025 s, 973 s, 913 w, 732 w; δ_H(400 MHz) 3.45 (1H, dd, *J* 9.7, 3.6, H-2′), 3.46–3.52 (1H, m, H-4′), 3.56–3.62 (2H,

stack, H-6′$_A$, H-6′$_B$), 3.66–3.72 (1H, m, H-5′), 3.79 (1H, app. t, *J* 10.0, H-6$_A$), 3.90 (1H, app. t, *J* 9.3, H-3′), 4.01 (1H, app. s, H-2), 4.12 (1H, dd, *J* 10.3, 4.5, H-6$_B$), 4.21–4.43 (6H, stack, H-3, H-4, H-5, three PhC*H*$_2$ hydrogens), 4.45–4.56, (2H, stack, PhC*H*$_2$), 4.65–4.80 (4H, stack, PhC*H*$_2$), 4.90 (1H, d, *J* 10.9, PhC*H*$_2$), 5.42 (1H, s, benzylidene C*H*), 5.45 (1H, d, *J* 3.5, H-1′), 5.49 (1H, d, *J* 1.1, H-1), 6.89–6.92 (2H, stack, Ph), 7.02–7.48 (33H, stack, Ph); δ_C(100 MHz) 65.3 (CH, C-5), 68.6 (CH$_2$, C-6, C-6′, resonance overlap), 70.6 (CH$_2$, PhCH$_2$), 70.9 (CH, C-5′), 72.8 (CH, C-3), 73.3 (CH$_2$, PhCH$_2$), 73.4 (CH$_2$, PhCH$_2$), 75.0 (CH$_2$, PhCH$_2$), 75.5 (CH$_2$, PhCH$_2$), 77.4 (CH, C-4′), 78.8 (CH, C-2′), 79.1 (CH, C-2), 79.5 (CH, C-4), 81.3 (CH, C-3′), 87.2 (CH, C-1), 97.0 (CH, C-1′), 102.4 (CH, benzylidene CH), [126.4, 127.2, 127.5, 127.6, 127.8, 127.9, 128.0, 128.1, 128.3, 128.5, 129.1, 129.3, 128.5 (CH, Ph, resonance overlap)], 133.8 (C, SPh *ipso* C), [137.3, 137.6, 137.9, 138.1, 138.4, 138.7 (C, Ph *ipso* C)]; *m/z* (TOF ES+) 995.4 ([M + Na]$^+$, 75%), 473.1 (100, [thioglycoside fragment + Na]$^+$); HRMS *m/z* (TOF ES+) 995.3808 [M + Na]$^+$, $C_{60}H_{60}O_{10}SNa$ requires 995.3805.

1,6-Di-*O*-acetyl-2,3,4-tri-*O*-benzyl-α,β-D-glucopyranose (115)

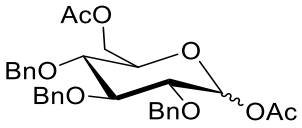

Concentrated H_2SO_4 (4 drops) was added to a solution of 2,3,4,6-Tetra-*O*-benzyl-D-glucopyranose (200 mg, 0.37 mmol) in acetic anhydride (1.5 mL) and acetic acid (0.5 mL). After 30 min at rt the reaction mixture was poured into ice-water (20 mL). The aqueous phase was extracted with CH_2Cl_2 (3 × 30 mL). The combined organic extracts were washed with brine (50 mL) and then dried (Na_2SO_4). The solvent was removed under reduced pressure and the residue purified by flash column chromatography (30% EtOAc in hexane) to yield the acetate **115** as a colourless syrup and as a mixture of anomers [α:β, 1.0 : 0.2 (as determined by ^{1}H-NMR), 162 mg, 82%]; Data for mixture unless specified otherwise: R_f = 0.5 (50% EtOAc in hexanes); δ_H(400 MHz, α-anomer) 2.03 (3H, s, C(O)C*H*$_3$), 2.16 (3H, s, C(O)C*H*$_3$), 3.54–3.60

(1H, m, H-4), 3.67 (1H, dd, *J* 9.6, 3.6, H-2), 3.91–4.01 (2H, stack, H-3, H-5), 4.23 (1H, dd, *J* 12.2, 2.6, H-6_A), 4.29 (1H, dd, *J* 12.2, 3.9, H-6_B), 4.57 (1H, A of AB, *J* 10.7, PhCH_AH_B), 4.64 (1H, A of AB, *J* 11.5, PhCH_CH_D), 4.71 (1H, B of AB, *J* 11.5, PhCH_CH_D), 4.83 (1H, A of AB, *J* 10.8, PhCH_EH_F), 4.89 (1H, B of AB, *J* 10.7, PhCH_AH_B), 4.99 (1H, B of AB, *J* 10.8, PhCH_EH_F), 6.32 (1H, d, *J* 3.5, H-1), 7.27–7.37 (15H, stack, Ph); δ_C(100 MHz, α-anomer) 20.8 (CH_3, C(O)CH_3), 21.1 (CH_3, C(O)CH_3), 62.7 (CH_2, C-6), 71.1 (CH, C-5), 73.2 (CH_2, PhCH_2), 75.3 (CH_2, PhCH_2), 75.8 (CH_2, PhCH_2), 76.6 (CH, C-4), 78.9 (CH, C-2), 81.6 (CH, C-3), 89.7 (CH, C-1), [127.8, 127.9, 128.10, 128.14, 128.2, 128.5, 128.6 (CH, Ar *C*H, resonance overlap)], [137.4, 137.6, 138.4 (C, Ar *C*)], [169.4, 170.4 (C, C=O)]; visible resonances for minor β-anomer: δ_H(400 MHz) 2.06 (3H, s, C(O)CH_3), 5.62 (1H, d, *J* 8.2, H-1); δ_C(100 MHz) 62.7 (CH_2, C-6), 73.7 (CH, C-5), 75.1 (CH_2, PhCH_2), 84.8 (CH, C-3), 93.8 (CH, C-1); *m/z* (TOF ES+) 557.2 ([M + Na]$^+$, 100%).

Data were in agreement with those reported in the literature.[181]

6-*O*-Acetyl-2,3,4-tri-*O*-benzyl-α,β-D-glucose (116)

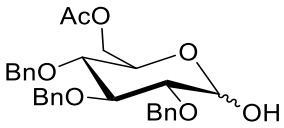

AcOH (15 μL, 0.27 mmol) and ethylenediamine (15 μL, 0.23 mmol) were added to a solution of diactate **115** (100 mg, 0.19 mmol) in THF (2 mL). After 24 h the THF was removed under reduced pressure and the crude residue was dissolved in CH_2Cl_2 (20 mL), washed with 2M HCl (20 mL), saturated sodium bicarbonate (20 mL) and then H_2O (3 × 50 mL). The organic layer was dried (Na_2SO_4), filtered and the filtrate was concentrated under reduced pressure. The crude residue was purified using flash column chromatography (30% EtOAc in hexanes) to give glucosyl **116** as a colourless syrup and a mixture of anomers [α:β, 1.0 : 0.64 (as determined by ^{1}H-NMR), 62 mg, 66%]; Data for mixture unless specified otherwise: R_f = 0.4

(50% EtOAc in hexanes); ν_{max}(film)/cm^{-1} 3031 w, 2873 w, 1739 s (C=O), 1496 m, 1454 m, 1363 m, 1235 s, 1147 m, 1067 vs, 1029 vs, 912 m, 748 s, 698 s; δ_H(400 MHz, α-anomer) 2.03 (3H, s, C(O)C*H*$_3$), 3.23 (1H, br s, O*H*), 3.48–3.60 (2H, stack, H-2, H-4), 4.02 (1H, spp. t, *J* 9.2, H-3), 4.08–4.12 (1H, m, H-5), 4.24–4.32 (2H, stack, H-6), 5.20 (1H, d, *J* 3.4, H-1), 4.58 (1H, A of AB, *J* 10.9, PhC*H*$_A$H$_B$), 4.70 (1H, A of AB, *J* 11.8, PhC*H*$_C$H$_D$), 4.78 (1H, B of AB, *J* 11.8, PhCH$_C$*H*$_D$), 4.84–4.91 (2H, stack, PhCH$_2$), 4.99 (1H, B of AB, *J* 10.8, PhCH$_E$*H*$_F$), 7.27–7.39 (15H, stack, Ar C*H*); δ_C(100 MHz, α-anomer) 20.9 (CH$_3$, C(O)*C*H$_3$), 63.0 (CH$_2$, C-6), 68.8 (CH, C-5), 73.3 (CH$_2$, Ph*C*H$_2$), 75.0 (CH$_2$, Ph*C*H$_2$), 75.7 (CH$_2$, Ph*C*H$_2$), 77.16 (CH, C-4), 80.0 (CH, C-2), 81.6 (CH, C-3), 91.1 (CH, C-1), [127.7, 127.77, 127.84, 127.9, 128.01, 128.05, 128.1, 128.4, 128.5 (CH, Ar *C*H, resonance overlap)], 137.6, 137.67, 137.73, 138.2, 138.3, 138.4 (C, Ar *C*, α+β) 170.8 (C, C=O); visible resonances for minor β-anomer: δ_H(400 MHz) 2.04 (3H, s, C(O)C*H*$_3$), 3.42 (1H, dd, *J* 9.1, 7.8, H-2), 3.67–3.72 (1H, m, H-3) δ_C(100 MHz) 21.0 (CH$_3$, C(O)*C*H$_3$), 63.1 (CH$_2$, C-6), 73.0 (CH, C-5), 74.8 (CH$_2$, Ph*C*H$_2$), 77.20 (CH, C-4), 83.0 (CH, C-2), 84.5 (CH, C-3), 97.4 (CH, C-1); *m/z* (TOF ES+) 515.2 ([M + Na]$^+$, 100%); HRMS *m/z* (TOF ES+) 515.2044 [M + Na]$^+$, $C_{29}H_{32}O_7Na$ requires 515.2046.

Data were in agreement with those reported in the literature.[62]

Phenyl [6′-*O*-acetyl-2′,3′,4′,-tri-*O*-benzyl-α-D-glucopyranosyl]-(1′→3)-[2-*O*-benzyl-4,6-*O*-benzylidene-1-thio-α-D-mannopyranoside] (118)

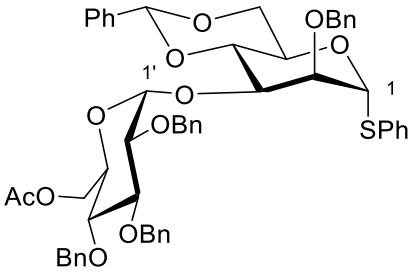

CBr_4 (101 mg, 0.30 mmol) and Ph_3P (80 mg, 0.30 mmol) were added sequentially to a solution of glucosyl **116** (50 mg, 0.10 mmol) in CH_2Cl_2 (3 mL) at rt. The reaction mixture was stirred for 3 h. In a separate flask, a solution of tetramethyl urea (TMU) (0.3 mL), Bu_4NBr (97 mg, 0.30 mmol) and acceptor **92** (45 mg, 0.10 mmol) CH_2Cl_2 (2 mL), were stirred over activated 3 Å MS for 30 min, after which time, this solution was added dropwise (2 min) *via* syringe to the solution containing the glycosyl donor. The reaction mixture was stirred at r.t. for 2 d until the donor was no longer being consumed (as judged by TLC). The reaction mixture was then filtered through a silica plug, washed with CH_2Cl_2 (30 mL) and concentrated under reduced pressure to provide the crude product. Purification of the residue by flash column chromatography (10% EtOAc in hexane) afforded glycoside **118** as a colourless oil (24 mg, 26%): R_f = 0.5 (25% EtOAc in hexanes); $[\alpha]_D^{22}$ = +109.3 (c = 1.0, $CHCl_3$); ν_{max}(film)/cm^{-1} 2910 vw, 1740 m (C=O), 1454 m, 1365 w, 1234 m, 1092 vs, 1039 vs, 1027 vs, 1004 s, 967 m, 907 m, 741 vs, 696 vs; δ_H(400 MHz) 2.00 (3H, s, CH_3), 3.30 (1H, app. t, *J* 9.4, H-4′), 3.41 (1H, dd, *J* 9.6, 3.6, H-2′), 3.71–3.83 (2H, stack, H-6$_A$, H-5′), 3.91 (1H, app. t, *J* 9.2, H-3′), 3.99–4.02 (1H, m, H-2), 4.08–4.19 (3H, stack, H-6$_B$, H-6′$_A$, H-6′$_B$), 4.22 (1H, d, *J* 12.3, PhCH_2), 4.25–4.39 (3H, stack, H-3, H-4, H-5), 4.45 (1H, d, *J* 11.0, PhCH_2), 4.49 (1H, d, *J* 12.3, PhCH_2), 4.67 (1H, d, *J* 10.9, PhCH_2), 4.72 (1H, A of AB, *J* 11.9, PhCH_AH$_B$), 4.76 (1H, B of AB, *J* 11.9, PhCH$_A$$H_B$), 4.80 (1H, d, *J* 11.0, PhCH_2), 4.92 (1H, d, *J* 10.9, PhCH_2), 5.39 (1H, d, *J* 3.6, H-1′), 5.42 (1H, s, benzylidene C*H*), 5.51 (1H, d, *J* 0.9, H-1), 6.88–6.91 (2H, stack, Ph), 7.05–7.40 (28H, stack, Ph); δ_C(100 MHz) 21.0 (*C*H$_3$), 63.5 (CH$_2$, C-6′), 65.3 (CH),

68.6 (CH_2, C-6), 69.4 (CH, C-5′), 70.6 (CH_2, $PhCH_2$), 73.0 (CH), 73.4 (CH_2, $PhCH_2$), 75.1 (CH_2, $PhCH_2$), 75.6 (CH_2, $PhCH_2$), 77.3 (CH, C-4′), 78.7 (CH, C-2′), 79.2 (CH, C-2), 79.5 (CH), 81.3 (CH, C-3′), 87.2 (CH, C-1), 96.9 (CH, C-1′), 102.6 (CH, benzylidene CH), [126.5 ,127.28 ,127.34 ,127.6 ,127.8 ,128.09 ,128.18 ,128.23 ,128.37 ,128.43 ,128.6 ,129.2 ,129.4 ,131.5 (CH, Ph, resonance overlap)], [133.7 ,137.3 ,137.5 ,137.99 ,138.03, 138.6 (C, Ph, ipso C)] ,170.9 (C, C=O); *m/z* (TOF ES+) 947.3 ([M + Na]$^+$, 100%; HRMS *m/z* (TOF ES+) 947.3462 [M + Na]$^+$, $C_{55}H_{56}O_{11}SNa$ requires 947.3441.

5‴′-Azidopentyl [2‴,3‴,4‴,6‴-tetra-*O*-benzyl-αβ-D-glucopyranosyl]-(1‴→3″)-[2″-*O*-benzyl-4″,6″-*O*-benzylidene-αβ-D-mannopyranosyl]-(1″→2′)-[3′,4′,6′-tri-*O*-benzyl-α-D-mannopyranosyl]-(1′→2)-[3,4,6-tri-*O*-benzyl-α-D-mannopyranoside] (119)

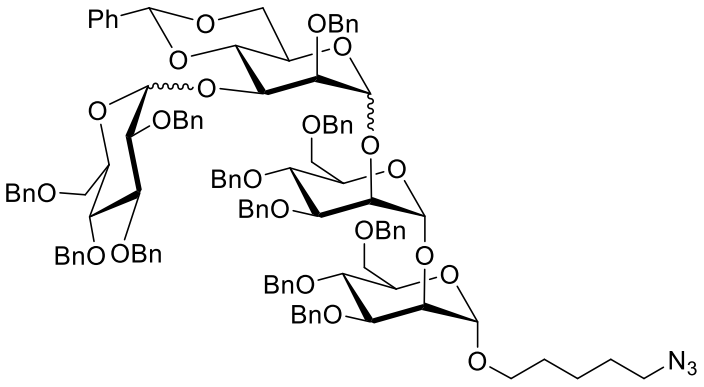

A solution of thioglycoside **105** (65 mg, 0.066 mmol) and acceptor **83** (65 mg, 0.066 mmol) in CH_2Cl_2 (2 mL) was stirred over activated 4 Å molecular sieves (70 mg) for 30 mins. NIS (30 mg, 0.132 mmol) was added and the mixture stirred for a further 10 min before cooling to –20 °C. TfOH (2 μL, 0.02 mmol) was added and after 2 h the reaction was quenched by addition of Et_3N (0.5 mL). The solution was diluted with CH_2Cl_2 (20 mL) before being filtered through a Celite pad. The filtrate was washed sequentially with $Na_2S_2O_3$ solution (20 mL), H_2O (20 mL) and brine (20 mL), dried (Na_2SO_4), filtered, and concentrated under reduced pressure. The residue was purified by flash column chromatography (10% EtOAc in hexanes) to afford

tetrasaccharide **119** as a colourless oil and as a mixture of anomers (27 mg, 22%): Data for mixture unless specified otherwise: R_f = 0.5 (25% EtOAc in hexanes); ν_{max}(film)/cm^{-1} 2923 m, 2862 m, 2094 m (N_3), 1495 m, 1453 m, 1361 m, 1279 m, 1209 m, 1052 br vs, 913 m, 814 m, 736 vs, 696 vs; δ_H(400 MHz) 1.20–1.27 (2H, stack), 1.35–1.50 (4H, stack), 3.07–3.18 (3H, stack), 3.37–3.47 (3H, stack), 3.45–3.66 (7H, stack), 3.71–3.77 (3H, stack), 3.78–3.88 (5H, stack), 3.89–3.96 (3H, stack), 4.02 (1H, dd, *J* 10.0, 4.8), 4.09–4.14 (2H, stack), 4.22 (1H, A of AB, *J* 12.3, PhC*H*$_A$H$_B$), 4.26–4.32 (2H, stack), 4.35–4.40 (2H, stack), 4.41–4.43 (2H, stack), 4.45–4.54 (7H, stack), 4.59–4.67 (5H, stack), 4.70–4.79 (3H, stack), 4.85–4.89 (2H, stack), 5.08 (1H, d, *J* 1.3), 5.10 (1H, d, *J* 1.1), 5.37 (1H, s, benzylidene C*H*), 5.47 (1H, d, *J* 3.5), 7.00–7.30 (60H, stack, Ar C*H*); δ_C(100 MHz) 23.3 (CH_2), 28.6 (CH_2), 29.0 (CH_2), 51.3 (CH_2), 64.6 (CH), 67.4 (CH_2), 68.1 (CH_2), 68.8 (CH_2), 69.4 (CH_2), 69.7 (CH_2), 70.7 (CH_2), 70.8 (CH), 71.9 (CH), 72.1 (CH), 73.3 (CH_2), 73.5 (CH_2), 74.9 (CH), 75.1 (CH_2), 75.1 (CH_2), 75.2 (CH_2), 75.3 (CH), 75.5 (CH_2), 76.0 (CH), 77.1 (CH), 77.7 (CH), 79.0 (CH), 79.2 (CH), 79.7 (CH), 81.4 (CH), 96.8, (CH), 98.7 (CH), 100.8 (CH), 101.1 (CH), 102.4 (CH, benzylidene *C*H), [126.5, 127.2, 127.3, 127.4, 127.5, 127.6, 127.7, 127.8, 128.0, 128.1, 128.23, 128.29, 128.34, 128.5, 128.6, 129.2 (CH, Ar *C*H, resonance overlap)], [137.5, 137.9, 138.0, 138.2, 138.3, 138.4, 138.6, 138.9 (C, Ar *C*, resonance overlap)]; *m/z* (TOF ES+) 1879.7 ([M + Na]$^+$, 20%), 951.4 (100).

Phenyl 2-*O*-benzoyl-4,6-*O*-benzylidene-1-thio-α-D-mannopyranose (120) and Phenyl 2,3-di-*O*-benzoyl-4,6-*O*-benzylidene-1-thio-α-D-mannopyranose (121)

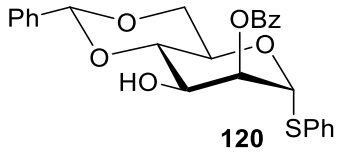

120

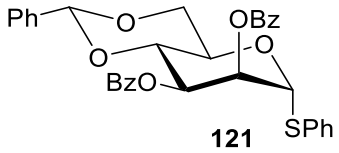

121

5% NaOH solution (7 mL) was added to solution of diol **86** (1.00 g, 2.77 mmol) and Bu_4HSO_4 (190 mg, 0.55 mmol) in CH_2Cl_2 (80 mL) at –3 °C. A solution of BzCl (0.35 mL, 3.05 mmol) in CH_2Cl_2 (5 mL) was added to the biphasic mixture over 5 min. After 35 min, the phases were separated and the aqueous phase was extracted with CH_2Cl_2 (2 × 10 mL). The combined organic fractions were washed sequentially with $NaHCO_3$ solution (50 mL) and brine (50 mL), dried (Na_2SO_4), filtered, and concentrated under reduced pressure. The residue was purified by flash column chromatography (10% EtOAc in hexanes) to afford in order of elution , bis-benzoate **121** as a white solid (410 mg, 26%): R_f = 0.5 (20% EtOAc in hexanes); m.p. 145–148 °C, lit.[64] 141-143 °C; $[\alpha]_D^{21}$ = +6.0 (c = 1.0, $CHCl_3$), lit.[64] $[\alpha]_D^{27}$ = +4.3 (c = 1.0, $CHCl_3$); ν_{max}(film)/cm^{-1} 1731 s (C=O), 1709 s (C=O), 1478 w, 1451 w, 1378 w, 1364 w, 1277 s, 1249 s, 1177 m, 1086 vs, 1066 vs, 1026 s, 1011 s, 1002 s, 964 s, 744 s, 713 vs, 697 vs, 689 vs; δ_H(400 MHz) 3.99 (1H, app. t, *J* 10.3, H-6$_A$), 4.35 (1H, dd, *J* 10.4, 4.9, H-6$_B$), 4.43 (1H, app. t, *J* 9.9, H-4), 4.65 (1H, app. td, *J* 9.9, 4.6, H-5), 5.69 (1H, d, *J* 1.3, H-1), 5.70 (1H, s, benzylidene CH), 5.84 (1H, dd, *J* 10.3, 3.4, H-3), 5.98 (1H, dd, *J* 3.4 1.3, H-2), 7.31–7.39 (8H, stack, Ph), 7.47–7.53 (5H, stack, Ph), 7.54–7.58 (2H, stack, Ph), 7.60–7.66 (1H, m, Ph), 7.92–7.97 (2H, stack, Ph), 8.06–8.11 (2H, stack , Ph); δ_C(100 MHz) 65.3 (CH, C-5), 68.6 (CH_2, C-6), 69.2 (CH, C-3), 72.5 (CH, C-2), 76.9 (CH, C-4), 87.0 (CH, C-1), 102.0 (CH, benzylidene CH), [126.2, 128.2, 128.3, 128.6, 129.1, 129.3 (CH, Ph)], [129.4, 129.5 (C, Ph *ipso* C)], [129.8, 129.9, 132.4 (CH, Ph)], 132.9 (C, Ph *ipso* C), [133.2, 133.6 (CH, Ph)], 137.0 (C, Ph *ipso* C), [165.3, 165.4 (C, C=O)]; *m/z* (TOF ES+) 591.1 ([M + Na]$^+$, 100%), followed by monobenzoate **120** (0.62 g,

48%): R_f = 0.29 (20% EtOAc in hexanes); m.p. 131–136 °C, lit.[64] 150–151 °C; $[\alpha]_D^{21}$ = +85.6 (c = 1.0, $CHCl_3$), lit.[64] $[\alpha]_D^{27}$ = +131.3 (c = 1.0, $CHCl_3$); ν_{max}(film)/cm^{-1} 3477 br w, 3061 w, 2868 w, 1721 s (C=O), 1382 m, 1266 s, 1091 vs, 1025 s, 1001 s, 965 s, 740 s, 710 s, 699 s; δ_H(400 MHz) 2.53 (1H, br s, O*H*), 3.82 (1H, app. t, *J* 10.3, H-6_A), 4.04 (1H, app. t, *J* 9.7, H-4), 4.21 (1H, dd, *J* 10.3, 4.9, H-6_B), 4.27 (1H, dd, *J* 9.9, 3.5, H-3), 4.37 (1H, app. dt, *J* 9.9, 4.9, H-5), 5.55 (1H, d, *J* 1.1, H-1), 5.59 (1H, s, benzylidene C*H*), 5.65 (1H, dd, *J* 3.5, 1.1, H-2), 7.20–7.55 (13H, stack, Ph), 7.99–8.03 (2H, stack, Ph); δ_C(100 MHz); 64.6 (CH, C-5), 68.0 (CH, C-3), 68.5 (CH_2, C-6), 74.1 (CH, C-2), 79.5 (CH, C-4), 87.0 (CH, C-1), 102.3 (CH, benzylidene CH), [126.3, 128.0, 128.4, 128.5, 129.2, 129.4, 129.9, 132.1 (CH, Ph)], 133.1 (C, Ph *ipso* C), 133.5 (CH, Ph) 137.0 (C, Ph *ipso* C, resonance overlap), 165.9 (C, C=O); *m/z* (TOF ES+) 487.1 ($[M + Na]^+$, 100%).

Data were in agreement with those reported in the literature.[64]

Methyl 2-*O*-acetyl-3,4,6-tri-*O*-benzyl-α-D-mannopyranose (122)

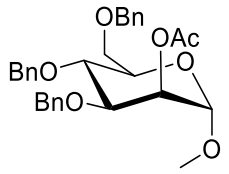

A solution of orthoester **44** (0.3 g, 0.59 mmol) in CH_2Cl_2 (2 mL) was stirred over activated powdered 4 Å molecular sieves (100 mg) for 30 min. The solution was then cooled to 0 °C and TMSOTf (11 µL, 0.061 mmol, 10 mol%) was added dropwise over 0.5 min. The reaction mixture was stirred for 1 h and then diluted with CH_2Cl_2 (10 mL) and filtered. The filtrate was washed with $NaHCO_3$ solution (3 × 10 mL). The aqueous phase was extracted with CH_2Cl_2 (2 × 50 mL). The combined organic extracts were washed with brine (100 mL) and then dried (Na_2SO_4). The solvent was removed under reduced pressure and the residue purified by flash column chromatography (15% EtOAc in hexane) to yield the acetate **122** as a colourless syrup

(0.26 g, 87%): R_f = 0.40 (30% EtOAc in hexanes); $[\alpha]_D^{21}$ = +432.8 (c = 1.0, $CHCl_3$), lit.[42] $[\alpha]_D^{19}$ = +29.2 (c = 5.8, $CHCl_3$); ν_{max}(film)/cm^{-1} 2910 w, 1744 s (C=O), 1496 w, 1453 m, 1366 m, 1286 w, 1233 vs, 1138 s, 1076 vs, 1059 vs, 1027 s, 971 s, 913 w, 847 w, 735 vs, 696 vs; δ_H(400 MHz) 2.08 (3H, s, acetyl CH_3), 3.28 (3H, s, OCH_3), 3.61–3.75 (3H, stack, H-5, H-6_A, H-6_B), 3.80 (1H, app. t, *J* 9.3, H-4), 3.89 (1H, dd, *J* 9.2, 3.2, H-3), 4.40 (1H, d, *J* 10.8, PhCH_2), 4.42–4.47 (2H, stack, PhCH_2), 4.58–4.67 (2H, stack, PhCH_2), 4.66 (1H, d, *J* 1.4, H-1), 4.78 (1H, d, *J* 10.8, PhCH_2), 5.29 (1H, dd, *J* 3.2, 1.6, H-2), 7.08–7.10 (2H, stack, Ph), 7.16–7.30 (13H, stack, Ph); δ_C(100 MHz) 21.2 (CH_3, acetyl CH_3), 55.0 (CH_3, OCH_3), 68.7 (CH, C-2), 68.9 (CH_2, C-6), 71.3 (CH, C-5), 71.8 (CH_2, $PhCH_2$), 73.5 (CH_2, $PhCH_2$), 74.3 (CH, C-4), 75.2 (CH_2, $PhCH_2$), 78.2 (CH, C-3), 98.8 (CH, C-1), [127.6, 127.77, 127.82, 128.1, 128.3, 128.4 (CH, Ph, resonance overlap)], [138.0, 138.2, 138.4 (C, Ph, *ipso* C)], 170.5 (C, C=O); *m/z* (TOF ES+) ($[M + Na]^+$, 100%).

Data were in agreement with those reported in the literature.[42]

Methyl 3,4,6-tri-*O*-benzyl-α-D-mannopyranose (123)

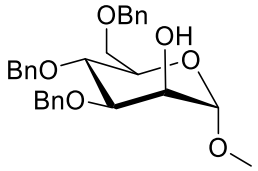

NaOMe (1.0 mL of a 0.5 M soln. in MeOH, 0.5 mmol) was added to a solution of acetate **122** (0.2 g, 0.39 mmol) in MeOH (10 mL). After stirring at rt for 3 h, the reaction mixture was neutralised by the addition of acidic ion-exchange resin [Dowex H CR-S, pre-washed sequentially with MeOH (100 mL) and $CHCl_3$ (50 mL)]. The solution was filtered and the resin washed sequentially with MeOH (2 × 20 mL) and $CHCl_3$ (2 × 20 mL). The filtrate was concentrated under reduced pressure and the residue purified by column chromatography (25% EtOAc in hexanes) to provide alcohol **123** as a colourless oil (0.176 g, 96%): R_f = 0.25 (30% EtOAc in hexanes); $[\alpha]_D^{21}$ = + 448.2 (c = 1.0, $CHCl_3$), lit.[42] $[\alpha]_D^{19}$ = +50.7 (c = 6.7, $CHCl_3$);

ν_{max}(film)/cm^{-1} 3368 br m (OH), 2910 w, 1637 m, 1453 m, 1363 w, 1209 w, 1098 s, 1055 s, 1025 m, 970 m, 907 w, 734 s, 696 s; δ_H(400 MHz) 3.38 (3H, s, OCH_3), 3.70–3.80 (3H, stack, H-6$_A$, H-6$_B$, H-5), 3.83–3.91 (2H, stack, H-3, H-4), 4.05 (1H, dd, *J* 2.6, 1.8, H-2), 4.52 (1H, d, *J* 10.9, PhCH_2), 4.56 (1H, d, *J* 12.2, PhCH_2), 4.67 (1H, d, *J* 12.2, PhCH_2), 4.70 (2H, AB quartet *J* 11.5, PhCH_2), 4.58 (1H, A of AB, *J* 11.6, PhCH_AH$_B$), 4.62 (1H, B of AB, *J* 11.6, PhCH$_A$$H_B$), 4.82 (1H, d, *J* 1.8, H-1), 4.84 (1H, d, *J* 10.9, PhCH_2), 7.16–7.21 (2H, stack, Ph), 7.25–7.40 (13H, stack, Ph); δ_C(100 MHz) 54.8 (CH_3, OMe) 68.2 (CH, C-2), 68.9 (CH_2, C-6), 70.9 (CH, C-5), 71.9 (CH_2, $PhCH_2$), 73.4 (CH_2, $PhCH_2$), 74.2 (CH, C-4), 75.0 (CH_2, $PhCH_2$), 80.1 (CH, C-3), 100.2 (CH, C-1), [127.5, 127.6, 127.8, 128.1, 128.3, 128.5, (CH, Ph, resonance overlap)], [137.9, 138.2, 138.3 (C, Ph, *ipso* C)]; *m/z* (TOF ES+) 487.2 ([M + Na]$^+$, 100%).

Data were in agreement with those reported in the literature.[42]

Methyl [2′,3′-di-*O*-benzoyl-4′,6′-*O*-benzylidene-α-D-mannopyranosyl]-(1′→2) [3,4,6-tri-*O*-benzyl-α-D-mannopyranoside] (124)

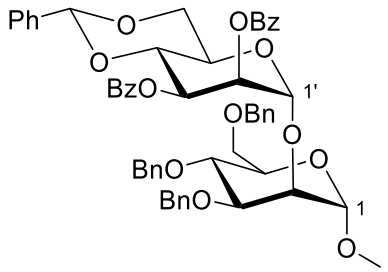

A solution of thioglycoside **121** (100 mg, 0.176 mmol) and acceptor **123** (100 mg, 0.215 mmol) in CH_2Cl_2 (2 mL) was stirred over activated 4 Å molecular sieves (150 mg) for 30 mins. NIS (79 mg, 0.352 mmol) was added and the mixture stirred for a further 10 min before cooling to –20 °C. TfOH (5 μL, 0.053 mmol) was added and after 2 h the reaction was quenched by addition of Et_3N (0.5 mL). The solution was diluted with CH_2Cl_2 (25 mL) before being filtered through a Celite pad. The filtrate was washed sequentially with $Na_2S_2O_3$ solution (20 mL), H_2O

(20 mL) and brine (20 mL), dried (Na_2SO_4), filtered, and concentrated under reduced pressure. The residue was purified by flash column chromatography (10% EtOAc in hexanes) to afford disaccharde **124** as a colourless oil (120 mg, 74%): R_f = 0.5 (25% EtOAc in hexanes); $[\alpha]_D^{21}$ = +359.2 (c = 1.0, $CHCl_3$); ν_{max}(film)/cm^{-1} 2911 w, 1729 s (C=O), 1452 m, 1364 w, 1314 w, 1272 s, 1218 w, 1176 w, 1135 m, 1093 vs, 1068 vs, 1058 vs, 1026 s, 969 m, 916 w, 751 m, 712 s, 698 s, 667 m; δ_H(400 MHz) 3.29 (3H, s, OCH_3), 3.67–3.74 (3H, stack, H-6, H-5), 3.81–3.89 (3H, stack, H-3, H-4, H-6′$_A$), 3.95–3.97 (1H, m, H-2), 4.12–4.24 (2H, stack, H-4′ and H-5′), 4.27 (1H, dd, *J* 10.2, 4.4, H-6′$_B$), 4.49 (1H, d, *J* 10.9, PhCH_2), 4.52–4.66 (4H, stack, 2 × PhCH_2), 4.74 (1H, d, *J* 1.7, H-1), 4.78 (1H, d, *J* 10.9, PhCH_2), 5.14 (1H, d, *J* 1.3, H-1′), 5.55 (1H, s, benzylidene C*H*), 5.80 (1H, dd, *J* 9.5, 3.5, H-3′), 5.84 (1H, dd, *J* 3.5, 1.3, H-2′), 6.96–7.02 (1H, m, Ph), 7.03–7.28 (17H, stack, Ph), 7.30–7.44 (7H, stack, Ph), 7.50–7.54 (1H, m, Ph), 7.80–7.84 (2H, stack, Ph), 7.96–8.00 (2H, stack, Ph); δ_C(100 MHz) 54.8 (CH_3, OCH_3), 64.3 (CH, C-4′), 68.9 (CH_2, C-6′), 69.0 (CH, C-3′), 69.4 (CH_2, C-6), 70.8 (CH, C-2′), 72.0 (CH, C-5), 72.6 (CH_2, $PhCH_2$), 73.5 (CH_2, $PhCH_2$), 75.0 (CH, C-4), 75.3 (CH_2, $PhCH_2$), 75.4 (CH, C-2), 77.0 (CH, C-5′), 80.0 (CH, C-3), 99.8 (CH, C-1), 100.2 (CH, C-1′), 102.0 (CH, benzylidene CH), [126.3, 127.5, 127.6, 127.8, 128.2, 128.3, 128.4, 128.6, 129.1, (CH, Ph, resonance overlap)],129.7 (C, Ph, *ipso* C), [129.8, 129.9, 133.0, 133.5 (CH, Ph)], [137.2, 138.3, 138.4, 138.6 (C, Ph, *ipso* C)], [165.1, 165.3 (C, C=O)]; *m/z* (TOF ES+) 945.3 ([M + Na]$^+$, 100%); HRMS *m/z* (TOF ES+) 945.3476 [M + Na]$^+$, $C_{55}H_{54}O_{13}Na$ requires 945.3462.

Phenyl [2′,3′,4′,6′-tetra-*O*-benzyl-α-D-glucopyranosyl]-(1′→3)-[2-*O*-benzoyl-4,6-*O*-benzylidene-1-thio-α-D-mannopyranoside] (125)

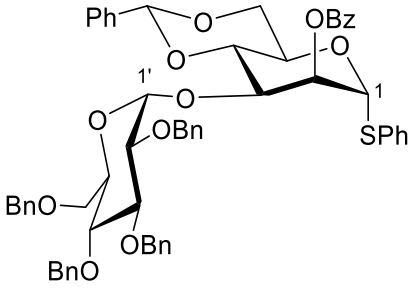

CBr_4 (430 mg, 1.29 mmol) and Ph_3P (338 mg, 1.29 mmol) were added sequentially to a solution of 2,3,4,6-tetra-*O*-benzyl-D-galactose **114** (227 mg, 0.42 mmol) in CH_2Cl_2 (5 mL) at rt. The reaction mixture was stirred for 3 h. In a separate flask, a solution of tetramethyl urea (TMU) (0.3 mL), Bu_4NBr (415 mg, 1.29 mmol) and acceptor **120** (200 mg, 0.43 mmol) in CH_2Cl_2 (5 mL), were stirred over activated 3 Å MS for 30 min, after which time, this solution was added dropwise (5 min) *via* syringe to the solution containing the glycosyl donor. The reaction mixture was stirred at r.t. for 3 d until the donor was no longer being consumed (as judged by TLC). The reaction mixture was then filtered through a silica plug, washed with CH_2Cl_2 (50 mL) and concentrated under reduced pressure to provide the crude product. Purification of the residue by flash column chromatography (10% EtOAc in hexane) afforded glycoside **125** as a colourless oil (236 mg, 57%): R_f = 0.6 (25% EtOAc in hexanes); $[\alpha]_D^{21}$ = +67.2 (c = 1.0, $CHCl_3$); ν_{max}(film)/cm^{-1} 3030 w, 3865 w, 1730 m (C=O), 1454 m, 1242 s, 1215 m, 1165 m, 1093 vs, 1059 vs, 1027 vs, 736 vs, 695 vs; δ_H(400 MHz) 3.39 (1H, dd, *J* 9.7, 3.7, H-2′), 3.48 (1H, app. t, *J* 9.5, H-4′), 3.58–3.64 (2H, stack, H-6′$_A$, H-6′$_B$), 3.68 (1H, app. t, *J* 9.3, H-3′), 3.76–3.84 (2H, stack, H-5′, H-6$_A$), 4.17 (1H, dd, *J* 10.3 4.8, H-6$_B$), 4.23–4.37 (3H, stack, H-4, PhC*H*$_2$), 4.38–4.46 (5H, stack, H-3, H-5, three Bn hydrogens), 4.54–4.70 (3H, stack, 3 × Bn hydrogens), 5.38 (1H, d, *J* 3.7, H-1′), 5.42 (1H, s, benzylidene C*H*), 5.59 (1H, d, *J* 1.2, H-1), 5.66 (1H, dd, *J* 3.4, 1.2, H-2), 6.87–6.91 (2H, stack, Ph), 6.99–7.44 (30H, stack, Ph), 7.47–7.52 (1H, m, Ph), 8.04–8.08 (2H, stack, Ph); δ_C(100 MHz) 65.0

(CH, C-5), 68.4 (CH_2, C-6′), 68.6 (CH_2, C-6), 70.8 (CH_2, $PhCH_2$), 70.9 (CH, C-5′), 71.7 (CH, C-3), 73.5 (CH_2, $PhCH_2$) 74.3 (CH, C-2), 74.5 (CH_2, $PhCH_2$ protecting 4′-*O*), 75.4 (CH_2, $PhCH_2$ protecting 3′-*O*), 77.2 (CH, C-4′), 79.0 (CH, C-2′), 79.7 (CH, C-4), 81.1 (CH, C-3′), 87.1 (CH, C-1), 97.5 (CH, C-1′), 102.4 (CH, benzylidene *C*H), [126.4, 127.0, 127.2, 127.4, 127.6, 128.0, 128.1, 128.2, 128.4, 128.5, 129.2, 129.4 (CH, Ph)], 129.8 (C, Ph *ipso* C), [130.0, 132.0 (CH, Ph)], 133.1 (C, Ph *ipso* C), 133.4 (CH, Ph), [137.1, 138.0, 138.4, 138.6, 138.8 (C, Ph *ipso* C)], 165.9 (C, C=O); *m/z* (TOF ES+) 1009.4 ($[M + Na]^+$, 100%); HRMS *m/z* (TOF ES+) 1009.3602 $[M + Na]^+$, $C_{60}H_{58}O_{11}SNa$ requires 1009.3598.

5-Azidopentyl [2‴″,3‴″,4‴″,6‴″-tetra-*O*-benzyl-α-D-glucopyranosyl]-(1‴″→3‴)-[4‴,6‴-*O*-benzylidene-α-D-mannopyranosyl]-(1‴→2″)-[3″,4″,6″-tri-*O*-benzyl-α-D-mannopyranosyl]-(1″→2′)-[3′,4′,6′-tri-*O*-benzyl-α-D-mannopyranoside] (127)

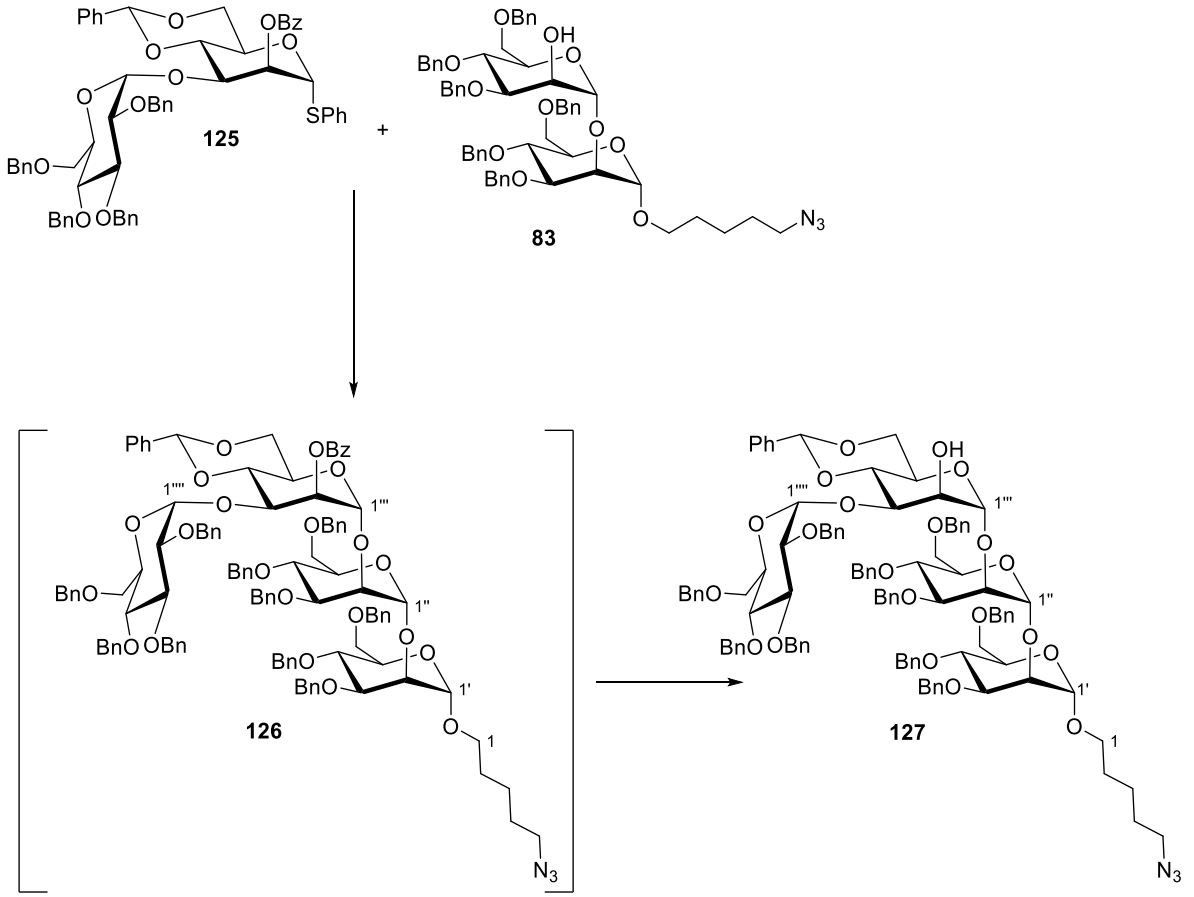

A solution of thioglycoside **125** (180 mg, 0.182 mmol) and acceptor **83** (180 mg, 0.182 mmol) in CH_2Cl_2 (2 mL) was stirred over activated 4 Å molecular sieves (200 mg) for 30 mins. NIS (82 mg, 0.364 mmol) was added and the mixture stirred for a further 10 min before cooling to –20 °C. TfOH (5 μL, 0.55 mmol) was added and after 2 h the reaction was quenched by addition of Et_3N (0.5 mL). The solution was diluted with CH_2Cl_2 (25 mL) before being filtered through a Celite pad. The filtrate was washed sequentially with $Na_2S_2O_3$ solution (20 mL), H_2O (20 mL) and brine (20 mL), dried (Na_2SO_4), filtered, and concentrated under reduced pressure. The residue was purified by flash column chromatography (10% EtOAc in hexanes) to afford tetrasaccharide **126** as a colourless oil and as a mixture of anomers (148 mg, 43%). Data for mixture unless specified otherwise: R_f = 0.5 (25% EtOAc in hexanes); ν_{max}(film)/cm^{-1} 2923 m,

2855 m, 2096 m (N_3), 1726 m (C=O), 1493 m, 1453 m, 1362 m, 1264 s, 1095 br vs, 737 s, 698 s; δ_H(400 MHz) 1.20–1.27 (2H, stack), 1.35–1.50 (4H, stack), 3.10–3.16 (3H, stack), 3.35 (1H, dd, *J* 9.6, 3.6), 3.43–3.57 (5H, stack), 3.60–3.83 (12H, stack), 3.85–4.10 (7H, stack), 4.13–4.24 (4H, stack), 4.31 (1H, A of AB, *J* 11.3, PhCH_AH_B), 4.37–4.60 (16H, stack), 4.67 (1H, B of AB, *J* 11.3, PhCH_2), 4.74 (1H, B of AB, *J* 10.7, PhCH_2), 4.78 (1H, B of AB, *J* 10.9), 4.83 (1H, d, *J* 1.55), 5.09 (1H, d, *J* 1.3), 5.13 (1H, d, *J* 1.5), 5.36 (1H, s, benzylidene C*H*), 5.39 (1H, d, *J* 3.5, H-2‴″), 5.56 (1H, dd, *J* 3.6, 1.44, H-1‴″), 7.00–7.30 (60H, stack, Ar C*H*); *m/z* (TOF ES+) 1893.7 ([M + Na]$^+$, 100%); NaOMe (0.5 mL of a 0.5 M soln. in MeOH, 0.25 mmol) was added to a solution of benzoate **126** (148 mg, mmol) in MeOH (3 mL). After stirring at rt for 3 h, the reaction mixture was neutralised by the addition of acidic ion-exchange resin [Dowex H CR-S, pre-washed sequentially with MeOH (20 mL) and $CHCl_3$ (20 mL)]. The solution was filtered and the resin washed sequentially with MeOH (2 × 20 mL) and $CHCl_3$ (2 × 20 mL). The filtrate was concentrated under reduced pressure and the residue purified by column chromatography (10% EtOAc in hexanes) to provide alcohol **127** as a colourless oil (0.111 g, 35% over two steps): R_f = 0.3 (25% EtOAC in hexanes); ν_{max}(film)/cm^{-1} 3398 br m (O–H), 3031 w, 2914 m, 2096 (N_3), 1496 m, 1453 m, 1361 m, 1280 w, 1210 w, 1134 s, 1093 vs, 1053 vs, 1027 vs, 913 m, 812 m, 736 vs, 696 vs; δ_H(900 MHz) 1.35–1.39 (2H, stack, H-3), 1.51–1.55 (2H, stack, H-2), 1.57–1.61 (2H, stack, H-4), 3.25–3.28 (3H, stack, H-1$_A$, H-5), 3.59–3.62 (2H, stack, H-1$_B$, H-2‴″), 3.64–3.71 (3H, stack, H-4‴″, H-6‴″) 3.75–3.78 (2H, stack, H-5′, H-6′$_A$), 3.79–3.82 (2H, stack, H-6″), 3.83–3.87 (4H, stack, H-4′, H-4″ H-6′$_B$, H-6‴$_A$) 3.94 (1H, ddd, *J* 10.1, 3.5, 2.2, H-5‴″), 3.96 (1H, dd, *J* 9.4, 3.0, H-3′), 3.99–4.01 (2H, stack, H-2′, H-3″), 4.04 (1H, app. t, *J* 9.3, H-3‴″), 4.06 (1H, ddd, *J* 9.8, 4.6, 3.3, H-5″), 4.11 (1H, app. dt, *J* 9.8, 5.0, H-5‴), 4.18 (1H, dd, *J* 10.3, 5.0, H-6‴$_B$), 4.21–4.22 (1H, m, H-2″), 4.28 (1H, dd, *J* 3.1, 1.4, H-2‴″), 4.30 (1H, app. t, *J* 9.6, H-4‴), 4.36 (1H, A of AB, *J* 12.2, PhCH_AH_B), 4.38 (1H, dd, *J* 9.8, 3.2, H-3‴), 4.45 (1H, A of AB, *J* 12.0, PhCH_CH_D), 4.47 (1H, A of AB, *J* 10.7, PhCH_EH_F), 4.54 (1H, A of AB, *J* 10.8, PhCH_KH_L), 4.58 (1H, B of AB, *J* 12.2, PhCH$_A$$H_B$), 4.60–4.65 (6H, stack, PhCH_2), 4.71–4.76 (4H, stack, PhCH_2), 4.85–4.90 (4H, stack, PhCH_2), 4.98 (1H, d, *J* 1.6, H-

1′), 5.03 (1H, A of AB, *J* 10.9, PhCH$_P$*H*$_Q$), 5.20 (1H, d, *J* 1.1, H-1‴), 5.24 (1H, d, *J* 1.5, H-1″), 5.52 (1H, d, *J* 3.8, H-1⁗), 5.57 (1H, s, benzylidene C*H*), 7.06–7.08 (2H, stack, Ar C*H*), 7.16–7.17 (2H, stack, Ar C*H*), 7.19–7.22 (4H, stack, Ar C*H*), 7.23–7.40 (43H, stack, Ar C*H*), (2H, stack, Ar C*H*), 7.42–7.44 (4H, stack, Ar C*H*); δ_C(100 MHz) 23.4 (CH_2, C-3), 28.6 (CH_2, C-4), 29.0 (CH_2, C-2), 51.3 (CH_2, C-5), 64.1 (CH, C-5‴), 67.3 (CH_2, C-1), 68.2 (CH_2, C-6⁗), 68.8 (CH_2, C-6‴), 69.4 (CH_2, C-6′), 69.6 (CH_2, C-6″), 70.7 (CH, C-5⁗), 71.1 (CH, C-2‴), 71.2 (CH_2, Ph*C*H$_2$), 71.9 (CH, C-5′), 72.10 (CH_2, Ph*C*H$_2$), 72.14 (CH, C-5″), 72.6 (CH_2, Ph*C*H$_2$), [73.3, 73.4 (CH_2, 3 × Ph*C*H$_2$ and CH, C-3‴, resonance overlap)], 74.9 (CH, C-4′), [75.1, 75.2 (CH_2, 3 × Ph*C*H$_2$ and CH, C-2′, C-4″, resonance overlap)], 75.3 (CH, C-2″), 75.6 (CH_2, Ph*C*H$_2$), 75.9 (CH, C-4″), 77.3 (CH, C-4⁗), 78.7 (CH, C-4‴), 79.0 (CH, C-2⁗), 79.1 (CH, C-3′), 79.6 (CH, C-3″), 81.4 (CH, C-3⁗), 97.0, (CH, C-1⁗), 98.7 (CH, C-1′), 101.1 (CH, C-1″), 101.8 (CH, C-1‴), 102.3 (CH, benzylidene *C*H), [126.3, 127.4, 127.6, 127.68, 127.71, 127.8, 127.9, 128.0, 128.2, 128.3, 128.5, 129.0 (CH, Ar *C*H, resonance overlap)], [137.3, 137.6, 138.0, 138.2, 138.3, 138.7 (C, Ar *C*, resonance overlap)]; *m/z* (TOF ES+) 1789.8 ([M + Na]$^+$, 70%), 906.4 ([M + 2Na], 100%), HRMS *m/z* (TOF ES+) 1788.7953 [M + Na]$^+$, $C_{106}H_{115}N_3O_{21}Na$ requires 1788.7921.

5′′′′-(Biotinamido)pentyl [α-D-glucopyranosyl]-(1′′′→3′′)-[α-D-mannopyranosyl]-(1′′→2′)-[α-D-mannopyranosyl]-(1′→2)-[α-D-mannopyranoside] (13)

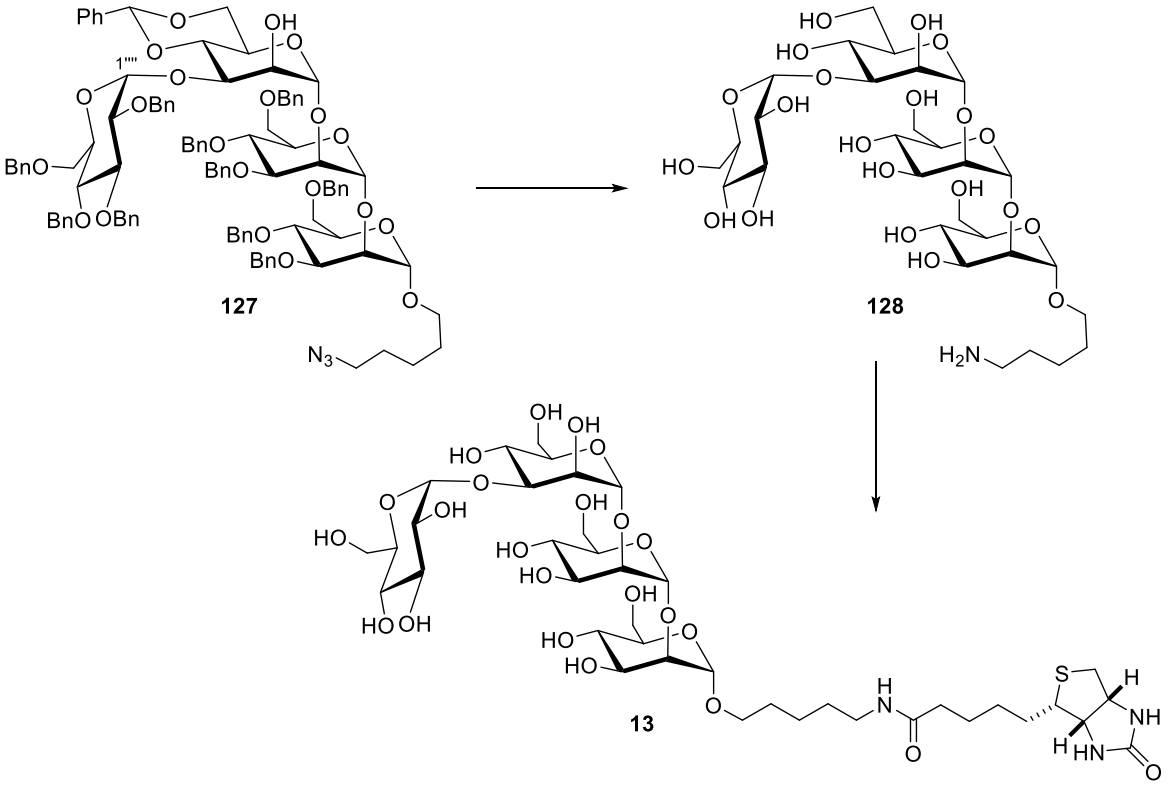

A flask containing a solution of tetrasaccharide **127** (110 mg, 0.062 mmol) in MeOH:AcOH (9:1, 10 mL) was purged with H_2 gas for 10 min. $Pd(OH)_2$ (2 mg, cat.) was then added and the mixture was stirred under a flow of H_2 for 24 h, after which time, the mixture was filtered through Celite, washing with MeOH (40 mL) and the filtrate was concentrated under reduced pressure. This procedure was repeated for another 24 h, until all of the protecting groups had been removed as evidenced by mass spectrometry analysis. Amine **128** was afforded as a white solid (21 mg, 45%): Selected data for amine **128**: *m/z* (TOF ES+) 752.8 ($[M + H]^+$, 50%), 774.7 ($[M + Na]^+$, 50%). Biotin NHS ester **65** (12 mg, 0.034 mmol) was added to a solution of amine **128** (21 mg, 0.028 mmol) in pyridine:H_2O (2 mL, 9:1). After 14 h at 60 °C, the reaction mixture was co-evaporated with toluene under reduced pressure and purified by flash column

chromatography (30% MeOH in EtOAC) to afford amide **13** (18 mg, 68%) as an off white foam: R_f = 0.3 (4:2:1, EtOAc:MeOH:H_2O); ν_{max}(film)/cm^{-1} 3300 br m (O–H), 2919 s, 2853 m, 1680 vs (C=O), 1635 s (C=O), 1591 m, 1457 m, 1400 m, 1360 m, 1246 m, 1206 m, 1128 s, 1090 vs, 1052 vs, 1029 vs, 919 m, 819 m, 700 m; δ_H(400 MHz,1:1 $CDCl_3$:CD_3OD) 1.33–176 (12H, stack), 2.01 (2H, t, *J* 7.3, H-1‴″), 2.67–2.74 (1H, m, H-8‴″$_A$), 2.94 (1H, dd, *J* 12.8, 4.9, H-8‴″$_B$), 3.15–3.25 (4H, stack), 3.37–3.90 (23H, stack), 4.01 (1H, m), 4.22–4.24 (1H, m), 4.31 (1H, dd, *J* 7.9, 4.4, H-6‴″), 4.50 (1H, dd, *J* 7.9, 4.3, H-7‴″), 4.97 (1H, d, *J* 1.7), 5.05–5.06 (1H, m), 5.15 (1H, d, *J* 3.9, H-1‴), 5.29 (1H, d, *J* 1.3) exchangeable hydrogens not observed; δ_C(100 MHz) 24.8, 27.0, 29.6, 29.8, 30.2, 30.3, 33.5, 36.9, 37.9, 40.3, 41.1, 57.1, 61.7, 63.0, 63.1, 63.2, 63.5, 67.8, 68.5, 69.2, 69.3, 71.1, 72.0, 72.1, 72.3, 74.1, 74.2, 74.7, 75.0, 75.1, 75.3, 80.5, 81.0, 81.5, 99.8, 101.8, 102.5, 104.2, 166.2, 176.1; *m/z* (TOF ES+) 1000.4 ([M + Na]$^+$, 100%); HRMS *m/z* (TOF ES+) 1000.3791 [M + Na]$^+$, $C_{39}H_{67}N_3O_{23}SNa$ requires 1000.3784**.**

5.3. Chapter 3

Imidazole-1-sulfonyl azide hydrochloride (182)

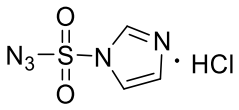

SO_2Cl_2 (16.1 mL, 200 mmol) was added dropwise over 30 min to an ice-cooled suspension of NaN_3 (13.0 g, 200 mmol) in dry CH_3CN (200 mL). The reaction mixture was stirred overnight at rt. Imidazole (25.9 g, 380 mmol) was then added portionwise over 1 h to the ice-cooled mixture and the resulting slurry was stirred for 3 h at rt. The mixture was then diluted with EtOAc (400 mL), washed sequentially with H_2O (2 × 400 mL) and $NaHCO_3$ solution (2 × 400 mL), dried over Na_2SO_4 and filtered. A solution of HCl in EtOH [obtained by dropwise addition of AcCl (21.2 mL, 300 mmol) to ice-cooled dry EtOH (75 mL)] was added dropwise over 10 min to the filtrate with stirring. The mixture was chilled in an ice bath, filtered and the filter cake washed with EtOAc (3 × 100 mL) to give azide **182** as a white solid (29.3 g, 70%): m.p. 103–104 °C, lit.[127] 100–102 °C; δ_H(400 MHz, D_2O) 7.64 (1H, app. s), 8.06 (1H, app. s), 7.43 (1H, app. s); δ_C(100 MHz, D_2O) 120.1 (CH), 123.1 (CH), 137.7 (CH); *m/z* (ASAP) 174.1 ([M – Cl]$^+$, 100%), 146.1 ([M – Cl – N_2]$^+$, 70%); HRMS *m/z* (ASAP) 174.0083 [M – Cl]$^+$, $C_3H_4N_5O_2S$ requires 174.0086.

Data were in agreement with those reported in the literature.[127]

(2*S*, 3*S*, 4*R*)-2-Azido-3, 4-*O*-isopropylidene-1, 3, 4-octadecanetriol (184)

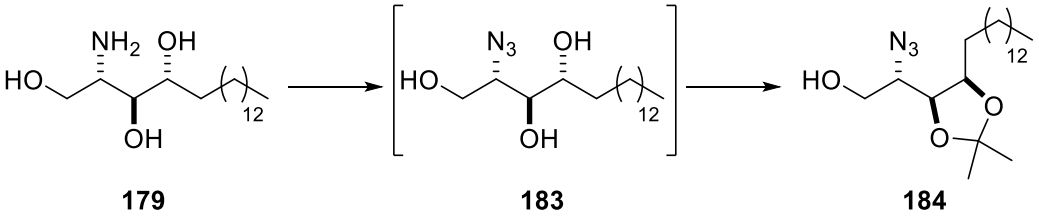

179 **183** **184**

A solution of imidazole-1-sulfonyl azide hydrochloride **182** (6.60 g, 31.5 mmol) in CH_2Cl_2 (50 mL) was added to a vigorously stirred solution of phytosphingosine **179** (6.00 g, 15.6 mmol), $CuSO_4$ (40 mg, 0.16 mmol) and K_2CO_3 (3.23 g, 23.4 mmol) in H_2O (47 mL). MeOH (157 mL) was added dropwise over 10 min and the mixture was stirred vigorously at rt for 18 h. The solution was then diluted with CH_2Cl_2 (400 mL) and washed sequentially with $NaHCO_3$ solution (100 mL), H_2O (70 mL) and brine (70 mL). The organic layer was dried over Na_2SO_4, filtered and the filtrate concentrated under reduced pressure. The crude azide **183** was isolated as a white solid and used directly in the next step without further purification (6.49 g, quant.): R_f = 0.7 (100% EtOAc); m.p. 91–94 °C (lit.[111] 92–94 °C); solubility issues prevented an optical rotation measurement data; ν_{max}(film)/cm^{-1} 3261 br w (O–H), 2916 s, 2847 s, 2096 s (N_3), 1590 w, 1461 m, 1248 m, 1098 w, 1058 s, 1008 m, 922 w, 857 m, 723 s; δ_H(300 MHz, $(CD_3)_2SO$) 0.85 (3H, t, *J* 6.8, C*H*$_3$), 1.21–1.30 (23H, stack, alkyl chain), 1.36–1.64 (3H, stack, alkyl chain), 3.23–3.38 (2H, stack), 3.48–3.65 (2H, stack), 3.71–3.79 (1H, m), 4.55 (1H, d, *J* 6.4, O*H*), 4.91 (1H, app t, *J* 4.9, O*H*), 5.04 (1H, d, *J* 5.7, O*H*); δ_C(100 MHz, $(CD_3)_2SO$) 14.0 (CH_3, *C*H$_3$), 22.1 (CH_2, alkyl chain), 25.1 (CH_2, alkyl chain), [28.7, 29.1, 29.2 (CH_2, alkyl chain, significant resonance overlap)], 31.3 (CH_2, alkyl chain), 33.0 (CH_2, alkyl chain), 60.0 (CH_2, *C*H$_2$OH), 65.4 (CH, *C*HN$_3$), [70.7, 74.5 (CH, 2 × *C*HOH)]; *m/z* (TOF ES+) 366.3 ([M + Na]$^+$, 100%); HRMS *m/z* (TOF ES+) 366.2727 [M + Na]$^+$, $C_{18}H_{37}N_3O_3Na$ requires 366.2733. Data were in agreement with those reported in the literature.[111] Concentrated H_2SO_4 (4 drops) was added to a solution of azide **183** (6.40 g, 18.6 mmol) in dry acetone (50 mL) at 0 °C. After stirring for 20 h, the reaction mixture was quenched by the addition of solid $NaHCO_3$ and then

concentrated under reduced pressure. The residue was partitioned between EtOAc (35 mL) and H_2O (30 mL). The layers were separated and the aqueous phase was extracted with EtOAc (3 × 20 mL). The combined organic layers were washed with brine (20 mL), then dried over Na_2SO_4, filtered and the filtrate concentrated under reduced pressure. The crude product was purified by column chromatography (20% EtOAc in hexanes) to give acetonide **184** as a white, low-melting point, amorphous solid (4.47 g, 63%): R_f = 0.6 (20% EtOAc in hexanes); $[\alpha]_D^{20}$ = +26.8 (c = 1.0, $CHCl_3$), lit. [111] $[\alpha]_D^{22}$ = + 23 (c = 1.0, $CHCl_3$); ν_{max}(film)/cm^{-1} 3435 br w (O–H), 2920 s, 2851 s, 2136 m, 2116 m, 2095 s (N_3), 1471 m, 1426 vw, 1382 w, 1370 w, 1317 w, 1261 m, 1208 s, 1165 m, 1102 m, 1065 m, 1019 s, 970 w, 883 m, 857 w, 826 w, 719 m; δ_H(300 MHz) 0.90 (3H, t, *J* 6.5, CH_2CH_3), 1.25–1.33 (23H, stack, alkyl chain), 1.35 [3H, s, $C(CH_3)_A(CH_3)_B$], 1.45 [3H, s, $C(CH_3)_A(CH_3)_B$], 1.53–1.67 (3H, stack, alkyl chain), 2.18 (1H, br s, O*H*), 3.45–3.53 (1H, m), 3.83–3.94 (1H, m), 3.95–4.06 (2H, stack), 4.16–4.24 (1H, m); δ_C(100 MHz) 14.4 (CH_3, CH_2CH_3), 22.9 (CH_2, alkyl chain), 25.8 [CH_3, $C(CH_3)_A(CH_3)_B$], 26.5 (CH_2, alkyl chain), 28.3 [CH_3, $C(CH_3)_A(CH_3)_B$], [29.6, 29.8, 29.9 (CH_2, alkyl chain, significant resonance overlap)], 32.2 (CH_2, alkyl chain), 61.4 (CH, C-2), 64.2 (CH_2, C-1), [76.9, 77.9 (CH, C-3, C-4)], 108.7 [C, $C(CH_3)_2$]; *m/z* (TOF ES+) 406.3 ([M + Na]$^+$, 30%), 356.3 (100, [M – N_2 + H]$^+$); HRMS *m/z* (TOF ES+) 406.3050 [M + Na]$^+$, $C_{21}H_{41}N_3O_3Na$ requires 406.3046**,** and then triol **183** (2.0 g, 31 %). Data were in agreement with those reported in the literature.[111]

(2*S*, 3*S*, 4*R*)-2-Azido-3, 4-*O*-isopropylidene-1-*O*-methanesulfonyl-1, 3, 4-octadecanetriol (185)

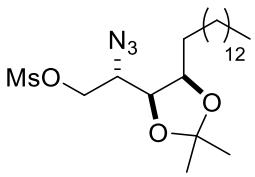

Et_3N (1.09 mL, 7.82 mmol) and MsCl (0.31 mL, 5.21 mmol) were added sequentially to a solution of alcohol **184** (1.00 g, 2.61 mmol) in THF (30 mL) at rt. The reaction mixture was

stirred for 3 h and then quenched with $NaHCO_3$ solution (20 mL). The phases were separated and the aqueous phase was extracted with EtOAc (3 × 20 mL). The combined organic layers were washed with brine (25 mL), dried over Na_2SO_4, filtered and the filtrate was concentrated under reduced pressure to yield mesylate **185** as a low-melting point, amorphous solid, which was used without further purification (1.13 g, 94%): R_f = 0.4 (15% EtOAc in hexanes); $[\alpha]_D^{20}$ = +6.0 (c = 1.0, $CHCl_3$) lit.[182] $[\alpha]_D^{21}$ +8.9 (c 0.45, $CHCl_3$); ν_{max}(film)/cm^{-1} 2995 w, 2944 m, 2918 vs, 2850 s, 2127 m, 2096 s (N_3), 1471 m, 1455 w, 1377 w, 1340 vs, 1324 s, 1280 w, 1252 m, 1224 s, 1167 s, 1109 m, 1067 m, 1032 m, 988 s, 967 vs, 951 s, 922 w, 879 m, 868 m, 856 m, 824 s, 799 w, 782 w, 737 m, 717 m, 653 w; δ_H(300 MHz) 0.87 (3H, t, *J* 6.7, CH_2CH_3), 1.23–1.30 (20H, stack, alkyl chain), 1.31 [3H, s, $C(CH_3)_A(CH_3)_B$], 1.33–1.39 (3H, stack, alkyl chain), 1.42 [3H, s, $C(CH_3)_A(CH_3)_B$], 1.51–1.66 (3H, stack, alkyl chain), 3.09 (3H, s, SO_2CH_3), 3.67–3.75 (1H, m), 3.85 (1H, dd, *J* 9.4, 5.5), 4.14–4.22 (1H, m), 4.30 (1H, dd, *J* 10.8, 7.6), 4.67 (1H, dd, *J* 10.8, 2.6); δ_C(100 MHz) 14.5 (CH_3, CH_2CH_3), 23.0 (CH_2, alkyl chain), 25.8 [CH_3, $C(CH_3)_A(CH_3)_B$], 26.9 (CH_2, alkyl chain), 28.4 [CH_3, $C(CH_3)_A(CH_3)_B$], [29.5, 29.7, 29.8, 29.9, 30.0 (CH_2, alkyl chain, significant resonance overlap)], 32.3 (CH_2, alkyl chain), 38.0 (CH_3, SO_2CH_3), 59.7 (CH, C-2), 70.3 (CH_2, C-1), [75.7, 77.9 (CH, *C*-3, *C*-4)], 109.0 [C, $C(CH_3)_2$]; *m/z* (TOF ES+) 484.3 ($[M + Na]^+$, 100%); HRMS *m/z* (TOF ES+) 484.2829 $[M + Na]^+$, $C_{22}H_{43}N_3O_5SNa$ requires 484.2821.

Data were in agreement with those reported in the literature.[182]

(2*S*, 3*S*, 4*R*)-1, 2-Imino-3, 4-*O*-isopropylidene-octadecane-3, 4-diol (186)

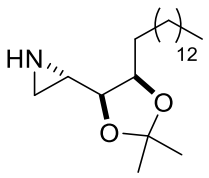

i-Pr_2NEt (2.35 mL, 13.5 mmol) and Ph_3P (3.07 g, 11.7 mmol) were added to a solution of mesylate **185** (4.15 g, 9.0 mmol) in THF–H_2O (90 mL, 8:1). The reaction mixture was heated

at 60 °C for 3 h and then cooled to rt. The mixture was washed with brine (60 mL) and the aqueous phase was extracted with Et_2O (2 × 80 mL). The organic layers were combined, dried with Na_2SO_4, filtered and the filtrate was concentrated under reduced pressure. The crude residue was purified first by trituration with hexane, which allowed the removal of the phosphine oxide by-product by filtration, then by column chromatography (30% EtOAc in hexanes) to yield aziridine **186** as a colourless oil (2.37 g, 77%): R_f = 0.2 (5% MeOH in $CHCl_3$); $[\alpha]_D^{20}$ = +6.0 (c = 1.0, $CHCl_3$) lit. [130] $[\alpha]_D^{20}$ = +7 (c = 1.0, $CHCl_3$); ν_{max}(film)/cm^{-1} 3308 vw (N-H), 2987 w, 2922 vs, 2853 s, 1466 m, 1378 m, 1368 m, 1245 m, 1214 s, 1165 m, 1090 m, 1049 s, 859 m, 721 w; δ_H(300 MHz) 0.87 (3H, t, *J* 6.9, CH_2CH_3), 1.22–1.31 (24H, stack, alkyl chain), 1.33 [3H, s, $C(CH_3)_A(CH_3)_B$], 1.46 [3H, s, $C(CH_3)_A(CH_3)_B$], 1.50–1.57 (1H, m), 1.59 (1H, d, *J* 3.6), 1.64–1.73 (2H, stack), 1.88 (1H, d, *J* 5.7), 2.07–2.14 (1H, m), 3.58 (1H, dd, *J* 7.5, 6.2), 4.20 (1H, app dt, *J* 7.5, 5.6); δ_C(100 MHz) 14.5 (CH_3, CH_2CH_3), 23.0 (CH_2, alkyl chain), 25.6 [CH_3, $C(CH_3)_A(CH_3)_B$], 27.0 (CH_2, alkyl chain), 28.2 [CH_3, $C(CH_3)_A(CH_3)_B$], 29.4 (CH, C-2), 29.7 (CH_2, alkyl chain), [29.9, 30.0, 30.1 (CH_2, alkyl chain and C-1, significant resonance overlap)], 30.3 (CH_2, alkyl chain), 32.3 (CH_2, alkyl chain), [78.3, 80.4 (CH, C-3, C-4)], 108.2 [C, $C(CH_3)_2$]; *m/z* (TOF ES+) 340.3 ($[M + H]^+$, 100%); HRMS *m/z* (TOF ES+) 340.3224 $[M + H]^+$, $C_{21}H_{42}NO_2$ requires 340.3216.

Data were in agreement with those reported in the literature.[130]

Hexacosanoic acid-2, 5-dioxo-1-pyrrolidinyl ester (189)

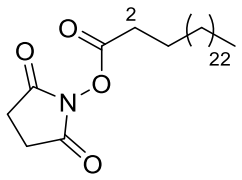

EDCI.HCl (450 mg, 2.72 mmol) and *N*-hydroxysuccinimide (348 mg, 3.02 mmol) were added sequentially to a solution of hexacosanoic acid (0.84 g, 2.12 mmol) in CH_2Cl_2 (30 mL). The reaction mixture was heated at 40 °C for 3 h, and then the mixture was poured into H_2O (20 mL) and extracted with Et_2O (60 mL). The organic layer was washed with brine (20 mL), dried over Na_2SO_4, and filtered. The solvent was removed under reduced pressure to give NHS ester **189** as a white foam (963 mg, 92%): R_f = 0.4 (25% EtOAc in hexanes); ν_{max}(film)/cm^{-1} 2956 w, 2917 vs, 2849 vs, 1819 m, 1787 m, 1740 vs (C=O), 1724 vs (C=O), 1463 m, 1430 w, 1409 w, 1296 w, 1255 w, 1208 vs, 1147 w, 1123 w, 1069 vs, 1061 vs, 1019 m, 1003 m, 993 m, 865 s, 811 m, 770 w, 722 m, 668 m, 654 s; δ_H(400 MHz) 0.88 (3H, t, *J* 6.9, CH_2CH_3), 1.22–1.35 (44H, stack, alkyl chain) 1.36–1.44 (2H, stack, H-4), 1.70–1.78 (2H, stack, *J* 7.5, H-3), 2.60 (2H, t, *J* 7.5, H-2), 2.81–2.86 (4H, stack, NHS C*H*); δ_C(100 MHz) 14.1 (CH_3, CH_2CH_3), [22.7, 24.6, 25.6, 28.8, 29.1, 29.4, 29.6, 29.7, 30.0, 30.1, 30.9, 31.9 (CH_2, alkyl chain, resonance overlap)], 168.7 (C, C=O, ester) 169.2(C, C=O, imide).

Data were in agreement with those reported in the literature.[183]

(2*S*, 3*S*, 4*R*)-1, 2-(Hexacosanoyl)imino-3,4-*O*-isopropylidene-octadecane-3, 4-diol (190)

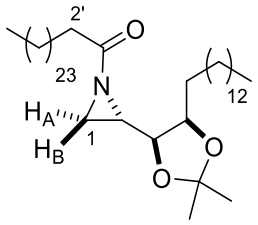

NHS ester **189** (290 mg, 0.589 mmol) and Et_3N (160 μL, 1.17 mmol) were added to a solution of aziridine **186** (200 mg, 0.589 mmol) in dry THF (10 mL). After stirring the reaction mixture for 12 h, the solvent was removed under reduced pressure. The crude mixture was purified by column chromatography (10% EtOAc in hexanes) to yield aziridine **190** as a white solid (313 mg, 74%): R_f = 0.5 (10% EtOAc in hexanes); m.p. 63–65 °C; $[\alpha]_D^{20}$ = –15.6 (c = 1.0, $CHCl_3$); ν_{max}(film)/cm^{-1} 2956 m, 2916 vs, 2848 vs, 1684 s (C=O), 1474 m, 1463 s, 1381 m, 1366 m, 1345 m, 1285 w, 1275 w, 1253 s, 1216 m, 1181 m, 1161 m, 1134 w, 1090 m, 1067 m, 1037 s, 979 w, 913 w, 875 m, 866 m, 846 w, 789 w, 728 m, 718 m, 668 m, 656 m; δ_H(400 MHz) 0.88 (6H, app. t, *J* 6.8, 2 × CH_2CH_3), 1.22–1.32 (68H, stack, alkyl chain), 1.34 (3H, s, $C(CH_3)_A(CH_3)_B$), 1.46 (3H, s, $C(CH_3)_A(CH_3)_B$), 1.60–1.66 (2H, stack, alkyl chain), 1.71–1.85 (2H, stack, alkyl chain), 2.22 (1H, dd, *J* 3.2, 0.6, H-1$_A$), 2.28 (1H, dd, *J* 6.0, 0.6, H-1$_B$), 2.30–2.47 (2H, stack, 2 × H-2′), 2.64 (1H, ddd, *J* 6.8, 6.0, 3.2, H-2), 3.78 (1H, app. t, *J* 6.4, H-3), 4.20 (1H, app. dt, *J* 8.6, 5.5, H-4); δ_C(100 MHz) 14.1 (CH_3, CH_2CH_3), 22.7 (CH_2, alkyl chain), 24.9 (CH_2, C-3′), 25.4 (CH_3, $C(CH_3)_A(CH_3)_B$), 26.6 (CH_2, alkyl chain), 27.9 (CH_3, $C(CH_3)_A(CH_3)_B$), 28.4 (CH_2, C-1), [29.4, 29.5, 29.7, 31.9 (CH_2, alkyl chain, resonance overlap)], 35.1 (CH, C-2), 36.7 (CH_2, C-2′), 77.8 (CH, C-4), 78.5 (CH, C-3), 108.1 (C, $C(CH_3)_2$), 185.7 (C, C=O); *m/z* (TOF ES+) 740.7 ([M + Na]$^+$, 100%); HRMS *m/z* (TOF ES+) 740.6898 [M + Na]$^+$, $C_{47}H_{91}NO_3Na$ requires 740.6897

(2*S*, 3*S*, 4*R*)-3,4-*O*-Isopropylidene-1, 2-(*para*-nitrobenzenesulfonyl)imino-octadecane-3, 4-diol (191)

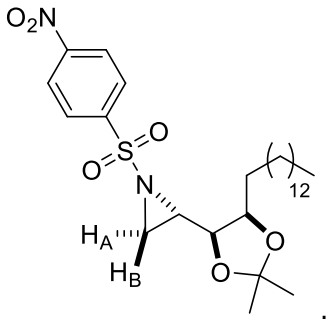

para-Nosyl chloride (109 mg, 0.59 mmol) was added to a solution of Et_3N (0.5 mL, 3.53 mmol) and aziridine **186** (168 mg, 0.59 mmol) in THF (5 mL). The reaction mixture was stirred at rt for 3 h, then quenched with $NaHCO_3$ solution (30 mL). The phases were separated and the aqueous phase was extracted with EtOAc (3 × 40 mL). The combined organic layers were dried (Na_2SO_4), filtered and the solvent removed under reduced pressure to give the crude product which was purified by column chromatography (10% EtOAc in hexanes) to yield sulfonamide **192** as a white solid yellow oil (143 mg, 55%): Rf = 0.5 (25% EtOAc in hexanes); $[\alpha]_D^{22}$ = –10.8 (c = 1.0, $CHCl_3$); ν_{max}(film)/cm^{-1} 2923 vs, 2853 s, 1606 w, 1533 s, 1465 m, 1369 m, 1348 s, 1312 m, 1217 m, 1161 s, 1090 m, 1061 m, 982 w, 855 m, 741 m, 686 w, 618 w; δ_H(400 MHz) 0.87 (3H, t, *J* 6.8, CH_2CH_3), 1.23–1.30 (23H, stack, alkyl chain), 1.32 [3H, s, $C(CH_3)_A(CH_3)_B$], 1.45 [3H, s, $C(CH_3)_A(CH_3)_B$], 1.47–1.67 (3H, stack, alkyl chain), 2.29 (1H, d, *J* 4.5, H-1_A), 2.70 (1H, d, *J* 7.0, H-1_B), 3.08 (1H, app. td, *J* 7.0, 4.5, H-2), 3.73 (1H, dd, *J* 6.7, 6.0, H-3), 4.15 (1H, ddd, *J* 9.6, 5.7, 4.0, H-4), 8.13–8.17 (2H, m, Ar C*H*), 8.37–8.41 (2H, m, Ar C*H*), δ_C(100 MHz) 14.1 (CH_3, CH_2CH_3), 22.7 (CH_2, alkyl chain), 25.2 [CH_3, $C(CH_3)_A(CH_3)_B$], 26.8 (CH_2, alkyl chain), 27.9 [CH_3, $C(CH_3)_A(CH_3)_B$], [29.4, 29.5, 29.6, 29.7, 31.9 (CH_2, alkyl chain, significant resonance overlap)], 32.1 (CH_2, C-1), 38.6 (CH, C-2), 77.5 (CH, C-4), 77.7 (CH, *C*-3), 108.6 [C, $C(CH_3)_2$], [124.4, 129.4, (CH, Ar *C*H)], [143.9, 150.7 (C, Ar *C*)]; *m/z* (TOF ES+) 547.3 ([M + Na]$^+$, 100%); HRMS *m/z* (TOF ES+) 547.2817 [M + Na]$^+$, $C_{27}H_{44}N_2O_6SNa$ requires 547.2818.

(2*S*, 3*S*, 4*R*)-3,4-*O*-Isopropylidene-1, 2-(*ortho*-nitrobenzenesulfonyl)imino-octadecane-3, 4-diol (192)

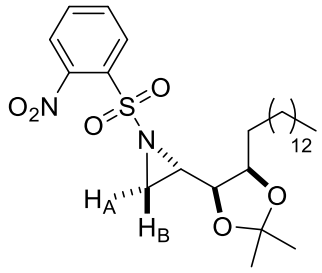

ortho-Nosyl chloride (208 mg, 1.18 mmol) was added to a solution of Et_3N (0.5 mL, 3.53 mmol) and aziridine **186** (320 mg, 1.18 mmol) in THF (10 mL). The reaction mixture was stirred at rt for 3 h, then quenched with $NaHCO_3$ solution (30 mL). The phases were separated and the aqueous phase was extracted with EtOAc (3 × 40 mL). The combined organic layers were dried (Na_2SO_4), filtered and the solvent removed under reduced pressure to give the crude product which was purified by column chromatography (10% EtOAc in hexanes) to yield sulfonamide **192** as a white solid yellow oil (321 mg, 65%): R_f = 0.4 (25% EtOAc in hexanes); $[\alpha]_D^{22}$ = –30.0 (c = 1.0, $CHCl_3$), lit.[130] $[\alpha]_D$ = –47 (c = 1.0, $CHCl_3$); ν_{max}(film)/cm^{-1} 3100 vw br, 2917 vs, 2849 s, 1594 vw, 1539 vs, 1473 m, 1461 m, 1441 w, 1407 vw, 1377 m, 1350 s, 1327 vs, 1310 m, 1244 m, 1215 m, 1162 vs , 1146 s, 1103 s, 1090 m, 1080 s, 1072 m, 1045 s, 1013 w, 999 m, 985 m, 952 m, 897 m, 882 s, 856 s, 787 s, 774 m, 744 s, 736 s, 717 m, 688 m, 672 m; δ_H(300 MHz) 0.87 (3H, t, *J* 6.8, CH_2CH_3), 1.23–1.30 (24H, stack, alkyl chain), 1.32 [3H, s, $C(CH_3)_A(CH_3)_B$], 1.44 [3H, s, $C(CH_3)_A(CH_3)_B$], 1.59–1.69 (2H, stack, alkyl chain), 2.50 (1H, d, *J* 4.7, H-1$_A$), 2.91 (1H, d, *J* 7.0, H-1$_B$), 3.16 (1H, ddd, *J* 7.0, 6.0, 4.7, H-2), 3.94 (1H, app t, *J* 6.0, H-3), 4.18–4.23 (1H, m, H-4), 7.71–7.79 (3H, stack, Ar C*H*), 8.17–8.21 (1H, m, Ar C*H)*; δ_C(100 MHz) 14.1 (CH_3, CH_2CH_3), 22.7 (CH_2, alkyl chain), 25.2 [CH_3, $C(CH_3)_A(CH_3)_B$], 26.7 (CH_2, alkyl chain), 27.8 [CH_3, $C(CH_3)_A(CH_3)_B$], [29.4, 29.5, 29.6, 29.7, 31.9 (CH_2, alkyl chain, significant resonance overlap)], 33.3 (CH_2, C-1), 39.9 (CH, C-2), 77.0 (CH, C-3), 78.3 (CH, *C*-

4), 108.5 [C, *C*$(CH_3)_2$], [124.4, 131.3, (CH, Ar *C*H)], 132.1 (C, Ar *C*), [132.2, 134.5 (CH, Ar *C*H), 148.5 (C, Ar *C*); *m/z* (TOF ES+) 547.3 ([M + Na]$^+$, 100%).

Data were in agreement with those reported in the literature.[130]

(2*S*, 3*S*, 4*R*)-3,4-*O*-Isopropylidene-1, 2-[*para*-(cyclohexyloxy)-benzenesulfonyl]imino-octadecane-3, 4-diol (196)

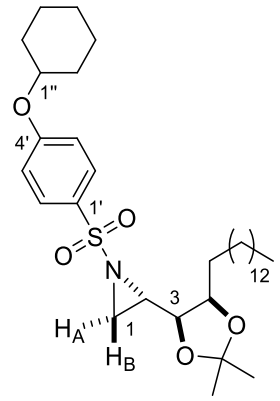

NaH (11 mg of a 60% dispersion in mineral oil, 0.23 mmol) was added to a solution of cyclohexanol (23 mg, 0.23 mmol) in DMF (1 mL) at 0 °C. After stirring for 1 h, a solution of aziridine **191** (100 mg, 0.19 mmol) in DMF (1 mL) was added. After 20 min at 0 °C, the reaction mixture was warmed to rt and stirred for a further 15 h. The reaction was then quenched with H_2O (25 mL) and extracted with EtOAc (5 × 30 mL). The combined organic layers were washed with brine (70 mL), dried using Na_2SO_4, filtered and the filtrate was concentrated under reduced pressure. The crude residue was purified using column chromatography (10% EtOAc) to yield aryl ether **196** as a colourless oil (63 mg, 58%.): R_f = 0.6 (20% EtOAc in hexanes); $[\alpha]_D^{22}$ = –14.8 (c = 1.0, $CHCl_3$); ν_{max}(film)/cm^{-1} 2923 vs, 2853 vs, 1593 s, 1495 m, 1458 m, 1370 m, 1256 s, 1217 m, 1158 vs, 1093 m, 1045 m, 926 w, 732 w; δ_H(400 MHz) 0.88 (3H, t, *J* 6.8, CH_2CH_3), 1.23–1.29 (23H, stack, alkyl chain), 1.31 [3H, s, $C(CH_3)_A(CH_3)_B$], 1.33–1.43 (3H, stack, alkyl chain and cyclohexyl ring), 1.45 [3H, s, $C(CH_3)_A(CH_3)_B$], 1.47–1.61 (6H, stack, alkyl chain and cyclohexyl ring), 1.76–1.85 (2H, stack, cyclohexyl ring), 1.95–2.02 (2H,

stack, cyclohexyl ring), 2.19 (1H, d, *J* 4.3, H-1_A), 2.58 (1H, d, *J* 7.0, H-1_B), 2.89 (1H, app. td, *J* 7.3, 4.6, H-2), 3.66 (1H, dd, *J* 7.3, 5.8, H-3), 4.11 (1H, ddd, *J* 9.6, 5.7, 4.0, H-4), 4.31–4.38 (1H, m, H-1″), 6.94–6.98 (2H, stack, Ar C*H*, H-3′), 7.80–7.84 (2H, m, Ar C*H*, H-2′); δ_C(100 MHz) 14.1 (CH_3, CH_2CH_3), 22.7 (CH_2, alkyl chain), 23.5 (CH_2, cyclohexyl) 25.3 [CH_3, $C(CH_3)_A(CH_3)_B$], 25.4 (CH_2, cyclohexyl), 26.8 (CH_2, alkyl chain), 28.0 [CH_3, $C(CH_3)_A(CH_3)_B$], [29.4, 29.5, 29.6, 29.7 (CH_2, alkyl chain, significant resonance overlap)], 31.1 (CH_2, C-1), [31.45, 31.49, 31.9 (CH_2, cyclohexyl resonance overlap)], 37.9 (CH, C-2), 75.8 (CH, C-1″), 77.6 (CH, C-4), 78.3 (CH, C-3), 108.4 [C, $C(CH_3)_2$], 115.7 (CH, C-3′), 128.5 (C, C-1′), 130.3 (CH, C-2′), 162.3 (C, C-4′); *m/z* (TOF ES+) 600.4 ([M + Na]$^+$, 100%); HRMS *m/z* (TOF ES+) 600.3696 [M + Na]$^+$, $C_{33}H_{55}NO_5SNa$ requires 600.3699.

(2*S*, 3*S*, 4*R*)-3,4-*O*-Isopropylidene-1, 2-(*para*-toluenesulfonyl)imino-octadecane-3, 4-diol (193)

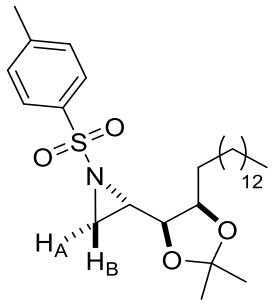

p-Tosyl chloride (1.37 g, 7.16 mmol) was added to a solution of Et_3N (1.36 mL, 9.72 mmol) and aziridine **186** (2.21 g, 6.51 mmol) in THF (65 mL). The reaction mixture was stirred at rt for 3 h and then quenched with $NaHCO_3$ solution (100 mL). The phases were separated and the aqueous phase was extracted with EtOAc (3 × 100 mL). The combined organic layers were dried (Na_2SO_4), filtered and the solvent removed under reduced pressure to give the crude product which was purified by column chromatography (10% EtOAc in hexanes) to yield sulfonamide **193** as a white solid (3.18 g, 85%): R_f = 0.5 (20% EtOAc in hexane); $[\alpha]_D^{20}$ = −22.0 (c = 1.0, $CHCl_3$); m.p. 43–44 °C; ν_{max}(film)/cm^{-1} 2920 s, 2851 s, 1597 vw, 1469 w, 1369

w, 1317 s, 1305 m, 1290 m, 1246 m, 1216 m, 1183 vw, 1156 vs, 1117 w, 1090 s, 1054 w, 1020 vw, 999 m, 933 m, 897 m, 878 m, 854 w, 830 w, 813 s, 724 s, 715 s, 700 s, 671 m, 653 s; δ_H(300 MHz) 0.88 (3H, t, *J* 6.7, CH_2CH_3), 1.21–1.29 (24H, stack, alkyl chain), 1.31 [3H, s, $C(CH_3)_A(CH_3)_B$], 1.44 [3H, s, $C(CH_3)_A(CH_3)_B$], 1.46–1.58 (2H, stack, alkyl chain), 2.20 (1H, d, *J* 4.4, H-1_A), 2.44 (3H, s, tosyl CH_3), 2.61 (1H, d, *J* 7.0, H-1_B), 2.92 (1H, app. td, *J* 7.0, 4.4, H-2), 3.66 (1H, dd, *J* 7.4, 5.7, H-3), 4.11 (1H, ddd, *J* 9.5, 5.7, 3.7, H-4), 7.31–7.36 (2H, Ar*H*), 7.80–7.84 (2H, m, Ar*H)*; δ_C(100 MHz) 14.1 (CH_3, CH_2CH_3), 21.7 (CH_3, tosyl CH_3), 22.7 (CH_2, alkyl chain), 25.3 [CH_3, $C(CH_3)_A(CH_3)_B$], 26.8 (CH_2, alkyl chain), 28.0 [CH_3, $C(CH_3)_A(CH_3)_B$], [29.4, 29.5, 29.7 (CH_2, alkyl chain, significant resonance overlap)], 31.2 (C-1), 31.9 (CH_2, alkyl chain), 37.9 (CH, C-2), 77.6 (CH, C-4), 78.3 (CH, C-3), 108.4 [C, $C(CH_3)_2$], 128.2 (CH, Ar), 129.7 (CH, Ar), 134.9 (C, Ar), 144.7 (C, Ar); *m/z* (TOF ES+) 494.3 ($[M + H]^+$, 100%); HRMS *m/z* (TOF ES+) 494.3298 $[M + Na]^+$, $C_{28}H_{47}NO_4SNa$ requires 494.3304.

(2*S*, 3*S*, 4*R*)-1-*O*-Cyclohexyl-3, 4-*O*-isopropylidene-2-toluenesulfonamido-1, 3, 4-octadecanetriol (198)

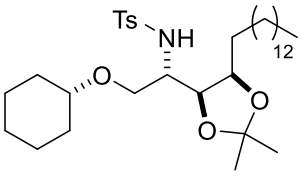

NaH (30 mg of a 60% dispersion in mineral oil, 1.21 mmol) was added to a solution of cyclohexanol (83 μL, 0.8 mmol) in DMF (1 mL) at 0 °C. After stirring for 1 h, a solution of aziridine **193** (100 mg, 0.2 mmol) in DMF (1 mL) was added. After 20 min at 0 °C, the reaction mixture was warmed to rt and stirred for a further 15 h. The reaction was then quenched with H_2O (25 mL) and extracted with EtOAc (5 × 30 mL). The combined organic layers were washed with brine (70 mL), dried using Na_2SO_4, filtered and the filtrate was concentrated under reduced pressure to yield ether **198** as a white non-amorphous solid (115 mg, quant.): Rf = 0.7 (25% EtOAc in hexanes); m.p. 79–81 °C; $[\alpha]_D^{22}$ = +29.2 (c = 1.0, $CHCl_3$); ν_{max}(film)/cm^{-1} 3308 br m (N–H), 2920 vs, 2850 s, 1598 w, 1468 m, 1438 m, 1329 s, 1244 s, 1220 m, 1158

s, 1086 s, 1061 s, 962 w, 816 m, 723 w, 670 s; δ_H(400 MHz) 0.87 (3H, t, *J* 6.8, CH_2CH_3), 1.09–1.21 (7H, stack, alkyl CH_2), 1.22–1.28 (23H, stack, CH_2 of alkyl chain), 1.28 [3H, s, $C(CH_3)_A(CH_3)_B$], 1.36 [3H, s, $C(CH_3)_A(CH_3)_B$], 1.40–1.50 (2H, stack), 1.52–1.70 (4H, stack), 2.42 (3H, s, tosyl CH_3), 2.89–2.96 (1H, m, H-1′), 3.00 (1H, dd, *J* 9.2, 3.0, H-1_A), 3.45–3.52 (2H, stack, H-1_B, H-2), 4.03–4.10 (2H, stack, H-3,H-4), 4.98 (1H, d, *J* 9.6, N-H), 7.28 (2H, AA′ of AA′ BB′, *J* 8.2, Ar C*H*), 7.75 (2H, BB′ of AA′ BB′, *J* 8.2, Ar C*H*); δ_C(100 MHz) 14.1 (CH_3, CH_2CH_3), 21.5 (CH_3, tosyl CH_3), 22.3 (CH_2), 22.7 (CH_2), 23.5 (CH_2), 23.7 (CH_2), 25.7 (CH_2), 25.8 [CH_3, $C(CH_3)_A(CH_3)_B$], 26.2 (CH_2), 28.1 [CH_3, $C(CH_3)_A(CH_3)_B$], [29.0, 29.4, 29.5, 29.7 (CH_2, alkyl chain, significant resonance overlap)], 31.6 (CH_2), 31.9 (CH_2), 53.1 (CH, C-2), 64.9 (CH_2, C-1), 75.9 (CH, C-3 or C-4), 77.3 (CH, C-1′), 77.7 (CH, C-4 or C-3), 107.6 [C, $C(CH_3)_2$], [127.1, 129.6 (CH, Ar *C*H)], [138.6, 143.5 (C, Ar *C*)]; *m/z* (TOF ES+) 614.4 ($[M + Na]^+$, 100%); HRMS m/z (TOF ES+) 614.3859 $[M + Na]^+$, $C_{34}H_{57}NO_5SNa$ requires 614.3855.

(3*S*, 4*S*, 5*S*, 6*S*)-4, 5-*O*-Isopropylidene-octa-1, 7-dien-3, 4, 5, 6-tetraol (176)

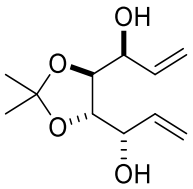

Preparation of $ZnCl_2$ solution:[184] Solid $ZnCl_2$ (4.0 g, 29.3 mmol) contained in a flame-dried Schlenk flask was fused by heating with a Bunsen burner under reduced pressure and then allowed to cool to rt. Dry THF (20 mL) was added under an argon atmosphere and the resulting mixture was sonicated until the $ZnCl_2$ had completely dissolved to yield a 1.4 M solution of $ZnCl_2$.

Preparation of divinylzinc:[185] Vinyl magnesium bromide (1.0 M in THF, 60 mL) and dry THF (20 mL) were added to a flask containing $ZnCl_2$ solution (1.4 M in THF, 20 mL, 29.3 mmol). The solution was heated under reflux for 4 h, after which time, the solution was cooled to rt.

The precipitated salts were allowed to settle and then the supernatant solution was transferred into a dry flask by filter cannula to yield a solution of divinylzinc (0.3 M in THF, 100 mL).

A solution of (2*R*, 3*R*)-dimethyl 2,3-*O*-isopropylidene tartrate **177** (2.0 g, 9.17 mmol) in toluene (25 mL) was degassed by bubbling argon through the solution for 10 min while sonicating. DIBALH (1.0 M in toluene, 18.3 mL, 18.3 mmol) was then added dropwise over 10 min to the solution at −78 °C. After 2.5 h, a solution of divinylzinc (0.3 M in THF, 100 mL, 29.3 mmol) was added. The reaction mixture was stirred for 2 h at −78 °C and then warmed to rt over 4 h. The reaction mixture was then cooled to 0 °C and the reaction carefully quenched by the dropwise addition of H_2O (30 mL) over 30 min. The mixture was filtered through Celite and the resulting solution was concentrated under reduced pressure. The crude product was re-dissolved with EtOAc (50 mL) and washed with H_2O (3 × 30 mL). The organic layer was washed with brine (20 mL), dried over Na_2SO_4, filtered and the filtrate concentrated under reduced pressure. The crude product was purified by column chromatography (25% EtOAc in hexanes) to give diene **176** (d.r: 5:1, major stereoisomer desired product) as a colourless oil (1.01 g, 55%): data on diastereoisomeric mixture unless specified otherwise: R_f = 0.2 (25% EtOAc in hexanes); ν_{max}(film)/cm^{-1} 3456 w (O–H), 3081 vw, 2939 w, 2874 w, 1640 w, 1426 w, 1381 s, 1372 s, 1315 w, 1239 s, 1213 m, 1165 m, 1136 m, 1082 m, 1040 m, 993 s, 925 s, 877 s, 811 m, 736 s, 698 s; δ_H(300 MHz) [1.40 (6H, s, C(*C*H$_3$)$_2$, major), 1.43 (6H, app s, C(*C*H$_3$)$_2$, minor)], [2.44–2.62 (2H, stack, O*H*, minor), 2.97 (2H, br s, O*H*, major)], [3.83–3.92 (2H, stack, 2 × C*H*O, major), 3.99–4.04 (2H, stack, 2 × C*H*O, minor)], [4.12–4.21 (2H, stack, 2 × C*H*O, major), 4.25–4.31 (2H, stack, 2 × C*H*O, minor)], 5.23–5.44 (4H, stack, 2 × CH=C*H*$_2$), 5.86–6.05 (2H, stack, 2 × C*H*=CH$_2$); δ_C(100 MHz) [26.9 (CH$_3$, acetal *C*H$_3$, major), 27.2 (CH$_3$, acetal *C*H$_3$, minor)], [71.6 (CH, *C*HO, minor), 72.6 (CH, *C*HO, minor), 73.6 (CH, *C*HO, major)], [79.0 (CH, *C*HO, minor), 80.2 (CH, *C*HO, minor), 81.7 (CH, *C*HOH, major)], 109.5 (C, acetal *C*, major), (acetal *C* for minor stereoisomer not observed), [116.5 (CH$_2$, CH=*C*H$_2$, minor), 117.2 (CH$_2$, CH=*C*H$_2$, major)], [136.1 (CH, *C*H=CH$_2$, minor), 136.9 (CH, *C*H=CH$_2$, major), 137.2 (CH,

*C*H=CH_2, minor)]; *m/z* (TOF ES+) 215.1 ([M + H]$^+$, 100%); HRMS *m/z* (TOF ES+) 215.1292 [M + H]$^+$, $C_{11}H_{19}O_4Na$ requires 215.1283.

Data were in agreement with those reported in the literature.[139-186]

(1*S*, 2*S*, 3*S*, 4*S*)-2, 3-*O*-Isopropylidene-cyclohex-5-en-1, 2, 3, 4-tetraol (202)

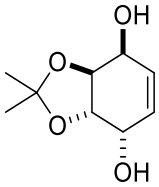

A solution of diene **176** (0.48 g, 2.2 mmol, 5:1 mixture of diastereoisomers) in CH_2Cl_2 (500 mL) was degassed by bubbling argon through the solution for 10 min while sonicating. Grubbs 2nd generation Ru metathesis catalyst (46 mg, 0.054 mmol) was then added and the solution was heated under reflux. After 2 h, the solution was concentrated under reduced pressure and the crude product purified by column chromatography (5% MeOH in $CHCl_3$) to give diol **202** as a colourless oil (0.32 g, 78%): R_f = 0.2 (5% MeOH in $CHCl_3$); $[\alpha]_D^{20}$ = +304.0 (c = 1.0, $CHCl_3$) lit.[136] $[\alpha]_D^{25}$ = +338.6 (c = 0.7, $CHCl_3$); ν_{max}(film)/cm^{-1} 3312 br m (O–H), 3043 vw, 2988 w, 2934 vw, 2902 w, 1449 w, 1368 m, 1335 w, 1279 w, 1247 m, 1230 m , 1210 m , 1171 m, 1148 s, 1129, s, 1116 s, 1091 vs, 1068 w, 1048 m, 1017 s, 992 w, 977 w, 967 m, 931 s, 839 vs, 795 m, 766 w, 732 m; δ_H(300 MHz) 1.48 [6H, s, C(C*H*$_3$)$_2$], 2.70 (2H, s, O*H*), 3.88–3.95 (2H, m, C*H*O), 4.53 (2H, app s, C*H*OH), 5.92–5.99 (2H, m, C*H*=C*H*); δ_C(100 MHz) 26.9 [CH_3, C(*C*H$_3$)$_2$], 64.8 (CH, *C*HO), 73.4 (CH, *C*HO), 110.5 [C, *C*(CH$_3$)$_2$], 130.4 (CH, =*C*H); *m/z* (TOF ES+) 209.1 ([M + Na]$^+$, 100%); HRMS *m/z* (TOF ES+) 209.0795 [M + Na]$^+$, $C_9H_{14}O_4Na$ requires 209.0790.

Data were in agreement with those reported in the literature.[139, 186]

(1*S*, 2*S*, 3*S*, 4*S*)-4-*O*-*tert*-Butyldimethylsilyl-2, 3-*O*-isopropylidene-cyclohex-5-en-1, 2, 3, 4-tetraol (163) and (1*S*, 2*S*, 3*S*, 4*S*)-1, 4-di-*O*-*tert*-butyldimethylsilyl-2, 3-*O*-isopropylidene-cyclohex-5-en-1, 2, 3, 4-tetraol (203)

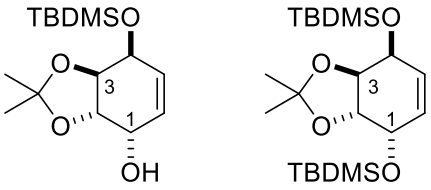

163 **203**

Imidazole (0.23 g, 3.31 mmol) and TBDMSCl (0.39 g, 1.61 mmol) were added sequentially to a solution of diol **202** (0.41 g, 2.22 mmol) in DMF (5 mL). After stirring overnight, the reaction mixture was diluted with EtOAc (30 mL) and washed sequentially with H_2O (10 mL) and NH_4Cl solution (10 mL). The organic layer was dried over Na_2SO_4, filtered and the filtrate concentrated under reduced pressure. The crude product was purified by column chromatography (20% EtOAc in hexanes) to give, in order of elution, bis-silyl ether **203** as a colourless oil (0.21 g, 23%): R_f = 0.9 (20% EtOAc in hexanes); $[\alpha]_D^{20}$ = +192.0 (c = 1.3, $CHCl_3$); ν_{max}(film)/cm^{-1} 3031 vw, 2987 vw, 2954 w, 2930 w, 2897 w, 2857 w, 1472 w, 1463 w, 1378 m, 1368 w, 1252 m, 1232 m, 1210 w, 1172 w, 1148 m, 1131 s, 1093 m, 1058 s, 1036 s, 1005 w, 971 m, 939 w, 919 w, 886 s, 854 m, 831 vs, 803 m, 775 vs, 712 w, 700 w, 681 w; δ_H(300 MHz) 0.08 [6H, s, 2 × Si(CH_3)$_A$(CH_3)$_B$], 0.09 [6H, s, 2 × Si(CH_3)$_A$(CH_3)$_B$], 0.88 [18H, s, C(CH_3)$_3$], 1.42 [6H, s, C(CH_3)$_2$], 3.92–3.96 (2H, stack, C*H*O), 4.43–4.47 (2H, stack, C*H*O), 5.75 (2H, dd, *J* 3.1, 1.6, C*H*=C*H*); δ_C(100 MHz) −4.8 [CH_3, Si(*C*$_a$H$_3$)(C$_b$H$_3$)], −4.5 [CH_3, Si(C$_a$H$_3$)(*C*$_b$H$_3$)], 18.3 [C, Si*C*(CH_3)$_3$], 25.8 [CH_3, SiC(*C*H_3)$_3$], 27.1 [CH_3, C(*C*H_3)$_2$], 66.1 (CH, *C*HO), 73.5 (CH, *C*HO), 109.8 [C, *C*(CH_3)$_2$], 130.2 (CH, =*C*H) and then silyl ether **163** as a colourless oil (0.38 g, 58%): R_f = 0.3 (20% EtOAc in hexanes); $[\alpha]_D^{20}$ = +19.6 (c = 1.0, $CHCl_3$); ν_{max}(film)/cm^{-1} 3431 w (O–H), 2987 w, 2953 w, 2930 m, 2892 w, 2856 m, 1472 w, 1462 w, 1371 m 1249 m, 1231 m, 1170 m, 1144 s, 1127 vs, 1090 vs, 1051 m, 1027 vs, 1006 w, 963 s, 935 m, 898 m, 832 vs,

777 vs; δ_H(400 MHz) 0.08 [3H, s, Si(C*H*$_3$)$_A$(CH$_3$)$_B$], 0.09 [3H, s, Si(CH$_3$)$_A$(C*H*$_3$)$_B$], 0.87 [9H, s, C(C*H*$_3$)$_3$], 1.437 [3H, s, C(C*H*$_3$)$_A$(CH$_3$)$_B$], 1.442 [3H, s, C(CH$_3$)$_A$(C*H*$_3$)$_B$], 2.29 (1H, br s, O*H*), 3.86 (1H, dd, *J* = 10.0, 3.4, H-3), 4.01 (1H, dd, *J* = 10.0, 3.7, H-2), 4.44–4.47 (1H, m, H-4), 4.48–4.51 (1H, m, H-1), 5.85–5.91 (2H, stack, C*H*=C*H*); δ_C(100 MHz) −4.8 [CH$_3$, Si(*C*H$_3$)$_A$(CH$_3$)$_B$], −4.6 [CH$_3$, Si(CH$_3$)$_A$(*C*H$_3$)$_B$], 18.4 [C, Si*C*(CH$_3$)$_3$], 25.9 [CH$_3$, C(*C*H$_3$)$_3$], 27.1 [CH$_3$, C(*C*H$_3$)$_2$], 65.2 (CH, C-1), 65.9 (CH, C-4), 73.2 (CH, C-2), 73.8 (CH, C-3), 110.3 [C, *C*(CH$_3$)$_2$], 128.5 (CH, *C*H=CH), 132.4 (CH, CH=*C*H); *m/z* (TOF ES+) 323.2 ([M + Na]$^+$, 100%); HRMS *m/z* (TOF ES+) 323.1656 [M + Na]$^+$, $C_{15}H_{28}O_4SiNa$ requires 323.1655.

(2*S*, 3*S*, 4*R*, 1′*S*, 2′*S*, 3′*S*, 4′*S*)-1-*O*-[4′-*O*-*tert*-Butyldimethylsilyl-2′, 3′-*O*-isopropylidene-2′, 3′, 4′-trihydroxycyclohex-5′-enyl]-3, 4-*O*-isopropylidene-2-toluenesulfonamido-1, 3, 4-octadecanetriol (209)

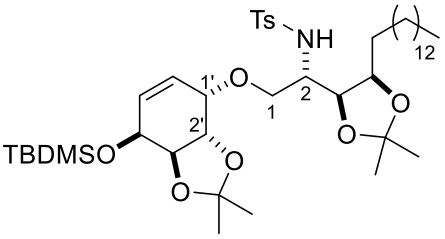

NaH (30 mg of a 60% dispersion in mineral oil, 1.21 mmol,) was added to a solution of cyclohexenol **163** (84 mg, 0.33 mmol) in DMF (0.37 mL) at 0 °C. After 1 h, a solution of aziridine **190** (150 mg, 0.303 mmol) in DMF (0.7 mL) was added. After 20 min at 0 °C, the reaction mixture was warmed to rt and stirred for a further 15 h. The reaction was quenched with H_2O (25 mL) and extracted with EtOAc (5 × 30 mL). The combined organic layers were washed with brine (70 mL), dried using Na_2SO_4, filtered and the filtrate was concentrated under reduced pressure. The crude mixture was purified by column chromatography (10% EtOAc in hexanes) to yield ether **209** as a colourless oil (115 mg, 58%): R_f = 0.7 (20% EtOAc in hexanes); $[\alpha]_D^{20}$ = +107.6 (c = 1.0, $CHCl_3$); ν_{max}(film)/cm^{-1} 3271 br vw (N–H), 2985 vw, 2925 m, 2854 m, 2216 m, 1695 w, 1589 w, 1491 w, 1459 w, 1438 w, 1378 m, 1334 w, 1268 w, 1246 w, 1221 w, 1189 m, 1168 m, 1148 w, 1129 w, 1091 w, 1065 m, 1025 w, 975 m, 923 w, 902 w,

834 m, 816 w, 800 w, 778 m, 760 s, 734 w, 706 w, 666 m; δ_H(500 MHz) 0.08–0.09 (6H, stack, Si(C*H*$_3$)$_2$), 0.86–0.89 (12H, stack, CH$_2$C*H*$_3$, C(C*H*$_3$)$_3$), 1.22–1.26 (22H, stack, C*H*$_2$ of alkyl chain), 1.27 (3H, s, C(C*H*$_3$)$_A$(CH$_3$)$_B$), 1.35 (3H, s, C(CH$_3$)$_A$(C*H*$_3$)$_B$), 1.38 (3H, s, C(C*H*$_3$)$_C$(CH$_3$)$_D$), 1.41–1.51 (2H, stack), 1.45 (3H, s, C(C*H*$_3$)$_C$(CH$_3$)$_D$), 1.57–1.65 (2H, stack), 2.45 (3H, s, tosyl C*H*$_3$), 3.02 (1H, dd, *J* 9.9, 3.3, H-1$_A$), 3.47–3.53 (1H, m, H-2), 3.70 (1H, dd, *J* 5.2, 3.5, H-1′), 3.76 (1H, dd, *J* 10.0, 3.6, H-3′), 3.92 (1H, dd, *J* 10.0, 3.5, H-2′), 4.01–4.10 (3H, stack, H-1$_B$, H-3, H-4), 4.40 (1H, dd, *J* 5.1, 3.6, H-4′), 5.00 (1H, d, *J* 9.8, N*H*), 5.64 (1H, dd, *J* 9.7, 5.2, 6′-*H*), 5.79 (1H, dd, *J* 9.7, 5.1, 5′-*H*), 7.29 (2H, AA′ of AA′ BB′, *J* 8.2, Ar*H*), 7.74 (2H, BB′ of AA′ BB′, *J* 8.2, Ar*H*); δ_C(100 MHz) −4.8 (CH$_3$, Si(*C*H$_3$)$_A$(CH$_3$)$_B$), −4.6 (CH$_3$, Si(CH$_3$)$_A$(*C*H$_3$)$_B$), 14.1 (CH$_3$, CH$_2$*C*H$_3$), 18.3 (C, Si*C*(CH$_3$)$_3$), 21.6 (CH$_3$, tosyl *C*H$_3$), 22.7 (CH$_2$), 25.8 (CH$_3$, SiC(*C*H$_3$)$_3$), 25.9 (CH$_3$, C(*C*H$_3$)$_A$(CH$_3$)$_B$), 26.8 (CH$_3$, (*C*H$_3$)$_C$(CH$_3$)$_D$), 26.9 (CH$_3$, C(CH$_3$)$_C$(*C*H$_3$)$_D$), 28.1 (CH$_3$, C(CH$_3$)$_A$(*C*H$_3$)$_B$), 26.3 (CH$_2$), [29.0, 29.4, 29.7 (CH$_2$, alkyl chain, significant resonance overlap)], 31.9 (CH$_2$), 53.2 (CH, C-2), 65.8 (CH, C-4′), 68.9 (CH$_2$, C-1), 73.5 (CH, C-1′), 73.85 (CH, C-3′), 73.94 (CH, C-2′), [75.8, 77.8 (CH, C-3, C-4)], 107.7 [C, chain acetal, *C*(CH$_3$)$_A$(CH$_3$)$_B$], 110.1 [C, cyclitol acetal, *C*(CH$_3$)$_C$(CH$_3$)$_D$], 126.9 (CH, Ar), 127.1 (CH, C-6′), 129.7 (CH, Ar), 131.9 (CH, C-5′), 138.7 (C, Ar), 143.6 (C, Ar); *m/z* (TOF ES+) 816.5 ([M + Na]$^+$, 100%); HRMS *m/z* (TOF ES+) 816.4897 [M + Na]$^+$, $C_{43}H_{75}NO_8SSiNa$ requires 816.4880.

(2*S*, 3*S*, 4*R*, 1′*S*, 2′*S*, 3′*S*, 4′*S*)-2-[(*N*-*tert*-Butoxycarbonyl)amino]-1-*O*-[4′-*O*-*tert*-butyldimethylsilyl-2′, 3′-*O*-isopropylidene-2′, 3′, 4′-trihydroxycyclohex-5′-enyl]-3, 4-*O*-isopropylidene-1, 3, 4-octadecanetriol (211)

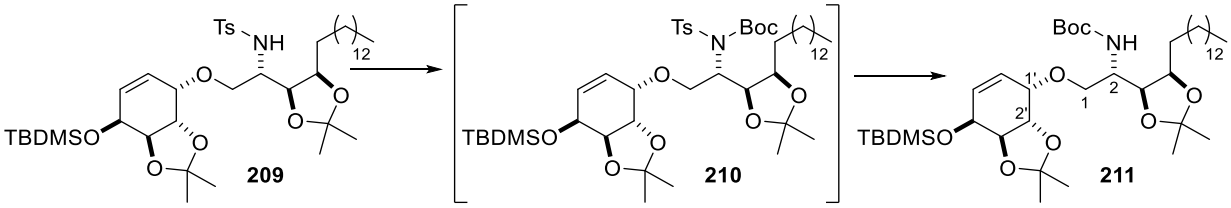

Boc_2O (38 mg, 0.18 mmol) and DMAP (5 mg, 10 weight %) were added to a solution of sulfonamide **209** (70 mg, 0.088 mmol) in CH_2Cl_2 (1 mL). The solution was stirred for 4 h and then the solvent was removed under reduced pressure to provide the crude product **210**, which was used directly in the next reaction without further purification: MeOH [1.1 mL (dried over activated 3 Å molecular sieves)] was charged to the flask containing the intermediate sulfonamide **210** (78 mg, 0.088 mmol). Mg powder (12 mg, 0.48 mmol) was added and the reaction mixture was sonicated in an ultrasound bath. After 30 min, the mixture was poured into hydrochloric acid (10 mL, 1.0 M) and extracted with Et_2O (3 × 15 mL). The combined organic phases were washed sequentially with $NaHCO_3$ solution (20 mL) and brine (20 mL), and dried with Na_2SO_4. The solvent was removed under pressure and the residue purified by flash column chromatography (20% EtOAc in hexanes) to give Boc amide **211** as a colourless oil (42 mg, 98% from **209**): R_f = 0.5 (10% EtOAc in hexanes); $[\alpha]_D^{20}$ = +108.0 (c = 1.0, $CHCl_3$); ν_{max}(film)/cm^{-1} 2926 vs, 2855 s, 1719 s (C=O), 1502 m, 1461 m, 1368 m, 1249 m, 1172 s, 1149 m, 1129 s, 1092 m, 1067 s, 1045 m, 1025 m, 985 w, 968 w, 922 vw, 834 m, 802 w, 705 w, 665 w; δ_H(400 MHz) 0.08–0.09 (6H, stack, Si(CH_3)$_2$), 0.85–0.89 (12H, stack, CH_2CH_3, SiC(CH_3)$_3$), 1.22–1.26 (23H, stack, CH_2 of alkyl chain), 1.30 (3H, s, C(CH_3)$_A$(CH$_3$)$_B$), 1.39 (3H, s, C(CH$_3$)$_A$(CH_3)$_B$), 1.40–1.43 (12H, stack, O(CH_3)$_3$), C(CH_3)$_C$(CH$_3$)$_D$), 1.50 (3H, s, C(CH$_3$)$_C$(CH_3)$_D$), 1.54–1.60 (3H, stack), 3.67 (1H, app d, *J* 9.0, H-1$_A$), 3.76–3.84 (1H, m, H-2),

3.90 (1H, dd, *J* 9.9, 3.5, 2′-*H* or 3′-*H*), 3.97–4.05 (2H, stack, H-1_B, H-2 or H-3), 4.06–4.13 (2H, stack, H-3, H-4), 4.20 (1H, app t, *J* 3.8, H-1′), 4.43 (1H, app t, *J* 4.0, H-4′), 4.88 (1H, d, *J* 9.1, N*H*), 5.79–5.86 (2H, stack, H-5′, H-6′); δ_C(100 MHz) −4.8 [CH_3, Si(CH_3)$_A$(CH_3)$_B$], −4.6 [CH_3, Si(CH_3)$_A$(CH_3)$_B$], 14.1 (CH_3, CH_2CH_3), 18.3 [C, SiC(CH_3)$_3$], 22.7 (CH_2), 25.7 (CH_3, C(CH_3)$_A$(CH_3)$_B$), 25.8 [CH_3, SiC(CH_3)$_3$], 26.6 (CH_2), 26.9 (CH_3, C(CH_3)$_C$(CH_3)$_D$), 27.1 (CH_3, C(CH_3)$_C$(CH_3)$_D$), 27.9 (CH_3, C(CH_3)$_A$(CH_3)$_B$), 28.4 [CH_3, OC(CH_3)$_3$], [28.9, 29.4, 29.5, 29.7 (CH_2, alkyl chain, significant resonance overlap)], 31.9 (CH_2), 50.3 (CH, C-2), 65.8 (CH, C-4′), 71.1 (CH_2, C-1), 73.0 (CH, C-1′), 73.8 (CH, C-3′), 74.0 (CH, C-2′), [76.6, 77.9 (CH, C-3, C-4)], 79.3 [C, OC(CH_3)$_3$] 107.7 [C, chain acetal C(CH_3)$_2$], 110.0 [C, cyclitol acetal C(CH_3)$_2$], 127.8 (CH, C-6′), 131.4 (CH, C-5′), 155.2 (C, C=O); *m/z* (TOF ES+) 762.5 ([M + Na]$^+$, 100%); HRMS *m/z* (TOF ES+) 762.5336 [M + Na]$^+$ $C_{41}H_{77}NO_8NaSi$ requires 762.5316.

(2*S*, 3*S*, 4*R*, 1′*S*, 2′*S*, 3′*S*, 4′*S*)-2-Hexacosanoylamino-1-*O*-[2′, 3′, 4′-trihydroxycyclohex-5′-enyl]-1, 3, 4-octadecanetriol (166)

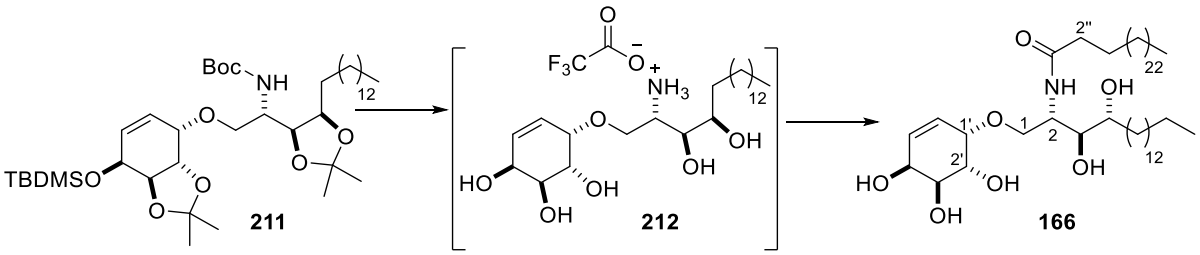

TFA (2 mL) was added to ether **211** (30 mg, 0.041 mmol). The mixture was stirred for 15 min before removing the TFA by bubbling argon through the mixture. Residual TFA was removed under reduced pressure. This procedure was repeated if necessary until all of the protecting groups had been removed as evidenced by TLC. The crude aminopolyol **212** was isolated, presumably as its TFA salt, as a yellow solid. [R_f = 0.3 (30% MeOH in $CHCl_3$)] and used without further purification in the next step: NHS ester **189** (20 mg, 0.041 mmol) and Et_3N (10 μL, 0.072 mmol) were added to a solution of aminopolyol **12** in dry THF (2 mL). After 12 h, the

solvent was removed under reduced pressure. The residue was purified by column chromatography (gradient: $CHCl_3$ → 5% MeOH in $CHCl_3$) to yield amide **166** as a white solid (17 mg, 52%): R_f = 0.3 (10% MeOH in $CHCl_3$); m.p. 80–83 °C; solubility issues prevented an optical rotation measurement; ν_{max}(film)/cm^{-1} 3303 br w (O–H, N–H), 2955 w, 2916 s, 2849 s, 1630 m (C=O), 1543 w, 1467 m, 1259 w, 1066 s, 926 w, 856 w, 801 w, 719 m; δ_H(400 MHz, 2:1 $CDCl_3$:CD_3OD) 0.84 (6H, t, *J* 6.8, 2 × CH_2CH_3), 1.12–1.27 (69H, stack, alkyl chain), 1.45–1.59 (3H, stack, alkyl chain), 2.12 (2H, app t, *J* 7.6, H-2″), 3.46–3.59 (2H, stack, H-3, H-4), 3.67 (1H, dd, *J* 9.6, 4.0, H-1$_A$), 3.76 (1H, dd, *J* 9.6, 3.6, H-1$_B$), 3.85 (1H, dd, *J* 8.2, 4.2, H-2′ or H-3′), 3.94–3.99 (2H, stack, H-3′ or H-2′, H-1′ or H-4′), 4.11–4.16 (1H, m, H-2), 4.24–4.27 (1H, m, H-4′ or H-1′), 5.79–5.84 (2H, stack, H-5′, H-6′), exchangeable hydrogens not observed; δ_C(100 MHz, 2:1 $CDCl_3$:CD_3OD) 14.3 (CH_3), 23.1 (CH_2), 26.3 (CH_2), [29.7, 29.8, 29.9, 30.0, 30.1, (CH_2, significant resonance overlap)], 32.4 (CH_2), 32.8 (CH_2), 36.9 (CH_2, C-2″), 50.6 (CH, C-2), 66.7 (CH, C-1′ or C-4′), 69.1 (CH, *C*HOH), 69.4 (CH_2, C-1), 70.1 (CH, C-2′ or C-3′), [72.7, 75.3 (CH, C-3, C-4)], 75.5 (CH, *C*HOH), [127.8, 130.7 (CH, *C*-5′, *C*-6′)], 174.8 (C, *C*=O); *m/z* (TOF ES+) 847.7 ([M + Na]$^+$, 70%), 489.1 (100); HRMS *m/z* (TOF ES+) 847.7240 [M + Na]$^+$, $C_{50}H_{97}NO_7Na$ requires 847.7241.

(2*S*, 3*S*, 4*R*, 1′*S*, 2′*S*, 3′*R*, 4′*S*)-2-[(*N*-*tert*-Butoxycarbonyl)amino]-1-*O*-[4′-*O*-*tert*-butyldimethylsilyl-2′, 3′-*O*-isopropylidene-2′, 3′, 4′-trihydroxycyclohexyl]-3, 4-*O*-isopropylidene-1, 3, 4-octadecanetriol (213)

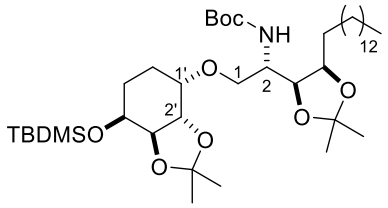

A flask containing a solution of alkene **211** (90 mg, 0.122 mmol) in MeOH (15 mL) was purged with H_2 gas for 10 min. Pd/C (0.01 g, 30 mol %) was then added and the mixture was stirred under a flow of H_2 for 12 h, after which time, the mixture was filtered through Celite, washing with MeOH (40 mL). The filtrate was concentrated under reduced pressure and the residue was purified by column chromatography (5% EtOAc in hexanes) to afford cyclohexane **213** as a colourless oil (78 mg, 86%): R_f = 0.5 (10% EtOAc in hexanes); $[\alpha]_D^{20}$ = +46.8 (c = 1.0, $CHCl_3$); δ_H(400 MHz) 0.05 (3H, s, Si(CH_3)$_A$(CH_3)$_B$), 0.07 (3H, s, Si(CH_3)$_A$(CH_3)$_B$), 0.85–0.89 (12H, stack, CH_2CH_3, SiC(CH_3)$_3$), 1.22–1.26 (22H, stack, alkyl chain), 1.30 (3H, s, C(CH_3)$_A$(CH_3)$_B$), 1.36 (3H, s, C(CH_3)$_C$(CH_3)$_D$), 1.39 (3H, s, C(CH_3)$_A$(CH_3)$_B$), 1.42 (9H, s, O(CH_3)$_3$), 1.44 (3H, s, C(CH_3)$_C$(CH_3)$_D$), 1.49–1.58 (4H, stack), 1.66–1.72 (4H, stack), 3.57 (1H, app d, *J* 8.3, H-1$_A$), 3.77–3.84 (1H, m, H-2), 3.87 (1H, dd, *J* 9.8, 2.1, H-2′ or H-3′), 3.94–4.10 (5H, stack), 4.29–4.32 (1H, m), 4.80 (1H, d, *J* 9.7, N*H*); δ_C(100 MHz) −5.1 [CH_3, Si(CH_3)$_A$(CH_3)$_B$], −4.7 [CH_3, Si(CH_3)$_A$(CH_3)$_B$], 14.1 (CH_3, CH_2CH_3), 18.1 [C, SiC(CH_3)$_3$], 22.7 (CH_2), 24.9 (CH_2), 25.7 [CH_3, SiC(CH_3)$_3$, C(CH_3)$_A$(CH_3)$_B$, resonance overlap], 26.4 (CH_2), 26.8 [CH_3, C(CH_3)$_C$(CH_3)$_D$], 26.9 (CH_3, C(CH_3)$_C$(CH_3)$_D$), 27.9 (CH_2), 28.1 (CH_3, C(CH_3)$_A$(CH_3)$_B$), 28.3 (CH_3, OC(CH_3)$_3$), [28.9, 29.3, 29.5, 29.7 (CH_2, alkyl chain, significant resonance overlap)], 31.9 (CH_2), 50.1 (CH, C-2), 67.4 (CH, *C*HO), 70.1 (CH_2, C-1), [74.5, 75.6, 75.7, 76.5, 77.9 (CH, *C*HO)], 79.4 (C, OC(CH_3)$_3$), 107.7 [C, chain acetal *C*(CH_3)$_2$], 108.6 [C, cyclitol acetal *C*(CH_3)$_2$], 155.1 (C, *C*=O).

(2*S*, 3*S*, 4*R*, 1′*S*, 2′*S*, 3′*S*, 4′*S*)-2-Hexacosanoylamino-1-*O*-[2′, 3′, 4′-trihydroxycyclohexyl]-1, 3, 4-octadecanetriol (16)

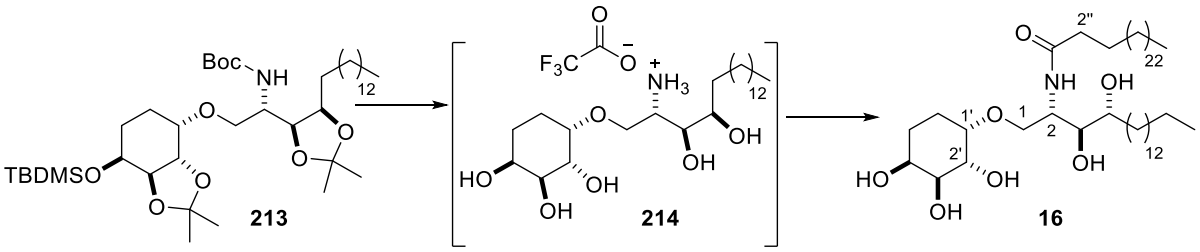

TFA (2 mL) was added to ether **213** (30 mg, 0.041 mmol). After 15 min, the TFA was removed by bubbling argon through the mixture. Any residual TFA was removed under reduced pressure. This procedure was repeated if necessary until all of the protecting groups had been removed as evidenced by TLC. The crude aminopolyol **214** was isolated, presumably as its TFA salt, as a yellow solid [R_f = 0.3 (30% MeOH in $CHCl_3$)] and used without further purification in the next step: NHS ester **19** (20 mg, 0.041 mmol) and Et_3N (10 μL, 0.072 mmol) were added to a solution of aminopolyol **214** in dry THF (2 mL). After 12 h the solvent was removed under reduced pressure. The crude mixture was purified by column chromatography (gradient: $CHCl_3$ → 5% MeOH in $CHCl_3$) to yield amide **16** as a white solid (24 mg, 73%): R_f = 0.3 (10% MeOH in $CHCl_3$); solubility issues prevented an optical rotation measurement; ν_{max}(film)/cm^{-1} 3342 br m (O–H, N–H), 2915 s, 2849 s, 2409 w, 1625 m (C=O), 1468 m, 1072 m, 1005 w, 849 w, 718 m; δ_H(300 MHz, 2:1 $CDCl_3$:CD_3OD) 0.84 (6H, t, *J* 6.7, 2 × CH_2CH_3), 1.18–1.32 (68H, stack, alkyl chain), 1.45–1.69 (8H, stack, CH_2 of cyclitol, alkyl chain), 2.12 (2H, app t, *J* 7.5, H-2*)*, 3.48–3.59 (3H, stack), 3.63–3.77 (4H, stack), 3.92–3.97 (1H, m), 4.10–4.18 (1H, m), 7.23 (1H, d, *J* 8.7, N*H*), O*H*s not observed; δ_C(100 MHz, 2:1 $CDCl_3$:CD_3OD) 14.3 (CH_3), 22.4 (CH_2), 23.1 (CH_2), 25.6 (CH_2), 26.3 (CH_2), 26.4 (CH_2), [29.8, 29.9, 30.0, 30.1, (CH_2, significant resonance overlap)], 32.3 (CH_2), 32.9 (CH_2), 36.9 (CH_2), 50.6 (CH, C-2), 68.7 (CH_2, C-1), 69.5 (CH, C-4′), 71.4 (CH, C-2′), 72.7 (CH, C-3′), 72.7 (CH, C-4), 75.3 (CH, C-3), 78.9

(CH, C-1′), 174.7 (C, *C*=O); *m/z* (TOF ES+) 849.1 ([M + Na]$^+$, 100%);%); HRMS *m/z* (TOF ES+) 848.7313 [M + Na]$^+$, $C_{50}H_{99}NO_7Na$ requires 848.7319.

Data were in agreement with those reported in the literature.[138]

(*Z*, *Z*, 2*S*, 3*S*, 4*R*, 1′*S*, 2′*S*, 3′*S*, 4′*S*)-2-Eicosa-11, 14-dienoylamino-1-*O*-[2′, 3′, 4′-trihydroxycyclohexyl]-1, 3, 4-octadecantriol (168)

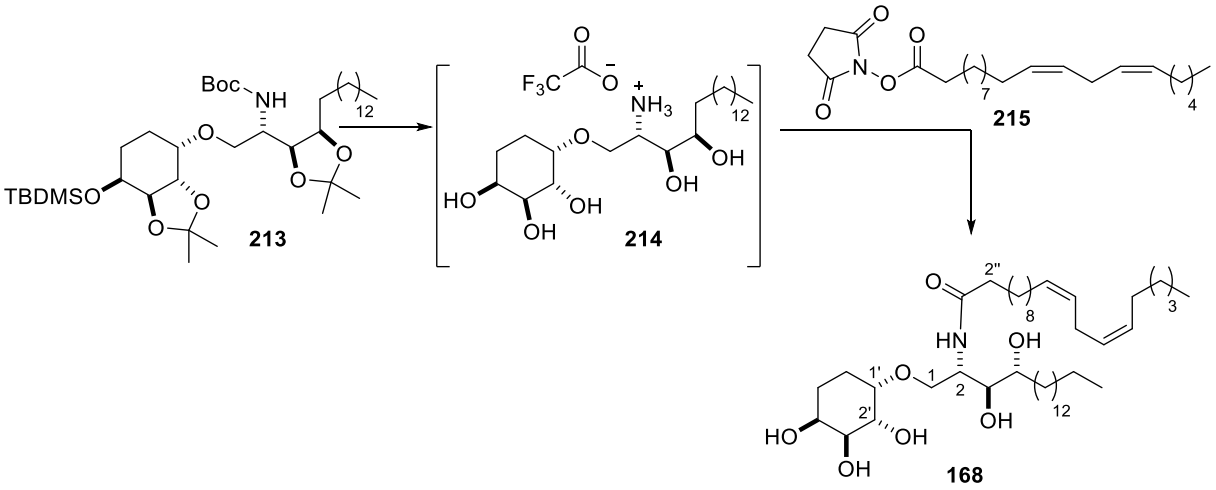

Preparation of (Z,Z)-Eicosa-11, 14-dienoic acid-2, 5-dioxo-1-pyrrolidinyl ester (**215**): EDCI.HCl (35 mg, 0.18 mmol), *N*-hydroxysuccinimide (23 mg, 0.20 mmol) and DMAP (5 mg, 0.04 mmol) were added to a solution of (*Z,Z*)-eicosa-11, 14-dienoic acid (50 mg, 0.16 mmol) in CH_2Cl_2 (1 mL). The solution was stirred in a sealed tube at 40 °C and the progress of the reaction monitored by TLC (40% Et_2O in petroleum ether b.p. 40–60 °C). After 12 h, the reaction mixture was poured into H_2O (5 mL) and extracted with Et_2O (3 × 10 mL). The combined organic layers were washed with brine (15 mL), dried with Na_2SO_4, filtered and the solution was concentrated under reduced pressure. The crude mixture was plugged quickly through a silica column (20% EtOAc in hexanes) and the NHS ester **215** used directly in the next step [R_f = 0.2 (40% Et_2O in petroleum ether b. p. 40–60 °C)]. TFA (2 mL) was added to ether **213** (30 mg, 0.041 mmol). After stirring for 15 min, the TFA was removed by bubbling argon through the mixture. Residual TFA was removed under reduced pressure. This procedure was repeated if necessary until all of the protecting groups had been removed as evidenced

by TLC. The crude aminopolyol **214** was isolated, presumably as its TFA salt, as a yellow solid [R_f = 0.3 (30% MeOH in $CHCl_3$)] and used without further purification in the next step: NHS ester **215** (20 mg, 0.041 mmol) and Et_3N (10 μL, 0.072 mmol) were added to a solution of aminopolyol **214** in dry THF (2 mL). After stirring the reaction mixture for 12 h, the solvent was removed under reduced pressure. The crude mixture was purified by column chromatography (gradient: $CHCl_3$ → 5% MeOH in $CHCl_3$) to yield amide **168** as a white solid (15 mg, 48%): R_f = 0.3 (10% MeOH in $CHCl_3$); m.p. 97–99 °C; solubility issues prevented an optical rotation measurement; ν_{max}(film)/cm^{-1} 3371 br w (O–H, N–H), 3010 w, 2917 s, 2850 s, 2466 w, 1626 s (C=O), 1545 w, 1454 m, 1401 w, 1368 w, 1341 w, 1322 w, 1286 w, 1260 w, 1072 s, 1009 m, 950 m, 904 w, 884 w, 814 w, 851 w, 720 s, 693 m; δ_H(400 MHz, 2:1 $CDCl_3$:CD_3OD) 0.75–0.84 (6H, stack, 2 × CH_2CH_3), 1.16–1.25 (44H, stack), 1.51–1.65 (6H, stack), 1.97 (4H, app q, *J* 6.8, 2 × CH_2CH_2CH=CH), 2.12 (2H, app t, *J* 7.6, H-2″), 2.69 (2H, app t, *J* 6.4, CH=CHCH_2CH=CH), 3.44–3.56 (3H, stack, 3 × C*H*O), 3.58–3.73 (4H, stack, 4 × C*H*O), 3.90–3.94 (1H, m, C*H*O), 4.06–4.12 (1H, m, H-2), 5.21–5.34 (4H, stack, 2 × C*H*=C*H*), 7.08 (1H, d, *J* 8.8, N*H*), O*H*s not observed; δ_C(100 MHz, 2:1 $CDCl_3$:CD_3OD) 14.2 (CH_3), 22.3 (CH_2), 23.0 (CH_2), 25.5 (CH_2), 25.9 (CH_2, CH=CH*C*H_2CH=CH), 26.2 (CH_2), [27.49, 27.53 (CH_2, CH_2CH_2CH=CH), [29.7, 29.8, 29.9, 30.0, 30.1, (CH_2, significant resonance overlap)], 31.8 (CH_2), 32.2 (CH_2), 33.0 (CH_2) 36.9 (CH_2, C-2″), 50.4 (CH, C-2), 68.7 (CH_2, C-1), [69.4, 71.3, 72.5, 72.6, 75.4, 78.8 (CH, *C*HO)], [128.2, 128.3, 130.4, 130.5 (CH,*C*H=CH)], 174.5 (C, *C*=O); *m/z* (TOF ES+) 761.8 ([M + H]$^+$, 100%); HRMS *m/z* (TOF ES+) 761.6148 [M + Na]$^+$, $C_{44}H_{84}NO_7Na$ requires 761.6145.

.

(2*S*, 3*S*, 4*R*, 1′*S*, 2′*S*, 3′*S*, 4′*S*)-3, 4-Di-*O*-acetyl-2-hexacosanoylamino-1-*O*-[2′, 3′, 4′-tri-*O*-acetyl-trihydroxycyclohexyl]-1, 3, 4-octadecanetriol (216)

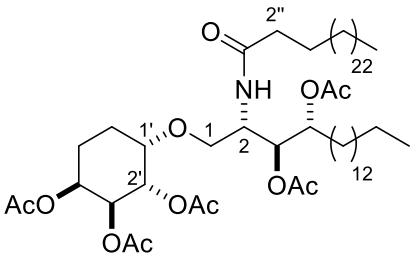

Ac_2O (8 μL, 0.51 mmol) was added dropwise over 20 s to a solution of pentaol **16** (18 mg, 0.017 mmol) in pyridine (1 mL). The reaction mixture was stirred at rt for 14 h, after which time, the volatiles were removed under reduced pressure. The residue was diluted with CH_2Cl_2 (15 mL), washed sequentially with H_2O (8 mL), $NaHCO_3$ solution (10 mL) and brine (5 mL), and then dried over Na_2SO_4. The mixture was filtered and the filtrate was concentrated under reduced pressure. The crude product was purified by flash chromatography (25% EtOAc in hexanes) to yield penta-acetate **216** as an off white amorphous solid (19 mg, 87%): R_f = 0.3 (25% EtOAc in hexanes); $[\alpha]_D^{20}$ = +41.6 (c = 1.0, $CHCl_3$); ν_{max}(film)/ cm^{-1} 3369 vw br (N–H), 2919 s, 2851 s, 1743 s (ester C=O), 1638 w (amide C=O), 1468 w, 1372 m, 1231 s, 1060 w; δ_H(300 MHz) 0.87 (6H, app t, *J* 6.8, 2 × CH_2CH_3), 1.12–1.28 (68H, stack, alkyl chain), 1.49–1.64 (5H, stack, alkyl chain, CH_2 of cyclitol), 1.67–1.76 (3H, stack, alkyl chain, CH_2 of cyclitol), 1.94 (3H, s, C(O)CH_3), 1.95 (3H, s, C(O)CH_3), 1.99 (3H, s, C(O)CH_3), 2.020 (3H, s, C(O)CH_3), 2.023 (3H, s, C(O)CH_3), 2.16 (2H, app t, *J* 7.6, H-2″), 3.37–3.44 (2H, stack, H-1), 3.63−3.68 (1H, m, H-1′ or H-4′), 4.21 (1H, ddd, *J* 9.4, 5.6, 2.8, H-2), 4.83 (1H, app td, *J* 10.0, 3.0, H-4), 5.08 (1H, dd, *J* 9.5, 2.6, H-2′ or H-3′), 5.15 (1H, dd, *J* 9.6, 3.0, H-3′ or H-2′), 5.19 (1H, dd, *J* 9.5, 2.5, H-3), 5.24−5.29 (1H, m, H-4′ or H-1′), 6.16 (1H, d, *J* 9.2, N*H*); δ_C(100 MHz) 14.1 (CH_3, 2 × CH_2CH_3), [20.8, 20.9, 21.1 (CH_3, C(O)CH_3, resonance overlap)], 22.7 (CH_2), 23.1 (CH_2), 25.6 (CH_2), 25.8 (CH_2), 27.6 (CH_2), [29.4, 29.7, 31.9 (CH_2, significant resonance overlap)], 36.8 (CH_2, C-2″), 48.2 (CH, C-2), 68.0 (CH_2, C-1), 69.4 (CH, C-1′ or C-4′ and C-2′ or C-3′, resonance overlap), 71.1 (CH, C-3 and C-3′ or C-2′, resonance overlap), 73.4 (CH, C-4), 76.4

(CH, C-4′ or C-1′), 169.83 (C, acetyl *C*=O), 170.02 (C, acetyl *C*=O), 170.2 (C, acetyl *C*=O), 170.6 (C, acetyl *C*=O), 171.1 (C, acetyl *C*=O), 172.9 (C, amide *C*=O); *m/z* (TOF ES+) 1058.7 ([M + Na]$^+$, 100%); HRMS *m/z* (TOF ES+) 1058.7420 [M + Na]$^+$, $C_{60}H_{109}NO_{12}Na$ requires 1058.7425.

(2*S*, 3*S*, 4*R*, 1′*S*, 2′*S*, 3′*S*, 4′*S*)-3, 4-Di-*O*-acetyl-2-hexacosathioylamino-1-*O*-[2′, 3′, 4′-tri-*O*-acetyl-trihydroxycyclohexyl]-1, 3, 4-octadecantriol (217)

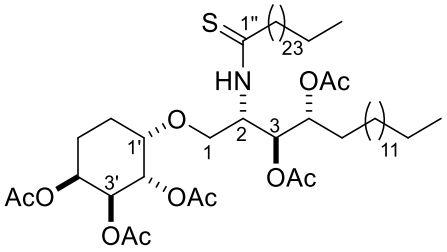

Lawesson′s reagent (8 mg, 0.02 mmol) was added to a solution of amide **216** (16 mg, 0.015 mmol) in toluene (1 mL) at rt. The reaction mixture was stirred at 80 °C for 4 h and then the solvent was removed under reduced pressure. The residue was diluted with CH_2Cl_2 (10 mL), washed sequentially with H_2O (5 mL), $NaHCO_3$ solution (10 mL) and brine (5 mL), and then dried over Na_2SO_4. The solution was filtered and the filtrate was concentrated under reduced pressure. The crude product was purified by flash chromatography (25% EtOAc in hexanes) to yield thioamide **217** as an off-white low melting point solid (14 mg, 93%): R_f = 0.3 (20% EtOAc in hexanes); $[\alpha]_D^{20}$ = +34.4 (c = 1.0, $CHCl_3$); ν_{max}(film)/cm^{-1} 2922 vs, 2852 s, 1744 vs (C=O), 1536 w, 1463 w, 1370 m, 1227 vs (C=S), 1058 m, 1023 m, 950 w, 832 vw, 720 w; δ_H(300 MHz) 0.88 (6H, app t, *J* 6.8, 2 × CH_2CH_3), 1.20–1.28 (68H, stack, alkyl chain), 1.57–1.81 (8H, stack, alkyl chain, CH_2 of cyclitol), 2.02 (3H, s, C(O)CH_3), 2.03 (3H, s, C(O)CH_3), 2.06 (3H, s, C(O)CH_3), 2.09 (3H, s, C(O)CH_3), 2.11 (3H, s, C(O)CH_3), 2.69 (2H, m, *J* 7.4, 2.5, H-2 ″), 3.54 (1H, app d, *J* 9.3, H-1$_A$), 3.66 (1H, dd, *J* 10.0, 3.1, H-1$_B$), 3.71−3.75 (1H, m, H-1′ or H-4′), 4.83 (1H, app td, *J* 10.1, 3.0, H-4), 5.04 (1H, app tt, *J* 8.9, 2.9, H-2), 5.16 (1H, dd, *J* 9.3, 2.5, H-2′ or H-3′), 5.23 (1H, dd, *J* 9.3, 2.5, H-3′ or H-2′), 5.29−5.34 (1H, m, H-4′ or H-1′),

5.40 (1H, dd, *J* 8.7, 2.7, H-3), 8.20−8.27 (1H*,* m, N*H*); δ_C(100 MHz) 14.1 (CH_3, 2 × CH_2CH_3), [20.8, 20.9, 21.1 (CH_3, $COCH_3$, resonance overlap)], 22.7 (CH_2), 23.2 (CH_2), 25.5 (CH_2), 25.8 (CH_2), 28.2 (CH_2), 28.9 (CH_2), [29.3, 29.4, 29.6, 29.7 (CH_2, significant resonance overlap)], 29.7 (CH_2), 31.9 (CH_2), 47.3 (CH_2, C-2″), 54.1 (CH, C-2), 66.4 (CH_2, C-1), 69.3 (CH, C-1′ or C-4′ and C-2′ or C-3′, resonance overlap), 70.8 (CH, C-3 and C-3′ or C-2′, resonance overlap), 73.4 (CH, C-4), 76.4 (CH, C-4′ or C-1′), 169.95 (C, acetyl C=O), 170.00 (C, acetyl C=O), 170.01 (C, acetyl C=O), 170.5 (C, acetyl C=O), 171.3 (C, acetyl C=O), 206.4 (C, C=S); *m/z* (TOF ES+) 1053.8 ($[M + H]^+$, 100%); HRMS *m/z* (TOF ES+) 1052.7820 $[M + H]^+$, $C_{60}H_{110}NO_{11}S$ requires 1052.7800.

(2*S*, 3*S*, 4*R*, 1′*S*, 2′*S*, 3′*S*, 4′*S*)-2-Hexacosathioylamino-1-*O*-[2′, 3′, 4′-trihydroxycyclohexyl]-1, 3, 4-octadecanetriol (167)

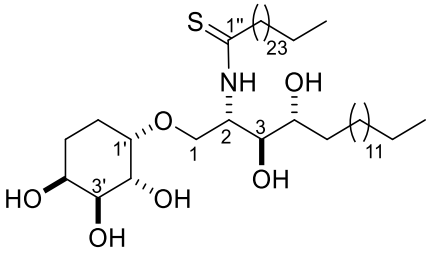

NaOMe (0.2 mL of a 1.0 M solution in MeOH, 0.2 mmol) was added to a solution of thioamide **217** (14 mg, 0.014 mmol) in MeOH (2.5 mL). After 2 h, the reaction mixture was neutralised by the addition of acidic ion-exchange resin [Dowex H CR-S, pre-washed with MeOH (100 mL) and $CHCl_3$ (50 mL)]. The solution was filtered and the resin washed with MeOH (25 mL) and $CHCl_3$–MeOH (25 mL, 9:1). The filtrate was concentrated under reduced pressure. Purification of the residue by column chromatography (gradient: $CHCl_3 \rightarrow$ 5% MeOH in $CHCl_3$) provided thioamide **167** as a pale white solid (8 mg, 74%): R_f = 0.3 (10% MeOH in $CHCl_3$); solubility issues prevented an optical rotation measurement; ν_{max}(film)/cm^{-1} 3377 br w (O–H), 2917 s, 2850 s, 2498 br w, 1648 w, 1467 m, 1377 w, 1260 m (C=S), 1071 m, 1017 m, 974 w, 800 s, 720 s, 663 s; δ_H(300 MHz, 2:1 $CDCl_3$:CD_3OD) 0.86 (6H, app t, *J* 6.7, 2 × CH_2CH_3), 1.20–1.32 (69H, stack, alkyl chain), 1.55–1.75 (7H, stack, CH_2 of cyclitol, alkyl chain), 2.64

(2H, app t, *J* 7.6, H-2″), 3.62–3.82 (6H, stack), 3.85 (1H, dd, *J* 9.8, 3.1), 4.01–4.04 (1H, m), 4.82–4.87 (1H, m), 8.95 (1H, d, *J* 8.3, N*H*), O*H*s not observed; δ_C(100 MHz, 2:1 $CDCl_3$:CD_3OD) 14.3 (CH_3), 22.4 (CH_2), 23.1 (CH_2), 25.6 (CH_2), 26.3 (CH_2), 26.4 (CH_2), [29.8, 29.9, 30.0, 30.1 (CH_2, significant resonance overlap)], 32.3 (CH_2), 32.9 (CH_2), 36.9 (CH_2), 56.5 (CH, C-2), 67.2 (CH_2, C-1), 69.6 (CH, C-4′), 71.5 (CH, C-2′), 72.6 (CH, C-3′), 72.7 (CH, C-4), 74.2 (CH, C-3), 78.8 (CH, C-1′), 205.6 (C, *C*=S); *m/z* (TOF ES+) 842.7 ([M + H]$^+$, 50%), 539.3 (100); HRMS *m/z* (TOF ES+) 842.7291 [M + H]$^+$, $C_{50}H_{100}NO_6S$ requires 842.7271.

11-(4′-Fluorophenyl)undec-10-ynoic acid (220)

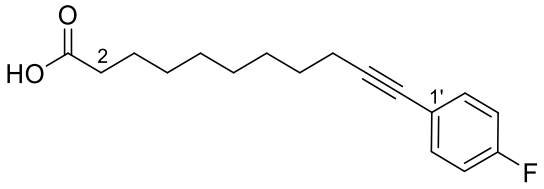

A solution of 4-fluoroiodobenzene (833 mg, 2.73 mmol) and undec-10-ynoic acid (500 mg, 3.76 mmol) in Et_3N (6 mL) was degassed by bubbling argon through the solution for 10 min while sonicating. $Pd(PPh_3)_2Cl_2$ (153 mg, 0.218 mmol) was added and the mixture was stirred. After 10 min, CuI (282 mg, 1.48 mmol) was added and the resulting mixture was heated under argon overnight at 50 °C. The reaction mixture was then cooled to rt before filtering through a pad of Celite to remove the insoluble ammonium salt generated in the reaction, rinsing with Et_2O (25 mL). The filtrate was concentrated under reduced pressure and the residue was purified by flash chromatography (10% MeOH in $CHCl_3$) to afford alkyne **220** as an off white solid (595 mg, 79 %): R_f = 0.6 (10% MeOH in $CHCl_3$); m.p. 64–65 °C; ν_{max}(film)/cm^{-1} 3675 w (O–H), 2926 m, 2917 br m, 2867 w, 2850 m, 1705 vs (C=O), 1600 w, 1505 s, 1467 s, 1451 w, 1427 m, 1410 m, 1345 w, 1327 m, 1288 w, 1264 w, 1252 m, 1217 vs, 1191 m, 1158 m, 1092 m, 1064 w, 1029 w, 1012 w, 921 m, 835 vs, 825 s, 814 m, 786 w, 746 w, 717 m, 676 w, 657 w; δ_H(400 MHz) 1.29–1.39 (6H, stack, alkyl chain), 1.40–1.48 (2H, m, alkyl chain), 1.54–1.69 (4H, stack, alkyl chain), 2.32–2.40 (4H, stack, H-2, H-9), 6.93–7.01 (2H, m, Ar), 7.32–7.39 (2H, m, Ar), O*H* not observed; δ_C(100 MHz) 19.3 (CH_2), 24.7 (CH_2), [29.7, 29.8, 28.9, 29.0,

29.1 (CH_2, alkyl chain)], 34.1 (CH_2), [79.5, 90.0 (C, C-10, C-11)], 115.4 (CH, d, *J*, 20.0, C-3′), 120.1 (C, Ar C-1′), 133.3 (CH, d, *J* 10.0, C-2′), 162.1 (C, d, *J* 250.0, C-4′), 180.0 (C, *C*=O); δ_F (282 MHz) −112.4 (tt, *J* 8.7, 5.4); *m/z* (TOF ES+) 299.1 ([M + Na]$^+$, 100%); HRMS *m/z* (TOF ES+) 299.1417 [M + Na]$^+$, $C_{17}H_{21}FO_2Na$ requires 299.1423.

Data were in agreement with those reported in the literature.[187]

11-(4′-Fluorophenyl)undecanoic acid (221)

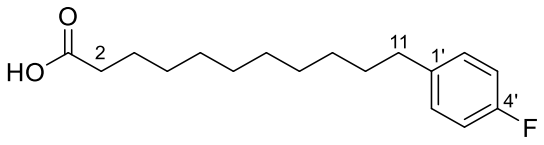

A flask containing a solution of alkyne **220** (200 mg, 0.724 mmol) in MeOH (25 mL) was purged with H_2 for 10 min. Pd/C (8 mg, 10% Pd) was added and the mixture was stirred under a flow of H_2 gas. After 12 h, the suspension was filtered through Celite, which was washed with MeOH (40 mL). The filtrate was concentrated under reduced pressure and the residue was purified by column chromatography (gradient: hexanes → 30% EtOAc in hexanes) to afford acid **221** as a white solid (0.19 g, 95%): R_f = 0.4 (5% MeOH in $CHCl_3$); m.p. 91–95 °C; ν_{max}(film)/cm^{-1} 3675 w (O–H), 2926 br m, 2914 m, 2867 w, 2850 m, 1694 s (C=O), 1605 w, 1507 s, 1470 m, 1459 w, 1428 m, 1405 m, 1348 w, 1325 w, 1286 w, 1265 m, 1240 s, 1217 vs, 1191 m, 1158 m, 1092 m, 1064 s, 1029 w, 1012 w, 919 m, 835 vs, 825 s, 817 s, 786 w, 750 m, 721 m, 678 w; δ_H(300 MHz) 1.24–1.35 (12H, stack, alkyl chain), 1.53–1.66 (4H, stack, alkyl chain), 2.35 (2H, t, *J* 7.5, H-2), 2.56 (2H, t, *J* 7.7, H-11), 6.92–6.98 (2H, m, Ar), 7.09–7.14 (2H, m, Ar), O*H* not observed; δ_C(100 MHz) [24.7, 29.1, 29.19, 29.24, 29.41, 29.46, 29.50 (CH_2, alkyl chain)], 31.6 (CH_2), 34.0 (CH_2), 35.2 (CH_2), 114.9 (CH, d, *J* 20.8, C-3′), 129.7 (CH, d, *J* 7.6, C-2′), 138.5 (C, d, *J* 2.0, C-1′), 161.1 (C, d, *J* 240.0, C-4′), 180.1 (C, *C*=O); δ_F (282 MHz) −118.3 (tt, *J* 8.8, 5.6); *m/z* (TOF ES+) 303.2 ([M + Na]$^+$, 100%); HRMS *m/z* (TOF ES+) 303.1745 [M + Na]$^+$, $C_{17}H_{25}FO_2Na$ requires 303.1736.

Data were in agreement with those reported in the literature.[187]

(2*S*, 3*S*, 4*R*, 1′*S*, 2′*S*, 3′*S*, 4′*S*)-2-[11″-(4‴-Fluorophenyl)undecanoylamino-1-*O*-[2′, 3′, 4′-trihydroxycyclohexyl]-1, 3, 4-octadecantriol (169)

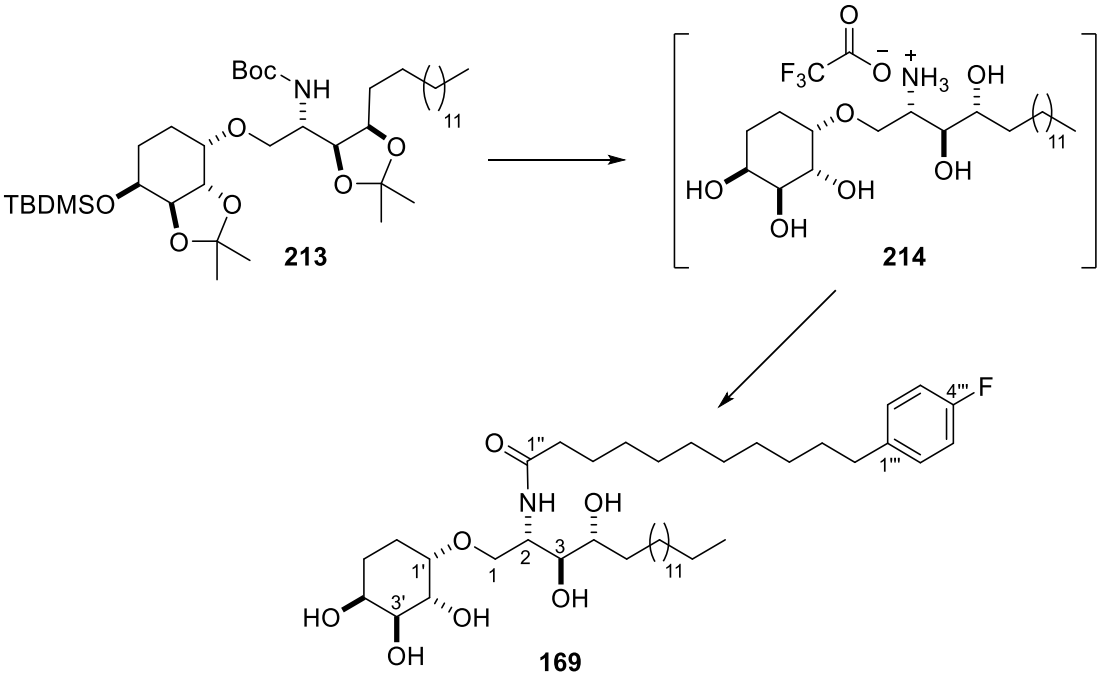

TFA (2 mL) was added to ether **213** (30 mg, 0.041 mmol). The mixture was stirred for 15 min before removing the TFA by bubbling argon through the mixture. Any residual TFA was removed under reduced pressure. This procedure was repeated if necessary until all of the protecting groups had been removed as evidenced by TLC. The crude aminopolyol **214** was obtained, presumably as its TFA salt, as a yellow solid [R_f = 0.3 (30% MeOH in $CHCl_3$)] and used without further purification. $(COCl)_2$ (2 mL) was added to acid **221** (11 mg, 0.041 mmol) and the resulting solution was heated at 70 °C for 2 h, after which time, the solution was cooled to rt, and the residual $(COCl)_2$ removed under a stream of dry argon. The residual volatiles were removed under reduced pressure. The resulting crude acyl chloride was dissolved in THF (0.5 mL) and added with vigorous stirring, to a solution of the crude aminopolyol **214** in THF/NaOAc (8 M) (1:1, 2 mL). Vigorous stirring was maintained for 2 h, after which time the reaction mixture was left to stand and the layers were separated. The aqueous layer was extracted with THF (3 × 2.0 mL) and the organic layers were combined and concentrated

under reduced pressure. The crude mixture was purified by column chromatography (gradient: $CHCl_3 \rightarrow$ 5% MeOH in $CHCl_3$) to yield amide **169** as a white solid (17 mg, 54%): R_f = 0.5 (10% MeOH in $CHCl_3$); solubility issues prevented an optical rotation measurement; ν_{max}(film)/cm^{-1} 3332 br w (O–H), 2922 s, 2852 m, 1648 m (C=O), 1541 m, 1593 s, 1464 m, 1253 m, 1221 m, 1079 s, 802 m, 765 m, 679 w; δ_H(300 MHz, 2:1 $CDCl_3$:CD_3OD) 0.85 (3H, t, *J* 6.7, CH_2CH_3), 1.19–1.38 (37H, stack), 1.50–1.70 (9H, stack), 2.16 (2H, app t, *J* 7.5), 2.53 (2H, app t, *J* 8.6), 3.48–3.78 (7H, stack), 3.92–3.99 (1H, m), 4.10–4.18 (1H, m), 6.86–6.96 (2H, m, Ar), 7.04–7.14 (2H, m, Ar), 7.22 (1H, d, *J* 8.6, N*H*), O*H*s not observed; δ_C(100 MHz, 2:1 $CDCl_3$:CD_3OD) 14.2 (CH_3, CH_2CH_3), 22.3 (CH_2), 22.9 (CH_2), 25.4 (CH_2), 26.1 (CH_2), [29.4, 29.5, 29.6, 29.7, 29.8, 29.9, 30.0 (CH_2, alkyl chain, resonance overlap)], 31.9 (CH_2), 32.2 (CH_2), 35.3 (CH_2), 36.8 (CH_2), 50.3 (CH, C-2), 68.7 (CH_2, C-1), [69.3, 71.2, 72.5, 72.6, 75.3, 78.8 (CH, *C*H-O, C-3, C-4, C-1′, C-2′, C-3′, C-4′)], 115.1 (CH, d, *J* 20.9, C-3‴), 130.0 (CH, d, *J* 3.2, C-2‴), 138.8 (C, d, *J* 3.2, C-1″) 161.5 (C, d, *J* 241.2, C-4‴) ,174.4 (C, C=O); δ_F (282 MHz) −115.0 (tt, *J* 8.8, 5.5); *m/z* (TOF ES+) 710.5 ($[M]^+$, 100%); HRMS *m/z* (TOF ES+) 710.5382 $[M]^+$, $C_{41}H_{73}NFO_7$ requires 710.5371.

(2*S*, 3*S*)-1-*O*-Benzyl-2,3-*O*-isopropylidene-1,2,3,4-butanetetraol (235)

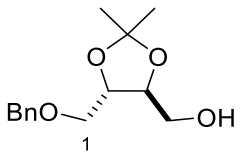

NaH (123 mg of a 60% dispersion in mineral oil, 3.08 mmol,) was added to a solution of (+)-2,3-*O*-isopropylidene-L-threitol (500 mg, 3.08 mmol) in THF (20 mL) at 0 °C. After 1 h, a solution of BnBr (527 mg, 3.08 mmol) in THF (5 mL) was added. The reaction mixture was warmed to rt and stirred for 16 h. The mixture was diluted with Et_2O (50 mL) and washed with NH_4Cl solution (50 mL). The aqueous layer was extracted with Et_2O (3 x 20 mL). The combined organic extracts were dried over Na_2SO_4, filtered and concentrated under reduced pressure.

The crude product was purified by column chromatography (10% EtOAc in hexanes → 20% EtOAc in hexanes) to afford benzyl ether **235** as a pale yellow oil (0.77 g, 76%). R_f = 0.2 (20% EtOAc in hexanes); $[\alpha]_D^{21}$ = +7.6 (c = 1.0, $CHCl_3$) lit.[188] $[\alpha]_D^{20}$ = +9.1 (c = 1.0, $CHCl_3$); ν_{max}(film)/cm^{-1} 3448 br m (O–H), 2986 m, 2931 m, 2868 m, 1454 m, 1370 s, 1249 s, 1213 s, 1167 m, 1076 vs, 1048 vs, 989 m, 902 m, 845 s, 737 s, 698 s, 606 w; δ_H(400 MHz) 1.35 (3H, s, C(C*H*$_3$)$_A$(CH$_3$)$_B$), 1.36 (3H, s, C(CH$_3$)$_A$(C*H*$_3$)$_B$), 2.51 (1H, br s, O*H*), 3.50 (1H, dd, *J* 9.9, 5.5, H-1$_A$), 3.57–3.64 (2H, stack, H-1$_B$, H-4$_A$), 3.69 (1H, app. dt, *J* 11.5, 3.8, H-4$_B$), 3.87 (1H, app. dt, *J* 8.4, 4.4, H-3), 3.99 (1H, app. dt, *J* 8.3, 5.3, H-2), 4.52 (2H, s, PhC*H*$_2$), 7.19–7.31 (5H, stack, Ar C*H*); δ_C(100 MHz) 26.8 [*C*H$_3$, C(*C*H$_3$)$_A$(CH$_3$)$_B$], 26.9 [*C*H$_3$, C(CH$_3$)$_A$(*C*H$_3$)$_B$], 62.3 (CH$_2$, C-4), 70.3 (CH$_2$, C-1), 73.6 (CH$_2$, Ph*C*H$_2$), 76.4 (CH, C-2), 79.5 (CH, C-3), 109.3 (C, *C*(CH$_3$)$_2$), [127.6, 127.7, 128.4 (CH, Ar CH)], 137.5 (C, Ar C); *m/z* (TOF ES+) 275.1 ([M + Na]$^+$, 100%).

Data were in agreement with those reported in the literature.[188]

(2*S*, 3*S*, 4*R*, 2′*S*, 3′*S*)-1-*O*-[4′-*O*-Benzyl-2′,3′-*O*-isopropylidene-2′,3′,4′-trihydroxybutyl]-2-toluenesulfonamido-3, 4-*O*-isopropylidene-1, 3, 4-octadecanetriol (236)

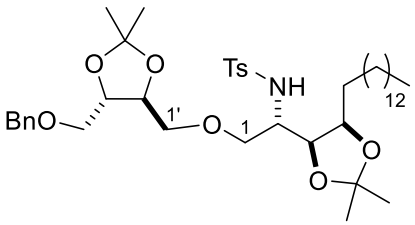

NaH (32 mg of a 60% dispersion in mineral oil, 0.8 mmol,) was added to a solution of benzyl ether **235** (200 mg, 0.793 mmol) in DMF (1 mL) at 0 °C. After stirring for 1 h, a solution of aziridine **193** (325 mg, 0.658 mmol) in DMF (1.5 mL) was added. After 20 min at 0 °C, the reaction mixture was warmed to rt and stirred for a further 15 h. The reaction mixture was then quenched with H_2O (25 mL) and extracted with EtOAc (5 × 30 mL). The combined organic fractions were washed with brine (70 mL), dried over Na_2SO_4, filtered and the filtrate was concentrated under reduced pressure. The residue was purified by column chromatography

(10% EtOAc in hexanes) to yield ether **236** as a colourless oil (314 mg, 64%): R_f = 0.3 (20% EtOAc in hexanes); $[\alpha]_D^{21}$ = +6.0 (c = 1.0, $CHCl_3$); ν_{max}(film)/cm^{-1} 3270 vw br (N–H), 2985 m, 2924 s, 2854 m, 1598 w, 1455 m, 1379 m, 1369 m, 1336 m, 1246 m, 1218 m, 1162 s, 1089 s, 848 w, 814 m, 736 w, 697 m, 666 m; δ_H(400 MHz) 0.88 (3H, t, *J* 6.8, CH_2CH_3), 1.23–1.28 (23H, stack, alkyl chain), 1.29 (3H, s, $C(CH_3)_A(CH_3)_B$), 1.36 (3H, s, $C(CH_3)_A(CH_3)_B$), 1.38 (3H, s, $C(CH_3)_C(CH_3)_D$), 1.41 (3H, s, $C(CH_3)_C(CH_3)_D$), 1.43–1.58 (3H, stack, alkyl chain), 2.41 (3H, s, Ar CH_3), 3.08 (1H, dd, *J* 9.8, 2.9, H-1_A), 3.23 (1H, dd, *J* 10.4, 4.7, H-$1'_A$), 3.46–3.56 (3H, stack, H-2, H-$1'_B$, H-$4'_A$), 3.57–3.65 (2H, stack, H-1_B, H-$4'_B$), 3.87 (1H, app. dt, *J* 8.2, 4.6, H-2′), 3.93–4.05 (3H, stack, H-3, H-4, H-3′), 4.56 (1H, A of AB, *J* 12.2, $PhCH_AH_B$), 4.61 (1H, B of AB, *J* 12.2, $PhCH_AH_B$), 5.31 (1H, d, *J* 9.7, N-H), 7.26–7.38 (7H, stack, Ar CH), 7.74–7.77 (2H, m, Ar CH); δ_C(100 MHz) 14.1 (CH_3, CH_2CH_3), 21.5 (CH_3, Ar CH_3), 22.7 (CH_2, alkyl chain), 25.8 [(CH_3, $C(CH_3)_A(CH_3)_B$], 26.4 (CH_2, alkyl chain), 27.0 (CH_3, $C(CH_3)_C(CH_3)_D$), $C(CH_3)_C(CH_3)_D$, resonance overlap], 28.0 (CH_3, $C(CH_3)_A(CH_3)_B$), [29.0, 29.4, 29.5, 29.7, 31.9 (CH_2, alkyl chain, resonance overlap)], 53.1 (CH, C-2), 69.5 (CH_2, C-1), 70.7 (CH_2, C-4′), 71.7 (CH_2, C-1′), 73.6 (CH_2, $PhCH_2$), [75.8, 77.2 (CH, C-3 or C-4 or C-3′)], 77.6 (CH, C-2′), 77.7 (CH, C-3 or C-4 or C-3′), 107.7 (C, $C(CH_3)_2$ phyto), 109.4 (C, $C(CH_3)_2$ thr), [127.1, 127.8, 128.4, 129.6 (CH, Ar CH, resonance overlap)], [137.7, 138.5, 143.5 (C, Ar C)]; *m/z* (TOF ES+) 768.4 ($[M + Na]^+$, 100%); *m/z* (TOF ES –) 744.5 ($[M - H]^-$, 100%); HRMS *m/z* (TOF ES–) 744.4506 ($[M - H]^-$), $C_{42}H_{66}NO_8$ requires 744.4509.

(2*S*, 3*S*, 4*R*, 2′*S*, 3′*S*)-1-*O*-[4′-*O*-Benzyl-2′,3′-*O*-isopropylidene-2′,3′,4′-trihydroxybutyl]-2-[(*N*-*tert*-butoxycarbonyl)amino]-3, 4-*O*-isopropylidene-1, 3, 4-octadecanetriol (238)

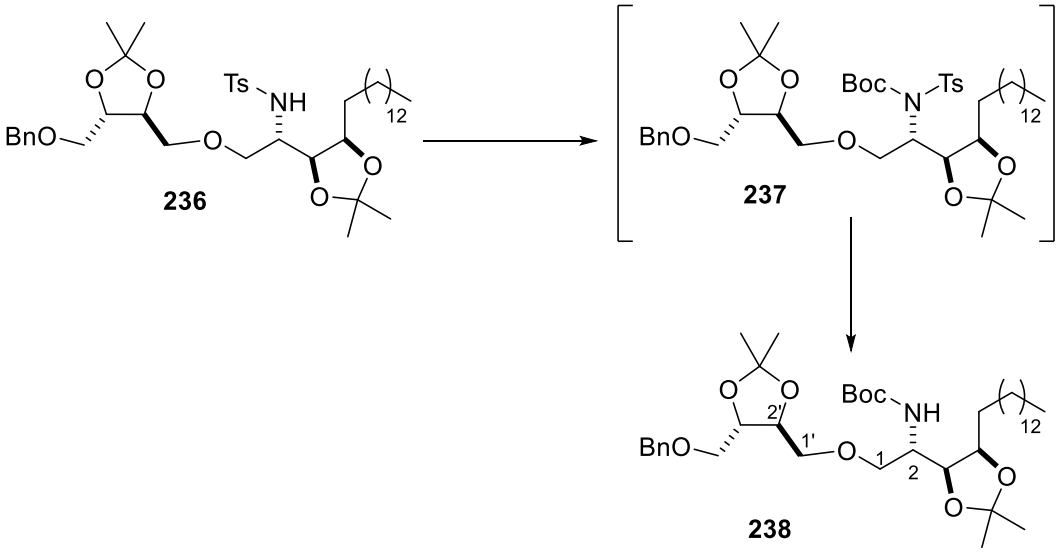

Boc_2O (150 mg, 0.687 mmol) and DMAP (25 mg, 10 weight %) were added to a solution of sulfonamide **236** (250 mg, 0.335 mmol) in CH_2Cl_2 (10 mL). The solution was stirred for 4 h and then the solvent was removed under reduced pressure to provide the crude product **237**, which was used directly in the next reaction without further purification: anhydrous MeOH (5 mL) was added to the flask containing carbamate **237** (283 mg, 0.335 mmol, based on 100% conversion). Mg powder (50 mg, 2.01 mmol) was added and the reaction mixture was sonicated in an ultrasound bath. After 30 min, the mixture was poured into hydrochloric acid (10 mL, 1.0 M) and extracted with Et_2O (3 × 20 mL). The combined organic phases were washed sequentially with $NaHCO_3$ solution (20 mL) and brine (20 mL), dried with Na_2SO_4 and filtered. The solvent was removed under reduced pressure and the residue purified by flash column chromatography (10% EtOAc in hexanes) to give Boc amide **238** as a colourless oil (150 mg, 65% over two steps): R_f = 0.5 (20% EtOAc in hexanes); $[\alpha]_D^{21}$ = +18.8 (c = 1.0, $CHCl_3$); ν_{max}(film)/cm^{-1} 3307 vw br (N–H), 2983 m, 2924 vs, 2854 s, 1717 s (C=O), 1499 m, 1455 m, 1367 s, 1247 s, 1218 s, 1169 vs, 1086 s, 1046 s, 852 m, 737 m, 697 m; δ_H(400 MHz) 0.87 (3H, t, *J* 6.8, CH_2CH_3), 1.23–1.29 (23H, stack, alkyl chain), 1.30 (3H, s, $C(CH_3)_A(CH_3)_B$),

1.39 (3H, s, $C(CH_3)_A(CH_3)_B$), 1.41–1.42 (6H, stack, $C(CH_3)_C(CH_3)_D$), 1.43 (9H, s, $C(CH_3)_3$), 1.49–1.55 (3H, stack, alkyl chain), 3.56 (1H, dd, *J* 9.7, 2.5, H-1_A), 3.58–3.63 (4H, stack, H-$1'_A$, H-$1'_B$, H-$4'_A$, H-$4'_B$), 3.71 (1H, dd, *J* 9.7, 3.5, H-1_B), 3.75–3.84 (1H, m, H-2), 3.92–4.00 (2H, stack, H-3,H-2′), 4.02–4.10 (2H, stack, H-4, H-3′), 4.57 (1H, A of AB, *J* 12.1, $PhCH_AH_B$), 4.61 (1H, B of AB, *J* 12.1, $PhCH_AH_B$), 4.82 (1H, d, *J* 9.7, N-H), 7.26–7.37 (5H, stack, Ar CH); δ_C(100 MHz) 14.1 (CH_3, CH_2CH_3), 22.7 (CH_2, alkyl chain), 25.8 (CH_3, $C(CH_3)_A(CH_3)_B$), 26.6 (CH_2, alkyl chain), 27.0 (CH_3, $C(CH_3)_C(CH_3)_D$, resonance overlap), 28.1 (CH_3, $C(CH_3)_A(CH_3)_B$), 28.3 (CH_3, $C(CH_3)_3$), [28.8, 29.3, 29.5, 29.7, 31.9 (CH_2, alkyl chain, resonance overlap)], 49.7 (CH, C-2), 70.6 (CH_2, C-4′), 71.6 (CH_2, C-1, C-1′, resonance overlap), 73.5 (CH_2, $PhCH_2$), [76.1, 77.2, 77.4, 77.9 (CH, C-3, C-4, C-2′, C-3′)], 79.4 (C, $C(CH_3)_3$), 107.8 (C, $C(CH_3)_2$ phyto), 109.5 (C, $C(CH_3)_2$ thr), [127.1, 128.4, (CH, Ar CH, resonance overlap)], 137.9 (C, Ar C), 155.0 (C, C=O); *m/z* (TOF ES+) 714.5 ($[M + Na]^+$, 100%); HRMS *m/z* (TOF ES+) 714.4922 $[M + Na]^+$, $C_{40}H_{69}NO_8Na$ requires 714.4921.

(2*S*, 3*S*, 4*R*, 2′*S*, 3′*S*)-2-[(*N*-*tert*-Butoxycarbonyl)amino]-1-*O*-[2′,3′-*O*-isopropylidene-2′,3′,4′-trihydroxybutyl]-3, 4-*O*-isopropylidene-1, 3, 4-octadecanetriol (239)

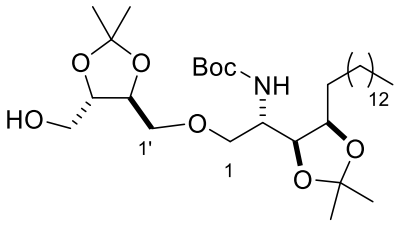

A flask containing a solution of benzyl ether **238** (120 mg, 0.173 mmol) in MeOH (10 mL) was purged with H_2 gas for 10 min. Pd/C (1 mg, 0.05 equiv) was then added and the mixture was stirred under a flow of H_2 for 4 h, after which time, the mixture was filtered through Celite, washing sequentially with MeOH (40 mL) and $CHCl_3$ (40 mL). The filtrate was concentrated under reduced pressure and the residue was purified by column chromatography (20% EtOAc in hexanes) to afford alcohol **239** as a colourless oil (82 mg, 79%): R_f = 0.2 (20% EtOAc in hexanes); $[\alpha]_D^{21}$ = +9.2 (c = 1.0, $CHCl_3$); ν_{max}(film)/cm^{-1} 3356 br m (O–H, N–H), 2983 m, 2923

vs, 2854 s, 1714 s (C=O), 1521 m, 1456 m, 1379 s, 1367 vs, 1246 vs, 1218 vs, 1167 vs, 1078 vs, 1045 vs, 1026 vs, 989 m, 847 s, 779 w, 721 w, 697 w; δ_H(400 MHz) 0.85 (3H, t, *J* 6.8, CH_2CH_3), 1.20–1.29 (23H, stack, alkyl chain), 1.30 (3H, s, $C(CH_3)_A(CH_3)_B$), 1.38–1.43 (18H, stack, $C(CH_3)_A(CH_3)_B$, $C(CH_3)_C(CH_3)_D$,), 1.48–1.57 (3H, stack, alkyl chain), 2.54 (1H, br s, O*H*), 3.56–3.78 (6H, stack, H-1_A, H-1_B, H-$1'_A$, H-$1'_B$, H-$4'_A$, H-$4'_B$), 3.79–3.89 (1H, m, H-2), 3.90–4.02 (3H, stack, H-3,H-2′, H-3′), 4.06–4.11 (1H, m, H-4), 4.79 (1H, d, *J* 9.7, N-H); δ_C(100 MHz) 14.1 (CH_3, CH_2CH_3), 22.7 (CH_2, alkyl chain), 25.7 (CH_3, $C(CH_3)_A(CH_3)_B$), 26.6 (CH_2, alkyl chain), [27.0, 28.0 (CH_3, $C(CH_3)_A(CH_3)_B$, $C(CH_3)_C(CH_3)_D$, resonance overlap)], 28.3 (CH_3, $C(CH_3)_3$), [28.7, 29.3, 29.5, 29.6, 31.9 (CH_2, alkyl chain, resonance overlap)], 49.4 (CH, C-2), 62.3 (CH_2, C-4′), 71.3 (CH_2, C-1), 71.8 (CH_2, C-1′), [76.4, 76.6, (CH, C-3 or C-2′ or C-3′)], 77.9 (CH, C-4), 79.0 (CH, C-3 or C-2′ or C-3′), 79.6 (C, $C(CH_3)_3$), 107.9 (C, $C(CH_3)_2$ phyto), 109.2 (C, $C(CH_3)_2$ thr), 155.1 (C, C=O); *m/z* (TOF ES+) 624.4 ($[M + Na]^+$, 100%); HRMS *m/z* (TOF ES+) 624.4453 $[M + Na]^+$, $C_{33}H_{63}NO_8Na$ requires 624.4451.

(2*S*, 3*S*, 4*R*, 2′*S*, 3′*S*)-2-Hexacosanoylamino-1-*O*-(2′, 3′, 4′-trihydroxybutyl)-1, 3, 4-octadecanetriol (14)

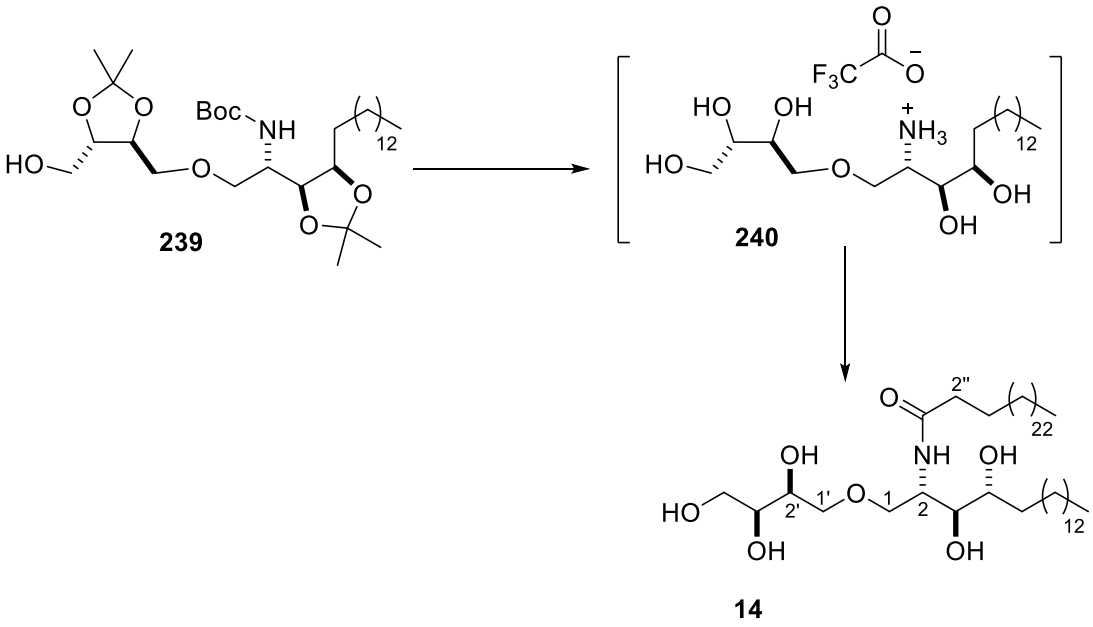

TFA (2 mL) was added to alcohol **239** (30 mg, 0.050 mmol). After stirring for 1 h, the TFA was removed by bubbling argon through the mixture. Residual TFA was removed under reduced pressure. This procedure was repeated if necessary until all of the protecting groups had been removed as evidenced by TLC. The crude aminopolyol was isolated presumably as its TFA salt and used without further purification in the next step: NHS ester **189** (30 mg, 0.06 mmol) and Et_3N (20 μL, 1.0 mmol) were added to a solution of aminopolyol **240** in dry THF (2 mL). After 12 h, the solvent was removed under reduced pressure. The residue was purified by column chromatography (gradient: $CHCl_3$ → 10% MeOH in $CHCl_3$) to yield ThrCer **14** as a white solid (24 mg, 62%): R_f = 0.3 (8% MeOH in $CHCl_3$); m.p. 106–111 °C, lit.[111] 107–109 °C; solubility issues prevented an optical rotation measurement; ν_{max}(film)/cm^{-1} 3393 br s (O–H, N–H), 2917 vs, 2849 vs, 1741 m, 1632 s (C=O), 1568 m, 1463 s, 1364 m, 1258 m, 1022 s, 968 w, 720 m; δ_H(400 MHz, 2:1 $CDCl_3$:CD_3OD) 0.84 (6H, t, *J* 6.7, 2 × CH_2CH_3), 1.20–1.30 (68H, stack, alkyl chain), 1.47–1.65 (4H, stack, alkyl chain), 2.17 (2H, app. t, *J* 7.6, H-2″), 3.48–3.65 (8H, stack, C*H*-OH), 3.70 (1H, dd, *J* 9.8, 4.5, H-1$_B$), 3.73– 3.77 (1H, m), 4.16 (1H, dd, *J* 9.0, 4.3, H-2) exchangeable protons not observed; δ_C(100 MHz, 2:1 $CDCl_3$:CD_3OD) 14.3

(CH_3, CH_2CH_3), [23.0, 26.3, 29.7, 29.9, 30.06, 30.09, 30.2, 32.3, 33.0 (CH_2, alkyl chain, resonance overlap)], 36.8 (CH_2, C-2″), 50.4 (CH, C-2), 63.8 (CH_2, C-4′), 70.7 (CH), 71.0 (CH_2, C-1), 72.5 (CH), 72.9 (CH), 73.4 (CH_2, C-1′), 75.2 (CH), 175.0 (C, *C*=O); *m/z* (TOF ES+) 822.7 ([M + Na]$^+$, 50%), 480.4 (100); HRMS *m/z* (TOF ES+) 822.7159 [M + Na]$^+$, $C_{48}H_{97}NO_7Na$ requires 822.7163.

Data were in agreement with those reported in the literature.[111]

(2*S*, 3*S*)-4-*O*-Benzyl-2,3-*O*-isopropylidene-1-*O*-tosyl-1,2,3,4-butanetetraol (244)

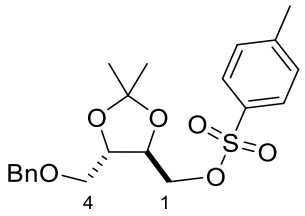

Et_3N (1.11 mL, 7.93 mmol) and DMAP (20 mg, 0.16 mmol) were added to a solution of benzyl ether **235** (1.00 g, 3.96 mmol) in CH_2Cl_2 (20 mL). The reaction mixture was cooled to 0 °C and a solution of TsCl (0.76 g, 4.00 mmol) in CH_2Cl_2 (10 mL) was added. The reaction mixture was warmed to rt. After 6 h, the reaction was quenched by adding H_2O (30 mL). Additional CH_2Cl_2 (20 mL) was added and the phases were separated. The combined organic phases were washed with brine (1 × 30 mL), dried over anhydrous Na_2SO_4, filtered and concentrated under reduced pressure. The residue was purified by flash column chromatography (10%EtOAc in hexanes) to provide tosylate **244** as a colourless oil (1.44 g, 89%): R_f = 0.5 (10% EtOAc in hexanes); $[\alpha]_D^{21}$ = –13.6 (c = 1.0, $CHCl_3$), [lit.[189] $[\alpha]_D^{26}$ = –9.3 (c = 2.5, $CHCl_3$); ν_{max}(film)/cm^{-1} 2987 w, 2869 w, 1598 w, 1496 w, 1454 m, 1362 s, 1307 w, 1292 w, 1248 m, 1213 m, 1189 s, 1175 vs, 1093 vs, 1028 m, 1019 m, 977 s, 907 m, 886 m, 848 m, 813 s, 785 s, 739 s, 698 s, 676 m, 663 s; δ_H(400 MHz) 1.34 (3H, s, C(C*H*$_3$)$_A$(CH$_3$)$_B$), 1.37 (3H, s, C(CH$_3$)$_A$(C*H*$_3$)$_B$), 2.43 (3H, s, Ar C*H*$_3$), 3.53 (1H, dd, *J* 10.1, 4.9, H-1$_A$), 3.61 (1H, dd, *J* 10.1, 4.8, H-1$_B$), 3.96–4.11 (3H, stack, H-2, H-3, H-4$_A$), 4.21 (1H, dd, *J* 10.3, 3.3, H-4$_B$), 4.54 (2H, s, PhC*H*$_2$), 7.27–7.38

(7H, stack, Ar C*H*), 7.75–7.79 (2H, m, Ar C*H*); δ_C(100 MHz) 21.7 (CH_3, Ar *C*H_3), 69.3 (CH_2, C-4), 70.1 (CH_2, C-1), 73.6 (CH_2, Ph*C*H_2), [76.27, 76.29 (CH, C-2, C-3)], 110.2 (C, *C*$(CH_3)_2$), [127.7, 127.8, 128.0, 128.5, 129.9 (CH, Ar CH)], [132.8, 137.7, 144.96 (C, Ar C)]; *m/z* (TOF ES+) 429.1 ([M + Na]$^+$, 100%).

Data were in agreement with those reported in the literature.[190]

(2*S*, 3*S*)-4-Azido-1-*O*-benzyl-2,3-*O*-isopropylidene-1,2,3-butanetriol (245)

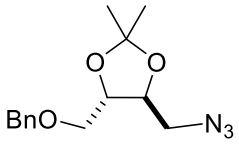

NaN_3 (160 mg, 2.46 mmol) was added to a solution of tosylate **244** (500 mg, 1.23 mmol) in DMF (15 mL). The solution was stirred for 6 h at 100 °C after which time, it was cooled to rt and H_2O (60 mL) was added. The phases were separated and the aqueous layer was extracted with EtOAc (5 × 50 mL). The combined organic layers were washed with brine (1 × 200 mL), dried with Na_2SO_4, filtered, and the filtrate evaporated under reduced pressure. The crude mixture was purified by column chromatography (10% EtOAc in hexanes) to yield azide **245** as a yellow oil (242 mg, 71%): R_f = 0.7 (25% EtOAc in hexanes); $[\alpha]_D^{24}$ = –56.8 (c = 1.0, $CHCl_3$); ν_{max}(film)/cm^{-1} 2933 w, 2863 w, 2099 vs (N_3), 1454 m, 1371 s, 1246 s, 1216 s, 1167 s, 1087 vs, 1028 m, 990 m, 901 m, 845 s, 804 w, 737 s, 698 s; δ_H(400 MHz) 1.43 (3H, s, C(C*H*$_3$)$_A$(CH_3)$_B$), 1.47 (3H, s, C(CH_3)$_A$(C*H*$_3$)$_B$), 3.30 (1H, dd, *J* 13.3, 5.0, H-4$_A$), 3.53–3.59 (2H, stack, H-1$_A$, H-4$_B$), 3.66 (1H, dd, *J* 10.0, 4.8, H-1$_B$), 4.00–4.10 (2H, stack, H-2, H-3), 4.57 (2H, s, PhC*H*$_2$), 7.27–7.38 (5H, stack, Ar C*H*); δ_C(100 MHz) 26.9 [CH_3, C(*C*H_3)$_A$(CH_3)$_B$], 27.0 [CH_3, C(CH_3)$_A$(*C*H_3)$_B$], 52.1 (CH_2, C-4), 70.2 (CH_2, C-1), 73.7 (CH_2, Ph*C*H_2), [76.6, 78.0 (CH, C-2, C-3)], 110.0 (C, *C*$(CH_3)_2$), [127.7, 127.8, 128.5, (CH, Ar CH)], 137.7 (C, Ar C); *m/z* (TOF ES+) 300.1 ([M + Na]$^+$, 100%); HRMS *m/z* (TOF ES+) 300.1320 [M + Na]$^+$, $C_{14}H_{19}N_3O_3Na$ requires 300.1324.

(2*S*, 3*S*)- 4-Amino-1-*O*-benzyl-2,3-*O*-isopropylidene-1,2,3-butanetriol (246)

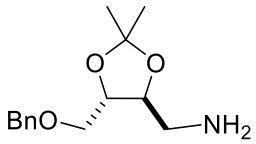

A flask containing a solution of azide **245** (100 mg, 0.360 mmol) in MeOH (10 mL) was purged with H_2 gas for 10 min. Pd/C (2 mg, 0.05 equiv.) was then added and the mixture was stirred under a flow of H_2. After 1.5 h, the mixture was filtered through Celite, washing sequentially with MeOH (40 mL) and $CHCl_3$ (40 mL). The filtrate was concentrated under reduced pressure and the residue was purified by column chromatography (30% EtOAc in hexanes) to afford amine **246** as a colourless oil (61 mg, 67%): R_f = 0.2 (10% MeOH in $CHCl_3$); solubility issues prevented an optical rotation measurement; ν_{max}(film)/cm^{-1} 3366 br vs (N–H), 1639 s, 1496 m, 1455m, 1373m, 1215 m, 1165m, 1091 m; δ_H(400 MHz) 1.40 (3H, s, C(C*H*$_3$)$_A$(CH$_3$)$_B$), 1.41 (3H, s, C(CH$_3$)$_A$(C*H*$_3$)$_B$), 2.82 (1H, dd, *J* 13.2, 6.3, H-4$_A$), 2.93 (1H, dd, *J* 13.2, 3.0, H-4$_B$), 3.55 (1H, dd, *J* 10.1, 4.9, H-1$_A$), 3.63 (1H, dd, *J* 10.1, 5.3, H-1$_B$), 3.85 (1H, ddd, *J* 8.1, 6.3, 3.0, H-3), 3.95 (1H, app. dt, *J* 8.1, 5.1, H-2), 4.56 (1H, A of AB, *J* 12.2, PhC*H*$_A$H$_B$), 4.59 (1H, B of AB, *J* 12.2, PhCH$_A$*H*$_B$), 7.26–7.37 (5H, stack, Ar C*H*); δ_C(100 MHz) 27.0 [CH$_3$, C(*C*H$_3$)$_A$(CH$_3$)$_B$], 27.2 [CH$_3$, C(CH$_3$)$_A$(*C*H$_3$)$_B$], 44.1 (CH$_2$, C-4), 70.8 (CH$_2$, C-1), 73.6 (CH$_2$, Ph*C*H$_2$), 77.3 (CH, C-2), 80.5 (CH, C-3), 109.2 (C, *C*(CH$_3$)$_2$), [127.70, 127.74, 128.4, (CH, Ar CH)], 137.7 (C, Ar C); *m/z* (TOF ES+) 252.2 ([M + H]$^+$, 100%).

Data were in agreement with those reported in the literature.[191]

(2*S*, 3*S*, 4*R*, 2′*S*, 3′*S*)-1-*N*-[4′-*O*-Benzyl-2′,3′-*O*-isopropylidene-2′, 3′, 4′-trihydroxybutanyl]-3, 4-*O*-isopropylidene-2-[*ortho*-nitrobenzenesulfonamido]-1-aminooctadecane-3, 4-diol (249)

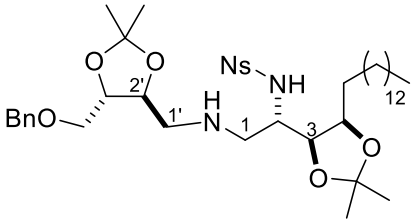

A solution of amine **246** (30 mg, 0.119 mmol) and aziridine **192** (63 mg, 0.120) in CH_3CN (2 mL) were heated under reflux in a sealed vial for 3 h. The solvent was then evaporated under reduced pressure and the crude product purified by column chromatography (20% EtOAc in hexanes) to yield amine **249** as a yellow oil (61 mg, 65%): R_f = 0.2 (EtOAc in hexanes); $[\alpha]_D^{20}$ = +49.6 (c = 1.0, $CHCl_3$); ν_{max}(film)/cm^{-1} 3317 br w (N–H), 2986 m, 2924 s, 2854 s, 1542 s, 1455 m, 1411 m, 1367 s, 1245 m, 1216 s, 1168 s, 1070 s, 853 m, 783 m, 737 s, 698 s, 668 m, 655 m; δ_H(400 MHz) 0.88 (3H, t, *J* 6.8, CH_2CH_3), 1.22–1.30 (23H, stack, alkyl chain), 1.28 (3H, s, $C(CH_3)_A(CH_3)_B$), 1.37 (6H, s, $C(CH_3)_C(CH_3)_D$), 1.38 (3H, s, $C(CH_3)_A(CH_3)_B$), 1.46–1.57 (2H, stack, alkyl chain), 1.58–1.67 (1H, m, alkyl chain), 2.27–2.39 (2H, stack, H-1_A, H-$1'_A$), 2.67 (1H, dd, *J* 12.3, 3.8, H-$1'_B$), 2.91 (1H, dd, *J* 12.8, 3.6, H-1_B), 3.51 (1H, dd, *J* 10.2, 4.8, H-$4'_A$), 3.58 (1H, dd, *J* 10.2, 5.1, H-$4'_B$), 3.65 (1H, app. dt, *J* 6.9, 3.5, H-2), 3.77–3.84 (1H, m, H-3), 3.99–4.05 (2H, stack, H-2′, H-3′), 4.10–4.16 (1H, m, H-4), 4.56–4.59 (2H, stack, $PhCH_2$), 7.28–7.39 (5H, stack, Ar CH), 7.57–7.77 (3H, stack, Ar CH), 8.10–8.14 (1H, m, Ar CH) NHs not observed; δ_C(100 MHz) 14.1 (CH_3, CH_2CH_3), 22.7 (CH_2), 25.4 [CH_3, $C(CH_3)_A(CH_3)_B$], 26.5 (CH_2), 27.0 [CH_3, $C(CH_3)_C(CH_3)_D$], 27.1 [CH_3, $C(CH_3)_C(CH_3)_D$], 27.7 [CH_3, $C(CH_3)_A(CH_3)_B$], [29.4, 29.5, 29.6, 29.7, 31.9 (CH_2, alkyl chain, resonance overlap)], 49.6 (CH_2, C-1), 51.3 (CH_2, C-1′), 53.8 (CH, C-2), 70.5 (CH_2, C-4′), 73.6 (CH_2, $PhCH_2$), [77.2, 77.6, 77.7, 77.9 (CH, C-3, C-4, C-2′, C-3′)], 107.9 (C, $C(CH_3)_2$ phyto), 109.0 (C, $C(CH_3)_2$ thr), [125.4, 127.8, 128.5, 130.4, 132.9, 133.4 (CH, Ar CH, resonance overlap)], [135.5, 138.0, 147.7 (C, Ar C)]; *m/z*

(TOF ES+) 776.5 ([M + H]$^+$, 100%); HRMS *m/z* (TOF ES+) 776.4521 [M + H]$^+$, $C_{41}H_{66}N_3O_9S$ requires 776.4520.

(2*S*, 3*S*, 4*R*, 2′*S*, 3′*S*)-2-Amino-1-*N*-[4′-*O*-benzyl-2′, 3′-*O*-isopropylidene-2′, 3′, 4′-trihydroxybutyl]-3, 4-*O*-isopropylidene-1-aminooctadecane-3, 4-diol (250)

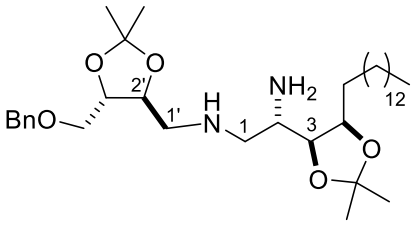

Thiophenol (15 μL, 0.14 mmol) and Cs_2CO_3 (34 mg, 0.105 mmol) were added to a solution of nosyl amide **192** (27 mg, 0.035 mmol) in CH_3CN (2 mL). After stirring at room temperature for 24 h, $NaHCO_3$ solution (20 mL) was added. The phases were separated and the aqueous phase was extracted with CH_2Cl_2 (3 × 20 mL). The combined organic extracts were dried with Na_2SO_4, filtered and the solvent was evaporated under reduced pressure. The residue was purified by column chromatography (30% EtOAc in hexanes) to give amine **250** as a colourless oil (18 mg, 86%): R_f = 0.2 (10% MeOH in $CHCl_3$); $[\alpha]_D^{21}$ = +3.6 (c = 0.6, $CHCl_3$); ν_{max}(film)/cm^{-1} 3305 vw br (N–H), 2985 w, 2923 s, 2853 s, 1590 w, 1454 m, 1378 s, 1368 s, 1242 m, 1215 s, 1166 s, 1073 s, 1028 m, 870 m, 847 m, 798 m, 753 vs, 696 s, 665 m; δ_H(400 MHz) 0.88 (3H, t, *J* 6.8, CH_2CH_3), 1.22–1.30 (23H, stack, alkyl chain), 1.31 (3H, s, $C(CH_3)_A(CH_3)_B$), 1.40 (6H, s, $C(CH_3)_A(CH_3)_B$, $C(CH_3)_C(CH_3)_D$, resonance overlap), 1.41 (3H, s $C(CH_3)_C(CH_3)_D$), 1.46–1.55 (3H, stack, alkyl chain), 2.55 (1H, app. td, *J* 8.9, 3.1, H-1$_A$), 2.78–2.85 (2H, stack, H-1′$_A$, H-1′$_B$), 2.88–2.95 (2H, stack, H-1$_B$, H-2), 3.57 (1H, dd, *J* 10.2, 4.2, H-4′$_A$), 3.63 (1H, dd, *J* 10.2, 4.9, H-4′$_B$), 3.75–3.81 (1H, m, H-3), 3.96–4.03 (2H, stack, H-2′, H-3′), 4.10–4.16 (1H, m, H-4), 4.56 (1H, A of AB, *J* 12.2, $PhCH_AH_B$), 4.60 (1H, B of AB, *J* 12.2, $PhCH_AH_B$), 7.27–7.35 (5H, stack, Ar CH); δ_C(100 MHz) 14.1 (CH_3, CH_2CH_3), 22.7 (CH_2, alkyl chain), 25.9 (CH_3, $C(CH_3)_A(CH_3)_B$), 26.2 (CH_2, alkyl chain), [27.0, 27.2, 28.3 (CH_3, $C(CH_3)_A(CH_3)_B$, $C(CH_3)_C(CH_3)_D$)], [29.4, 29.6, 29.7, 31.9 (CH_2, alkyl chain, resonance overlap)], 49.9 (CH, C-

2), 52.0 (CH_2, C-1 or C-1′), 54.1 (CH_2, C-1′ or C-1), 70.7 (CH_2, C-4′), 73.6 (CH_2, Ph*C*H_2), [77.9, 78.0, 78.2, 80.7 (CH, C-3, C-4, C-2′, C-3′)], 107.9 (C, *C*$(CH_3)_2$ phyto), 109.3 (C, *C*$(CH_3)_2$ thr), [127.7, 128.4 (CH, Ar CH, resonance overlap)], 137.9 (C, Ar C); *m/z* (TOF ES+) 591.5 ([M + H]$^+$, 100%); HRMS *m/z* (TOF ES+) 591.4735 [M + H]$^+$, $C_{35}H_{63}N_2O_5$ requires 591.4737.

(2*R*, 3*S*)-4-*O*-Benzyl-2,3-*O*-isopropylidene-2,3,4-trihydroxybutyl ethanethioate (253)

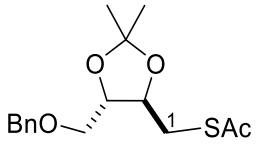

A suspension of Cs_2CO_3 (320 mg, 0.984 mmol) and thioacetic acid (144 μL, 1.97 mmol) in DMF (5 mL) was stirred in absence of light until all of the Cs_2CO_3 had dissolved. A solution of tosylate **244** (200 mg, 0.492 mmol) in DMF (1 mL) was then added. After 20 h, the reaction mixture was diluted with H_2O (20 mL) and extracted with EtOAc (5 × 20 mL). The combined organic extracts were washed with brine (75 mL), dried over Na_2SO_4, filtered and the filtrate concentrated under reduced pressure. The crude product was purified by column chromatography to yield thioester **253** as a colourless oil (148 mg, 97%): R_f = 0.6 (20% EtOac in hexanes); $[\alpha]_D^{21}$ = +31.6 (c = 1.0, $CHCl_3$); ν_{max}(film)/cm^{-1} 1691 vs (C=O), 1496 w, 1454 m, 1379 m, 1369 m, 1238 m, 1213 m, 1164 m, 1132 s, 1093 vs, 1023 m, 954 m, 912 m, 871 m, 828 m, 737 vs, 698 vs; δ_H(400 MHz) 1.40 (3H, s, C(C*H*$_3$)$_A$(CH_3)$_B$), 1.43 (3H, s, C(CH_3)$_A$(C*H*$_3$)$_B$), 2.33 (3H, s, C(O)C*H*$_3$), 3.06 (1H, dd, *J* 14.0, 6.3, H-1$_A$), 3.26 (1H, dd, *J* 14.0, 4.3, H-1$_B$), 3.58–3.65 (2H, stack, H-4$_A$, H-4$_B$), 3.91 (1H, app. dt, *J* 8.0, 4.7, H-3), 4.00 (1H, ddd, *J* 8.0, 6.3, 4.3, H-2), 4.60 (2H, s, PhC*H*$_2$), 7.26–7.37 (5H, stack, Ar C*H*); δ_C(100 MHz) 26.98 (CH_3, C(*C*H$_3$)$_A$(CH_3)$_B$), 27.01 (CH_3, C(CH_3)$_A$(*C*H$_3$)$_B$), 30.4 (CH_3, C(O)*C*H$_3$), 31.3 (CH_2, C-1), 70.1 (CH_2, C-4), 73.5 (CH_2, Ph*C*H_2), 76.6 (CH, C-2), 79.1 (CH, C-3), 109.5 (C, *C*$(CH_3)_2$), [127.6, 128.3, (CH, Ar CH, resonance overlap)], 137.8 (C, Ar C), 195.0 (C, C=O); *m/z* (TOF ES+)

333.1 ([M + Na]$^+$, 100%); HRMS *m/z* (TOF ES+) 333.1139 [M + Na]$^+$, $C_{16}H_{22}O_4SNa$ requires 333.1136.

(2*S*, 3*S*, 4*R*, 2′*R*, 3′*S*)-1-*S*-[4′-*O*-Benzyl-2′, 3′-*O*-isopropylidene-2′,3′,4′-trihydroxybutyl]-3, 4-*O*-isopropylidene-1-mercapto-2-toluenesulfonamido-3, 4-octadecanediol (255)

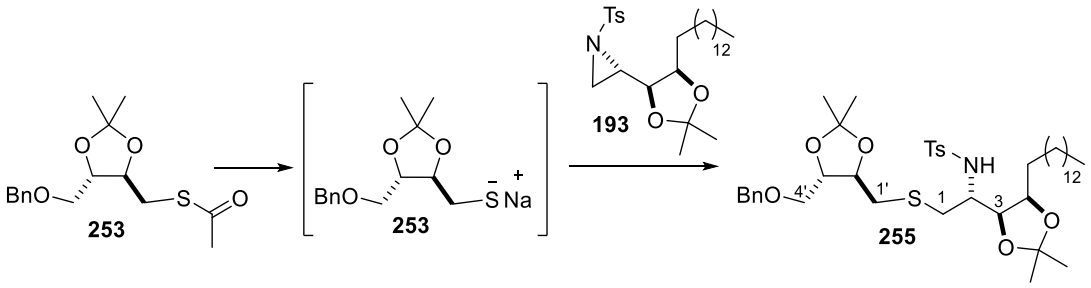

NaOMe (0.5 mL of a 1.0 M soln. in MeOH) was added to a solution of thioacetate **253** (75 mg, 0.24 mmol) and aziridine **193** (120 mg, 0.24 mmol) in THF (5 mL). After 6 h, the reaction mixture was neutralised by the addition of acidic ion-exchange resin [Dowex H CR-S, pre-washed sequentially with MeOH (100 mL) and $CHCl_3$ (50 mL)]. The solution was filtered through Celite and the solvent evaporated under reduced pressure. The crude mixture was purified by flash column chromatography to give thioether **255** as a colourless oil (125 mg, 68%): R_f = 0.4 (20% EtOAc I hexanes); $[\alpha]_D^{20}$ = +21.2 (c = 1.0, $CHCl_3$); ν_{max}(film)/cm^{-1} 3263 w br (N–H), 2985 m, 2923 s, 2854 m, 1598 w, 1496 w, 1454 m, 1379 m, 1369 m, 1335 m, 1242 m, 1216 m, 1159 vs, 1092 vs, 1061 s, 927 m, 864 m, 814 m, 736 m, 698 vs; δ_H(400 MHz) 0.88 (3H, t, *J* 6.8, CH_2CH_3), 1.21–1.28 (23H, stack, alkyl chain), 1.28 (3H, s, $C(CH_3)_A(CH_3)_B$), 1.36 (3H, s, $C(CH_3)_A(CH_3)_B$), 1.42 (6H, s, $C(CH_3)_C(CH_3)_D$), 1.45–1.50 (3H, stack, alkyl chain), 2.41 (3H, s, Ar CH_3), 2.51 (1H, dd, *J* 14.3, 3.4, H-1$_A$), 2.58 (1H, dd, *J* 14.2, 4.1, H-1′$_A$), 2.65 (1H, dd, *J* 14.2, 5.5, H-1′$_B$), 2.92 (1H, dd, *J* 14.3, 4.4, H-1$_B$), 3.52–3.68 (3H, stack, H-4′$_A$, H-4′$_B$, H-2), 3.87–3.97 (2H, stack, H-2′, H-3′), 4.03–4.15 (2H, stack, H-3,H-4), 4.56 (2H, app. s, $PhCH_2$), 5.65 (1H, d, *J* 9.5, N*H*), 7.26–7.37 (7H, stack, Ar CH), 7.73–7.77 (2H, m, Ar CH); δ_C(100 MHz) 14.1 (CH_3, CH_2CH_3), 21.6 (CH_3, Ar CH_3), 22.7 (CH_2, alkyl chain), 25.7 (CH_3, $C(CH_3)_A(CH_3)_B$), 26.4 (CH_2, alkyl chain), 27.1, (CH_3, $C(CH_3)_C(CH_3)_D$), 27.8 [CH_3, $C(CH_3)_A(CH_3)_B$], [29.2, 29.4,

29.5, 29.7, 31.9 (CH_2, alkyl chain, resonance overlap)], 31.9 (CH_2, C-1′), 36.2 (CH_2, C-1), 52.6 (CH, C-2), 70.1 (CH_2, C-4′), 73.6 (CH_2, Ph*C*H_2), [77.1, 77.6 (CH, C-3, C-4)], [78.4, 78.7 (CH, C-2′, C-3′)], 107.9 (C, *C*$(CH_3)_2$ phyto), 109.6 (C, *C*$(CH_3)_2$ thr), [127.2, 127.7, 127.8, 128.5, 129.7 (CH, Ar CH)], [137.8, 138.3, 143.6 (C, Ar C)]; *m/z* (TOF ES+) 784.4 ($[M + Na]^+$, 100%); HRMS *m/z* (TOF ES+) 784.4259 $[M + Na]^+$, $C_{42}H_{67}NO_7S_2Na$ requires 784.4257.

(2*S*, 3*S*, 4*R*, 2′*R*, 3′*S*)-1-*S*-[4′-*O*-Benzyl-2′, 3′-*O*-isopropylidene-2′,3′,4′-trihydroxybutyl]- 2-[(*N*-*tert*-butoxycarbonyl)amino]-3, 4-*O*-isopropylidene-1-mercapto-3, 4-octadecanediol (256)

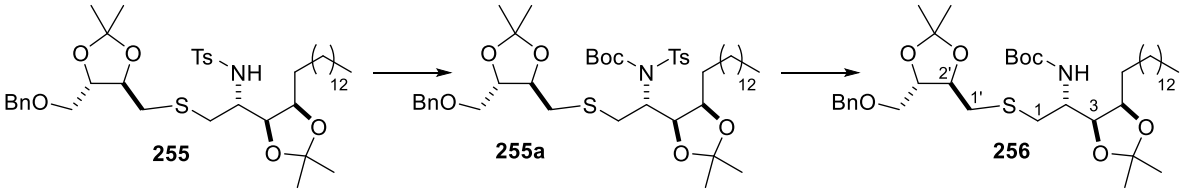

Boc_2O (0.236 mg, 0.18 mmol) and DMAP (10 mg, 10 weight %) were added to a solution of sulfonamide **255** (90 mg, 0.12 mmol) in CH_2Cl_2 (2 mL). The solution was stirred for 4 h and then the solvent was removed under reduced pressure to provide the crude product **255a**, which was used directly in the next reaction without further purification: anhydrous MeOH (2 mL) was added to the flask containing the intermediate carbamate **255a**. Mg powder (17 mg, 0.71 mmol) was added and the reaction mixture was sonicated in an ultrasound bath. After 30 min, the mixture was poured into hydrochloric acid (10 mL, 1.0 M) and extracted with Et_2O (3 × 20 mL). The combined organic phases were washed sequentially with $NaHCO_3$ solution (20 mL) and brine (20 mL), dried with Na_2SO_4 and filtered. The solvent was removed under pressure and the residue purified by flash column chromatography (20% EtOAc in hexanes) to give Boc amide **256** as a colourless oil (58 mg, 70% from **255**): R_f = 0.6 (20% EtOAc in hexanes); $[\alpha]_D^{21}$ = +10.0 (c = 1.0, $CHCl_3$); ν_{max}(film)/cm^{-1} 3342 br w (N–H), 2982 m, 2923 s, 2853 s, 1715 s (C=O), 1497 m, 1454 m, 1378 m, 1366 s, 1298 m, 1243 s, 1216 s, 1164 vs, 1090 s, 1073 s, 1041 s, 1018 s, 869 s, 800 m, 750 s, 735 s, 697 s, 665 m; δ_H(400 MHz) 0.88

(3H, t, *J* 6.8, CH_2CH_3), 1.23–1.29 (23H, stack, alkyl chain), 1.31 (3H, s, $C(CH_3)_A(CH_3)_B$), 1.40 (3H, s, $C(CH_3)_A(CH_3)_B$), 1.41 (3H, s, $C(CH_3)_C(CH_3)_D$), 1.43 (12H, s, $C(CH_3)_C(CH_3)_D$, $C(CH_3)_3$, resonance overlap), 1.49–1.56 (3H, stack, alkyl chain), 2.77–2.85 (3H, stack, H-1_A, H-$1'_A$, H-$1'_B$), 2.93 (1H, dd, *J* 13.9, 3.4, H-1_B), 3.60–3.65 (2H, stack, H-4′), 3.85–3.93 (1H, m, H-2), 3.95–4.05 (3H, stack, H-3, H-2′, H-3′), 4.07–4.13 (1H, m, H-4), 4.58 (2H, app. s, $PhCH_2$), 4.88 (1H, d, *J* 9.5, N*H*), 7.25–7.37 (5H, stack, Ar CH); δ_C(100 MHz) 14.1 (CH_3, CH_2CH_3), 22.7 (CH_2, alkyl chain), 25.7 [CH_3, $C(CH_3)_A(CH_3)_B$], 26.6 (CH_2, alkyl chain), 27.1 [CH_3, $C(CH_3)_C(CH_3)_D$], 27.2 [CH_3, $C(CH_3)_C(CH_3)_D$], 27.9 [CH_3, $C(CH_3)_A(CH_3)_B$], 28.4 [CH_3, $C(CH_3)_3$], [29.1, 29.4, 29.6, 29.7, 31.9 (CH_2, alkyl chain, resonance overlap)], 35.6 (CH_2, C-1′), 36.3 (CH_2, C-1), 49.5 (CH, C-2), 70.5 (CH_2, C-4′), 73.6 (CH_2, $PhCH_2$), [77.8, 77.9, 78.5, 79.3 (CH, C-3, C-4, C-2′, C-3′)], 79.6 (C, $C(CH_3)_3$), 108.0 (C, $C(CH_3)_2$ phyto), 109.5 (C, $C(CH_3)_2$ thr), [127.1, 128.4, (CH, Ar CH, resonance overlap)], 137.9 (C, Ar C), 155.1 (C, C=O); *m/z* (TOF ES+) 730.5 ($[M + Na]^+$, 100%); HRMS *m/z* (TOF ES+) 730.4691 $[M + Na]^+$, $C_{40}H_{69}NO_7SNa$ requires 730.4692.

(2*S*, 3*S*, 4*R*, 2′*R*, 3′*S*)-1-*S*-[4′-*O*-Benzyl-2′,3′,4′-trihydroxybutyl]-2-(hexacosanoyl)amino-1-mercapto-3, 4-octadecanediol (258)

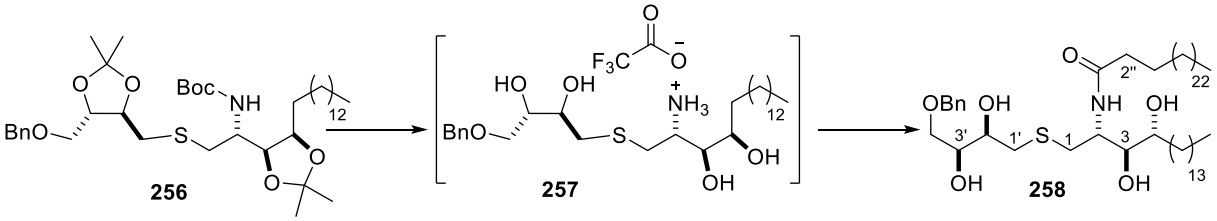

TFA (2 mL) was added to Boc amide **256** (52 mg, 0.073 mmol). After 1 h, the TFA was removed by bubbling argon through the mixture. Residual TFA was removed under reduced pressure. The crude aminopolyol **257** was isolated presumably as its TFA salt and used without further purification in the next step: NHS ester **189** (54 mg, 0.15 mmol) and Et_3N (30 μL, 0.22 mmol) were added to a solution of aminopolyol **257** (assuming 100% conversion in the first step) in dry THF (2 mL). After 12 h, the solvent was removed under reduced pressure. The crude mixture was purified by column chromatography (gradient: $CHCl_3$ → 5% MeOH in

$CHCl_3$) to yield amide **258** as a white solid (31 mg, 47% over two steps): R_f = 0.5 (10% MeOH in $CHCl_3$); solubility issues prevented an optical rotation measurement; ν_{max}(film)/cm^{-1} 3301 br m (O–H, N–H), 2917 vs, 2849 vs, 1639 m (C=O), 1531 m, 1467 m, 1454 m, 1366 w, 1250 w, 1172 w, 1055 m, 1028 m, 906 w, 719 s, 696 s; δ_H(400 MHz, 2:1 $CDCl_3$:CD_3OD) 0.84 (6H, t, *J* 6.8, 2 × CH_2CH_3), 1.17–1.34 (68H, stack, alkyl chain), 1.46–1.69 (4H, stack, alkyl chain), 2.17 (2H, app. td, *J* 7.3, 2.4, H-2″) 2.61–2.73 (3H, stack, H-1$_A$, H-1′$_A$, H-1′$_B$), 2.90 (1H, dd *J* 13.9, 3.7, H-1$_B$), 3.38–3.48 (2H, stack, H-3, H-4), 3.54 (1H, dd, *J* 9.9, 6.1, H-4′$_A$), 3.58 (1H, dd, *J* 9.9, 4.9, H-4′$_B$), 3.72 (1H, ddd, *J* 8.8, 5.6, 3.2, H-2′), 3.78 (1H, ddd, *J* 6.1, 4.9, 3.2, H-3′), 4.20 (1H, app. dt, *J* 9.3, 3.4, H-2), 4.51 (1H, A of AB, *J* 11.9, PhCH_ACH$_B$), 4.54 (1H, B of AB, *J* 11.9, PhCH$_A$CH_B), 7.22–7.32 (5H, stack, Ar C*H*), exchangeable protons not observed; δ_C(100 MHz, 2:1 $CDCl_3$:CD_3OD) 14.3 (CH_3, CH_2CH_3), [23.0, 26.1, 26.2, 29.67, 29.74, 29.9, 30.0, 32.2, 33.0 (CH_2, alkyl chain, resonance overlap)], 33.4 (CH_2, C-1), 33.5 (CH_2, alkyl chain), 36.0 (CH_2, C-1′), 36.9 (CH_2, C-2″), 51.1 (CH, C-2), [71.4, 71.5 (CH, C-2′, C-3′), 72.2 (CH_2, C-4′), 72.4 (CH, C-3), 73.8 (CH_2, PhCH_2), 76.4 (CH, C-4), [128.1, 128.2, 128.7, (CH, Ar CH)], 175.3 (C, C=O), Ar C not observed; *m/z* (TOF ES+) 928.75 ([M + Na]$^+$, 90%), 929.74 (100); HRMS *m/z* (TOF ES+) 928.7405 [M + Na]$^+$, $C_{55}H_{103}NO_6SNa$ requires 928.7404.

(2*R*, 3*S*)-4-*O*-Benzyl-1-iodo-2, 3-*O*-isopropylidene-2, 3, 4-butanetriol (265)

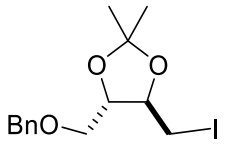

Imidazole (227 mg, 3.33 mmol), Ph_3P (457 mg, 1.74 mmol) and a solution of I_2 (442 mg, 1.74 mmol) in THF (1 mL) were added sequentially to a solution of alcohol **235** (400 mg, 1.59 mmol) in dry THF (10 mL) at 0 °C. After 2 h, the reaction mixture was quenched with H_2O (20 mL) and extracted with Et_2O (3 × 20 mL). The combined organic layers were washed with brine (1 × 40 mL), dried over anhydrous Na_2SO_4, filtered and concentrated under reduced pressure.

The residue was purified by column chromatography (10% Et_2O in hexanes) to afford iodide **265** as a colourless oil (564 mg, 96%): R_f = 0.8 (25% EtOAc in hexanes); $[\alpha]_D^{24}$ = –4.0 (c = 1.0, $CHCl_3$), lit.[192] $[\alpha]_D^{26}$ = –8.6 (c = 2.5, $CHCl_3$); ν_{max}(film)/cm^{-1} 3029 w, 2986 w, 2933 w, 2863 w, 1496 w, 1453 m, 1379 s, 1370 s, 1321 w, 1236 s, 1210 s, 1170 s, 1090 vs, 1072 vs, 1028 s, 1007 s, 908 m, 885 m, 860 s, 818 m, 779 w, 735 vs, 697 vs; δ_H(400 MHz) 1.42 (3H, s, C(CH_3)$_A$(CH_3)$_B$), 1.47 (3H, s, C(CH_3)$_A$(CH_3)$_B$), 3.28 (1H, dd, *J* 10.6, 5.3, H-1$_A$), 3.35 (1H, dd, *J* 10.6, 5.1, H-1$_B$), 3.61–3.69 (2H, stack, H-4), 3.87 (1H, app. dt, *J* 7.4, 5.2, H-2), 3.97 (1H, app. dt, *J* 7.4, 5.1, H-3), 4.59 (2H, app. s, PhCH_2), 7.27–7.39 (5H, stack, Ar C*H*); δ_C(100 MHz) 6.4 (CH_2, C-1), [27.3, 27.4 (CH_3, C(CH_3)$_A$(CH_3)$_B$], 70.5 (CH_2, C-4), 73.6 (CH_2, Ph*C*H_2), 77.7 (CH, C-2), 80.1 (CH, C-3), 109.8 (C, *C*(CH_3)$_2$), [127.7, 127.8, 128.5, (CH, Ar CH)], 137.8 (C, Ar C); *m/z* (TOF ES+) 385.0 ([M + Na]$^+$, 100%); HRMS *m/z* (TOF ES+) 385.0273 [M + Na]$^+$, $C_{14}H_{19}IO_3Na$ requires 385.0277.

Data were in agreement with those reported in the literature.[192]

(2*S*, 3*S*)-1-*O*-Benzyl-2, 3-*O*-isopropylidene-4-[2′-trimethylsilyl-1′,3′-dithian-2′-yl]-2, 3, 4-butanetriol (266) and (2*S*, 3*S*)-1-*O*-benzyl-2, 3-*O*-isopropylidene-4-(1′,3′-dithian-2′-yl)-2, 3, 4-butanetriol (267)

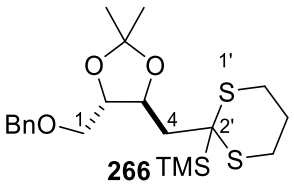

266

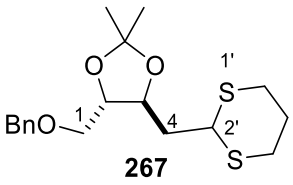

267

n-BuLi (1.0 mL, 2.5 M in THF, 2.48 mmol) was added to a solution of 2-trimethylsilyl-1, 3-dithiane (0.31 mL, 2.48 mmol) in THF (3 mL) and HMPA (0.3 mL) at –30 °C. The solution was stirred for 1 h at –30 °C before adding a solution of iodide **265** (225 mg, 0.621 mmol) in THF (3 mL) and HMPA (0.3 mL). The resulting mixture was warmed to rt. After 14 h, the solution was neutralised with NH_4Cl solution (40 mL) and extracted with Et_2O (3 × 50 mL). The

combined organic phases were washed with brine (50 mL), dried over Na_2SO_4, filtered and concentrated under reduced pressure. The residue was purified by column chromatography (20% EtOAc in hexanes) to yield, in order of elution, silyl dithiane **266** as a colourless oil (184 mg, 69%): R_f = 0.7 (20% Et_2O in hexane); $[\alpha]_D^{20}$ = –13.2 (c = 1.0, $CHCl_3$); ν_{max}(film)/cm^{-1} 2984 m, 2900 m, 1637 w, 1497 w, 1454 m, 1422 m, 1369 m, 1245 s, 1215 m, 1167 m, 1072 s, 1028 m, 987 m, 906 m, 876 s, 841 vs, 733 s, 715 s, 697 vs; δ_H(400 MHz) 0.21 (9H, s, Si(CH_3)$_3$), 1.35 (3H, s, C(CH_3)$_A$(CH$_3$)$_B$), 1.41 (3H, s, C(CH$_3$)$_A$(CH_3)$_B$), 1.73–1.80 (2H, stack, H-5′$_A$, H-5′$_B$), 2.14–2.21 (2H, stack, H-4′$_A$ or H-6′$_A$, H-4$_A$), 2.32–2.38 (1H, m, H-4′$_A$ or H-6′$_A$), 2.70–2.83 (2H, stack, H-4′$_B$ or H-6′$_B$, H-4$_B$), 2.86–2.96 (1H, m, H-4′$_B$ or H-6′$_B$), 3.59 (1H, dd, *J* 9.8, 5.8, H-1$_A$), 3.73 (1H, dd, *J* 9.8, 5.2, H-1$_B$), 3.87 (1H, app. dt, *J* 8.5, 5.5, H-2), 4.08 (1H, app. t, *J* 8.3, H-3), 4.55 (1H, d, *J* 11.8, A of AB, PhCH_AH$_B$), 4.62 (1H, d, *J*, 11.8, B of AB, PhCH$_A$$H_B$), 7.25–7.39 (5H, stack, Ar C*H*); δ_C(100 MHz) –2.9 [CH$_3$, Si(*C*H$_3$)$_3$], [22.5, 23.1 (CH$_2$, C-4′, C-6′)], 24.9 (CH$_2$, C-5′), 26.7 [CH$_3$, C(*C*H$_3$)$_A$(CH$_3$)$_B$], 27.2 [CH$_3$, C(CH$_3$)$_A$(*C*H$_3$)$_2$], 37.7 (C, C-2′), 40.1 (CH$_2$, C-4), 71.1 (CH$_2$, C-1), 73.7 (CH$_2$, Ph*C*H$_2$), 77.4 (CH, C-3), 79.3 (CH, C-2), 109.2 (C, *C*(CH$_3$)$_2$), [127.8, 127.9, 128.4 (CH, Ar *C*H)], 137.9 (C, Ar *C*); *m/z* (TOF ES+) 449.2 ([M + Na]$^+$, 100%); HRMS *m/z* (TOF ES+) 449.1619 [M + Na]$^+$, $C_{21}H_{34}O_3S_2SiNa$ requires 449.1616, followed by dithiane **267** as a colourless oil (56 mg, 25%): R_f = 0.5 (20% Et_2O in hexane); $[\alpha]_D^{20}$ = –7.6 (c = 1.0., $CHCl_3$); lit.[154] (R,R enantiomer) $[\alpha]_D^{25}$ = +14.5 (c = 0.97, $CHCl_3$); ν_{max}(film)/cm^{-1} 2985 m, 2932 m, 2900 m, 1496 w, 1453 m, 1422 m, 1369 s, 1242 s, 1213 s, 1162 m, 1091 vs, 1069 vs, 1028 s, 1012 s, 907 m, 895 m, 867 m, 844 s, 798 m, 741 vs, 697 vs, 667 m; δ_H(400 MHz) 1.40 (3H, s, C(CH_3)$_A$(CH$_3$)$_B$), 1.41 (3H, s, C(CH$_3$)$_A$(CH_3)$_B$), 1.80–1.92 (1H, m, H-5′$_A$), 1.98–2.02 (2H, stack, H-4), 2.05–2.13 (1H, m, H-5′$_B$), 2.76–2.89 (4H, stack, H-4′$_A$, H-4′$_B$, H-6′$_A$, H-6′), 3.53 (1H, dd, *J* 10.1, 4.8, H-1$_A$), 3.60 (1H, dd, *J* 10.1, 5.6, H-1$_B$), 3.86 (1H, app. dt, *J* 7.9, 5.2, H-2), 4.09–4.15 (1H, m, H-3), 4.19–4.23 (1H, m, H-2′), 4.55 (1H, d, *J* 12.2, A of AB, PhCH_AH$_B$), 4.61 (1H, d, *J* 12.2, B of AB, PhCH$_A$$H_B$), 7.25–7.37 (5H, stack, Ar C*H*); δ_C(100 MHz) 25.8 (CH$_2$, C-5′), 27.0 (CH$_3$, C(*C*H$_3$)$_A$(CH$_3$)$_B$), 27.2 (CH$_3$, C(CH$_3$)$_A$(*C*H$_3$)$_B$), [29.7, 30.1 (CH$_2$, C-4′, C-6′), 39.6 (CH$_2$, C-4), 43.7 (CH, C-2′), 70.4 (CH$_2$, C-1), 73.5 (CH$_2$, Ph*C*H$_2$), 75.2 (CH, C-3), 79.8 (CH, C-

4), 109.4 (C, *C*$(CH_3)_2$), [127.7, 128.4 (CH, Ar *C*H, resonance overlap)], 137.9 (C, Ar *C*); *m/z* (TOF ES+) 377.1 ([M + Na]$^+$, 100%); HRMS *m/z* (TOF ES+) 377.1222 [M + Na]$^+$, $C_{18}H_{26}O_3S_2Na$ requires 377.1221.

(2*S*, 3*S*)-1-*O*-Benzyl-2, 3-*O*-isopropylidene-4-(1′,3′-dithian-2′-yl)-2, 3, 4-butanetriol (267)

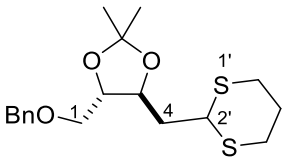

TBAF (0.3 mL, 1.0 M in THF, 0.3 mmol) was added to a solution of silyl dithiane **266** (182 mg, 0.138 mmol) in THF (2 mL). After 14 h, the reaction mixture was concentrated under reduced pressure. The residue was dissolved in EtOAc (30 mL). The resulting solution was washed sequentially with H_2O (3 × 20 mL) and brine (1 × 20 mL), then dried with Na_2SO_4, filtered and the filtrate was concentrated under reduced pressure. The residue was purified by column chromatography to yield dithiane **266** as a colourless oil (76 mg, quant.).

Data in agreement with those obtained for the same compound prepared from **265**.

(2*S*, 3*S*, 4*R*)-3, 4-*O*-Isopropylidene-2-toluenesulfonamido-1-[2′-trimethylsilyl-1′, 3′-dithian-2′-yl)]-1, 3, 4-octadecanetriol (269)

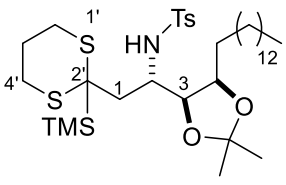

n-BuLi (0.33 mL, 2.5 M in hexanes, 0.81 mmol) was added to a solution of 2-trimethylsilyl-1,3-dithiane (156 mg, 0.81 mmol) in anhydrous THF (2.5 mL) at –23 °C. The solution was stirred for 1 h while maintaining the temperature at –23 °C. A solution of aziridine **193** (200 mg, 0.405

mmol) in THF (2.5 mL) was then added and the resulting mixture was warmed to rt. After stirring overnight, the solution was neutralised with NH_4Cl solution (40 mL) and the mixture extracted with Et_2O (3 × 50 mL). The combined organic phases were washed with brine (50 mL), dried over Na_2SO_4, filtered and concentrated under reduced pressure. The residue was purified by column chromatography (20% EtOAc in hexanes) to yield silyl dithiane **269** as a colourless oil (155 mg, 56%): R_f = 0.6 (20% EtOAc in hexanes); $[\alpha]_D^{21}$ = –16.8 (c = 1.0, $CHCl_3$); ν_{max}(film)/cm^{-1} 3304 br w (N–H), 2923 vs, 2854 s, 1599 w, 1452 m, 1379 m, 1339 m, 1248 s, 1216 m, 1155 vs, 1094 m, 1057 s, 954 w, 844 vs, 814 m, 758 w, 713 w, 663 m; δ_H(400 MHz) 0.21 (9H, s, Si(C*H*$_3$)$_3$), 0.88 (3H, t, *J* 6.8, CH_2CH_3), 1.22 (3H, s, C(C*H*$_3$)$_A$(CH$_3$)$_B$), 1.23–1.33 (23H, stack, alkyl chain, resonance overlap), 1.36 (3H, s, C(CH$_3$)$_A$(C*H*$_3$)$_B$), 1.37–1.46 (3H, stack, alkyl chain), 1.79–1.90 (1H, m, dithiane C*H*), 1.97–2.05 (1H, m, dithiane C*H*), 2.35–2.45 (4H, stack, H-1$_A$, Ar C*H*$_3$), 2.53– 2.60 (2H, stack, dithiane), 2.78 (1H, dd, *J* 15.8, 9.2, H-1$_B$), 3.01 (1H, ddd, *J* 14.0, 11.0, 2.8, dithiane C*H*), 3.10 (1H, ddd, *J* 14.0, 11.2, 2.9, dithiane C*H*), 3.44–3.50 (1H, m, H-4), 3.67–3.73 (1H, m, H-2), 4.41 (1H, app. t, *J* 6.3, H-3), 5.77 (1H, d, *J* 4.1, N*H*), 7.29 (2H, AA′ of AA′BB′, *J* 8.2, Ar C*H*), 7.78 (2H, BB′ of AA′BB′, *J* 8.2, Ar C*H*); δ_C(100 MHz) –2.5 [CH$_3$, Si(*C*H$_3$)$_3$], 14.1 (CH$_3$, CH$_2$*C*H$_3$), 21.5 (CH$_3$, Ar *C*H$_3$), 22.7 (CH$_2$, alkyl chain), [24.1, 24.87, 24.92 (CH$_2$, 3 × dithiane *C*H$_2$)], 25.2 [CH$_3$, C(*C*H$_3$)$_A$(CH$_3$)$_B$], 26.3 (CH$_2$, alkyl chain), 27.2 [CH$_3$, C(CH$_3$)$_A$(*C*H$_3$)$_B$], [29.4, 29.56, 29.62, 29.7, 31.9 (CH$_2$, alkyl chain, resonance overlap)], 36.3 (C, C-2′), 39.2 (CH$_2$, C-1), 54.7 (CH, C-2), 76.98 (CH, C-3), 77.2 (CH, C-4), 107.4 (C, *C*(CH$_3$)$_2$), [127.0, 129.5 (CH, Ar CH)], [139.4, 143.3 (C, Ar C)]; *m/z* (TOF ES+) 708.4 ([M + Na]$^+$, 100%); HRMS *m/z* (TOF ES+) 708.3585 [M + Na]$^+$, $C_{35}H_{63}NO_4S_3SiNa$ requires 708.3586.

(2*S*, 3*S*, 4*R*)-1-(1′,3′-Dithian-2′-yl)-3, 4-*O*-isopropylidene-2-toluenesulfonamido-3, 4-octadecanediol (270)

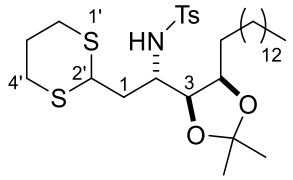

TBAF (1.0 mL, 1.0 M in THF, 1.0 mmol) was added to a solution of silyl dithiane **269** (155 mg, 0.226 mmol) in THF (3.5 mL). After 4 h, the reaction mixture was concentrated under reduced pressure. The residue was dissolved in EtOAc (30 mL) and washed sequentially with H_2O (3 × 20 mL) and brine (1 × 20 mL), then dried with Na_2SO_4, filtered and the filtrate concentrated under reduced pressure. The residue was purified by column chromatography to yield dithiane **270** as a colourless oil (120 mg, 87%): R_f = 0.3 (20% EtOAc in hexanes); $[\alpha]_D^{21}$ = –49.6 (c = 1.0, $CHCl_3$); ν_{max}(film)/cm^{-1} 3244 br w (N–H), 2908 vs, 2852 s, 1599 w, 1461 m, 1433 m, 1378 m, 1332 m, 1258 w, 1216 m, 1156 s, 1093 m, 1044 s, 976 w, 953 m, 859 w, 815 m, 773 w, 663 m; δ_H(400 MHz) 0.87 (3H, t, *J* 6.8, CH_2CH_3), 1.20–1.35 (23H, stack, alkyl chain, $C(CH_3)_A(CH_3)_B$, resonance overlap), 1.39 (3H, s, $C(CH_3)_A(CH_3)_B$), 1.41–1.54 (2H, stack, alkyl chain), 1.58–1.67 (1H, m, alkyl chain), 1.70–1.84 (2H, stack, dithiane, H-1_A), 1.88–2.05 (2H, stack, dithiane, H-1_B), 2.37–2.46 (4H, stack, dithiane. Ar CH_3), 2.62– 2.80 (3H, stack, dithiane), 3.59 (1H, app. t, *J* 9.3, H-2), 3.73 (1H, dd, *J* 11.5, 2.4, H-2′), 4.04–4.13 (2H, stack, H-3,H-4), 5.08 (1H, d, *J* 9.2, N*H*), 7.30 (2H, AA′ of AA′BB′, *J* 8.2, Ar C*H*), 7.80 (2H, BB′ of AA′BB′, *J* 8.2, Ar C*H*); δ_C(100 MHz) 14.1 (CH_3, CH_2CH_3), 21.5 (CH_3, Ar CH_3), 22.7 (CH_2, alkyl chain), 24.9 [CH_3, $C(CH_3)_A(CH_3)_B$], 25.8 (CH_2, dithiane), 26.2 [CH_3, $C(CH_3)_A(CH_3)_B$], 26.8 (CH_2, alkyl chain), [28.7, 29.4, 29.5, 29.6, 29.7 (CH_2, alkyl chain, dithane CH_2, resonance overlap)], 30.4 (CH_2, dithiane CH_2), 31.9 (CH_2, alkyl chain), 37.7 (CH_2, C-1), 43.6 (CH, C-2′), 52.1 (CH, C-2), [77.2, 80.2 (CH, C-3, C-4)], 108.1 (C, $C(CH_3)_2$), [127.3, 129.7 (CH, Ar CH)], [138.2, 143.3 (C, Ar C)]; *m/z* (TOF ES+) 636.3 ([M + Na]$^+$, 100%); HRMS *m/z* (TOF ES+) 636.3192 [M + Na]$^+$, $C_{32}H_{55}NO_4S_3Na$ requires 636.3191.

5.4. Chapter 4

13-Trimethylsilyl-12-tridecynoic acid (304)

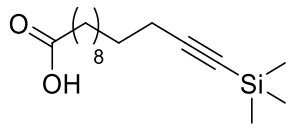

*n*BuLi (4.97 mL, 12.4 mmol, 2.5 M solution in hexanes) was added to a solution of (trimethylsilyl)acetylene (1.56 mL, 11.3 mmol) in THF (10 mL) at –78 °C. After 30 min, a solution of 11-bromoundecanoic acid (1.00 g, 3.77 mmol) in dry THF (6 mL) and anhydrous HMPA (4 mL) was added via syringe over 10 min at –78 °C. The reaction mixture was stirred for 2 h at –78 °C, then at rt for12 h. The reaction was then quenched with NH_4Cl solution (50 mL) and extracted with Et_2O (3 × 50 mL). The combined organic extracts were washed with brine (100 mL), dried using Na_2SO_4, filtered, and the filtrate concentrated under reduced pressure. The residue was purified by flash column chromatography (20% EtOAc/hexane) to give silyl alkyne **304** as a colourless oil (0.892 g, 88%): R_f = 0.4 (20% EtOAc in hexanes); ν_{max}(film)/cm^{-1} O*H* not observed, 2927 s, 2855 m, 2174 m (alkynyl C≡C), 1708 vs (C=O), 1412 m, 1283 m, 1248 s, 1028 w, 931 w, 839 vs, 759 s, 721 w, 698 m; δ_H(400 MHz) 0.01 (9H, s, Si(C*H*$_3$)$_3$), 1.11–1.25 (12H, stack, alkyl chain), 1.32–1.40 (2H, m, H-3), 1.45–1.53 (2H, m, H-10), 2.06 (2H, t, *J* 7.2, H-2), 2.20 (2H, t, *J* 7.5, H-11) OH not observed; δ_C(100 MHz) 0.16 (CH_3, Si(*C*H$_3$)$_3$), 19.8 (CH_2, C-11), 24.7 (CH_2, C-10), [28.6, 28.8, 29.0, 29.2, 29.3, 29.4 (CH_2, alkyl chain, resonance overlap)], 34.0 (CH_2, C-2), 84.2 (C, C-12), 107.7 (C, C-13), 180.1 (C, C-1); *m/z* (TOF ES+) 305.2 ([M + Na]$^+$, 30%), 337.2 (100); HRMS *m/z* (TOF ES+) 305.1910 [M + Na]$^+$, $C_{16}H_{30}O_2SiNa$ requires 305.1913.

Tridec-12-ynoic acid (301)

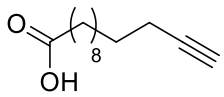

TBAF (6.0 mL of a 1.0 M solution in THF, 6.0 mmol) was added to a solution of silyl alkyne **304** (816 mg, 2.89 mmol) in THF (20 mL). After 14 h, the solution was concentrated under reduced pressure and the residue was dissolved in EtOAc (50 mL). The organic layer was washed sequentially with H_2O (3 × 40 mL) and brine (1 × 50 mL), then dried with Na_2SO_4, filtered and the filtrate was concentrated under reduced pressure. The residue was purified by column chromatography to yield alkyne **301** as a white, low-melting point, amorphous solid (504 mg, 84%): R_f = 0.3 (20% EtOAc in hexanes); ν_{max}(film)/cm^{-1} 3287 m (alkynyl C–H), 3037 br m (O–H), 2916 vs, 2848 vs, 2115 vw (alkynyl C≡C), 1697 vs (C=O), 1471 s, 1452 s, 1432 s, 1409 s, 1346 m, 1324 m, 1300 s, 1272 s, 1258 s, 1243 s, 1215 s, 1190 m, 1122 w, 1107 w, 1067 w, 1053 w, 899 s, 720 m, 731 m, 682 s, 666 vs, 649 s, 628 vs; δ_H(400 MHz) 1.19–1.35 (12H, stack, alkyl chain), 1.41–1.49 (2H, stack, alkyl chain), 1.52–1.62 (2H, stack, H-10), 1.87 (1H, t, *J* 2.7, H-13), 2.11 (2H, td, *J* 7.1, 2.7, H-11), 2.28 (2H, t, *J* 7.5, H-2), O*H* not observed; δ_C(100 MHz) 18.4 (CH_2, C-11), 24.6 (CH_2, C-10), [28.5, 28.7, 29.0, 29.2, 29.3, 29.4 (CH_2, alkyl chain, resonance overlap)], 34.0 (CH_2, C-2), 68.0 (CH, C-13), 84.8 (C, C-12), 180.1 (C, C-1); *m/z* (TOF ES+) 211.2 ([M + H]$^+$, 70%), 193.2 (100, [M–OH]$^+$); HRMS *m/z* (TOF ES+) 211.1697 [M + Na]$^+$, $C_{13}H_{23}O_2$ requires 211.1698.

Methyl tridec-12-ynoate (305)

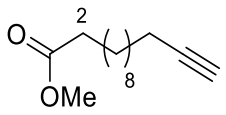

Concentrated H_2SO_4 (6 drops) was added to a suspension of acid **301** (864 mg, 4.11 mmol) in MeOH (40 mL). After 14 h, at rt the reaction mixture was neutralised by the addition of solid $NaHCO_3$. The mixture was then filtered through Celite, washing with MeOH (30 mL) and then CH_2Cl_2 (40 mL). The filtrate was concentrated under reduced pressure and the crude mixture purified by flash column chromatography (5% EtOAc in hexanes) to give methyl ester **305** as a colourless oil (842 mg, 91%): R_f = 0.7 (10% EtOAc in hexanes); ν_{max}(film)/cm^{-1} 3297 w (alkynyl C–H), 2930 s, 2856 m, 2117 vw (alkynyl C≡C) 1736 vs (C=O), 1435 m, 1361 w, 1238 m, 1195 s, 1170 s, 1100 m, 1017 w, 863 w, 724 w, 628 s; δ_H(400 MHz) 1.25–1.32 (12H, stack,alkyl chain), 1.33–1.40 (2H, stack, alkyl chain), 1.45–1.54 (2H, m, H-10), 1.55–1.64 (2H, m, H-3), 1.91 (1H, t, *J* 2.6, H-13), 2.15 (2H, td, *J* 7.1, 2.6, H-11), 2.28 (1H, t, *J* 7.5, H-2), 3.64 (3H, s, OC*H*$_3$); δ_C(100 MHz) 18.4 (CH_2, C-11), [24.9, 28.4, 28.7, 28.9, 29.1 (CH_2, alkyl chain, resonance overlap)], 34.1 (CH_2, C-1), 51.4 (CH_3, O*C*H$_3$), 68.1 (CH, C-13), 84.7 (C-12), 174.3 (C, *C*=O); *m/z* (TOF ES+) 225.2 ([M + H]$^+$, 30%), 193.2 ([M – OMe + H]$^+$, 100%) ; HRMS *m/z* (TOF ES+) 225.1851 [M + H]$^+$, $C_{14}H_{25}O_2$ requires 225.1855.

Methyl 13-(3′-benzoylphenyl)-tridec-12-ynoate (307)

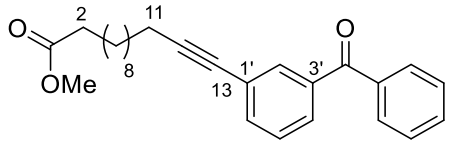

A solution of 3-bromo benzophenone (277 mg, 1.06 mmol) and methyl ester **305** (670 mg, 3.18 mmol) in Et_2NH (40 mL) was degassed using argon under sonication for 15 min. $[Pd(Ph_3P)_2Cl_2]$ (148 mg, 0.212 mmol) and CuI (20 mg, 0.106 mmol) were added and the reaction mixture was heated at reflux for 4 h. The solution was then filtered through Celite, washing with CH_2Cl_2 (50 mL). The filtrate was evaporated under pressure and the residue purified by column chromatography (5% EtOAc in hexanes) to yield alkyne **307** as a colourless oil (273 mg, 66%): R_f = 0.4 (20% EtOAc in hexanes); ν_{max}(film)/cm^{-1} 2926 vs, 2854 s, 1737 vs (C=O, ester), 1661 vs (C=O, ketone), 1596 w, 1575 w, 1447 m ,1435 m, 1363 w, 1318 m, 1287 s, 1234 s, 1196 m, 1171 s, 1075 m, 1075 m, 943 w, 907 w, 816 w, 786 w, 718 vs, 697 s; δ_H(400 MHz) 1.24–1.32 (10H, stack, alkyl chain), 1.39–1.52 (2H, stack, alkyl chain), 1.54–1.64 (4H, stack, alkyl chain), 2.28 (2H, t, *J* 7.6, H-11), 2.38 (2H, t, *J* 7.1, H-2), 3.64 (3H, s, C*H*$_3$), 7.39 (1H, app. t, *J* 7.8, Ar C*H*), 7.45–7.50 (2H, stack, Ar C*H*), 7.56–7.60 (2H, stack, Ar C*H*), 7.67 (1H, app. dt, *J* 7.8 1.4, Ar C*H*) 7.76–7.77 (1H, m, Ar C*H*), 7.78–7.79 (2H, stack, Ar C*H*); δ_C(100 MHz) 19.4 (CH_2, C-11), [24.9, 28.6, 28.8, 28.9, 29.1, 29.2, 29.39, 29.42 (CH_2, alkyl chain)], 34.1 (CH_2, C-2), 51.4 (CH_3, O*C*H$_3$), 79.7 (C, C-13), 91.8 (C, C-12), 124.5 (C, Ar C), [128.2, 128.3, 128.8, 130.0, 132.5, 133.0, 135.2 (CH, Ar CH), [137.3, 137.7 (C, Ar C)], 177.3 (C, ester *C*=O), 196.1 (C, ketone *C*=O); *m/z* (TOF ES+) 427.2 ([M + Na]$^+$, 100%); HRMS *m/z* (TOF ES+) 427.2247 [M + Na]$^+$, $C_{27}H_{32}O_3Na$ requires 427.2249.

Methyl 13-(3′-benzoylphenyl)-tridecanoate (309)

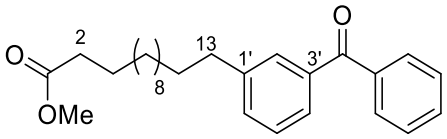

A flask containing a solution of alkyne **307** (200 mg, 0.49 mmol) in MeOH (15 mL) was purged with H_2 gas for 10 min. Pd/C (5 mg, 0.1 equiv) was then added and the mixture was stirred under a flow of H_2 for 15 min, after which time, the mixture was filtered through Celite, washing with MeOH (40 mL) and then CH_2Cl_2 (40 mL). The filtrate was concentrated under reduced pressure and the residue was purified by column chromatography (10% EtOAc in hexanes) to afford ester **309** as a white, low-melting point, amoprhous solid (170 mg, 85%): R_f = 0.7 (20% EtOAc in hexanes); ν_{max}(film)/cm^{-1} 2924 vs, 2853 vs, 1737 vs (C=O, ester), 1659 vs (C=O, ketone), 1598 m, 1581 w, 1447 s, 1435 s, 1361 w, 1316 s, 1278 vs, 1203 s, 1172 s, 1104 w, 1000 w, 977 w, 907 w, 838 w, 781 m, 709 vs, 719 vs; δ_H(400 MHz) 1.22–1.37 (16H, stack, alkyl chain), 1.56–1.67 (4H, stack, H-3, H-12), 2.30 (2H, t, *J* 7.6, H-2), 2.66 (2H, t, *J* 7.7, H-13), 3.66 (3H, s, OC*H*$_3$), 7.35–7.42 (2H, stack, Ar C*H*), 7.45–7.50 (2H, stack, Ar C*H*), 7.56–7.61 (2H, stack, Ar C*H*), 7.62–7.64 (1H, m, Ar C*H*), 7.78–7.82 (2H, stack, Ar C*H*); δ_C(100 MHz) 25.0 (CH_2, C-3), [29.2, 29.3, 29.5, 29.6 (CH_2, alkyl chain, resonance overlap)], 31.4 (CH_2, C-12), 34.1 (CH_2, C-2), 35.8 (CH_2, C-13), 51.4 (CH_3, O*C*H$_3$), [127.6, 128.1, 128.2, 129.9, 130.1, 132.3, 132.6 (CH, Ar CH)], [137.6, 137.8, 143.2 (C, Ar C)], 174.3 (C, ester *C*=O), 197.0 (C, ketone *C*=O); *m/z* (TOF ES+) 431.3 ([M + Na]$^+$, 100%); HRMS *m/z* (TOF ES+) 431.2563 [M + Na]$^+$, $C_{27}H_{36}O_3Na$ requires 431.2562.

13-(3′-benzoylphenyl)-tridecanoic acid (294)

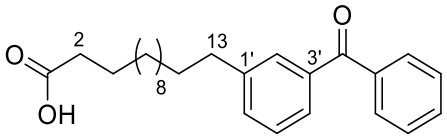

1 M NaOH (0.36 mL, 0.36 mmol) was added to a solution of ester **309** (100 mg, 0.24 mmol) in THF (0.36 mL) and MeOH (0.36 mL). After 2 h at rt the organic solvents were removed and the solution acidified with 1 M HCl (5 mL). The aqueous layer was extracted with EtOAc (3 × 30 mL). The combined organic layers were washed with brine (1 × 50 mL), dried with Na_2SO_4, filtered and the filtrate was concentrated under reduced pressure. The residue was purified by column chromatography to yield carboxylic acid **294** as a white amorphous solid (89 mg, 91%): R_f = 0.3 (20% EtOAc in hexanes); m.p. 68–70 °C; ν_{max}(film)/cm^{-1} 3059 br m (O–H), 2919 vs, 2848 vs,1689 vs (C=O), 1655 vs (C=O), 1600 m, 1581 w, 1480 w, 1460 m, 1434 s, 1409 m, 1343 w, 1322 m, 1305 s, 1279 vs, 1259 s, 1234 s, 1206 s, 1189 m, 1164 w, 1135 w, 1115 w, 1076 w, 1025 w, 988 m, 970 m, 927 s, 908 s, 837 s, 807 m, 759 w, 726 vs, 707 vs, 687 vs; δ_H(400 MHz) 1.23–1.36 (16H, stack, alkyl chain), 1.58–1.68 (4H, stack, H-3, H-12), 2.34 (2H, t, *J* 7.5, H-2), 2.67 (2H, t, *J* 7.7, H-13), 7.35–7.43 (2H, stack, Ar C*H*), 7.45–7.51 (2H, stack, Ar C*H*), 7.56–7.61 (2H, stack, Ar C*H*), 7.62–7.64 (1H, m, Ar C*H*), 7.79–7.82 (2H, stack, Ar C*H*) O*H* not observed; δ_C(100 MHz) [24.7, 29.1, 29.3, 29.4, 29.5, 29.6, 31.4 (CH_2, alkyl chain, resonance overlap)], 34.0 (CH_2, C-2), 35.8 (CH_2, C-13), [127.6, 128.1, 128.2, 129.9, 130.1, 132.3, 132.6 (CH, Ar CH)], [137.6, 137.8, 143.2 (C, Ar C)], 179.6 (C, acid *C*=O), 197.1 (C, ketone *C*=O); *m/z* (TOF ES+) 417.2 ([M + Na]$^+$, 100%); HRMS *m/z* (TOF ES+) 417.2408 [M + Na]$^+$, $C_{26}H_{34}O_3Na$ requires 417.2406.

Succinimidyl 13-(3′-benzoylphenyl)-tridecanoate (310)

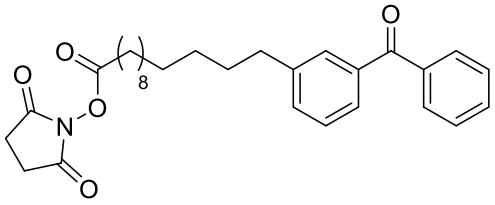

EDCI.HCl (62 mg, 0.32 mmol), *N*-hydroxysuccinimide (30 mg, 0.26 mmol) and DMAP (2 mg, cat.) were added to a solution of acid **294** (85 mg, 0.22 mmol) in CH_2Cl_2 (2 mL). The reaction mixture was heated at 40 °C for 12 h and then poured into H_2O (20 mL). The mixture was extracted with Et_2O (3 × 20 mL). The combined organic fractions were washed with brine (20 mL), dried over Na_2SO_4, and filtered. The solvent was removed under reduced pressure to give NHS ester **310** (100 g, 94%) as an amorphous solid; R_f = 0.5 (40% EtOAc in hexanes); m.p. 66–68 °C; ν_{max}(film)/cm^{-1} 2924 s, 2853 m, 1814 m, 1784 m, 1727 vs (C=O), 1657 s (C=O), 1598 w, 1580 w, 1447 m, 1431 m, 1365 m, 1316 m, 1279 s, 1213 vs, 1134 w, 1086 vs, 994 w, 814 w, 783 w, 721 s, 709 m; δ_H(400 MHz) 1.22–1.35 (14H, stack, alkyl chain), 1.35–1.41 (2H, stack, H-4), 1.58–1.66 (2H, m, H-12), 1.68–1.75 (2H, m, H-3), 2.57 (2H, t, *J* 7.5, H-2), 2.65 (2H, app. t, *J* 7.7, H-13), 2.77–2.81 (4H, stack, NHS C*H*$_2$), 7.35–7.42 (2H, stack, Ar C*H*), 7.45–7.50 (2H, stack, Ar C*H*), 7.56–7.61 (2H, stack, Ar C*H*), 7.62–7.64 (1H, m, Ar C*H*), 7.78–7.82 (2H, stack, Ar C*H*); δ_C(100 MHz) 24.6 (CH_2, C-3), 25.6 (CH_2, NHS C*H*$_2$), [28.8, 29.1, 29.2, 29.3, 29.4, 29.5 (CH_2, alkyl chain, resonance overlap)], 30.9 (CH_2, C-2), 31.4 (CH_2, C-12), 35.8 (CH_2, C-13), [127.6, 128.1, 128.2, 129.9, 130.0, 132.3, 132.6 (CH, Ar CH)], [137.6, 137.8, 143.2 (C, Ar C)], 168.7 (C, ester *C*=O), 169.3 (C, NHS *C*=O), 196.9 (C, ketone *C*=O); *m/z* (TOF ES+) 514.3 ([M + Na]$^+$, 100%); HRMS *m/z* (TOF ES+) 514.2572 [M + Na]$^+$, $C_{30}H_{37}NO_5$ requires 514.2569.

11-*O*-Benzyl-1-bromo-undecan-11-ol (312)

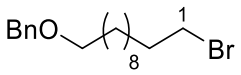

NaH (95 mg of a 60% dispersion in mineral oil, 2.39 mmol,) was added to a solution of 1-bromo-undecan-1-ol (500 mg, 1.99 mmol) in THF (10 mL) at 0 °C. After 1 h, a solution of BnBr (410 mg, 2.39 mmol) in THF (5 mL) was added. The reaction mixture was warmed to rt and stirred for 16 h. The mixture was diluted with Et_2O (20 mL) and washed with NH_4Cl solution (25 mL). The aqueous layer was extracted with Et_2O (3 x 20 mL). The combined organic extracts were dried over Na_2SO_4, filtered and concentrated under reduced pressure. The crude product was purified by column chromatography (5% EtOAc in hexanes) to afford benzyl ether **312** as a pale yellow oil (678 mg, quant.): R_f = 0.7 (5% EtOAc in hexanes); ν_{max}(film)/cm^{-1} 2924 vs, 2852 s, 1719 m, 1453 m, 1361 w, 1273 s, 1204 w, 1099 s, 1072 m, 1027 w, 735 m, 712 s, 697 s; δ_H(400 MHz) 1.18–1.38 (14H, stack, alkyl chain), 1.50–1.60 (2H, m, H-2 or H-10), 1.72–1.83 (2H, m, H-10 or H-2), 3.30–3.41 (4H, stack, H-1, H-11), 4.43 (2H, s, PhC*H*$_2$), 7.18–7.28 (5H, stack, Ar C*H*); δ_C(100 MHz) [26.2, 28.2, 28.8, 29.4, 29.46, 29.53, 29.8 (CH_2, alkyl chain, resonance overlap)], 32.8 (CH_2, C-2 or C-10), 34.0 (CH_2, C-1), 70.5 (CH_2, C-11), 72.9 (CH_2, Ph*C*H$_2$), [127.5, 127.6, 128.3 (CH, Ar *C*H)], 138.7 (C, Ar *C*); *m/z* (TOF ES+) 363.1 ([M + Na]$^+$, 100%); HRMS *m/z* (TOF ES+) 363.1297 [M + Na]$^+$, $C_{18}H_{29}O^{79}BrNa$ requires 363.1299.

1-*O*-Benzyl-tridec-12-yn-1-ol (313)

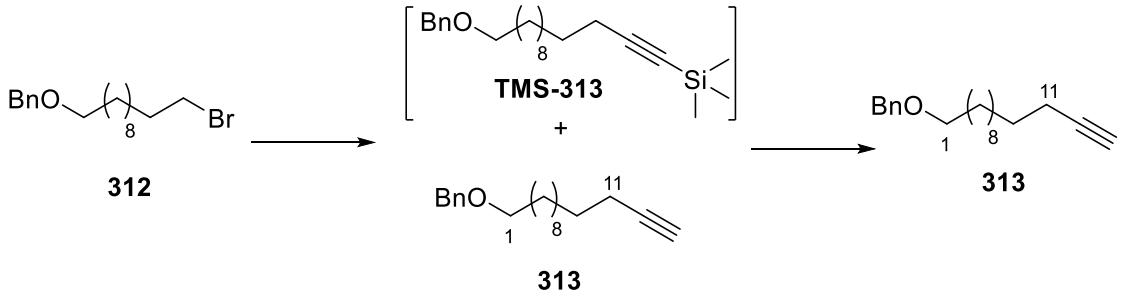

*n*BuLi (0.64 mL, 1.61 mmol, 2.5 M solution in hexanes) was added to a solution of (trimethylsilyl)acetylene (0.23 mL, 1.61 mmol) in THF (4 mL) at –78 °C. After 30 min, the solution was warmed to –30 °C and a solution of bromide **312** (500 mg, 1.46 mmol) in dry THF (4 mL) and anhydrous HMPA (1 mL) was added via syringe over 5 min. After 15 min the reaction mixture was warmed to 0 °C for 5h and then to rt for an additional 12 h. The reaction was then quenched with NH_4Cl solution (20 mL) and extracted with Et_2O (3 × 30 mL). The combined organic extracts were washed with brine (50 mL), dried using Na_2SO_4, filtered, and the filtrate concentrated under reduced pressure to yield an inseparable mixture of silyl alkyne **TMS-313** and alkyne **313**, which was directly used without further purification. Assuming full conversion of the starting material, TBAF (2.0 mL of a 1.0 M solution in THF, 2.0 mmol) was added to a solution of the mixture (482 mg) in THF (10 mL). After 14 h, the solution was concentrated under reduced pressure and the residue was dissolved in EtOAc (20 mL). The organic layer was washed sequentially with H_2O (3 × 15 mL) and brine (1 × 15 mL), then dried with Na_2SO_4, filtered and the filtrate was concentrated under reduced pressure. The residue was purified by column chromatography to yield alkyne **313** as a colour oil (504 mg, 83% over two steps): R_f = 0.7 (5% EtOAc in hexanes); ν_{max}(film)/cm^{-1} 3309 m (alkyne C–H), 2924 vs, 2852 vs, 2123 vw (alkyne C≡C), 1454 m, 1362 m, 1204 w, 1099 vs, 1028 m, 734 s, 696 s; δ_H(400 MHz) 1.11–1.15 (10H, stack, alkyl chain), 1.19–1.28 (4H, stack, alkyl chain), 1.33–1.41 (2H, m, H-10), 1.43–1.50 (2H, m, H-2), 1.79 (1H, t, *J* 2.7, H-13), 2.03 (2H, td, *J* 7.1, 2.7, H-11), 3.31 (2H, t, *J* 6.7, H-1), 4.35 (2H, s, PhCH_2), 7.10–7.16 (1H, m, Ar C*H*), 7.18–7.21 (4H, stack, Ar C*H*); δ_C(100 MHz) 18.4 (CH_2, C-11), 26.2 (CH_2), 28.5 (CH_2, C-10), [28.8, 29.1, 29.49,

29.55, 29.6 (CH_2, alkyl chain, resonance overlap)], 29.9 (CH_2, C-2), 68.1 (CH, C-13), 70.5 (CH_2, C-1), 72.9 (CH_2, Ph*C*H_2), 84.8 (C, C-12), [127.5, 127.6, 128.3 (CH, Ar *C*H)], 138.8 (C, Ar *C*); *m/z* (TOF ES+) 309.2 ([M + Na]$^+$, 100%); HRMS *m/z* (TOF ES+) 309.2192 [M + Na]$^+$, $C_{20}H_{30}ONa$ requires 309.2194.

3-Benzoylphenylmethanol (298)

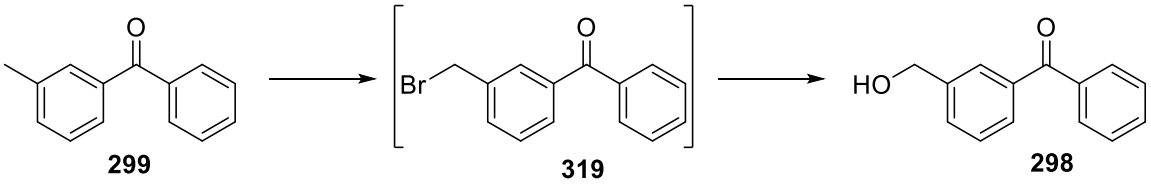

299 **319** **298**

N-Bromo succinimide (0.55 g, 3.06 mmol) and benzoyl peroxide (62 mg, 0.26 mmol) were added to a solution of 3-methylbenzophenone (500 mg, 2.55 mmol) in benzene (15 mL). After 12 h at reflux the reaction was concentrated under reduced pressure and the resulting residue was diluted with EtOAc (30 mL). The mixture was washed with H_2O (3 × 20 mL), brine (20 mL), dried (Na_2SO_4), filtered and the filtrate was concentrated under reduced pressure the resulting residue was used direcly without further purification in the next step: $CaCO_3$ (1.28 g, 12.8 mmol) was added to a solution of the crude bromide **319** (assuming 100% conversion in the first step) in dioxane:water (1:1, 20 mL). After 14 h at reflux, the reaction was cooled to rt and quenched with 2M HCl (25 mL) and extracted with CH_2Cl_2 (3 × 50 mL). The combined organic layers were washed with water (75 mL) brine (75 mL), dried using Na_2SO_4, filtered and the filtrate was concentrated under reduced pressure. The residue was purified using flash column chromatography (20% EtOAc in hexanes) to yield alcohol **298** as a colourless oil (411 mg, 76%, over two steps): R_f = 0.1 (20% EtOAc in hexanes); ν_{max}(film)/cm^{-1} 3388 br m (O-H), 1650 vs (C=O), 1596 s, 1577 m, 1447 m, 1362 w, 1314 s, 1281 vs, 1205 s, 1179 m, 1132 m, 1024 m, 1000 m, 965 m, 929 w, 904 w, 836 w, 816 w, 781 m, 720 vs, 709 vs, 696 vs; δ_H(400 MHz) 3.09 (1H, br s, O*H*), 4.69 (2H, s, CH_2OH), 7.39–7.47 (3H, stack, Ar CH), 7.53–7.59 (2H, stack, Ar CH), 7.62–7.65 (1H, m, Ar CH), 7.72–7.76 (3H, stack, Ar CH); δ_C(100 MHz) 64.4

(CH_2, CH_2OH), [128.1, 128.2, 128.3, 129.1, 130.0, 130.1, 132.5 (CH, Ar CH)], [137.3, 137.6, 141.3 (C, Ar *C*)], 196.9 (C, *C*=O); *m/z* (TOF ES+) 212.1 ($[M]^+$, 30%), 77.0 (100,Ph^+).

Data were in agreement with those reported in the literature.[193]

11-*O*-[3′-Benzoylphenylmethoxy]undecanoic acid (296)

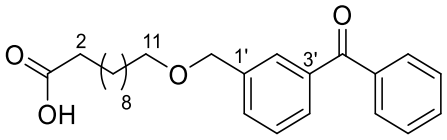

NaH (113 mg of a 60% dispersion in mineral oil, 2.82 mmol) was added to a solution of alcohol **298** (200 mg, 0.94 mmol) in DMF (10 mL) at 0 °C. After stirring for 1 h, a solution of 11-bromo undecanoic acid (166 mg, 0.63 mmol) in DMF (5 mL) was added. After 20 min at 0 °C, the reaction mixture was warmed to rt and stirred for a further 15 h. The reaction was then quenched with 2M HCl (25 mL) and extracted with EtOAc (5 × 30 mL). The combined organic layers were washed with water (75 mL) brine (75 mL), dried using Na_2SO_4, filtered and the filtrate was concentrated under reduced pressure. The residue was purified using flash column chromatography (20% EtOAc in hexanes) to yield ether **296** as a colourless oil (234 mg, 83%.): R_f = 0.4 (40% EtOAc in hexanes); ν_{max}(film)/cm^{-1} 3303 vbr s (O–H), 2927 vs, 2855 s, 1706 vs (C=O), 1658 vs (C=O), 1599 m, 1448 w, 1282 s, 1208 m, 1100 m, 715 vs; δ_H(400 MHz) 1.22–1.38 (12H, stack, alkyl chain), 1.57–1.66 (4H, stack, alkyl chain), 2.33 (2H, t, *J* 7.5, H-2), 3.49 (2H, t, *J* 6.6, H-11), 4.56 (2H, s, CH_2Ar), 7.43–7.50 (3H, stack, Ar C*H*), 7.56–7.61 (2H, stack, Ar C*H*), 7.68–7.72 (1H, m, Ar C*H*), 7.76–7.81 (3H, stack, Ar C*H*); δ_C(100 MHz) [24.7, 26.2, 29.0, 29.2, 29.35, 29.43, 29.5, 29.7 (CH_2, alkyl chain)], 34.1 (CH_2, C-2), 70.8 (CH_2, C-11), 72.3 (CH_2, Ar CH_2), [128.29, 128.34, 129.1, 129.3, 130.1, 131.1, 132.5 (CH, Ar CH)], [137.6, 137.7, 139.1 (C, Ar C)], 179.9 (C, acid *C*=O), 196.8 (C, ketone *C*=O); *m/z* (TOF ES+) 419.2 ([M + Na]$^+$, 100%); HRMS *m/z* (TOF ES+) 419.2202 [M + Na]$^+$, $C_{25}H_{32}O_4Na$ requires 419.2198.

Succinimidyl-11-*O*-[3′-Benzoylphenylmethoxyl]undecanoate (320)

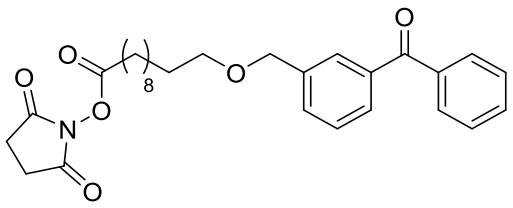

EDCI.HCl (47 mg, 0.24 mmol) and *N*-hydroxysuccinimide (31 mg, 0.27 mmol) were added to a solution of carboxylic acid **296** (88 mg, 0.22 mmol) in CH_2Cl_2 (3 mL). After 12 h at 40 °C, the mixture was poured into H_2O (20 mL) and extracted with Et_2O (60 mL). The organic layer was washed with brine (20 mL), dried over Na_2SO_4, and filtered. The solvent was removed under reduced pressure to give NHS ester **320** as a glassy non-amorphous solid(95 mg, 90%): R_f = 0.5 (40% EtOAc in hexanes); ν_{max}(film)/cm^{-1} 2928 m, 2854 m, 1813 m, 1784 m, 1737 vs (C=O), 1658 s (C=O), 1598 w, 1447 w, 1362 m, 1317 m, 1282 m, 1250 w, 1205 s, 1179 m, 1131 m, 1103 m, 1067 s, 994 w, 970 w, 815 w, 783 w, 721 m, 712 m; δ_H(400 MHz) 1.24–1.40 (12H, stack, alkyl chain), 1.57–1.64 (2H, stack, alkyl chain), 1.68–1.76 (2H, stack, alkyl chain), 2.58 (2H, t, *J* 7.5, H-2), 2.79 (4H, stack, NHS), 3.48 (2H, t, *J* 6.6, H-11), 4.56 (2H, s, C*H*$_2$Ar), 7.43–7.51 (3H, stack, Ar C*H*), 7.55–7.61 (2H, stack, Ar C*H*), 7.67–7.71 (1H, m, Ar C*H*), 7.75–7.81 (3H, stack, Ar C*H*); δ_C(100 MHz) [24.6, 25.6, 26.2, 28.7, 29.0, 29.3, 29.4, 29.7, 30.9 (CH_2, alkyl chain, resonance overlap)], 34.1 (CH_2, C-2), 70.8 (CH_2, C-11), 72.3 (CH_2, Ar *C*H_2), [128.29, 128.34, 129.0, 129.3, 130.1, 131.6, 132.4 (CH, Ar CH)], [137.6, 137.7, 139.2 (C, Ar C)], 168.7 (C, ester *C*=O)169.2 (C, NHS *C*=O), 196.7 (C, benzophenone *C*=O); *m/z* (TOF ES+) 516.2 ([M + Na]$^+$, 100%); HRMS *m/z* (TOF ES+) 516.2359 [M + Na]$^+$, $C_{29}H_{35}NO_6Na$ requires 516.2362.

(2*S*, 3*S, 4R*)-2-[(*N-tert*-Butoxycarbony)amino]-1, 3, 4-octadecanetriol (322)

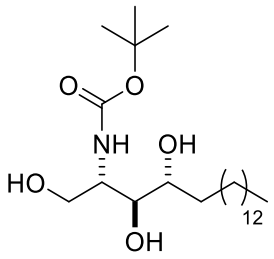

Et_3N (2.2 mL, 15.7 mmol) and Boc_2O (3.02 g, 13.2 mmol) were added sequentially to a solution of phytosphingosine **179** (4.0 g, 12.5 mmol) in THF (100 mL). The solution was stirred vigorously for 14 h after which time the reaction mixture was concentrated under reduced pressure. Recrystallisation of the residue from EtOAc (100 mL) yielded carbamate **322** as white crystals (5.49 g, 96%): R_f = 0.2 (5% MeOH in $CHCl_3$); m.p. 80–82 °C (lit.[52] 86–88 °C); solubility issues prevented an optical rotation measurement; ν_{max}(film)/cm^{-1} 3306 br m (O–H, N–H), 2953 w, 2918 s, 2851 s, 1669 vs C=O, 1545 s, 1468 m, 1392 w, 1356 m, 1304 m, 1253 m, 1170 s, 1107 w, 1060 s, 1043 s, 1028 s, 927 w, 872 w, 783 w, 720 m; δ_H(400 MHz) 0.84 (3H, t, *J* 6.8, CH_2CH_3), 1.20–1.30 (24H, stack, alkyl chain), 1.41 (9H, s, $C(CH_3)_3$), 1.47–1.56 (1H, m, alkyl chain), 1.60–1.69 (1H, m, alkyl chain), 3.49–3.57 (2H, stack, H-3,H-4), 3.63–3.69 (1H, m, H-1_A), 3.70–3.78 (2H, stack, H-1_B, H-2); δ_C(100 MHz) 14.5 (CH_3, CH_2CH_3), [23.2, 26.5 (CH_2, alkyl chain)], 28.8 [CH_3, $C(CH_3)_3$], [29.9, 30.3, 32.5, 33.3 (CH_2, alkyl chain, resonance overlap)], 53.1 (CH, C-2), 62.0 (CH_2, C-1), [73.1, 76.3 (CH, C-3, C-4)], 80.3 (C, $C(CH_3)_3$), 157.1 (C, C=O); *m/z* (TOF ES+) 440.3 ([M + Na]$^+$, 100%).

Data were in agreement with those reported in the literature.[52]

(2*S*, 3*S, 4R*)-2-[(*N-tert*-butoxycarbonyl)amino]- 1-*O-tert*-Butyldiphenylsilyl-1, 3, 4-octadecanetriol (323)

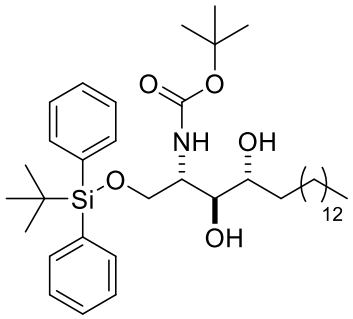

TBDPSCl (3.71 mL, 14.3 mmol) was added to a solution of carbamate **322** (5.00 g, 11.9 mmol) in pyrdine (50 mL). After 12 h, the reaction mixure was concentrated under reduced pressure. The residue was dissolved with EtOAc (100 mL) and the resulting solution sequentially washed with H_2O (3 × 50 mL) and brine (1 × 50 mL), and dried using Na_2SO_4. The solution was filtered and concentrated under reduced pressure and the residue was purified by flash column chromatography (20% EtOAc in hexanes) to provide pure silyl ether **323** as colourless oil (7.2 g, 92%): R_f = 0.7 (30% EtOAc in hexanes); $[\alpha]_D^{21}$ = +12.8 (c = 1.0, $CHCl_3$), lit.[194] $[\alpha]_D^{25}$ = +13.6 (c = 0.3, $CHCl_3$);; ν_{max}(film)/cm^{-1} 3424 br w (O–H, N–H), 2924 s, 2854 s, 1690 m (C=O), 1501 m, 1467 m, 1427 m, 1391 m, 1366 m, 1323 w, 1246 w, 1168 s, 1113 s, 1064 s, 857 w, 822 w, 779 w, 739 w, 700 vs, 608 s; δ_H(400 MHz) 0.88 (3H, t, *J* 6.9, CH_2CH_3), 1.09 (9H, s, $SiC(CH_3)_3$), 1.23–1.33 (25H, stack, alkyl chain), 1.43 (9H, s, $OC(CH_3)_3$), 1.66–1.75 (1H, stack, alkyl chain), 2.51 (1H, br d, *J* 5.3, OH), 3.05 (1H, br d, *J* 6.9, OH), 3.60–3.69 (2H, stack, H-3,H-4), 3.79–3.89 (2H, stack, H-1_A, H-2), 3.98 (1H, app. d, *J* 9.0, H-1_B), 5.16 (1H, d, *J* 8.2, N*H*), 7.36–7.48 (6H, stack, Ar C*H*), 7.62–7.70 (4H, stack, Ar C*H*); δ_C(100 MHz) 14.1 (CH_3, CH_2CH_3), 19.2 (C, $SiC(CH_3)_3$), 22.7 (CH_2, alkyl chain), 26.0 (CH_2, alkyl chain), 26.9 (CH_3, $SiC(CH_3)_3$), 28.4 (CH_3, $C(CH_3)_3$), [29.4, 29.67, 29.73, 31.9, 33.1 (CH_2, alkyl chain, resonance overlap)], 52.1 (CH, C-2), 64.1 (CH_2, C-1), [73.5, 75.7 (CH, C-4, C-3)], 79.7 (C, $OC(CH_3)_3$),

[127.9, 130.0 (CH, Ar)], [132.4, 132.6 (C, Ar)], [135.5, 135.6 (CH, Ar)], 155.7 (C, C=O); *m/z* (TOF ES+) 678.5 ([M + Na]$^+$, 100%).

Data were in agreement with those reported in the literature.[194]

(2*S*, 3*S*, 4*R*)-2-[(*N*-*tert*-butoxycarbonyl)amino]-1-*O*-*tert*-Butyldiphenylsilyloxy-3, 4-*O*-isopropylidene-1, 3, 4-octadecanetriol (324)

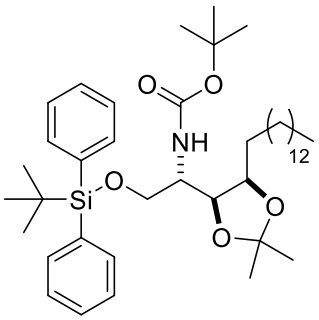

Concentrated H_2SO_4 (4 drops) was added to a solution of silyl ether **323** (4.80 g, 7.33 mmol) in dry acetone (50 mL) at 0 °C. After 20 h the reaction mixture was quenched by the addition of solid $NaHCO_3$ and then concentrated under reduced pressure. The residue was partitioned between EtOAc (35 mL) and H_2O (30 mL). The layers were separated and the aqueous phase was extracted with EtOAc (3 × 20 mL). The combined organic layers were washed with brine (20 mL), then dried over Na_2SO_4, filtered and the filtrate concentrated under reduced pressure. The crude product was purified by column chromatography (5% EtOAc in hexanes) to give acetonide **324** as a colourless oil (4.32 g, 84%): R_f = 0.7 (10% EtOAc in hexanes); $[\alpha]_D^{21}$ = +18.0 (c = 1.0, $CHCl_3$), ν_{max}(film)/cm^{-1} 3425 br w (N–H), 2925 s, 2854 s, 1720 s, 1707 s (C=O), 1496 m, 1466 m, 1428 m, 1390 m, 1378 m, 1366 s, 1247 m, 1218 m, 1167 s, 1109 s, 1045 s, 1027 m, 955 w, 866 w, 822 m, 780 w, 739 m, 700 vs, 615 w; δ_H(400 MHz) 0.89 (3H, t, *J* 6.8, CH_2CH_3), 1.07 (9H, s, $SiC(CH_3)_3$), 1.22–1.32 (23H, stack, alkyl chain), 1.35–1.37 (6H, stack, $C(CH_3)_A(CH_3)_B$), 1.46 (9H, s, $OC(CH_3)_3$), 1.50–1.56 (3H, stack, alkyl chain), 3.70–3.85 (2H, stack, H-2, H-1_A), 3.92 (1H, dd, *J* 9.9, 2.8, H-1_B), 4.10–4.16 (1H, m, H-4), 4.20 (1H, dd, *J* 9.1, 5.6, H-3), 4.80 (1H, d, *J* 9.9, N*H*), 7.35–7.45 (6H, stack, Ar C*H*), 7.64–7.73 (4H, stack, Ar C*H*);

δ_C(100 MHz) 14.1 (CH_3, CH_2CH_3), 19.3 (C, $SiC(CH_3)_3$), 22.7 (CH_2, alkyl chain), 25.9 (CH_3, $C(CH_3)_A(CH_3)_B$), 26.3 (CH_2, alkyl chain), 26.8 (CH_3, $SiC(CH_3)_3$), 28.2 (CH_3, $C(CH_3)_A(CH_3)_B$), 28.4 (CH_3, $C(CH_3)_3$), [29.1, 29.3, 29.5, 29.7, 31.9 (CH_2, alkyl chain, resonance overlap)], 51.0 (CH, C-2), 63.9 (CH_2, C-1), 75.9 (CH, C-4), 77.9 (CH, C-3), 79.4 (C, $OC(CH_3)_3$), 107.8 (C, $C(CH_3)_2$), [127.6, 127.7, 129.66, 129.68 (CH, Ar)], [133.3, 133.5 (C, Ar)], [135.5, 135.6 (CH, Ar)], 155.1 (C, *C*=O); *m/z* (TOF ES+) 718.5 ([M + Na]$^+$, 100%); HRMS *m/z* (TOF ES+) 718.4844 [M + Na]$^+$, $C_{42}H_{69}NO_5SiNa$ requires 718.4843.

(2*S*, 3*S,* 4*R*)-2-[(*N-tert*-Butoxycarbonyl)amino]-3, 4-*O*-isopropylidene-1, 3, 4 octadecanetriol (325)

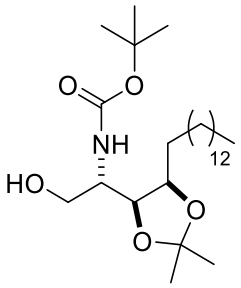

TBAF (8.6 mL, 1.0 M in THF, 8.6 mmol) was added to a solution of acetonide **324** (5.00 g, 7.18 mmol) in THF (50 mL). After 14 h, the reaction mixture was concentrated under reduced pressure. The residue was dissolved in EtOAc (100 mL). The resulting solution was washed sequentially with H_2O (3 × 50 mL) and brine (1 × 50 mL), dried with Na_2SO_4, filtered and the filtrate was concentrated under reduced pressure. The residue was purified by column chromatography to yield alcohol **325** as a white amorphous solid (2.79 g, 85%): R_f = 0.1 (20% EtOAc in hexanes); $[\alpha]_D^{21}$ = +6.0 (c = 1.0, $CHCl_3$), lit. $[\alpha]_D^{21}$ = +6.0 (c = 1.0, $CHCl_3$); ν_{max}(film)/cm^{-1} 3347 br m (O–H, N–H), 2984 w, 2918 vs, 2850 s, 1683 vs (C=O), 1665 m, 1529 vs, 1467 m, 1390 w, 1366 s, 1310 w, 1275 w, 1246 s, 1220 s, 1167 vs, 1065 s, 1041 s, 1018 s, 997 m, 919 w, 903 w, 867 w, 796 w, 781 w, 763 w, 745 w, 720 m, 678 m; δ_H(400 MHz) 0.88 (3H, t, *J* 6.8, CH_2CH_3), 1.23–1.30 (22H, stack, alkyl chain), 1.33 (3H, s, $C(CH_3)_A(CH_3)_B$), 1.44

(9H, s, OC(C*H*$_3$)$_3$), 1.45 (3H, s, C(CH$_3$)$_A$(C*H*$_3$)$_B$), 1.52–1.65 (4H, stack, alkyl chain), 2.30 (1H, br s, O*H*), 3.66–3.73 (1H, m, H-1$_A$), 3.73–3.81 (1H, m, H-2), 3.81–3.87 (1H, m, H-1$_B$), 4.08 (1H, app. t, *J* 6.2, H-3), 4.17 (1H, dd, *J* 12.1, 6.9, H-4), 4.95 (1H, d, *J* 8.8, N*H*); δ_C(100 MHz) 14.1 (CH$_3$, CH$_2$*C*H$_3$), 22.7 (CH$_2$, alkyl chain), 25.3 (CH$_3$, C(*C*H$_3$)$_A$(CH$_3$)$_B$), 26.7 (CH$_2$, alkyl chain), 27.6 (CH$_3$, C(CH$_3$)$_A$(*C*H$_3$)$_B$), 28.3 (CH$_3$, OC(*C*H$_3$)$_3$), [29.3, 29.5, 29.6, 29.7, 31.9 (CH$_2$, alkyl chain, resonance overlap)], 51.1 (CH, C-2), 63.8 (CH$_2$, C-1), 77.8 (CH, C-4), 78.2 (CH, C-3), 79.7 (C, O*C*(CH$_3$)$_3$), 108.1 (C, *C*(CH$_3$)$_2$), 155.4 (C, *C*=O); *m/z* (TOF ES+) 480.4 ([M + Na]$^+$, 100%).

Data were in agreement with those reported in the literature.[195]

1, 2, 3, 4, 6-Penta-*O*-trimethylsilyl-α-D-galactopyranoside (330)

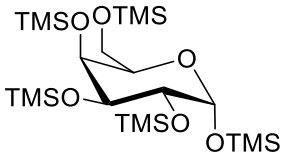

HMDS (50 mL, 0.24 mol) and TMSCl (25 mL, 0.20 mol) were added sequentially to a solution of D-galactose (5.0 g, 55.5 mmol) in pyridine (100 mL). The solution was heated at 75 ºC for 1 h under an Ar atmosphere and then cooled to rt. The mixture was poured into ice-H_2O (250 mL) and extracted with hexane (3 × 150 mL). The combined organic extracts were washed with H_2O (3 × 150 mL), dried ($MgSO_4$) and concentrated under reduced pressure to afford per-silylated galactose **330** as a viscous, colourless oil (15.0 g, 91%, α-anomer only): R_f = 0.2 (4% EtOAc in hexanes); $[\alpha]_D^{22}$ = +32.0 (c = 1.0, $CHCl_3$), lit.[52] $[\alpha]_D^{20}$ = +67.9 (c = 0.5, $CHCl_3$); ν_{max}(film)/cm^{-1} 2956 m, 2901 w, 1459 w, 1402 w, 1383 w, 1248 s, 1154 m, 1103 m, 1071 s, 1051 m, 968 m, 892 m, 865 s, 832 vs, 747 s, 682 m; δ_H(400 MHz) 0.10 (9H, s, Si(C*H*$_3$)$_3$), 0.11 (9H, s, Si(C*H*$_3$)$_3$), 0.13 (9H, s, Si(C*H*$_3$)$_3$), 0.14 (18H, s, Si(C*H*$_3$)$_3$), 3.53 (1H, dd, *J* 9.6, 5.6, H-6$_A$), 3.63 (1H, dd, 9.6, 7.9, H-6$_B$), 3.81–3.83 (2H, stack, incl. H-2), 3.88–3.92 (2H, stack, incl. H-5), 5.05 (1H, d, *J* 2.2, H-1); δ_C(100 MHz) [–0.5, 0.2, 0.3, 0.5, 0.6, CH$_3$, Si(*C*H$_3$)$_3$], 61.2, (CH$_2$,

C-6), 67.0 (CH), 70.5 (CH), 71.1 (CH), 72.3 (CH), 94.6 (CH, C-1); *m/z* (TOF ES+) 563.25 ([M + Na]$^+$, 100%).

Data were in agreement with those reported in the literature.[52]

(2*S*, 3*S,* 4*R*)-2-[*N-tert*-Butoxycarbonylamino]-1-*O*-α-D-galactopyranosyl-3,4-*O*-isopropylidene-1, 3, 4-octadecanetriol (331) and (2*S*, 3*S,* 4*R*)-2-[*N-tert*-butoxycarbonylamino]-1-*O*-α-D-galactopyranosyl-1, 3, 4-octadecantriol (332)

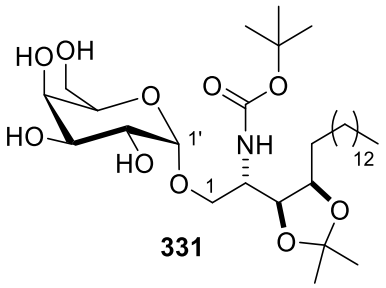

331

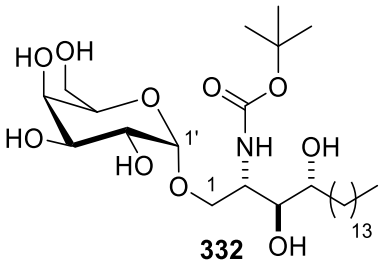

332

TMSI (1.87 mL, 13.1 mmol) was added to a solution of per-silylated galactose **330** (7.1 g, 13.1 mmol) in CH_2Cl_2 (50 mL) at 0 °C. The reaction mixture was stirred under an Ar atmosphere for 1 h before the solvent was removed under reduced pressure. The residue was dissolved in anhydrous toluene (20 mL) and the solvent was removed under reduced pressure to remove any traces if HI. The resulting glycosyl iodide intermediate **95** was dissolved in CH_2Cl_2 (20 mL) and kept under an Ar atmosphere. Activated 4 Å molecular sieves (2.20 g) were added to a separate flask containing *n*-Bu_4NI (8.45 g, 26.2 mmol), *i*-Pr_2NEt (3.5 mL, 20.1 mmol) and alcohol **325** (2.00 g, 4.37 mmol) in CH_2Cl_2 (30 mL). After 30 min, the solution of glycosyl iodide **95** in CH_2Cl_2 was added to the solution containing the alcohol and the resulting mixture was stirred overnight. The solution was filtered through Celite and after removal of the solvent under reduced pressure, Et_2O (50 mL) and H_2O (50 mL) were added and the phases were separated. The organic phase was dried (Na_2SO_4) and then concentrated under reduced pressure. $CHCl_3$:MeOH:2 M HCl (40 mL total volume, 10:10:3) was added to the resulting residue. After stirring for 20 min, $CHCl_3$ (17.5 mL) and H_2O (7.5 mL) were added at which point

the mixture separated into two phases. The top phase was isolated and concentrated under reduced pressure. Purification of the residue by flash column chromatography (1% MeOH in $CHCl_3$ → 10% MeOH in $CHCl_3$) afforded, in order of elution, glycoside **331** as a colourless syrup (1.30 g, 48%, α-anomer only): R_f = 0.3 (10% MeOH in $CHCl_3$); solubility issues prevented an optical rotation measurement; ν_{max}(film)/cm^{-1} 3352 br m (O–H, N–H), 2923 s, 2853 s, 1686 s (C=O), 1526 w, 1458 w, 1367 s, 1248 s, 1220 s, 1161 s, 1043 vs, 1023 vs, 974 w, 867 w, 770 w; δ_H(400 MHz, 2:1 $CDCl_3$:CD_3OD) 0.84 (3H, t, *J* 6.8, CH_2CH_3), 1.20–1.28 (23H, stack, alkyl chain), 1.29 (3H, s, $C(CH_3)_A(CH_3)_B$), 1.38 (3H, s, $C(CH_3)_A(CH_3)_B$), 1.40 (9H, s, $OC(CH_3)_3$), 1.45–1.51 (3H, stack, alkyl chain), 3.68–3.81 (8H, stack, incl. H-2, H-1$_A$, H-1$_B$, H-2′, H-6′$_A$, H-6′$_B$), 3.92–3.94 (1H, m, sugar C*H*), 4.03–4.11 (2H, stack, H-3, H-4), 4.89 (1H, d, *J* 2.7, H-1′), exchangeable protons not observed; δ_C(100 MHz, 2:1 $CDCl_3$:CD_3OD) 14.5 (CH_3, CH_2CH_3), 23.2 (CH_2, alkyl chain), 26.1 (CH_3, $C(CH_3)_A(CH_3)_B$), 26.9 (CH_2, alkyl chain), 28.6 (CH_3, $C(CH_3)_A(CH_3)_B$), 28.8 (CH_3, $OC(CH_3)_3$), [29.9, 30.1, 30.2, 32.4 (CH_2, alkyl chain, resonance overlap)], 50.6 (CH, C-2), 62.5 (CH_2, C-1), 69.1 (CH_2, C-6′), [69.9, 70.4, 70.9, (CH, C-2′, C-3′, C-4′, C-5′, resonance overlap)], 76.0 (CH, C-4), 78.7 (CH, C-3), 80.1 (C, $OC(CH_3)_3$), 100.2 (CH, C-1′), 108.7 1 (C, $C(CH_3)_2$), 156.4 (C, *C*=O); *m/z* (TOF ES+) 642.4 ([M + Na]$^+$, 100%); HRMS *m/z* (TOF ES+) 642.4196 [M + Na]$^+$, $C_{32}H_{61}NO_{10}Na$ requires 642.4193 and then glycoside **332** as a white foam (0.71 g, 28%, α-anomer only): R_f = 0.1 (10% MeOH in $CHCl_3$); solubility issues prevented an optical rotation measurement; ν_{max}(film)/cm^{-1} 3334 br s (O–H, N–H), 2917 s, 2849 s, 1692 s, 1679 s (C=O), 1526 s, 1464 m, 1392 m, 1366 m, 1316 m, 1296 m, 1246 s, 1169 s, 1134 s, 1081 s, 1039 vs, 1001 s, 978 m, 937 w, 882 w, 823 w, 785 w, 764 w, 719 w; δ_H(400 MHz, 2:1 $CDCl_3$:CD_3OD) 0.84 (3H, t, *J* 6.8, CH_2CH_3), 1.20–1.30 (24H, stack, alkyl chain), 1.41 (9H, s, $OC(CH_3)_3$), 1.47–1.57 (1H, m, alkyl chain), 1.60–1.69 (1H, m, alkyl chain), 3.48–3.57 (2H, stack, H-3, H-4), 3.63 (1H, dd, *J* 11.9, 6.0, H-6′$_A$), 3.67–3.81 (5H, stack, incl. H-1$_A$, H-1$_B$, H-2′), 3.82–3.88 (2H, stack, H-2, H-6′$_B$), 3.90–3.93 (1H, m, sugar C*H*), 4.87 (1H, d, *J* 3.6, H-1′); δ_C(100 MHz, 2:1 $CDCl_3$:CD_3OD) 14.5 (CH_3, CH_2CH_3), [23.2, 26.5 (CH_2, alkyl chain)], 28.8 (CH_3, $OC(CH_3)_3$), [29.9, 30.3, 32.5, 33.1 (CH_2, alkyl chain, resonance

overlap)], 51.8 (CH, C-2), 62.4 (CH_2, C-6′), 68.3 (CH_2, C-1), [69.5, 70.4, 70.9, 71.3 (CH, C-2′, C-3′, C-4′, C-5′)], [72.6, 75.7 (CH, C-3, C-4)], 80.3 (C, O*C*$(CH_3)_3$), 100.3 (CH, C-1′), 156.9 (C, *C*=O); *m/z* (TOF ES+) 602.4 ([M + Na]$^+$, 100%); HRMS *m/z* (TOF ES+) 602.3882 [M + Na]$^+$, $C_{29}H_{57}NO_{10}Na$ requires 602.3880.

(2*S*, 3*S*, 4*R*)-2-[11″-*O*-(3‴-Benzoylphenylmethoxy)-undecanoylamino]-1-*O*-α-D-galactopyranosyl-1, 3, 4-octadecanetriol (333)

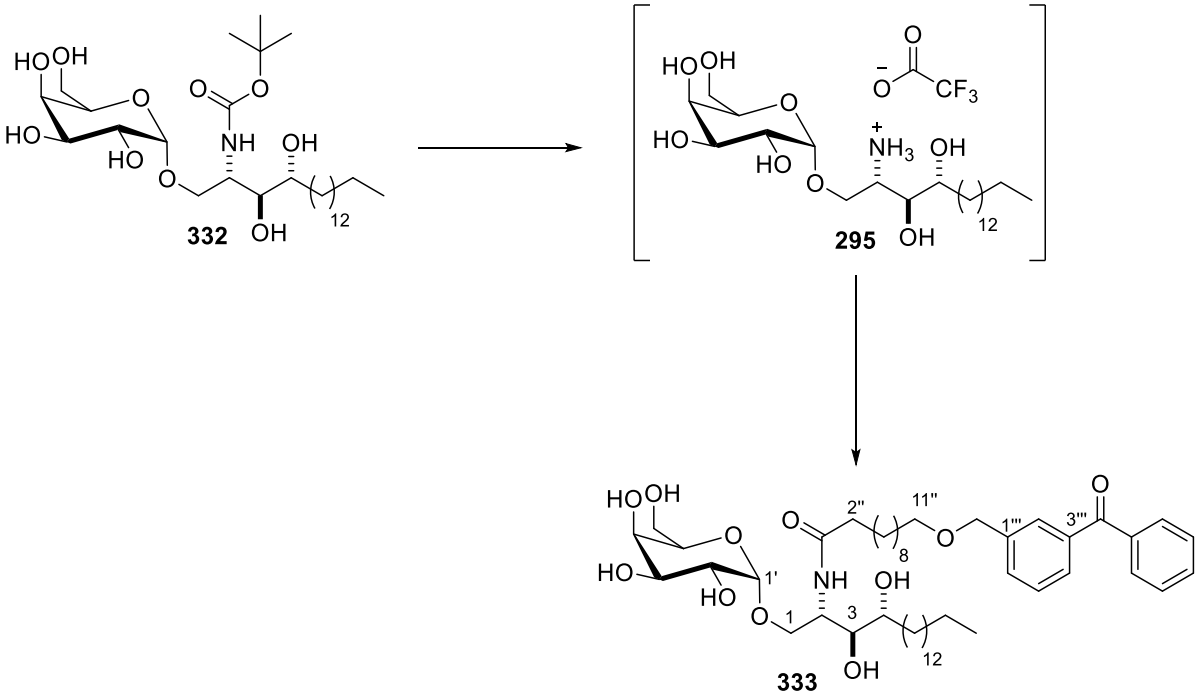

TFA (2 mL) was added to a flask containing glycoside **332** (30 mg, 0.052 mmol). After 30 min, the solvent was removed under reduced pressure. The residue was dissolved in THF (2 mL) followed by addition Et_3N (30 μL, 0.215 mmol) and NHS ester **320** (31 mg, 0.062 mmol). After 14 h at 50 °C, the reaction mixture was concentrated under reduced pressure and purified by flash column chromatography (1% MeOH in $CHCl_3$ →10% MeOH in $CHCl_3$) to afford amide **333** as a colourless syrup (21 mg, 48%): R_f = 0.1 (10% MeOH in $CHCl_3$); solubility issues prevented an optical rotation measurement; ν_{max}(film)/cm^{-1} 3350 br m (O–H, N–H), 2923 m, 2851 m, 1672 vs br (C=O), 1449 m, 1399 w, 1360 w, 1317 w, 1283 w, 1243 w, 1200 vs, 1180

s, 1129 vs, 1072 m, 1034 m, 976 w, 833 m, 799 m, 719 m; δ_H(400 MHz, 2:1 $CDCl_3$:CD_3OD) 0.84 (3H, t, *J* 6.7, CH_2CH_3), 1.2–1.33 (38H, stack, alkyl chain), 1.50–1.67 (5H, stack, alkyl chain), 1.71–1.78 (1H, m, alkyl chain), 2.17 (2H, app. t, *J* 7.7, H-2″), 3.48 (2H, t, *J* 6.6, H-11″), 3.51–3.55 (2H, stack, H-3, H-4), 3.66 (1H, dd, *J* 10.7, 4.4, H-1_A), 3.68–3.80 (4H, stack), 3.85 (1H, dd, *J* 10.7, 4.7, H-1_B), 3.90 (1H, app. d, *J* 3.0), 4.14–4.19 (1H, m, H-2), 4.31 (1H, t, *J* 6.67), 4.55 (2H, s, $ArCH_2$), 4.87 (1H, d, *J* 3.7, H-1′), 7.45–7.51 (3H, Ar C*H*), 7.56–7.63 (2H, stack, Ar C*H*), 7.66–7.69 (1H, m, Ar C*H*), 7.71–7.78 (3H, stack, Ar C*H*), exchangeable protons not observed; δ_C(100 MHz, 2:1 $CDCl_3$:CD_3OD) 14.3 (CH_3, CH_2CH_3), [23.1, 26.3, 29.7, 29.8, 29.9, 30.07, 30.13, 31.5, 32.3, 32.9 (CH_2, alkyl chain, resonance overlap)], 36.9 (CH_2, C-2″), 50.8 (CH, C-2), 62.3 (CH_2, C-6′), 67.8 (CH_2, C-1), [69.4, 70.3, 70.7, 71.1 (CH, C-2′, C-3′, C-4′, C-5′)], 71.3 (CH_2, C-11″), 72.5 (CH, C-3 or C-4), 72.7 (CH_2, $ArCH_2$), 75.1 (CH, C-4 or C-3)], 100.1 (CH, C-1′), [128.8, 128.95, 129.00, 129.8, 130.5, 131.4, 133.2 (CH, Ar *C*H)], 175.0 (C, *C*=O), ketone *C*=O or Ar *C* not observed; *m/z* (TOF ES+) 880.5 ($[M + Na]^+$, 100%); HRMS *m/z* (TOF ES+) 880.5549 $[M + Na]^+$, $C_{49}H_{79}NO_{11}Na$ requires 880.5551.

(2*S*, 3*S*, 4*R*)-2-[13″-(3‴-Benzoylphenyl)tridecanoylamino]-1-*O*-α-D-galactopyranosyl-1, 3, 4-octadecanetriol (334)

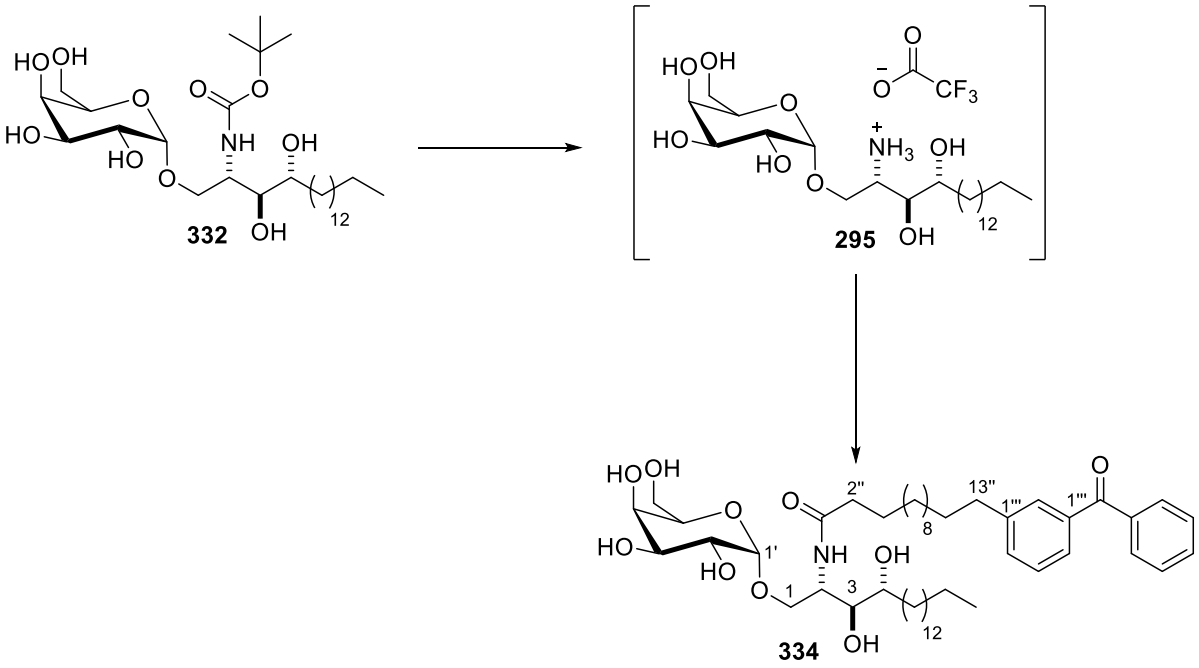

TFA (2 mL) was added to a flask containing glycoside **332** (30 mg, 0.052 mmol). After 30 min, the solvent was removed under reduced pressure. The residue was dissolved in pyridine:H_2O (2 mL, 9:1) and then NHS ester **310** (32 mg, 0.063 mmol) was added. After 14 h at 60 °C, the reaction mixture was co-evaporated with toluene under reduced pressure and purified by flash column chromatography (1% MeOH in $CHCl_3$ →10% MeOH in $CHCl_3$) to afford amide **334** (22 mg, 50%) as a glassy foam: R_f = 0.1 (10% MeOH in $CHCl_3$); solubility issues prevented an optical rotation measurement; ν_{max}(film)/cm^{-1} 3355 br m (O–H, N–H), 2917 vs, 2849 s, 1731 w, 1657 m (C=O), 1638 m, 1465 m, 1348 w, 1316 w, 1280 m, 1207 w, 1153 m, 1061 m, 1029 m, 799 w, 719 m, 644 w, 612 w; δ_H(400 MHz, 2:1 $CDCl_3$:CD_3OD) 0.84 (3H, t, *J* 6.8, CH_2CH_3), 1.20–1.35 (40H, stack, alkyl chain), 1.50–1.67 (6H, stack, alkyl chain), 2.17 (2H, app. t, *J* 7.7, H-2″), 2.65 (2H, app. t, *J* 7.7, H-13″), 3.49–3.54 (2H, stack, H-3, H-4), 3.62–3.79 (6H, stack, incl. H-1$_A$, H-2′, H-6′$_A$, H-6′$_B$), 3.84 (1H, dd, *J* 10.7, 4.6, H-1$_B$), 3.90 (1H, app. d, *J* 3.0), 4.13–4.20 (1H, m, H-2), 4.87 (1H, d, *J* 3.7, H-1′), 7.35–7.43 (2H, Ar C*H*), 7.45–7.50 (2H, stack, Ar

C*H*), 7.53–7.61 (3H, stack, Ar C*H*), 7.73–7.77 (2H, stack, Ar C*H*), exchangeable protons not observed; δ_C(100 MHz, 2:1 $CDCl_3$:CD_3OD) 14.3 (CH_3, CH_2CH_3), [23.1, 26.3, 29.7, 29.8, 29.86, 29.89, 30.07, 30.13, 31.8, 32.3, (CH_2, alkyl chain, resonance overlap)], 32.9 (CH_2, C-13″), 36.9 (CH_2, C-2″), 50.9 (CH, C-2), 62.3 (CH_2, C-6′), 67.8 (CH_2, C-1), [69.4, 70.2, 70.7, 71.3 (CH, C-2′, C-3′, C-4′, C-5′)], [72.4, 75.1 (CH, C-3, C-4)], 100.2 (CH, C-1′), [128.1, 128.7, 128.8, 130.4, 130.5, 133.1, 133.4 (CH, Ar *C*H)], [137.9, 138.1, 143.8 (C, Ar *C*)], 175.0 (C, *C*=O), ketone *C*=O not observed; *m/z* (TOF ES+) 878.6 ([M + Na]$^+$, 100%); HRMS *m/z* (TOF ES+) 878.5762 [M + Na]$^+$, $C_{50}H_{81}NO_{10}Na$ requires 878.5758.

(2*S*, 3*S,* 4*R*)-1-Azido-3, 4-*O*-isopropylidene-2-(*ortho*-nitrobenzenesulfonamido)-3, 4-octadecanediol (348)

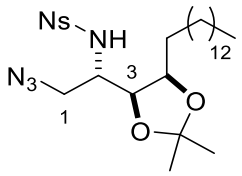

NaN_3 (20 mg, 0.31 mmol) was added to a solution of nosyl aziridine **192** (100 mg, 0.21 mmol) in CH_3CN:H_2O (3 mL; 9:1). After 2 h heating at reflux, the reaction flask was cooled to rt and the CH_3CN was removed under reduced pressure. The residue was dissolved in EtOAc (40 mL) and the mixture was washed sequentially with H_2O (3 × 30 mL), brine (30 mL), dried using Na_2SO_4, filtered and the filtrate concentrated under reduced pressure. The residue was purified by flash column chromatography (10% EtOAc in hexanes) to give azide **348** as a yellow oil (78 mg, 72%): R_f = 0.7 (20% EtOAc in hexanes); $[\alpha]_D^{21}$ = +80.0 (c = 1.0, $CHCl_3$), lit.[130] $[\alpha]_D$ = +11 (c = 1.0, $CHCl_3$); ν_{max}(film)/cm^{-1} 3336 w br (N–H), 2923 s, 2853 s, 2104 s (N_3), 1541 vs, 1442 m, 1421 m, 1354 s, 1300 m, 1251 m, 1217 m, 1167 s, 1123 m, 1059 s, 958 w, 854 m, 783 m, 740 m, 731 m, 700 w, 655 m; δ_H(400 MHz) 0.88 (3H, t, *J* 6.8, CH_2CH_3), 1.22–1.30 (22H, stack, alkyl chain, resonance overlap), 1.33 (3H, s, $C(CH_3)_A(CH_3)_B$), 1.40 (3H, s, $C(CH_3)_A(CH_3)_B$), 1.47–1.67 (4H, stack, alkyl chain), 3.28 (1H, dd, *J* 12.7, 3.0, H-1$_A$), 3.58 (1H,

dd, *J* 12.7, 4.5, H-1_B), 3.78–3.84 (1H, m, H-2), 4.04 (1H, dd, *J* 7.9, 5.7, H-3), 4.18 (1H, ddd, *J* 9.5, 5.7, 3.6, H-4), 5.73 (1H, d, *J* 9.8, N-H), 7.73–7.80 (2H, stack, Ar C*H*), 7.91–7.98 (1H, m, Ar C*H*), 8.13–8.20 (1H, m, Ar C*H*); δ_C(100 MHz) 14.1 (CH_3, CH_2CH_3), 22.7 (CH_2, alkyl chain), 25.4 [CH_3, $C(CH_3)_A(CH_3)_B$], 26.5 (CH_2, alkyl chain), 27.7 (CH_3, $C(CH_3)_A(CH_3)_B$), [29.2, 29.3, 29.47, 29.52, 29.6, 29.7, 31.9 (CH_2, alkyl chain, resonance overlap)], 52.6 (CH, C-1), 53.8 (CH, C-2), 76.5 (CH, C-3), 77.4 (CH, C-4), 108.3 (C, $C(CH_3)_2$), [125.8, 130.1, 133.2, 133.7 (CH, Ar CH)], [135.5, 147.6 (C, Ar C)]; *m/z* (TOF ES+) 590.3 ([M + Na]$^+$, 100%).

Data were in agreement with those reported in the literature.[130]

(2*S*, 3*S*, 4*R*)-2-Amino-1-azido-3, 4-*O*-isopropylidene-3, 4-octadecanediol (349)

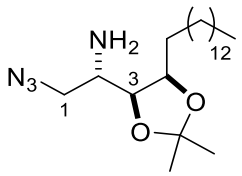

Thiophenol (19 μL, 0.18 mmol) and Cs_2CO_3 (45 mg, 0.14 mmol) were added sequentially to a solution of azide **348** (26 mg, 0.046 mmol) in anhydrous CH_3CN (1 mL). After 16 h, the reaction was quenched by the addition of $NaHCO_3$ solution (20 mL). The phases were partitioned and the aqueous phase was extracted with CH_2Cl_2 (3 × 30 mL). The combined organic fractions were dried with Na_2SO_4, filtered and the filtrate was concentrated under reduced pressure. The residue was purified by flash column chromatography (20% EtOAc in hexanes) to afford amine **349** as a colourless oil (14 mg, 83%): R_f = 0.3 (EtOAc in hexanes); $[\alpha]_D^{21}$ = + 20.0 (c = 1.0, $CHCl_3$), lit.[130] $[\alpha]_D$ = + 19.0 (c = 1.0, $CHCl_3$); ν_{max}(film)/cm^{-1} 3369 w (N–H), 2923 vs, 2853 s, 2102 s (N_3), 1678 w, 1461 m, 1379 m, 1369 m, 1246 m, 1218 m, 1167 m, 1059 s, 871 m, 799 m, 722 m; δ_H(400 MHz) 0.88 (3H, t, *J* 6.8, CH_2CH_3), 1.24–1.28 (21H, stack, alkyl chain), 1.33 (3H, s, $C(CH_3)_A(CH_3)_B$), 1.41 (3H, s, $C(CH_3)_A(CH_3)_B$), 1.44–1.58 (5H, stack, alkyl chain), 2.98 (1H, ddd, *J* 9.1, 6.4, 3.0, H-2), 3.44 (1H, dd, *J* 12.2, 6.4, H-1_A), 3.57 (1H, dd, *J* 12.2, 3.0,

H-1_B), 3.84 (1H, dd, *J* 9.1, 5.6, H-3), 4.16 (1H, ddd, *J* 9.1, 5.6, 3.6, H-4), N*H* not observed; δ_C(100 MHz)) 14.1 (CH_3, CH_2CH_3), 22.7 (CH_2, alkyl chain), 25.8 [CH_3, $C(CH_3)_A(CH_3)_B$, 26.2 (CH_2, alkyl chain), 28.2 [CH_3, $C(CH_3)_A(CH_3)_B$], [29.3, 29.6, 29.7, 29.8, 31.9 (CH_2, alkyl chain, resonance overlap)], 50.4 (CH, C-2), 56.6 (CH_2, C-1), 77.7 (CH, C-4), 79.0 (CH, C-3), 108.1 (C, $C(CH_3)_2$); *m/z* (TOF ES+) 405.3 ($[M + Na]^+$, 30%), 383.3 ($[M + H]^+$, 50%), 325.3 (100%).

Data were in agreement with those reported in the literature.[130]

(2*S*, 3*S,* 4*R*)-1-Azido-2-[13′-(3″-benzoylphenyl)tridecanoylamino] -3, 4-*O*-isopropylidene-3, 4-octadecanediol (350)

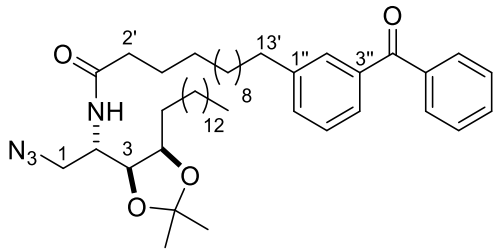

Et_3N (100 μL, 0.66 mmol) and NHS ester **310** (115 mg, 0.242 mmol) were added to a flask containing amine **349** (84 mg, 0.22 mmol) in THF (2 mL), After heating at 50 °C for 14 h, the reaction mixture was concentrated under reduced pressure and the residue purified by flash column chromatography (10% EtOAc in hexanes) to afford amide **350** as a colourless oil (125 mg, 76%): R_f = 0.4 (20% EtOAc in hexanes); $[\alpha]_D^{21}$ = +17.6 (c = 1.0, $CHCl_3$); ν_{max}(film)/cm^{-1} 3303 w (N–H), 2914 vs, 2848 s, 2118 s (N_3), 1645 vs (C=O), 1598 w, 1579 m, 1547 s, 1469 s, 1441 m, 1416 m, 1380 m, 1350 m, 1309 m, 1279 s, 1255 s, 1217 m, 1165 m, 1129 w, 1073 s, 1062 s, 1015 w, 998 w, 986 w, 972 w, 909 w, 864 m, 838 w, 809 w, 784 m, 709 vs, 702 vs, 691 s, 633 m, 606 w; δ_H(400 MHz) 0.88 (3H, t, *J* 6.8, CH_2CH_3), 1.22–1.28 (40H, stack, alkyl chain), 1.33 (3H, s, $C(CH_3)_A(CH_3)_B$), 1.42 (3H, s, $C(CH_3)_A(CH_3)_B$), 1.45–1.55 (2H, stack, alkyl chain), 1.57–1.67 (4H, stack, alkyl chain), 2.16 (2H, app. td, *J* 7.6, 4.1, H-2′), 2.66 (2H, app. t, *J* 7.8, H-13′), 3.47 (1H, dd, *J* 12.4, 3.0, H-1_A), 3.65 (1H, dd, *J* 12.4, 4.1, H-1_B), 4.03 (1H, dd, *J*

8.7, 5.6, H-3), 4.07–4.13 (1H, m, H-4), 4.22 (1H, m, H-2), 5.69 (1H, d, *J* 9.3, N*H*), 7.34–7.42 (2H, stack, Ar C*H*), 7.45–7.50 (2H, stack, Ar C*H*), 7.55–7.61 (2H, stack, Ar C*H*), 7.61–7.64 (1H, m, Ar C*H*), 7.78–7.82 (2H, stack, Ar C*H*); δ_C(100 MHz) 14.1 (CH_3, CH_2CH_3), 22.7 (CH_2, alkyl chain), 25.6 (CH_3, $C(CH_3)_A(CH_3)_B$), [25.7, 26.5 (CH_2, alkyl chain)], 27.9 (CH_3, $C(CH_3)_A(CH_3)_B$), [29.1, 29.2, 29.3, 29.4, 29.45, 29.49, 29.54, 29.6, 29.7, 31.4, 31.9, (CH_2, alkyl chain, resonance overlap)], 35.8 (CH, C-13′), 36.8 (CH_2, C-2′), 48.0 (CH, C-2) 53.0 (CH_2, C-1), 76.2 (CH, C-3), 77.6 (CH, C-4), 108.3 (C, $C(CH_3)_2$), [127.6, 128.1, 128.2, 129.8, 130.0, 132.6, 133.7 (CH, Ar CH)], [137.5, 137.8, 143.2 (C, Ar C)], 172.5 (C, amide *C*=O), 197.1 (C, ketone *C*=O); *m/z* (TOF ES+) 781.6 ([M + Na]$^+$, 100%); HRMS *m/z* (TOF ES+) 781.5610 [M + Na]$^+$, $C_{47}H_{74}N_4O_4Na$ requires 781.5608

(2*S*, 3*S*, 4*R*)-1-Azido-2-[13′-(3″-benzoylphenyl)tridecanoylamino]-3, 4-octadecanediol (342)

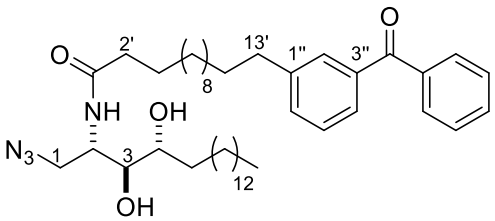

TFA (5 drops) and H_2O (2 drops) were added to a solution of amide **350** (120 mg, 0.16 mmol) in CH_2Cl_2 (2 mL). After 12 h, the solvent was removed under reduced pressure. EtOAc (40 mL) was added to the residue and the solution was washed with $NaHCO_3$ solution (3 × 25 mL), dried with Na_2SO_4, filtered and the filtrate was concentrated under reduced pressure. The residue was purified by column chromatography (30% EtOAc in hexanes) to yield diol **342** as an off-white amorphous solid (63 mg, 56%): R_f = 0.1 (30% EtOAc in hexanes); solubility issues prevented an optical rotation measurement; ν_{max}(film)/cm^{-1} 3274 br s (O–H, N–H), 2921 vs, 2852 vs, 2100 vs (N_3), 1660 s (C=O), 1642 vs (C=O), 1598 w, 1581 s, 1533 m, 1466 m, 1447 m, 1316 m, 1279 vs, 1207 w, 1178 w, 1149 w, 1098 w, 1047 w, 960 w, 812 w, 779 m, 718 vs,

709 vs; δ_H(400 MHz)) 0.87 (3H, t, *J* 6.8, CH_2CH_3), 1.22–1.35 (40H, stack, alkyl chain), 1.38–1.55 (2H, stack, alkyl chain), 1.57–1.70 (4H, stack, alkyl chain), 2.20 (2H, app. dd, *J* 8.1, 7.0, H-2′), 2.46 (1H, br s, O*H*), 2.66 (2H, app. t, *J* 7.7, H-13′), 3.42 (1H, br s, O*H*), 3.56–3.63 (3H, stack, H-1_A, H-3, H-4), 3.77 (1H, dd, *J* 12.6, 5.7, H-1_B), 4.12–4.18 (1H, m, H-2), 6.18 (1H, d, *J* 8.3, N*H*), 7.35–7.42 (2H, stack, Ar C*H*), 7.45–7.50 (2H, stack, Ar C*H*), 7.56–7.61 (2H, stack, Ar C*H*), 7.61–7.64 (1H, m, Ar C*H*), 7.78–7.82 (2H, stack, Ar C*H*); δ_C(100 MHz) 14.1 (CH_3, CH_2CH_3), [22.7, 25.6, 28.8, 29.25, 29.33, 29.4, 29.5, 29.57, 29.65, 29.7, 31.4, 31.9, 33.0 (CH_2, alkyl chain, resonance overlap)], 35.8 (CH, C-13′), 36.8 (CH_2, C-2′), 50.7 (CH, C-2), 51.4 (CH_2, C-1), [73.0, 75.1 (CH, C-3, C-4)], [127.7, 128.1, 128.3, 129.9, 130.1, 132.4, 132.7 (CH, Ar CH)], [137.5, 137.8, 143.2 (C, Ar C)], 174.0 (C, amide *C*=O), 197.2 (C, ketone *C*=O); *m/z* (TOF ES+) 741.5 ([M + Na]$^+$, 100%); HRMS *m/z* (TOF ES+) 741.5298 [M + Na]$^+$, $C_{44}H_{70}N_4O_4Na$ requires 741.5295.

(2*S*, 3*S,* 4*R*)-1-(4′-(Propan-3″-ol)-1H-1′,2′,3′-triazol-1′-yl)-2-[13‴-(3⁗-benzoylphenyl)tridecanoylamino]-octadecan-3,4-diol (351)

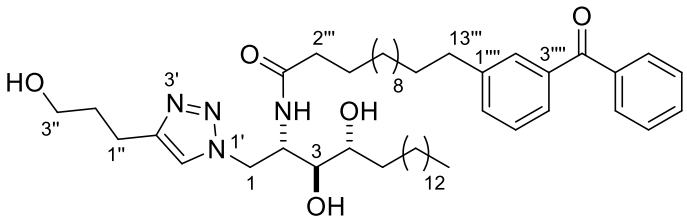

Freshly prepared solutions of $CuSO_4$ solution (12 μL of 0.5 M solution, 0.006 mmol) and sodium ascorbate solution (20 μL of 1.0 M solution, 0.0020 mmol) were added to a solution of diol **342** (27 mg, 0.0375 mmol) and 4-pentynol (4 mg, 0.045 mmol) in H_2O:THF (2 mL, 2:1). After heating the reaction mixture at 80 °C for 5 h, the solvent was evaporated under reduced pressure and the residue was purified by flash column chromatography (1% MeOH in $CHCl_3$ → 10% MeOH in $CHCl_3$) to afford triazole **351** as a white solid (27 mg, 90%): R_f = 0.5 (10% MeOH in $CHCl_3$); m.p. 143–147 °C; solubility issues prevented an optical rotation

measurement; ν_{max}(film)/cm^{-1} 3337 br w (O-H, N–H), 2918 vs, 2848 s, 1657 m (C=O), 1632 s (C=O), 1579 w, 1464 m, 1309 w, 1279 m, 1208 w, 1149 w, 1072 m, 1028 w, 971 w, 909 w, 720 m; δ_H(400 MHz, 2:1 $CDCl_3$:CD_3OD) 0.83 (3H, t, *J* 6.8, CH_2CH_3), 1.17–1.32 (40H, stack, alkyl chain), 1.36–1.45 (3H, stack, alkyl chain), 1.46–1.65 (3H, stack, alkyl chain),1.78–1.86 (2H, stack, H-2″), 1.99–2.04 (2H, stack, H-2‴), 2.63 (2H, app. t, *J* 7.7, H-13‴), 2.71 (2H, app. t, *J* 7.4, H-1″), 3.40–3.49 (2H, stack, H-3, H-4), 3.53 (2H, app.t, *J* 6.3, H-3″), 4.40 (1H, app. dt, *J* 8.4, 4.7, H-2), 4.48–4.59 (2H, stack, H-1), 7.32–7.40 (2H, stack, Ar C*H*), 7.42–7.49 (3H, stack, Ar C*H*), 7.52–7.59 (3H, stack, Ar C*H*), 7.72–7.76 (2H, stack, Ar C*H*) exchangeable protons not observed; δ_C(100 MHz, 2:1 $CDCl_3$:CD_3OD) 14.2 (CH_3, CH_2CH_3), 21.8 (CH_2, C-1″), [22.8 25.8, 26.0, 29.4, 29.5, 29.66, 29.68, 29.8, 29.9, 31.6 (CH_2, alkyl chain, resonance overlap)], [32.0, 32.1, 32.8 (CH_2, alkyl chain including C-2″)], 36.0 (CH_2, C-13‴), 36.5 (CH_2, C-2‴), 49.8 (CH_2, C-1), 51.2 (CH, C-2), 61.1 (CH_2, C-3″), [72.3, 75.0 (CH, C-3, C-4)], 122.9 (CH, Ar CH, triazole), [127.8, 128.4, 128.5, 130.1, 130.3, 132.8, 133.1 (CH, Ar CH)], [143.4, 143.5, 147.7 (C, Ar C)], 174.9 (C, amide *C*=O), triazole *C* and ketone *C*=O not observed; *m/z* (TOF ES+) 825.6 ([M + Na]$^+$, 100%); HRMS *m/z* (TOF ES+) 825.5868 [M + Na]$^+$, $C_{49}H_{78}N_4O_5Na$ requires 825.5870.

(3*S*, 4*S,* 5*R*)-4, 5-*O*-Isopropylidene-2-(*ortho*-nitrobenzenesulfonamido)-1-nonadecanenitrile-4, 5-diol (352)

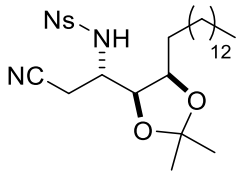

NaCN (14 mg, 0.29 mmol) was added to a solution of nosyl aziridine **192** (100 mg, 0.19 mmol) in CH_3CN:H_2O (2 mL; 9:1). After heating at reflux for 3 h, the flask was cooled to rt and the CH_3CN was removed under reduced pressure. EtOAc (40 mL) was added and the solution was washed sequentially with H_2O (3 × 25 mL) and brine (30 mL), dried using Na_2SO_4, filtered

and the filtrate concentrated under reduced pressure. The residue was purified by flash column chromatography (10% EtOAc in hexanes) to give nitrile **352** as a yellow oil (72 mg, 64%): R_f = 0.6 (20% EtOAc in hexanes); $[\alpha]_D^{21}$ = + 42.8 (c = 1.0, $CHCl_3$), lit.[130] $[\alpha]_D$ = + 9.3 (c = 1.0, $CHCl_3$); ν_{max}(film)/cm^{-1} 3352 w br (N–H), 2989 w, 2922 vs, 2852 s, 2244 w (CN), 1597 w, 1534 vs, 1469 m, 1443 m, 1427 s, 1396 m, 1346 vs, 1247 m, 1219 m, 1168 vs, 1115 m, 1052 s, 932 w, 857 m, 824 m, 787 s, 739 s, 730 m, 686 m, 654 s; δ_H(400 MHz) 0.88 (3H, t, *J* 6.8, CH_2CH_3), 1.22–1.30 (24H, stack, alkyl chain, resonance overlap), 1.33 (3H, s, $C(CH_3)_A(CH_3)_B$), 1.41 (3H, s, $C(CH_3)_A(CH_3)_B$), 1.43–1.51 (2H, stack, alkyl chain), 2.63 (1H, dd, *J* 17.1, 4.0, H-2_A), 2.73 (1H, dd, *J* 17.1, 5.7, H-2_B) 3.91–3.98 (1H, m, H-3), 4.13 (1H, app. t, *J* 6.4, H-4), 4.19 (1H, ddd, *J* 9.3, 5.9, 3.2, H-5), 5.78–5.84 (1H, m, N*H*), 7.75–7.80 (2H, stack, Ar C*H*), 7.90–7.96 (1H, m, Ar C*H*), 8.15–8.20 (1H, m, Ar C*H*); δ_C(100 MHz) 14.1 (CH_3, CH_2CH_3), 21.9 (CH_2, C-2), 22.7 (CH_2, alkyl chain), 25.1 (CH_3, $C(CH_3)_A(CH_3)_B$), 26.6 (CH_2, alkyl chain), 27.4 [CH_3, $C(CH_3)_A(CH_3)_B$], [29.2, 29.4, 29.45, 29.51, 29.6, 29.7, 31.9 (CH_2, alkyl chain, resonance overlap)], 51.2 (CH, C-3), 77.1 (CH, C-5), 77.8 (CH, C-4), 108.7 (C, $C(CH_3)_2$), 116.4 (C, C-1), [125.8, 130.2, 133.3, 134.1 (CH, Ar CH)], [135.0, 147.7 (C, Ar C)]; *m/z* (TOF ES+) 574.3 ([M + Na]$^+$, 100%).

Data were in agreement with those reported in the literature.[130]

(3*S*, 4*S,* 5*R*)-2-Amino-4, 5-*O*-Isopropylidene-1-nonadecanenitrile-4, 5-diol (353)

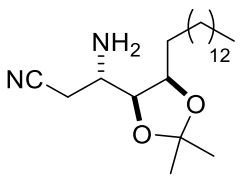

Thiophenol (27 μL, 0.26 mmol) and Cs_2CO_3 (64 mg, 0.20 mmol) were added sequentially to a solution of nitrile **353** (36 mg, 0.065 mmol) in CH_3CN (2 mL). After 16 h, the reaction was quenched by addition of $NaHCO_3$ solution (20 mL). The mixture was extracted with CH_2Cl_2 (3 × 30 mL). The combined organic layers were dried with Na_2SO_4, filtered and the filtrate

concentrated under reduced pressure. The residue was purified by flash column chromatography (20% EtOAc in hexanes) to afford amine **353** as a colourless oil (22 mg, 92%): R_f = 0.2 (20% EtOAc in hexanes); $[\alpha]_D^{21}$ = +11.2 (c = 1.0, $CHCl_3$); ν_{max}(film)/cm^{-1} 3387 vw (NH_2) 2922 vs, 2852 s, 2249 w (CN), 1620 w, 1465 m, 1370 m, 1246 m, 1218 s, 1166 m, 1069 m, 871 m, 797 w, 766 w; δ_H(400 MHz) 0.88 (3H, t, *J* 6.8, CH_2CH_3), 1.24–1.30 (21H, stack, alkyl chain), 1.33 (3H, s, $C(CH_3)_A(CH_3)_B$), 1.40 (3H, s, $C(CH_3)_A(CH_3)_B$), 1.42–1.60 (5H, stack, alkyl chain), 2.52 (1H, dd, *J* 16.7, 7.4, H-2_A), 2.72 (1H, dd, *J* 16.7, 3.5, H-2_B), 3.14 (1H, ddd, *J* 8.8, 7.4, 3.5, H-3), 3.82 (1H, dd, *J* 8.8, 5.7, H-4), 4.17 (1H, ddd, *J* 10.6, 5.7, 2.5, H-5), NH_2 not observed; δ_C(100 MHz) 14.1 (CH_3, CH_2CH_3), 22.7 (CH_2, C-2), 25.4 (CH_2, alkyl chain), 25.7 (CH_3, $C(CH_3)_A(CH_3)_B$), 26.3 (CH_2, alkyl chain), 28.1 (CH_3, $C(CH_3)_A(CH_3)_B$), [29.4, 29.66, 29.68, 31.9 (CH_2, alkyl chain, resonance overlap)], 48.0 (CH, C-3), 77.6 (CH, C-5), 80.1 (CH, C-4), 108.1 (C, $C(CH_3)_2$), 118.2 (C, C-1); *m/z* (TOF ES+) 367.3 ($[M + H]^+$, 100%); HRMS *m/z* (TOF ES+) 367.3319 $[M + H]^+$, $C_{22}H_{43}N_2O_2$ requires 367.3325.

(4*S*, 5*S,* 6*R*)-5, 6-*O*-Isopropylidene-4-(*ortho*-nitrobenzenesulfonamido)-1-trimethylsilyl-eicos-1-yne-5, 6-diol (354)

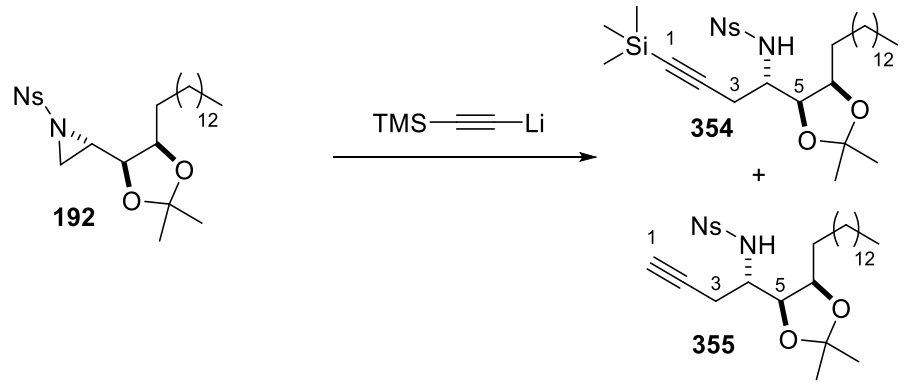

*n*BuLi (0.35 mL, 0.88 mmol, 2.5 M solution in hexanes) was added to a solution of (trimethylsilyl)acetylene (0.12 mL, 0.88 mmol) in THF:HMPA (1.5 mL, 10:1) at –78 °C. After 30 min, a solution of Ns-aziridine **192** (155 mg, 0.30 mmol) in THF:HMPA (0.5 mL, 10:1) was added via syringe at –78 °C. The reaction mixture was stirred for 2 h at –78 °C, then at rt for12

h. The reaction was then quenched with NH_4Cl solution (20 mL) and extracted with Et_2O (3 × 30 mL). The combined organic extracts were washed with brine (50 mL), dried using Na_2SO_4, filtered, and the filtrate concentrated under reduced pressure. The residue was purified by flash column chromatography (10% EtOAc/hexane) to give in order of elution silyl alkyne **354** as a colourless oil (0.086 g, 46%): R_f = 0.6 (20% EtOAc in hexanes); $[\alpha]_D^{21}$ = +136.0 (c = 1.0, $CHCl_3$); ν_{max}(film)/cm^{-1} 3324 w (N–H), 2924 vs, 2854 s, 2175 w (C≡C), 1542 vs, 1442 m, 1420 s, 1355 vs, 1249 s, 1218 m, 1173 vs, 1123 m, 1059 m, 844 vs, 784 m, 759 m, 740 m, 699 m, 655 m; δ_H(400 MHz) 0.08 (9H, s, Si(CH_3)$_3$), 0.87 (3H, t, *J* 6.8, CH_2CH_3), 1.22–1.30 (23H, stack, alkyl chain, resonance overlap), 1.33 (3H, s, C(CH_3)$_A$(CH$_3$)$_B$), 1.39 (3H, s, C(CH$_3$)$_A$(CH_3)$_B$), 1.50–1.65 (2H, stack, alkyl chain), 1.67–1.77 (1H, m, alkyl chain), 2.22 (1H, dd, *J* 17.2, 4.5, H-3$_A$), 2.62 (1H, dd, *J* 17.2, 3.2, H-3$_B$) 3.81–3.89 (1H, m, H-4), 4.10 (1H, dd, *J* 9.1, 5.4, H-5), 4.19 (1H, ddd, *J* 10.4, 5.4, 3.1, H-6), 5.96 (1H, d, *J* 10.1, N*H*), 7.73–7.79 (2H, stack, Ar C*H*), 7.93–7.98 (1H, m, Ar C*H*), 8.13–8.18 (1H, m, Ar C*H*); δ_C(100 MHz) –0.2 (CH$_3$, Si(*C*H$_3$)$_3$), 14.1 (CH$_3$, CH$_2$*C*H$_3$), 22.7 (CH$_2$, alkyl chain), 23.0 (CH$_2$, C-3), 25.6 [CH$_3$, C(*C*H$_3$)$_A$(CH$_3$)$_B$], 26.3 (CH$_2$, alkyl chain), 28.0 [CH$_3$, C(CH$_3$)$_A$(*C*H$_3$)$_B$], [29.3, 29.48, 29.58, 29.64, 29.67, 31.9 (CH$_2$, alkyl chain, resonance overlap)], 51.9 (CH, C-4), 76.4 (CH, C-5), 77.6 (CH, C-6), 89.1 (C, C-2), 99.9 (C, C-1) 108.0 (C, *C*(CH$_3$)$_2$), [125.8, 130.1, 133.4, 133.6 (CH, Ar CH)], [135.9, 147.6 (C, Ar C)]; *m/z* (TOF ES+) 645.3 ([M + Na]$^+$, 100%); HRMS *m/z* (TOF ES+) 645.3372 [M + Na]$^+$, $C_{32}H_{54}N_2O_6SiNa$ requires 645.337, followed by alkyne **355** as a colourless oil (0.039 g, 25%): R_f = 0.5 (20% EtOAc in hexanes); $[\alpha]_D^{21}$ = +89.2 (c = 1.0, $CHCl_3$); ν_{max}(film)/cm^{-1} 3311 w (N–H), 2923 vs, 2853 s, 1541 vs, 1460 m, 1442 m, 1421 m, 1353 vs, 1302 w, 1245 m, 1216 m, 1169 vs, 1124 m, 1056 s, 945 w, 854 m, 783 m, 755 vs, 741 vs, 699 m, 655 s; δ_H(400 MHz) 0.87 (3H, t, *J* 6.8, CH_2CH_3), 1.24–1.30 (23H, stack, alkyl chain, resonance overlap), 1.33 (3H, s, C(CH_3)$_A$(CH$_3$)$_B$), 1.40 (3H, s, C(CH$_3$)$_A$(CH_3)$_B$), 1.48–1.62 (2H, stack, alkyl chain), 1.63–1.72 (1H, m, alkyl chain), 1.82 (1H, app. t, *J* 2.6, H-1), 2.25 (1H, ddd, *J* 17.2, 4.1, 2.6, H-3$_A$), 2.57 (1H, ddd, *J* 17.2, 4.2, 2.6, H-3$_B$), 3.84 (1H, app. ddt, *J* 9.8, 8.1, 4.2, H-4), 4.13 (1H, dd, *J* 8.1, 5.7, H-5), 4.15–4.22 (1H, m, H-6), 5.86 (1H, d, *J* 9.8, N*H*), 7.72–7.79 (2H, stack, Ar C*H*), 7.93–

7.98 (1H, m, Ar C*H*), 8.14–8.20 (1H, m, Ar C*H*); δ_C(100 MHz) 14.1 (CH_3, CH_2CH_3), 21.8 (CH_2, C-3), 22.7 (CH_2, alkyl chain), 25.5 [CH_3, $C(CH_3)_A(CH_3)_B$], 26.5 (CH_2, alkyl chain), 27.8 [CH_3, $C(CH_3)_A(CH_3)_B$), [29.2, 29.4, 29.5, 29.6, 29.7, 31.9 (CH_2, alkyl chain, resonance overlap)], 52.5 (CH, C-4), 71.9 (CH, C-1), 77.1 (CH, C-5), 77.6 (CH, C-6), 78.4 (C, C-2), 108.2 (C, $C(CH_3)_2$), [125.8, 130.3, 133.3, 133.6 (CH, Ar CH)], [135.8, 147.6 (C, Ar C)]; *m/z* (TOF ES+) 573.3 ([M + Na]$^+$, 100%); HRMS *m/z* (TOF ES+) 573.2977 [M + Na]$^+$, $C_{29}H_{46}N_2O_6SNa$ requires 573.2974.

(4*S*, 5*S,* 6*R*)-5, 6-*O*-Isopropylidene-4-(*ortho*-nitrobenzenesulfonamido)-eicos-1-yne-5, 6-diol (355)

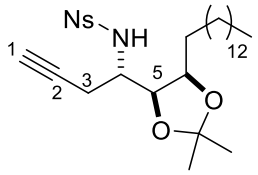

TBAF (0.3 mL of a 1.0 M solution in THF, 0.3 mmol) was added to a solution of silyl alkyne **354** (86 mg, 0.14 mmol) in THF (2 mL). After 14 h, the reaction mixture was concentrated under reduced pressure. The residue was dissolved in EtOAc (30 mL). The solution was washed sequentially with H_2O (3 × 20 mL) and brine (1 × 20 mL). The combined organic layers were dried with Na_2SO_4, filtered and the filtrate was concentrated under reduced pressure. The residue was purified by flash column chromatography to yield alkyne **355** as a colourless oil (76 mg, quant.).

Data in agreement with those obtained for the same compound prepared from **192** (see p 282).

(4*S*, 5*S,* 6*R*)- 4-Amino-5, 6-*O*-isopropylidene-eicos-1-yne-5, 6-diol (356)

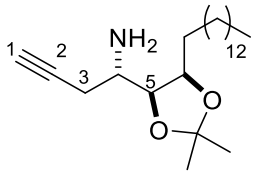

Thiophenol (76 μL, 0.74 mmol) and Cs_2CO_3 (181 mg, 0.556 mmol) were sequentially added to a solution of alkyne **355** (101 mg, 0.185 mmol) in anhydrous CH_3CN (2 mL). After 16 h, the reaction was quenched by addition of $NaHCO_3$ solution (20 mL). The mixture was extracted with CH_2Cl_2 (3 × 30 mL). The combined organic fractions were dried with Na_2SO_4, filtered and the filtrate was concentrated under reduced pressure. The residue was purified by flash column chromatography (1% MeOH in $CHCl_3$ → 10% MeOH in $CHCl_3$) to afford amine **356** as a colourless oil (52 g, 77%): R_f = 0.3 (20% EtOAc in hexanes); $[\alpha]_D^{21}$ = +20.0 (c = 1.0, $CHCl_3$); ν_{max}(film)/cm^{-1} 3311 m (alkynyl C–H), 3291 vw (N–H) 2923 vs, 2853 vs, 1463 m, 1378 m, 1369 m, 1245 m, 1218 s, 1165 w, 1070 w, 869 w, 722 w; δ_H(400 MHz) 0.87 (3H, t, *J* 6.8, CH_2CH_3), 1.23–1.29 (23H, stack, alkyl chain, resonance overlap), 1.32 (3H, s, $C(CH_3)_A(CH_3)_B$), 1.40 (3H, s, $C(CH_3)_A(CH_3)_B$), 1.45–1.60 (3H, stack, alkyl chain), 2.03 (1H, app. t, *J* 2.6, H-1), 2.34 (1H, ddd, *J* 16.8, 7.5, 2.6, H-3$_A$), 2.58 (1H, app. dt, *J* 16.8, 3.0, H-3$_B$), 2.96 (1H, ddd, *J* 9.0, 7.5, 3.4, H-4), 3.83 (1H, dd, *J* 9.0, 5.6, H-5), 4.11–4.16 (1H, m, H-6), NH_2 not observed; δ_C(100 MHz) 14.1 (CH_3, CH_2CH_3), 22.7 (CH_2, alkyl chain), 25.8 (CH_2, C-3), 25.9 (CH_3, $C(CH_3)_A(CH_3)_B$), 26.2 (CH_2, alkyl chain), 28.3 (CH_3, $C(CH_3)_A(CH_3)_B$), [29.4, 29.6, 29.7, 29.8, 31.9 (CH_2, alkyl chain, resonance overlap)], 49.2 (CH, C-4), 70.7 (CH, C-1), 77.9 (CH, C-6), 80.3 (CH, C-5), 81.3 (C, C-2), 107.8 (C, $C(CH_3)_2$); *m/z* (TOF ES+) 388.3 ([M + Na]$^+$, 100%); HRMS *m/z* (TOF ES+) 388.3188 [M + Na]$^+$, $C_{23}H_{43}NO_2Na$ requires 388.3191.

(4*S*, 5*S,* 6*R*)-4-[13′-(3″-benzoylphenyl)tridecanoylamino]-5, 6-*O*-isopropylidene-eicos-1-yne-5, 6-diol (357)

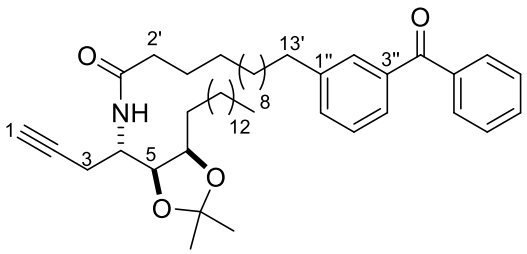

NHS ester **310** (61 mg, 0.12 mmol) was added to a solution of amine **356** (45 mg, 0.12 mmol) in pyridine:H_2O (9:1, 3 mL). After heating at 50 °C for 14 h, the reaction mixture was concentrated under reduced pressure and the residue was purified by flash column chromatography (10% EtOAc in hexanes) to afford amide **357** as a colourless oil (55 mg, 60%): R_f = 0.4 (20% EtOAc in hexanes); $[\alpha]_D^{21}$ = +15.6 (c = 1.0, $CHCl_3$); ν_{max}(film)/cm^{-1} 3303 m (alkynyl C–H), 3254 w (N–H), 2915 vs, 2848 s, 1649 s (C=O), 1598 w, 1543 m, 1468 m, 1380 w, 1310 w, 1277m, 1247 w, 1222 w, 1177w, 1070 w, 864 w, 773 w, 720 w; δ_H(400 MHz) 0.87 (3H, t, *J* 6.8, CH_2CH_3), 1.22–1.33 (40H, stack, alkyl chain), 1.34 (3H, s, $C(CH_3)_A(CH_3)_B$), 1.42 (3H, s, $C(CH_3)_A(CH_3)_B$), 1.45–1.56 (2H, stack, alkyl chain), 1.58–1.66 (4H, stack, alkyl chain), 1.99 (1H, app. t, *J* 2.6, H-1), 2.17 (2H, m, H-2′), 2.50 (ddd, *J* 16.9, 4.0, 2.8, H-3_A), 2.60 (ddd, *J* 16.9, 5.0, 2.6, H-3_B), 2.66 (2H, app. t, *J* 7.7, H-13′), 4.07– 4.12 (2H, stack, H-5, H-6), 4.18–4.26 (1H, m, H-4), 5.63 (1H, d, *J* 9.5, N*H*), 7.34–7.42 (2H, stack, Ar C*H*), 7.45–7.50 (2H, stack, Ar C*H*), 7.55–7.61 (2H, stack, Ar C*H*), 7.61–7.64 (1H, m, Ar C*H*), 7.78–7.82 (2H, stack, Ar C*H*); δ_C(100 MHz) 14.1 (CH_3, CH_2CH_3), 21.9 (CH_2, C-3), 22.6 (CH_2, alkyl chain), 25.6 (CH_3, $C(CH_3)_A(CH_3)_B$), [25.7, 26.6 (CH_2, alkyl chain)], 27.8 (CH_3, $C(CH_3)_A(CH_3)_B$), [29.1, 29.3, 29.4, 29.5, 29.6, 29.7, 31.4, 31.9, (CH_2, alkyl chain, resonance overlap)], 35.8 (CH, C-13′), 36.9 (CH_2, C-2′), 46.3 (CH, C-4), 70.7 (CH, C-1), [77.3, 77.7 (CH, C-5, C-6)], 80.3 (C, C-2), 108.1 (C, $C(CH_3)_2$), [127.6, 128.1, 128.2, 129.9, 130.1, 132.3, 132.6 (CH, Ar CH, resonance overlap)], [137.6, 137.8, 143.2 (C, Ar C)], 172.5 (C, amide *C*=O), 197.0 (C, ketone *C*=O); *m/z*

(TOF ES+) 742.6 ([M + H]$^+$, 100%); HRMS *m/z* (TOF ES+) 742.5772 [M + H]$^+$, $C_{49}H_{76}N\,O_4$ requires 742.5774.

(4*S*, 5*S,* 6*R*)-4-[13′-(3″-benzoylphenyl)tridecanoylamino]-eicos-1-yne-5, 6-diol (344)

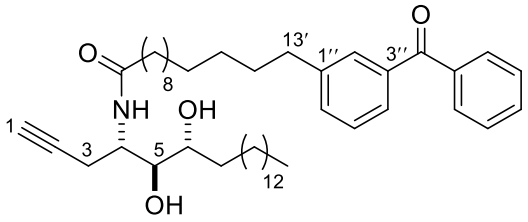

TFA (6 drops) was added to a solution of amide **357** (50 mg, 0.067 mmol) in CH_2Cl_2 (2 mL). After 12 h, the mixture was concentrated under reduced pressure. The residue was dissolved in EtOAc (40 mL) and the solution was washed with $NaHCO_3$ solution (3 × 25 mL), then dried with Na_2SO_4, filtered and the filtrate was concentrated under reduced pressure. The crude product was purified by column chromatography (30% EtOAc in hexanes) to yield diol **344** as a white amorphous solid (38 mg, 85%): R_f = 0.1 (30% EtOAc in hexanes); solubility issues prevented an optical rotation measurement; ν_{max}(film)/cm^{-1} 3304 br m (O–H, alkynyl C–H), 2921 vs, 2851 vs, 1641 vs (C=O), 1598 w, 1537 m, 1465 m, 1316 m, 1279 s, 1206 w, 1139 w, 1068 w, 1026 w, 719 s; δ_H(400 MHz) 0.87 (3H, t, *J* 6.8, CH_2CH_3), 1.22–1.35 (41H, stack, alkyl chain), 1.58–1.69 (5H, stack, alkyl chain), 2.03 (1H, app. t, *J* 2.6, H-1), 2.20 (2H, app. dd, *J* 8.0, 7.1, H-2′), 2.56 (1H, ddd, *J* 17.1, 4.7, 2.6, H-3$_A$), 2.66 (2H, app. t, *J* 7.7, H-13′), 2.73 (1H, ddd, *J* 17.1, 6.4, 2.6, H-3$_B$), 3.60–3.65 (2H, stack, H-5, H-6), 4.11–4.18 (1H, m, H-4), 6.11 (1H, d, *J* 8.5, N*H*), 7.35–7.42 (2H, stack, Ar C*H*), 7.45–7.50 (2H, stack, Ar C*H*), 7.56–7.61 (2H, stack, Ar C*H*), 7.61–7.64 (1H, m, Ar C*H*), 7.78–7.82 (2H, stack, Ar C*H*) O*H*s not observed; δ_C(100 MHz) 14.1 (CH_3, CH_2CH_3), 20.0 (CH_2, C-3), [22.7, 25.7, 25.9, 29.2, 29.4, 29.5, 29.6, 29.65, 29.72, 31.4, 31.9, 33.0 (CH_2, alkyl chain, resonance overlap)], 35.8 (CH_2, C-13′), 36.8 (CH_2, C-2′), 49.8 (CH, C-4), 70.9 (CH, C-1), [73.2, 75.6 (CH, C-5, C-6)], 81.3 (C, C-2), [127.6, 128.1, 128.2, 129.9, 130.1, 132.3, 132.6 (CH, Ar CH, resonance overlap)], [137.6, 137.8,

143.2 (C, Ar C)], 173.8 (C, amide *C*=O), 197.1 (C, ketone *C*=O); *m/z* (TOF ES+) 724.5 ([M + Na]$^+$, 100%); HRMS *m/z* (TOF ES+) 724.5278 [M + Na]$^+$, $C_{46}H_{71}NO_4Na$ requires 724.5281.

(2*S*, 3*S,* 4*R*)-1-[1′-(3″-Hydroxypropyl)-1*H*-1′,2′,3′-triazol-4′-yl]-2-[13‴-(3‴″-benzoylphenyl)tridecanoylamino]-octadecan-3,4-diol (358)

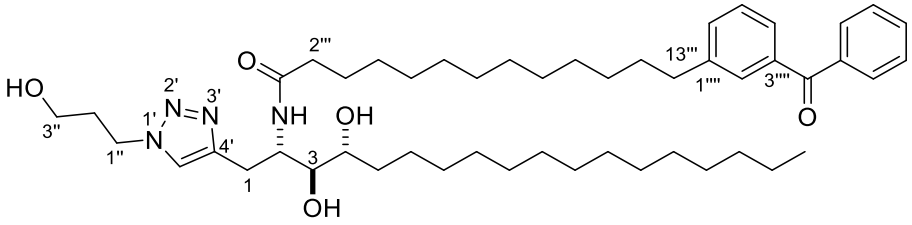

Freshly prepared $CuSO_4$ solution (8 μL of a 0.5 M solution, 0.004 mmol) and sodium ascorbate solution (63 μL of 1.0 M solution, 0.016 mmol) were added to a solution of diol **344** (28 g, 0.040 mmol) and 3-azidopropan-1-ol (6 mg, 0.06 mmol) in H_2O:THF (1.5 mL, 2:1) After heating at 80 °C for 5 h, the solvent was evaporated under reduced pressure. The residue was purified by flash column chromatography (1% MeOH in $CHCl_3$ → 10% MeOH in $CHCl_3$) to afford triazole **358** as a white solid (25 mg, 78%): R_f = 0.5 (10% MeOH in $CHCl_3$); m.p. 144–147 °C; solubility issues prevented an optical rotation measurement; ν_{max}(film)/cm^{-1} 3236 br m (O–H, N–H), 2918 s, 2849 s, 1656 m (C=O), 1633 s (C=O), 1560 m, 1468 m, 1339 w, 1278 m, 1066 s, 720 m; δ_H(400 MHz, 2:1 $CDCl_3$:CD_3OD) 0.84 (3H, t, *J* 6.9, CH_2CH_3), 1.19–1.33 (42H, stack, alkyl chain), 1.36–1.70 (4H, stack, alkyl chain), 2.00–2.08 (4H, stack, H-2″, H-2‴), 2.64 (2H, app. t, *J* 7.7, H-13‴), 2.85 (1H, dd, *J* 15.1, 10.2, H-1$_A$), 3.05 (1H, dd, *J* 15.1, 3.4, H-1$_B$) 3.39–3.53 (4H, stack, H-3, H-4, H-3″), 4.26–4.32 (1H, m, H-2), 4.41 (2H, t, *J* 6.9, H-1″), 7.34–7.42 (2H, stack, Ar C*H*), 7.43–7.49 (2H, stack, Ar C*H*), 7.53–7.61 (4H, stack, Ar C*H*), 7.73–7.77 (2H, stack, Ar C*H*), exchangeable protons not observed; δ_C(100 MHz, 2:1 $CDCl_3$:CD_3OD) 14.3 (CH_3, CH_2CH_3), 23.0 (CH_2, alkyl chain), 25.8 (CH_2, C-1), 26.2 (CH_2,alkyl chain), [29.6, 29.7, 29.8, 29.9, 30.0, 30.1, 31.8, 32.3 (CH_2, alkyl chain, resonance overlap)], 32.9 (CH_2, C-2″), 33.2 (CH_2, alkyl chain), 36.1 (CH_2,C-13‴), 36.8 (CH_2, C-2‴), 47.4 (CH_2, C-1″), 51.3 (CH, C-2), 58.3

(CH_2, C-3″), [72.5, 76.7 (CH, C-3, C-4)], 123.5 (CH, Ar CH, triazole), [128.0, 128.6, 128.7, 130.3, 130.4, 133.0, 133.3 (CH, Ar CH)], [137.8, 138.0, 143.7 (C, Ar C)], 174.9 (C, amide *C*=O), triazole *C* and ketone *C*=O not observed; *m/z* (TOF ES+) 803.6 ($[M + H]^+$, 100%); HRMS *m/z* (TOF ES+) 803.6054 [M + H], $C_{49}H_{79}N_4O_5$ requires 803.6050.

Chapter 5

References

6. References

1. Reece, J. B.; Campbell, N. A., *Campbell biology*. Benjamin Cummings / Pearson: Boston, 2011.
2. Maverakis, E.; Kim, K.; Shimoda, M.; Gershwin, M. E.; Patel, F.; Wilken, R.; Raychaudhuri, S.; Ruhaak, L. R.; Lebrilla, C. B. *J. Autoimmun.* **2015,** 57, 1-13.
3. Mogensen, T. H. *Clin. Microbiol. Rev.* **2009,** 22, (2), 240-273.
4. Janeway, C., Immunobiology : the immune system in health and disease. 6th ed. ed.; Garland Science: New York :, 2005.
5. OpenStax, Adaptive Immune Response. OpenStax CNX. Jun 21, 2013 http://cnx.org/contents/7ad6686e-c53e-45bb-aaa2-15327dff8d3e@6
6. Gascoigne, N. R. J. *Nat. Rev. Immunol.* **2008,** 8, (11), 895-900.
7. Genesis, R. Unbiased next generation T cell receptor (TCR)/B cell receptor (BCR) repertoire analysis. http://www.repertoire.co.jp/wprepgen/en/technology/detailed_repertoire
8. National Institute of Allergy and Infectious Diseases (U.S.); National Cancer Institute (U.S.), Understanding the immune system : how it works. In *NIH publication no. 03-5423*, U.S. Dept. of Health and Human Services, National Institutes of Health National Cancer Institute: [Bethesda, Md.?], 2003; p 57 p.
9. Berger, A. *BMJ* **2000,** 321, (7258), 424.
10. Vantourout, P.; Hayday, A. *Nat. Rev. Immunol.* **2013,** 13, (2), 88-100.
11. Kjer-Nielsen, L.; Patel, O.; Corbett, A. J.; Le Nours, J.; Meehan, B.; Liu, L.; Bhati, M.; Chen, Z.; Kostenko, L.; Reantragoon, R.; Williamson, N. A.; Purcell, A. W.; Dudek, N. L.; McConville, M. J.; O/'Hair, R. A. J.; Khairallah, G. N.; Godfrey, D. I.; Fairlie, D. P.; Rossjohn, J.; McCluskey, J. *Nature* **2012,** 491, (7426), 717-723.
12. Corbett, A. J.; Eckle, S. B. G.; Birkinshaw, R. W.; Liu, L.; Patel, O.; Mahony, J.; Chen, Z.; Reantragoon, R.; Meehan, B.; Cao, H.; Williamson, N. A.; Strugnell, R. A.; Van

Sinderen, D.; Mak, J. Y. W.; Fairlie, D. P.; Kjer-Nielsen, L.; Rossjohn, J.; McCluskey, J. *Nature* **2014,** 509, (7500), 361-365.

13. Ussher, J. E.; Klenerman, P.; Willberg, C. B. *Front. Immunol.* **2014,** 5, 450.
14. Gold, M. C.; Eid, T.; Smyk-Pearson, S.; Eberling, Y.; Swarbrick, G. M.; Langley, S. M.; Streeter, P. R.; Lewinsohn, D. A.; Lewinsohn, D. M. *Mucosal Immunol.* **2013,** 6, (1), 35-44.
15. Gold, M. C.; Cerri, S.; Smyk-Pearson, S.; Cansler, M. E.; Vogt, T. M.; Delepine, J.; Winata, E.; Swarbrick, G. M.; Chua, W. J.; Yu, Y. Y.; Lantz, O.; Cook, M. S.; Null, M. D.; Jacoby, D. B.; Harriff, M. J.; Lewinsohn, D. A.; Hansen, T. H.; Lewinsohn, D. M. *PLoS Biol.* **2010,** 8, (6), e1000407.
16. Budd, R. C.; Miescher, G. C.; Howe, R. C.; Lees, R. K.; Bron, C.; MacDonald, H. R. *J. Exp. Med.* **1987,** 166, (2), 577-82.
17. Fowlkes, B. J.; Kruisbeek, A. M.; Ton-That, H.; Weston, M. A.; Coligan, J. E.; Schwartz, R. H.; Pardoll, D. M. *Nature* **1987,** 329, (6136), 251-4.
18. Ceredig, R.; Lynch, F.; Newman, P. *Proc. Natl. Acad. Sci. U.S.A.* **1987,** 84, (23), 8578-82.
19. Godfrey, D. I.; MacDonald, H. R.; Kronenberg, M.; Smyth, M. J.; Van Kaer, L. *Nat. Rev. Immunol.* **2004,** 4, (3), 231-7.
20. Morita, M.; Motoki, K.; Akimoto, K.; Natori, T.; Sakai, T.; Sawa, E.; Yamaji, K.; Koezuka, Y.; Kobayashi, E.; Fukushima, H. *J. Med. Chem.* **1995,** 38, (12), 2176-87.
21. Bendelac, A.; Savage, P. B.; Teyton, L. *Annu. Rev. Immunol.* **2007,** 25, 297-336.
22. Kobayashi, K. S.; van den Elsen, P. J. *Nat. Rev. Immunol.* **2012,** 12, (12), 813-820.
23. and, A. L. H.; Yeager, M. *Annual Review of Genetics* **1998,** 32, (1), 415-435.
24. Parcej, D.; Tampe, R. *Nat. Chem. Biol.* **2010,** 6, (8), 572-80.
25. Mendlovic, F.; Conconi, M. *Nature Education* **2010**.
26. Satoh, T.; Yamaguchi, T.; Kato, K. *Molecules* **2015,** 20, (2), 2475-91.
27. Kozlov, G.; Pocanschi, C. L.; Rosenauer, A.; Bastos-Aristizabal, S.; Gorelik, A.; Williams, D. B.; Gehring, K. *J. Biol. Chem.* **2010,** 285, (49), 38612-38620.

28. Kapoor, M.; Ellgaard, L.; Gopalakrishnapai, J.; Schirra, C.; Gemma, E.; Oscarson, S.; Helenius, A.; Surolia, A. *Biochemistry* **2004,** 43, (1), 97-106.

29. Kapoor, M.; Srinivas, H.; Kandiah, E.; Gemma, E.; Ellgaard, L.; Oscarson, S.; Helenius, A.; Surolia, A. *J. Biol. Chem.* **2003,** 278, (8), 6194-6200.

30. Demchenko, A. V., General Aspects of the Glycosidic Bond Formation. In *Handbook of Chemical Glycosylation*, Wiley-VCH Verlag GmbH & Co. KGaA: 2008; pp 1-27.

31. Jain, R. K.; Liu, X. G.; Oruganti, S. R.; Chandrasekaran, E. V.; Matta, K. L. *Carbohydr. Res.* **1995,** 271, (2), 185-96.

32. Sato, S.; Mori, M.; Ito, Y.; Ogawa, t. *Carbohydr. Res.* **1986,** 155, C6-C10.

33. Cherif, S.; Clavel, J.-M.; Monneret, C. *J. Carbohyd. Chem.* **2002,** 21, (1-2), 123-130.

34. Cherif, S.; Clavel, J.-M.; Monneret, C. *J. Carbohyd. Chem.* **1998,** 17, (8), 1203-1218.

35. Gemma, E.; Lahmann, M.; Oscarson, S. *Carbohydr. Res.* **2005,** 340, (16), 2558-62.

36. Ogawa, T.; Katano, K.; Sasajima, K.; Matsui, M. *Tetrahedron* **1981,** 37, (16), 2779-2786.

37. Kobashi, Y.; Mukaiyama, T. *Chem. Lett.* **2004,** 33, (7), 874-875.

38. Iwamoto, S.; Kasahara, Y.; Kamei, K.; Seko, A.; Takeda, Y.; Ito, Y.; Matsuo, I. *Biosci. Biotech. Bioch.* **2014,** 78, (6), 927-36.

39. Lemieux, R. U.; Suemitsu, R.; Gunner, S. W. *Can. J. Chem.* **1968,** 46, (6), 1040-1041.

40. Iino, K.; Iwamoto, S.; Kasahara, Y.; Matsuda, K.; Tonozuka, T.; Nishikawa, A.; Ito, Y.; Matsuo, I. *Tetrahedron Lett.* **2012,** 53, (33), 4452-4456.

41. Diamandis, E. P.; Christopoulos, T. K. *Clin. Chem.* **1991,** 37, (5), 625-36.

42. Beignet, J.; Tiernan, J.; Woo, C. H.; Kariuki, B. M.; Cox, L. R. *J. Org. Chem.* **2004,** 69, (19), 6341-56.

43. L'Abbe, G. *Chem. Rev.* **1969,** 69, (3), 345-363.

44. MinHuang; Huu-AnhTran; LuisBohé; Crich, D., Phenyl 4,6-O-Benzylidene-1-thio-α-d-mannopyranoside. In *Carbohydrate Chemistry*, CRC Press: 2014; pp 175-182.

45. Sanapala, S. R.; Kulkarni, S. S. *Chem. Eur. J.* **2014,** 20, (13), 3578-3583.

46. Szurmai, Z.; Balatoni, L.; Lipták, A. *Carbohydr. Res.* **1994,** 254, 301-309.

47. Staněk, J., Preparation of selectively alkylated saccharides as synthetic intermediates. In *Carbohydrate Chemistry*, Springer Berlin Heidelberg: Berlin, Heidelberg, 1990; pp 209-256.

48. Garegg, P. J.; Iversen, T.; Oscarson, S. *Carbohydr. Res.* **1976,** 50, (2), C12-C14.

49. Crich, D.; Li, W.; Li, H. *J. Am. Chem. Soc.* **2004,** 126, (46), 15081-15086.

50. Matsuo, I.; Wada, M.; Manabe, S.; Yamaguchi, Y.; Otake, K.; Kato, K.; Ito, Y. *J. Am. Chem. Soc.* **2003,** 125, (12), 3402-3403.

51. Garegg, P. J.; Kvarnström, I.; Niklasson, A.; Niklasson, G.; Svensson, S. C. T. *J. Carbohyd. Chem.* **1993,** 12, (7), 933-953.

52. Jervis, P. J.; Cox, L. R.; Besra, G. S. *J. Org. Chem.* **2011,** 76, (1), 320-323.

53. Schombs, M.; Park, F. E.; Du, W.; Kulkarni, S. S.; Gervay-Hague, J. *J. Org. Chem.* **2010,** 75, (15), 4891-4898.

54. Du, W.; Gervay-Hague, J. *Org. Lett.* **2005,** 7, (10), 2063-2065.

55. Du, W.; Kulkarni, S. S.; Gervay-Hague, J. *Chem. Commun.* **2007**, (23), 2336-2338.

56. Davis, R. A.; Fettinger, J. C.; Gervay-Hague, J. *J. Org. Chem.* **2014,** 79, (17), 8447-8452.

57. Wonjo, J. Novel glycolipids in CD1d-mediated immunity: synthesis of new agonists of CD1d. Ph.D., University of Birmingham, 2012.

58. Shingu, Y.; Nishida, Y.; Dohi, H.; Matsuda, K.; Kobayashi, K. *J. Carbohyd. Chem.* **2002,** 21, (6), 605-611.

59. Nishida, Y.; Ohrui, H.; Meguro, H.; Ishizawa, M.; Matsuda, K.; Taki, T.; Handa, S.; Yamamoto, N. *Tetrahedron Lett.* **1994,** 35, (30), 5465-5468.

60. Shingu, Y.; Nishida, Y.; Dohi, H.; Kobayashi, K. *Org. Biomol. Chem.* **2003,** 1, (14), 2518-2521.

61. Nishida, Y.; Shingu, Y.; Dohi, H.; Kobayashi, K. *Org. Lett.* **2003,** 5, (14), 2377-2380.

62. Tambie, M. S.; Jalsa, N. K. *J. Carbohyd. Chem.* **2015,** 34, (9), 545-559.

63. Eby, R.; J. Sondheimer, S.; Schuerch, C. *Carbohydr. Res.* **1979,** 73, (1), 273-276.

64. Franzyk, H.; Meldal, M.; Paulsen, H.; Bock, K. *J. Chem. Soc., Perkin Trans. 1* **1995**, (22), 2883-2898.

65. Mootoo, D. R.; Konradsson, P.; Udodong, U.; Fraser-Reid, B. *J. Am. Chem. Soc.* **1988,** 110, (16), 5583-5584.

66. Fraser-Reid, B.; Wu, Z.; Andrews, C. W.; Skowronski, E.; Bowen, J. P. *J. Am. Chem. Soc.* **1991,** 113, (4), 1434-1435.

67. Duus, J. Ø.; Gotfredsen, C. H.; Bock, K. *Chem. Rev.* **2000,** 100, (12), 4589-4614.

68. Bock, K.; Thøgersen, H. *Ann. R. NMR S.* **1983,** 13, 1-57.

69. Despras, G.; Robert, R.; Sendid, B.; Machez, E.; Poulain, D.; Mallet, J.-M. *Bioorg. Med. Chem.* **2012,** 20, (5), 1817-1831.

70. Brigl, M.; Brenner, M. B. *Annu. Rev. Immunol.* **2004,** 22, 817-890.

71. Calabi, F.; Jarvis, J. M.; Martin, L.; Milstein, C. *Eur. J. Immunol.* **1989,** 19, (2), 285-292.

72. Young, D. C.; Moody, D. B. *Glycobiology* **2006,** 16, (7), 103r-112r.

73. Barral, D. C.; Brenner, M. B. *Nat. Rev. Immunol.* **2007,** 7, (12), 929-941.

74. Porubsky, S.; Speak, A. O.; Luckow, B.; Cerundolo, V.; Platt, F. M.; Gröne, H.-J. *Proc. Natl. Acad. Sci. U.S.A.* **2007,** 104, (14), 5977-5982.

75. Kain, L.; Webb, B.; Anderson, Brian L.; Deng, S.; Holt, M.; Costanzo, A.; Zhao, M.; Self, K.; Teyton, A.; Everett, C.; Kronenberg, M.; Zajonc, Dirk M.; Bendelac, A.; Savage, Paul B.; Teyton, L. *Immunity* 41, (4), 543-554.

76. Kronenberg, M.; Gapin, L. *Nat. Rev. Immunol.* **2002,** 2, (8), 557-568.

77. Joyce, S. *Cell. Mol. Life. Sci.* **2001,** 58, (3), 442-469.

78. Godfrey, D. I.; Berzins, S. P. *Nat. Rev. Immunol.* **2007,** 7, (7), 505-18.

79. Natori, T.; Koezuka, Y.; Higa, T. *Tetrahedron Lett.* **1993,** 34, (35), 5591-5592.

80. Kaer, L. V. *Nat. Rev. Immunol.* **2005,** 5, (1), 31-42.

81. Ishikawa, A.; Motohashi, S.; Ishikawa, E.; Fuchida, H.; Higashino, K.; Otsuji, M.; Iizasa, T.; Nakayama, T.; Taniguchi, M.; Fujisawa, T. *Clin. Cancer Res.* **2005,** 11, (5), 1910-1917.

82. Uchida, T.; Horiguchi, S.; Tanaka, Y.; Yamamoto, H.; Kunii, N.; Motohashi, S.; Taniguchi, M.; Nakayama, T.; Okamoto, Y. *Cancer Immunol. Immun.* **2008,** 57, (3), 337-345.

83. Koch, M.; Stronge, V. S.; Shepherd, D.; Gadola, S. D.; Mathew, B.; Ritter, G.; Fersht, A. R.; Besra, G. S.; Schmidt, R. R.; Jones, E. Y.; Cerundolo, V. *Nature Immunology* **2005,** 6, (8), 819-826.

84. Zajonc, D. M.; Cantu, C.; Mattner, J.; Zhou, D.; Savage, P. B.; Bendelac, A.; Wilson, I. A.; Teyton, L. *Nat. Immunol.* **2005,** 6, (8), 810-818.

85. Rossjohn, J.; Pellicci, D. G.; Patel, O.; Gapin, L.; Godfrey, D. I. *Nat. Rev. Immunol.* **2012,** 12, (12), 845-857.

86. Pellicci, D. G.; Patel, O.; Kjer-Nielsen, L.; Pang, S. S.; Sullivan, L. C.; Kyparissoudis, K.; Brooks, A. G.; Reid, H. H.; Gras, S.; Lucet, I. S.; Koh, R.; Smyth, M. J.; Mallevaey, T.; Matsuda, J. L.; Gapin, L.; McCluskey, J.; Godfrey, D. I.; Rossjohn, J. *Immunity* **2009,** 31, (1), 47-59.

87. Wojno, J.; Jukes, J. P.; Ghadbane, H.; Shepherd, D.; Besra, G. S.; Cerundolo, V.; Cox, L. R. *ACS Chem. Biol.* **2012,** 7, (5), 847-55.

88. Borg, N. A.; Wun, K. S.; Kjer-Nielsen, L.; Wilce, M. C.; Pellicci, D. G.; Koh, R.; Besra, G. S.; Bharadwaj, M.; Godfrey, D. I.; McCluskey, J.; Rossjohn, J. *Nature* **2007,** 448, (7149), 44-9.

89. Chang, Y. J.; Huang, J. R.; Tsai, Y. C.; Hung, J. T.; Wu, D.; Fujio, M.; Wong, C. H.; Yu, A. L. *Proc. Natl. Acad. Sci. U S A* **2007,** 104, (25), 10299-304.

90. Miyamoto, K.; Miyake, S.; Yamamura, T. *Nature* **2001,** 413, (6855), 531-4.

91. Iijima, H.; Kimura, K.; Sakai, T.; Uchimura, A.; Shimizu, T.; Ueno, H.; Natori, T.; Koezuka, Y. *Bioorg. Med. Chem.* **1998,** 6, (10), 1905-10.

92. Brossay, L.; Naidenko, O.; Burdin, N.; Matsuda, J.; Sakai, T.; Kronenberg, M. *J Immunol* **1998,** 161, (10), 5124-8.

93. Leung, L.; Tomassi, C.; Van Beneden, K.; Decruy, T.; Elewaut, D.; Elliott, T.; Al-Shamkhani, A.; Ottensmeier, C.; Van Calenbergh, S.; Werner, J.; Williams, T.; Linclau, B. *Org. Lett.* **2008,** 10, (20), 4433-6.

94. Fujio, M.; Wu, D.; Garcia-Navarro, R.; Ho, D. D.; Tsuji, M.; Wong, C. H. *J. Am. Chem. Soc.* **2006,** 128, (28), 9022-3.

95. Forestier, C.; Takaki, T.; Molano, A.; Im, J. S.; Baine, I.; Jerud, E. S.; Illarionov, P.; Ndonye, R.; Howell, A. R.; Santamaria, P.; Besra, G. S.; DiLorenzo, T. P.; Porcelli, S. A. *J. Immunol.* **2007,** 178, (3), 1415-1425.

96. Yu, K. O. A.; Im, J. S.; Molano, A.; Dutronc, Y.; Illarionov, P. A.; Forestier, C.; Fujiwara, N.; Arias, I.; Miyake, S.; Yamamura, T.; Chang, Y.-T.; Besra, G. S.; Porcelli, S. A. *Proc. Natl. Acad. Sci. U.S.A.* **2005,** 102, (9), 3383-3388.

97. Wu, T.-N.; Lin, K.-H.; Chang, Y.-J.; Huang, J.-R.; Cheng, J.-Y.; Yu, A. L.; Wong, C.-H. *Proc. Natl. Acad. Sci. U.S.A.* **2011,** 108, (42), 17275-17280.

98. Li, X.; Fujio, M.; Imamura, M.; Wu, D.; Vasan, S.; Wong, C.-H.; Ho, D. D.; Tsuji, M. *Proc. Natl. Acad. Sci. U.S.A.* **2010,** 107, (29), 13010-13015.

99. Schiefner, A.; Fujio, M.; Wu, D.; Wong, C.-H.; Wilson, I. A. *J. Mol. Biol.* **2009,** 394, (1), 71-82.

100. Koch, M.; Stronge, V. S.; Shepherd, D.; Gadola, S. D.; Mathew, B.; Ritter, G.; Fersht, A. R.; Besra, G. S.; Schmidt, R. R.; Jones, E. Y.; Cerundolo, V. *Nat. Immunol.* **2005,** 6, (8), 819-826.

101. E. Hénon; M. Dauchez; A. Haudrechy; A. Blanchet. *Tetrahedron* **2008,** 64, 9480-8489.

102. Leung, L.; Tomassi, C.; Van Beneden, K.; Decruy, T.; Trappeniers, M.; Elewaut, D.; Gao, Y.; Elliott, T.; Al-Shamkhani, A.; Ottensmeier, C.; Werner, J. M.; Williams, A.; Van Calenbergh, S.; Linclau, B. *ChemMedChem* **2009,** 4, (3), 329-34.

103. Tashiro, T.; Hongo, N.; Nakagawa, R.; Seino, K.; Watarai, H.; Ishii, Y.; Taniguchi, M.; Mori, K. *Bioorg. Med. Chem.* **2008,** 16, (19), 8896-906.

104. Lee, T.; Cho, M.; Ko, S. Y.; Youn, H. J.; Baek, D. J.; Cho, W. J.; Kang, C. Y.; Kim, S. *J. Med. Chem.* **2007,** 50, (3), 585-9.

105. Tashiro, T.; Shigeura, T.; Watarai, H.; Taniguchi, M.; Mori, K. *Bioorg. Med. Chem.* **2012,** 20, (14), 4540-8.

106. Venkataswamy, M. M.; Porcelli, S. A. *Semin. Immunol.* **2010,** 22, (2), 68-78.

107. Sullivan, B. A.; Nagarajan, N. A.; Wingender, G.; Wang, J.; Scott, I.; Tsuji, M.; Franck, R. W.; Porcelli, S. A.; Zajonc, D. M.; Kronenberg, M. *J. Immunol.* **2010,** 184, (1), 141-153.

108. Schmieg, J.; Yang, G.; Franck, R. W.; Tsuji, M. *J. Exp. Med.* **2003,** 198, (11), 1631-41.

109. Tashiro, T.; Nakagawa, R.; Inoue, S.; Shiozaki, M.; Watarai, H.; Taniguchi, M.; Mori, K. *Tetrahedron Lett* **2008,** 49, (48), 6827-6830.

110. Trappeniers, M.; Van Beneden, K.; Decruy, T.; Hillaert, U.; Linclau, B.; Elewaut, D.; Van Calenbergh, S. *J. Am. Chem. Soc.* **2008,** 130, (49), 16468-9.

111. Diaz, Y. R. G.; Wojno, J.; Cox, L. R.; Besra, G. S. *Tetrahedron-Asymmetry* **2009,** 20, (6-8), 747-753.

112. Yu, T.-F. The Synthesis and Evaluation of Chemical Adjuvants for Modulating Immunity. University of Birmingham, Birmingham, 2012.

113. Jukes, J. P.; Gileadi, U.; Ghadbane, H.; Yu, T. F.; Shepherd, D.; Cox, L. R.; Besra, G. S.; Cerundolo, V. *Eur. J. Immunol.* **2016,** 46, (5), 1224-1234.

114. Silk, J. D.; Salio, M.; Reddy, B. G.; Shepherd, D.; Gileadi, U.; Brown, J.; Masri, S. H.; Polzella, P.; Ritter, G.; Besra, G. S.; Jones, E. Y.; Schmidt, R. R.; Cerundolo, V. *J. Immunol.* **2008,** 180, (10), 6452-6.

115. Li, X.; Fujio, M.; Imamura, M.; Wu, D.; Vasan, S.; Wong, C. H.; Ho, D. D.; Tsuji, M. *Proc. Natl. Acad. Sci. U.S.A.* **2010,** 107, (29), 13010-5.

116. Yu, S. H.; Park, J. J.; Chung, S. K. *Tetrahedron-Asymmetry* **2006,** 17, (21), 3030-3036.

117. Ottesen, L. K.; Jaroszewski, J. W.; Franzyk, H. *J. Org. Chem.* **2010,** 75, (15), 4983-4991.

118. Stanetty, C.; Blaukopf, M. K.; Lachmann, B.; Noe, C. R. *Eur. J. Org. Chem.* **2011**, (17), 3126-3130.

119. Prasad, B. A. B.; Sanghi, R.; Singh, V. K. *Tetrahedron* **2002,** 58, (36), 7355-7363.

120. Paul, B. J.; Willis, J.; Martinot, T. A.; Ghiviriga, I.; Abboud, K. A.; Hudlicky, T. *J. Am. Chem. Soc.* **2002,** 124, (35), 10416-26.

121. Tsunoda, H.; Ogawa, S. *Liebigs Ann.* **1995**, (2), 267-277.

122. Roemmele, R. C.; Rapoport, H. *J. Org. Chem.* **1988,** 53, (10), 2367-2371.

123. Vedejs, E.; Lin, S. Z. *J. Org. Chem.* **1994,** 59, (7), 1602-1603.

124. Alonso, E.; Ramon, D. J.; Yus, M. *Tetrahedron* **1997,** 53, (42), 14355-14368.

125. Berkessel, A.; Schröder, M.; Sklorz, C. A.; Tabanella, S.; Vogl, N.; Lex, J.; Neudörfl, J. M. *J. Org. Chem.* **2004,** 69, (9), 3050-3056.

126. Chandrasekhar, S.; Mahipal, B.; Kavitha, M. *J. Org. Chem.* **2009,** 74, (24), 9531-9534.

127. Goddard-Borger, E. D.; Stick, R. V. *Org. Lett.* **2007,** 9, (19), 3797-3800.

128. Vasella, A.; Witzig, C.; Chiara, J. L.; Martinlomas, M. *Helv. Chim. Acta.* **1991,** 74, (8), 2073-2077.

129. Alper, P. B.; Hung, S. C.; Wong, C. H. *Tetrahedron Lett.* **1996,** 37, (34), 6029-6032.

130. Harrak, Y.; Llebaria, A.; Delgado, A. *Eur. J. Org. Chem.* **2008**, (27), 4647-4654.

131. Loudon, J. D.; Shulman, N. *J. Chem. Soc.* **1941**, 722-727.

132. Nyasse, B.; Grehn, L.; Ragnarsson, U. *Chem. Commun.* **1997**, (11), 1017-1018.

133. Jørgensen, M.; Iversen, E. H.; Paulsen, A. L.; Madsen, R. *J. Org. Chem.* **2001,** 66, (13), 4630-4634.

134. Bartocha, B.; Kaesz, H. D.; Stone, F. G. A. *Z. Naturforsch. B* **1959,** 14 b, 352-353.

135. Kwon, Y.-U.; Lee, C.; Chung, S.-K. *J. Org. Chem.* **2002,** 67, (10), 3327-3338.

136. Chang, Y.-K.; Lo, H.-J.; Yan, T.-H. *Org. Lett.* **2009,** 11, (19), 4278-4281.

137. Kwon, Y. U.; Chung, S. K. *Org. Lett.* **2001,** 3, (19), 3013-6.

138. Yu, T.-F. The synthesis and evaluation of chemical adjuvants for modulating immunity. Ph.D., University of Birmingham, 2013.

139. Ackermann, L.; El Tom, D.; Furstner, A. *Tetrahedron* **2000,** 56, (15), 2195-2202.

140. Chérest, M.; Felkin, H.; Prudent, N. *Tetrahedron Lett.* **1968,** 9, (18), 2199-2204.

141. Bricard, G.; Venkataswamy, M. M.; Yu, K. O.; Im, J. S.; Ndonye, R. M.; Howell, A. R.; Veerapen, N.; Illarionov, P. A.; Besra, G. S.; Li, Q.; Chang, Y. T.; Porcelli, S. A. *PLoS One* **2010,** 5, (12), e14374.

142. Fujii, S.-i.; Shimizu, K.; Hemmi, H.; Fukui, M.; Bonito, A. J.; Chen, G.; Franck, R. W.; Tsuji, M.; Steinman, R. M. *Proc. Natl. Acad. Sci. U.S.A.* **2006,** 103, (30), 11252-11257.

143. Yang, G.; Schmieg, J.; Tsuji, M.; Franck, R. W. *Angew. Chem. Int. Ed.* **2004,** 43, (29), 3818-3822.

144. Hogan, A. E.; O'Reilly, V.; Dunne, M. R.; Dere, R. T.; Zeng, S. G.; O'Brien, C.; Amu, S.; Fallon, P. G.; Exley, M. A.; O'Farrelly, C.; Zhu, X.; Doherty, D. G. *Clin. Immunol.* **2011,** 140, (2), 196-207.

145. Chennamadhavuni, D.; Howell, A. R. *Tetrahedron Lett.* **2015,** 56, (23), 3583-3586.

146. Harrak, Y.; Barra, C. M.; Delgado, A.; Castaño, A. R.; Llebaria, A. *J. Am. Chem. Soc.* **2011,** 133, (31), 12079-12084.

147. Harrak, Y.; Barra, C. M.; Bedia, C.; Delgado, A.; Castaño, A. R.; Llebaria, A. *ChemMedChem* **2009,** 4, (10), 1608-1613.

148. Garcia Diaz, Y. R.; Wojno, J.; Cox, L. R.; Besra, G. S. *Tetrahedron-Asymmetry* **2009,** 20, (6–8), 747-753.

149. Alcaide, A.; Llebaria, A. *J. Org. Chem.* **2014,** 79, (7), 2993-3029.

150. Zhu, X.; Dere, R. T.; Jiang, J. *Tetrahedron Lett.* **2011,** 52, (38), 4971-4974.

151. Dere, R. T.; Zhu, X. *Org. Lett.* **2008,** 10, (20), 4641-4644.

152. Sakakibara, K.; Nozaki, K. *Org. Biomol. Chem.* **2009,** 7, (3), 502-507.

153. Howson, W.; Osborn, H. M. I.; Sweeney, J. *J. Chem. Soc., Perkin Trans. 1* **1995**, (19), 2439-2445.

154. Enders, D.; Lenzen, A.; Backes, M.; Janeck, C.; Catlin, K.; Lannou, M.-I.; Runsink, J.; Raabe, G. *J. Org. Chem.* **2005,** 70, (25), 10538-10551.

155. Singh, A.; Thornton, E. R.; Westheimer, F. H. *J. Biol. Chem.* **1962,** 237, (9), PC3006-PC3008.

156. Qvit, N.; Monderer-Rothkoff, G.; Ido, A.; Shalev, D. E.; Amster-Choder, O.; Gilon, C. *Biopolymers* **2008,** 90, (4), 526-36.

157. Hilbold, B.; Perrault, M.; Ehret, C.; Niu, S. L.; Frisch, B.; Pecheur, E. I.; Bourel-Bonnet, L. *Bioorg. Med. Chem.* **2011,** 19, (24), 7464-73.

158. Dubinsky, L.; Krom, B. P.; Meijler, M. M. *Bioorg. Med. Chem.* **2012,** 20, (2), 554-70.

159. Galardy, R. E.; Craig, L. C.; Printz, M. P. *Nat. New Biol.* **1973,** 242, (117), 127-8.

160. Sumranjit, J.; Chung, S. J. *Molecules* **2013,** 18, (9), 10425-51.

161. Sonogashira, K.; Tohda, Y.; Hagihara, N. *Tetrahedron Lett.* **1975,** 16, (50), 4467-4470.

162. Quesada, E.; Ardhammar, M.; Nordén, B.; Miesch, M.; Duportail, G.; Bonzi-Coulibaly, Y.; Nakatani, Y.; Ourisson, G. *Helv. Chim. Acta.* **2000,** 83, (9), 2464-2476.

163. Lee, T.; Cho, M.; Ko, S.-Y.; Youn, H.-J.; Baek, D. J.; Cho, W.-J.; Kang, C.-Y.; Kim, S. *J. Med. Chem.* **2007,** 50, (3), 585-589.

164. Jervis, P. J.; Graham, L. M.; Foster, E. L.; Cox, L. R.; Porcelli, S. A.; Besra, G. S. *Bioorg. Med. Chem. Lett.* **2012,** 22, (13), 4348-4352.

165. Gorantla, J. N.; Faseela, A.; Lankalapalli, R. S. *Chem. Phys. Lipids* **2016,** 194, 158-164.

166. McKay, Craig S.; Finn, M. G. *Chem. Biol* **2014,** 21, (9), 1075-1101.

167. Bisai, A.; Pandey, G.; Pandey, M. K.; Singh, V. K. *Tetrahedron Lett.* **2003,** 44, (31), 5839-5841.

168. Jervis, P. J.; Moulis, M.; Jukes, J.-P.; Ghadbane, H.; Cox, L. R.; Cerundolo, V.; Besra, G. S. *Carbohydr. Res.* **2012,** 356, 152-162.

169. Meldal, M.; Tornoe, C. W. *Chem. Rev.* **2008,** 108, (8), 2952-3015.

170. Xia, Y.; Li, W.; Qu, F. Q.; Fan, Z. J.; Liu, X. F.; Berro, C.; Rauzy, E.; Peng, L. *Org. Biomol. Chem.* **2007,** 5, (11), 1695-1701.

171. Xia, Y.; Fan, Z. J.; Yao, J. H.; Liao, Q.; Li, W.; Qu, F. Q.; Peng, L. *Bioorg. Med. Chem. Lett.* **2006,** 16, (10), 2693-2698.

172. Turner, J. J.; Leeuwenburgh, M. A.; van der Marel, G. A.; van Boom, J. H. *Tetrahedron Lett.* **2001,** 42, (49), 8713-8716.

173. Trost, B. M.; Machacek, M. R.; Faulk, B. D. *J. Am. Chem. Soc.* **2006,** 128, (20), 6745-6754.

174. Hsu, C.-H.; Chu, K.-C.; Lin, Y.-S.; Han, J.-L.; Peng, Y.-S.; Ren, C.-T.; Wu, C.-Y.; Wong, C.-H. *Chem. Eur. J.* **2010,** 16, (6), 1754-1760.

175. Tennant-Eyles, R. J.; Davis, B. G.; Fairbanks, A. J. *Tetrahedron-Asymmetry* **2003,** 14, (9), 1201-1210.

176. Weng, S.-S.; Lin, Y.-D.; Chen, C.-T. *Org. Lett.* **2006,** 8, (24), 5633-5636.

177. Ekholm, F. S.; Poláková, M.; Pawłowicz, A. J.; Leino, R. *Synthesis* **2009,** 2009, (04), 567-576.

178. Crich, D.; Li, W. J.; Li, H. M. *J. Am. Chem. Soc.* **2004,** 126, (46), 15081-15086.

179. Jervis, P. J.; Veerapen, N.; Bricard, G.; Cox, L. R.; Porcelli, S. A.; Besra, G. S. *Bioorg. Med. Chem. Lett.* **2010,** 20, (12), 3475-3478.

180. Bucher, C.; Gilmour, R. *Angew. Chem. Int. Ed.* **2010,** 49, (46), 8724-8728.

181. Ková, P.; Yeh, H. J. C.; Jung, G. L. *J. Carbohyd. Chem.* **1987,** 6, (3), 423-439.

182. Dere, R. T.; Zhu, X. M. *Org. Lett.* **2008,** 10, (20), 4641-4644.

183. Kim, S.; Song, S.; Lee, T.; Jung, S.; Kim, D. *Synthesis-Stuttgart* **2004**, (6), 847-850.

184. Soucy, R. L.; Kozhinov, D.; Behar, V. *J. Org. Chem.* **2002,** 67, (6), 1947-1952.

185. Tobler, E.; J, F. D., Divinylizinc and method of making. Google Patents: 1963.

186. Lo, H. J.; Chang, Y. K.; Yan, T. H. *Org. Lett.* **2012,** 14, (23), 5896-5899.

187. Liu, Z.; Bittman, R. *Org. Lett.* **2012,** 14, (2), 620-623.

188. Fernandes, R. A. *Eur. J. Org. Chem.* **2007**, (30), 5064-5070.

189. Suemune, H.; Harabe, T.; Sakai, K. *Chem. Pharm. Bull.* **1988,** 36, (9), 3632-3637.

190. Wang, L.; Zhu, W. *Tetrahedron Lett.* **2013,** 54, (49), 6729-6731.

191. Danieli, E.; Trabocchi, A.; Menchi, G.; Guarna, A. *Eur. J. Org. Chem.* **2005,** 2005, (20), 4372-4381.

192. Prasad, K. R.; Swain, B. *J. Org. Chem.* **2011,** 76, (7), 2029-2039.

193. Mitchell, D.; Lukeman, M.; Lehnherr, D.; Wan, P. *Org. Lett.* **2005,** 7, (15), 3387-3389.

194. Lee, Y. M.; Baek, D. J.; Lee, S.; Kim, D.; Kim, S. *J. Org. Chem.* **2011,** 76, (2), 408-416.

195. Chen, G.; Schmieg, J.; Tsuji, M.; Franck, R. W. *Org. Lett.* **2004,** 6, (22), 4077-4080.